

*The McGraw-Hill Companies*

# **FLOW IN OPEN CHANNELS**

Third Edition

## About the Author



**K Subramanya** is a retired Professor of Civil Engineering at the Indian Institute of Technology, Kanpur, India. He obtained his Bachelor's degree in Civil Engineering from Mysore University and a Master's degree from the University of Madras. Further, he obtained another Master's degree and a PhD degree from the University of Alberta, Edmonton, Canada. He has taught at IIT Kanpur for over 30 years and has extensive teaching experience in the areas of *Open Channel Hydraulics*, *Fluid Mechanics* and *Hydrology*. He has authored several successful books for McGraw-Hill Education India; besides the current book, his other books include *Engineering Hydrology* (3<sup>rd</sup> Ed., TMH 2008), and *1000 Solved Problems in Fluid Mechanics* (TMH 2005).

Dr Subramanya has published over eighty technical papers in national and international journals and conferences. He is a Fellow of the Institution of Engineers (India); Fellow of Indian Society for Hydraulics, Member of Indian Society of Technical Education and Member of Indian Water Resources Association.

Currently, he resides in Bangalore and is active as a practicing consultant in Water Resources Engineering.

The McGraw-Hill Companies

# FLOW IN OPEN CHANNELS

Third Edition

**K Subramanya**

*Former Professor  
Department of Civil Engineering  
Indian Institute of Technology  
Kanpur*



**Tata McGraw-Hill Publishing Company Limited**

NEW DELHI

---

*McGraw-Hill Offices*

**New Delhi** New York St. Louis San Francisco Auckland Bogotá  
Caracas Kuala Lumpur Lisbon London Madrid Mexico City  
Milan Montreal San Juan Santiago Singapore Sydney Tokyo Toronto



**Tata McGraw-Hill**

Published by the Tata McGraw-Hill Publishing Company Limited,  
7 West Patel Nagar, New Delhi 110 008.

Copyright © 2009, 1997, 1986 by Tata McGraw-Hill Publishing Company Limited.

No part of this publication may be reproduced or distributed in any form or by any means, electronic, mechanical, photocopying, recording, or otherwise or stored in a database or retrieval system without the prior written permission of the publishers. The program listings (if any) may be entered, stored and executed in a computer system, but they may not be reproduced for publication.

This edition can be exported from India only by the publishers,  
Tata McGraw-Hill Publishing Company Limited

ISBN (13): 978-0-07-008695-1

ISBN (10): 0-07-008695-8

Managing Director: *Ajay Shukla*

General Manager: Publishing—SEM & Tech Ed: *Vibha Mahajan*

Sponsoring Editor: *Shukti Mukherjee*

Jr Editorial Executive: *Surabhi Shukla*

Executive—Editorial Services: *Sohini Mukherjee*

Senior Production Manager: *P L Pandita*

General Manager: Marketing—Higher Education & School: *Michael J Cruz*

Product Manager: SEM & Tech Ed: *Biju Ganesan*

Controller—Production: *Rajender P Ghansela*

Asst. General Manager—Production: *B L Dogra*

Information contained in this work has been obtained by Tata McGraw-Hill, from sources believed to be reliable. However, neither Tata McGraw-Hill nor its authors guarantee the accuracy or completeness of any information published herein, and neither Tata McGraw Hill nor its authors shall be responsible for any errors, omissions, or damages arising out of use of this information. This work is published with the understanding that Tata McGraw-Hill and its authors are supplying information but are not attempting to render engineering or other professional services. If such services are required, the assistance of an appropriate professional should be sought.

Typeset at Mukesh Technologies Pvt. Ltd., #10, 100 Feet Road, Ellapillaichavadi,  
Pondicherry 605 005 and printed at Rashtriya Printers, M-135, Panchsheel Garden,  
Naveen Shahdara, Delhi 110 032

Cover Printer: Rashtriya Printers

RCXACDDFDRBYA

*To  
My Father*

सुप्रणीतो जलीघो हि कुक्षे कार्यमुत्तमम् ।  
घ्नन्धं जडं बलं प्राहुः प्रणेतव्यं विचक्षणेः ॥

महाभारत

*Only a well-designed channel performs its functions best.  
A blind inert force necessitates intelligent control.*

**MAHABHARATA**



# Contents

<i>Preface</i>	<i>xi</i>
<i>Guided Tour</i>	<i>xv</i>
<b>1. Flow in Open Channels</b>	<b>1</b>
1.1 Introduction	1
1.2 Types of Channels	1
1.3 Classification of Flows	2
1.4 Velocity Distribution	5
1.5 One-Dimensional Method of Flow Analysis	7
1.6 Pressure Distribution	10
1.7 Pressure Distribution in Curvilinear Flows	13
1.8 Flows with Small Water-Surface Curvature	17
1.9 Equation of Continuity	19
1.10 Energy Equation	22
1.11 Momentum Equation	26
References	30
Problems	30
Objective Questions	38
<b>2. Energy–Depth Relationships</b>	<b>42</b>
2.1 Specific Energy	42
2.2 Critical Depth	43
2.3 Calculation of the Critical Depth	47
2.4 Section Factor $Z$	51
2.5 First Hydraulic Exponent $M$	51
2.6 Computations	54
2.7 Transitions	60
References	73
Problems	73
Objective Questions	78
<b>3. Uniform Flow</b>	<b>85</b>
3.1 Introduction	85
3.2 Chezy Equation	85
3.3 Darcy–Weisbach Friction Factor $f$	86
3.4 Manning’s Formula	89
3.5 Other Resistance Formulae	91
3.6 Velocity Distribution	91
3.7 Shear Stress Distribution	94
3.8 Resistance Formula for Practical Use	96
3.9 Manning’s Roughness Coefficient $n$	96
3.10 Equivalent Roughness	101
3.11 Uniform Flow Computations	104
3.12 Standard Lined Canal Sections	114
3.13 Maximum Discharge of a Channel of the Second Kind	117
3.14 Hydraulically Efficient Channel Section	119
3.15 The Second Hydraulic Exponent $N$	123
3.16 Compound Channels	125
3.17 Critical Slope	131

3.18	Generalised-Flow Relation	134
3.19	Design of Irrigation Canals	139
	References	144
	Problems	145
	Objective Questions	151
<b>4.</b>	<b>Gradually Varied Flow Theory</b>	<b>157</b>
4.1	Introduction	157
4.2	Differential Equation of GVF	157
4.3	Classification of Flow Profiles	160
4.4	Some Features of Flow Profiles	166
4.5	Control Sections	169
4.6	Analysis of Flow Profile	172
4.7	Transitional Depth	180
	Problems	183
	Objective Questions	185
<b>5.</b>	<b>Gradually Varied Flow Computations</b>	<b>189</b>
5.1	Introduction	189
5.2	Direct Integration of GVF Differential Equation	190
5.3	Bresse's Solution	195
5.4	Channels with Considerable Variation in Hydraulic Exponents	199
5.5	Direct Integration for Circular Channels	200
5.6	Simple Numerical Solutions of GVF Problems	203
5.7	Advanced Numerical Methods	221
5.8	Flow Profiles in Divided Channels	223
5.9	Role of End Conditions	225
	References	232
	Problems	233
	Objective Questions	236
<b>6.</b>	<b>Rapidly Varied Flow-1—Hydraulic Jump</b>	<b>248</b>
6.1	Introduction	248
6.2	The Momentum Equation Formulation for the Jump	249
6.3	Hydraulic Jump in a Horizontal Rectangular Channel	250
6.4	Jumps in Horizontal Non-Rectangular Channels	265
6.5	Jumps on a Sloping Floor	274
6.6	Use of the Jump as an Energy Dissipator	279
6.7	Location of the Jump	281
	References	286
	Problems	287
	Objective Questions	293
<b>7.</b>	<b>Rapidly Varied Flow-2</b>	<b>295</b>
7.1	Introduction	295
7.2	Sharp-Crested Weir	295
7.3	Special Sharp-Crested Weirs	305
7.4	Ogee Spillway	316
7.5	Broad-Crested Weir	326
7.6	Critical-Depth Flumes	332
7.7	End Depth in a Free Overfall	334
7.8	Sluice-Gate Flow	346
7.9	Culvert Hydraulics	352



<i>References</i>	358	
<i>Problems</i>	360	
<i>Objective Questions</i>	363	
<b>8. Spatially Varied Flow</b>		<b>366</b>
8.1 Introduction	366	
8.2 SVF with Increasing Discharge	366	
8.3 SVF with Decreasing Discharge	377	
8.4 Side Weir	379	
8.5 Bottom Racks	388	
<i>References</i>	395	
<i>Problems</i>	396	
<i>Objective Questions</i>	398	
<b>9. Supercritical-Flow Transitions</b>		<b>401</b>
9.1 Introduction	401	
9.2 Response to a Disturbance	401	
9.3 Gradual Change in the Boundary	404	
9.4 Flow at a Corner	411	
9.5 Wave Interactions and Reflections	418	
9.6 Contractions	421	
9.7 Supercritical Expansions	426	
9.8 Stability of Supercritical Flows	430	
<i>References</i>	432	
<i>Problems</i>	432	
<i>Objective Questions</i>	435	
<b>10. Unsteady Flows</b>		<b>437</b>
10.1 Introduction	437	
10.2 Gradually Varied Unsteady Flow (GVUF)	438	
10.3 Uniformly Progressive Wave	444	
10.4 Numerical Methods	447	
10.5 Rapidly Varied Unsteady Flow—Positive Surges	458	
10.6 Rapidly Varied Unsteady Flow—Negative Surges	467	
<i>References</i>	478	
<i>Problems</i>	479	
<i>Objective Questions</i>	481	
<b>11. Hydraulics of Mobile Bed Channels</b>		<b>483</b>
11.1 Introduction	483	
11.2 Initiation of Motion of Sediment	483	
11.3 Bed Forms	487	
11.4 Sediment Load	494	
11.5 Design of Stable Channels Carrying Clear Water [Critical Tractive Force Approach]	503	
11.6 Regime Channels	507	
11.7 Scour	511	
<i>References</i>	522	
<i>Problems</i>	523	
<i>Objective Questions</i>	526	
<b>Answers to Problems</b>		<b>531</b>
<b>Answers to Objective Questions</b>		<b>541</b>
<b>Index</b>		<b>543</b>



# Preface

This third edition of *Flow in Open Channels* marks the silver jubilee of the book which first appeared in a different format of two volumes in 1982. A revised first edition combining the two volumes into a single volume was released in 1986. The second edition of the book which came out in 1997 had substantial improvement of the material from that of the first revised edition and was very well received as reflected in more than 25 reprints of that edition. This third edition is being brought out by incorporating advances in the subject matter, changes in the technology and related practices. Further, certain topics in the earlier edition that could be considered to be irrelevant or of marginal value due to advancement of knowledge of the subject and technology have been deleted.

In this third edition, the scope of the book is defined to provide source material in the form of a textbook that would meet all the requirements of the undergraduate course and most of the requirements of a post-graduate course in open-channel hydraulics as taught in a typical Indian university. Towards this, the following procedures have been adopted:

- Careful pruning of the material dealing with obsolete practices from the earlier edition of the book
- Addition of specific topics/ recent significant developments in the subject matter of some chapters to bring the chapter contents up to date. This has resulted in inclusion of detailed coverage on
  - Flow through culverts
  - Discharge estimation in compound channels
  - Scour at bridge constrictions
- Further, many existing sections have been revised through more precise and better presentations. These include substantive improvement to Section 10.6 which deals with negative surges in rapidly varied unsteady flow and Section 5.7.4 dealing with backwater curves in natural channels.
- Additional worked examples and additional figures at appropriate locations have been provided for easy comprehension of the subject matter.
- Major deletions from the previous edition for reasons of being of marginal value include
  - Pruning of Tables 2A.2 at the end of Chapter 2, Table 3A-1 at the end of Chapter 3 and Table 5A-1 of Chapter 5
  - Section 5.3 dealing with a procedure for estimation of  $N$  and  $M$  for a trapezoidal channel, and Section 5.9 dealing with graphical methods of GVF computations
  - Computer Program PROFIL-94 at the end of Chapter 5

The book in the present form contains eleven chapters. Chapters 1 and 2 contain the introduction to the basic principles and energy-depth relationships in open-channel flow. Various aspects of critical flow, its computation and use in analysis of transitions

are dealt in detail in Chapter 2. Uniform flow resistance and computations are dealt in great detail in Chapter 3. This chapter also includes several aspects relating to compound channels. Gradually varied flow theory and computations of varied flow profiles are discussed in ample detail in chapters 4 and 5 with sufficient coverage of control points and backwater curve computations in natural channels.

Hydraulic jump phenomenon in channels of different shapes is dealt in substantial detail in Chapter 6. Chapter 7 contains thorough treatment of some important rapidly varied flow situations which include flow-measuring devices, spillways and culverts. Spatially varied flow theory with specific reference to side channel spillways, side weirs and bottom-rack devices is covered in Chapter 8. A brief description of the transitions in supercritical flows is presented in Chapter 9. An introduction to the important flow situation of unsteady flow in open channels is provided in Chapter 10. The last chapter provides a brief introduction to the hydraulics of mobile bed channels.

The contents of the book, which cover essentially all the important normally accepted basic areas of open-channel flow, are presented in simple, lucid style. A basic knowledge of fluid mechanics is assumed and the mathematics is kept at the minimal level. Details of advanced numerical methods and their computational procedures are intentionally not included with the belief that the interested reader will source the background and details in appropriate specialized literature on the subject. Each chapter includes a set of worked examples, a list of problems for practice and a set of objective questions for clear comprehension of the subject matter. The Table of problems distribution given at the beginning of problems set in each chapter will be of particular use to teachers to select problems for class work, assignments, quizzes and examinations. The problems are designed to further the student's capabilities of analysis and application. A total of 314 problems and 240 objective questions, with answers to the above, provided at the end of the book will be of immense use to teachers and students alike.

The Online Learning Center of the book can be accessed at <http://www.mhhe.com/subramanya/foc3e>. It contains the following material:

**For Instructors**

- Solution Manual
- Power Point Lecture Slides

**For Students**

- Web links for additional reading
- Interactive Objective Questions

A typical undergraduate course in *Open-Channel Flow* includes major portions of chapters 1 through 6 and selected portions of chapters 7, 10 and 11. In this selection, a few sections, such as Sec.1.8, Sec.3.16, Sec. 3.17, Sec. 5.5, Sec. 5.6, Sec. 5.7.3, and Sec. 5.7.4, Sec. 5.8, Sec. 5.9, Sec. 6.4, Sec. 6.5 and Sec. 6.8 could be excluded to achieve a simple introductory course. A typical post-graduate course would include all the eleven chapters with more emphasis on advanced portions of each chapter and supplemented by additional appropriate reference material.

In addition to students taking formal courses in Open-Channel Flow offered in University engineering colleges, the book is useful to students appearing for AMIE

examinations. Candidates taking competitive examinations like Central Engineering Services examinations and Central Civil Services examinations will find this book useful in their preparations related to the topic of water-resources engineering. Practicing engineers in the domain of water-resources engineering will find this book a useful reference source. Further, the book is self-sufficient to be used in self-study of the subject of open-channel flow.

I am grateful to the American Society of Civil Engineers, USA, for permission to reproduce several figures and tables from their publications; the Indian Journal of Technology, New Delhi, for permission to reproduce three figures; Mr M Bos of the International Institute of Land Reclamation and Improvement, Wageningen, The Netherlands, for photographs of the hydraulic jump and weir flow; the US Department of Interior, Water and Power Resources Service, USA, for the photograph of the side-channel spillway of the Hoover Dam; Dr Chandra Nalluri, of the University of New Castle-upon – Tyne, England, for the tables of Keifer and Chu functions and *The Citizen, Gloucester, England*, for the photograph of Severn Bore.

I would like express my sincere thanks to all those who have directly and indirectly helped me in bringing out this revised edition, especially the reviewers who gave noteworthy suggestions.

They are

<b>Suman Sharma</b>	<i>TRUBA College of Engineering and Technology Indore, Madhya Pradesh</i>
<b>Achintya</b>	<i>Muzaffarpur Institute of Technology Muzaffarpur, Bihar</i>
<b>Anima Gupta</b>	<i>Government Women's Polytechnic Patna, Bihar</i>
<b>D R Pachpande</b>	<i>JT Mahajan College of Engineering Jalgaon, Maharashtra</i>
<b>V Subramania Bharathi</b>	<i>Bannari Amman Institute of Technology Anna University, Coimbatore, Tamil Nadu</i>
<b>K V Jaya Kumar</b>	<i>National Institute of Technology Warangal, Andhra Pradesh</i>

Comments and suggestions for further improvement of the book would be greatly appreciated. I could be contacted at the following e-mail address: *subramanyak1@gmail.com*

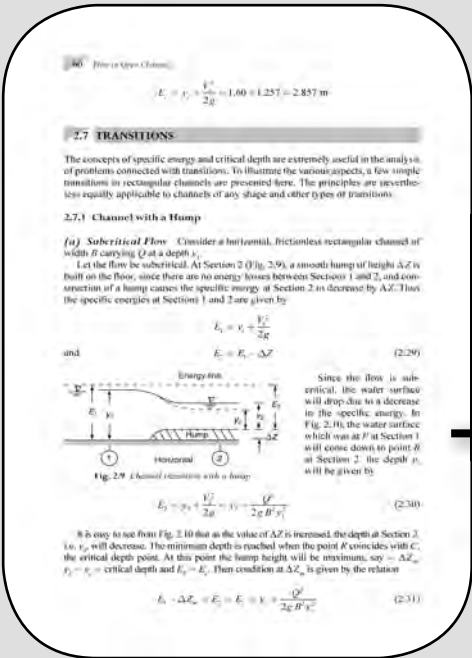
**K SUBRAMANYA**



# Guided Tour

## Introduction

Each chapter begins with an Introduction that gives a brief summary of the background and contents of the chapter.



## Sections and Sub-sections

Each chapter has been neatly divided into sections and sub-sections so that the subject matter is studied in a logical progression of ideas and concepts.

478 Flow in Open Channels

Wave Profile: The profile at any time  $t$  is given as

$$(x - ct) = E_0 y^2 + 2\sqrt{gD_0} y - 3\sqrt{gD_0} t \quad (10.71)$$

where  $y$  = depth of flow at any  $(x, t)$ .

**Example 10.8**

A reservoir having water to a depth of 40 m undergoes an instantaneous ideal dam break. Estimate the depth and discharge intensity at the dam site and the water surface profile of the negative wave 3 seconds after the dam break.

**Solution:** The water surface profile with positive  $x$  in the downstream of the gate axis, is by Eq. 10.65 is

$$\begin{aligned} (x) &= (3\sqrt{gD_0} - 2\sqrt{gD_0}) t \\ (x) &= (3\sqrt{9.81} \times 3 - 2\sqrt{9.81} \times 3) t \\ y &= 39.62t - 9.396\sqrt{t} \end{aligned}$$

At  $t = 0$ ,  $y = y_0 = (39.62/9.396) = 17.78$  m.

Velocity at  $x = 0$ ,  $v = V_0 = \frac{2}{3}\sqrt{gD_0} = \frac{2}{3}\sqrt{9.81} \times 40 = 13.21$  m/s

Profile after 3 seconds:  $x = 39.62 \times 3 - 9.396 \times 3\sqrt{3}$

$$x = 118.86 - 28.188\sqrt{3}$$

**Example 10.9**

A wide rectangular horizontal channel is passing a discharge of 1.5 m<sup>3</sup>/s/m at a depth of 3.0 m. The flow is controlled by a sluice gate at the downstream end. If the gate is abruptly raised by a certain extent to pass a flow of 3.0 m<sup>3</sup>/s/m to the downstream, estimate (i) the new depth and velocity of flow in the channel at a section when the negative surge has passed; (ii) the maximum wave velocity of the negative surge; and (iii) profile of the negative surge.

**Solution:** This is a case of Type-4 surge, where the negative wave moves upstream. Using the suffix 1 for the conditions before the passage and 2 for conditions after the passage of the negative wave and suffix 0 to the position of the gate.

Velocity at any section

$$\begin{aligned} V = V_1 &= 2\sqrt{gD_0} - 2\sqrt{gD_0}. \text{ Here } y_1 = 3.0 \text{ m and } V_1 = 1.5/3.0 = 0.5 \text{ m/s.} \\ 4 &= 0.5 + 2\sqrt{9.81} \times 3.0 = 2\sqrt{9.81} \times 3 \\ &= 11.35 - 6.264\sqrt{y_2} \quad (10.72) \end{aligned}$$

Worked Examples

Worked Examples, totaling to 122, are provided in sufficient number in each chapter and at appropriate locations to aid in understanding of the text material.

Photographs

Photographs of important flow phenomenon are presented at appropriate locations.

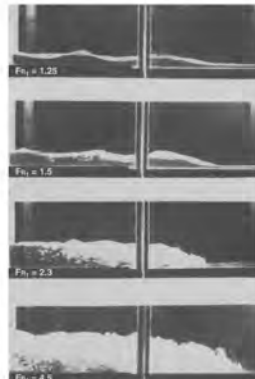


Fig. 6.5 Hydraulic jumps at different Froude numbers (Courtesy: M G Bos)  
[Note: The flow is right to left]

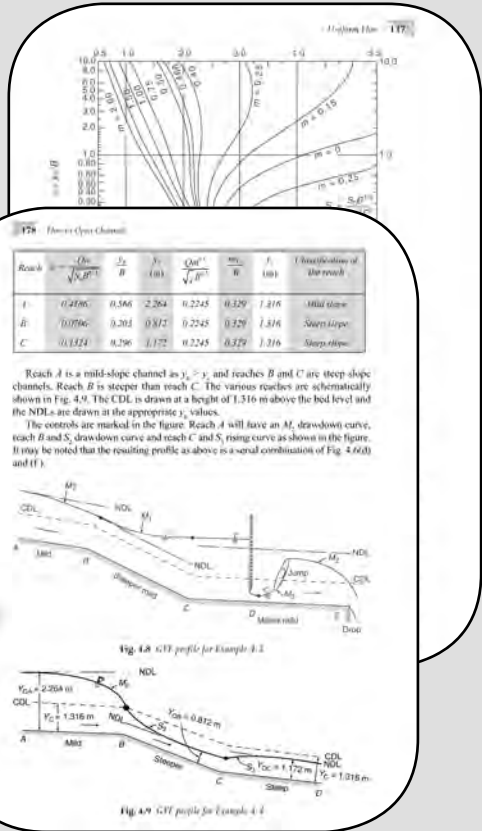
Substituting for  $y_2$  in the expression for  $\frac{E_2}{y_1}$  given above,

$$\frac{16g^{-3/2} E_1}{g^{3/2} y_1^3} \frac{(-3 + \sqrt{1 + 8F_1^2})}{(F_1)^{3/2} (-1 + \sqrt{1 + 8F_1^2})} = f(F_1) \quad (6.8)$$



Illustrations

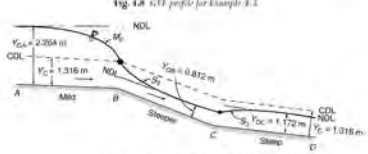
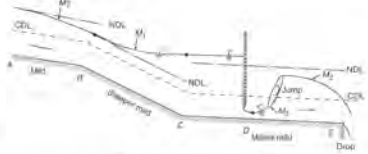
Illustrations are essential tools in books on Engineering subjects. Ample illustrations are provided in each chapter to illustrate the concepts, functional relationships and to provide definition sketches for mathematical models.



178 Three-Crest Channel

Reach	$\frac{S_0}{\sqrt{1+m^2}}$	$\frac{S_0}{B}$	$S_0$ (m)	$\frac{Q_{crit}^2}{gB^3}$	$\frac{y_c}{B}$	$f$ (m)	Classification of the reach
A	0.2196	0.566	2.264	0.2245	0.329	1.816	Mild slope
B	0.0796	0.201	0.812	0.2245	0.329	1.816	Steep slope
C	0.1324	0.296	1.172	0.2245	0.329	1.816	Sharp slope

Reach A is a mild-slope channel as  $y_1 > y_c$  and reaches B and C are steep-slope channels. Reach B is steeper than reach C. The various reaches are schematically shown in Fig. 4.9. The CDL is drawn at a height of 1.316 m above the bed level and the NDLs are drawn at the appropriate  $y_c$  values. The controls are marked in the figure. Reach A will have an  $M_2$  draw-down curve, reach B and S<sub>2</sub> draw-down curve and reach C and S<sub>1</sub> rising curve as shown in the figure. It may be noted that the resulting profile as above is a serial combination of Fig. 4.6(a) and (f).



Problem Distribution

A table of Problem Distribution is provided at the top of each set of Problems. These are very helpful to teachers in setting class work, assignments, quizzes and examinations.

Rapidly Used Exam-1 Hydraulic Jump 287

**2 PROBLEMS**

Problem Distribution

Type	Problems
1. Elements of jump in a rectangular channel	6.1-6.10
2. Jump below a sluice gate	6.11, 6.23, 6.24, 6.31, 6.32
3. Jump below an overflow spillway	6.12, 6.14
4. Jump at an oblique weir	6.15, 6.30
5. Jump at a width change	6.16
6. Jump on a sloping floor	6.17, 6.25, 6.27
7. Jump in sloping (angular) channels	6.18, 6.22, 6.26
8. Location of the jump	6.23, 6.24
9. Forced hydraulic jump	6.28
10. Circular hydraulic jump	6.29
11. Repelled jump	6.31, 6.32

(Hydro engineers stated the channel to be frictionless for purposes of hydraulic jump calculations.)

6.1 A hydraulic jump occurs in a horizontal rectangular channel with sequent depths of 0.70 m and 4.2 m. Calculate the rate of flow per unit width, energy loss and the initial Froude number.

6.2 A hydraulic jump occurs in a horizontal rectangular channel in an initial Froude number of 10.0. What percentage of initial energy is lost in this jump?

6.3 The following table gives some of the possible types of problems associated with a hydraulic jump occurring in a rectangular channel. Complete the following table. [Note that Problems 6.3(c) requires a trial-and-error approach. Assume  $F_1$ , find  $y_2$ ,  $y_1$ , and check  $E_1$ . Repeat till satisfactory values are obtained.]

Probs	$F_1$	$y_1$ (m)	$q$ (m <sup>3</sup> /s/m)	$F_2$	$y_2$ (m)	$E_1$ (m)	$E_2$ (m)	$E_1/E_2$
a		0.75						2.90
b			2.00					1.75
c	11.50	0.350		1.00	0.90			
d						0.15	0.00	

6.4 A hydraulic jump in a rectangular channel has the Froude number at the beginning of the jump  $F_1 = 5$ . Find the Froude number  $F_2$  at the end of the jump.

6.5 Show that the Froude numbers  $F_1$  and  $F_2$  in a hydraulic jump occurring in a rectangular channel are related by:

(a)  $F_2^2 = \frac{8F_1^2}{-1 + \sqrt{1 + 8F_1^2}}$  (b)  $F_1^2 = \frac{8F_2^2}{-1 + \sqrt{1 + 8F_2^2}}$

6.6 A rectangular channel carrying a supercritical stream is to be provided with a hydraulic jump type of energy dissipator. If it is desired to have an energy loss of 5 m in the jump when the inlet Froude number is 8.5, determine the sequent depths.

6.7 Show that in a hydraulic jump formed in a horizontal, frictionless, rectangular channel the energy loss  $E_L$  relative to the critical depth  $y_c$  can be expressed as

Problems with Answers

Each chapter contains a set of practice problems, totaling to 314 problems in the book. Solutions to these require not only application of the material covered in the book but also enables the student to strive towards good comprehension of the subject matter. Answers are provided for all the problem sets at the end of the book.

116. Flow in Open Channel:

9.8 A channel has multiple-roughness types in its perimeter. Assuming that the total discharge in the channel is equal to the sum of discharges in the partial areas, show that the equivalent roughness is given by

$$n = \frac{PR^{4/3}}{\sum (P_i R_i^{4/3})}$$

Supercritical Flow Transition 419



Fig. 9.21 Problem 9.9

9.9 A 3.0-m wide horizontal frictionless rectangular channel has an enlarging section as shown in Fig. 9.22. Calculate the expansion waves at  $\theta$  for an initial Froude number of 2.0 with a depth of flow of 0.50 m. Sketch a few Froude lines and graphically determine their reflections and interactions.



Fig. 9.22 Problem 9.11

9.12 An asymmetrical contraction, as in Fig. 9.12, has  $F_1 = 4.0$ ,  $\theta_1 = 5^\circ$  and  $\theta_2 = 8^\circ$ . Calculate  $F_2$ ,  $F_3$ ,  $\beta_1$ ,  $\beta_2$ ,  $\beta_3$  and  $\beta_4$ . Sketch the shock waves and streamlines.

9.13 Design symmetrical contractions for the following sets of data and fill in Table 9.2.

Table 9.2 Problem 9.13

$M$ No	$F_1$	$\beta_1$ ( $^\circ$ )	$\theta_1$ ( $^\circ$ )	$F_2$	$\beta_2$ ( $^\circ$ )	$\theta_2$ ( $^\circ$ )	$F_3$	$\beta_3$ ( $^\circ$ )	$\theta_3$ ( $^\circ$ )	$\beta_4$ ( $^\circ$ )
1	5.0	0.70	0.0	-	-	3.0	-	-	-	-
2	6.0	0.50	4.0	-	-	-	-	2.0	-	-
3	4.0	0.60	-	-	2.3	-	-	-	6.0	-
4	-	-	-	1.50	2.0	-	-	-	-	18

9.14 For values of  $F_1 = 4.0$  and  $\theta_1/\theta_2 = 2.0$ , sketch a preliminary design of an expansion.

9.15 If a bridge is to be built across a supercritical stream, from the consideration of mechanics of flow, what factors govern the shape of the bridge piers, span and shape of abutments? Which of these factors will be different in subcritical flow?

9.16 The division of supercritical flow at a branch channel or a side weir can be solved by treating the problem as a particular type of channel transition. Considering a simple 90° branch channel, indicate an algorithm for calculating the branch-channel discharge for given main channel flow properties.

Specific Head Flow 199

8.3 The differential equation of SVF with decreasing discharge has one extra term in the numerator on the right-hand side when compared to the corresponding OVE equation. This term is

- (a)  $\frac{2v(\partial Q_c)}{\partial t^2}$
- (b)  $\frac{2v(\partial Q_c)}{\partial t}$
- (c)  $\frac{2v(\partial Q_c)}{\partial t}$
- (d)  $\frac{v(\partial Q_c)}{\partial t}$

8.4 The transitional profile in a lateral spillway channel is

- (a) independent of the roughness of the channel
- (b) independent of rate of lateral flow
- (c) independent of channel geometry
- (d) independent of the bottom slope of the channel

8.5 The flow profile in a side spillway channel can be determined by using

- (a) Standard step method
- (b) Standard Range-Kutta method
- (c) De Marchi equation
- (d) Muskhelishvili equation

8.6 A lateral spillway channel in rectangular in cross-section with a bottom width of 4.0 m. At a certain flow the critical depth was found to be 0.5 m and occurred at a distance of 5.53 m from the upstream end. The lateral inflow rate in  $m^3/s$  is

- (a) 0.20
- (b) 0.40
- (c) 0.80
- (d) 1.10

8.7 The De Marchi varied-flow function is

- (a) used in SVF over bottom racks
- (b) used in SVF in lateral spillway channels
- (c) meant for side weirs in frictionless rectangular channels
- (d) meant for subcritical flow only

8.8 The De Marchi coefficient of discharge  $C_{dw}$  for a side weir is

- (a) independent of the Froude number
- (b) same as that of a normal weir
- (c) essentially a function of inlet Froude number,  $F_1$
- (d) approaches unity as  $F_1 \rightarrow 0$

8.9 A rectangular channel 2.7 m wide has a discharge of 2.0  $m^3/s$  at a depth of 0.8 m. The coefficient of discharge  $C_{dw}$  of a side weir introduced in a side of this channel with a crest height of 0.2 m above the bed is

- (a) 0.574
- (b) 0.611
- (c) 0.286
- (d) 0.851

8.10 To achieve uniformly discharging side weirs the area of flow  $A$  in any section distant  $x$  from the upstream end of the weir is related as

- (a)  $A = A_0 + 3xv$
- (b)  $A = A_0 + 5xv$
- (c)  $A = A_0$
- (d)  $A = e^{3xv}$

8.11 A side weir is provided in the side of channel. If  $E =$  specific energy is assumed constant, at any section within the length of the side weir, the discharge  $Q$  in the channel is given by

- (a)  $Q = \text{constant}$
- (b)  $Q = H_0 \sqrt{2g(E - y)^2}$
- (c)  $Q = \frac{By}{\sqrt{2E - y}}$
- (d)  $Q = Bv\sqrt{2g(E - y)}$

Objective Questions

Each chapter contains a set of Objective Questions, totaling to 240 questions in the book. This enables the user to obtain clear comprehension of the subject matter. Answers to all the Objective Question sets are provided at the end of the book.

## References

At the end of each chapter, a comprehensive list of references are provided.

### REFERENCES

- Bradley, J N and Peterka, A J 'The Hydraulic Design of Stilling Basins, Hydraulic Jumps on a Horizontal Apert', *J. of Hyd. Div., Proc. ASCE*, Paper No. 1401, October 1957, pp 1401-1-25.
- Samtani, P K and Rathie, P N, 'Exact Solution of Sequent Depth Problems', *J. of Irr and Drainage Engrg.*, Vol. 131, No. 6, Nov./Dec. 2004, pp 520-522.
- Ejzenberg, I A, *Hydraulic Energy Dissipators*, McGraw-Hill, New York, 1999.
- Rajaratnam, N, 'Hydraulic Jumps', Chapter in *Advances in Hydraulics*, ed Chow, V T Vol. 4, Academic Press, New York, 1967, pp 198-280.
- Subramanya K, 'Some Studies on Turbulent Wall Jets in Hydraulic Engineering', *Ph D thesis*, Univ. of Alberta, Edmonton, Canada, Oct. 1967.
- Rajaratnam, N and Subramanya K, 'Profile of the Hydraulic Jump', *J. of Hyd Div., Proc.*, ASCE, Paper No. 5931, May 1968, pp 663-675.
- Leschusser, H J and Kartha, V C, 'Effects of Inflow Condition on Hydraulic Jump', *J. of Hyd. Div., Proc.*, ASCE, Paper No. 9088, Aug 1972, pp 1267-1285.
- Silvester, R, 'Hydraulic Jumps in all Shapes of Horizontal Channels', *J. of Hyd. Div., Proc.*, ASCE, Jan 1961, pp 23-55.
- Argyropoulos, P A, 'Theoretical and Experimental Analysis of the Hydraulic Jump in a Sloping Parabolic Flume', *Proc. IAHR, Lisbon*, Vol. 2, 1957, pp 12-1-20.
- Argyropoulos, P A, 'The Hydraulic Jump and the Effect of Turbulence on Hydraulic Structures', *Proc. IAHR, Durbeswijk, Yugoslavia*, 1964, pp 173-185.
- Bradley, J N and Peterka, A J 'Hydraulic Design of Stilling Basin, Stilling Basin with Sloping Apron (Basin V)', *J. of Hyd. Div., Proc.*, ASCE, Paper No. 1405, Oct 1957, pp 1405-1-32.
- Henderson, F M *Open Channel Flow*, Macmillan, New York, 1966.
- Bradley, J N and Peterka, A J 'Hydraulic Design of Stilling Basins' in Symposium on Stilling Basins and Energy Dissipators', *ASCE, Proc. Symp. Series No. 5, Paper Nos. 1401 to 1406*, June 1961, pp 1401-1 to 1406-17 (also in *J. of Hyd. Div., Proc.*, ASCE, Vol. 83, No. HV 5, Oct. 1957).
- Forsesh, J W and Skrinde, R A 'Control of the Hydraulic Jump by Sills', *Trans. ASCE*, Vol. 115, 1950, pp 973-1022.
- Hsu, T Y, 'Discussion on Control of the Hydraulic Jump by Sills', *Trans.*, ASCE, Vol. 115, 1950, pp 998-991.
- Moore, W L, and Morgan, C W 'Hydraulic Jump in an Abrupt Drop', *Trans.*, ASCE, Vol. 124, 1959, pp 507-524.
- Harleman, D R F, 'Effect of Baffle Piers on Stilling Basin Performance', *J. of Resour Res. of Civil Engineers*, Vol. 42, 1955, pp 84-89.
- Kotsovos, H J and Ahmad, D 'Circular Hydraulic Jump', *J. of Hyd. Div., Proc.*, ASCE, Jan 1969, pp 409-422.
- Arthabharanam, A and Wan, W C, 'Characteristics of a Circular Jump in a Radial Wall Jet', *J. of Hyd. Res., IAHR*, Vol. 13, No. 3, 1973, pp 239-262.
- Lewson, J D and Phillips, B E 'Circular Hydraulic Jump', *J. of Hyd. Engrg.*, ASCE, Vol. 109, No. 4, April, 1983, pp 505-518.
- Arthabharanam, A and Abella, V 'Hydraulic Jump with a Gradually Expanding Channel', *J. of Hyd. Div., Proc.*, ASCE, Jan. 1971, pp 31-42.
- Khaliifa A M and McCorquodale, J A 'Ballial Hydraulic Jump', *J. of Hyd. Div., Proc.*, ASCE, Sept. 1979, pp 1003-1078.

## Online Resources

To effectively use the internet resources, references to relevant web addresses are provided in the text and a list of useful websites related to Open Channel Hydraulics is provided at the end of the book.

### SOME USEFUL WEBSITES RELATED TO OPEN CHANNEL HYDRAULICS

- USGS - Surface Water Field Techniques  
<http://www.usgs.gov>
- US Department of Transportation, Federal Highway Administration  
<http://www.fhwa.dot.gov/engineering/hydraulics/index.cfm>
- US Bureau of Reclamation, USA  
[http://www.usbr.gov/pms/hydraulics\\_inh/](http://www.usbr.gov/pms/hydraulics_inh/)
- Hydrologic Center, US Army Corps of Engineers  
<http://www.hcc.usace.army.mil/>
- W M Keck Laboratory of Hydraulics and Water Resources Technical Reports administration.  
<http://www.cultechlibr.library.cultech.edu/>
- Dr. Victor Miguel Ponce - Online Open Channel Hydraulics.  
<http://www.victormiguelponce.com>  
<http://onlinechannel.sdsu.edu/>
- Fluid Flow Calculations web site of LMNO Engineering Research and Software, Ltd.  
<http://www.lmneng.com>

# Introduction

# 1

## 1.1 INTRODUCTION

An open channel is a conduit in which a liquid flows with a free surface. The free surface is actually an interface between the moving liquid and an overlying fluid medium and will have constant pressure. In civil engineering applications; water is the most common liquid with air at atmospheric pressure as the overlying fluid. As such, our attention will be chiefly focused on the flow of water with a free surface. The prime motivating force for open channel flow is gravity.

In engineering practice, activities for utilization of water resources involve open channels of varying magnitudes in one way or the other. Flows in natural rivers, streams and rivulets; artificial, i.e. man-made canals for transmitting water from a source to a place of need, such as for irrigation, water supply and hydropower generation; sewers that carry domestic or industrial waste waters; navigation channels—are all examples of open channels in their diverse roles. It is evident that the size, shape and roughness of open channels vary over a sizeable range, covering a few orders of magnitude. Thus the flow in a road side gutter, flow of water in an irrigation canal and flows in the mighty rivers, such as the Ganga and the Brahmaputra, all have a free surface and as such are open channels, governed by the same general laws of fluid mechanics. Basically, all open channels have a bottom slope and the mechanism of flow is akin to the movement of a mass down an inclined plane due to gravity. The component of the weight of the liquid along the slope acts as the driving force. The boundary resistance at the perimeter acts as the resisting force. Water flow in open channels is largely in the turbulent regime with negligible surface tension effects. In addition, the fact that water behaves as an incompressible fluid leads one to appreciate the importance of the force due to gravity as the major force and the Froude number as the prime non-dimensional number governing the flow phenomenon in open channels.

## 1.2 TYPES OF CHANNELS

### 1.2.1 Prismatic and Non-prismatic Channels

A channel in which the cross-sectional shape and size and also the bottom slope are constant is termed as a prismatic channel. Most of the man-made (artificial) channels are prismatic channels over long stretches. The rectangle, trapezoid, triangle

and circle are some of the commonly used shapes in manmade channels. All natural channels generally have varying cross-sections and consequently are non-prismatic.

### 1.2.2 Rigid and Mobile Boundary Channels

On the basis of the nature of the boundary open channels can be broadly classified into two types: (i) rigid channels, and (ii) mobile boundary channels.

Rigid channels are those in which the boundary is not deformable in the sense that the shape, planiform and roughness magnitudes are not functions of the flow parameters. Typical examples include lined canals, sewers and non-erodible unlined canals. The flow velocity and shear-stress distribution will be such that no major scour, erosion or deposition takes place in the channel and the channel geometry and roughness are essentially constant with respect to time. The rigid channels can be considered to have only one degree of freedom; for a given channel geometry the only change that may take place is the depth of flow which may vary with space and time depending upon the nature of the flow. This book is concerned essentially with the study of rigid boundary channels.

In contrast to the above, we have many unlined channels in alluvium—both man-made channels and natural rivers—in which the boundaries undergo deformation due to the continuous process of erosion and deposition due to the flow. The boundary of the channel is mobile in such cases and the flow carries considerable amounts of sediment through suspension and in contact with the bed. Such channels are classified as mobile-boundary channels. The resistance to flow, quantity of sediment transported, channel geometry and planiform, all depend on the interaction of the flow with the channel boundaries. A general mobile-boundary channel can be considered to have four degrees of freedom. For a given channel not only the depth of flow but also the bed width, longitudinal slope and planiform (or layout) of the channel may undergo changes with space and time depending on the type of flow. Mobile-boundary channels, usually treated under the topic of *sediment transport* or *sediment engineering*,<sup>1,2</sup> attract considerable attention of the hydraulic engineer and their study constitutes a major area of multi-disciplinary interest.

Mobile-boundary channels are dealt briefly in Chapter 11. The discussion in rest of the book is confined to rigid-boundary open channels only. Unless specifically stated, the term *channel* is used in this book to mean the rigid-boundary channels.

## 1.3 CLASSIFICATION OF FLOWS

### 1.3.1 Steady and Unsteady Flows

A steady flow occurs when the flow properties, such as the depth or discharge at a section do not change with time. As a corollary, if the depth or discharge changes with time the flow is termed *unsteady*.

In practical applications, due to the turbulent nature of the flow and also due to the interaction of various forces, such as wind, surface tension, etc., at the surface there will always be some fluctuations of the flow properties with respect to time. To

account for these, the definition of steady flow is somewhat generalised and the classification is done on the basis of gross characteristics of the flow. Thus, for example, if there are ripples resulting in small fluctuations of depth in a canal due to wind blowing over the free surface and if the nature of the water-surface profile due to the action of an obstruction is to be studied, the flow is not termed unsteady. In this case, a time average of depth taken over a sufficiently long time interval would indicate a constant depth at a section and as such for the study of gross characteristics the flow would be taken as steady. However, if the characteristics of the ripples were to be studied, certainly an unsteady wave movement at the surface is warranted. Similarly, a depth or discharge slowly varying with respect to time may be approximated for certain calculations to be steady over short time intervals.

Flood flows in rivers and rapidly varying surges in canals are some examples of unsteady flows. Unsteady flows are considerably more difficult to analyse than steady flows. Fortunately, a large number of open channel problems encountered in practice can be treated as steady-state situations to obtain meaningful results. A substantial portion of this book deals with steady-state flows and only a few relatively simple cases of unsteady flow problems are presented in Chapter 10.

### 1.3.2 Uniform and Non-uniform Flows

If the flow properties, say the depth of flow, in an open channel remain constant along the length of the channel, the flow is said to be *uniform*. As a corollary of this, a flow in which the flow properties vary along the channel is termed as *non-uniform flow* or *varied flow*.

A prismatic channel carrying a certain discharge with a constant velocity is an example of uniform flow [Fig. 1.1(a)]. In this case the depth of flow will be constant along the channel length and hence the free surface will be parallel to the bed. It is easy to see that an unsteady uniform flow is practically impossible, and hence the term uniform flow is used for *steady uniform flow*.

Flow in a non-prismatic channel and flow with varying velocities in a prismatic channel are examples of *varied flow*. Varied flow can be either steady or unsteady.

### 1.3.3 Gradually Varied and Rapidly Varied Flows

If the change of depth in a varied flow is gradual so that the curvature of streamlines is not excessive, such a flow is said to be a *gradually varied flow* (GVF). Frictional resistance plays an important role in these flows. The backing up of water in a stream due to a dam or drooping of the water surface due to a sudden drop in a canal bed are examples of steady GVF. The passage of a flood wave in a river is a case of unsteady GVF [Fig. 1.1(b)].

If the curvature in a varied flow is large and the depth changes appreciably over short lengths, such a phenomenon is termed as *rapidly varied flow* (RVF). The frictional resistance is relatively insignificant in such cases and it is usual to regard RVF as a local phenomenon. A hydraulic jump occurring below a spillway or a sluice gate is an example of steady RVF. A surge moving up a canal [Fig. 1.1(c)] and a bore traveling up a river are examples of unsteady RVF.

4 Flow in Open Channels

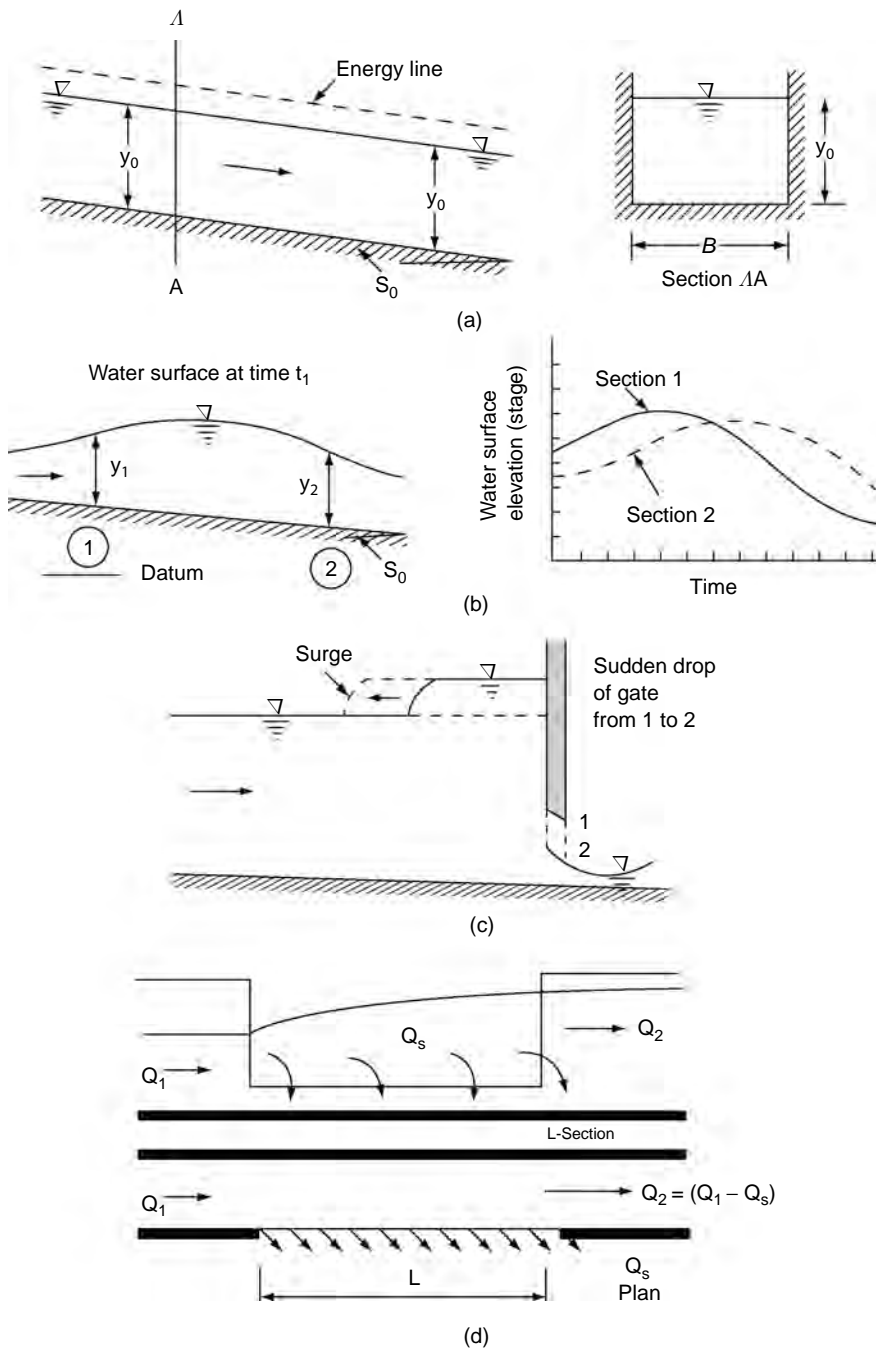


**Fig. 1.1** Various types of open channel flows: (a) Uniform flow, (b) Gradually varied flow (c) Rapidly varied flow and (d) Side Weir: Spatially varied flow

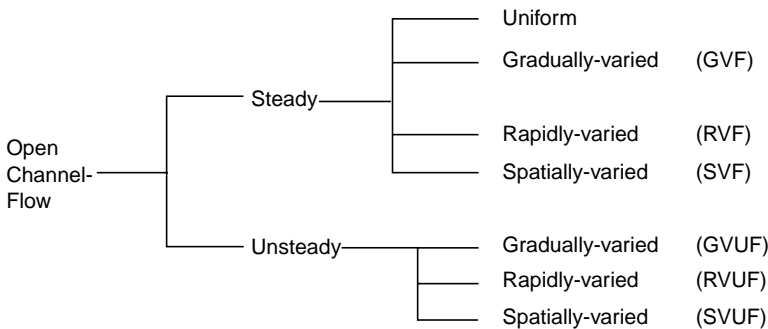
### 1.3.4 Spatially Varied Flow

Varied flow classified as GVF and RVF assumes that no flow is externally added to or taken out of the canal system. The volume of water in a known time interval is conserved in the channel system. In steady-varied flow the discharge is constant at all sections. However, if some flow is added to or abstracted from the system the resulting varied flow is known as a *spatially varied flow* (SVF).

SVF can be steady or unsteady. In the steady SVF the discharge while being steady-varies along the channel length. The flow over a side weir is an example of steady SVF [Fig. 1.1(d)]. The production of surface runoff due to rainfall, known as overland flow, is a typical example of unsteady SVF.

**Classification.** Thus open channel flows are classified for purposes of identification and analysis as follows:

Figure 1.1(a) to (d) shows some typical examples of the above types of flows



## 1.4 VELOCITY DISTRIBUTION

The presence of corners and boundaries in an open channel causes the velocity vectors of the flow to have components not only in the longitudinal and lateral direction but also in normal direction to the flow. In a macro-analysis, one is concerned only with the major component, viz., the longitudinal component,  $v_x$ . The other two components being small are ignored and  $v_x$  is designated as  $v$ . The distribution of  $v$  in a channel is dependent on the geometry of the channel. Figure 1.2(a) and (b) show isovels (contours of equal velocity) of  $v$  for a natural and rectangular channel respectively. The influence of the channel geometry is apparent. The velocity  $v$  is zero at the solid boundaries and gradually increases with distance from the boundary. The maximum velocity of the cross-section occurs at a certain distance below the free surface. This dip of the maximum velocity point, giving surface velocities which are less than the maximum velocity, is due to secondary currents and is a function of the aspect ratio (ratio of depth to width) of the channel. Thus for a deep narrow channel, the location of the maximum velocity point will be much lower from the water surface than for a wider channel of the same depth. This characteristic location



6 Flow in Open Channels

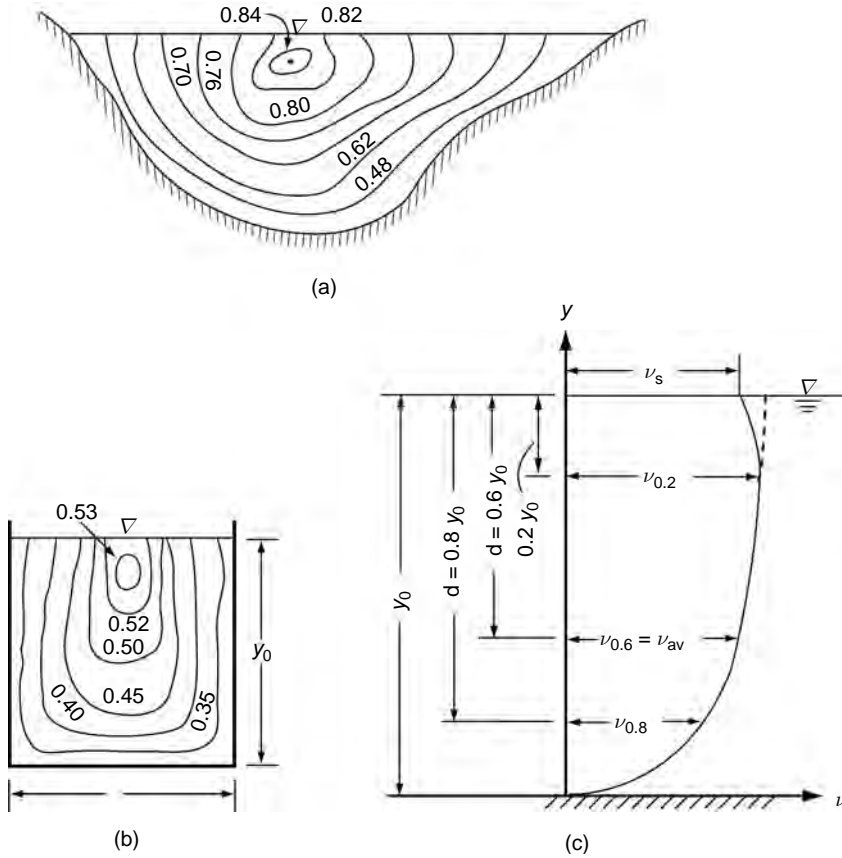


Fig. 1.2 Velocity distribution in open channels: (a) Natural channel (b) Rectangular channel and (c) Typical velocity profile

of the maximum velocity point below the surface has nothing to do with the wind shear on the free surface.

A typical velocity profile at a section in a plane normal to the direction of flow is presented in Fig. 1.2(c). The profile can be roughly described by a logarithmic distribution or a power-law distribution up to the maximum velocity point (Section 3.7). Field observations in rivers and canals have shown that the average velocity at any vertical  $v_{av}$ , occurs at a level of  $0.6 y_0$  from the free surface, where  $y_0 =$  depth of flow. Further, it is found that

$$v_{av} = \frac{v_{0.2} + v_{0.8}}{2} \tag{1.1}$$

in which  $v_{0.2} =$  velocity at a depth of  $0.2 y_0$  from the free surface, and  $v_{0.8} =$  velocity at a depth of  $0.8 y_0$  from the free surface. This property of the velocity distribution is

commonly used in stream-gauging practice to determine the discharge using the area-velocity method. The surface velocity  $v_s$  is related to the average velocity  $v_{av}$  as

$$v_{av} = kv_s \quad (1.2)$$

where,  $k$  = a coefficient with a value between 0.8 and 0.95. The proper value of  $k$  depends on the channel section and has to be determined by field calibrations. Knowing  $k$ , one can estimate the average velocity in an open channel by using floats and other surface velocity measuring devices.

## 1.5 ONE-DIMENSIONAL METHOD OF FLOW ANALYSIS

Flow properties, such as velocity and pressure gradient in a general open channel flow situation can be expected to have components in the longitudinal as well as in the normal directions. The analysis of such a three-dimensional problem is very complex. However, for the purpose of obtaining engineering solutions, a majority of open channel flow problems are analysed by one-dimensional analysis where only the mean or representative properties of a cross section are considered and their variations in the longitudinal direction is analysed. This method when properly used not only simplifies the problem but also gives meaningful results.

Regarding velocity, a mean velocity  $V$  for the entire cross-section is defined on the basis of the longitudinal component of the velocity  $v$  as

$$V = \frac{1}{A} \int_A v dA \quad (1.3)$$

This velocity  $V$  is used as a representative velocity at a cross-section. The discharge past a section can then be expressed as

$$Q = \int v dA = VA \quad (1.4)$$

The following important features specific to one dimensional open channel flow are to be noted:

- A single elevation represents the water surface perpendicular to the flow.
- Velocities in directions other than the direction of the main axis of flow are not considered.

**Kinetic Energy** The flux of the kinetic energy flowing past a section can also be expressed in terms of  $V$ . But in this case, a correction factor  $\alpha$  will be needed as the kinetic energy per unit weight  $V^2/2g$  will not be the same as  $v^2/2g$  averaged over the cross-section area. An expression for  $\alpha$  can be obtained as follows:

For an elemental area  $dA$ , the flux of kinetic energy through it is equal to

$$\left( \frac{\text{mass}}{\text{time}} \right) \left( \frac{\text{KE}}{\text{mass}} \right) = (\rho v dA) \frac{v^2}{2}$$

## 8 Flow in Open Channels

For the total area, the kinetic energy flux

$$= \int_A \frac{\rho}{2} v^3 dA = \alpha \frac{\rho}{2} V^3 A \quad (1.5)$$

from which

$$\alpha = \frac{\int v^3 dA}{V^3 A} \quad (1.6)$$

or for discrete values of  $v$ ,

$$\alpha = \frac{\sum v^3 \Delta A}{V^3 A} \quad (1.7)$$

$\alpha$  is known as the *kinetic energy correction factor* and is equal to or greater than unity.

The kinetic energy per unit weight of fluid can then be written as  $\alpha \frac{V^2}{2g}$ .

**Momentum** Similarly, the flux of momentum at a section is also expressed in terms of  $V$  and a correction factor  $\beta$ . Considering an elemental area  $dA$ , the flux of momentum in the longitudinal direction through this elemental area

$$= \left( \frac{\text{mass}}{\text{time}} \times \text{velocity} \right) = (\rho v dA)(v)$$

For the total area, the momentum flux

$$= \int \rho v^2 dA = \beta \rho V^2 A \quad (1.8)$$

which gives

$$\beta = \frac{\int v^2 dA}{V^2 A} = \frac{\sum v^2 \Delta A}{V^2 A} \quad (1.9)$$

$\beta$  is known as the *momentum correction factor* and is equal to or greater than unity.

**Values of  $\alpha$  and  $\beta$**  The coefficients  $\alpha$  and  $\beta$  are both unity in the case of uniform velocity distribution. For any other velocity distribution  $\alpha > \beta > 1.0$ . The higher the non-uniformity of velocity distribution, the greater will be the values of the coefficients. Generally, large and deep channels of regular cross sections and with fairly straight alignments exhibit lower values of the coefficients. Conversely, small channels with irregular cross sections contribute to larger values of  $\alpha$  and  $\beta$ . A few measured values of  $\alpha$  and  $\beta$  are reported by King<sup>3</sup>. It appears that for straight prismatic channels,  $\alpha$  and  $\beta$  are of the order of 1.10 and 1.05 respectively. In compound channels, i.e. channels with one or two flood banks,  $\alpha$  and  $\beta$  may, in certain cases reach very high values, of the order of 2.0 (see Compound channels in Sec. 5.7.3).

Generally, one can assume  $\alpha = \beta = 1.0$  when the channels are straight, prismatic and uniform flow or GVF takes place. In local phenomenon, it is desirable to include estimated values of these coefficients in the analysis. For natural channels, the following values of  $\alpha$  and  $\beta$  are suggested for practical use<sup>7</sup>:

Channels	Values of $\alpha$		Values of $\beta$	
	Range	Average	Range	Average
Natural channels and torrents	1.15 – 1.50	1.30	1.05 – 1.17	1.10
River valleys, overflowed	1.50 – 2.00	1.75	1.17 – 1.33	1.25

It is usual practice to assume  $\alpha = \beta = 1.0$  when no other specific information about the coefficients are available.

**Example 1.1** | The velocity distribution in a rectangular channel of width  $B$  and depth of flow  $y_0$  was approximated as  $v = k_1\sqrt{y}$  in which  $k_1 = a$  constant. Calculate the average velocity for the cross section and correction coefficients  $\alpha$  and  $\beta$ .

*Solution* Area of cross section  $A = By_0$

$$\begin{aligned} \text{Average velocity } V &= \frac{1}{By_0} \int_0^{y_0} v(B dy) \\ &= \frac{1}{y_0} \int_0^{y_0} k_1\sqrt{y} dy = \frac{2}{3} k_1\sqrt{y_0} \end{aligned}$$

Kinetic energy correction factor

$$\alpha = \frac{\int_0^{y_0} v^3(B dy)}{V^3 B y_0} = \frac{\int_0^{y_0} k_1^3 y^{3/2} B dy}{\left(\frac{2}{3} k_1\sqrt{y_0}\right)^3 B y_0} = 1.35$$

Momentum correction factor

$$\beta = \frac{\int_0^{y_0} v^2(B dy)}{V^2 B y_0} = \frac{\int_0^{y_0} k_1^2 y B dy}{\left(\frac{2}{3} k_1\sqrt{y_0}\right)^2 B y_0} = 1.125$$

**Example 1.2** | The velocity distribution in an open channel could be approximated as in Fig. 1.3. Determine the kinetic energy correction factor  $\alpha$  and momentum correction factor  $\beta$  for this velocity profile.

10 Flow in Open Channels

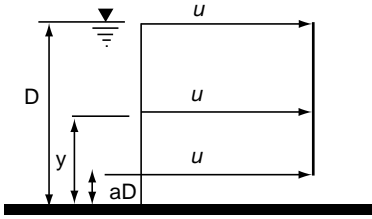


Fig. 1.3 Velocity distribution of Example 1.2

**Solution** From Fig. 1.3  $VD = u(1-a)D$

$$V = (1-a)u$$

$$\alpha = \frac{\int_{aD}^D u^3 dy}{V^3 D} = \frac{u^3 (D-aD)}{u^3 (1-a)^3 D} = \frac{1}{(1-a)^2}$$

$$\beta = \frac{\int_{aD}^D u^2 dy}{V^2 D} = \frac{u^2 D(1-a)}{u^2 (1-a)^2 D} = \frac{1}{(1-a)}$$

**Pressure** In some curvilinear flows, the piezometric pressure head may have non-linear variations with depth. The piezometric head  $h_p$  at any depth  $y$  from the free surface can be expressed as

$$\begin{aligned} h_p &= Z_0 + y + (h_1 - y) + \Delta h \\ h_p &= Z_0 + h_1 + \Delta h \end{aligned} \tag{1.10}$$

in which  $Z_0$  = elevation of the bed,  $h_1$  pressure head at the bed if linear variation of pressure with depth existed and  $\Delta h$  = deviation from the linear pressure head variation at any depth  $y$ . For one-dimensional analysis, a representative piezometric head for the section called *effective piezometric head*,  $h_{ep}$ , is defined as

$$h_{ep} = Z_0 + h_1 + \frac{1}{h_1} \int_0^{h_1} (\Delta h) dy \tag{1.11}$$

$$= Z_0 + h_1 + \overline{\Delta h} \tag{1.11a}$$

Usually hydrostatic pressure variation is considered as the reference linear variation.

## 1.6 PRESSURE DISTRIBUTION

The intensity of pressure for a liquid at its free surface is equal to that of the surrounding atmosphere. Since the atmospheric pressure is commonly taken as a reference and of value equal to zero, the free surface of the liquid is thus a surface of zero pressure. The distribution of pressure in an open channel flow is governed by the acceleration due to gravity  $g$  and other accelerations and is given by the Euler's equation as below:

In any arbitrary direction  $s$ ,

$$-\frac{\partial(p + \gamma Z)}{\partial s} = \rho a_s \tag{1.12}$$

and in the direction normal to  $s$  direction, i.e., in the  $n$  direction,

$$-\frac{\partial}{\partial n}(p + \gamma Z) = \rho a_n \tag{1.13}$$

in which  $p$  = pressure,  $a_s$  = acceleration component in the  $s$  direction,  $a_n$  = acceleration in the  $n$  direction and  $Z$  = elevation measured above a datum.

Consider the  $s$  direction along the streamline and the  $n$  direction across it. The direction of the normal towards the centre of curvature is considered as positive. We are interested in studying the pressure distribution in the  $n$ -direction. The normal acceleration of any streamline at a section is given by

$$a_n = \frac{v^2}{r} \tag{1.14}$$

where  $v$  = velocity of flow along the streamline of radius of curvature  $r$ .

**Hydrostatic Pressure Distribution** The normal acceleration  $a_n$  will be zero

- (i) if  $v = 0$ , i.e., when there is no motion, or
- (ii) if  $r \rightarrow \infty$ , i.e., when the streamlines are straight lines.

Consider the case of no motion, i.e. the still water case (Fig. 1.4(a)). From Eq. 1.13, since  $a_n = 0$ , taking  $n$  in the  $Z$  direction and integrating

$$\frac{p}{\gamma} + Z = \text{constant} = C \tag{1.15}$$

At the free surface [point 1 in Fig. 1.3(a)]  $p_1/\gamma = 0$  and  $Z = Z_1$ , giving  $C = Z_1$ . At any point A at a depth  $y$  below the free surface,

$$\frac{p_A}{\gamma} = (Z_1 - Z_A) = y$$

i.e. 
$$p_A = \gamma y \tag{1.16}$$

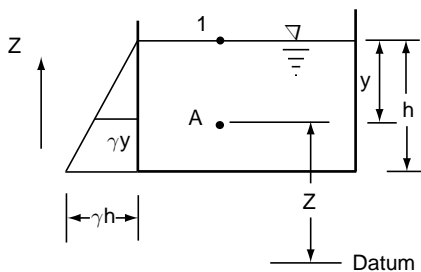


Fig. 1.4(a) Pressure distribution in still water

This linear variation of pressure with depth having the constant of proportionality equal to the unit weight of the liquid is known as *hydrostatic-pressure distribution*.

**Channels with Small Slope** Let us consider a channel with a very small value of the longitudinal slope  $\theta$ . Let  $\theta \sim \sin \theta \sim 1/1000$ . For such channels the vertical section is practically the same

as the normal section. If a flow takes place in this channel with the water surface parallel to the bed, i.e. uniform flow, the streamlines will be straight lines and as such in a vertical direction [Section 0–1 in Fig. 1.4(b)] the normal acceleration  $a_n = 0$ .

Following the argument of the previous paragraph, the pressure distribution at the Section 0 – 1 will be hydrostatic. At any point A at a depth  $y$  below the water surface,

12 Flow in Open Channels

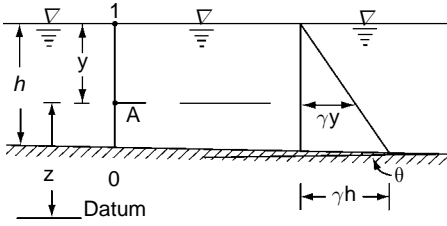


Fig. 1.4(b) Pressure distribution in a channel with small slope

$$\frac{p}{\gamma} = y \quad \text{and} \quad \frac{p}{\gamma} + Z = Z_1$$

= Elevation of water surface

Thus the piezometric head at any point in the channel will be equal to the water-surface elevation. The hydraulic grade line will therefore lie essentially on the water surface.

**Channels with Large Slope** Figure 1.5 shows a uniform free-surface flow in a channel with a large value of inclination  $\theta$ . The flow is uniform, i.e. the water surface is parallel to the bed. An element of length  $\Delta L$  and unit width is considered at the Section 0–1.

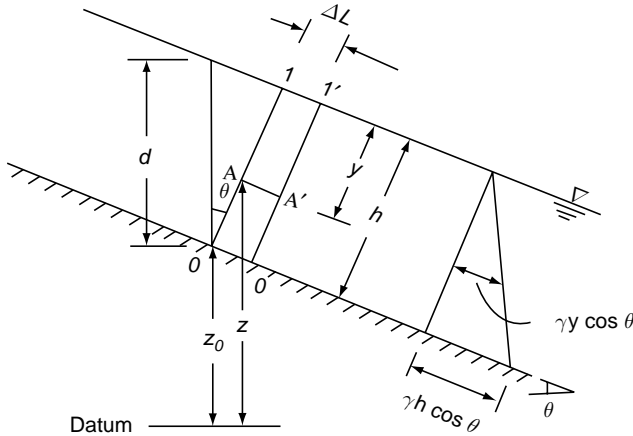


Fig. 1.5 Pressure distribution in a channel with large slope

At any point A at a depth y measured normal to the water surface, the weight of column A1 1'A' =  $\gamma \Delta L y$  and acts vertically downwards. The pressure at AA' supports the normal component of the column A1 1'A'. Thus

$$p_A \Delta L = \gamma y \Delta L \cos \theta \quad (1.17)$$

i.e. 
$$p_A = \gamma y \cos \theta \quad (1.18)$$

or 
$$p_A / \gamma = y \cos \theta \quad (1.18a)$$

The pressure  $p_A$  varies linearly with the depth y but the constant of proportionality is  $\gamma \cos \theta$ . If  $h$  = normal depth of flow, the pressure on the bed at point 0,  $p_0 = \gamma h \cos \theta$ .

If  $d$  = vertical depth to water surface measured at the point O, then  $h = d \cos \theta$  and the pressure head at point O, on the bed is given by

$$\frac{p_0}{\gamma} = h \cos \theta = d \cos^2 \theta \quad (1.19)$$

The piezometric height at any point  $A = Z + y \cos \theta = Z_0 + h \cos \theta$ . Thus for channels with large values of the slope, the conventionally defined hydraulic gradient line does not lie on the water surface.

Channels of large slopes are encountered rarely in practice except, typically in spillways and chutes. On the other hand, most of the canals, streams and rivers with which a hydraulic engineer is commonly associated will have slopes ( $\sin \theta$ ) smaller than  $1/100$ . For such cases  $\cos \theta \approx 1.0$ . As such, in further sections of this book the term  $\cos \theta$  in the expression for the pressure will be omitted with the knowledge that it has to be used as in Eq. 1.18 if  $\theta$  is large.

### 1.7 PRESSURE DISTRIBUTION IN CURVILINEAR FLOWS

Figure 1.6(a) shows a curvilinear flow in a vertical plane on an upward convex surface. For simplicity consider a Section 01A2 in which the  $r$  direction and  $Z$  direction coincide. Replacing the  $n$  direction in Eq. 1.13 by  $(-r)$  direction,

$$\frac{\partial}{\partial r} \left[ \frac{p}{\gamma} + Z \right] = \frac{a_n}{g} \tag{1.20}$$

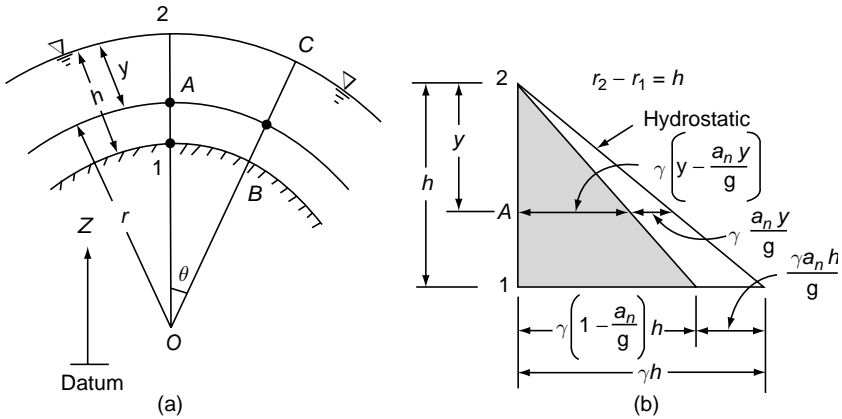


Fig. 1.6 Convex curvilinear flow

Let us assume a simple case in which  $a_n$  = constant. Then, the integration of Eq. 1.20 yields

$$\frac{p}{\gamma} + Z = \frac{a_n}{g} r + C \tag{1.21}$$

in which  $C$  = constant. With the boundary condition that at point 2 which lies on the free surface,  $r = r_2$  and  $p/\gamma = 0$  and  $Z = Z_2$ ,

$$\frac{p}{\gamma} = (Z_2 - Z) - \frac{a_n}{g} (r_2 - r) \tag{1.22}$$



14 Flow in Open Channels

Let  $Z_2 - Z =$  depth below the free surface of any point  $A$  in the Section  $O1A2 = y$ . Then for point  $A$ ,

$$(r_2 - r) = y = (Z_2 - Z)$$

and

$$\frac{P}{\gamma} = y - \frac{a_n}{g} y \tag{1.23}$$

Equation 1.23 shows that the pressure is less than the pressure obtained by the hydrostatic distribution [Fig. 1.6(b)].

For any normal direction  $OBC$  in Fig. 1.6(a), at point  $C$ ,  $(p/\gamma)_c = 0$ ,  $r_c = r_2$ , and for any point at a radial distance  $r$  from the origin  $O$ , by Eq. 1.22

$$\frac{P}{\gamma} = (Z_c - Z) - \frac{a_n}{g} (r_2 - r)$$

But

$$Z_c - Z = (r_2 - r) \cos \theta,$$

giving

$$\frac{P}{\gamma} = (r_2 - r) \cos \theta - \frac{a_n}{g} (r_2 - r) \tag{1.24}$$

It may be noted that when  $a_n = 0$ , Eq. 1.24 is the same as Eq. 1.18a, for the flow down a steep slope.

If the curvature is convex downwards, (i.e.  $r$  direction is opposite to  $Z$  direction) following the argument as above, for constant  $a_n$ , the pressure at any point  $A$  at a depth  $y$  below the free surface in a vertical Section  $O1A2$  [Fig. 1.7(a)] can be shown to be

$$\frac{P}{\gamma} = y + \frac{a_n}{g} y \tag{1.25}$$

The pressure distribution in a vertical section is as shown in Fig. 1.7(b).

Thus it is seen that for a curvilinear flow in a vertical plane, an additional pressure will be imposed on the hydrostatic pressure distribution. The extra pressure will be additive if the curvature is convex downwards and subtractive if it is convex upwards.

**Normal Acceleration** In the previous discussion on curvilinear flows, the normal acceleration  $a_n$  was assumed to be constant. However, it is known that at any point in a curvilinear flow,  $a_n = \frac{v^2}{r}$ , where  $v =$  velocity and  $r =$  radius of curvature of the streamline at that point.

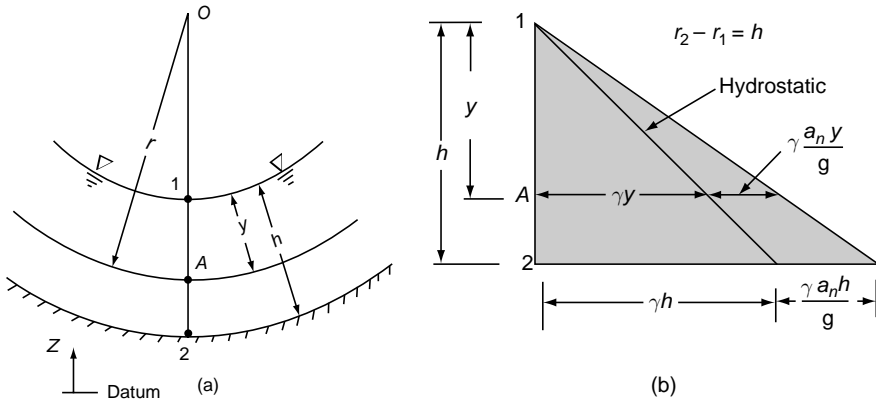


Fig. 1.7 Concave curvilinear flow

In general, one can write  $v = f(r)$  and the pressure distribution can then be expressed by

$$\left(\frac{p}{\gamma} + Z\right) = \int \frac{v^2}{gr} dr + \text{Const} \tag{1.26}$$

This expression can be evaluated if  $v = f(r)$  is known. For simple analysis, the following functional forms are used in appropriate circumstances:

- (i)  $v = \text{constant} = V = \text{mean velocity of flow}$
- (ii)  $v = c/r$ , (free-vortex model)
- (iii)  $v = cr$ , (forced-vortex model)
- (iv)  $a_n = \text{constant} = V^2/R$ , where  $R = \text{radius of curvature at mid-depth}$ .

**Example 1.3**

At a section in a rectangular channel, the pressure distribution was recorded as shown in Fig. 1.8. Determine the effective piezometric head for this section. Take the hydrostatic pressure distribution as the reference.

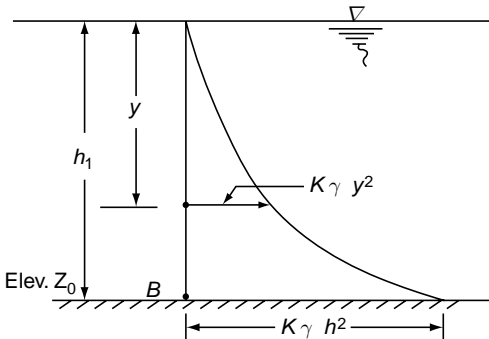


Fig.1.8 Example 1.3

*Solution*  $Z_0 = \text{elevation of the bed of channel above the datum}$   
 $h_1 = \text{depth of flow at the section OB}$

Let  $h_p = \text{piezometric head at point A, depth } y \text{ below the free surface}$

Then  $h_p = Z_0 + ky^2 + (h_1 - y)$

Putting  $h_p = Z_0 + h_1 + \Delta h$

$\Delta h = ky^2 - y$

Effective piezometric head, by Eq. 1.11 is

$$\begin{aligned} h_{ep} &= Z_0 + h_1 + \frac{1}{h_1} \int_0^{h_1} (\Delta h) dy \\ &= Z_0 + h_1 + \frac{1}{h_1} \int_0^{h_1} (ky^2 - y) dy \\ h_{ep} &= Z_0 + \frac{h_1}{2} + \frac{kh_1^2}{2} \end{aligned}$$

**Example 1.4**

A spillway bucket has a radius of curvature  $R$  as shown in Fig. 1.9. (a) Obtain an expression for the pressure distribution at a radial section of inclination  $\theta$  to the vertical. Assume the velocity at any radial section to be uniform and the depth of flow  $h$  to be constant. (b) What is the effective piezometric head for the above pressure distribution?

*Solution* (a) Consider the Section 012. Velocity =  $V =$  constant across 12. Depth of flow =  $h$ . From Eq. 1.26, since the curvature is convex downwards

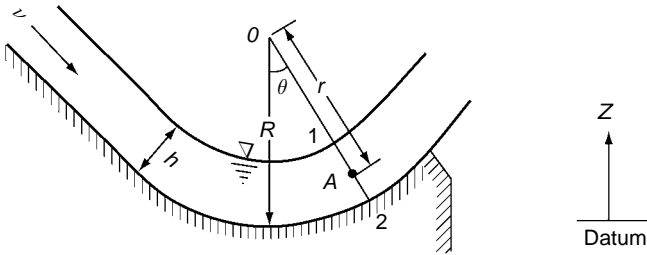


Fig. 1.9 Example 1.4

$$\begin{aligned} \left( \frac{p}{\gamma} + Z \right) &= \int \frac{v^2}{gr} dr + \text{Const} \\ \frac{p}{\gamma} + Z &= \frac{V^2}{g} \ln r + C \end{aligned} \tag{1.27}$$

At the point 1,  $p/\gamma = 0, Z = Z_1, r = R - h$

$$C = Z_1 - \frac{V^2}{g} \ln(R - h)$$

At any point A, at radial distance  $r$  from  $O$

$$\frac{p}{\gamma} = (Z_1 - Z) \frac{V^2}{g} \ln \left( \frac{r}{R - h} \right) \tag{1.28}$$

But  $(Z_1 - Z) = (r - R + h) \cos \theta$

$$\frac{p}{\gamma} = (r - R + h) \cos \theta + \frac{V^2}{g} \ln \left( \frac{r}{R-h} \right) \quad (1.29)$$

Equation 1.29 represents the pressure distribution at any point  $(r, \theta)$ . At point 2,  $r = R$ ,  $p = p_2$ .

(b) Effective piezometric head,  $h_{ep}$ :

From Eq. 1.28 the piezometric head  $h_p$  at A is

$$h_p = \left( \frac{p}{\gamma} + Z \right)_A = Z_1 + \frac{V^2}{g} \ln \left( \frac{r}{R-h} \right)$$

Noting that  $Z_1 = Z_2 + h \cos \theta$  and expressing  $h_p$  in the form of Eq. 1.10

$$h_p = Z_2 + h \cos \theta + \Delta h$$

Where

$$\Delta h = \frac{V^2}{g} \ln \frac{r}{R-h}$$

The effective piezometric head  $h_{ep}$  from Eq. 1.11 is

$$h_{ep} = Z_2 + h \cos \theta + \frac{1}{h \cos \theta} \int_{R-h}^R \frac{V^2}{g} \ln \frac{r}{R-h} dr$$

on integration,

$$\begin{aligned} h_{ep} &= Z_2 + h \cos \theta + \frac{V^2}{gh \cos \theta} \left[ -h + R \ln \frac{R}{R-h} \right] \\ &= Z_2 + h \cos \theta + \frac{V^2 \left( -\frac{h}{R} + \ln \frac{1}{1-h/R} \right)}{gR \left( \frac{h}{R} \right) \cos \theta} \end{aligned} \quad (1.30)$$

It may be noted that when  $R \rightarrow \infty$  and  $h/R \rightarrow 0$ ,  $h_{ep} \rightarrow Z_2 + h \cos \theta$

## 1.8 FLOWS WITH SMALL WATER-SURFACE CURVATURE

Consider a free-surface flow with a convex upward water surface over a horizontal bed (Fig. 1.10). For this water surface,  $d^2h/dx^2$  is negative. The radius of curvature of the free surface is given by

$$\frac{1}{r_1} = \frac{\frac{d^2h}{dx^2}}{\left[ 1 + \left( \frac{dh}{dx} \right)^2 \right]^{3/2}} \approx \frac{d^2h}{dx^2} \quad (1.31)$$

18 Flow in Open Channels

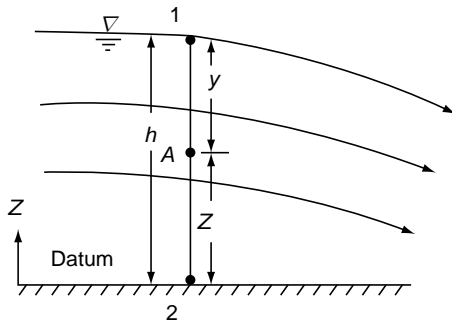


Fig. 1.10 Definition sketch of flow with small water-surface curvature

Assuming linear variation of the curvature with depth, at any point A at a depth  $y$  below the free surface, the radius of curvature  $r$  is given by

$$\frac{1}{r} = \frac{d^2h}{dx^2} \left( \frac{h-y}{h} \right) \quad (1.32)$$

If the velocity at any depth is assumed to be constant and equal to the mean velocity  $V$  in the section, the normal acceleration  $a_n$  at point A is given by

$$a_n = \frac{V^2}{r} = \frac{V^2}{h} (h-y) \frac{d^2h}{dx^2} = K(h-y) \quad (1.33)$$

where  $K = (V^2/h)d^2h/dx^2$ . Taking the channel bed as the datum, the piezometric head  $h_p$  at point A is then by Eq. 1.26

$$h_p = \left( \frac{p}{\gamma} + Z \right) = \int \frac{K}{g} (h-y) dy + \text{Const}$$

i.e.

$$h_p = \frac{K}{g} \left( hy - \frac{y^2}{2} \right) + C \quad (1.34)$$

Using the boundary condition; at  $y = 0$ ,  $p/\gamma = 0$ ,  $Z = h$  and  $h_p = h$ , leads to  $C = h$ ,

$$h_p = h + \frac{K}{g} \left( hy - \frac{y^2}{2} \right) \quad (1.35)$$

Equation 1.35 gives the variation of the piezometric head with the depth  $y$  below the free surface. Designing  $h_p = h + \Delta h$

$$\Delta h = \frac{K}{g} \left( hy - \frac{y^2}{2} \right)$$

The mean value of  $\Delta h$

$$\begin{aligned} \overline{\Delta h} &= \frac{1}{h} \int_0^A \Delta h dy \\ &= \frac{K}{gh} \int_0^A \left( hy - \frac{y^2}{2} \right) dy = \frac{Kh^2}{3g} \end{aligned}$$

The *effective piezometric head*  $h_{ep}$  at the section with the channel bed as the datum can now be expressed as

$$h_{ep} = h + \frac{Kh^2}{3g} \quad (1.36)$$

It may be noted that  $d^2h/dx^2$  and hence  $K$  is negative for convex upward curvature and positive for concave upward curvature. Substituting for  $K$ , Eq. 1.36 reads as

$$h_{ep} = h + \frac{1}{3} \frac{V^2 h}{g} \frac{d^2 h}{dx^2} \quad (1.37)$$

This equation, attributed to Boussinesq<sup>4</sup> finds application in solving problems with small departures from the hydrostatic pressure distribution due to the curvature of the water surface.

## 1.9 EQUATION OF CONTINUITY

The continuity equation is a statement of the law of conservation of matter. In open-channel flows, since we deal with incompressible fluids, this equation is relatively simple and much more for the cases of steady flow.

**Steady Flow** In a steady flow the volumetric rate of flow (discharge in  $m^3/s$ ) past various section must be the same. Thus in a varied flow, if  $Q$  = discharge,  $V$  = mean velocity and  $A$  = area of cross-section with suffixes representing the sections to which they refer

$$Q = VA = V_1 A_1 = V_2 A_2 = \dots \quad (1.38)$$

If the velocity distribution is given, the discharge is obtained by integration as in Eq. 1.4. It should be kept in mind that the area element and the velocity through this area element must be perpendicular to each other.

In a steady spatially-varied flow, the discharge at various sections will not be the same. A budgeting of inflows and outflows of a reach is necessary. Consider, for example, an SVF with increasing discharge as in Fig. 1.11. The rate of addition of discharge =  $dQ/dx = q_*$ . The discharge at any section at a distance  $x$  from Section 1

$$= Q = Q_1 + \int_0^x q_* dx \quad (1.39)$$

If  $q_* = \text{constant}$ ,  $Q = Q_1 + q_* x$  and  $Q_2 = Q_1 + q_* L$

**Unsteady Flow** In the unsteady flow of incompressible fluids, if we consider a reach of the channel, the continuity equation states that the net discharge going out of all the boundary surfaces of the reach is equal to the rate of depletion of the storage within it.

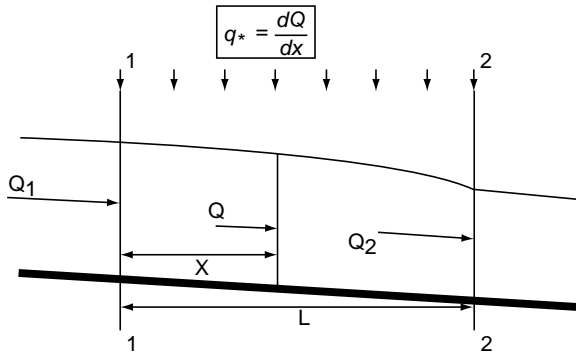


Fig. 1.11 Spatially varied flow

In Fig. 1.12, if  $Q_2 > Q_1$ , more flow goes out than what is coming into Section 1. The excess volume of outflow in a time  $\Delta t$  is made good by the depletion of storage within the reach bounded by Sections 1 and 2. As a result of this the water surface will start falling. If  $\Delta t =$  distance between Sections 1 and 2,

$$Q_2 - Q_1 = \frac{\partial Q}{\partial x} \Delta x$$

The excess volume rate of flow in a time  $\Delta t = (\partial Q / \partial x) \Delta x \Delta t$ . If the top width of the canal at any depth  $y$  is  $T$ ,  $\partial A / \partial y = T$ . The storage volume at depth  $y = A \cdot \Delta x$ . The rate of decrease of storage  $= -\Delta x \frac{\partial A}{\partial y} \frac{\partial y}{\partial t} = -T \Delta x \frac{\partial y}{\partial t}$ . The decrease in storage in time

$$\Delta t = \left( -T \Delta x \frac{\partial y}{\partial t} \right) \Delta t. \text{ By continuity } \frac{\partial Q}{\partial x} \Delta x \Delta t = -T \frac{\partial y}{\partial t} \Delta x \Delta t.$$

$$\text{or } \frac{\partial Q}{\partial x} + T \frac{\partial y}{\partial t} = 0 \tag{1.40}$$

Equation 1.40 is the basic equation of continuity for unsteady, open-channel flow.

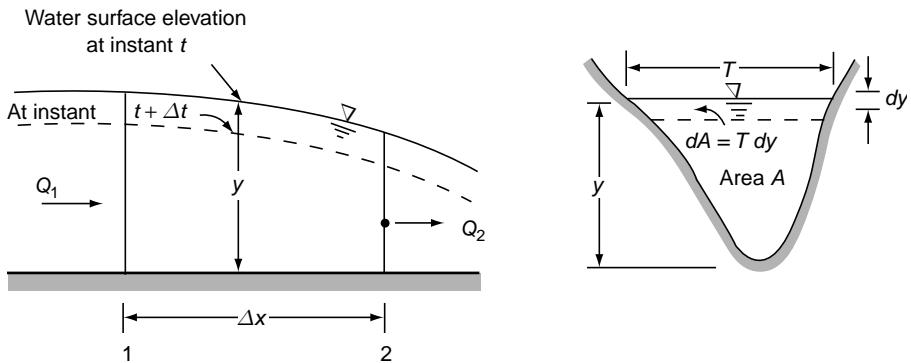


Fig. 1.12 Definition sketch of unsteady flow

**Example 1.5** The velocity distribution in the plane of a vertical sluice gate discharging free is shown in Fig. 1.13. Calculate the discharge per unit width of the gate.

Location	1	2	3	4	5	6	7
Velocity (m/s)	2.3	2.5	2.6	2.6	2.5	2.1	0.0
$\theta$ (degrees)	5	10	15	20	25	30	–
$y$ (m)	0.05	0.10	0.15	0.20	0.25	0.30	0.35

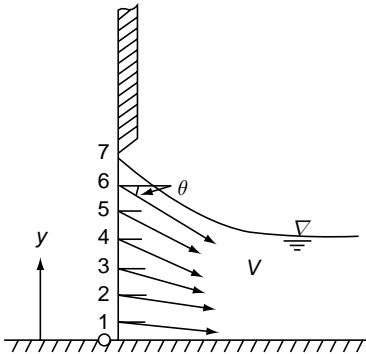


Fig. 1.13 Example 1.5

**Solution** The component of velocity normal to the  $y$ -axis is calculated as  $V_n = V \cos \theta$ . The discharge per unit width  $q = \sum V_n \Delta y$ . The velocity is zero at the boundaries, i.e., at end sections 0 and 7 and this should be noted in calculating average velocities relating to the end sections. The calculations are done in tabular form as shown below. In the table  $\Delta q =$  discharge in the element between two sections = Col 5  $\times$  Col 6.

The total discharge per unit width is  $0.690 \text{ m}^3/\text{s}/\text{m}$ .

1	2	3	4	5	6	7
Section	$V =$ Velocity (m/s)	$\theta^\circ$	$V_n = V \cos \theta$ (m/s)	Average $V_n$ (m/s)	$\Delta y$ (m)	$\Delta q_3$ ( $\text{m}^3/\text{s}/\text{m}$ )
0	0	0	0.000		0	0
1	2.3	5	2.291	1.146	0.05	0.057
2	2.5	10	2.462	2.377	0.05	0.119
3	2.6	15	2.511	2.487	0.05	0.124
4	2.6	20	2.443	2.477	0.05	0.124
5	2.5	25	2.266	2.354	0.05	0.118
6	2.1	30	1.819	2.042	0.05	0.102
7	0	0	0.000	0.090	0.05	0.045
<b>Total Discharge = <math>q =</math></b>						<b>0.690</b>

**Example 1.6**

While measuring the discharge in a small stream it was found that the depth of flow increases at the ratio of 0.10 m/h. If the discharge at that section was  $25 \text{ m}^3/\text{s}$  and the surface width of the stream was 20m, estimate the discharge at a section 1 km upstream.

**Solution** This is a case of unsteady flow and the continuity equation Eq. 1.40 will be used.

$$T \frac{\partial y}{\partial t} = \frac{20 \times 0.10}{60 \times 60} = 0.000556$$



By Eq. 1.36,

$$\begin{aligned} \frac{Q_2 - Q_1}{\Delta x} &= \frac{\partial Q}{\partial x} = -T \frac{\partial y}{\partial t} \\ Q_1 &= \text{discharge at the upstream section} \\ &= Q_2 + T \frac{\partial y}{\partial t} \Delta x = 25.0 + 1000 \times 0.000556 \\ &= 25.556 \text{ m}^3/\text{s} \end{aligned}$$

### 1.10 ENERGY EQUATION

In the one-dimensional analysis of steady open-channel flow, the energy equation in the form of the Bernoulli equation is used. According to this equation, the total energy at a downstream section differs from the total energy at the upstream section by an amount equal to the loss of energy between the sections.

Figure 1.14 shows a steady varied flow in a channel. If the effect of the curvature on the pressure distribution is neglected, the total energy head (in N.m/newton of fluid) at any point A at a depth  $d$  below the water surface is

$$H = Z_A + d \cos \theta + \alpha \frac{V^2}{2g} \tag{1.41}$$

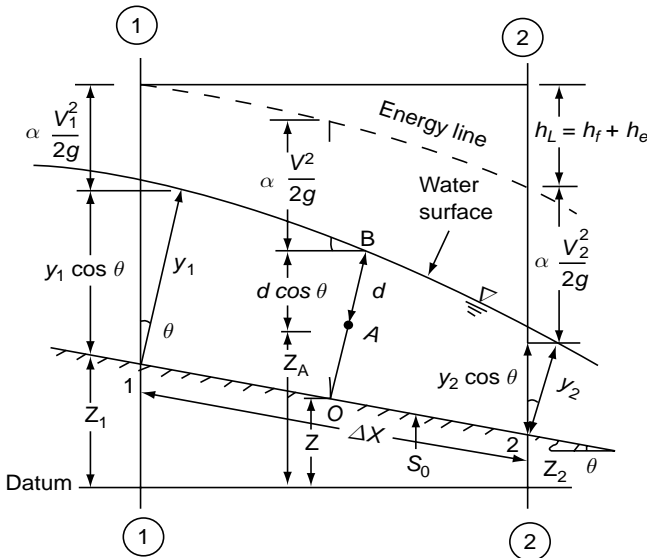


Fig.1.14 Definition sketch for the energy equation

This total energy will be constant for all values of  $d$  from zero to  $y$  at a normal section through point A (i.e. Section OAB), where  $y$  = depth of flow measured normal to the bed. Thus the total energy at any section whose bed is at an elevation  $Z$  above the datum is

$$H = Z + y \cos \theta + \alpha V^2/2g \tag{1.42}$$

In Fig. 1.14, the total energy at a point on the bed is plotted along the vertical through that point. Thus the elevation of energy line on the line 1–1 represents the total energy at any point on the normal section through point 1. The total energies at normal sections through 1 and 2 are therefore

$$H_1 = Z_1 + y_1 \cos \theta + \alpha_1 \frac{V_1^2}{2g}$$

$$H_2 = Z_2 + y_2 \cos \theta + \alpha_2 \frac{V_2^2}{2g}$$

respectively. The term  $(Z + y \cos \theta) = h$  represents the elevation of the hydraulic grade line above the datum.

If the slope of the channel  $\theta$  is small,  $\cos \theta \approx 1.0$ , the normal section is practically the same as the vertical section and the total energy at any section can be written as

$$H = Z + y + \alpha \frac{V^2}{2g} \quad (1.43)$$

Since most of the channels in practice happen to have small values of  $\theta$  ( $\theta < 10^\circ$ ), the term  $\cos \theta$  is usually neglected. Thus the energy equation is written as Eq. 1.40 in subsequent sections of this book, with the realisation that the slope term will be included if  $\cos \theta$  is appreciably different from unity.

Due to energy losses between Sections 1 and 2, the energy head  $H_1$  will be larger than  $H_2$  and  $H_1 - H_2 = h_L =$  head loss. Normally, the head loss ( $h_L$ ) can be considered to be made up of frictional losses ( $h_f$ ) and eddy or form loss ( $h_e$ ) such that  $h_L = h_f + h_e$ . For prismatic channels,  $h_e = 0$ . One can observe that for channels of small slope the piezometric head line essentially coincides with the free surface. The energy line which is a plot of  $H$  vs  $x$  is a dropping line in the longitudinal ( $x$ ) direction. The difference of the ordinates between the energy line and free surface represents the velocity head at that section. In general, the bottom profile, water-surface and energy line will have distinct slopes at a given section. The bed slope is a geometric parameter of the channel. The slope of the energy line depends on the resistance characteristics of the channel and is discussed in Chapter 3. Discussions on the water-surface profiles are presented in chapter 4 and 5.

In designating the total energy by Eq. 1.41 or 1.42, hydrostatic pressure distribution was assumed. However, if the curvature effects in a vertical plane are appreciable, the pressure distribution at a section may have a non-linear variation with the depth  $d$ . In such cases the effective piezometric head  $h_{ep}$  as defined in Eq. 1.11 will be used to represent the total energy at a section as

$$H = h_{ep} + \alpha \frac{V^2}{2g} \quad (1.44)$$

**Example 1.7** | The width of a horizontal rectangular channel is reduced from 3.5 m to 2.5 m and the floor is raised by 0.25 m in elevation at a given section. At the upstream section, the depth of flow is 2.0 m and the kinetic energy correction

24 Flow in Open Channels

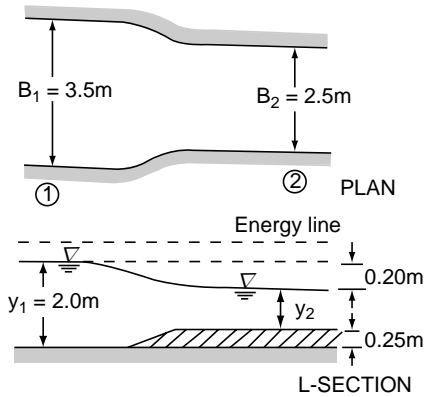


Fig. 1.15 Example 1.7

factor  $\alpha$  is 1.15. If the drop in the water surface elevation at the contraction is 0.20 m, calculate the discharge if (a) the energy loss is neglected, and (b) the energy loss is one-tenth of the upstream velocity head. [The kinetic energy correction factor at the contracted section may be assumed to be unity].

Solution Referring to Fig. 1.15,  
 $y_1 = 2.0$  m

$$y_2 = 2.0 - 0.25 - 0.20 = 1.55 \text{ m}$$

By continuity

$$B_1 y_1 V_1 = B_2 y_2 V_2$$

$$V_1 = \frac{2.5 \times 1.55}{3.5 \times 2.0} V_2 = 0.5536 V_2$$

(a) When there is no energy loss

By energy equation applied to Sections 1 and 2,

$$Z_1 + y_1 + \alpha_1 \frac{V_1^2}{2g} = (Z_1 + \Delta Z) + y_2 + \alpha_2 \frac{V_2^2}{2g}$$

$$\alpha_1 = 1.15 \text{ and } \alpha_2 = 1.0$$

$$\frac{V_2^2 - (1.15 V_1^2)}{2g} = y_1 - y_2 - \Delta Z$$

$$\frac{V_2^2}{2g} [1 - (1.15)(0.5536)^2] = 2.00 - 1.55 - 0.25$$

$$0.6476 \frac{V_2^2}{2 \times 9.81} = 0.2$$

$$V_2 = 2.462 \text{ m/s}$$

$$\text{Discharge } Q = 2.5 \times 1.55 \times 2.462 = 9.54 \text{ m}^3/\text{s}$$

(b) When there is an energy loss

$$H_L = 0.1 \left[ \alpha_1 \frac{V_1^2}{2g} \right] = 0.115 \frac{V_1^2}{2g}$$

By energy equation,

$$Z_1 + y_1 + \alpha_1 \frac{V_1^2}{2g} = (Z_1 + \Delta Z) + y_2 + \alpha_2 \frac{V_2^2}{2g} + H_L$$

$$\left[ \alpha_2 \frac{V_2^2}{2g} - \alpha_1 \frac{V_1^2}{2g} + H_L \right] = y_1 - y_2 - \Delta Z$$

Substituting  $\alpha_2 = 1.0$ ,  $\alpha_1 = 1.15$  and  $H_L = 0.115 \frac{V_1^2}{2g}$

$$\frac{V_2^2}{2g} - 1.15 \frac{V_1^2}{2g} - 0.115 \frac{V_1^2}{2g} = 2.00 - 1.55 - 0.25$$

Since  $V_1 = 0.5536V_2$

$$\frac{V_2^2}{2g} \left[ 1 - (0.9)(1.15)(0.5536)^2 \right] = 0.2$$

$$\frac{0.6826 V_2^2}{2 \times 9.81} = 0.2$$

$V_2 = 2.397$  m/s and discharge  $Q = 2.5 \times 1.55 \times 2.397 = 9.289$  m<sup>3</sup>/s

**Example 1.8** A sluice gate in a 2.0-m wide horizontal rectangular channel is discharging freely as shown in Fig. 1.16. If the depths a small distance upstream ( $y_1$ ) and downstream ( $y_2$ ) are 2.5 m and 0.20 m respectively, estimate the discharge in the channel (i) by neglecting energy losses at the gate, and (ii) by assuming the energy loss at the gate to be 10% of the upstream depth  $y_1$ .

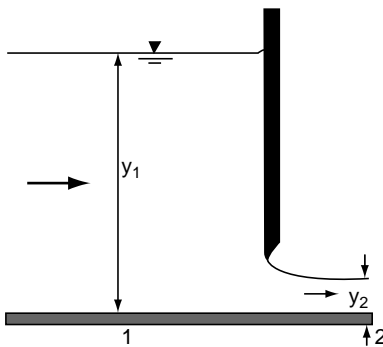


Fig. 1.16 Free flow from a sluice gate – Example 1.8

**Solution** Referring to Fig. 1.16,  $y_1 = 2.5$  m and  $y_2 = 0.20$  m

$$B y_1 V_1 = B y_2 V_2$$

$$V_2 = \frac{y_1}{y_2} V_1 = \frac{2.5}{0.20} \times V_1 = 12.5 V_1$$

(i) When there is no energy loss

$$Z_1 + y_1 + \frac{V_1^2}{2g} = Z_2 + y_2 + \frac{V_2^2}{2g}$$

Since the channel is horizontal,  $Z_1 = Z_2$  and

$$\frac{V_2^2}{2g} - \frac{V_1^2}{2g} = (y_1 - y_2)$$

$$\frac{V_1^2}{2g}[(12.5)^2 - 1] = 2.50 - 0.20 = 2.30$$

$$\frac{V_1^2}{2g} = \frac{2.30}{155.25} = 0.01481 \text{ and } V_1 = 0.539 \text{ m/s.}$$

$$\text{Discharge } Q = By_1V_1 = 2.0 \times 2.5 \times 0.539 = 2.696 \text{ m}^3/\text{s.}$$

(ii) When there is energy loss

$$H_L = \text{Energy loss} = 0.10 y_1 = 0.25 \text{ m}$$

$$y_1 + \frac{V_1^2}{2g} = y_2 + \frac{V_2^2}{2g} + H_L$$

$$\frac{V_2^2}{2g} - \frac{V_1^2}{2g} = (y_1 - y_2 - H_L)$$

$$\frac{V_1^2}{2g}[(12.5)^2 - 1] = 2.50 - 0.20 - 0.25 = 2.05$$

$$\frac{V_1^2}{2g} = \frac{2.05}{155.25} = 0.0132 \text{ and } V_1 = 0.509 \text{ m/s}$$

$$\text{Discharge } Q = By_1V_1 = 2.0 \times 2.5 \times 0.509 = 2.545 \text{ m}^3/\text{s.}$$

## 1.11 MOMENTUM EQUATION

**Steady Flow** Momentum is a vector quantity. The momentum equation commonly used in most of the open channel flow problems is the *linear-momentum equation*. This equation states that the algebraic sum of all external forces, acting in a given direction on a fluid mass equals the time rate of change of linear-momentum of the fluid mass in the direction. In a steady flow the rate of change of momentum in a given direction will be equal to the net flux of momentum in that direction.

Figure 1.17 shows a *control volume* (a volume fixed in space) bounded by Sections 1 and 2, the boundary and a surface lying above the free surface. The various forces acting on the control volume in the longitudinal direction are as follows:

- (i) Pressure forces acting on the control surfaces,  $F_1$  and  $F_2$ .
- (ii) Tangential force on the bed,  $F_3$ ,
- (iii) Body force, i.e., the component of the weight of the fluid in the longitudinal direction,  $F_4$ .

By the linear-momentum equation in the longitudinal direction for a steady-flow discharge of  $Q$ ,

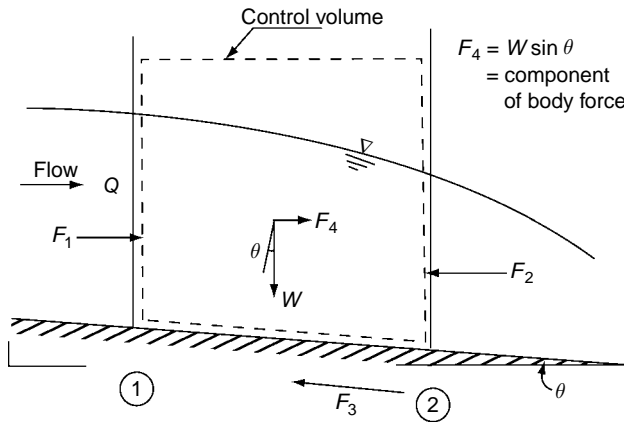


Fig.1.17 Definition sketch for the momentum equation

$\Sigma F_1 = F_1 - F_2 - F_3 + F_4 = M_2 - M_1$  (1.45)  
 in which  $M_1 = \beta_1 \rho Q V_1$  = momentum flux entering the control volume,  $M_2 = \beta_2 \rho Q V_2$  = momentum flux leaving the control volume.

In practical applications of the momentum equation, the proper identification of the geometry of the control volume and the various forces acting on it are very important. The momentum equation is a particularly useful tool in analysing rapidly varied flow (RVF) situations where energy losses are complex and cannot be easily estimated. It is also very helpful in estimating forces on a fluid mass. Detailed information on the basis of the momentum equation and selection of the control volume are available in books dealing with the mechanics of fluids.<sup>5,6</sup>

**Example 1.9**

Estimate the force, on a sluice gate shown in Fig. 1.18.

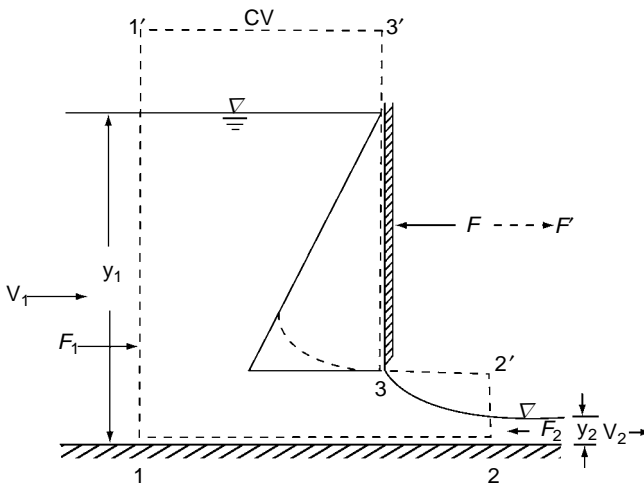


Fig. 1.18 Forces in a sluice gate flow-Example 1.9

*Solution* Consider a unit width of the channel. The force exerted on the fluid by the gate is  $F$ , as shown in the figure. This is equal and opposite to the force exerted by the fluid on the gate,  $F'$ .

Consider the control volume as shown by dotted lines in the figure. Section 1 is sufficiently far away from the efflux section and hydrostatic pressure distribution can be assumed. The frictional force on the bed between Sections 1 and 2 is neglected. Also assumed are  $\beta_1 = \beta_2 = 1.0$ . Section 2 is at the vena contracta of the jet where the streamlines are parallel to the bed. The forces acting on the control volume in the longitudinal direction are

$$F_1 = \text{pressure force on the control surface at Section 1} = \frac{1}{2} \gamma y_1^2$$

$$F_2 = \text{pressure force on the control surface at Section 2} = \frac{1}{2} \gamma y_2^2 \quad \text{acting in a direction opposing } F_1.$$

$$F = \text{reaction force of the gate on the Section 3}$$

By the momentum equation, Eq. 1.45,

$$\frac{1}{2} \gamma y_1^2 - \frac{1}{2} \gamma y_2^2 - F = \rho q (V_2 - V_1) \quad (1.46)$$

in which  $q = \text{discharge per unit width} = V_1 y_1 = V_2 y_2$ . Simplifying Eq. 1.46,

$$F = \frac{1}{2} \gamma \frac{(y_1 - y_2)}{y_1 y_2} \left( y_1 y_2 (y_1 + y_2) - \frac{2q^2}{g} \right) \quad (1.47)$$

If the loss of energy between Sections 1 and 2 is assumed to be negligible, by the energy equation with  $\alpha_1 = \alpha_2 = 1.0$

$$y_1 + \frac{V_1^2}{2g} = y_2 + \frac{V_2^2}{2g} \quad (1.48)$$

Substituting

$$V_1 = \frac{q}{y_1} \quad \text{and} \quad V_2 = \frac{q}{y_2}$$

$$\frac{q^2}{g} = \frac{2y_1^2 y_2^2}{(y_1 + y_2)}$$

and by Eq. 1.43,

$$F = \frac{1}{2} \gamma \frac{(y_1 - y_2)^3}{(y_1 + y_2)} \quad (1.49)$$

The force on the gate  $F'$  would be equal and opposite to  $F$ .

**Example 1.10** Figure 1.19 shows a hydraulic jump in a horizontal apron aided by a two dimensional block on the apron. Obtain an expression for the drag force per unit length of the block.

**Solution** Consider a control volume surrounding the block as shown in Fig. 1.19. A unit width of apron is considered. The drag force on the block would have a reaction force =  $F_D$  on the control surface, acting in the upstream direction as shown in Fig. 1.19. Assume, a frictionless, horizontal channel and hydrostatic pressure distribution at Sections 1 and 2.

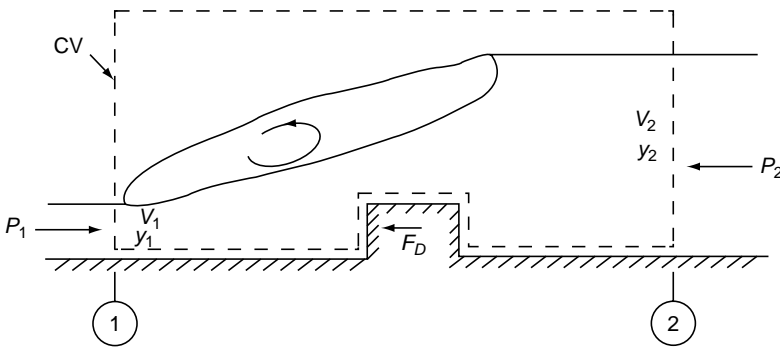


Fig. 1.19 Example 1.10

By momentum equation, Eq. 1.45, in the direction of the flow

$$P_1 - F_D - P_2 = M_2 - M_1$$

$$\frac{1}{2} \gamma y_1^2 - F_D - \frac{1}{2} \gamma y_2^2 = \rho q (\beta_2 V_2 - \beta_1 V_1)$$

where  $q$  = discharge per unit width of apron =  $y_1 V_1 = y_2 V_2$ .

Assuming  $\beta_1 = \beta_2 = 1.0$

$$\begin{aligned} F_D &= \frac{1}{2} \gamma y_1^2 - \frac{1}{2} \gamma y_2^2 = \rho q^2 \left( \frac{1}{y_2} - \frac{1}{y_1} \right) \\ &= \frac{\gamma}{2} \left[ y_1^2 - y_2^2 + \frac{q^2}{g} \left( \frac{y_2 - y_1}{y_1 y_2} \right) \right] \end{aligned}$$

**Unsteady Flow** In unsteady flow, the linear-momentum equation will have an additional term over and above that of the steady flow equation to include the rate of change of momentum in the control volume. The momentum equation would then state that in an unsteady flow the algebraic sum of all external forces in a given direction on a fluid mass equals the net change of the linear-momentum flux of the fluid mass in that direction plus the time rate of increase of momentum in that direction within the control volume. An application of the momentum equation in unsteady flows is given in Chapter 10. For details on the momentum equation in unsteady flow consult References 5 and 6.



**Specific Force** The steady-state momentum equation (Eq. 1.45) takes a simple form if the tangential force  $F_3$  and body force  $F_4$  are both zero. In that case

$$F_1 - F_2 = M_2 - M_1$$

or

$$F_1 + M_1 = F_2 + M_2$$

Denoting  $\frac{1}{\gamma}(F + M) = P_s$

$$(P_s)_1 = (P_s)_2 \tag{1.50}$$

The term  $P_s$  is known as the *specific force* and represents the sum of the pressure force and momentum flux per unit weight of the fluid at a section. Equation (1.50) states that the specific force is constant in a horizontal, frictionless channel. This fact can be advantageously used to solve some flow situations. An application of the specific force relationship to obtain an expression for the depth at the end of a hydraulic jump is given in Section 6.4. In a majority of applications the force  $F$  is taken as due to hydrostatic pressure distribution and hence is given by,  $F = \gamma A\bar{y}$  where  $\bar{y}$  is the depth of the centre of gravity of the flow area.



## REFERENCES

1. Graf, W H, *Hydraulics of Sediment Transport*, McGraw-Hill, New York, 1971.
2. ASCE, *Sedimentation Engineering*, American Soc. of Civil Engrs., Manual No. 54, New York, 1977.
3. King, H W, *Handbook of Hydraulics*, McGraw-Hill, New York, 1954, pp 7–12.
4. Jaeger, C, *Engineering Fluid Mechanics*, Blackie and Son, London, 1957.
5. White, F M, *Fluid Mechanics*, 3rd ed., McGraw-Hill, New York, 1994.
6. Daily, J W and Harleman, D R F, *Fluid Dynamics*, Addison-Wesley, New York, 1966.
7. Chow, V T, *Open Channel Hydraulics*, McGraw-Hill, New York, 1959.



## PROBLEMS

### Problem Distribution

Topic	Problems
Classification	1.1
$\alpha$ and $\beta$	1.2 – 1.6
Pressure distribution	1.7 – 1.14
Continuity equation	1.15 – 1.17
Energy equation	1.18 – 1.22
Momentum equation	1.23 – 1.31

- 1.1 Classify the following open-channel flow situations:
- (a) Flow from a sluice gate
  - (b) Flow in a main irrigation canal
  - (c) A river during flood

- (d) Breaking of a dam
  - (e) Flow over a spillway
  - (f) Sudden opening of a sluice gate
  - (g) Spreading of irrigation water on a field
  - (h) Flow in a sewer
- 1.2 The Velocity distributions along the vertical in an open channel are as shown in Fig. 1.20. Determine the kinetic energy correction factor  $\alpha$  and momentum correction factor  $\beta$  for both the velocity profiles.

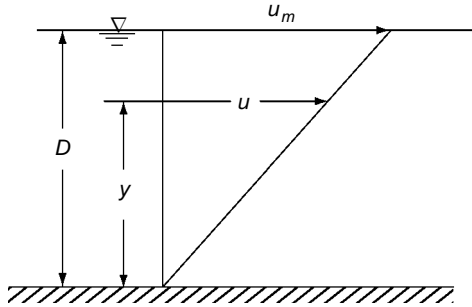


Fig. 1.20 Problem 1.2

- 1.3 The velocity distribution along a vertical in a channel can be expressed as  $v/v_{\max} = (y/y_0)^{1/n}$  where  $y_0 =$  depth of flow,  $v =$  velocity at any height  $y$  above the bed and  $n =$  a constant. Find the values of  $\alpha$  and  $\beta$ .
- 1.4 For the velocity distribution given in Fig. 1.21, find  $\alpha$  and  $\beta$ .

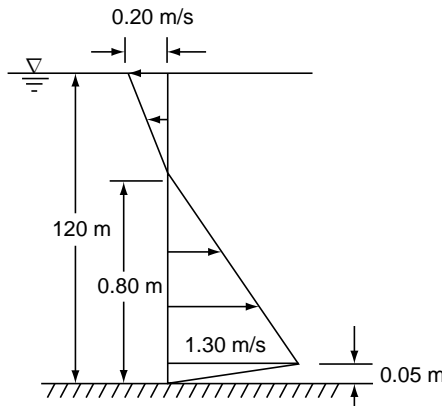


Fig. 1.21 Problem 1.4

- 1.5 The velocity distribution in a channel is given by  $u = u(y)$ . By representing  $u = V + \delta u$ , where  $V =$  mean velocity and  $\delta u =$  deviation from the mean, show that
- $$\alpha \approx 1 + 3\eta \quad \text{and} \quad \beta \approx 1 + \eta$$

where

$$\eta = \frac{1}{AV^2} \int_A (\delta u)^2 dA$$

- 1.6 A rectangular channel curved in the vertical plane is 2.0 m wide and has a centreline radius of 5.0 m. The velocity distribution at a radial section can be considered to be an irrotational vortex, i.e.  $v = C/r$ . The depth of flow is 1.50 m and is constant along the channel.

32 Flow in Open Channels

For a discharge of  $6.0 \text{ m}^2/\text{s}$ , find (a) the velocity distribution, (b) the average velocity, and (c) the correction factors  $\alpha$  and  $\beta$ .

- 1.7 For the following two pressure distributions [Fig. 1.22 (a) and (b)] in an open channel flow, calculate the effective piezometric head. Take the hydrostatic pressure distribution as the reference.

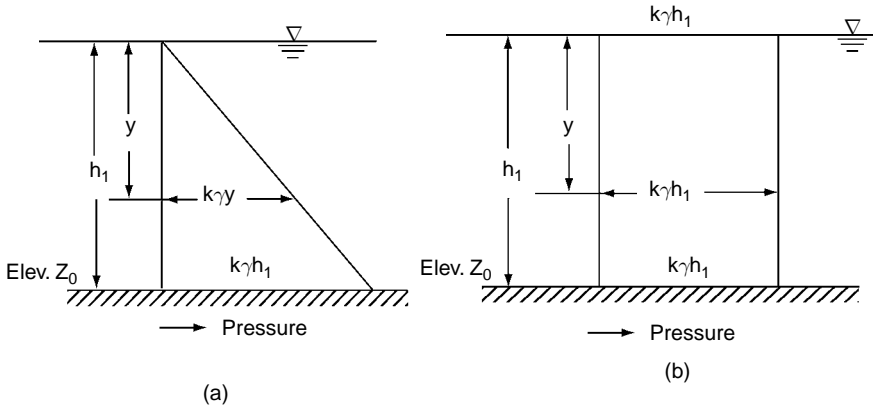


Fig. 1.22 Problem 1.7

- 1.8 A rectangular channel has a convex curvature in a vertical plane on its bed. At a section the bed has an inclination of  $30^\circ$  to the horizontal and the depth measured normal to the flow is  $0.75 \text{ m}$ . A certain flow produces a normal acceleration of  $0.4 g$  which can be assumed to be constant throughout the depth. Determine the pressure distribution and compare it with the hydrostatic distribution.
- 1.9 For the situation detailed in Problem 1.8, determine the pressure distribution if the boundary has a concave curvature to the flow and the rest of the data remain same.
- 1.10 In a flow over a certain spillway crest the normal acceleration  $a_n$  can be assumed to be constant. Show that the pressure on the crest is atmospheric when  $a_n = g \cos \theta$ , where  $\theta =$  inclination of the normal to the surface with the vertical.
- 1.11 Assuming the flow in the spillway bucket of Example 1.3 to be an irrotational vortex ( $v = C/r$ ) at a constant depth  $h$  in the curved portion, show that

$$\frac{p_2}{\gamma} = h \cos \theta + \frac{v_1^2 - v_2^2}{2g}$$

- 1.12 If the flow Problem 1.11 is assumed to be a forced vortex ( $v = Cr$ ), show that

$$\frac{p_2}{\gamma} = h \cos \theta + \frac{v_2^2 - v_1^2}{2g}$$

- 1.13 A spillway crest having a circular arc of radius  $6.0 \text{ m}$  is shown in Fig. 1.23. Estimate the pressure at point 1 when the discharge intensity is  $5.0 \text{ m}^3/\text{s}$  per metre width by assuming:

- Velocity is constant across 1–2
- Velocity varies linearly with the radius ( $v = Cr$ )
- Velocity is inversely proportional to the radius ( $v = C/r$ )
- Normal acceleration is constant at a value corresponding to average values of velocity and radius

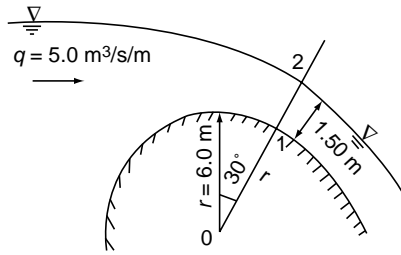


Fig. 1.23 Problem 1.13

- 1.14 At a free overflow in a wide horizontal rectangular channel the depth at the brink was found to be 0.86 m. At a section that is 5 m upstream of the brink, the depth was noted as 1.20 m. The discharge per unit width of the channel is estimated as 4.12 m<sup>3</sup>/s per m width. Assuming the water surface profile between the above two sections to be given by  $y = Ax^2 + B$ , where  $x$  is measured from the upstream section, determine the
- pressure distribution at a 2.5 m upstream section of the brink, and
  - effective piezometric head at (i)  $x = 1.0$  m, and (ii)  $x = 2.5$  m.
- 1.15 In the moving-boat method of discharge measurement of rivers the magnitude and direction of the velocity of a stream relative to the moving boat ( $V_R$  and  $\theta$ ) are measured. The depth of the stream is also simultaneously recorded. Estimate the discharge in a river (Fig. 1.24) using the following moving-boat data. Assume the velocity to be uniform in a vertical section.

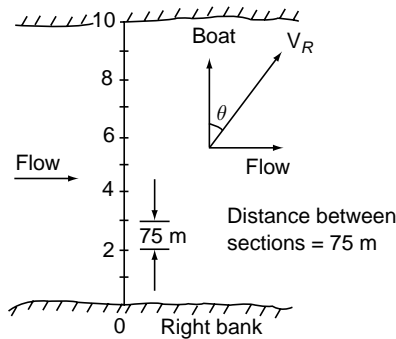


Fig. 1.24 Problem 1.15

Section	$V_R$ (m/s)	$\theta$ (degrees)	Depth (m)
1	1.75	55	1.8
2	1.84	57	2.5
3	2.00	60	3.5
4	2.28	64	4.0
5	2.28	64	4.0
6	2.20	63	4.0
7	2.00	60	3.0
8	1.84	57	2.5
9	1.70	54	2.0

34 Flow in Open Channels

- 1.16 In a rectangular channel, the flow has a free overfall. The velocity measurement at the end section where the flow was curvilinear is indicated in Fig. 1.25. Estimate the discharge per unit width of the channel.

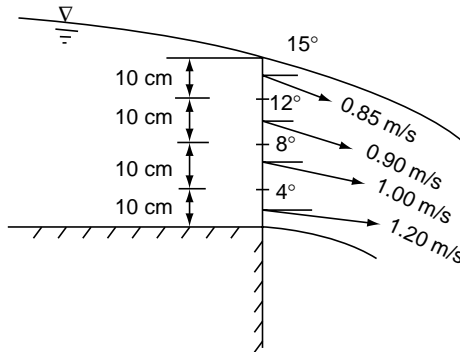


Fig. 1.25 Problem 1.16

- 1.17 Figure 1.26 shows the velocity distribution in a submerged sluice-gate flow. Estimate the discharge per unit width of the gate.

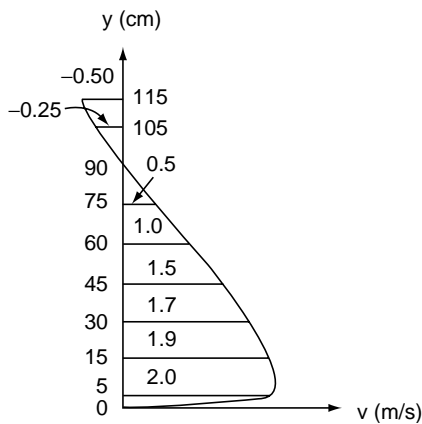


Fig. 1.26 Problem 1.17

- 1.18 A skijump spillway has an exit angle of  $40^\circ$  (Fig. 1.27). If the flow over it has a velocity of 20 m/s, neglecting all losses, estimate the maximum elevation of the outflow trajectory.

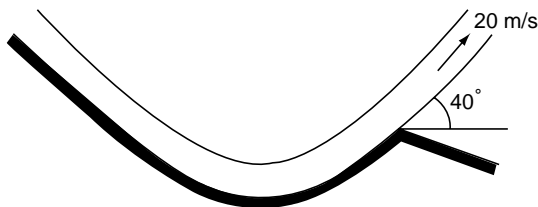


Fig. 1.27 Problem 1.18

1.19 Figure 1.28 shows a sluice gate in a rectangular channel. Fill the missing data in the following table:

Case	$y_1$ (m)	$y_2$ (m)	$q$ ( $m^2/s/m$ )	Losses
(a)	-	0.30	2.5	neglect
(b)	4.0	-	2.0	neglect
(c)	4.0	-	2.0	$0.1 V_2^2/2g$
(d)	3.0	0.25	-	neglect

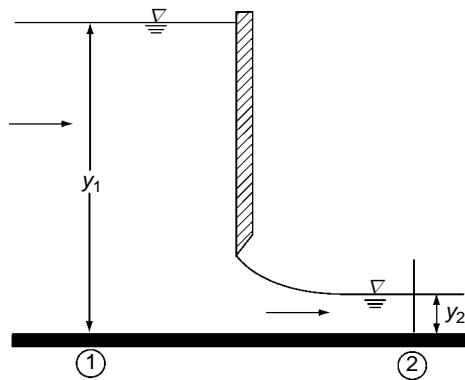


Fig. 1.28 Problem 1.19

- 1.20 A transition in a cross drainage canal works consists of a rectangular canal 2.0-m wide changing into a trapezoidal canal section of 3.0 m bottom width and side slopes 1.5 horizontal: 1 vertical. The depths of flow of 1.5 m in the rectangular section and 1.0 m in the trapezoidal section for a discharge of 10.0  $m^3/s$  is envisaged. If a loss of energy = (0.2 x difference of velocity heads) is to be included, calculate the difference in water surface and bed elevations of the two end sections of the transition. Sketch the longitudinal section of the transition, showing the water-surface elevations and the energy line.
- 1.21 Gradually varied flow is found to occur in a channel having an inclination of  $10^\circ$  with the horizontal. At the normal Section A, the elevation of the bed is 15.00 m, the elevation of the water surface is 16.30 m and the velocity of flow is 3.0 m/s. At the normal Section B, the elevation of the bed is 14.60 m and the water surface elevation is 15.80 m. Calculate the elevations of total energy and hydraulic grade lines at normal Sections A and B. Assume the values of the kinetic energy correction factor at A and B as 1.03 and 1.02, respectively.
- 1.22 An expansion in a horizontal rectangular channel takes place from a width of 2.0 m to 3.0 m. The depths of flow for a discharge of 7.20  $m^3/s$  are 1.20 m and 1.40 m in the narrower and wider sections respectively. Estimate the energy loss in the transition. Assume the kinetic energy correction coefficient  $\alpha$  to have values of 1.05 and 1.15 at the inlet and outlet of the transition, respectively.
- 1.23 Figure 1.29 shows the flow over a spillway. The depths of water are  $h_1$  and  $h_2$  and  $V_1$  is the upstream approach velocity. Estimate the horizontal force on the spillway structure.

Is the data enough to calculate the vertical component of the force on the spillway also? If not, what additional information is needed?

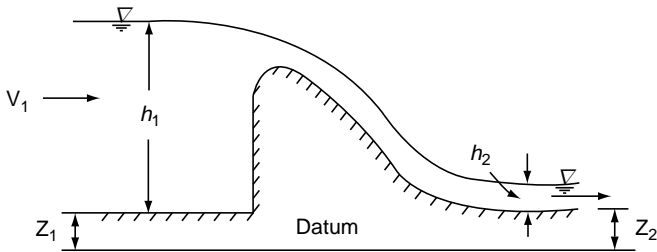


Fig. 1.29 Problem 1.23

- 1.24 Afflux is the net differential water-surface elevation between the upstream and downstream sections of a constriction to the flow. A 15 m wide rectangular canal, has a two-span bridge at a section. The bridge pier is 0.80 m wide and its coefficient of drag  $C_D$  is estimated as 2.0. If the depth of flow downstream of the bridge is 2.0 m for a discharge of  $80 \text{ m}^3/\text{s}$  in the canal, estimate the afflux due to the bridge.  
(Hint: The drag force on the bridge pier =  $C_D a \rho V_1^2/2$ , where  $a$  = projected area of the pier offered to the flow.)
- 1.25 A high-velocity flow from a hydraulic structure has a velocity of 6.0 m/s and a depth of 0.40 m. It is deflected upwards at the end of a horizontal apron through an angle of  $45^\circ$  into the atmosphere as a jet by an end sill. Calculate the force on the sill per unit width.
- 1.26 In Problem 1.19 (a, b, c and d), determine the force per m width of the sluice gate.
- 1.27 Analyse the force on a sluice gate (Example 1.7) when it is discharging under submerged conditions. What additional assumptions are required?
- 1.28 Figure 1.30 shows a submerged flow over a sharp-crested weir in a rectangular channel. If the discharge per unit width is  $1.8 \text{ m}^3/\text{s}/\text{m}$ , estimate the energy loss due to the weir. What is the force on the weir plate?

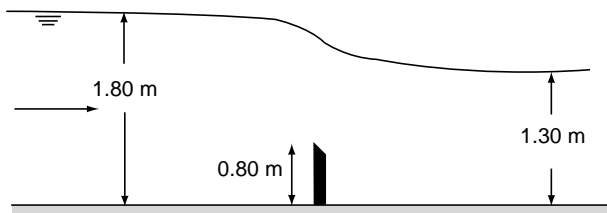


Fig. 1.30 Problem 1.28

- 1.29 A hydraulic jump assisted by a two-dimensional block is formed on a horizontal apron as shown in Fig. 1.31. Estimate the force  $F_D$  in kN/m width on the block when a discharge of  $6.64 \text{ m}^3/\text{s}$  per m width enters the apron at a depth of 0.5 m and leaves it at a depth of 3.6 m.

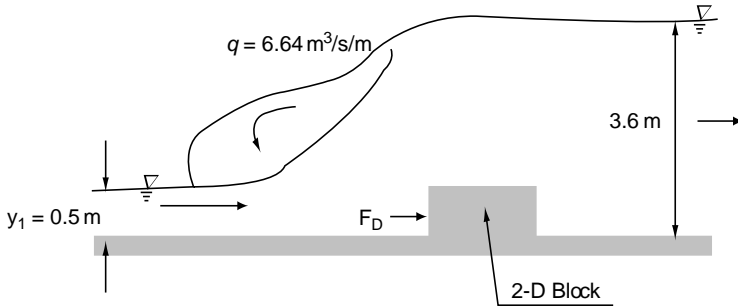


Fig. 1.31 Problem 1.29

- 1.30 Figure 1.32 shows a free overfall in a horizontal frictionless rectangular channel. Assuming the flow to be horizontal at Section 1 and the pressure at the brink of Section 2 to be atmospheric throughout the depth, show that

$$\frac{y_e}{y_0} = \frac{2F_0^2}{(2F_0^2 + 1)}$$

where  $F_0^2 = \frac{q^2}{g y_0^3}$  and  $q$  = discharge per unit width.

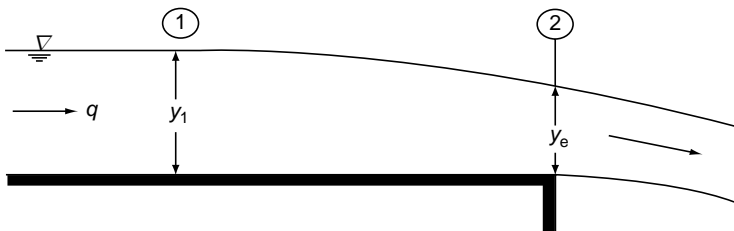


Fig. 1.32 Problem 1.30

- 1.31 Figure 1.33 shows a free overfall at the end of a horizontal, rectangular and frictionless prismatic channel. The space below the lower nappe is fully ventilated. It can be assumed that the water leaves the brink horizontally at a brink depth of  $y_e$ . Considering the control volume shown in the figure, show that the back-up depth of water  $y_1$  below the nappe is given by

$$\left[ \frac{y_1}{y_2} \right]^2 = 1 + 2F_2^2 \left[ 1 - \frac{y_2}{y_e} \right]$$

where  $F_2 = \frac{q}{y_2 \sqrt{g y_2}}$  and  $q$  = discharge per unit width of the channel.



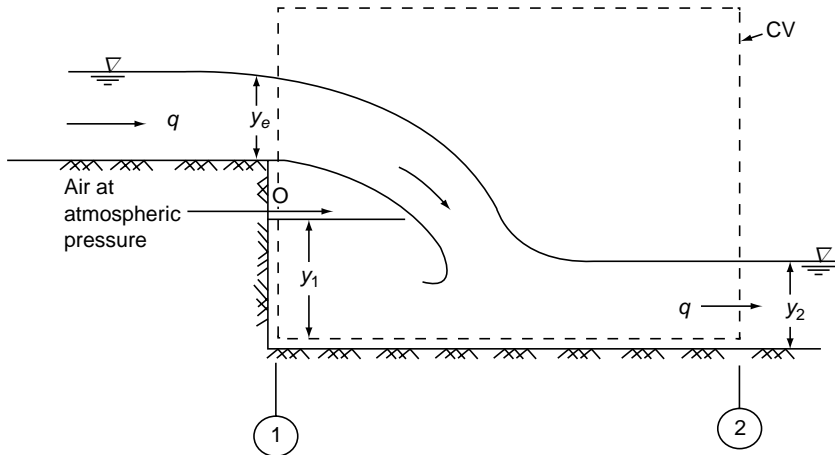


Fig. 1.33 Problem 1.31

## OBJECTIVE QUESTIONS

- 1.1 Steady flow in an open channel exists when the
  - (a) flow is uniform
  - (b) depth does not change with time
  - (c) channel is frictionless
  - (d) channel bed is not curved
- 1.2 In a steady spatially-varied flow in a prismatic open channel, the
  - (a) depth does not change along the channel length
  - (b) discharge is constant along its length
  - (c) discharge varies along the length of channel
  - (d) discharge varies with respect to time
- 1.3 A flood wave while passing down a river section protected by embankments, spills over the embankment at certain locations. The flow is classified as
  - (a) steady GVF
  - (b) unsteady RVF
  - (c) steady SVF
  - (d) unsteady SVF
- 1.4 In the uniform flow in a channel of small bed slope, the hydraulic grade line
  - (a) coincides with the bed
  - (b) is considerably below the free surface
  - (c) is considerably above the free surface
  - (d) essentially coincides with the free surface
- 1.5 A uniform flow takes place in a steep channel of large slope. The hydraulic gradient line
  - (a) coincides with the bed
  - (b) essentially coincides with the free surface
  - (c) is above the free surface
  - (d) is below the free surface
- 1.6 One-dimensional method of flow analysis means
  - (a) uniform flow
  - (b) steady uniform flow
  - (c) neglecting the variations in the transverse directions
  - (d) neglecting the variations in the longitudinal direction
- 1.7 At a section in a channel expansion, the velocity over a quarter of the cross-section is zero and is uniform over the remaining three-fourths of the area. The kinetic energy correction factor  $\alpha$  is

- (a) 1.78      (b) 1.33      (c) 1.67      (d) 2.00
- 1.8 The velocity distribution in a vertical in a channel gives a rectangular plot when the velocity as abscissa is plotted against height above the bed as ordinate. The kinetic energy correction for this distribution is  
 (a) greater than zero but less than unity      (c) equal to unity  
 (b) less than zero      (d) greater than unity
- 1.9 The momentum correction factor  $\beta$  is given by  $\beta$   
 (a)  $\frac{1}{V^3 A} \int v^3 dA$       (c)  $\frac{1}{V^2 A} \int v^2 dA$   
 (b)  $\frac{1}{VA} \int v dA$       (d)  $\frac{1}{V^3 A} \int v^2 dA$
- [In the above,  $V =$  average velocity  $= \frac{1}{A} \int v dA$ ]
- 1.10 For Question 1.7 above, the momentum correction factor  $\beta$  is  
 (a) 2.33      (b) 1.33      (c) 1.67      (d) 1.78
- 1.11 A steep chute is inclined at  $45^\circ$  to the horizontal and carries a flow at a depth of 0.75 m. The pressure at the bed of the chute in  $N/m^2$  is  
 (a) 7358      (b) 3679      (c) 5203      (d) 10401
- 1.12 A steep channel has a depth of flow, measured normal to the bed, of  $h$ . If the inclination of the channel to the horizontal is  $\theta$ , the overturning moment of a side wall is  
 (a)  $\frac{1}{6} \gamma h^3 \cos^4 \theta$       (c)  $\frac{1}{6} \gamma h^3 \cos \theta$   
 (b)  $\frac{1}{6} \gamma h^3 \cos^2 \theta$       (d)  $\frac{1}{6} \gamma h^3 / \cos \theta$
- 1.13 In an inclined channel the pressure at a depth  $y$  is calculated as  $\gamma y$ . If this value is to be accurate within 2 per cent of the true value, the maximum inclination of the channel is  
 (a)  $78^\circ 30'$       (b)  $11^\circ 29'$       (c)  $11^\circ 22'$       (d)  $8^\circ 8'$
- 1.14 Flow takes place over a spillway crest, which can be assumed to be an arc of a circle, at a depth of  $y_0$ . The pressure at any point located on the crest will be  
 (a)  $= \gamma y_0 \cos \theta$       (c) always zero  
 (b)  $< \gamma y_0 \cos \theta$       (d) always below atmospheric pressure.
- 1.15 A channel with very small value of longitudinal slope  $S_0$  has its water surface parallel to its bed. With the channel bed as the datum, the variation of the piezometric head  $H_p$  with distance above the bed  $y$  in this channel can be represented by the following:

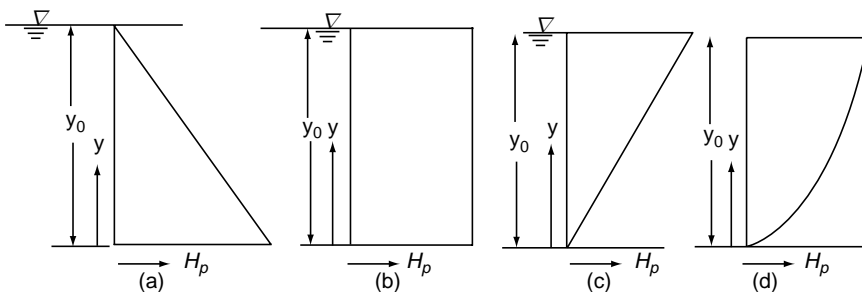


Fig. 1.34 Objective Question 1.15

- 1.16 A curvilinear flow in a vertical plane has a depth of flow of  $h$  and the pressure is found to be uniform at  $h$  throughout. The effective piezometric head measured with respect to the bed as the datum is  
 (a)  $1/2 h$  (b)  $1/3 h$  (c)  $2/3 h$  (d)  $3/2 h$
- 1.17 The velocity and depth of flow in a 3.0 m wide rectangular channel are 2.0 m/s and 2.5 m, respectively. If the channel has its width enlarged to 3.5 m at a section, the discharge past that section is  
 (a)  $10.0 \text{ m}^3/\text{s}$  (b)  $20.0 \text{ m}^3/\text{s}$  (c)  $15.0 \text{ m}^3/\text{s}$  (d)  $17.5 \text{ m}^3/\text{s}$
- 1.18 Figure 1.35 shows the velocity distribution at two Sections A and B in a canal. The canal is rectangular in cross section and has widths of 2.0 m at A and 3.5 m at B. Section A is upstream of B. From the data one can infer that  
 (a) the discharge in the canal is constant in the reach AB.  
 (b) Certain amount of flow is being added into the canal in the reach AB.  
 (c) Some amount of flow is being extracted out of the canal in the reach AB.  
 (d) The discharge per unit width of the canal is constant in the reach AB.

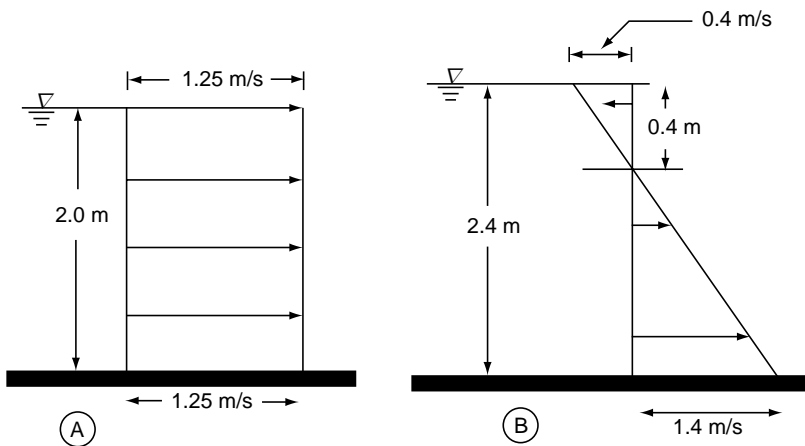


Fig. 1.35 Objective Question 1.18

- 1.19 A sluice gate in a small pond discharges a flow having  $10.0 \text{ m}^2$  flow area and a velocity of 4.0 m/s. If the pond has a surface area of 1.0 hectare, the rate at which the water surface falls in the pond is  
 (a) 0.25 m/s (b) 4 cm/s (c) 4 mm/s (d) 4.0 m/s
- 1.20 For an open channel flow to take place between two sections,  
 (a) the channel bed must always slope in the direction of the flow  
 (b) the upstream depth must be larger than the downstream depth  
 (c) the upstream momentum must be larger than the downstream momentum  
 (d) the total energy at the upstream end must be larger than the total energy at the downstream section
- 1.21 A steep rectangular channel has a slope of  $30^\circ$  with the horizontal. At a section the bed is 1.20 m above the datum, the depth of flow is 0.70 m the discharge is  $3.10 \text{ m}^3/\text{s}$  per metre width. The total energy head at that section by assuming  $\alpha = 1.10$  is  
 (a) 3.00 m (b) 2.91 m (c) 1.90 m (d) 3.10 m
- 1.22 The width of a rectangular channel is reduced from 3.5 m to 2.5 m at a transition structure. The depth of flow upstream of the contraction is 1.5 m. The change in the bottom elevation required to cause zero change in the water surface elevation is  
 (a)  $-2.1$  (b)  $-0.6$  (c)  $+0.6$  (d)  $-0.2$  m

- 1.23 The total energy head for an open channel flow is written with usual notation as  $H = z + y + V^2/2g$ . In this each of the terms represent
- (a) energy in kg m/kg mass of fluid
  - (b) energy in N m/N of fluid
  - (c) power in kW/kg mass of fluid
  - (d) energy in N m/ mass of fluid
- 1.24 Piezometric head is the sum of
- (a) pressure head, datum head and velocity head
  - (b) datum head and velocity head
  - (c) pressure head and velocity head
  - (d) pressure head and datum head
- 1.25 The difference between total head line and piezometric head line represents
- (a) the velocity head
  - (b) the pressure head
  - (c) the elevation of the bed of the channel
  - (d) the depth of flow
- 1.26 The momentum equation in  $x$ -direction as  $\Sigma F_x = \rho Q_j (V_{x2} - V_{x1})$  has the assumption that the flow is
- (a) steady
  - (b) unsteady
  - (c) uniform
  - (d) frictionless
- 1.27 Normally in a stream the ratio of the surface velocity at a location to the average velocity in the vertical through that location
- (a) is greater than 1.0
  - (b) will be between 0.8 and 0.95
  - (c) is less than or greater than unity depending on the type of flow
  - (d) is equal to 0.6
- 1.28 The specific force is constant
- (a) in all frictionless channels irrespective of the magnitude of the longitudinal slope
  - (b) in horizontal, frictionless channels of any shape
  - (c) in all horizontal channels of any shape
  - (d) in any open channel

# Energy–Depth Relationships

## 2

### 2.1 SPECIFIC ENERGY

The *total energy* of a channel flow referred to a datum is given by Eq.1.39 as

$$H = Z + y \cos \theta + \alpha \frac{V^2}{2g}$$

If the datum coincides with the channel bed at the section, the resulting expression is known as *specific energy* and is denoted by  $E$ . Thus

$$E = y \cos \theta + \alpha \frac{V^2}{2g} \quad (2.1)$$

When  $\cos \theta = 1.0$  and  $\alpha = 1.0$ ,

$$E = y + \frac{V^2}{2g} \quad (2.2)$$

The concept of specific energy, introduced by Bakhmeteff, is very useful in defining critical depth and in the analysis of flow problems. It may be noted that while the total energy in a real fluid flow always decreases in the downstream direction, the specific energy is constant for a uniform flow and can either decrease or increase in a varied flow, since the elevation of the bed of the channel relative to the elevation of the total energy line, determines the specific energy. If the frictional resistance of the flow can be neglected, the total energy in non-uniform flow will be constant at all sections while the specific energy for such flows, however, will be constant only for a horizontal bed channel and in all other cases the specific energy will vary.

To simplify the expressions it will be assumed, for use in all further analysis, that the specific energy is given by Eq. 2.2, i.e.,  $\cos \theta = 1.0$  and  $\alpha = 1.0$ . This is with the knowledge that  $\cos \theta$  and  $\alpha$  can be appended to  $y$  and  $(V^2/2g)$  terms respectively, without difficulty if warranted.

## 2.2 CRITICAL DEPTH

**Constant Discharge Situation** Since the specific energy

$$E = y + \frac{V^2}{2g} = y + \frac{Q^2}{2gA^2} \tag{2.2a}$$

for a channel of known geometry,  $E = f(y, Q)$  keeping  $Q = \text{constant} = Q_1$  the variation of  $E$  with  $y$  is represented by a cubic parabola Fig. 2.1. It is seen that there are two positive roots for the equation of  $E$  indicating that any particular discharge  $Q_1$  can be passed in a given channel at two depths and still maintain the same specific energy  $E$ . In Fig. 2.1 the ordinate  $PP'$  represents the condition for a specific energy of  $E_1$ . The depths of flow can be either  $PR = y_1$  or  $PR' = y'_1$ . These two possible depths having the same specific energy are known as *alternate depths*. In Fig. 2.1, a line ( $OS$ ) drawn such that  $E = y$  (i.e. at  $45^\circ$  to the abscissa) is the asymptote of the upper limb of the specific energy curve. It may be noticed that the intercept  $P'R'$  or  $P'R$  represents the velocity head. Of the two alternate depths, one ( $PR = y_1$ ) is smaller and has a large velocity head while the other ( $PR' = y'_1$ ) has a larger depth and consequently a smaller velocity head. For a given  $Q_1$  as the specific energy is increased the difference between the two alternate depths increases. On the other hand, if  $E$  is decreased, the difference ( $y'_1 - y_1$ ) will decrease and at a certain value  $E = E_c$ , the two depths will merge with each other (point  $C$  in Fig. 2.1). No value for  $y$  can be obtained when  $E < E_c$ , denoting that the flow under the given conditions is not possible in this region. The condition of minimum specific energy is known as the *critical-flow condition* and the corresponding depth  $y_c$  is known as the *critical depth*.

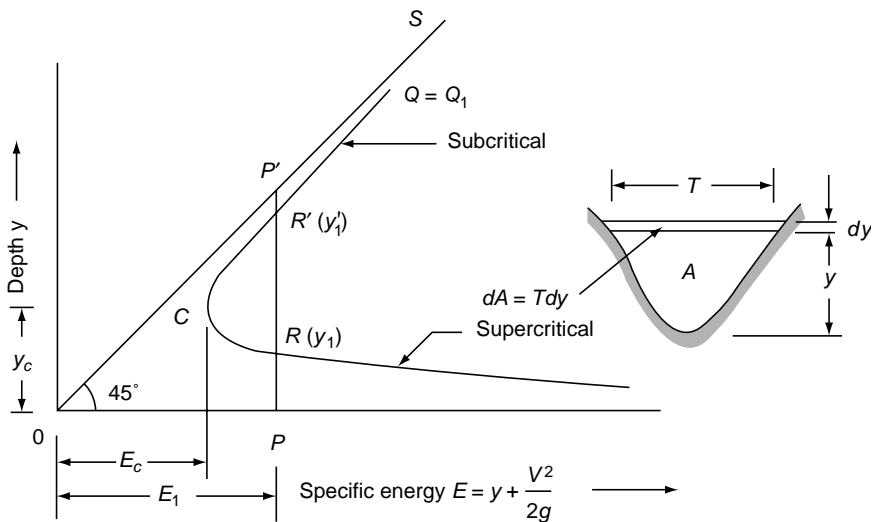


Fig. 2.1 Definition sketch of specific energy

At critical depth, the specific energy is minimum. Thus differentiating Eq. 2.2a with respect to  $y$  (keeping  $Q$  constant) and equating to zero,

$$\frac{dE}{dy} = 1 - \frac{Q^2}{gA^3} \frac{dA}{dy} = 0 \quad (2.3)$$

But  $\frac{dA}{dy} = T =$  top width, i.e. width of the channel at the water surface.

Designating the critical-flow conditions by the suffix 'c',

$$\frac{Q^2 T_c}{gA_c^3} = 1 \quad (2.4)$$

or 
$$\frac{Q^2}{g} = \frac{A_c^3}{T_c} \quad (2.4a)$$

If an  $\alpha$  value other than unity is to be used, Eq. 2.4 will become

$$\frac{\alpha Q^2 T_c}{gA_c^3} = 1.0 \quad (2.5)$$

Equation 2.4 or 2.5 is the basic equation governing the critical-flow conditions in a channel. It may be noted that the critical-flow condition is governed solely by the channel geometry and discharge (and  $\alpha$ ). Other channel properties such as the bed slope and roughness do not influence the critical-flow condition for any given  $Q$ . If the Froude number of the flow is define as

$$F = V / \left( \sqrt{gA/T} \right) \quad (2.6)$$

it is easy to see that by using  $F$  in Eq. 2.4, at the critical flow  $y = y_c$  and  $F = F_c = 1.0$ . We thus get an important result that the critical flow corresponds to the minimum specific energy and at this condition the Froude number of the flow is unity. For a channel with large longitudinal slope  $\theta$  and having a flow with an energy correction factor of  $\alpha$ , the Froude number  $F$  will be defined as

$$F = V / \left( \sqrt{\frac{1}{\alpha} g \frac{A}{T} \cos \theta} \right) \quad (2.6a)$$

Referring to Fig. 2.1, considering any specific energy other than  $E_c$ , (say ordinate  $PP'$  at  $E = E_1$ ) the Froude number of the flow corresponding to both the alternate depths will be different from unity as  $y_1$  or  $y'_1 \neq y_c$ . At the lower limb,  $CR$  of the specific-energy curve, the depth  $y_1 < y_c$ . As such,  $V'_1 > V_c$  and  $F_1 > 1.0$ . This region is called the *supercritical flow* region. In the upper limb  $CR'$ ,  $y'_1 > y_c$ . As such  $V'_1 < V_c$  and  $F'_1 < 1.0$ . This denotes the *subcritical flow* region.

**Discharge as a Variable** In the above section the critical-flow condition was derived by keeping the discharge constant. The specific-energy diagram can be plotted

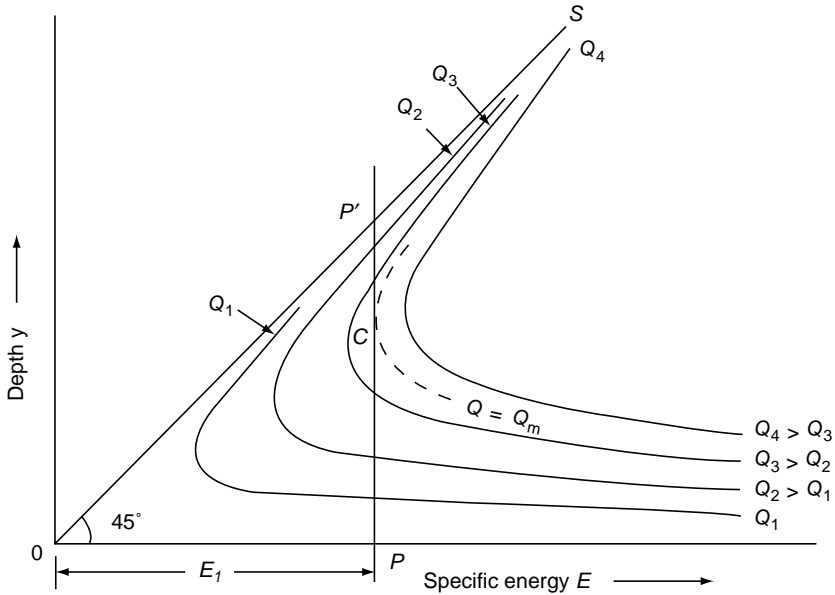


Fig. 2.2 Specific energy for varying discharges

for different discharges  $Q = Q_i = \text{constant}$  ( $i = 1, 2, 3 \dots$ ), as in Fig. 2.2. In this figure,  $Q_1 < Q_2 < Q_3 < \dots$  and is constant along the respective  $E$  vs  $y$  plots. Consider a section  $PP'$  in this plot. It is seen that for the ordinate  $PP'$ ,  $E = E_1 = \text{constant}$ . Different  $Q$  curves give different intercepts. The difference between the alternate depths decreases as the  $Q$  value increases. It is possible to imagine a value of  $Q = Q_m$  at a point  $C$  at which the corresponding specific-energy curve would be just tangential to the ordinate  $PP'$ . The dotted line in Fig. 2.2 indicating  $Q = Q_m$  represents the maximum value of discharge that can be passed in the channel while maintaining the specific energy at a constant value ( $E_1$ ). Any specific energy curve of higher  $Q$  value (i.e.  $Q > Q_m$ ) will have no intercept with the ordinate  $PP'$  and hence there will be no depth at which such a discharge can be passed in the channel with the given specific energy. Since by Eq. 2.2a

$$E = y + \frac{Q^2}{2gA^2}$$

$$Q = A\sqrt{2g(E - y)} \tag{2.7}$$

The condition for maximum discharge can be obtained by differentiating Eq. 2.7 with respect to  $y$  and equating it to zero while keeping  $E = \text{constant}$ .

Thus 
$$\frac{dQ}{dy} = \sqrt{2g(E - y)} \frac{dA}{dy} - \frac{gA}{\sqrt{2g(E - y)}} = 0$$

By putting 
$$\frac{dA}{dy} = T \text{ and } \frac{Q}{A} = \sqrt{2g(E - y)}$$
 yields



$$\frac{Q^2 T}{gA^3} = 1.0 \quad (2.8)$$

This is same as Eq. 2.4 and hence represents the critical-flow conditions. Hence, the critical-flow condition also corresponds to the condition for maximum discharge in a channel for a fixed specific energy.

**Example 2.1** | A 2.5-m wide rectangular channel has a specific energy of 1.50 m when carrying a discharge of 6.48 m<sup>3</sup>/s. Calculate the alternate depths and corresponding Froude numbers.

*Solution* From Eq. 2.2a

$$\begin{aligned} E &= y + \frac{V^2}{2g} = y + \frac{Q^2}{2gB^2 y^2} \\ 1.5 &= y + \frac{(6.48)^2}{2 \times 9.81 \times (2.5)^2 y^2} \\ &= y + \frac{0.34243}{y^2} \end{aligned}$$

Solving this equation by trial and error, the alternate depths  $y_1$  and  $y_2$  are obtained as  $y_1 = 1.296$  m and  $y_2 = 0.625$  m.

$$\text{Froude number} \quad F = \frac{V}{\sqrt{gy}} = \frac{6.48}{(2.5y)\sqrt{9.81y}} = \frac{0.82756}{y^{3/2}},$$

At  $y_1 = 1.296$  m,  $F_1 = 0.561$ ; and

at  $y_2 = 0.625$  m,  $F_2 = 1.675$

The depth  $y_1 = 1.296$  m is in the subcritical flow region and the depth  $y = 0.625$  m is in the supercritical flow region.

**Example 2.2** | A flow of 5.0 m<sup>3</sup>/s is passing at a depth of 1.5 m through a rectangular channel of 2.5 m width. The kinetic energy correction factor  $\alpha$  is found to be 1.20. What is the specific energy of the flow? What is the value of the depth alternate to the existing depth if  $\alpha = 1.0$  is assumed for the alternate flow?

$$\text{Solution} \quad V_1 = \frac{Q}{A_1} = \frac{5.0}{(2.5 \times 1.5)} = 1.33 \text{ m/s}$$

$$\alpha_1 \frac{V_1^2}{2g} = 1.20 \times \frac{(1.33)^2}{2 \times 9.81} = 0.1087 \text{ m}$$

Specific energy  $E_1 = y_1 + \alpha_1 \frac{V_1^2}{2g} = 1.5 + 0.1087$   
 $= 1.6087 \text{ m}$

For the alternate depth  $y_2$ ,

$$y_2 + \frac{(5.0)^2}{2 \times 9.81 (2.5y_2)^2} = 1.6087 \dots \text{ (since } \alpha_2 = 1.0 \text{)}$$

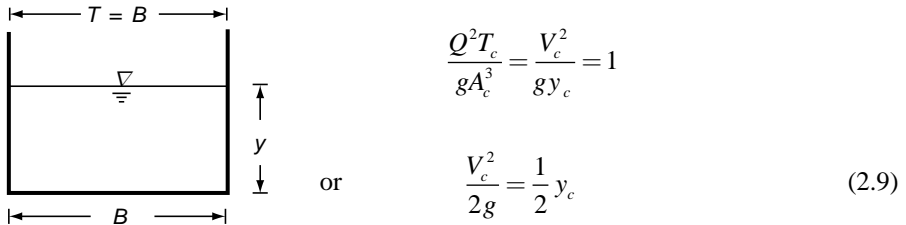
i.e.  $y_2 + \frac{0.2039}{y_2^2} = 1.6087$

By trial and error,  $y_2 = 0.413 \text{ m}$

### 2.3 CALCULATION OF THE CRITICAL DEPTH

Using Eq. 2.4, expressions for the critical depth in channels of various geometric shapes can be obtained as follows:

**Rectangular Section** For a rectangular section,  $A = By$  and  $T = B$  (Fig. 2.3). Hence by Eq. 2.4



$$\frac{Q^2 T_c}{g A_c^3} = \frac{V_c^2}{g y_c} = 1$$

$$\text{or} \quad \frac{V_c^2}{2g} = \frac{1}{2} y_c \quad (2.9)$$

Fig. 2.3 Rectangular channel

Specific energy at critical depth  $E_c = y_c + \frac{V_c^2}{2g} = \frac{3}{2} y_c$  (2.10)

Note that Eq. 2.10 is independent of the width of the channel.

Also, if  $q =$  discharge per unit width  $= Q/B$ ,

$$\frac{q^2}{g} = y_c^3$$

i.e.  $y_c = \left( \frac{q^2}{g} \right)^{1/3}$  (2.11)

Since  $A/T = y$ , from Eq. 2.6, the Froude number for a rectangular channel will be defined as

$$F = \frac{V}{\sqrt{gy}} \quad (2.12)$$

**Triangular Channel** For a triangular channel having a side slope of  $m$  horizontal: 1 vertical (Fig. 2.4),  $A = my^2$  and  $T = 2my$ .

By Eq. 2.4a,

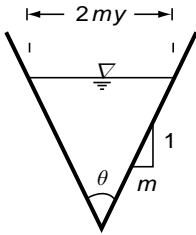


Fig. 2.4 Triangular channel

$$\frac{Q^2}{g} = \frac{A_c^3}{T_c} = \frac{m^3 y_c^6}{2my_c} = \frac{m^2 y_c^5}{2} \quad (2.13)$$

$$\text{Hence } y_c = \left( \frac{2Q^2}{gm^2} \right)^{1/5} \quad (2.14)$$

The specific energy at critical depth  $E_c = y_c + \frac{V_c^2}{2g}$

$$= y_c + \frac{Q^2}{2gA_c^2} = y_c + \frac{m^2 y_c^5}{4m^2 y_c^4}$$

i.e.  $E_c = 1.25y_c \quad (2.15)$

It is noted that Eq. 2.15 is independent of the side slope  $m$  of the channel. Since  $A/T = y/2$ , the Froude number for a triangular channel is defined by using Eq. 2.6 as

$$F = \frac{V\sqrt{2}}{\sqrt{gy}} \quad (2.16)$$

**Circular Channel** Let  $D$  be the diameter of a circular channel (Fig. 2.5) and  $2\theta$  be the angle in radians subtended by the water surface at the centre.

$A$  = area of the flow section

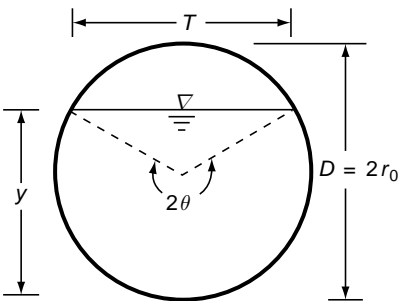


Fig. 2.5 Circular channel

= area of the sector + area of the triangular portion

$$= \frac{1}{2} r_0^2 2\theta + \frac{1}{2} \cdot 2r_0 \sin(\pi - \theta) r_0 \cos(\pi - \theta)$$

$$= \frac{1}{2} (r_0^2 2\theta - r_0^2 \sin 2\theta)$$

$$A = \frac{D^2}{8} (2\theta - \sin 2\theta)$$

Top width  $T = D \sin \theta$

$$2\theta = 2 \cos^{-1} \left( 1 - \frac{2y}{D} \right) = f(y/D)$$

and

Substituting these in Eq. 2.4a yields

$$\frac{Q^2}{g} = \frac{\left[ \frac{D^2}{8} (2\theta_c - \sin 2\theta_c) \right]^3}{D \sin \theta_c} \quad (2.17)$$

Since explicit solutions for  $y_c$  cannot be obtained from Eq. 2.17, a non-dimensional representation of Eq. 2.17 is obtained as

$$\frac{Q^2}{\sqrt{gD^5}} = \frac{0.044194 (2\theta_c - \sin 2\theta_c)^{3/2}}{(\sin \theta_c)^{1/2}} = f(y_c/D) \quad (2.18)$$

This function is evaluated and is given in Table 2A.1 of Appendix 2A at the end of this chapter as an aid for the estimation of  $y_c$ .

Since  $A/T = fn\left(\frac{y}{D}\right)$ , the Froude number for a given  $Q$  at any depth  $y$  will be

$$F = \frac{V}{\sqrt{g(A/T)}} = \frac{Q}{\sqrt{g(A^3/T)}} = fn(y/D)$$

The following are two empirical equations that have been proposed for quick and accurate estimation of critical depth in circular channels:

*Empirical relationships for critical depth in circular channels*

Sl.No	Equation	Details
1	$\frac{y_c}{D} = [0.77F_D^{-6} + 1.0]^{-0.085}$ <p>where <math>F_D = \frac{Q}{D^2 \sqrt{gD}} = \frac{Z}{D^{2.5}}</math></p>	Swamee P K (1993)(Ref. 4).
2	$y_c = \frac{1.01}{D^{0.265}} \left( \frac{Q}{\sqrt{g}} \right)^{0.506}$ <p>for <math>0.02 &lt; \frac{y_c}{D} \leq 0.85</math></p>	Straub W O (1978)(Ref. 5).

**Trapezoidal Channel** For a trapezoidal channel having a bottom width of  $B$  and side slopes of  $m$  horizontal: 1 vertical (Fig. 2.6)

Area  $A = (B + my)y$   
 and Top width  $T = (B + 2my)$

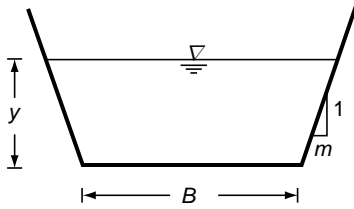


Fig. 2.6 Trapezoidal channel

At the critical flow

$$\frac{Q^2}{g} = \frac{A_c^3}{T_c} = \frac{(B + my_c)^3 y_c^3}{(B + 2my_c)} \quad (2.19)$$

Here also an explicit expression for the critical depth  $y_c$  is not possible. The non-dimensional representation of Eq. 2.19 facilitates the solution of  $y_c$  by the aid of tables or graphs. Rewriting the right-hand side of Eq. 2.19 as

$$\begin{aligned} \frac{(B + my_c)^3 y_c^3}{B + 2my_c} &= \frac{B^3 \left(1 + \frac{my_c}{B}\right)^3 y_c^3}{B \left(1 + \frac{2my_c}{B}\right)} \\ &= \frac{B^5 (1 + \zeta_c)^3 \zeta_c^3}{m^3 (1 + 2\zeta_c)} \quad \text{where } \zeta_c = \frac{m y_c}{B} \end{aligned}$$

gives 
$$\frac{Q^2 m^3}{g B^5} = \frac{(1 + \zeta_c)^3 \zeta_c^3}{(1 + 2\zeta_c)} \quad (2.20)$$

or 
$$\frac{Q m^{3/2}}{\sqrt{g} B^{5/2}} = \psi = \frac{(1 + \zeta_c)^{3/2} \zeta_c^{3/2}}{(1 + 2\zeta_c)^{1/2}} \quad (2.20a)$$

Equation 2.20a can easily be evaluated for various value of  $\zeta_c$  and plotted as  $\psi$  vs  $\zeta_c$ . It may be noted that if  $\alpha > 1$ ,  $\psi$  can be defined as

$$\psi = \left( \frac{\alpha Q^2 m^3}{g B^5} \right)^{1/2} \quad (2.21)$$

Table 2A - 2 which gives values of  $\psi$  for different values of  $\zeta_c$  is provided at the end of this chapter. This table is very useful in quick solution of problems related to critical depth in trapezoidal channels.

Since  $A/T = \frac{(B + my)y}{(B + 2my)} = \frac{\left(1 + \frac{my}{B}\right)y}{\left(1 + 2\frac{my}{B}\right)}$  the Froude number at any depth  $y$  is

$$F = \frac{V}{\sqrt{gA/T}} = \frac{Q/A}{\sqrt{gA/T}} = fn (my/B) \text{ for a given discharge } Q.$$

Further the specific energy at critical depth,  $E_c$  is a function of  $(my_c/B)$  and it can be shown that (Problem 2.7)

$$\frac{E_c}{y_c} = \frac{1(3+5\zeta_c)}{2(1+2\zeta_c)}$$

where 
$$\zeta_c = \frac{my_c}{B}$$

## 2.4 SECTION FACTOR $Z$

The expression  $A\sqrt{A/T}$  is a function of the depth  $y$  for a given channel geometry and is known as the *section factor*  $Z$ .

Thus 
$$Z = A\sqrt{A/T} \quad (2.22)$$

At the critical-flow condition,  $y = y_c$  and

$$Z_c = A_c\sqrt{A_c/T_c} = Q/\sqrt{g} \quad (2.23)$$

which is a convenient parameter for analysing the role of the critical depth in a flow problem.

As a corollary of Eq. 2.23, if  $Z$  is the section factor for any depth of flow  $y$ , then

$$Q_c = \sqrt{g} Z \quad (2.24)$$

where  $Q_c$  represents the discharge that would make the depth  $y$  critical and is known as the *critical discharge*.

Note that the left-hand side of Eq. 2.18 is a non-dimensional form of the section factor (as  $Z/D^{2.5}$ ) for circular channels.

## 2.5 FIRST HYDRAULIC EXPONENT $M$

In many computations involving a wide range of depths in a channel, such as in the GVF computations, it is convenient to express the variation of  $Z$  with  $y$  in an exponential form.

The  $(Z - y)$  relationship

$$Z^2 = C_1 y^M \quad (2.25)$$

is found to be very advantageous. In this equation  $C_1$  is a coefficient and  $M$  is an exponent called the *first hydraulic exponent*. It is found that generally  $M$  is a slowly-varying

function of the aspect ratio for most of the channel shapes. The variation of  $M$  and  $\zeta = \frac{my}{B}$  for a trapezoidal channel is indicated in Fig. 2.7.

The value of  $M$  for a given channel can be determined by preparing a plot of  $Z$  vs  $y$  on a log-log scale. If  $M$  is constant between two points  $(Z_1, y_1)$  and  $(Z_2, y_2)$  in this plot, the value of  $M$  is determined as

$$M = 2 \frac{\log(Z_2/Z_1)}{\log(y_2/y_1)} \tag{2.26}$$

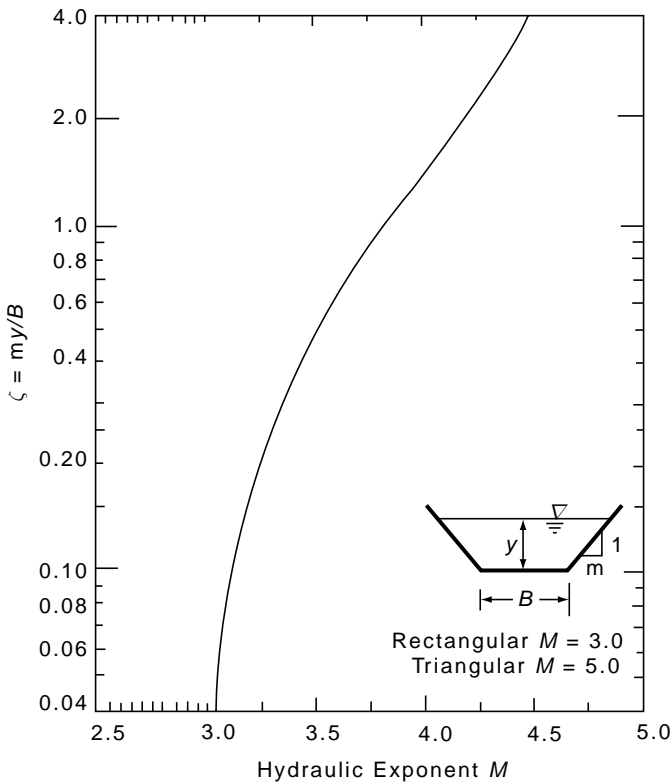


Fig. 2.7 Variation of first hydraulic exponent  $M$  in a trapezoidal channel

In Eq. 2.26, instead of  $Z$ , a non-dimensionalised  $Z$  value can also be used. For a trapezoidal channel, Eq. 2.20a represents a non-dimensionalised value of  $Z$ , if the suffix 'c' is removed. Hence the slope of  $\psi$  vs  $my/B$  on a log-log plot, such as in Fig. 2.7, can be used to obtain the value of  $M$  at any value of  $\zeta$ . It may be noted that  $M$  for a trapezoidal channel is a unique function of  $my/B$  and will have a value in the range 3.0 to 5.0.

An estimate of  $M$  can also be obtained by the relation

$$M = \frac{y}{A} \left( 3T - \frac{A}{T} \frac{dT}{dy} \right) \quad (2.27)$$

**Example 2.3** Obtain the value of the first hydraulic exponent  $M$  for (a) rectangular channel, and (b) an exponential channel where the area  $A$  is given as  $A = K_1 y^a$

*Solution* (a) For a rectangular channel  $A = By$  and  $T = B$

By Eq. 2.25,  $z^2 = \frac{A^2}{T} = B^2 y^3 = C_1 y^M$

By equating the exponents on both sides,  $M = 3.0$

[Note: The above value of  $M$  can also be obtained directly by using Eq. 2.27]

(b) 
$$A = K_1 y^a$$

$$T = \frac{dA}{dy} = K_1 a y^{(a-1)}$$

By Eq. 2.27, 
$$M = \frac{y}{A} \left( 3T - \frac{A}{T} \frac{dT}{dy} \right)$$

$$M = \frac{y}{K_1 y^a} \left[ 3K_1 a y^{(a-1)} - \frac{K_1 y^a}{K_1 a y^{(a-1)}} \left\{ K_1 a (a-1) y^{(a-2)} \right\} \right]$$

$$= 3a - a + 1 = 2a + 1$$

**Example 2.4** It is required to have a channel in which the Froude number  $F$  remains constant at all depths. If the specific energy  $E$  is kept constant, show that for such a channel  $\frac{T}{B} = \left[ \frac{E}{E-y} \right]^{1+\frac{F^2}{2}}$  where  $T$  and  $B$  are the top width and bottom width of the channel respectively.

*Solution* 
$$E = y + \frac{V^2}{2g} = y + \frac{Q^2}{2gA^2} = y + \frac{F^2}{2} \left( \frac{A}{T} \right)$$

$$E - y = \frac{AF^2}{2T} \quad (2.28)$$



Differentiating with respect to  $y$  and noting that  $F$  is constant,

$$\frac{dE}{dx} - 1 = \frac{F^2}{2} \left[ \frac{\left( T \frac{dA}{dy} - A \frac{dT}{dy} \right)}{T^2} \right]$$

Since  $E$  is constant,  $\frac{dE}{dy} = 0$ . Also  $\frac{dA}{dy} = T$

Hence, 
$$\frac{F^2}{2} \left( 1 - \frac{A}{T^2} \frac{dT}{dy} \right) = -1$$

$$\frac{AF^2}{2T} \frac{1}{T} \frac{dT}{dy} = \left( 1 + \frac{F^2}{2} \right)$$

Substituting for  $\left( \frac{AF^2}{2T} \right)$  from Eq. 2.28,  $(E - y) \left( \frac{1}{T} \frac{dT}{dy} \right) = \left( 1 + \frac{F^2}{2} \right)$

$$\frac{dT}{T} = \left( 1 + \frac{F^2}{2} \right) \frac{dy}{(E - y)}$$

On integration  $\ln T = \left( 1 + \frac{F^2}{2} \right) (-\ln(E - y)) + C$

At  $y = 0$ ,  $T = B$  and hence  $C = \ln B + \left( 1 + \frac{F^2}{2} \right) \ln E$

$\therefore \ln \frac{T}{B} = \left( 1 + \frac{F^2}{2} \right) \ln \left( \frac{E}{E - y} \right)$

or 
$$\frac{T}{B} = \left[ \frac{E}{E - Y} \right]^{\left( 1 + \frac{F^2}{2} \right)}$$

## 2.6 COMPUTATIONS

The problems concerning critical depth involve the following parameters: geometry of the channel,  $Q$  or  $E$  or  $y_c$ . For rectangular and triangular channel sections, most of the problems involve explicit relationships for the variable and a few problems involve trial and error solutions. However, for trapezoidal, circular and most other regular geometrical shapes of channel sections, many of the problems have to be solved by trial and error procedure. Tables 2A.1 and 2A.2 are helpful

in problems connected with circular and trapezoidal channels respectively. Examples 2.5 to 2.8 illustrate some of the typical problems and the approach to their solutions. The graphical solutions and monographs which were in use some decades back are obsolete now. With the general availability of computers, a large number of elegant numerical methods are available to solve non-linear algebraic equations and the solutions of critical depth and related critical flow problems in channels of all shapes, including natural channels, is no longer difficult.

**Example 2.5** Calculate the critical depth and the corresponding specific energy for a discharge of  $5.0 \text{ m}^3/\text{s}$  in the following channels:

- (a) Rectangular channel,  $B = 2.0 \text{ m}$
- (b) Triangular channel,  $m = 0.5$
- (c) Trapezoidal channel,  $B = 2.0 \text{ m}$ ,  $m = 1.5$
- (d) Circular channel,  $D = 2.0 \text{ m}$

*Solution* (a) Rectangular Channel

$$q = Q/B = \frac{5.0}{2.0} = 2.5 \text{ m}^3/\text{s}/\text{m}$$

$$y_c = (q^2/g)^{1/3} = \left[ \frac{(2.5)^2}{9.81} \right]^{1/3} = 0.860 \text{ m}$$

Since for a rectangular channel  $\frac{E_c}{y_c} = 1.5$ ,  $E_c = 1.290 \text{ m}$

(b) Triangular Channel

From Eq. 2.14

$$y_c = \left( \frac{2Q^2}{gm^2} \right)^{1/5} = \left[ \frac{2 \times (5)^2}{9.81 \times (0.5)^2} \right]^{1/5} = 1.828 \text{ m}$$

Since for a triangular channel  $\frac{E_c}{y_c} = 1.25$ ,  $E_c = 2.284 \text{ m}$

(c) Trapezoidal Channel

$$\Psi = \frac{Qm^{3/2}}{\sqrt{g}B^{5/2}} = \frac{5.0 \times (1.5)^{3/2}}{\sqrt{9.81} \times (2.0)^{5/2}} = 0.51843$$

## 56 Flow in Open Channels

Using Table 2A.2 the corresponding value of

$$\zeta_c = \frac{my_c}{B} = 0.536$$

$$y_c = 0.715 \text{ m}$$

$$A_c = (2.0 + 1.5 \times 0.715) \times 0.715 = 2.197 \text{ m}^2$$

$$V_c = 5.0 / 2.197 = 2.276 \text{ m/s}$$

$$V_c^2 / 2g = 0.265 \text{ m}$$

$$E_c = y_c + \frac{V_c^2}{2g} = 0.715 + 0.264 = 0.979 \text{ m}$$

(d) *Circular Channel*

$$Z_c = \frac{Q}{\sqrt{g}} = \frac{5.0}{\sqrt{9.81}} = 1.5964$$

$$\frac{Z_c}{D^{2.5}} = \frac{1.5964}{(2.0)^{2.5}} = 0.2822$$

From Table 2A.1 showing the relationship of  $\frac{Z}{D^{2.5}}$  with  $y/D$ , the value of  $y_c/D$  corresponding to  $\frac{Z_c}{D^{2.5}} = 0.2822$  is found by suitable linear interpolation as  $y_c/D = 0.537$  and hence  $y_c = 1.074 \text{ m}$ .

*Determination of  $y_c$  by empirical equations*

1. By Swamee's equation

$$F_D = \frac{Q}{D^2 \sqrt{gD}} = \frac{5.0}{(2.0)^2 \sqrt{9.81 \times 2.0}} = 0.2822$$

$$\frac{y_c}{D} = [0.77 F_D^{-6} + 1.0]^{-0.085}$$

$$\frac{y_c}{2.0} = [0.77 (0.2822)^{-6} + 1.0]^{-0.085} = 0.5363$$

$$y_c = 1.072 \text{ m}$$

2. By Straub's equation

$$y_c = \frac{1.01}{D^{0.265}} \left( \frac{Q}{\sqrt{g}} \right)^{0.506}$$

$$y_c = \frac{1.01}{(2.0)^{0.265}} \left( \frac{5.0}{\sqrt{9.81}} \right)^{0.506} = 1.065 \text{ m}$$

**Example 2.6** A trapezoidal channel with a bed width of 4.0 m and side slopes of 1.5 H: 1 V carries a certain discharge. (a) Based on observations, if the critical depth of the flow is estimated as 1.70 m, calculate the discharge in the channel. (b) If this discharge is observed to be flowing at a depth of 2.50 m in a reach, estimate the Froude number of the flow in that reach.

**Solution** (a) At critical depth, area  $A_c = (B + m y_c) y_c$   
 $= [4.0 + (1.5 \times 1.70)] \times 1.70 = 11.135 \text{ m}^2$   
 Top width  $T_c = (B + 2 m y_c)$   
 $= [4.0 + (2 \times 1.5 \times 1.70)] = 9.10 \text{ m}$

At critical flow, by Eq. 2.4a  $\frac{Q^2}{g} = \frac{A_c^3}{T_c} = \frac{(11.135)^3}{9.10} = 151.715$

Discharge  $Q = 38.579 \text{ m}^3/\text{s}$

(b) When the depth of flow  $y = 2.50 \text{ m}$

Area  $A = (B + m y) y = [4.0 + (1.5 \times 2.50)] \times 2.50 = 19.375 \text{ m}^2$

Top width  $T = (B + 2 m y) = [4.0 + (2 \times 1.5 \times 2.50)] = 11.5 \text{ m}$

$A/T = 19.375/11.50 = 1.685 \text{ m}$

$V = \frac{Q}{A} = \frac{38.579}{19.375} = 1.991 \text{ m/s}$

Froude number  $F = \frac{V}{\sqrt{g(\frac{A}{T})}} = \frac{1.991}{\sqrt{9.81 \times 1.685}} = 0.490$

**Example 2.7** Calculate the bottom width of a channel required to carry a discharge of  $15.0 \text{ m}^3/\text{s}$  as a critical flow at a depth of 1.2 m, if the channel section is (a) rectangular, and (b) trapezoidal with side slope 1.5 horizontal: 1 vertical.

**Solution** (a) *Rectangular Section*  
 The solution here is straightforward.

$$y_c = \left( \frac{q^2}{g} \right)^{1/3} \quad \text{i.e.} \quad q = \sqrt{g y_c^3}$$

$$q = \sqrt{9.81(1.2)^3} = 4.117 \text{ m}^3/\text{s/m}$$

$$B = \text{bottom width} = \frac{15.0}{4.117} = 3.643 \text{ m}$$

(b) *Trapezoidal Channel*

The solution in this case is by trial-and-error.

$$A_c = (B + 1.5 \times 1.2) \times 1.2 = (B + 1.8) \times 1.2$$

$$T_c = (B + 2 \times 1.5 \times 1.2) = (B + 3.6)$$

$$\frac{Q^2}{g} = \frac{A_c^3}{T_c}$$

$$\frac{(B + 1.8)^3 \times (1.2)^3}{(B + 3.6)} = \frac{(15)^2}{9.81}$$

$$\frac{(B + 1.8)^3}{(B + 3.6)} = 13.273$$

By trial-and-error  $B = 2.535 \text{ m}$

**Example 2.8** Find the critical depth for a specific energy head of 1.5 m in the following channels:

- (a) Rectangular channel,  $B = 2.0 \text{ m}$
- (b) Triangular channel,  $m = 1.5$
- (c) Trapezoidal channel,  $B = 2.0 \text{ m}$  and  $m = 1.0$
- (d) Circular channel,  $D = 1.50 \text{ m}$

*Solution* (a) *Rectangular Channel*

By Eq. 2.10  $E_c = \frac{3}{2} y_c = 1.50 \text{ m}$

$$y_c = \frac{1.50 \times 2}{3} = 1.00 \text{ m}$$

(b) *Triangular Channel*

By Eq. 2.15  $E_c = 1.25 y_c = 1.50 \text{ m}$

$$y_c = \frac{1.50}{1.25} = 1.20 \text{ m}$$

(c) *Trapezoidal Channel*

$$E_c = y_c + \frac{V_c^2}{2g} = y_c + \frac{Q^2}{2gA_c^2}$$

Since by Eq. 2.4a 
$$\frac{Q^2}{g} = A_c^3 / T_c, E_c = y_c + \frac{A_c}{2T_c}$$

$$1.5 = y_c + \frac{(2.0 + y_c)y_c}{2(2.0 + 2y_c)}$$

Solving by trial-and-error,  $y_c = 1.095$  m.

(d) *Circular Channel*

$$E_c = y_c + \frac{A_c}{2T_c}$$

By non-dimensionalising with respect to the diameter  $D$ .

$$\frac{y_c}{D} + \frac{(A_c/D^2)}{2(T_c/D)} = \frac{E_c}{D} = \frac{1.5}{1.5} = 1.0$$

From Table 2A.1, values of  $(A_c / D^2)$  and  $(T_c / D)$  for a chosen  $(y_c / D)$  are read and a trial-and-error procedure is adopted to solve for  $y_c / D$ . It is found that  $\frac{y_c}{D} = 0.69$  and  $y_c = 0.69 \times 1.50 = 1.035$  m

**Example 2.9** | Water is flowing a critical depth at a section in a  $\Delta$  shaped channel, with side slope of 0.5 H: 1 V. (Fig. 2.8). If the critical depth is 1.6 m, estimate the discharge in the channel and the specific energy at the critical depth section.

*Solution* (i) Here  $m = -0.5$

$$T_c = 3.0 - (2 \times 0.5 \times 1.6) = 1.40 \text{ m}$$

$$A_c = \frac{(3.0 + 1.4)}{2} \times 1.60 = 3.52 \text{ m}^2$$

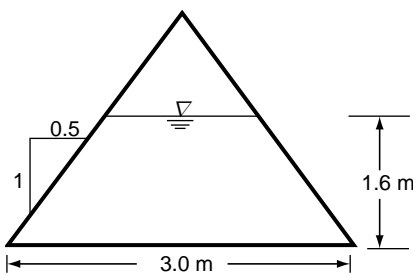


Fig. 2.8 Example 2.9

$$\frac{Q^2}{g} = \frac{A_c^3}{T_c} = \frac{(3.52)^3}{1.40} = 31.153$$

Discharge  $Q = 17.48 \text{ m}^3/\text{s}$

(ii)  $V_c = \frac{Q}{A_c} = \frac{17.48}{3.52} = 4.966 \text{ m/s}$

$$\frac{V_c^2}{2g} = \frac{(4.966)^2}{2 \times 9.81} = 1.257 \text{ m}$$

$$E_c = y_c + \frac{V_c^2}{2g} = 1.60 + 1.257 = 2.857 \text{ m}$$

## 2.7 TRANSITIONS

The concepts of specific energy and critical depth are extremely useful in the analysis of problems connected with transitions. To illustrate the various aspects, a few simple transitions in rectangular channels are presented here. The principles are nevertheless equally applicable to channels of any shape and other types of transitions.

### 2.7.1 Channel with a Hump

**(a) Subcritical Flow** Consider a horizontal, frictionless rectangular channel of width  $B$  carrying  $Q$  at a depth  $y_1$ .

Let the flow be subcritical. At Section 2 (Fig. 2.9), a smooth hump of height  $\Delta Z$  is built on the floor, since there are no energy losses between Sections 1 and 2, and construction of a hump causes the specific energy at Section 2 to decrease by  $\Delta Z$ . Thus the specific energies at Sections 1 and 2 are given by

$$E_1 = y_1 + \frac{V_1^2}{2g}$$

and

$$E_2 = E_1 - \Delta Z \tag{2.29}$$

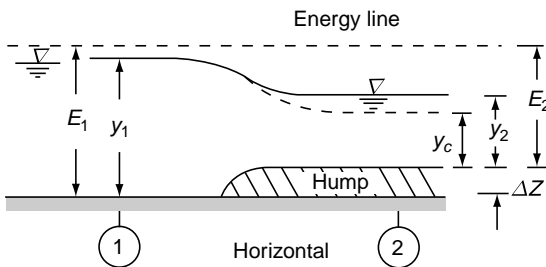


Fig. 2.9 Channel transition with a hump

Since the flow is subcritical, the water surface will drop due to a decrease in the specific energy. In Fig. 2.10, the water surface which was at  $P$  at Section 1 will come down to point  $R$  at Section 2. the depth  $y_2$  will be given by

$$E_2 = y_2 + \frac{V_2^2}{2g} = y_2 + \frac{Q^2}{2g B^2 y_2^2} \tag{2.30}$$

It is easy to see from Fig. 2.10 that as the value of  $\Delta Z$  is increased, the depth at Section 2, i.e.  $y_2$ , will decrease. The minimum depth is reached when the point  $R$  coincides with  $C$ , the critical depth point. At this point the hump height will be maximum, say =  $\Delta Z_m$ ,  $y_2 = y_c =$  critical depth and  $E_2 = E_c$ . Then condition at  $\Delta Z_m$  is given by the relation

$$E_1 - \Delta Z_m = E_2 = E_c = y_c + \frac{Q^2}{2g B^2 y_c^2} \tag{2.31}$$

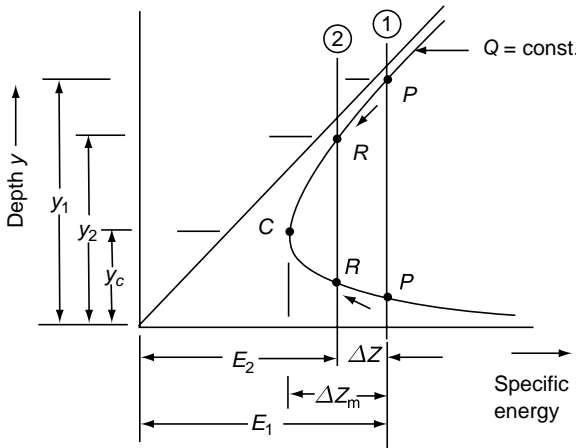


Fig. 2.10 Specific-energy diagram for Fig. 2.9

The question naturally arises as to what happens when  $\Delta Z > \Delta Z_m$ . From Fig. 2.10 it is seen that the flow is not possible with the given conditions, viz. with the given specific energy. The upstream depth has to increase to cause an increase in the specific energy at Section 1. If this modified depth is represented by  $y'_1$ , then

$$E'_1 = y'_1 + \frac{Q^2}{2gB^2 y_1'^2} \quad \{ \text{with } E'_1 > E_1 \text{ and } y'_1 > y_1 \} \quad (2.32)$$

At Section 2 the flow will continue at the minimum specific energy level, i.e., at the critical condition. At this condition,  $y_2 = y_c$  and

$$E'_1 - \Delta Z = E_2 = E_c = y_c + \frac{Q^2}{2gB^2 y_c^2} \quad (2.33)$$

Recollecting the various sequences, when  $0 < \Delta Z < \Delta Z_m$  the upstream water level remains stationary at  $y_1$  while the depth of flow at Section 2 decreases with  $\Delta Z$  reaching a minimum value of  $y_c$  at  $\Delta Z = \Delta Z_m$  (Fig. 2.11). With further increase in the value of  $\Delta Z$ , i.e. for  $\Delta Z > \Delta Z_m$ ,  $y_1$  will change to  $y'_1$  while  $y_2$  will continue to remain at  $y_c$ .

The variation of  $y_1$  and  $y_2$  with  $\Delta Z$  in the subcritical regime can be clearly noticed in Fig. 2.11.

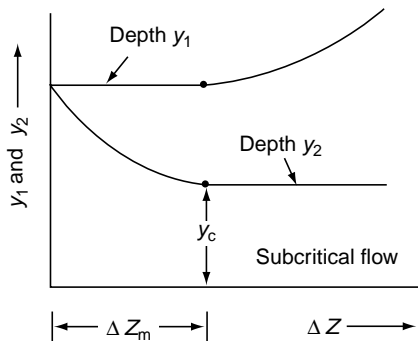


Fig. 2.11 Variation of  $y_1$  and  $y_2$  in subcritical flow over a hump

### Minimum Size of Hump for Critical Flow

(i) *Frictionless situation* Consider a smooth, frictionless, streamlined hump of height  $\Delta Z$  placed at a section in a rectangular channel carrying subcritical flow. The relationship between the specific energies at a section upstream of the hump ( $E_1$ ) and at section on the hump ( $E_2$ ) is given as

$$E_1 = E_2 + \Delta Z \quad (2.34)$$



Let  $\Delta Z_m$  be the height of the hump that would cause critical flow to occur over the hump (i.e., at Section 2) without changing the upstream specific energy. Any value of  $\Delta Z > \Delta Z_m$  would cause critical flow over the hump but the upstream specific energy would change to a value greater than  $E_1$ . Thus  $\Delta Z_m$  could also be called as the minimum height of a streamlined, frictionless hump that has to be provided to cause critical flow over the hump. An expression for the value of  $\Delta Z_m$  is obtained as below:

Since at  $\Delta Z = \Delta Z_m, E_2 = E_c = \frac{3}{2} y_c$  and Eq. 2.28 would now read as

$$E_1 = E_c + \Delta Z_m$$

$$\Delta Z_m = E_1 - \frac{3}{2} y_c$$

$$\frac{\Delta Z_m}{y_1} = \frac{E_1}{y_1} - \frac{3}{2} \frac{y_c}{y_1} = \left( 1 + \frac{F_1^2}{2} - \frac{3}{2} \left( \frac{q^2}{g} \right)^{1/3} \frac{1}{y_1} \right)$$

$$\frac{\Delta Z_m}{y_1} = \left( 1 + \frac{F_1^2}{2} - \frac{3}{2} F_1^{2/3} \right) \tag{2.35}$$

(ii) When there is energy loss due to the hump Let  $h_L$  = energy loss in the transition due to the hump. The energy Eq. 2.34 will now be written as

$$E_1 = E_2 + \Delta Z + h_L \tag{2.36}$$

Following the same procedure as in the frictionless case and noting that  $E_2 = E_c$ , Eq. 2.35 will be modified as

$$\left( \frac{\Delta Z_m}{y_1} + \frac{h_L}{y_1} \right) = \left( 1 + \frac{F_1^2}{2} - \frac{3}{2} F_1^{2/3} \right) \tag{2.37}$$

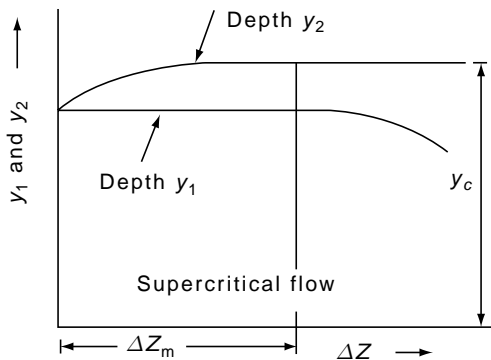


Fig. 2.12 Variation of  $y_1$  and  $y_2$  in supercritical flow over a hump

Comparing Eq. 2.37 with Eq. 2.35, it may be noted that the effect of energy loss in the transition due to shape and friction is equivalent to that of a hump placed in the downstream section.

**(b) Supercritical Flow** If  $y_1$  is in the supercritical flow regime, Fig. 2.12 shows that the depth of flow increases due to the reduction of specific energy. In Fig. 2.10 point  $P'$  corresponds to  $y_1$  and

point  $R'$  to depth at the Section 2. Up to the critical depth,  $y_2$  increases to reach  $y_c$  at  $\Delta Z = \Delta Z_m$ . For  $\Delta Z > \Delta Z_m$ , the depth over the hump  $y_2 = y_c$  will remain constant and the upstream depth  $y_1$  will change. It will decrease to have a higher specific energy  $E_1'$ . The variation of the depths  $y_1$  and  $y_2$  with  $\Delta Z$  in the supercritical flow is shown in Fig. 2.12.

**Example 2.10** | A rectangular channel has a width of 2.0 m and carries a discharge of 4.80 m<sup>3</sup>/s with a depth of 1.60 m. at a certain section a small, smooth hump with a flat top and of height 0.10 m is proposed to be built. Calculate the likely change in the water surface. Neglect the energy loss.

**Solution** Let the suffixes 1 and 2 refer to the upstream and downstream sections respectively as in Fig. 2.9.

$$q = \frac{4.80}{2.0} = 2.40 \text{ m}^3/\text{s}/\text{m}$$

$$V_1 = \frac{2.40}{1.6} = 1.50 \text{ m/s}, \quad \frac{V_1^2}{2g} = 0.115 \text{ m}$$

$F_1 = V_1 / \sqrt{g y_1} = 0.379$ , hence the upstream flow is subcritical and the hump will cause a drop in the watersurface elevation.

$$E_1 = 1.60 + 0.115 = 1.715 \text{ m}$$

At Section 2,

$$E_2 = E_1 - \Delta Z = 1.715 - 0.10 = 1.615 \text{ m}$$

$$y_c = \left( \frac{(2.4)^2}{9.81} \right)^{1/3} = 0.837 \text{ m}$$

$$E_c = 1.5 y_c = 1.256 \text{ m}$$

The minimum specific energy at Section 2,  $E_{c2}$  is less than  $E_2$ , the available specific energy at that section. Hence  $y_2 > y_c$  and the upstream depth  $y_1$  will remain unchanged. The depth  $y_2$  is calculated by solving the specific energy relation

$$y_2 + \frac{V_2^2}{2g} = E_2$$

i.e. 
$$y_2 + \frac{(2.4)^2}{2 \times 9.81 \times y_2^2} = 1.615$$

Solving by trial-and-error,  $y_2 = 1.481 \text{ m}$ .

**Example 2.11** (a) In example 2.10, if the height of the hump is 0.5 m, estimate the water surface elevation on the hump and at a section upstream of the hump. (b) Estimate the minimum size of the hump to cause critical flow over the hump.

**Solution** (a) From Example 2.10:  $F_1 = 0.379$ ,  $E_1 = 1.715$  m and  $y_c = y_{c2} = 0.837$  m.

Available specific energy at Section 2 =  $E_2 = E_1 - \Delta Z$

$$E_2 = 1.715 - 0.500 = 1.215 \text{ m}$$

$$E_2 = 1.5 y_{c2} = 1.256 \text{ m.}$$

The minimum specific energy at the Section 2 is greater than  $E_2$ , the available specific energy at that section. Hence, the depth at Section 2 will be at the critical depth. Thus  $y_2 = y_{c2} = 1.256$  m. The upstream depth  $y_1$  will increase to a depth  $y'_1$ , such that the new specific energy at the upstream Section 1 is

$$E'_1 = E_{c2} + \Delta Z$$

Thus 
$$E'_1 = y'_1 + \frac{V_1'^2}{2g} = E_{c2} + \Delta Z$$

$$y'_1 + \frac{q^2}{2g y_1'^2} = 1.256 + 0.500 = 1.756$$

$$y'_1 + \frac{(2.4)^2}{2 \times 981 \times y_1'^2} = 1.756$$

$$y'_1 + \frac{0.2936}{y_1'^2} = 1.756$$

Solving by trial-and-error and selecting the positive root which gives  $y'_1 > y_2$ ,  $y'_1 = 1.648$  m

The nature of the water surface is shown in Fig. 2.13.

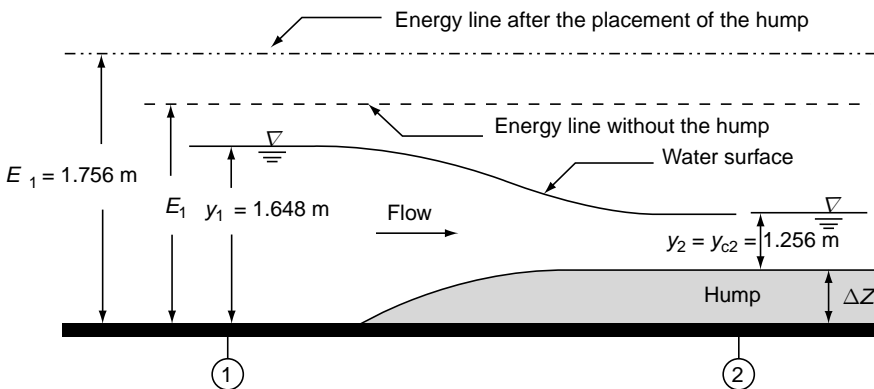


Fig. 2.13 Example 2.11

(b) Here,  $F_1 = 0.379$  and  $y_1 = 1.6$  m. By use of Eq. 2.35

$$\frac{\Delta Z_m}{y_1} = \left( 1 + \frac{F_1^2}{2} - \frac{3}{2} F_1^{2/3} \right)$$

$$\frac{\Delta Z_m}{1.6} = \left( 1 + \frac{(0.379)^2}{2} - \frac{3}{2} (0.379)^{2/3} \right) = 0.2866$$

$$\Delta Z_m = 0.459 \text{ m}$$

**Alternatively,**  $\Delta Z_m = E_1 - E_c = 1.715 - 1.256 = 0.459$  m

**Example 2.12** | A 2.5-m wide rectangular channel carries 6.0 m<sup>3</sup>/s of flow at a depth of 0.50 m. Calculate the minimum height of a streamlined, flat-topped hump required to be placed at a section to cause critical flow over the hump. The energy loss over the hump can be taken as 10% of the upstream velocity head.

**Solution** Discharge intensity  $q = 6.0/2.5 = 2.40$  m<sup>3</sup>/s/m

$$V_1 = 2.4/0.5 = 4.8 \text{ m/s}, \quad \frac{V_1^2}{2g} = 1.174 \text{ m}$$

$$\text{Energy loss, } h_L = 0.1 \times \frac{V_1^2}{2g} = 0.1174$$

$$\text{Froude number, } F_1 = \frac{V_1}{\sqrt{g y_1}} = \frac{4.8}{\sqrt{9.81 \times 0.5}} = 2.167$$

$$\text{By Eq. (2.37) } \left( \frac{\Delta Z_m}{y_1} + \frac{h_L}{y_1} \right) = \left( 1 + \frac{F_1^2}{2} - \frac{3}{2} F_1^{2/3} \right)$$

$$\left( \frac{\Delta Z_m}{0.5} + 0.1174 \right) = \left( 1 + \frac{(2.167)^2}{2} - \frac{3}{2} (2.167)^{2/3} \right)$$

$$\frac{\Delta Z_m}{0.5} = 0.6017 \text{ and } \Delta Z_m = 0.301 \text{ m}$$

**Alternatively,**  $\Delta Z_m = E_1 - E_c - h_L$

$$E_c = 1.5 y_c = 1.5 \times \left( \frac{q^2}{g} \right)^{1/3}$$

$$= 1.5 \times \left( \frac{(2.4)^2}{9.81} \right)^{1/3} = 1.256 \text{ m}$$

$$h_L = 0.1174 \text{ m and } E_1 = y_1 + \frac{V_1^2}{2g} = 0.5 + 1.174 = 1.674 \text{ m}$$

$$\Delta Z_m = 1.674 - 1.256 - 0.1174 = 0.301 \text{ m}$$

### 2.7.2 Transition with a Change in Width

**(a) Subcritical flow in a Width Constriction** Consider a frictionless horizontal channel of width  $B_1$  carrying a discharge  $Q$  at a depth  $y_1$  as in Fig. 2.14. At the Section 2 the channel width has been constricted to  $B_2$  by a smooth transition. Since there are no losses involved and since the bed elevations at Sections 1 and 2 are the same, the specific energy at Section 1 is equal to the specific energy at the Section 2.

$$E_1 = y_1 + \frac{V_1^2}{2g} = y_1 + \frac{Q^2}{2gB_1^2 y_1^2}$$

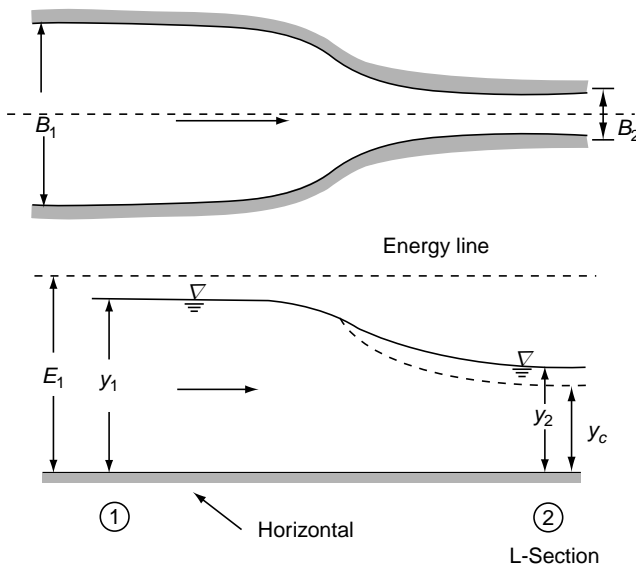


Fig. 2.14 Transition with width constriction

and

$$E_2 = y_2 + \frac{V_2^2}{2g} = y_2 + \frac{Q^2}{2gB_2^2 y_2^2}$$

It is convenient to analyse the flow in terms of the discharge intensity  $q = Q/B$ . At Section 1,  $q_1 = Q/B_1$  and at Section 2,  $q_2 = Q/B_2$ . Since  $B_2 < B_1$ ,  $q_2 > q_1$ . In the specific energy diagram (Fig. 2.15) drawn with the discharge intensity as the third parameter, point  $P$  on the curve  $q_1$  corresponds to depth  $y_1$  and specific energy  $E_1$ , since at Section 2,  $E_2 = E_1$  and  $q = q_2$ , the point  $P$  will move vertically downward to point  $R$  on the curve  $q_2$  to reach the depth  $y_2$ . Thus, in subcritical flow the depth

$y_2 < y_1$ . If  $B_2$  is made smaller, then  $q_2$  will increase and  $y_2$  will decrease. The limit of the contracted width  $B_2 = B_{2m}$  is obviously reached when corresponding to  $E_1$ , the discharge intensity  $q_2 = q_m$ , i.e., the maximum discharge intensity for a given specific energy (critical-flow condition) will prevail. At this minimum width,  $y_2 =$  critical depth at Section 2,  $y_{cm}$  and

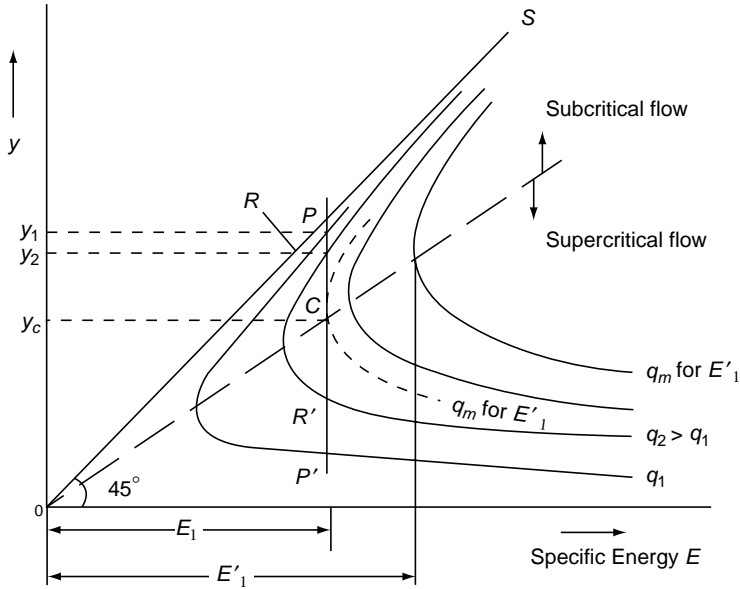


Fig. 2.15 Specific energy diagram for transition of Fig. 2.14

$$E_1 = E_{cm} = y_{cm} + \frac{Q^2}{2g(B_{2m})^2 y_{cm}^2} \quad (2.38)$$

For a rectangular channel, at critical flow  $y_c = \frac{2}{3} E_c$

Since  $E_1 = E_{cm}$

$$y_2 = y_{cm} = \frac{2}{3} E_{cm} = \frac{2}{3} E_1 \quad (2.39)$$

and  $y_c = \left( \frac{Q^2}{B_{2m}^2 g} \right)^{1/3}$  or  $B_{2m} = \sqrt{\frac{Q^2}{g y_{cm}^3}}$

i.e.  $B_{2m} = \sqrt{\frac{27Q^2}{8gE_1^3}} \quad (2.40)$

If  $B_2 < B_{2m}$ , the discharge intensity  $q_2$  will be larger than  $q_m$  the maximum discharge intensity consistent with  $E_1$ . The flow will not, therefore, be possible with the

given upstream conditions. The upstream depth will have to increase to  $y_1$  so that a new specific energy  $E'_1 = y'_1 + \frac{Q^2}{2g(B_1^2 y_1'^2)}$  is formed which will just be sufficient to cause critical flow at Section 2. It may be noted that the new critical depth at Section 2 for a rectangular channel is

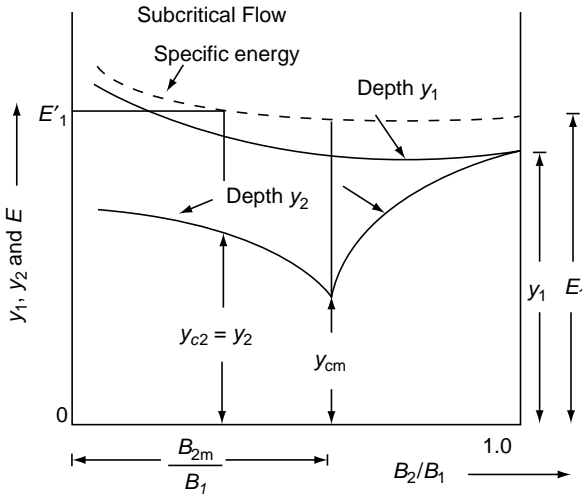


Fig. 2.16 Variation of  $y_1$  and  $y_2$  in subcritical flow in a width constriction

$$y_{c2} = \left[ \frac{Q^2}{B_2^2 g} \right]^{1/3} = (q_2^2 / g)^{1/3}$$

and 
$$E_{c2} = y_{c2} + \frac{V_{c2}^2}{2g} = 1.5 y_{c2}$$

Since  $B_2 < B_{2m}$ ,  $y_{c2}$  will be larger than  $y_{cm}$ . Further,  $E'_1 = E_{c2} = 1.5 y_{c2}$ . Thus even though critical flow prevails for all  $B_2 < B_{2m}$ , the depth at Section 2 is not constant as in the hump case but increases as  $y'_1$  and hence  $E'_1$  rises. The variation of  $y_1$ ,  $y_2$  and  $E$  with  $B_2 / B_1$  is shown schematically in Fig. 2.16.

**(b) Supercritical Flow in a Width Constriction** If the upstream depth  $y_1$  is in the supercritical flow regime, a reduction of the flow width and hence an increase in the discharge intensity causes a rise in depth  $y_2$ . In Fig. 2.15, point  $P'$  corresponds to  $y_1$  and point  $R'$  to  $y_2$ . As the width  $B_2$  is decreased,  $R'$  moves up till it becomes critical at  $B_2 = B_{2m}$ . Any further reduction in  $B_2$  causes the upstream depth to decrease to  $y'_1$  so that  $E_1$  rises to  $E'_1$ . At Section 2, critical depth  $y'_c$  corresponding to the new specific energy  $E'_1$  will prevail. The variation of  $y_1$ ,  $y_2$  and  $E$  with  $B_2 / B_1$  in supercritical flow regime is indicated in Fig. 2.17.

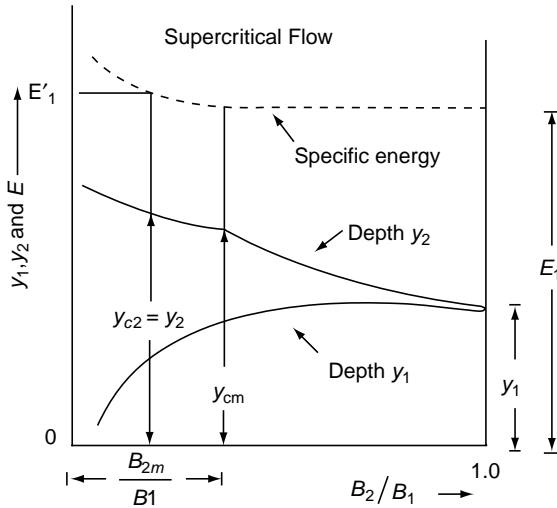


Fig. 2.17 Variation of  $y_1$  and  $y_2$  in supercritical flow in a width constriction

**Choking** In the case of channel with a hump, and also in the case of a width constriction, it is observed that the upstream water-surface elevation is not affected by the conditions at Section 2 till a critical stage is first achieved. Thus in the case of a hump for all  $\Delta Z > \Delta Z_m$ , the upstream water depth is constant and for all  $\Delta Z > \Delta Z_m$  the upstream depth is different from  $y_1$ . Similarly, in the case of the width constriction, for  $B_2 \geq B_{2m}$ , the upstream depth  $y_1$  is constant; while for all  $B_2 < B_{2m}$ , the upstream depth undergoes a change. This onset of critical condition at Section 2 is a prerequisite to choking. Thus all cases with  $\Delta Z > \Delta Z_m$  or  $B_2 < B_{2m}$  are known as *choked conditions*. Obviously, choked conditions are undesirable and need to be watched in the design of culverts and other surface-drainage features involving channel transitions.

**Example 2.13**

A rectangular channel is 3.5 m wide and conveys a discharge of 15.0 m<sup>3</sup>/s at a depth of 2.0 m. It is proposed to reduce the width of the channel at a hydraulic structure. Assuming the transition to be horizontal and the flow to be frictionless determine the water surface elevations upstream and downstream of the constriction when the constricted width is (a) 2.50 m, and (b) 2.20 m.

**Solution** Let suffixes 1 and 2 denote sections upstream and downstream of the transition respectively. Discharge  $Q = B_1 y_1 V_1$

$$V_1 = \frac{15.0}{3.5 \times 2.0} = 2.143 \text{ m/s}$$

$$F_1 = \text{Froude number} = \frac{V_1}{\sqrt{g y_1}} = \frac{2.143}{\sqrt{9.81 \times 2.0}} = 0.484$$

The upstream flow is subcritical and the transition will cause a drop in the water surface.

$$E_1 = y_1 + \frac{V_1^2}{2g} = 2.0 + \frac{(2.143)^2}{2 \times 9.81} = 2.234 \text{ m}$$



70 Flow in Open Channels

Let  $B_{2m}$  = minimum width at Section 2 which does not cause choking.

Then 
$$E_{cm} = E_1 = 2.234 \text{ m}$$

$$y_{cm} = \frac{2}{3} E_{cm} = \frac{2}{3} \times 2.234 = 1.489 \text{ m}$$

Since 
$$y_{cm}^3 = \left[ \frac{Q^2}{g B_{2m}^2} \right]$$

$$B_{2m} = \left[ \frac{Q^2}{g y_{c2}^3} \right]^{1/2} = \left[ \frac{(15.0)^2}{9.81 \times (1.489)^3} \right]^{1/2} = 2.636 \text{ m}$$

(a) When  $B_1 = 2.50 \text{ m}$

$B_2 < B_{2m}$  and hence choking conditions prevail. The depth at the Section 2 =  $y_2 = y_{c2}$ . The upstream depth  $y_1$  will increase to  $y'$ .

Actually 
$$q_2 = \frac{15.0}{2.0} = 6.0 \text{ m}^3/\text{s}/\text{m}$$

$$y_{c2} = \left[ \frac{q_2^2}{g} \right]^{1/3} = \left[ \frac{(6.0)^2}{9.81} \right]^{1/3} = 1.542 \text{ m}$$

$$E_{c2} = 1.5 y_{c2} = 1.5 \times 1.542 = 2.3136 \text{ m}$$

At the upstream Section 1:

$$E'_1 = E_{c2} = 2.3136 \text{ with new upstream depth of } y_1 \text{ such that } q_1 = y_1 V_1 = 15/3.5 = 4.2857 \text{ m}^3/\text{s}/\text{m}.$$

Hence 
$$y'_1 = \frac{V_1'^2}{2g} = 2.3136$$

$$y'_1 + \frac{(4.2857)^2}{2 \times 9.81 \times y_1'^2} = 2.3136$$

$$y'_1 + \frac{0.9362}{y_1'^2} = 2.3136$$

Solving by the trial and error and selecting a root that gives subcritical flow,

$$y'_1 = 2.102 \text{ m}$$

(b) When  $B_2 = 2.20 \text{ m}$

As  $B_2 < B_{2m}$  choking conditions prevail.

Depth at Section 2 =  $y_2 = y_{c2}$

$$q_2 = \frac{15.0}{2.20} = 6.8182 \text{ m}^2/\text{s}/\text{m}$$

$$y_{c2} = \left[ \frac{(6.8182)^2}{9.81} \right]^{1/3} = 1.6797 \text{ m}$$

$$E_{c2} = 1.5y_{c2} = 2.5195 \text{ m}$$

At upstream Section 1: New upstream depth =  $y'_1$  and

$$E'_1 = E_{c2} = 2.5195 \text{ m}$$

$$q_1 = V'_1 y'_1 = 15/3.5 = 4.2857 \text{ m}^3/\text{s}/\text{m}$$

Hence 
$$y'_1 = \frac{V_1'^2}{2g y'_1} = 2.5195$$

$$y'_1 + \frac{(4.2857)^2}{2 \times 9.81 \times y_1'^2} = 2.5195$$

$$y'_1 + \frac{0.9362}{y_1'^2} = 2.5195$$

Solving by trial and error, the appropriate depth to give subcritical flow is

$$y'_1 = 2.350 \text{ m}$$

[Note that for the same discharge when  $B_2 < B_{2m}$  (i.e., under choking conditions) the depth at the critical section will be different from  $y_{cm}$  and depends on the value of  $B_2$ ].

### 2.7.3 General Transition

A transition in its general form may have a change of channel shape, provision of a hump or a depression and contraction or expansion of channel width, in any combination. In addition, there may be various degrees of loss of energy at various components. However, the basic dependence of the depths of flow on the channel geometry and specific energy of flow will remain the same. Many complicated transition situations can be analysed by using the principles of specific energy and critical depth.

In subcritical flow transitions the emphasis is essentially to provide smooth and gradual changes in the boundary to prevent flow separation and consequent energy losses. Details about subcritical flow transitions are available in Ref. 1, 2 and 3. The transitions in supercritical flow, however, are different and involve suppression of shock waves related disturbances and are explained in Chapter 9.

**Example 2.14** | A discharge of  $16.0 \text{ m}^3/\text{s}$  flows with a depth of  $2.0 \text{ m}$  in a  $4.0 \text{ m}$  wide rectangular channel. At a downstream section the width is reduced to  $3.5 \text{ m}$  and the channel bed is raised by  $\Delta Z$ . Analyse the water-surface elevation in the transitions when (a)  $\Delta Z = 0.02 \text{ m}$ , and (b)  $\Delta Z = 0.35 \text{ m}$ .

## 72 Flow in Open Channels

**Solution** Let the suffixes 1 and 2 refer to the upstream and downstream sections respectively.

At the upstream section,  $V_1 = \frac{16}{4 \times 2} = 2.0$  m/s

$$F_1 = \text{Froude number} = \frac{V_1}{\sqrt{g y_1}} = \frac{2.0}{\sqrt{9.81 \times 2.0}} = 0.452$$

The upstream flow is subcritical and the transition will cause a drop in the water surface elevation.

$$V_1^2/2g = 0.204 \text{ m}$$

$$E_1 = 2.0 + 0.204 = 2.204 \text{ m}$$

$q_2$  = discharge intensity at the downstream section

$$= \frac{Q}{B_2} = \frac{16.0}{3.5} = 4.571 \text{ m}^3/\text{s}/\text{m}$$

$y_{c2}$  = critical depth corresponding to  $q_2$

$$= \left( \frac{q_2^2}{g} \right)^{1/3} = \left[ \frac{(4.571)^2}{9.81} \right]^{1/3} = 1.287 \text{ m}$$

$$E_{c2} = \frac{3}{2} y_{c2} = 1.930 \text{ m}$$

(a) When  $\Delta Z = 0.20$  m

$E_2$  = available specific energy at Section 2

$$= E_1 - \Delta Z = 2.204 - 0.20 = 2.004 \text{ m} > E_{c2}$$

Hence the depth  $y_2 > y_{c2}$  and the upstream depth will remain unchanged at  $y_1$ .

$$y_2 + \frac{V_2^2}{2g} + \Delta Z = E_1$$

$$y_2 + \frac{(4.571)^2}{2 \times 9.81 \times y_2^2} = 2.204 - 0.20$$

$$y_2 + \frac{1.065}{y_2^2} = 2.004$$

Solving by trial and error,  $y_2 = 1.575$  m.

Hence when  $\Delta Z = 0.20$  m,  $y_1 = 2.00$  m and  $y_2 = 1.575$  m

(b) When  $\Delta Z = 0.35$ ,

$E_2$  = available specific energy at Section 2

$$= 2.204 - 0.350 = 1.854 \text{ m} < E_{c2}$$

Hence the contraction will be working under choked conditions. The upstream depth must rise to create a higher total head. The depth of flow at Section 2 will be critical with  $y_2 = y_{c2} = 1.287$  m.

If the new upstream depth is  $y'_1$

$$y'_1 + \frac{Q^2}{2gB_1^2 y_1'^2} = E_{c2} + \Delta Z = 1.930 + 0.350$$

$$y'_1 + \frac{(16)^2}{2 \times 9.81 \times (4.0)^2 \times y_1'^2} = 2.28$$

i.e.  $y'_1 + \frac{0.8155}{y_1'^2} = 2.280$

By trial-and-error,  $y'_1 = 2.094$  m.

The upstream depth will therefore rise by 0.094 m due to the choked condition at the constriction. Hence, when  $\Delta Z = 0.35$  m

$$y_1 = 2.094 \text{ m and } y_2 = y_{c2} = 1.287 \text{ m.}$$



## REFERENCES

1. Vittal, N and Chiranjeevi, V V ‘Open Channel Transitions : Rational Methods of Design’, *J of Hyd. Engg.*, ASCE, Vol. 109, NO. 1, Jan. 1983, pp 99–115.
2. Vittal, N et. al., ‘Hydraulic Design of Flume Aqueducts’, *J. of Hyd. Engg.*, ASCE, Vol. 119, No. 2, Feb. 1993, pp 284–289.
3. Swamee, P K and Basak, B C ‘Comprehensive Open–Channel Expansion Transition Design’, *J. of Irr. & Dri. Engg.*, ASCE, Vol. 119, No. 1, Jan./Feb., 1993, pp 1–17.
4. Swamee, P K ‘Critical Depth Equations for Irrigation Canals’, *J. of Irr. & Dri. Engg.*, ASCE, Vol. 119, No. 2, March 1993, pp 400–409.
5. Straub, W Ö ‘A Quick and Easy Way to Calculate Critical and Conjugate Depths in Circular Channels’, *Civil Engineering*, Dec. 1978, 99.70–71.



## PROBLEMS

### Problem Distribution

Topics	Problems
<i>Specific energy and alternate depths</i>	2.1 – 2.7
<i>Minimum specific energy and critical depth</i>	2.8 – 2.16
<i>Computations involving critical depth</i>	2.17 – 2.27; 2.29
<i>First hydraulic exponent, M</i>	2.30 – 2.32
<i>Transitions</i>	
1. <i>with hump/ drop</i>	2.33 – 2.35
2. <i>with change in width</i>	2.36 – 2.38
3. <i>General</i>	2.39 – 2.44
<i>Miscellaneous concepts</i>	2.28

74 Flow in Open Channels

2.1 In a rectangular channel  $F_1$  and  $F_2$  are the Froude numbers corresponding to the alternate depths of a certain discharge. Show that

$$\left(\frac{F_2}{F_1}\right)^{2/3} = \frac{2 + F_2^2}{2 + F_1^2}$$

2.2 Show that in a triangular channel, the Froude number corresponding to alternate depths are given by

$$\frac{F_1}{F_2} = \frac{(4 + F_1^2)^{5/2}}{(4 + F_2^2)^{5/2}}$$

2.3 A 5.0 m wide rectangular channel carries 20 m<sup>3</sup>/s of discharge at a depth of 2.0 m. The width beyond a certain section is to be changed to 3.5 m. If it is desired to keep the water-surface elevation unaffected by this change, what modifications are needed to the bottom elevation?

2.4 Find the alternate depths corresponding to a specific head of 2.0 m and a discharge of 6.0 m<sup>3</sup>/s in (a) a trapezoidal channel,  $B = 0.9$  m,  $m = 1.0$ , (b) triangular channel,  $m = 1.5$ , (c) circular channel,  $D = 2.50$  m. (Use the trial and error method. For Part (c) use Table 2A.1)

2.5 If  $y_1$  and  $y_2$  are alternate depths in a rectangular channel show that

$$\frac{2y_1^2 y_2^2}{(y_1 + y_2)} = y_c^3$$

and hence the specific energy,  $E = \frac{y_1^2 + y_1 y_2 + y_2^2}{(y_1 + y_2)}$

2.6 If  $y_1$  and  $y_2$  are the alternate depths in a triangular channel show that

$$\frac{4y_1^4 y_2^4}{(y_1^2 + y_2^2)(y_1 + y_2)} = y_c^5$$

where  $y_c$  = critical depth. Show further that the specific energy  $E$  is given by

$$\frac{E}{y_1} = \frac{\eta^4 + \eta^3 + \eta^2 + \eta + 1}{(1 + \eta^2)(1 + \eta)}$$

where  $\eta = y_2/y_1$

2.7 A trapezoidal channel has a bottom width of 6.0 m and side slopes of 1: 1. The depth of flow is 1.5 m at a discharge of 15 m<sup>3</sup>/s. Determine the specific energy and alternate depth.

2.8 Show that for a trapezoidal channel the minimum specific energy  $E_c$  is related to the critical depth  $y_c$  as

$$E_c = \frac{y_c}{2} \left[ \frac{3 + 5\zeta_c}{1 + 2\zeta_c} \right] \quad \text{where } \zeta_c = \frac{m y_c}{B}$$

2.9 Prove that the alternate depths in an exponential channel ( $A = k_1 y^a$ ) are given by

$$\frac{2a y_1^{2a} y_2^{2a} (y_1 - y_2)}{(y_1^{2a} - y_2^{2a})} = y_c^{2a+1}$$

- 2.10 Show that in an exponential channel ( $A = k_1 y^a$ ) the minimum specific energy  $E_c$  and the critical depth  $y_c$  are related as

$$\frac{E_c}{y_c} = 1 + \frac{1}{2a}$$

- 2.11 A parabolic channel has its profile given by  $x^2 = 4ay$ . Obtain an expression for the relative specific energy at the critical flow,  $E_c / y_c$  for this channel.
- 2.12 Show that for a horizontal frictionless channel the minimum specific force for a specified discharge is obtained at the critical depth.
- 2.13 A channel in which the area is related to the depth as ( $A = k_1 y^a$ ) in which  $k_1$  and  $a$  are constants is called an exponential channel. Show that the critical depth for an exponential channel is given by

$$y_c = \left( \frac{Q^2}{g} \frac{a}{k_1^2} \right)^{1/(2a+1)}$$

- 2.14 An exponential channel ( $A = k_1 y^a$ ) carries a flow with a Froude number  $F_0$  at a depth of flow of  $y_0$ . Show that the critical depth  $y_c$  is given by

$$\frac{y_c}{y_0} = F_0^x \quad \text{where } x = 2/(2a+1)$$

- 2.15 If it is desired to have a channel in which the flow is critical at all stages, show that the cross section of such a channel is given by.

$$T^2 h^2 = \frac{Q^3}{8g}$$

in which  $T$  = top width and  $h$  = depth of the water surface below the energy line.

- 2.16 Show that in a parabolic channel ( $x = c\sqrt{y}$ ) the area can be expressed in terms of the top width  $T$  as

$$A = \frac{2}{3}Ty$$

Further, show that the critical depth in such a parabolic channel is given by

$$y_c = \left[ \frac{27}{8} \frac{Q^2}{gT_c^2} \right]^{1/3} = \left[ \frac{27}{32} \frac{Q^2}{gc^2} \right]^{1/4}$$

- 2.17 A channel has a cross section given by the relationship  $A = y^{2.5}$ . For a critical depth of 0.5 m in this channel, estimate the (i) discharge and (ii) specific energy.
- 2.18 A triangular channel has an apex angle of  $60^\circ$  and carries a flow with a velocity of 2.0 m/s and depth of 1.25 m. (a) Is the flow subcritical or super-critical? (b) What is the critical depth? (c) What is the specific energy? (d) What is the alternate depth possible for this specific energy?
- 2.19 Fill the missing data in the following table connected with critical depth computations in rectangular channels:

Case	$Q$ ( $m^3/s$ )	$B$ ( $m$ )	$y_c$ ( $m$ )	$E_c$ ( $m$ )
(a)	–	3.0	0.50	–
(b)	5.60	–	0.80	–
(c)	7.50	2.5	–	–
(d)	–	2.0	–	0.60

2.20 Fill in the missing data in the following table connected with critical depth computation in triangular channels:

Case	$Q$ ( $m^3/s$ )	Side Slope = $m$	$y_c$ ( $m$ )	$E_c$ ( $m$ )
(i)	1.50	1.25	–	–
(ii)	–	1.50	0.30	–
(iii)	–	1.00	–	0.60

2.21 Fill in the missing data in the following table relating critical depth in trapezoidal channels:

Case	$m$	$B$ ( $m$ )	$y_c$ ( $m$ )	$Q$ ( $m^3/s$ )	$E_c$ ( $m$ )
(a)	1.5	3.5	–	5.0	–
(b)	2.0	2.0	0.30	–	–
(c)	1.5	–	0.40	2.641	–
(d)	2.0	4.0	–	–	1.111

- 2.22 Calculate the discharges and specific energies corresponding to the following critical depths in circular channels: (a)  $y_c = 0.375$  m,  $D = 1.50$  m, and (b)  $y_c = 0.40$  m,  $D = 2.0$  m.
- 2.23 What is the critical depth corresponding to a discharge of  $5.0$   $m^3/s$  in (a) a trapezoidal channel of  $B = 0.80$  m and  $m = 1.5$ , and (b) a circular channel of  $D = 1.50$  m?
- 2.24 In a circular channel of diameter  $D = 1.50$  m, the critical depth  $y_c$  is known to occur at a specific energy of  $1.80$  m. Estimate the value of  $y_c$ .
- 2.25 A circular channel is to carry a discharge of  $558$  litres/s. Find the diameter of the conduit such that the flow is critical when the conduit is running quarter full.
- 2.26 A circular culvert of  $1.20$ -m diameter is flowing half full and the flow is in critical state. Estimate the discharge and the specific energy.
- 2.27 A brick-lined sewer has a semicircular bottom and vertical side walls  $0.60$  m apart. If the depth of flow at a section where the flow is known to be at a critical state is  $0.60$  m, estimate the discharge in the sewer.
- 2.28 A rectangular channel section is to have critical flow and at the same time the wetted perimeter is to be minimum. Show that for these two conditions to occur simultaneously, the width of the channel must be equal to  $8/9$  times the minimum specific-energy head.

- 2.29 Water flows in a  $\Delta$  shaped channel shown in Fig 2.18. Critical depth is known to occur at a section in this canal. Estimate the discharge and specific energy corresponding to an observed critical depth of 1.40 m.

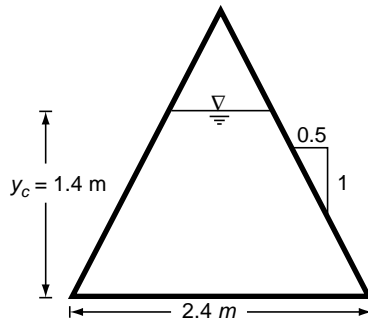


Fig. 2.18 Problem 2.29

- 2.30 For an exponential channel ( $A = k_1 y^n$ ) obtain explicit expressions for the (i) critical depth, (ii) Froude number, (iii) Hydraulic exponent  $M$ .
- 2.31 Derive the approximate expression for the first hydraulic exponent  $M$  given by Eq. (2.27) as

$$M = \frac{y}{A} \left( 3T - \frac{A}{T} \frac{dT}{dy} \right)$$

- 2.32 Estimate the value of the first hydraulic exponent  $M$  for the following cases:
- Trapezoidal channel with  $B = 4.0$  m,  $m = 2.0$  and  $y = 0.20$ ; 1.0; 2.0; and 4.0 m. [Hint: Use Eq. (2.27)].
  - Circular channel of diameter  $D = 2.0$  m with  $y = 0.20$ ; 0.8; and 1.6 m. [Hint: Use Eq. (2.27) and Table 2A.1]
- 2.33 A 5.0-m wide rectangular channel carries a discharge of  $6.40 \text{ m}^3/\text{s}$  at a depth of 0.8 m. At a section there is a smooth drop of 0.22 m in the bed. What is the water surface elevation downstream of the drop?
- 2.34 A rectangular channel is 4.0 m wide and carries a discharge of  $20 \text{ m}^3/\text{s}$  at a depth of 2.0 m. At a certain section it is proposed to build a hump. Calculate the water surface elevations at upstream of the hump and over the hump if the hump height is (a) 0.33 m and (b) 0.20 m. (Assume no loss of energy at the hump.)
- 2.35 A uniform flow of  $12.0 \text{ m}^3/\text{s}$  occurs in a long rectangular channel of 5.0 m width and depth of flow of 1.50 m. A flat hump is to be built at a certain section. Assuming a loss of head equal to the upstream velocity head, compute the minimum height of the hump to provide critical flow. What will happen (a) if the height of the hump is higher than the computed value and (b) if the energy loss is less than the assumed value?
- 2.36 A rectangular channel is 3.0 m wide and carries a flow of  $1.85 \text{ m}^3/\text{s}$  at a depth of 0.50 m. A contraction of the channel width is required at a certain section. Find the greatest allowable contraction in the width for the upstream flow to be possible as specified.
- 2.37 A rectangular channel is 2.5 m wide and conveys a discharge of  $2.75 \text{ m}^3/\text{s}$  at a depth of 0.90 m. A contraction of width is proposed at a section in this canal. Calculate the water surface elevations in the contracted section as well as in an upstream 2.5 m wide section when the width of the proposed contraction is (a) 2.0 m and (b) 1.5 m. (Neglect energy losses in the transition).



## 78 Flow in Open Channels

- 2.38 A 3.0-m wide horizontal rectangular channel is narrowed to a width of 1.5 m to cause critical flow in the contracted section. If the depth in the contracted section is 0.8 m, calculate the discharge in the channel and the possible depths of flow and corresponding Froude numbers in the 3.0 m wide section. Neglect energy losses in the transition.
- 2.39 A rectangular channel is 3.0 m wide and carries a discharge of  $15.0 \text{ m}^3/\text{s}$  at a depth of 2.0 m. At a certain section of the channel it is proposed to reduce the width to 2.0 m and to alter the bed elevation by  $\Delta Z$  to obtain critical flow at the contracted section without altering the upstream depth. What should be the value of  $\Delta Z$ ?
- 2.40 Water flows at a velocity of 1.0 m/s and a depth of 2.0 m in an open channel of rectangular cross section and bed-width of 3.0 m. At certain section the width is reduced to 1.80 m and the bed is raised by 0.65 m. Will the upstream depth be affected and if so, to what extent?
- 2.41 A 3-m wide rectangular channel carries  $3 \text{ m}^3/\text{s}$  of water at a depth of 1.0 m. If the width is to be reduced to 2.0 m and bed raised by 10 cm, what would be the depth of flow in the contracted section? Neglect the loss of energy in transition. What maximum rise in the bed level of the contracted section is possible without affecting the depth of flow upstream of the transition?
- 2.42 Water flows in a 3.0-m wide rectangular channel at a velocity of 2.5 m/s and a depth of 1.8 m. If at a section there is a smooth upward step of 0.30 m, what width is needed at that section to enable the critical flow to occur on the hump without any change in the upstream depth?
- 2.43 A 3.0-m wide rectangular channel carries a flow at 1.25 m depth. At a certain section the width is reduced to 2.5 m and the channel bed raised by 0.20 m through a streamlined hump. (a) Estimate the discharge in the channel when the water surface drops by 0.15 m over the hump. (b) What change in the bed elevation at the contracted section would make the water surface have the same elevation upstream and downstream of the contraction? (The energy losses in the contraction can be neglected).
- 2.44 A 1.5-m wide rectangular channel carries a discharge of  $5.0 \text{ m}^3/\text{s}$  at a depth of 1.5 m. At a section the channel undergoes transition to a triangular section of side slopes 2 horizontal: 1 vertical. If the flow in the triangular section is to be critical without changing the upstream water surface, find the location of the vertex of the triangular section relative to the bed of the rectangular channel. What is the drop/rise in the water surface at the transition? Assume zero energy loss at the transition.

## OBJECTIVE QUESTIONS

- 2.1 The term *alternate depths* is used in open channel flow to denote the depths
- having the same kinetic energy for a given discharge
  - having the same specific force for a given discharge
  - having the same specific energy for a given discharge
  - having the same total energy for a given discharge
- 2.2 The two alternate depths in a 4.0 m wide rectangular channel are 3.86 m and 1.0 m respectively. The discharge in the channel in  $\text{m}^3/\text{s}$  is
- 15
  - 1.5
  - 7.76
  - 31.0
- 2.3 In a rectangular channel, the alternate depths are 1.0 m and 2.0 m respectively. The specific energy head in m is
- 3.38
  - 1.33
  - 2.33
  - 3.0

- 2.4 A rectangular channel carries a certain flow for which the alternate depths are found to be 3.0 m and 1.0 m. The critical depth in m for this flow is  
 (a) 2.65 (b) 1.65 (c) 0.65 (d) 1.33
- 2.5 The critical flow condition in a channel is given by  
 (a)  $\frac{\alpha QT^2}{gA^3} = 1$  (b)  $\frac{\alpha Q^2 T^2}{gA^3} = 1$   
 (c)  $\frac{\alpha Q^2 T}{gA^3} = 1$  (d)  $\frac{\alpha QT}{gA^3} = 1$
- 2.6 In defining a Froude number applicable to open channels of any shape, the length parameter used is the  
 (a) ratio of area to top width (c) depth of flow  
 (b) ratio of area to wetted perimeter (d) square root of the area
- 2.7 For a triangular channel of side slopes  $m$  horizontal : 1 vertical, the Froude number is given by  $F =$   
 (a)  $\frac{m}{\sqrt{gy}}$  (b)  $\frac{V}{\sqrt{2gy}}$  (c)  $\frac{V\sqrt{2}}{gy}$  (d)  $\frac{V}{\sqrt{gy}}$
- 2.8 A triangular channel has a vertex angle of  $90^\circ$  and carries a discharge of  $1.90 \text{ m}^3/\text{s}$  at a depth of 0.8 m. The Froude number of the flow is  
 (a) 0.68 (b) 1.06 (c) 0.75 (d) 1.50
- 2.9 A triangular channel of apex angle of  $120^\circ$  carries a discharge of  $1573 \text{ l/s}$ . The critical depth in m is  
 (a) 0.600 (b) 0.700 (c) 0.800 (d) 0.632
- 2.10 A triangular channel of apex angle of  $60^\circ$  has a critical depth of 0.25 m. The discharge in  $\text{l/s}$  is  
 (a) 60 (b) 640 (c) 160 (d) 40
- 2.11 At critical depth  
 (a) the discharge is minimum for a given specific energy  
 (b) the discharge is maximum for a given specific force  
 (c) the discharge is maximum for a given specific energy  
 (d) the discharge is minimum for a given specific force
- 2.12 For a given open channel carrying a certain discharge the critical depth depends on  
 (a) the geometry of the channel (c) the roughness of the channel  
 (b) the viscosity of water (d) the longitudinal slope of the channel
- 2.13 In a triangular channel the value of  $E_c / y_c$  is  
 (a) 1.25 (b) 2.5 (c) 3.33 (d) 1.5
- 2.14 In a parabolic channel ( $x^2 = 4ay$ ) the value of  $E_c / y_c$  is  
 (a) 1.5 (b) 2.0 (c) 3.33 (d) 1.25
- 2.15 In an exponential channel (Area  $A = k y^a$ ) the ratio of specific energy at critical depth  $E_c$  to the critical depth  $y_c$  is  
 (a)  $\left[ \frac{2a+1}{2a} \right]$  (b)  $2a$  (c)  $\frac{a+1}{a}$  (d)  $\frac{3}{2}a$
- 2.16 In a rectangular channel carrying uniform flow with a specific energy  $E$  and depth of flow  $= y_0$  the ratio  $E / y_c$  is equal to

$$(a) \left(\frac{y_0}{y_c}\right)^2 + \frac{1}{2(y_0/y_c)^2} \quad (b) \left(\frac{y_c}{y_0}\right) + 2\left(\frac{y_c}{y_0}\right)^2$$

$$(c) 2\left(\frac{y_c}{y_0}\right) + \frac{1}{2(y_c/y_0)^2} \quad (d) \left(\frac{y_0}{y_c}\right) + \frac{1}{2(y_0/y_c)^2}$$

- 2.17 If  $F_0$  = Froude number of flow in rectangular channel at a depth of flow =  $y_0$  then  $y_c / y_0 =$
- (a)  $\sqrt{F_0}$       (b)  $F_0^{2/3}$       (c)  $F_0^{1/3}$       (d)  $F_0^{3/2}$
- 2.18 Supercritical flow at Froude number of  $F_0 = 2.0$  occurs at a depth of 0.63 m in a rectangular channel. The critical depth in m is
- (a) 0.857      (b) 0.735      (c) 1.000      (d) 0.500
- 2.19 The Froude number of a flow in a rectangular channel is 0.73. If the depth of flow is 1.50 m, the specific energy in metres is
- (a) 1.90      (b) 1.50      (c) 1.73      (d) 0.73
- 2.20 A trapezoidal channel of bed width of 3.5 m and side slope of 1.5 H: 1 V carries a flow of 9.0 m<sup>3</sup>/s with a depth of 2.0 m. The Froude number of flow is
- (a) 0.156      (b) 0.189      (c) 0.013      (d) 0.506
- 2.21 For a triangular channel the first hydraulic exponent  $M$  is
- (a) 2.0      (b) 3.0      (c) 5.0      (d) 5.33
- 2.22 For a trapezoidal canal section with side slope of  $m$  horizontal : 1 vertical the value of the first hydraulic exponent  $M$  is
- (a) a constant at all stages  
 (b) a function of  $S_0$  and Manning's coefficient  $n$   
 (c) a function  $my/B$   
 (d) a function of  $y/B$  only
- 2.23 In a rectangular channel with subcritical flow the height of a hump to be built to cause subcritical flow over it was calculated by neglecting energy losses. If, after building the hump, it is found that the energy losses in the transition are appreciable, the effect of this hump on the flow will be
- (a) to make the flow over the hump subcritical  
 (b) to make the flow over the hump supercritical  
 (c) to cause the depth of flow upstream of the hump to raise  
 (d) to lower the upstream water surface
- 2.24 For an exponential channel ( $A = ky^a$ ) the first hydraulic exponent  $M$  is
- (a)  $(a + 1)$       (b)  $(2a)$       (c)  $(2a + 1)$       (d)  $a^2$
- 2.25 The flow in a rectangular channel is subcritical. If the width is expanded at a certain section, the water surface
- (a) at a downstream section will drop  
 (b) at the downstream section will rise  
 (c) at the upstream section will rise  
 (d) at the upstream section will drop
- 2.26 A bottom rack in a channel is used to withdraw a part of the discharge flowing in a canal. If the flow is subcritical throughout, this will cause
- (a) a rise in the water surface on the rack  
 (b) a drop in the water surface over the rack  
 (c) a jump over the rack  
 (d) a lowering of the water surface upstream of the rack.

- 2.27 The flow in a channel is at critical depth. If at a section  $M$  a small hump of height  $\Delta Z$  is built on the bed of the channel, the flow will be
- (a) critical upstream of  $M$
  - (b) critical at  $M$
  - (c) subcritical at  $M$
  - (d) supercritical at  $M$



**APPENDIX 2A**

Two tables which are useful in various open channel flow computations are presented here.

1. Table 2A.1 contains the geometric elements of a circular channel in a non-dimensional fashion. The column  $(Z/D^{2.5}) = f(y/D)$  is useful in calculating critical depths by using Eq. (2.18). At critical depth,  $y = y_c$  and

$$(Z/D^{2.5}) = (Q/\sqrt{g}D^{2.5}).$$

The last column,  $AR^{2/3}/D^{8/3}$ , will be useful in the calculation of normal depths as will be explained in Chapter 3 (Eq. (3.29)). At normal depth,

$$\phi(y_0/D) = \frac{AR^{2/3}}{D^{8/3}} = \frac{Qn}{\sqrt{S_0}D^{8/3}}$$

2. Table 2A.2 contains the values of  $\psi = f(\zeta_c)$  for computation of critical depth in trapezoidal channels. At the critical depth  $y_c'$

$$\psi = \left( \frac{\alpha Q^2 m^3}{g B^5} \right)^{1/2} \text{ and } \zeta_c = \frac{m y_c}{B}$$

**Table 2A.1** Elements of Circular Channels\*

$y/D$	$2\theta(\text{radians})$	$A/D^2$	$P/D$	$T/D$	$Z/D^{2.5}$	$AR^{2/3}/D^{8/3}$
0.01	0.40067 E+00	0.13293 E-02	0.20033 E+00	0.19900 E+00	0.10865 E-03	0.46941 E-04
0.02	0.56759 E+00	0.37485 E-02	0.28379 E+00	0.28000 E+00	0.43372 E-03	0.20946 E-03
0.03	0.69633 E+00	0.68655 E-02	0.34817 E+00	0.34117 E+00	0.97392 E-03	0.50111 E-03
0.04	0.80543 E+00	0.10538 E-01	0.40272 E+00	0.39192 E+00	0.17279 E-02	0.92878 E-03
0.05	0.90205 E+00	0.14681 E-01	0.45103 E+00	0.43589 E+00	0.26944 E-02	0.14967 E-02
0.06	0.98987 E+00	0.19239 E-01	0.49493 E+00	0.47497 E+00	0.38721 E-02	0.22078 E-02
0.07	0.10711 E+01	0.24168 E-01	0.53553 E+00	0.51029 E+00	0.52597 E-02	0.30636 E-02
0.08	0.11470 E+01	0.29435 E-01	0.57351 E+00	0.54259 E+00	0.68559 E-02	0.40652 E-02
0.09	0.12188 E+01	0.35012 E-01	0.60939 E+00	0.57236 E+00	0.86594 E-02	0.52131 E-02
0.10	0.12870 E+01	0.40875 E-01	0.64350 E+00	0.60000 E+00	0.10669 E-01	0.65073 E-02
0.11	0.13523 E+01	0.47006 E-01	0.67613 E+00	0.62578 E+00	0.12883 E-01	0.79475 E-02
0.12	0.14150 E+01	0.53385 E-01	0.70748 E+00	0.64992 E+00	0.15300 E-01	0.95329 E-02
0.13	0.14755 E+01	0.59999 E-01	0.73773 E+00	0.67261 E+00	0.17920 E-01	0.11263 E-01
0.14	0.15340 E+01	0.66833 E-01	0.76699 E+00	0.69397 E+00	0.20740 E-01	0.13136 E-01
0.15	0.15908 E+01	0.73875 E-01	0.79540 E+00	0.71414 E+00	0.23760 E-01	0.15151 E-01
0.16	1.64607	0.08111	0.82303	0.73321	0.02698	0.01731
0.17	1.69996	0.08854	0.84998	0.75127	0.03039	0.01960
0.18	1.75260	0.09613	0.87630	0.76837	0.03400	0.02203

82 Flow in Open Channels

Table 2A.1 (Continued)

$y/D$	$2\theta(\text{radians})$	$A/D^2$	$P/D$	$T/D$	$Z/D^{2.5}$	$AR^{2/3}/D^{8/3}$
0.19	1.80411	0.10390	0.90205	0.78460	0.03781	0.02460
0.20	1.85459	0.11182	0.92730	0.80000	0.04181	0.02729
0.21	1.90414	0.11990	0.95207	0.81462	0.04600	0.03012
0.22	1.95282	0.12811	0.97641	0.82849	0.05038	0.03308
0.23	2.00072	0.13647	1.00036	0.84167	0.05495	0.03616
0.24	2.04789	0.14494	1.02395	0.85417	0.05971	0.03937
0.25	2.09440	0.15355	1.04720	0.86603	0.06465	0.04270
0.26	2.14028	0.16226	1.07014	0.87727	0.06979	0.04614
0.27	2.18560	0.17109	1.09280	0.88792	0.07510	0.04970
0.28	2.23040	0.18002	1.11520	0.89800	0.08060	0.05337
0.29	2.27470	0.18905	1.13735	0.90752	0.08628	0.05715
0.30	2.31856	0.19817	1.15928	0.91652	0.09215	0.06104
0.31	2.36200	0.20738	1.18100	0.92499	0.09819	0.06503
0.32	2.40506	0.21667	1.20253	0.93295	0.10441	0.06912
0.33	2.44776	0.22603	1.22388	0.94043	0.11081	0.07330
0.34	2.49013	0.23547	1.24507	0.94742	0.11739	0.07758
0.35	2.53221	0.24498	1.26610	0.95394	0.12415	0.08195
0.36	2.57400	0.25455	1.28700	0.96000	0.13108	0.08641
0.37	2.61555	0.26418	1.30777	0.96561	0.13818	0.09095
0.38	2.65686	0.27386	1.32843	0.97077	0.14546	0.09557
0.39	2.69796	0.28359	1.34898	0.97550	0.15291	0.10027
0.40	2.73888	0.29337	1.36944	0.97980	0.16053	0.10503
0.41	2.77962	0.30319	1.38981	0.98367	0.16832	0.10987
0.42	2.82021	0.31304	1.41011	0.98712	0.17629	0.11477
0.43	2.86067	0.32293	1.43033	0.99015	0.18442	0.11973
0.44	2.90101	0.33284	1.45051	0.99277	0.19272	0.12475
0.45	2.94126	0.34278	1.47063	0.99499	0.20120	0.12983
0.46	2.98142	0.35274	1.49071	0.99679	0.20984	0.13495
0.47	3.02152	0.36272	1.51076	0.99820	0.21865	0.14011
0.48	3.06157	0.37270	1.53079	0.99920	0.22763	0.14532
0.49	3.10159	0.38270	1.55080	0.99980	0.23677	0.15057
0.50	3.14159	0.39270	1.57080	1.00000	0.24609	0.15584
0.51	3.18160	0.40270	1.59080	0.99980	0.25557	0.16115
0.52	3.22161	0.41269	1.61081	0.99920	0.26523	0.16648
0.53	3.26166	0.42268	1.63083	0.99820	0.27505	0.17182
0.54	3.30176	0.43266	1.65088	0.99679	0.28504	0.17719
0.55	3.34193	0.44262	1.67096	0.99499	0.29521	0.18256
0.56	3.38217	0.45255	1.69109	0.99277	0.30555	0.18794
0.57	3.42252	0.46247	1.71126	0.99015	0.31606	0.19331
0.58	3.46297	0.47236	1.73149	0.98712	0.32675	0.19869
0.59	3.50357	0.48221	1.75178	0.98367	0.33762	0.20405
0.60	3.54431	0.49203	1.77215	0.97980	0.34867	0.20940
0.61	3.58522	0.50181	1.79261	0.97550	0.35991	0.21473
0.62	3.62632	0.51154	1.81316	0.97077	0.37133	0.22004
0.63	3.66764	0.52122	1.83382	0.96561	0.38294	0.22532

y/D	2θ(radians)	A/D <sup>2</sup>	P/D	T/D	Z/D <sup>2.5</sup>	AR <sup>2.5</sup> /D <sup>8/3</sup>
0.64	3.70918	0.53085	1.85459	0.96000	0.39475	0.23056
0.65	3.75098	0.54042	1.87549	0.95394	0.40676	0.23576
0.66	3.79305	0.54992	1.89653	0.94742	0.41897	0.24092
0.67	3.83543	0.55936	1.91771	0.94043	0.43140	0.24602
0.68	3.87813	0.56873	1.93906	0.93295	0.44405	0.25106
0.69	3.92119	0.57802	1.96059	0.92499	0.45693	0.25604
0.70	3.96463	0.58723	1.98231	0.91652	0.47005	0.26095
0.71	4.00848	0.59635	2.00424	0.90752	0.48342	0.26579
0.72	4.05279	0.60538	2.02639	0.89800	0.49705	0.27054
0.73	4.09758	0.61431	2.04879	0.88702	0.51097	0.27520
0.74	4.14290	0.62313	2.07145	0.87727	0.52518	0.27976
0.75	4.18879	0.63185	2.09440	0.86603	0.53971	0.28422
0.76	4.23529	0.64045	2.11765	0.85417	0.55457	0.28856
0.77	4.28247	0.64893	2.14123	0.84167	0.56981	0.29279
0.78	4.33036	0.65728	2.16518	0.82849	0.58544	0.29689
0.79	4.37905	0.66550	2.18953	0.81462	0.60151	0.30085
0.80	4.42859	0.67357	2.21430	0.80000	0.61806	0.30466
0.81	4.47908	0.68150	2.23954	0.78460	0.63514	0.30832
0.82	4.53059	0.68926	2.26529	0.76837	0.65282	0.31181
0.83	4.58323	0.69686	2.29162	0.75127	0.67116	0.31513
0.84	4.63712	0.70429	2.31856	0.73321	0.69025	0.31825
0.85	4.69239	0.71152	2.34619	0.71414	0.71022	0.32117
0.86	4.74920	0.71856	2.37460	0.69397	0.73119	0.32388
0.87	4.80773	0.72540	2.40387	0.67261	0.75333	0.32635
0.88	4.86822	0.73201	2.43411	0.64992	0.77687	0.32858
0.89	4.93092	0.73839	2.46546	0.62578	0.80208	0.33053
0.90	4.99618	0.74452	2.49809	0.60000	0.82936	0.33219
0.91	5.06441	0.75039	2.53221	0.57236	0.85919	0.33354
0.92	5.13616	0.75596	2.56808	0.54259	0.89231	0.33453
0.93	5.21213	0.76123	2.60607	0.51029	0.92974	0.33512
0.94	5.29332	0.76616	2.64666	0.47497	0.97307	0.33527
0.95	5.38113	0.77072	2.69057	0.43589	1.02483	0.33491
0.96	5.47775	0.77486	2.73888	0.39192	1.08953	0.33393
0.97	5.58685	0.77853	2.79343	0.34117	1.17605	0.33218
0.98	5.71560	0.78165	2.85780	0.28000	1.30599	0.32936
0.99	5.88252	0.78407	2.94126	0.19900	1.55635	0.32476
1.00	6.28319	0.78540	3.14159	0.00000		0.31169

\*The notations 'E + a' represents 10<sup>a</sup> and 'E - a' represents 10<sup>-a</sup>. Thus for example

$$0.13523\text{E}+01 = 1.3523$$

$$0.47006\text{E}-01 = 0.047006$$

Table 2A. 2 Values of  $\psi$  for computation of critical depth in trapezoidal channels

$\xi$	$\psi$	$\xi$	$\psi$	$\xi$	$\psi$	$\xi$	$\psi$	$\xi$	$\psi$
0.100	0.0333042	0.330	0.2256807	0.560	0.5607910	0.790	1.0469124	1.020	1.6962526
0.105	0.0359281	0.335	0.2314360	0.565	0.5697107	0.795	1.0592476	1.025	1.7122746
0.110	0.0386272	0.340	0.2372580	0.570	0.5787019	0.800	1.0716601	1.030	1.7283798
0.115	0.0414006	0.345	0.2431469	0.575	0.5877645	0.805	1.0841500	1.035	1.7445682
0.120	0.0442474	0.350	0.2491026	0.580	0.5968989	0.810	1.0967174	1.040	1.7608400
0.125	0.0471671	0.355	0.2551252	0.585	0.6061050	0.815	1.1093625	1.045	1.7771953
0.130	0.0501588	0.360	0.2612149	0.590	0.6153829	0.820	1.1220854	1.050	1.7936343
0.135	0.0532222	0.365	0.2673716	0.595	0.6247330	0.825	1.1348861	1.055	1.8101570
0.140	0.0563565	0.370	0.2735954	0.600	0.6341551	0.830	1.1477649	1.060	1.8267635
0.145	0.0595615	0.375	0.2798865	0.605	0.6436496	0.835	1.1607219	1.065	1.8434541
0.150	0.0628365	0.380	0.2862449	0.610	0.6532164	0.840	1.1737572	1.070	1.8602288
0.155	0.0661812	0.385	0.2926706	0.615	0.6628558	0.845	1.1868709	1.075	1.8770877
0.160	0.0695953	0.390	0.2991638	0.620	0.6725678	0.850	1.2000631	1.080	1.8940310
0.165	0.0730784	0.395	0.3057246	0.625	0.6823525	0.855	1.2133341	1.085	1.9110589
0.170	0.0766302	0.400	0.3123531	0.630	0.6922102	0.860	1.2266838	1.090	1.9281713
0.175	0.0802504	0.405	0.3190493	0.635	0.7021409	0.865	1.2401125	1.095	1.9453685
0.180	0.0839387	0.410	0.3258133	0.640	0.7121448	0.870	1.2536203	1.100	1.9626506
0.185	0.0876950	0.415	0.3326452	0.645	0.7222220	0.875	1.2672072	1.105	1.9800176
0.190	0.0915190	0.420	0.3395452	0.650	0.7323725	0.880	1.2808735	1.110	1.9974698
0.195	0.0954105	0.425	0.3465132	0.655	0.7425966	0.885	1.2946192	1.115	2.0150072
0.200	0.0993694	0.430	0.3535495	0.660	0.7528944	0.890	1.3084445	1.120	2.0326299
0.205	0.1033955	0.435	0.3606541	0.665	0.7632659	0.895	1.3223496	1.125	2.0503382
0.210	0.1074887	0.440	0.3678272	0.670	0.7737114	0.900	1.3363344	1.130	2.0681321
0.215	0.1116488	0.445	0.3750688	0.675	0.7842309	0.905	1.3503992	1.135	2.0860117
0.220	0.1158757	0.450	0.3823789	0.680	0.7948246	0.910	1.3645441	1.140	2.1039771
0.225	0.1201694	0.455	0.3897579	0.685	0.8054926	0.915	1.3787693	1.145	2.1220286
0.230	0.1245297	0.460	0.3972056	0.690	0.8162350	0.920	1.3930747	1.150	2.1401661
0.235	0.1289566	0.465	0.4047224	0.695	0.8270520	0.925	1.4074607	1.155	2.1583899
0.240	0.1334500	0.470	0.4123082	0.700	0.8379437	0.930	1.4219272	1.160	2.1767000
0.245	0.13890098	0.475	0.4199631	0.705	0.8489102	0.935	1.4364745	1.165	2.1950965
0.250	0.1426361	0.480	0.4276873	0.710	0.8599516	0.940	1.4511026	1.170	2.2135797
0.255	0.1473287	0.485	0.4354810	0.715	0.8710681	0.945	1.4658118	1.175	2.2321496
0.260	0.1520877	0.490	0.4433441	0.720	0.8822598	0.950	1.4806020	1.180	2.2508063
0.265	0.1569130	0.495	0.4512768	0.725	0.8935269	0.955	1.4954734	1.185	2.2695499
0.270	0.1618046	0.500	0.4592793	0.730	0.9048694	0.960	1.5104263	1.190	2.2883806
0.275	0.1667625	0.505	0.4673517	0.735	0.9162875	0.965	1.5254606	1.195	2.3072986
0.280	0.1717868	0.510	0.4754940	0.740	0.9277813	0.970	1.5405765	1.200	2.3263038
0.285	0.1768773	0.515	0.4837063	0.745	0.9393510	0.975	1.5557742	1.205	2.3453965
0.290	0.1820342	0.520	0.4919889	0.750	0.9509966	0.980	1.5710537	1.210	2.3645767
0.295	0.1872575	0.525	0.5003418	0.755	0.9627183	0.985	1.5864153	1.215	2.3838447
0.300	0.1925471	0.530	0.5087651	0.760	0.9745163	0.990	1.6018590	1.220	2.4032004
0.305	0.1979031	0.535	0.5172590	0.765	0.9863907	0.995	1.6173849	1.225	2.4226440
0.310	0.2033256	0.540	0.5258236	0.770	0.9983415	1.000	1.6329932	1.230	2.4421757
0.315	0.2088145	0.545	0.5344589	0.775	1.0103690	1.005	1.6486840	1.235	2.4617956
0.320	0.2143700	0.550	0.5431652	0.780	1.0224732	1.010	1.6644574	1.240	2.4815037
0.325	0.2199920	0.555	0.5519425	0.785	1.0346543	1.015	1.6803135	1.245	2.5013003
0.330	0.2256807	0.560	0.5607910	0.790	1.0469124	1.020	1.6962526	1.250	2.5211853

In Table 2A. 2  $\xi = \frac{my_c}{B}$   
 $\psi = \frac{\alpha Q^2 m^3}{gB^5}$

# Uniform Flow

# 3

## 3.1 INTRODUCTION

A flow is said to be uniform if its properties remain constant with respect to distance. As mentioned earlier, the term uniform flow in open channels is understood to mean steady uniform flow. The depth of flow remains constant at all sections in a uniform flow (Fig. 3.1). Considering two Sections 1 and 2, the depths

$$\begin{aligned}y_1 &= y_2 = y_0 \\ A_1 &= A_2 = A_0\end{aligned}$$

and hence

Since  $Q = AV = \text{constant}$ , it follows that in uniform flow  $V_1 = V_2 = V$ . Thus in a uniform flow, the depth of flow, area of cross-section and velocity of flow remain constant along the channel. It is obvious, therefore, that uniform flow is possible only in prismatic channels. The trace of the water surface and channel bottom slope are parallel in uniform flow (Fig. 3.1). Further, since  $V = \text{constant}$ , the energy line will be at a constant elevation above the water surface. As such, the slope of the energy line  $S_f$ , slope of the water surface  $S_w$  and bottom slope  $S_0$  will all be equal to each other.

## 3.2 CHEZY EQUATION

By definition there is no acceleration in uniform flow. By applying the momentum equation to a control volume encompassing Sections 1 and 2, distance  $L$  apart, as shown in Fig. 3.1,

$$P_1 - W \sin \theta - F_f - P_2 = M_2 - M_1 \quad (3.1)$$

where  $P_1$  and  $P_2$  are the pressure forces and  $M_1$  and  $M_2$  are the momentum fluxes at Sections 1 and 2 respectively  $W = \text{weight to fluid in the control volume}$  and  $F_f = \text{shear force at the boundary}$ .

Since the flow is uniform,

$$\begin{aligned}\text{Also,} \quad P_1 &= P_2 & \text{and} & \quad M_1 = M_2 \\ W &= \gamma AL & \text{and} & \quad F_f = \tau_0 PL\end{aligned}$$



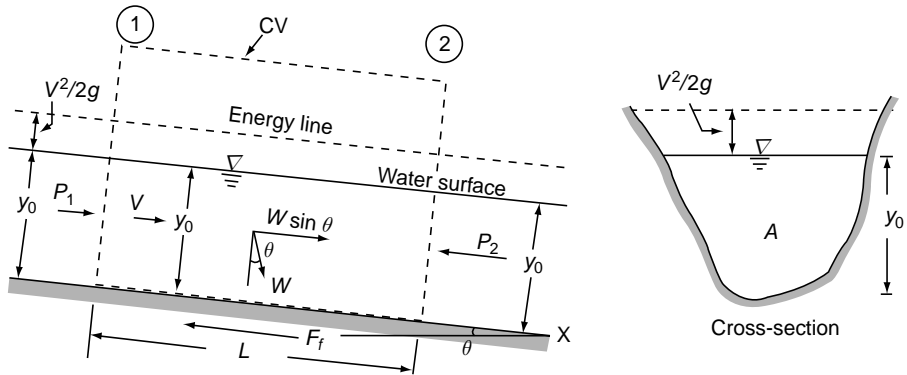


Fig. 3.1 Uniform flow

where  $\tau_0$  = average shear stress on the wetted perimeter of length  $P$  and  $\gamma$  = unit weight of water. Replacing  $\sin \theta$  by  $S_0$  (= bottom slope), Eq. 3.1 can be written as

$$\gamma ALS_0 = \tau_0 PL$$

or

$$\tau_0 = \gamma \frac{A}{P} S_0 = \gamma RS_0 \quad (3.2)$$

where  $R = A/P$  is defined as the *hydraulic radius*.  $R$  is a length parameter accounting for the shape of the channel. It plays a very important role in developing flow equations which are common to all shapes of channels.

Expressing the average shear stress  $\tau_0$  as  $\tau_0 = k\rho V^2$ , where  $k$  = a coefficient which depends on the nature of the surface and flow parameters, Eq. 3.2 is written as

$$k\rho V^2 = \gamma RS_0$$

leading to

$$V = C \sqrt{RS_0} \quad (3.3)$$

where  $C = \sqrt{\frac{\gamma}{\rho k}}$  = a coefficient which depends on the nature of the surface and the flow. Equation 3.3 is known as the *Chezy formula* after the French engineer Antoine Chezy, who is credited with developing this basic simple relationship in 1769. The dimensions of  $C$  are  $[L^{1/2} T^{-1}]$  and it can be made dimensionless by dividing it by  $\sqrt{g}$ . The coefficient  $C$  is known as the Chezy coefficient.

### 3.3 DARCY–WEISBACH FRICTION FACTOR $f$

Incompressible, turbulent flow over plates, in pipes and ducts have been extensively studied in the fluid mechanics discipline. From the time of Prandtl (1875–1953) and

Von Karman (1881–1963) research by numerous eminent investigators has enabled considerable understanding of turbulent flow and associated useful practical applications. The basics of velocity distribution and shear resistance in a turbulent flow are available in any good text on fluid mechanics<sup>1,2</sup>.

Only relevant information necessary for our study is summed up in this section.

**Pipe Flow** A surface can be termed hydraulically smooth, rough or in transition depending on the relative thickness of the roughness magnitude to the thickness of the laminar sub-layer. The classification is as follows:

$$\frac{\varepsilon_s \nu_*}{\nu} < 4 \text{ — hydraulically-smooth wall}$$

$$4 < \frac{\varepsilon_s \nu_*}{\nu} < 60 \text{ — transitional regime}$$

$$\frac{\varepsilon_s \nu_*}{\nu} > 60 \text{ — full rough flow}$$

where  $\varepsilon_s$  = equivalent sand grain roughness,  $\nu_* = \sqrt{\tau_0 / \rho} = \sqrt{gRS_0}$  = shear velocity and

$\nu$  = kinematic viscosity.

For pipe flow, the Darcy–Weisbach equation is

$$h_f = f \frac{L}{D} \frac{V^2}{2g} \quad (3.4)$$

where  $h_f$  = head loss due to friction in a pipe of diameter  $D$  and length  $L$ ;  $f$  = Darcy–Weisbach friction factor. For smooth pipes,  $f$  is found to be a function of the Reynolds number  $\left( \mathbf{Re} = \frac{VD}{\nu} \right)$  only. For rough turbulent flows,  $f$  is a function of the relative roughness ( $\varepsilon_s/D$ ) and type of roughness and is independent of the Reynolds number. In the transition regime, both the Reynolds number and relative roughness play important roles. The roughness magnitudes for commercial pipes are expressed as equivalent sand-grain roughness  $\varepsilon_s$ . The extensive experimental investigations of pipe flow have yielded the following generally accepted relations for the variation of  $f$  in various regimes of flow:

1. For smooth walls and  $\mathbf{Re} < 10^5$

$$f = \frac{0.316}{\mathbf{Re}^{1/4}} \quad (\text{Blasius formula}) \quad (3.5)$$

2. For smooth walls and  $\mathbf{Re} > 10^5$

$$\frac{1}{\sqrt{f}} = 2.0 \log \mathbf{Re} \sqrt{f} - 0.8 \quad (\text{Karman–Prandtl equation}) \quad (3.6)$$

88 Flow in Open Channels

3. For rough boundaries and  $\mathbf{Re} > 10^5$

$$\frac{1}{\sqrt{f}} = -2 \log \frac{\varepsilon_s}{D} + 1.14 \quad (\text{Karman-Prandtl equation}) \quad (3.7)$$

4. For the transition zone

$$\frac{1}{\sqrt{f}} + 2 \log \frac{\varepsilon_s}{D} = 1.14 - 2 \log \left( 1 + 9.35 \frac{D/\varepsilon_s}{\mathbf{Re}\sqrt{f}} \right) \quad (\text{Colebrook-White equation}) \quad (3.8)$$

It is usual to show the variation of  $f$  with  $\mathbf{Re}$  and  $\frac{\varepsilon_s}{D}$  by a three-parameter graph known as the *Moody chart*.

Studies on non-circular conduits, such as rectangular, oval and triangular shapes have shown that by introducing the hydraulic radius  $R$ , the formulae developed for pipes are applicable for non-circular ducts also. Since for a circular shape  $R = D/4$ , by replacing  $D$  by  $4R$ , Eqs 3.5 to 3.8 can be used for any duct shape provided the conduit areas are close enough to the area of a circumscribing circle or semicircle.

**Open Channels** For purposes of flow resistance which essentially takes place in a thin layer adjacent to the wall, an open channel can be considered to be a conduit cut into two. The hydraulic radius would then be the appropriate length parameter and prediction of friction factor  $f$  can be done by using Eqs 3.5 to 3.8. It should be remembered that  $\mathbf{Re} = \frac{4RV}{\nu}$  and the relative roughness is  $(\varepsilon_s/4R)$ .

Equation 3.4 can then be written for an open channel flow as

$$h_f = f \frac{L}{4R} \frac{V^2}{2g}$$

which on rearranging gives

$$V = \sqrt{\frac{8g}{f}} \sqrt{R} \cdot \sqrt{h_f/L} \quad (3.9)$$

Noting that for uniform flow in an open channel  $h_f/L = \text{slope of the energy line} = S_f = S_0$ , it may be seen that Eq. 3.9 is the same as Eq. 3.3 (Chezy formula) with

$$C = \sqrt{8g/f} \quad (3.10)$$

For convenience of use, Eq. 3.10 along with Eqs 3.5 to 3.8 can be used to prepare a modified Moody chart showing the variation of  $C$  with

$$\left( \mathbf{Re} = \frac{4RV}{\nu} \right) \text{ and } \left( \frac{4R}{\varepsilon_s} \right)$$

If  $f$  is to be calculated by using one of the Eqs 3.5 to 3.8, Eqs 3.6 to 3.8 are inconvenient to use as  $f$  is involved on both sides of the equations. Simplified empirical forms of Eqs 3.6 and 3.8, which are accurate enough for all practical purposes, are given by Jain<sup>3</sup> as follows:

$$\frac{1}{\sqrt{f}} = 1.80 \log \mathbf{Re} - 1.5146 \quad (\text{in lieu of Eq. (3.6)}) \quad (3.6a)$$

and 
$$\frac{1}{\sqrt{f}} = 1.14 - 2.0 \log \left( \frac{\varepsilon_s}{4R} + \frac{21.25}{\mathbf{Re}^{0.9}} \right) \quad (\text{in lieu of Eq. (3.8)}) \quad (3.8a)$$

Equation (3.8a) is valid for  $5000 \leq \mathbf{Re} \leq 10^8$  and  $10^{-6} < \frac{\varepsilon_s}{4R} < 10^{-2}$ .

These two equations are very useful for obtaining explicit solutions of many flow-resistance problems.

Generally, the open channels that are encountered in the field are very large in size and also in the magnitude of roughness elements. Consequently, high Reynolds numbers and large relative roughnesses are operative with the result that most of the open channels have rough turbulent-flow regimes. Due to paucity of reliable experimental or field data on channels covering a wide range of parameters, values of  $\varepsilon_s$  are not available to the same degree of confidence as for pipe materials. However, Table 3.1 can be used to estimate the values of  $\varepsilon_s$  for some common open channel surfaces.

**Table 3.1** Values of  $\varepsilon_s$  for some Common Channel Surfaces

Sl. No.	Surface	Equivalent Roughness $\varepsilon_s$ in mm
1	Glass	$3 \times 10^{-4}$
2	Very smooth concrete surface	0.15–0.30
3	Glazed sewer pipe	0.60
4	Gunite (smooth)	0.50–1.5
5	Rough concrete	3.0–4.5
6	Earth channels (straight, uniform)	3.0
7	Rubble masonry	6.0
8	Untreated gunite	3.0–10.0

### 3.4 MANNING'S FORMULA

A resistance formula proposed by Robert Manning, an Irish engineer, for uniform flow in open channels, is

$$V = \frac{1}{n} R^{2/3} S_0^{1/2} \quad (3.11)$$

where  $n$  = a roughness coefficient known as Manning's  $n$ . This coefficient is essentially a function of the nature of boundary surface. It may be noted that the dimensions of  $n$  are  $[L^{-1/3} T]$ . Equation 3.11 is popularly known as the Manning's formula. Owing to its simplicity and acceptable degree of accuracy in a variety of practical applications, the Manning's formula is probably the most widely used uniform flow formula in the world.

Comparing Eq. 3.11 with the Chezy formula, Eq. 3.3, we have

$$C = \frac{1}{n} R^{1/6} \tag{3.12}$$

From Eq. 3.10,

$$C = \sqrt{\frac{8g}{f}} = \frac{1}{n} R^{1/6}$$

i.e.

$$f = \left( \frac{n^2}{R^{1/3}} \right) (8g) \tag{3.13}$$

Since Eq. 3.13 does not contain velocity term (and hence the Reynolds number), we can compare Eq. 3.13 with Eq. 3.7, i.e., the Prandtl-Karman relationship for rough turbulent flow. If Eq. 3.7 is plotted as  $f$  vs.  $\frac{4R}{\epsilon_s}$  on a log-log paper, a smooth curve that can be approximated to a straight line with a slope of  $\left(-\frac{1}{3}\right)$  is obtained (Fig 3.2). From this the term  $f$  can be expressed as

$$f \propto \left( \frac{4R}{\epsilon_s} \right)^{-1/3} \quad \text{or} \quad f \propto \left( \frac{\epsilon_s}{R} \right)^{1/3}$$

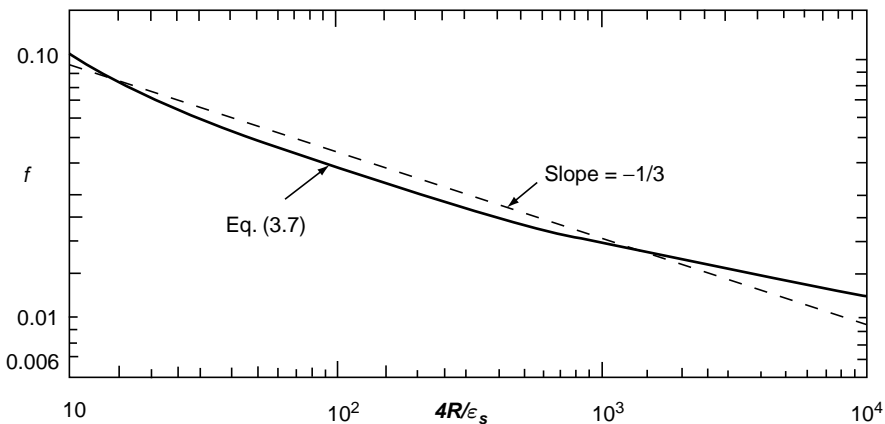


Fig. 3.2 Variation of  $f$  in fully rough flow

Since from Eq. 3.13,  $f \propto \frac{n^2}{R^{1/3}}$ , it follows that  $n \propto \varepsilon_s^{1/6}$ . Conversely, if  $n \propto \varepsilon_s^{1/6}$ , the Manning's formula and Darcy–Weisbach formula both represent rough turbulent flow  $\left( \frac{\varepsilon_s v_*}{\nu} > 60 \right)$ .

### 3.5 OTHER RESISTANCE FORMULAE

Several forms of expressions for the Chezy coefficient  $C$  have been proposed by different investigators in the past. Many of these are archaic and are of historic interest only. A few selected ones are listed below:

#### 1. Pavlovski formula

$$C = \frac{1}{n} R^x \quad (3.14)$$

in which  $x = 2.5 \sqrt{n} - 0.13 - 0.75 \sqrt{R} (\sqrt{n} - 0.10)$  and  $n =$  Manning's coefficient. This formula appears to be in use in Russia.

#### 2. Ganguillet and Kutter Formula

$$C = \frac{23 + \frac{1}{n} + \frac{0.00155}{S_0}}{1 + \left[ 23 + \frac{0.00155}{S_0} \right] \frac{n}{\sqrt{R}}} \quad (3.15)$$

in which  $n =$  Manning's coefficient.

#### 3. Bazin's formula

$$C = \frac{87.0}{1 + M/R} \quad (3.16)$$

in which  $M =$  a coefficient dependent on the surface roughness.

### 3.6 VELOCITY DISTRIBUTION

#### (a) Wide Channels

(i) *Velocity-defect Law* In channels with large aspect ratio  $B/y_0$ , as for example in rivers and very large canals, the flow can be considered to be essentially two dimensional. The fully developed velocity distributions are similar to the logarithmic

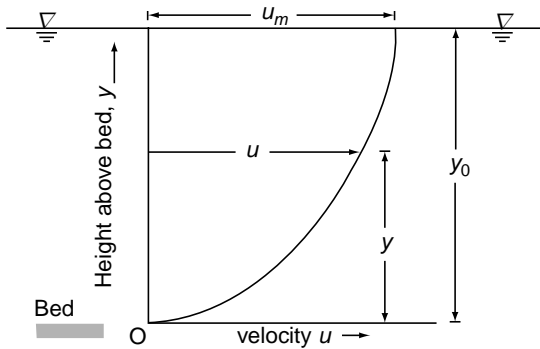


Fig. 3.3 Velocity profile in a wide open channel

form of velocity-defect law found in turbulent flow in pipes. The maximum velocity  $u_m$  occurs essentially at the water surface, (Fig. 3.3). The velocity  $u$  at a height  $y$  above the bed in a channel having uniform flow at a depth  $y_0$  is given by the velocity-defect law for  $y/y_0 > 0.15$  as

$$\begin{aligned} \frac{u_m - u}{u_*} &= \frac{1}{k} \ln \frac{y}{y_0} \\ &= -\frac{2.3}{k} \log_{10} (y/y_0) \end{aligned} \quad (3.17)$$

where  $u_* = \text{shear velocity} = \sqrt{\tau_0 / \rho} = \sqrt{gRS_0}$ ,  $R = \text{hydraulic radius}$ ,  $S_0 = \text{longitudinal slope}$ , and  $k = \text{Karman constant} = 0.41$  for open channel flows<sup>5</sup>.

This equation is applicable to both rough and smooth boundaries alike. Assuming the velocity distribution of Eq. 3.17 is applicable to the entire depth  $y_0$ , the velocity  $u$  can be expressed in terms of the average velocity

$$\begin{aligned} V &= \frac{1}{y_0} \int_0^{y_0} u \, dy \quad \text{as} \\ u &= V + \frac{u_*}{k} \left( 1 + \ln \frac{y}{y_0} \right) \end{aligned} \quad (3.18)$$

From Eq. 3.18, it follows that

$$V = u_m - \frac{u_*}{k} \quad (3.19)$$

(ii) *Law of the Wall* For smooth boundaries, the law of the wall as

$$\frac{u}{u_*} = \frac{1}{k} \ln \frac{yu_*}{\nu} + A_s \quad (3.20)$$

is found applicable in the inner wall region ( $y/y_0 < 0.20$ ). The values of the constants are found to be  $k = 0.41$  and  $A_s = 5.29$  regardless of the Froude number and Reynolds number of the flow<sup>5</sup>. Further, there is an overlap zone between the law of the wall region and the velocity-defect law region.

For completely rough turbulent flows, the velocity distribution in the wall region ( $y/y_0 < 0.20$ ) is given by

$$\frac{u}{u_*} = \frac{1}{k} \ln \frac{y}{\varepsilon_s} + A_r \quad (3.21)$$

where  $\varepsilon_s$  = equivalent sand grain roughness. It has been found that  $k$  is a universal constant irrespective of the roughness size<sup>5</sup>. Values of  $k = 0.41$  and  $A_r = 8.5$  are appropriate.

For further details of the velocity distributions Ref. [5] can be consulted.

**(b) Channels with Small Aspect Ratio** In channels which are not wide enough to have two dimensional flow, the resistance of the sides will be significant to alter the two-dimensional nature of the velocity distribution given by Eq. 3.17. The most important feature of the velocity distributions in such channels is the occurrence of *velocity-dip*, where the maximum velocity occurs not at the free surface but rather some distance below it, (Fig. 3.4) Various investigations have inferred the secondary currents as responsible for this velocity-dip phenomenon<sup>4</sup>. The critical ratio of  $B/y_0$  above which the velocity-dip becomes insignificant has been found to be about 5.0. Based on this the channels with  $B/y_0 \leq 5$  can be classified as *narrow channels*.

Typical velocity distributions in rectangular channels with  $B/y_0 = 1.0$  and 6.0 are shown in Figures 3.5(a) and (b) respectively.

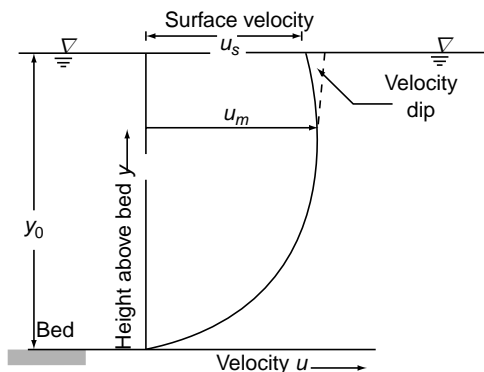


Fig. 3.4 Velocity profile in a narrow channel



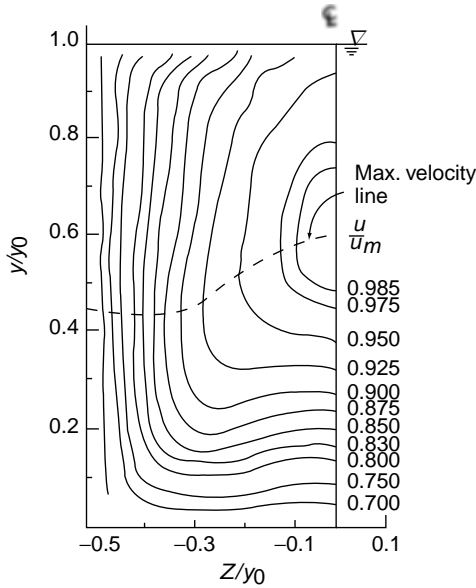


Fig. 3.5(a) Typical velocity distribution in a narrow channel,  $B/y_0 = 1.0$ . (Ref. 4)

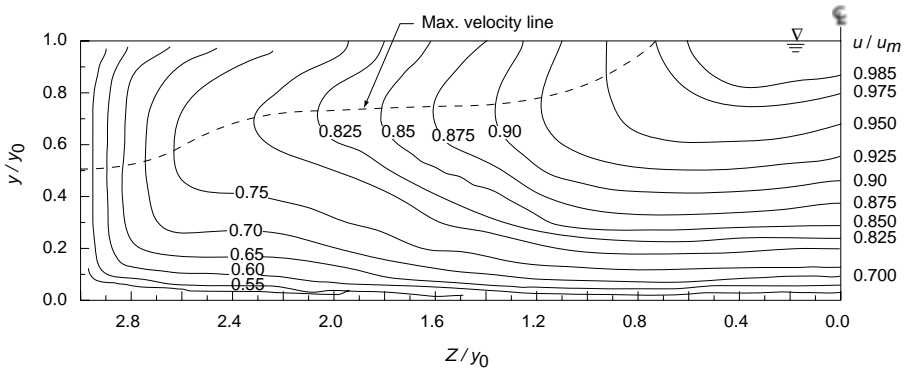


Fig. 3.5(b) Typical velocity distribution in a rectangular channel with  $B/y_0 = 6.0$ . (Ref. 47)

### 3.7 SHEAR STRESS DISTRIBUTION

The average shear stress  $\tau_0$  on the boundary of a channel is, by Eq. 3.2, given as  $\tau_0 = \gamma RS_0$ . However, this shear stress is not uniformly distributed over the boundary. It is zero at the intersection of the water surface with the boundary and also at the corners in the boundary. As such, the boundary shear stress  $\tau_0$  will have certain local maxima on the side as well as on the bed. The turbulence of the flow and the presence of secondary cur-

rents in the channel also contribute to the non-uniformity of the shear stress distribution. A knowledge of the shear stress distribution in a channel is of interest not only in the understanding of the mechanics of flow but also in certain problems involving sediment transport and design of stable channels in non-cohesive material (Chapter 11).

*Preston tube*<sup>5</sup> is a very convenient device for the boundary shear stress measurements in a laboratory channel. Distributions of boundary shear stress by using Preston tube in rectangular, trapezoidal and compound channels have been reported<sup>6,7</sup>. Isaacs and Macintosh<sup>8</sup> report the use of a modified Preston tube to measure shear stress in open channels.

Lane<sup>9</sup> obtained the shear stress distributions on the sides and bed of trapezoidal and rectangular channels by the use of membrane analogy. A typical distribution of the boundary shear stress on the side ( $\tau_s$ ) and bed ( $\tau_b$ ) in a trapezoidal channel of  $B/y_0 = 4.0$  and side slope  $m = 1.5$  obtained by Lane is shown in Fig 3.6. The variation of the maximum shear stress on the bed  $\tau_{bm}$  and on the sides  $\tau_{sm}$  in rectangular and trapezoidal channels is shown in Fig. 3.7. It is noted from the figure that for trapezoidal sections approximately  $\tau_{sm} \approx 0.76 \gamma y_0 S_0$  and  $\tau_{bm} \approx \gamma y_0 S_0$  when  $B/y_0 \gtrsim 6.0$ .

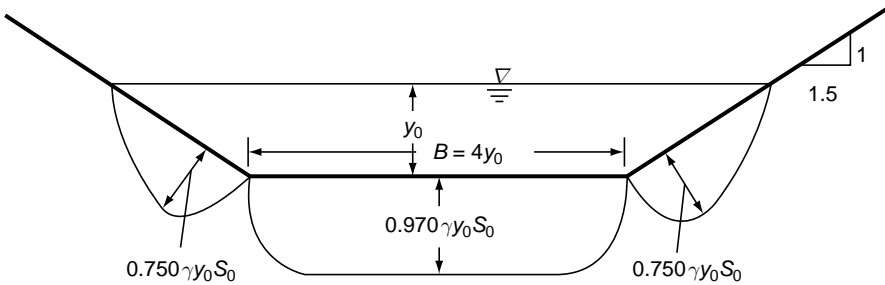


Fig. 3.6 Variation of boundary shear stress in a trapezoidal channel with  $B/y_0 = 4$  and  $m = 1.5$

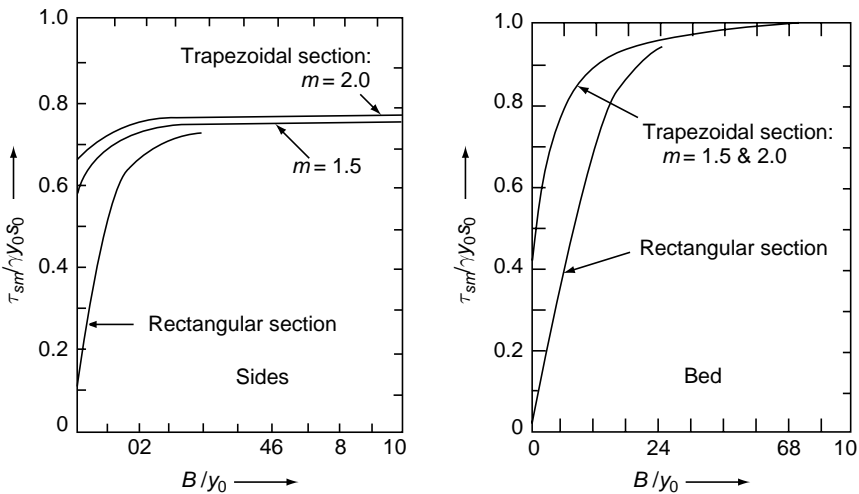


Fig. 3.7 Variation of maximum shear stress on bed and sides of smooth channels

### 3.8 RESISTANCE FORMULA FOR PRACTICAL USE

Since a majority of the open channel flow are in the rough turbulent range, the Manning's formula (Eq. 3.11) is the most convenient one for practical use. Since, it is simple in form and is also backed by considerable amount of experience, it is the most preferred choice of hydraulic engineers. However, it has a limitation in that it cannot adequately represent the resistance in situations where the Reynolds number effect is predominant and this must be borne in mind. In the book, the Manning's formula is used as the resistance equation.

The Darcy–weissbach coefficient  $f$  used with the Chezy formula is also an equally effective way of representing the resistance in uniform flow. However, field engineers generally do not prefer this approach, partly because of the inadequate information to assist in the estimation of  $\varepsilon_s$  and partly because it is not sufficiently backed by experimental or field observational data. It should be realized that for open channel flows with hydrodynamically smooth boundaries, it is perhaps the only approach available to estimate the resistance.

### 3.9 MANNING'S ROUGHNESS COEFFICIENT $n$

In the Manning's formula, all the terms except  $n$  are capable of direct measurement. The roughness coefficient, being a parameter representing the integrated effects of the channel cross-sectional resistance, is to be estimated. The selection of a value for  $n$  is subjective, based on one's own experience and engineering judgement. However, a few aids are available which reduce to a certain extent the subjectiveness in the selection of an appropriate value of  $n$  for a given channel. These include:

1. Photographs of selected typical reaches of canals, their description and measured values of  $n$ <sup>10,11</sup>. These act as type values and by comparing the channel under question with a figure and description set that resembles it most, one can estimate the value of  $n$  fairly well. Movies, stereoscopic colour photographs and video recordings of selected typical reaches are other possible effective aids under the category.
2. A comprehensive list of various types of channels, their descriptions with the associates range of values of  $n$ . Some typical values of  $n$  for various normally encountered channel surfaces prepared from information gathered from various sources<sup>10,11,12,13</sup> are presented in Table 3.2.

Estimation of correct  $n$ -value of natural channels is of utmost importance in practical problems associated with backwater computations, flood flow estimation, routing and management. The photographs of man-made and natural channels with corresponding values of  $n$  given by Chow<sup>10</sup>, Barnes<sup>11</sup> and Arcemont and Schnieder<sup>14</sup> are very useful in obtaining a first estimate of roughness coefficient in such situations.

Cowan<sup>15</sup> has developed a procedure to estimate the value of roughness factor  $n$  of natural channels in a systematic way by giving weightages to various important factors that affect the roughness coefficient. According to Cowan.

$$n = (n_b + n_1 + n_2 + n_3 + n_4) m$$

Table 3.2 Values of Roughness Coefficient  $n$ 

Sl. No.	Surface Characteristics	Range of $n$
(a)	<i>Lined channels with straight alignment</i>	
1	Concrete (a) formed, no finish	0.013–0.017
	(b) Trowel finish	0.011–0.015
	(c) Float finish	0.013–0.015
	(d) Gunite, good section	0.016–0.019
	(e) Gunite, wavy section	0.018–0.022
2	Concrete bottom, float finish, sides as indicated	
	(a) Dressed stone in mortar	0.015–0.017
	(b) Random stone in mortar	0.017–0.020
	(c) Cement rubble masonry	0.020–0.025
	(d) Cement-rubble masonry, plastered	0.016–0.020
	(e) Dry rubble (rip-rap)	0.020–0.030
3	Tile	0.016–0.018
4	Brick	0.014–0.017
5	Sewers (concrete, A.C., vitrified-clay pipes)	0.012–0.015
6	Asphalt (i) Smooth	0.013
	(ii) Rough	0.016
7	Concrete lined, excavated rock	
	(i) good section	0.017–0.020
	(ii) irregular section	0.022–0.027
8	Laboratory flumes-smooth metal bed and glass or perspex sides	0.009–0.010
(b)	<i>Unlined, non-erodible channels</i>	
1	Earth, straight and uniform	
	(i) clean, recently completed	0.016–0.020
	(ii) clean, after weathering	0.018–0.025
	(iii) gravel, uniform section, clean	0.022–0.030
	(iv) with short grass, few weeds	0.022–0.033
2	Channels with weeds and brush, uncut	
	(i) dense weeds, high as flow depth	0.05–0.12
	(ii) clean bottom, brush on sides	0.04–0.08
	(iii) dense weeds or aquatic plants in deep channels	0.03–0.035
	(iv) grass, some weeds	0.025–0.033
3	Rock	0.025–0.045
(c)	<i>Natural channels</i>	
1	Smooth natural earth channel, free from growth, little curvature	0.020
2	Earth channels, considerably covered with small growth	0.035
3	Mountain streams in clean loose cobbles, rivers with variable section with some vegetation on the banks	0.04–0.05
4	Rivers with fairly straight alignment, obstructed by small trees, very little under brush	0.06–0.075
5	Rivers with irregular alignment and cross-section, covered with growth of virgin timber and occasional patches of bushes and small trees	0.125

98 Flow in Open Channels

Where  $n_b$  = a base value of  $n$  for a straight uniform smooth channel in natural material

$n_1$  = correction for surface irregularities

$n_2$  = correction for variation in shape and size of the cross section

$n_3$  = correction for obstructions

$n_4$  = correction for vegetation and flow conditions

$m$  = correction for meandering of the channel

Values of the  $n_b$  and the other five correction factors are given in Chow<sup>10</sup> and in Ref. (14).

**Example 3.1** | A 2.0-m wide rectangular channel carries water at 20°C at a depth of 0.5 m. The channel is laid on a slope of 0.0004. Find the hydrodynamic nature of the surface if the channel is made of (a) very smooth concrete and (b) rough concrete.

**Solution** Hydraulic radius  $R = \frac{2 \times 0.5}{(2 + 2 \times 0.5)} = 0.333 \text{ m}$

$$\tau_0 = \gamma R S_0 = (9.81 \times 10^3) \times 0.333 \times 0.0004 = 1.308 \text{ N/m}^2$$

$$v_* = \text{shear velocity} = \sqrt{\frac{\tau_0}{\rho}} = \sqrt{\left(\frac{1.308}{10^3}\right)} = 0.03617 \text{ m/s}$$

(a) For a smooth concrete surface

From Table 3.1  $\varepsilon_s = 0.25 \text{ mm} = 0.00025 \text{ m}$

$\nu$  at 20°C =  $10^{-6} \text{ m}^2/\text{s}$

$$\frac{\varepsilon_s \nu_*}{\nu} = \frac{0.00025 \times 0.03617}{10^{-6}} = 9.04$$

Since this value is slightly greater than 4.0, the boundary is hydrodynamically in the early transition from smooth to rough surface

(b) For a rough concrete surface

From Table 3.1,  $\varepsilon_s = 3.5 \text{ mm} = 0.0035$

$$\frac{\varepsilon_s \nu_*}{\nu} = 126.6$$

Since this value is greater than 60, the boundary is hydrodynamically rough.

**Example 3.2** | For the two cases in Example 3.1, estimate the discharge in the channel using (i) the Chezy formula with Dancy–Weisbach  $f$ , and (ii) the Manning’s formula.

**Solution** Case (a): Smooth concrete channel

(i)  $\varepsilon_s = 0.25 \text{ mm}$  and  $\frac{\varepsilon_s}{4R} = \frac{0.25}{4 \times 0.33 \times 10^3} = 1.894 \times 10^{-4}$

Since the boundary is in the transitional stage, Eq. 3.8a would be used.

$$\frac{1}{\sqrt{f}} = 1.14 - 2.0 \log \left( \frac{\varepsilon_s}{4R} + \frac{21.25}{\mathbf{Re}^{0.9}} \right)$$

Here,  $\mathbf{Re}$  is not known to start with and hence a trial and error method has to be adopted. By trial

$$\begin{aligned} f &= 0.0145 \\ C &= \sqrt{8g/f} = 73.6 \\ V &= C \sqrt{RS_0} = 73.6 \times \sqrt{0.333 \times 0.0004} = 0.850 \text{ m/s} \\ Q &= AV = 0.850 \text{ m}^3/\text{s} \end{aligned}$$

(ii) Referring to Table 3.2, the value of  $n$  for smooth trowel-finished concrete can be taken as 0.012, By Manning's formula (Eq. 3.11),

$$\begin{aligned} V &= \frac{1}{0.012} \times (0.333)^{2/3} \times (0.0004)^{1/2} \\ &= 0.801 \text{ m/s} \\ Q &= AV = 0.801 \text{ m}^3/\text{s} \end{aligned}$$

Case (b): Rough concrete channel

$$(i) \varepsilon_s = 3.5 \text{ mm} \quad \text{and} \quad \frac{\varepsilon_s}{4R} = 2.625 \times 10^{-3}$$

Since the flow is in the rough-turbulent state, by Eq. 3.7,

$$\begin{aligned} \frac{1}{\sqrt{f}} &= 1.14 - 2 \log (2.625 \times 10^{-3}) \\ f &= 0.025 \\ C &= \sqrt{\left( \frac{8 \times 9.81}{0.025} \right)} = 56.0 \\ V &= 56 \times \sqrt{0.333 \times 0.0004} = 0.647 \text{ m/s} \\ Q &= AV = 0.647 \text{ m}^3/\text{s} \end{aligned}$$

(ii) By the Manning's Formula

From Table 3.2, for rough concrete,  $n = 0.015$  is appropriate

$$\begin{aligned} V &= \frac{1}{0.015} \times (0.333)^{2/3} \times (0.0004)^{1/2} \\ &= 0.641 \text{ m}^3/\text{s} \\ Q &= 0.641 \text{ m}^3/\text{s} \end{aligned}$$

[The following may be noted:

1. The subjectiveness involved in selecting proper value of  $\varepsilon_s$  and  $n$ .
2. The ease of calculations by using Manning's formula.
3. Reasonably accurate results can be obtained by the Manning's formula in rough-turbulent flows.]

**Empirical Formulae for  $n$**  Many empirical formulae have been presented for estimating Manning's coefficient  $n$  in natural streams. These relate  $n$  to the bed-particle size. The most popular form under this type is the Strickler formula:

$$n = \frac{d_{50}^{1/6}}{21.1} \quad (3.22)$$

Where  $d_{50}$  is in metres and represents the particle size in which 50 per cent of the bed material is finer. For mixtures of bed materials with considerable coarse-grained sizes, Eq. 3.17 has been modified by Meyer *et al.* as

$$n = \frac{d_{90}^{1/6}}{26} \quad (3.23)$$

Where  $d_{90}$  = size in metres in which 90 per cent of the particles are finer than  $d_{90}$ . This equation is reported to be useful in predicting  $n$  in mountain streams paved with coarse gravel and cobbles.

**Factors Affecting  $n$**  The Manning's  $n$  is essentially a coefficient representing the integrated effect of a large number of factors contributing to the energy loss in a reach. Some important factors are: (a) Surface roughness, (b) vegetation, (c) cross-section irregularity and (d) irregular alignment of channel. The chief among these are the characteristics of the surface. The dependence of the value of  $n$  on the surface roughness is indicated in Tables 3.1 and 3.2. Since  $n$  is proportional to  $(\epsilon_s)^{1/6}$ , a large variation in the absolute roughness magnitude of a surface causes correspondingly a small change in the value of  $n$ . The importance of other factors are indicated in Cowan's method of estimation of  $n$ , as mentioned earlier.

The vegetation on the channel perimeter acts as a flexible roughness element. At low velocities and small depths vegetations, such as grass and weeds, can act as a rigid roughness element which bends and deforms at higher velocities and depths of flow to yield lower resistance. For grass-covered channels, the value of  $n$  is known to decrease as the product  $VR$  increases. The type of grass and density of coverage also influence the value of  $n$ . For other types of vegetation, such as brush, trees in flood plains, etc. the only recourse is to account for their presence by suitably increasing the values of  $n$  given in Table 3.2, which of course is highly subjective.

Channel irregularities and curvature, especially in natural streams, produce energy losses which are difficult to evaluate separately. As such, they are combined with the boundary resistance by suitably increasing the value of  $n$ . The procedure is sometimes also applied to account for other types of form losses, such as obstructions that may occur in a reach of channel.

An interesting feature of the roughness coefficient is observed in some large rivers, where values of  $n$  at high stages have been found to be smaller when compared to the values of  $n$  at low stages. Typically,  $n$  can change from a value, such as 0.05 at low stages to 0.02 at high stages. No satisfactory explanation is available for this phenomenon. Another instance of similar, but possibly unrelated, variation of  $n$  with the stage is found in the flow through circular channels, such as sewers and tile

drains. In this case the largest value of  $n$  is found to occur when the depth of flow  $y_0 = 0.25 D$  and the least value at  $y_0 = D$ , where  $D =$  diameter of the channel. The range of variation of  $n$  is about 30 per cent.

The resistance to flow in alluvial channels is complex owing to the interaction of the flow, fluid and boundary. Detailed information on this is available in standard treatises on sediment transport (Section 11.3).

### 3.10 EQUIVALENT ROUGHNESS

In some channels different parts of the channel perimeter may have different roughnesses. Canals in which only the sides are lined, laboratory flumes with glass side walls and rough bed, natural rivers with sandy bed and sides with vegetation, flood plains with different land uses are some typical examples. For such channels it is necessary to determine an equivalent roughness coefficient that can be applied to the entire cross-sectional perimeter for use in Manning’s formula. This *equivalent roughness*, also called the *composite roughness*, represents a weighted average value for the roughness coefficient.

A large number of formulae, proposed by various investigators for calculating equivalent roughness of multi-roughness channel are available in literature. All of them are based on some assumptions and are approximately effective to the same degree. One of the commonly used method due to Horton (1933) and Einstein (1934) is described below. Table 3.3 lists several proposed formulae for equivalent roughness. For calculating subareas the dividing lines can be vertical lines or bisector of angles at the break in the geometry of the roughness element.

#### 3.10.1 Horton’s Method of Equivalent Roughness Estimation:

Consider a channel having its perimeter composed of  $N$  types of roughness,  $P_1, P_2, \dots, P_i, \dots, P_N$  are the lengths of these  $N$  parts and  $n_1, n_2, \dots, n_i, \dots, n_N$  are the respective roughness coefficients (Fig. 3.8). Let each part  $P_i$  be associated with a partial area  $A_i$  such that

$$\sum_{i=1}^N A_i = A_1 + A_2 + \dots + A_i + \dots + A_N = A = \text{total area}$$

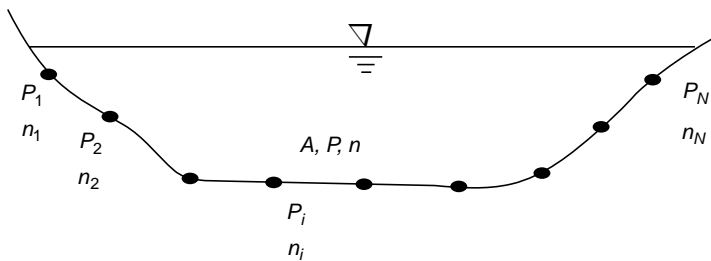


Fig. 3.8 Multi-roughness type perimeter



It is assumed that the mean velocity in each partial area is the mean velocity  $V$  for the entire area of flow, i.e.,

$$V_1 = V_2 = \dots = V_i = \dots = V_N = V$$

By the Manning's formula

$$\begin{aligned} S_0^{1/2} &= \frac{V_1 n_1}{R_1^{2/3}} = \frac{V_2 n_2}{R_2^{2/3}} = \dots = \frac{V_i n_i}{R_i^{2/3}} = \dots = \frac{V_N n_N}{R_N^{2/3}} \\ &= \frac{Vn}{R^{2/3}} \end{aligned} \quad (3.24)$$

Where  $n$  = equivalent roughness

From Eq. 3.24

$$\left(\frac{A_i}{A}\right)^{2/3} = \frac{n_i P_i^{2/3}}{nP^{2/3}}$$

$$A_i = A \frac{n_i^{3/2} P_i}{n^{3/2} P} \quad (3.25)$$

$$\sum A_i = A = A \frac{\sum (n_i^{3/2} P_i)}{n^{3/2} P}$$

i.e.

$$n = \frac{\left(\sum n_i^{3/2} P_i\right)^{2/3}}{P^{2/3}} \quad (3.26)$$

This equation affords a means of estimating the equivalent roughness of a channel having multiple roughness types in its perimeter. This formula was independently developed by Horton in 1933 and by Einstein in 1934. However, Eq. 3.26 is popularly known as Horton's formula

If the Darcy-Weisbach friction formula is used under the same assumption of (i) Velocity being equal in all the partial areas, and (ii) slope  $S_0$  is common to all partial areas, then

$$h_f / L = S_0 = \frac{fV^2}{8gR} = \frac{fV^2 P}{8gA}$$

Hence

$$\frac{V^2}{8gS_0} = \frac{A}{Pf} = \frac{A_i}{P_i f_i}$$

Thus

$$A_i/A = \frac{P_i f_i}{P f} \text{ and on summation } \sum_i^N A_i / A = \frac{\sum_i^N P_i f_i}{P f} = 1$$

i.e. 
$$\sum P_i f_i = Pf$$

or 
$$f = \frac{\sum P_i f_i}{P} \tag{3.27}$$

Table 3.3 lists some of the equations proposed for estimation of equivalent roughness. This list is extracted from Ref. 16 which contains a list of 17 equations for composite roughness calculation.

**Table 3.3** Equations for Equivalent Roughness Coefficient (Ref.10,16)

Sl. No	Investigator	$n_e$	Concept
1	Horton (1933); Einstein (1934)	$= \left[ \frac{1}{P} \sum (n_i^{3/2} P_i) \right]^{2/3}$	Mean Velocity is constant in all subareas.
2	Pavlovskii (1931) Muhlhofer (1933) Einstein and Banks (1950)	$= \left[ \frac{1}{P} \sum (n_i^2 P_i) \right]^{1/2}$	Total resistance force $F$ is sum of subarea resistance forces, $\sum F_i$
3	Lotter (1932)	$= \frac{PR^{5/3}}{\sum \frac{P_i R_i^{5/3}}{n_i}}$	Total discharge is sum of subarea discharges
4	Felkel (1960)	$= \frac{P}{\sum \frac{P_i}{n_i}}$	Total discharge is sum of subarea discharges
5	Krishnamurthy and Christensen (1972)	$= \exp \left[ \frac{\sum P_i h_i^{3/2} \ln n_i}{\sum P_i h_i^{3/2}} \right]$	Logarithmic velocity distribution over depth $h$ for wide channel
6	Yen (1991)	$= \frac{\sum (n_i P_i)}{P}$	Total shear velocity is weighted sum of subarea shear velocity

**Example 3.3** An earthen trapezoidal channel ( $n = 0.025$ ) has a bottom width of 5.0 m, side slopes of 1.5 horizontal: 1 vertical and a uniform flow depth of 1.1 m. In an economic study to remedy excessive seepage from the canal two proposals, viz (a) to line the sides only, and (b) to line the bed only are considered. If the lining is of smooth concrete ( $n = 0.012$ ), determine the equivalent roughness in the above two cases by using (i) Horton’s formula, and by (ii) Pavlovskii formula.

**Solution** Case (a) Lining of the sides only  
 Here for the bed:  $n_1 = 0.025$ , and  $P_1 = 5.0$  m.

For the sides:  $n_2 = n_3 = 0.012$ , and  $P_2 = P_3 = 1.10 \times \sqrt{1 + (1.5)^2} = 1.983$  m

(i) Equivalent roughness  $n_e$  by Horton's formula:  $n_e = \left[ \frac{1}{P} \sum (n_i^{3/2} P_i) \right]^{2/3}$

$$n_e = \frac{[5.0 \times (0.025)^{3/2} + 1.983 \times (0.012)^{3/2} + 1.983 \times (0.012)^{3/2}]^{2/3}}{[5.0 + 1.983 + 1.983]^{2/3}} = \frac{0.085448}{4.31584} = 0.0198$$

(ii) Equivalent roughness  $n_e$  by Pavlovskii formula:  $n_e = \left[ \frac{1}{P} \sum (n_i^2 P_i) \right]^{1/2}$

$$n_e = \frac{[5.0 \times (0.025)^2 + 1.983 \times (0.012)^2 + 1.983 \times (0.012)^2]^{1/2}}{[5.0 + 1.983 + 1.983]^{1/2}} = \frac{0.060796}{2.99433} = 0.0203$$

Case (b) Lining of the bed only

Here for the bed:  $n_1 = 0.012$  and  $P_1 = 5.0$  m.

For the sides:  $n_2 = n_3 = 0.025$ , and  $P_2 = P_3 = 1.10 \times \sqrt{1 + 1.5^2} = 1.983$  m

(i) Equivalent roughness  $n_e$  by Horton's formula:  $n_e = \left[ \frac{1}{P} \sum (n_i^{3/2} P_i) \right]^{2/3}$

$$n_e = \frac{[5.0 \times (0.012)^{3/2} + 1.983 \times (0.025)^{3/2} + 1.983 \times (0.025)^{3/2}]^{2/3}}{[5.0 + 1.983 + 1.983]^{2/3}} = \frac{0.079107}{4.31584} = 0.01833$$

(ii) Equivalent roughness  $n_e$  by Pavlovskii formula:  $n_e = \left[ \frac{1}{P} \sum (n_i^2 P_i) \right]^{1/2}$

$$n_e = \frac{[5.0 \times (0.012)^2 + 1.983 \times (0.025)^2 + 1.983 \times (0.025)^2]^{1/2}}{[5.0 + 1.983 + 1.983]^{1/2}} = \frac{0.05656}{2.99433} = 0.01889$$

### 3.11 UNIFORM FLOW COMPUTATIONS

The Manning's formula (Eq. 3.11) and the continuity equation,  $Q = AV$  form the basic equations for uniform-flow computations. The discharge  $Q$  is then given by

$$Q = \frac{1}{n} AR^{2/3} S_0^{1/2} \quad (3.28)$$

$$= K \sqrt{S_0} \quad (3.28a)$$

where,  $K = \frac{1}{n} AR^{2/3}$  is called the *conveyance* of the channel and expresses the discharge capacity of the channel per unit longitudinal slope. The term  $nK = AR^{2/3}$  is sometimes called *the section factor for uniform-flow computations*.

For a given channel,  $AR^{2/3}$  is a function of the depth of flow. For example, consider a trapezoidal section of bottom width =  $B$  and side slope  $m$  horizontal: 1 vertical. Then,

$$\begin{aligned}
 A &= (B + my)y \\
 P &= (B + 2y \sqrt{m^2 + 1}) \\
 R &= \frac{(B + my)y}{(B + 2y \sqrt{m^2 + 1})} \\
 AR^{2/3} &= \frac{(B + my)^{5/3} y^{5/3}}{(B + 2y \sqrt{m^2 + 1})^{2/3}} = f(B, m, y) \tag{3.29}
 \end{aligned}$$

For a given channel,  $B$  and  $m$  are fixed and  $AR^{2/3} = f(y)$ . Figure 3.9 shows the relationship of Eq. 3.29 in a non-dimensional manner by plotting  $\phi = \frac{AR^{2/3}}{B^{8/3}}$  vs  $y/B$  for different values of  $m$ . It may be seen that for  $m \geq 0$ , there is only one value  $y/B$  for each value of  $\phi$ , indicating that for  $m \geq 0$ ,  $AR^{2/3}$  is a single-valued function of  $y$ . This is also true for any other shape of channel provided that the top width is either constant or increases with depth. We shall denote these channels as *channels of the first kind*.

Since  $AR^{2/3} = \frac{Qn}{\sqrt{S_0}}$  and if  $n$  and  $S_0$  are fixed for a channel, the channels of the first kind have a unique depth in uniform flow associated with each discharge. This depth is called the *normal depth*. Thus the normal depth is defined as the depth of flow at which a given discharge flows as uniform flow in a given channel. The normal depth

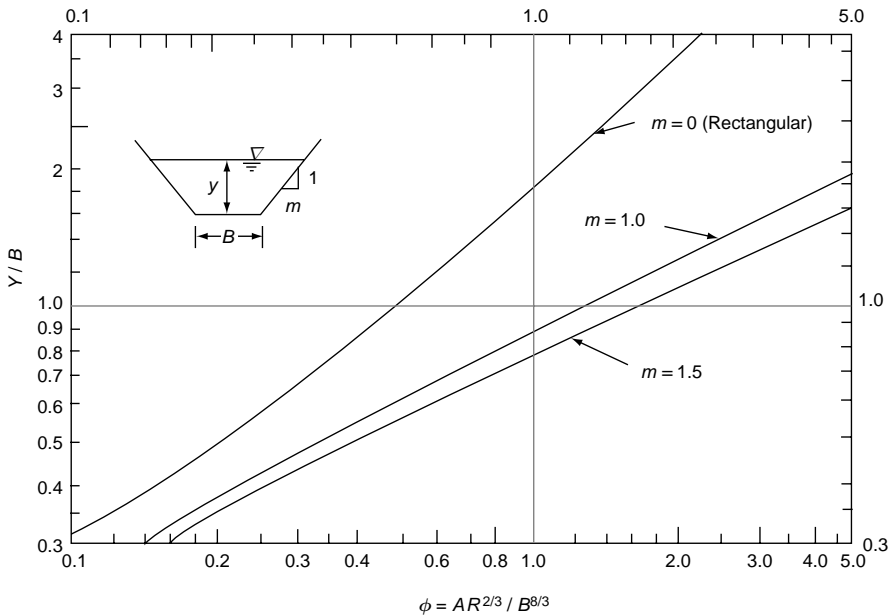


Fig. 3.9 Variation of  $\phi$  with  $y/B$  in trapezoidal channels

is designated as  $y_0$ , the suffix '0' being usually used to indicate uniform-flow conditions. The channels of the first kind thus have one normal depth only.

While a majority of the channels belong to the first kind, sometimes one encounters channels with closing top width. Circular and ovoid sewers are typical examples of this category, Channels with a closing top-width can be designated as *channels of the second kind*.

The variation of  $AR^{2/3}$  with depth of flow in two geometries of channels of second kind is shown in Fig. 3.10. It may be seen that in some ranges of depth,  $AR^{2/3}$  is not a single valued function of depth. For example

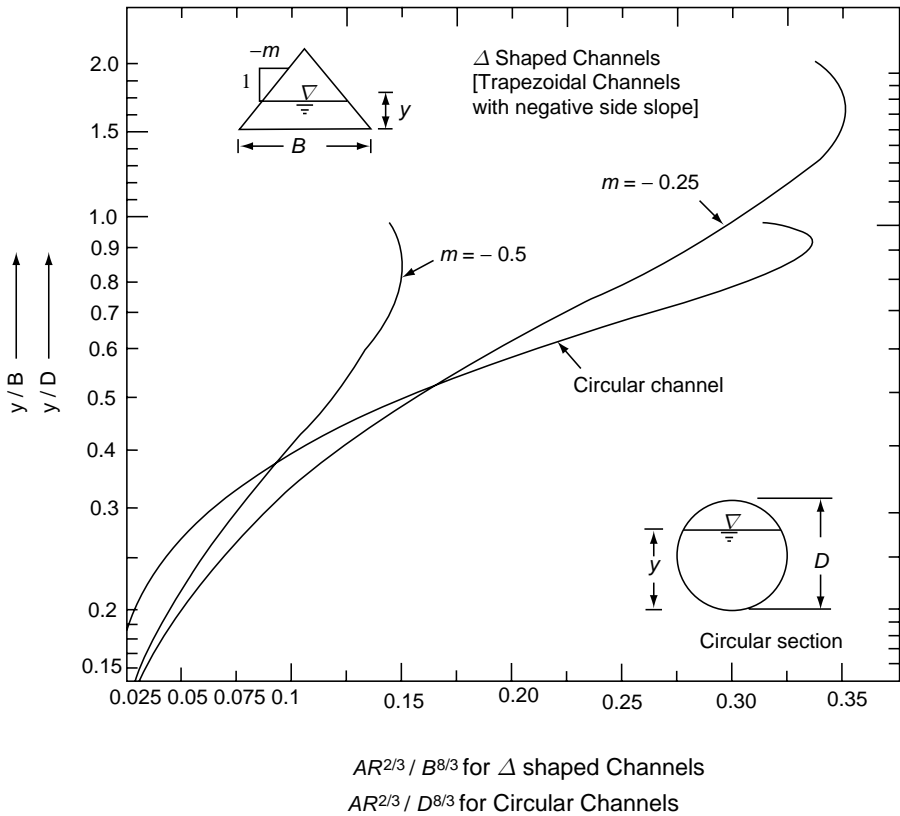


Fig. 3.10 Variation of  $AR^{2/3}$  in channels of the second kind

- (i) for circular channels the range  $\frac{y}{D} > 0.82$  has two values of  $y$  for a given value of  $AR^{2/3}$ .
- (ii) for  $\Delta$  shaped channels the following ranges of  $y/B$ , which depend on the value of side slope  $m$ , have two depths for a given value of  $AR^{2/3}$ :
  - for  $m = -0.25$ , the range  $\frac{y}{B} > 0.71$
  - for  $m = -0.50$ , the range  $\frac{y}{B} > 1.30$

As can be seen from Fig. 3.10, the channels of the second kind will have a finite depth of flow at which  $AR^{2/3}$ , and hence the discharge for a given channel is maximum.

**Types of Problems** Uniform flow computation problems are relatively simple. The available relations are

1. Manning's formula
2. Continuity equation
3. Geometry of the cross section

The basic variables in uniform flow situations can be the discharge  $Q$ , velocity of flow  $V$ , normal depth  $y_0$ , roughness coefficient  $n$ , channel slope  $S_0$  and the geometric elements (e, g.,  $B$  and  $m$  for a trapezoidal channel), There can be many other derived variables accompanied by corresponding relationships. From among the above, the following five types of basic problems are recognized.

Problem type	Given	Required
1	$y_0, n, S_0, \text{Geometric elements}$	$Q \text{ and } V$
2	$Q, y_0, n, \text{Geometric elements}$	$S_0$
3	$Q, y_0, S_0, \text{Geometric elements}$	$n$
4	$Q, n, S_0, \text{Geometric elements}$	$y_0$
5	$Q, y_0, n, S_0, \text{Geometry}$	Geometric elements

Problems of the types 1, 2 and 3 normally have explicit solutions and hence do not present any difficulty in their calculations. Problems of the types 4 and 5 usually do not have explicit solutions and as such may involve trial-and-error solutions procedures. A typical example for each type of problem is given below.

**Example 3.4** A trapezoidal channel is 10.0 m wide and has a side slope of 1.5 horizontal: 1 vertical. The bed slope is 0.0003. The channel is lined with smooth concrete of  $n = 0.012$ . Compute the mean velocity and discharge for a depth of flow of 3.0 m.

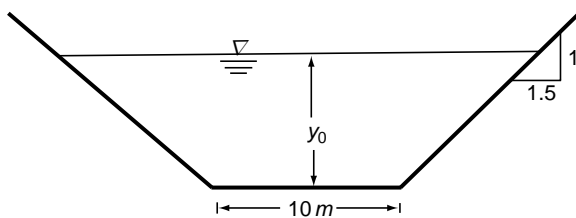


Fig. 3.11 Example 3.4

**Solution** Let  $y_0 =$  uniform flow depth  
 Here  $B = 10.0$  m and side slope  $m = 1.5$   
 Area  $A = (B + my) y$   
 $= (10.0 + 1.5 \times 3.0) 3.0 = 43.50 \text{ m}^2$   
 Wetted perimeter  $P = B + 2y \sqrt{m^2 + 1}$   
 $= 10.0 + 2 \sqrt{2.25 + 1} \times 3.0 = 20.817 \text{ m}$

Hydraulic radius  $R = \frac{A}{P} = 2.090 \text{ m}$

Mean velocity  $V = \frac{1}{n} R^{2/3} S_0^{1/2}$   
 $= \frac{1}{0.012} \times (2.09)^{2/3} \times (0.0003)^{1/2}$   
 $= 2.36 \text{ m/s}$

Discharge  $Q = AV = 102.63 \text{ m}^3/\text{s}$

**Example 3.5** In the channel of Example 3.4, find the bottom slope necessary to carry only  $50 \text{ m}^3/\text{s}$  of the discharge at a depth of  $3.0 \text{ m}$ .

Solution  $A = 43.50 \text{ m}^2$   
 $P = 20.817 \text{ m}$   
 $R = 2.09 \text{ m}$   
 $S_0 = \frac{Q^2 n^2}{A^2 R^{4/3}} = \frac{(50.0)^2 \times (0.012)^2}{(43.5)^2 \times (2.09)^{4/3}}$   
 $= 0.0000712$

**Example 3.6** A triangular channel with an apex angle of  $75^\circ$  carries a flow of  $1.2 \text{ m}^3/\text{s}$  at a depth of  $0.80 \text{ m}$ . If the bed slope is  $0.009$ , find the roughness coefficient of the channel.

Solution  $y_0 = \text{normal depth} = 0.80 \text{ m}$

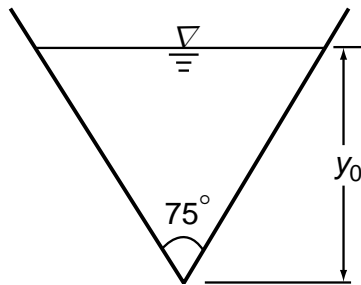


Fig. 3.12 Example 3.6

Referring to Fig. 3.12

Area  $A = \frac{1}{2} \times 0.80 \times 2 \times 0.8 \tan\left(\frac{75}{2}\right)$   
 $= 0.491 \text{ m}^2$

$$\begin{aligned}
 \text{Wetted perimeter} \quad P &= 2 \times 0.8 \times \sec 37.5^\circ = 2.0168 \text{ m} \\
 R &= A/P = 0.243 \text{ m} \\
 n &= \frac{AR^{2/3}S_0^{1/2}}{Q} = \frac{(0.491) \times (0.243)^{2/3} \times (0.009)^{1/2}}{1.20} \\
 n &= 0.0151
 \end{aligned}$$

**Example 3.7** | A 5.0-m wide trapezoidal channel having a side slope of 1.5 horizontal: 1 vertical is laid on a slope of 0.00035. The roughness coefficient  $n = 0.015$ . Find the normal depth for a discharge of 20 m<sup>3</sup>/s through this channel.

*Solution* Let

$$\begin{aligned}
 y_0 &= \text{normal depth} \\
 \text{Area} \quad A &= (5.0 + 1.5 y_0) y_0 \\
 \text{Wetted perimeter} \quad P &= 5.0 + 2\sqrt{3.25} y_0 \\
 &= 5.0 + 3.606 y_0 \\
 R &= A/P = \frac{(5.0 + 1.5 y_0) y_0}{(5.0 + 3.606 y_0)}
 \end{aligned}$$

$$\begin{aligned}
 \text{The section factor } AR^{2/3} &= \frac{Qn}{\sqrt{S_0}} \\
 \frac{(5.0 + 1.5 y_0)^{5/3} y_0^{5/3}}{(5.0 + 3.606 y_0)^{2/3}} &= \frac{20 \times 0.015}{(0.00035)^{1/2}} = 16.036
 \end{aligned}$$

Algebraically,  $y_0$  can be found from the above equation by the trial-and-error method. The normal depth is found to be 1.820 m

**Example 3.8** | A concrete-lined trapezoidal channel ( $n = 0.015$ ) is to have a side slope of 1.0 horizontal: 1 vertical. The bottom slope is to be 0.0004. Find the bottom width of the channel necessary to carry 100 m<sup>3</sup>/s of discharge at a normal depth of 2.50 m.

*Solution* Let  $B$  = bottom width. Here,  $y_0$  = normal depth = 2.50 m,  $m = 1.0$

$$\begin{aligned}
 \text{Area} \quad A &= (B + 2.5) \times 2.5 \\
 \text{Wetted perimeter} \quad P &= (B + 2\sqrt{2} \times 2.5) = B + 7.071
 \end{aligned}$$

$$\frac{Qn}{\sqrt{S_0}} = \frac{100 \times 0.015}{\sqrt{0.0004}} = 75 = AR^{2/3}$$

$$\frac{[(B + 2.5) \times 2.5]^{5/3}}{(B + 7.071)^{2/3}} = 75.0$$

By trial-and-error  $B = 16.33$  m.



### 3.11.1 Computation of Normal Depth

It is evident from Example 3.7 that the calculation of normal depth for a trapezoidal channel involves a trial-and-error solution. This is true for many other channel shapes also. Since practically all open channel problems involve normal depth, special attention towards providing aids for quicker calculations of normal depth is warranted. A few aids for computing normal depth in some common channel sections are given below.

#### 3.11.2 Rectangular Channel

(a) *Wide Rectangular Channel* For a rectangular channel, (Fig. 3.13)

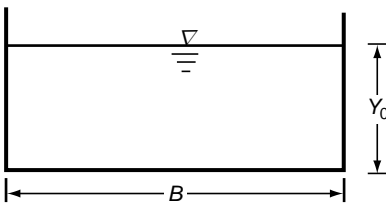


Fig. 3.13 Rectangular channel

Area  $A = By_0$   
 Wetter perimeter  $P = B + 2y_0$   
 Hydraulic radius

$$R = \frac{By_0}{B + 2y_0} = \frac{y_0}{1 + 2y_0 / B}$$

As  $y_0/B$ , the aspect ratio of the channel decreases,  $R \rightarrow y_0$ . Such channels with large bed-widths as compared to their respective depths are known as *wide rectangular channels*. In these channels, the hydraulic radius approximates to the depth of flow.

Considering a unit width of a wide rectangular channel,

$$A = y_0, R = y_0 \quad \text{and} \quad B = 1.0$$

$$\frac{Q}{B} = q = \text{discharge per unit width} = \frac{1}{n} y_0^{5/3} S_0^{1/2}$$

$$y_0 = \left[ \frac{qn}{\sqrt{S_0}} \right]^{3/5} \tag{3.30}$$

This approximation of a wide rectangular channel is found applicable to rectangular channels with  $y_0/B < 0.02$ .

(b) *Rectangular Channels with  $y_0/B \geq 0.02$*  For these channels  $\frac{Qn}{\sqrt{S_0}} = AR^{2/3}$

$$AR^{2/3} = \frac{(By_0)^{5/3}}{(B + 2y_0)^{2/3}} = \frac{(y_0 / B)^{5/3}}{(1 + 2y_0 / B)^{2/3}} B^{8/3}$$

$$\frac{Qn}{\sqrt{S_0} B^{8/3}} = \frac{AR^{2/3}}{B^{8/3}} = \frac{(\eta_0)^{5/3}}{(1 + 2\eta_0)^{2/3}} = \phi(\eta_0) \tag{3.31}$$

Where  $\eta_0 = \frac{y_0}{B}$

Tables of  $\phi(\eta_0)$  vs  $\eta_0$  will provide a non-dimensional graphical solution aid for general application. Since  $\phi = \frac{Qn}{\sqrt{S_0} B^{8/3}}$ , one can easily find  $y_0/B$  from this table for any combination of  $Q$ ,  $n$ ,  $S_0$  and  $B$  in a rectangular channel.

### 3.11.3 Trapezoidal Channel

Following a procedure similar to the above, for a trapezoidal section of side slope  $m : 1$ , (Fig. 3.14)

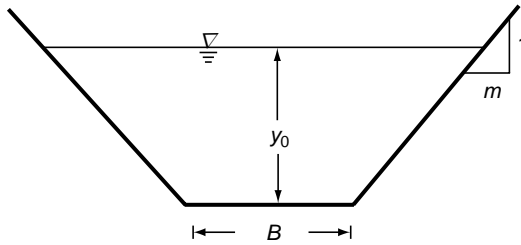


Fig. 3.14 Trapezoidal channel

Area  $A = (B + my_0) y_0$

Wetter perimeter  $P = (B + 2\sqrt{m^2 + 1} y_0)$

Hydraulic radius  $R = A/P = \frac{(B + my_0)y_0}{(B + 2\sqrt{m^2 + 1} y_0)}$

$$\frac{Qn}{\sqrt{S_0}} = AR^{2/3} = \frac{(B + my_0)^{5/3} y_0^{5/3}}{(B + 2\sqrt{m^2 + 1} y_0)^{2/3}}$$

Non-dimensionalising the variables,

$$\frac{AR^{2/3}}{B^{8/3}} = \frac{Qn}{\sqrt{S_0} B^{8/3}} = \frac{(1 + m\eta_0)^{5/3} (\eta_0)^{5/3}}{(1 + 2\sqrt{m^2 + 1} \eta_0)^{2/3}} = \phi(\eta_0, m) \tag{3.32}$$

Where  $\eta_0 = y_0/B$

Equation 3.32 could be represented as curves or Tables of  $\phi$  vs  $\eta_0$  with  $m$  as the third parameter to provide a general normal depth solution aid. It may be noted that  $m = 0$  is the case of a rectangular channel. Table 3A.1 given in Appendix 3A at the end of this chapter gives values of  $\phi$  for  $\eta_0$  in the range 0.1 to 1.70 and  $m$  in the range 0 to 2.5. Values of  $\eta_0$  are close enough for linear interpolation between successive values. This table will be useful in quick solution of a variety of uniform flow problems in rectangular and trapezoidal channels. Similar table of  $\phi$  vs  $\eta_0$  for any desired  $m$  values and ranges of  $\eta_0$  can be prepared very easily by using a spread sheet such as MS Excel.

**Example 3.9** A trapezoidal channel with a bed width of 5.0 m and side slopes of 1.5 H: 1 V is laid on a slope of 0.0004. Find the normal depth corresponding to discharges of (i) 10.0 m<sup>3</sup>/s, and (ii) 20.0 m<sup>3</sup>/s in this channel. Use Table 3A.1 and take  $n = 0.015$  for both cases.

**Solution** For  $Q = 10.0$  m<sup>3</sup>/s

$$\phi = \frac{Qn}{\sqrt{S_0} B^{8/3}} = \frac{10.0 \times 0.015}{(0.0004)^{1/2} \times (5.0)^{8/3}} = 0.1026$$

Looking up in Table 3A.1 under  $m = 1.5$

$$\phi = 0.10211 \quad \text{for } \eta_0 = 0.240$$

$$\phi = 0.10597 \quad \text{for } \eta_0 = 0.245$$

By linear interpolation  $\eta_0 = 0.24063$  for  $\phi = 0.1026$ .

Thus normal depth  $y_0 = 0.24063 \times 5.0 = 1.203$  m

For  $Q = 20.0$  m<sup>3</sup>/s.

$$\phi = \frac{Qn}{\sqrt{S_0} B^{8/3}} = \frac{20.0 \times 0.015}{(0.0004)^{1/2} \times (5.0)^{8/3}} = 0.2052$$

Looking up in Table 3 A.1 under  $m = 1.5$

$$\phi = 0.20382 \quad \text{for } \eta_0 = 0.350$$

$$\phi = 0.20930 \quad \text{for } \eta_0 = 0.355$$

By linear interpolation  $\eta_0 = 0.3513$  for  $\phi = 0.2052$ .

Thus normal depth  $y_0 = 0.3513 \times 5.0 = 1.756$  m

### 3.11.4 Circular Channel

Let  $D$  be diameter of a circular channel (Fig 3.15) and  $2\theta$  be the angle in radians subtended by the water surface at the centre.

$A$  = area of the flow section

= area of the sector OMN – area of the triangle OMN

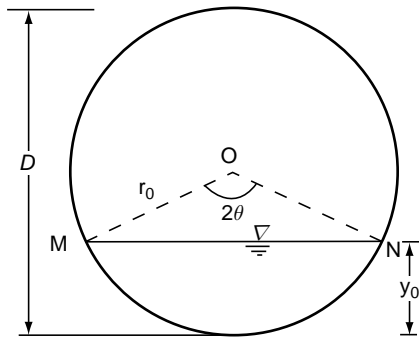


Fig. 3.15 Circular channel

$$\begin{aligned} A &= \frac{1}{2} r_0^2 2\theta - \frac{1}{2} \cdot 2r_0 \sin \theta \cdot r_0 \cos \theta \\ &= \frac{1}{2} (r_0^2 2\theta - r_0^2 \sin 2\theta) \\ &= \frac{D^2}{8} (2\theta - \sin 2\theta) \end{aligned} \quad (3.33)$$

$$\begin{aligned} P &= \text{wetted perimeter} \\ &= 2r_0 \theta = D\theta \end{aligned} \quad (3.34)$$

$$\text{Also } \cos \theta = \frac{r_0 - y_0}{r_0} = \left(1 - \frac{2y_0}{D}\right)$$

$$\text{Hence } \theta = f(y_0/D)$$

$$Q = \frac{1}{n} AR^{2/3} S_0^{1/2}$$

Assuming  $n = \text{constant}$  for all depths

$$\frac{Qn}{\sqrt{S_0}} = \frac{A^{5/3}}{P^{2/3}} = \frac{D^{10/3}}{8^{5/3}} \frac{(2\theta - \sin 2\theta)^{5/3}}{(D_\theta)^{2/3}}$$

Non-dimensionalising both sides

$$\begin{aligned} \frac{Qn}{\sqrt{S_0} D^{8/3}} &= \frac{AR^{2/3}}{D^{8/3}} = \frac{1}{32} \frac{(\theta - \sin 2\theta)^{5/3}}{\theta^{2/3}} \\ &= \phi(y_0/D) \end{aligned} \quad (3.35)$$

The functional relationship of Eq. 3.35 has been evaluated for various values of  $y_0/D$  and is given in Table 2A.1 in Appendix 2A. Besides  $AR^{2/3}/D^{8/3}$ , other geometric elements of a circular channel are also given in the table which is very handy in solving problems related to circular channels. Using this table, with linear interpolations wherever necessary, the normal depth for a given  $D$ ,  $Q$ ,  $n$  and  $S_0$  in a circular channel can be determined easily. The graphical plot of Eq. 3.35 is also shown in Fig. 3.10.

As noted earlier, for depths of flow greater than  $0.82D$ , there will be two normal depths in a circular channel. In practice, it is usual to restrict the depth of flow to a value of  $0.8D$  to avoid the region of two normal depths. In the region  $y/D > 0.82$ , a small disturbance in the water surface may lead the water surface to seek alternate normal depths, thus contributing to the instability of the water surface.

**Example 3.10** | A trunk sewer pipe of 2.0-m diameter is laid on a slope of 0.0004. Find the depth of flow when the discharge is  $2.0 \text{ m}^3/\text{s}$ . (Assume  $n = 0.014$ .)

$$\begin{aligned} \text{Solution } \frac{AR^{2/3}}{D^{8/3}} &= \frac{Qn}{\sqrt{S_0} D^{8/3}} = \frac{2.0 \times 0.014}{\sqrt{0.0004} \times (2.0)^{8/3}} \\ &= 0.22049 \end{aligned}$$

$$\begin{aligned} \text{From Table 2A. 2, } \frac{AR^{2/3}}{D^{8/3}} &= 0.22004 \text{ at } \frac{y_0}{D} = 0.62 \\ &= 0.22532 \text{ at } y_0/D = 0.63 \end{aligned}$$

$$\text{By interpolation, for } AR^{2/3}/D^{8/3} = 0.22049, y_0/D = 0.621$$

$$\text{The normal depth of flow } y_0 = 1.242 \text{ m}$$

[Note: The advantage of using Table 2A.1 in calculating the normal depth in circular channels can be appreciated if one tries to solve this problem by trial and error]

### 3.12 STANDARD LINED CANAL SECTIONS

Canals are very often lined to reduce seepage losses and related problems. Exposed hard surface lining using materials such as cement concrete, brick tiles, asphaltic concrete and stone masonry form one of the important category of canal lining and especially so for canals with large discharges. For such hard surface lined canals the cross-section recommended by Indian Standards (IS: 4745 – 1968)<sup>12</sup> consists of a trapezoidal cross-section with corners rounded off with a radius equal to the full supply depth, (Fig. 3.16). For discharges less than 55 m<sup>3</sup>/s, a triangular lined section with bottom portion rounded off with a radius equal to full supply depth, (Fig. 3.17), is recommended by the Central Water Commission. (CWC), India. For convenience and ease of identification, the above two channel sections are termed *standard lined canal sections* and, in particular, as *standard lined trapezoidal section* and *standard lined triangular section* respectively. Note that the standard lined triangular section is the limiting case of the standard lined trapezoidal section with  $B = 0$ . These standard lined sections have interesting geometrical properties which are beneficial in the solution of some uniform flow problems.

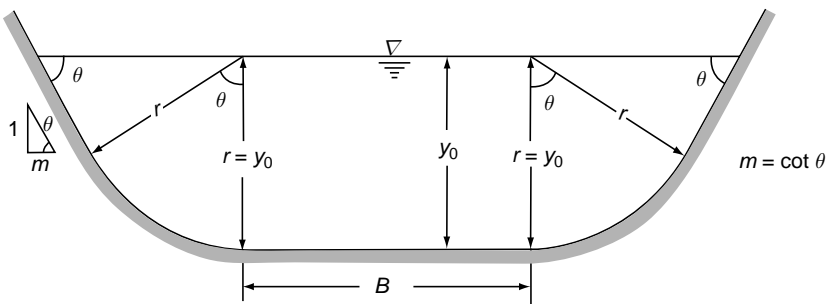


Fig. 3.16 Standard lined trapezoidal channel section for  $Q > 55 \text{ m}^3/\text{s}$

**Standard Lined Trapezoidal Section** Referring to Fig. 3.16, the full supply depth = normal depth at design discharge =  $y_0$ . At normal depth

$$\begin{aligned} \text{Area} \quad A &= By_0 + my_0^2 + y_0^2 \theta \\ &= (B + y_0 \varepsilon) y_0 \end{aligned} \quad (3.36)$$

$$\text{Where} \quad \varepsilon = m + \theta = \left( m + \tan^{-1} \frac{1}{m} \right) \quad (3.37)$$

$$\text{Wetter perimeter} \quad P = B + 2my_0 + 2y_0 \theta = B + 2y_0 \varepsilon \quad (3.38)$$

$$\text{Hydraulic radius} \quad R = A/P = \frac{(B + y_0 \varepsilon) y_0}{B + 2y_0 \varepsilon}$$

By Manning's formula

$$Q = \frac{1}{n} \left[ \frac{(B + y_0 \varepsilon)^{5/3} y_0^{5/3}}{(B + 2y_0 \varepsilon)^{2/3}} \right] S_0^{1/2}$$

Non-dimensionalising the variables,

$$\frac{Qn \varepsilon^{5/3}}{S_0^{1/2} B^{8/3}} = \phi_1(\eta_0) = \frac{(1 + \eta_0)^{5/3} \eta_0^{5/3}}{(1 + 2\eta_0)^{2/3}} \quad (3.39)$$

Where

$$\eta_0 = \left( \frac{y_0 \varepsilon}{B} \right)$$

From Eq. 3.39 the function  $\phi_1$  can be easily evaluated for various values of  $\eta_0$ . A table of  $\phi_1$  vs  $\eta_0$  or a curve of  $\phi_1$  vs  $\eta_0$  affords a quick method for the solution of many types of problems associated with lined trapezoidal channels.

**Standard Lined Triangular Section** Referring to Fig. 3. 17, at normal depth  $y_0$ ,

Area  $A = 2 \left( \frac{m y_0^2}{2} \right) + \theta y_0^2 = \varepsilon y_0^2 \quad (3.40)$

Where as before  $\varepsilon = m + \theta = \left( m + \tan^{-1} \frac{1}{m} \right)$

Wetted perimeter  $P = 2y_0 \varepsilon \quad (3.41)$

and hydraulic radius  $R = A/P = y_0/2 \quad (3.42)$

By Manning's formula  $Q = \frac{1}{n} (\varepsilon y_0^2) (y_0 / 2)^{2/3} S_0^{1/2}$

or  $\phi_T = \frac{Qn}{S_0^{1/2} y_0^{8/3} \varepsilon} = 0.63 \quad (3.43)$

By using Eq. 3.43 elements of standard lined triangular channels in uniform flow can be easily determined.

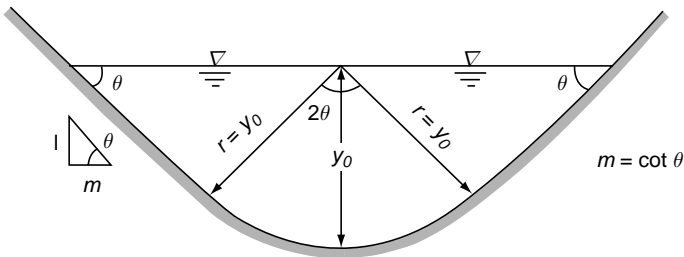


Fig. 3.17 Standard lined triangular channel section for  $Q \leq 55 \text{ m}^3/\text{s}$

**Example 3.11** A standard lined trapezoidal canal section is to be designed to convey  $100 \text{ m}^3/\text{s}$  of flow. The side slopes are to be 1.5 horizontal: 1 vertical and Manning's  $n = 0.016$ . The longitudinal slope of the bed is 1 in 5000. If a bed width of 10.0 m is preferred what would be the normal depth?

**Solution** Referring to Fig. 3.16,  $m = \text{side slope} = 1.5$

$$\varepsilon = m + \tan^{-1} \frac{1}{m} = 1.5 + \tan^{-1}(1/1.5) = 2.088$$

Further, here  $Q = 100.0 \text{ m}^3/\text{s}$ ,  $n = 0.016$ ,  $S_0 = 0.0002$ ,  $B = 10.0 \text{ m}$

$$\phi_1 = \frac{Qn\varepsilon^{5/3}}{S_0^{1/2}B^{8/3}} = \frac{100 \times 0.016 \times (2.088)^{5/3}}{(0.0002) \times (10.0)^{8/3}} = 0.8314$$

By Eq.(3.39) 
$$\phi_1 = \frac{(1 + \eta_0)^{5/3} \eta_0^{5/3}}{(1 + 2\eta_0)^{2/3}} = 0.8314$$

On Simplifying, 
$$\frac{(1 + \eta_0)^{5/3} \eta_0^{5/3}}{(1 + 2\eta_0)^{2/5}} = 0.8951$$

On solving by trial and error 
$$\eta_0 = \frac{y_0\varepsilon}{B} = 0.74$$

The normal depth 
$$y_0 = \frac{0.74 \times 10.0}{2.088} = 3.544 \text{ m}$$

**Example 3.12** Show that for a standard lined trapezoidal canal section with side slopes of  $m$  horizontal: 1 vertical, and carrying a discharge of  $Q$  with a velocity  $V_s$ ,

$$\eta_0 = \frac{1}{2} \left[ -1 + \sqrt{1 + \frac{4}{M - 4}} \right]$$

Where  $\eta_0 = \frac{y_0\varepsilon}{B}$ ;  $\varepsilon = m + \tan^{-1} \frac{1}{m}$ ;  $M = \frac{QS_0^{3/2}}{V_s^4 n^3 \varepsilon}$  and  $n$  is Manning's coefficient.

Also examine the situation when (i)  $M \rightarrow 4$  and (ii)  $M < 4$ .

**Solution** For a standard lined trapezoidal canal section (Fig.3.16)

Area  $A = (B + y_0\varepsilon) y_0 = Q/V_s$  (3.44)

Perimeter  $P = (B + 2 y_0\varepsilon)$

Hydraulic radius  $R = A/P = \frac{Q}{V_s P}$  (3.45)

From Manning's formula  $V_s = \frac{1}{n} R^{2/3} S_0^{1/2}$

i.e  $R^2 = \frac{V_s^3 n^3}{S_0^{3/2}}$  (3.46)

Substituting for  $R$  in Eq. 3.45  $\frac{Q^2}{V_s^2 P^2} = \frac{V_s^3 n^3}{S_0^{3/2}}$

Hence 
$$P^2 = \frac{Q^2 S_0^{3/2}}{V_s^5 P^3} = B^2 \left( 1 + \frac{2y_0 \varepsilon}{B} \right)^2 \quad (3.47)$$

Putting 
$$\eta_0 = \frac{y_0 \varepsilon}{B}$$

from Eq. 3.44 
$$B^2 = \varepsilon \left( \frac{Q}{V_s} \right) \frac{1}{(1 + \eta_0) \eta_0}$$

Substituting for  $B^2$  in Eq. 3.47 
$$\begin{aligned} \frac{(1 + 2\eta_0)^2}{\eta_0^2 + \eta_0} &= \frac{Q^2 S_0^{3/2}}{V_s^5 n^3} \left[ \frac{V_s}{\varepsilon Q} \right] \\ &= \frac{Q S_0^{3/2}}{V_s^4 n^3} = M \end{aligned}$$

Hence 
$$\begin{aligned} 1 + 4\eta_0^2 + 4\eta_0 &= M\eta_0^2 + M\eta_0 \\ (M - 4)\eta_0^2 + (M - 4)\eta_0 - 1 &= 0 \end{aligned}$$

On solving 
$$\eta_0 = \frac{1}{2} \left[ -1 + \sqrt{1 + \frac{4}{M - 4}} \right]$$

- (i) When  $M \rightarrow 4$ ,  $\eta_0 = \frac{y_0 \varepsilon}{B} \rightarrow \infty$ , since  $y_0$  and  $\varepsilon$  are finite values this corresponds to  $B \rightarrow 0$ . Thus  $M = 4$ , corresponds to the case of standard lined triangular channel section.
- (ii) When  $M < 4$ ,  $\eta_0$  is imaginary and hence this is not physically realisable proposition.

[Note: The expression for  $\eta_0$  in terms of  $M$  derived as above is very useful in solving some uniform flow problems relating to standard lined trapezoidal sections where  $V_s$  is known, (for e.g. Problem 3.28)].

### 3.13 MAXIMUM DISCHARGE OF A CHANNEL OF THE SECOND KIND

It was shown in Section 3.11 that the channels of the second kind have two normal depths in a certain range and there exists a finite depth at which these sections carry maximum discharge. The condition for maximum discharge can be expressed as

$$\frac{dQ}{dy} = 0 \quad (3.48)$$



118 Flow in Open Channels

Assuming  $n$  = constant at all depths, for a constant  $S_0$ , Eq. 3.48 can be rewritten as

$$\frac{d}{dy}(AR^{2/3}) = 0 \quad (3.49)$$

i.e. 
$$\frac{d}{dy}(A^5 / P^2) = 0 \quad (3.49a)$$

Knowing  $AR^{2/3} = f(y)$  for a given channel, Eq. 3.49 can be used to evaluate the depth for maximum discharge.

**Example 3.13** | Analyse the maximum discharge in a circular channel.

*Solution* Referring to Fig. 3.15, from Eq. 3.33

$$A = \frac{D^2}{8}(2\theta - \sin 2\theta)$$

and from Eq. 3.34  $P = D\theta$

For the maximum discharge, from Eq. 3.49a

$$\frac{d}{d\theta}(A^5 / P^2) = 0$$

i.e. 
$$5P \frac{dA}{d\theta} - 2A \frac{dP}{d\theta} = 0$$

$$5D\theta \frac{D^2}{8}(2 - 2 \cos 2\theta) - 2 \frac{D^2}{8}(2\theta - \sin 2\theta) D = 0$$

$$3\theta - 5\theta \cos 2\theta + \sin 2\theta = 0$$

The solution of this equation is obtained as  $\theta = 150^\circ 11'$ ,

$$y_0/D = \frac{1 - \cos \theta}{2} = 0.938$$

Hence the depth of flow for maximum discharge  $y_0 = 0.938 D$

At 
$$y_0/D = 0.935, \quad \left( \frac{AR^{2/3}}{D^{8/3}} \right) = 0.3353$$

Also when 
$$y_0/D = 1.0, \quad \left( \frac{AR^{2/3}}{D^{8/3}} \right) = 0.3117$$

Hence if  $Q_f$  = discharge with  $y_0 = D$ , i.e. the pipe running just full, and  $Q_m$  = maximum discharge then

$$\frac{Q_m}{Q_f} = \frac{0.3353}{0.3117} = 1.0757$$

Thus the maximum discharge will be 7.6 per cent more than the pipe full discharge.

[Note that if chezy formula with a constant  $C$  is used, Eq. 3.49 would become  $\frac{d}{dy} (AR^{1/2}) = 0$ . The solution would correspondingly change. The depth for maximum discharge would be  $y_0 = 0.95D$ .]

### 3.14 HYDRAULICALLY EFFICIENT CHANNEL SECTION

The conveyance of a channel section of a given area increases with a decrease in its perimeter. Hence a channel section having the minimum perimeter for a given area of flow provides the maximum value of the conveyance. With the slope, roughness coefficient and area of flow fixed, a minimum perimeter section will represent the *hydraulically efficient* section as it conveys the maximum discharge. This channel section is also called the *best section*.

Of all the various possible open channel sections, the semicircular shape has the least amount of perimeter for a given area. However, for any other selected geometrical shape, the relationship between the various geometric elements to form an efficient section can be obtained as follows.

**(a) Rectangular Section** Bottom width =  $B$  and depth of flow =  $y$

Area of flow  $A = By = \text{constant}$

Wetted perimeter  $P = B + 2y$

$$= \frac{A}{y} + 2y$$

If  $P$  is to be minimum with  $A = \text{constant}$ ,

$$\frac{dP}{dy} = -\frac{A}{y^2} + 2 = 0$$

Which gives  $A = 2y_e^2$

i.e.  $y_e = B_e/2, B_e = 2y_e$  and  $R_e = \frac{y_e}{2}$  (3.50)

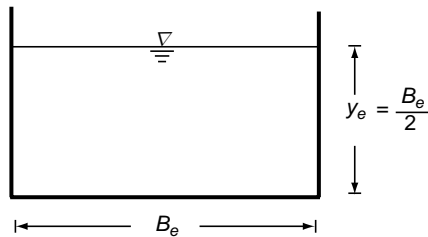


Fig. 3.18 Hydraulically efficient rectangular channel

The suffix ‘ $e$ ’ denotes the geometric elements of a hydraulically efficient section. Thus it is seen that for a rectangular channel when the depth of flow is equal to half the bottom width, i.e., when the channel section is a half-square, a hydraulically efficient section is obtained (Fig. 3.18).

**(b) Trapezoidal Section** Bottom width =  $B$ , side slope =  $m$  horizontal: 1 vertical

Area  $A = (B + my)y = \text{constant}$

$$B = \frac{A}{y} - my \tag{3.51}$$

Wetter perimeter  $B + 2y\sqrt{m^2 + 1}$

$$= \frac{A}{y} - my + 2y\sqrt{m^2 + 1} \quad (3.52)$$

Keeping  $A$  and  $m$  as fixed, for a hydraulically efficient section,

$$\frac{dP}{dy} = -\frac{A}{y^2} - m + 2\sqrt{m^2 + 1} = 0$$

i.e.  $A = (2\sqrt{1 + m^2} - m)y_e^2 \quad (3.53)$

Substituting in eqs 3.51 and 3.52

$$B_e = 2y_e(\sqrt{1 + m^2} - m) \quad (3.54)$$

$$P_e = 2y_e(2\sqrt{1 + m^2} - m) \quad (3.55)$$

$$R_e = \frac{(2\sqrt{1 + m^2} - m)y_e^2}{2(2\sqrt{1 + m^2} - m)y_e} = y_e / 2 \quad (3.56)$$

A hydraulically efficient trapezoidal section having the proportions given by Eqs 3.53 to 3.56 is indicated in Fig. 3.19. Let  $O$  be centre of the water surface.  $OS$  and  $OT$  are perpendiculars drawn to the bed and sides respectively.

$$OS = y_e$$

$$OT = OR \sin\theta = \frac{OR}{\sqrt{m^2 + 1}}$$

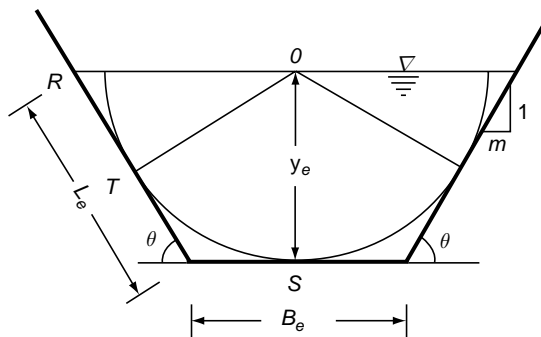


Fig. 3.19 Hydraulically efficient trapezoidal channel

$$OR = \frac{1}{2} B_e + my_e.$$

Substituting for  $B_e$  from Eq. 3.50,

$$OR = y_e \sqrt{1 + m^2}$$

$$OT = OS = y_e$$

Thus the proportions of a hydraulically efficient trapezoidal section will be such that a semicircle can be inscribed in it.

In the above analysis, the side slope  $m$  was held constant. However, if  $m$  is allowed to vary, the optimum value of  $m$  to make  $P_e$  most efficient is obtained by putting

$$\frac{dP_e}{dm} = 0, \text{ from Eqs 3.55 and 3.53}$$

$$P_e = 2\sqrt{A(2\sqrt{1+m^2} - m)} \quad (3.57)$$

Setting  $\frac{dp_e}{dm} = 0$  in Eq. 3.57 gives

$$m_{em} = \frac{1}{\sqrt{3}} = \cot \theta$$

$$\theta_{em} = 60^\circ$$

Where the suffix 'em' denotes the most efficient section, Further.

$$p_{em} = 2y_{em} \left( 2\sqrt{1+1/3} - \frac{1}{\sqrt{3}} \right) = 2\sqrt{3} y_{em} \quad (3.58a)$$

$$B_{em} = 2y_{em} \left( 2\sqrt{1+1/3} - \frac{1}{\sqrt{3}} \right) = \frac{2}{\sqrt{3}} y_{em} \quad (3.58b)$$

$$A = \left( 2\sqrt{1+1/3} - \frac{1}{\sqrt{3}} \right) y_{em}^2 = \sqrt{3} y_{em}^2 \quad (3.58c)$$

If  $L$  = length of the inclined side of the canal, it is easily seen that

$$L_{em} = \frac{2}{\sqrt{3}} y_{em} = B_{em}$$

Thus the hydraulically most efficient trapezoidal section is one-half of a regular hexagon.

Using the above approach, the relationship between the various geometrical elements to make different channel shapes hydraulically efficient can be determined. Table 3.4 contains the geometrical relation of some most efficient sections.

### 3.14.1 Uniform flow in Most Efficient Channels

It is seen from Table 3.4 that the area  $A$  and hydraulic radius  $R$  of a most efficient hydraulic section can be represented as

$A_{em} = k_1 y_{em}^2$  and  $R = K_2 y_{em}$  where  $K_1$  and  $K_2$  are constants which depend upon the channel shape. Thus the discharge in uniform flow through a most efficient channel section can be represented as

$$Q = \frac{1}{n} (K_1 y_{em}^2) \times (K_2 y_{em})^{2/3} \times (S_0^{1/2})$$

$$\frac{Qn}{y_{em}^{8/3} S_0^{1/2}} = K_{em} \quad (3.59)$$

where  $K_{em} = K_1 K_2^{2/3}$  is a constant unique to each channel shape. Thus for rectangular shape, from Table 3.4,  $K_1 = 2$  and  $K_2 = 1/2$  and hence  $K_{em} = 1.260$ . similarly, values

**Table 3.4** Proportions of Some Most Efficient Sections

Sl. No	Channel Shape	Area ( $A_{em}$ )	Wetted Perimeter ( $P_{em}$ )	Width ( $B_{em}$ )	Hydraulic Radius ( $R_{em}$ )	Top width ( $T_{em}$ )	$\frac{Qn}{y_{em}^{8/3} S_0^{1/2}} = K_{em}$
1	Rectangle (Half square)	$2 y_{em}^2$	$4 y_{em}$	$2 y_{em}$	$\frac{y_{em}}{2}$	$2 y_{em}$	1.260
2	Trapezoidal (Half regular hexagon, $m = \frac{1}{\sqrt{3}}$ )	$\sqrt{3} y_{em}^2$	$2\sqrt{3} y_{em}$	$\frac{2}{\sqrt{3}} y_{em}$	$\frac{y_{em}}{2}$	$\frac{4 y_{em}}{\sqrt{3}}$	1.091
3	Circular (semi-circular)	$\frac{\pi}{2} y_{em}^2$	$\pi y_{em}$	$D = 2 y_{em}$	$\frac{y_{em}}{2}$	$2 y_{em}$	0.9895
4	Triangle (Vertex angle = $90^\circ$ )	$y_{em}^2$	$2\sqrt{3} y_{em}$	–	$\frac{y_{em}}{2\sqrt{2}}$	$2 y_{em}$	0.500

of  $K_{em}$  for other channel shapes are calculated and shown in Col. 8 of Table 3.4. The use of  $K_{em}$  in calculating parameters of uniform flow in most efficient channel sections is shown in Example 3.15 and 3.16.

**Example 3.14** | A slightly rough brick-lined ( $n = 0.017$ ) trapezoidal channel carrying a discharge of  $25.0 \text{ m}^3/\text{s}$  is to have a longitudinal slope of  $0.0004$ . Analyse the proportions of an efficient trapezoidal channel section having a side slope of 1.5 horizontal: 1 vertical.

**Solution** For an efficient trapezoidal section having a side slope of  $m$ , by Eq. 3.53

$$A_e = (2 \times \sqrt{1+m^2} - m) y_e^2 = (2 \times \sqrt{1+(1.5)^2} - 1.5) y_e^2$$

$$R_e = y_e/2 \text{ and } Q = 25.0 \text{ m}^3/\text{s}$$

Substituting a Manning's formula,

$$25.0 = \frac{1}{0.017} \times (2.1056 y_e^2) \times (y_e/2)^{2/3} \times (0.0004)^{1/2}$$

$$y_e = 2.830 \text{ m}$$

$$\text{By Eq. (3.54), } B_e = 2y_e(\sqrt{1+m^2} - m) = 2 \times 2.830 \times (\sqrt{1+(1.5)^2} - (1.5)) = 1.714 \text{ m}$$

**Example 3.15** | When the normal depth of flow in most efficient circular concrete ( $n = 0.014$ ) section laid on a bed slope of  $0.005$  is  $0.50 \text{ m}$ , estimate the discharge.

**Solutions** For the most efficient circular section

From Table 3.4,  $\frac{Qn}{y_{em}^{8/3} S_0^{1/2}} = 0.9895$ . In the present case  $y_{em} = 0.5$  and  $S_0 = 0.005$ .

$$\text{Hence } Q = \frac{0.9895}{0.014} \times (0.5)^{8/3} \times (0.005)^{1/2} = 0.787 \text{ m}^3/\text{s}.$$

**Example 3.16** Determine the normal depth, bed width and sides slopes of a most efficient trapezoidal channel section to carry a discharge of 25 m<sup>3</sup>/s. The longitudinal slope of the channel is to be 0.0009 and Manning's  $n$  can be taken as 0.015.

**Solution** For the most efficient trapezoidal section

From Table 3.4,  $\frac{Qn}{y_{em}^{8/3} S_0^{1/2}} = 1.091$ . In the present case  $Q = 25.0$  m<sup>3</sup>/s and  $S_0 = 0.0009$ .

$$\text{Hence } y_{em}^{-8/3} = \frac{1.091 \times (0.0009)^{1/2}}{25.0 \times 0.015} = 0.08728$$

$$y_{em} = 2.50 \text{ m}$$

$$\text{Also, from Table 3.4, } B_{em} = \frac{2}{\sqrt{3}} y_{em} = \frac{2}{\sqrt{3}} \times 2.50 = 2.887 \text{ m}$$

$$\text{Sides slope of most efficient trapezoidal channel section, } m = \frac{1}{\sqrt{3}} = 0.57735$$

### 3.15 THE SECOND HYDRAULIC EXPONENT $N$

The conveyance of a channel is in general a function of the depth of flow. In calculations involving gradually varied flow, for purposes of integration, Bakhmeteff introduced the following assumption

$$K^2 = C_2 y^N \quad (3.60)$$

Where  $C_2$  = a coefficient and  $N$  = an exponent called here as the *second hydraulic exponent* to distinguish it from the first hydraulic exponent  $M$  associated with the critical depth. It is found that the second hydraulic exponent  $N$  is essentially constant for a channel over a wide range of depths. Alternatively,  $N$  is usually a slowly varying function of the aspect ratio of the channel.

To determine  $N$  for any channel, a plot of  $\log K$  vs  $\log y$  is prepared. If  $N$  is constant between two points  $(K_1, y_1)$  and  $(K_2, y_2)$  in this plot, it is determined as

$$N = 2 \frac{\log (K_1 / K_2)}{\log (y_1 / y_2)}$$

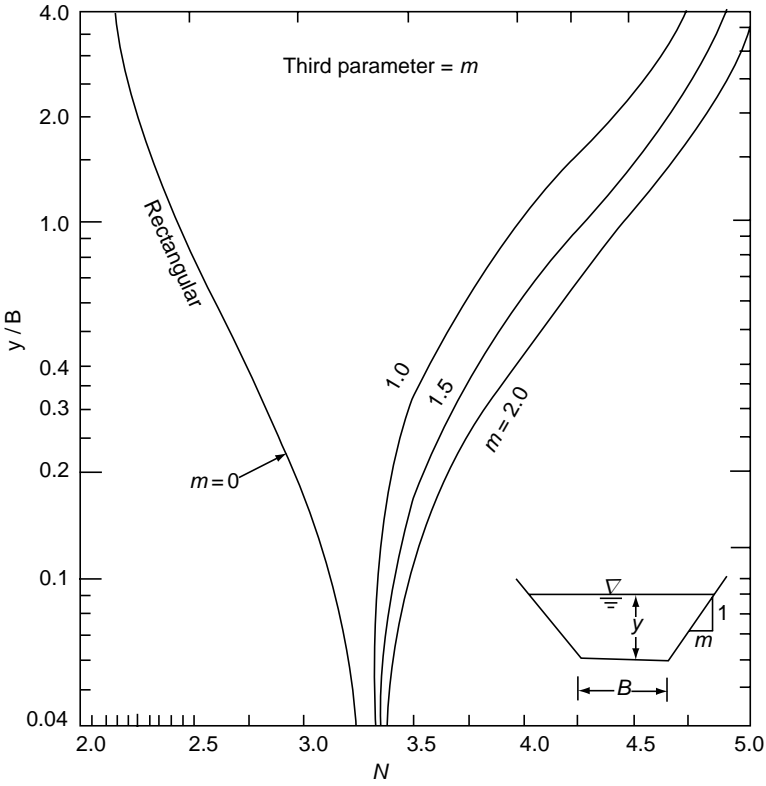


Fig. 3.20 Variation of the second hydraulic exponent  $N$  in trapezoidal channels

For a trapezoidal channel, if  $\phi = \frac{AR^{2/3}}{B^{8/3}}$  given in Table 3A.1 is plotted against  $\eta = y/B$  on a log paper, from the slope of the curve at any  $\eta$ , the value of  $N$  at that point can be estimated. Figure 3.20 shows the variation of  $N$  for trapezoidal channels. The values of  $N$  in this curve have been generated based on the slope of the  $\log K - \log y$  relation using a computer. Figure 3.20 is useful in the quick estimation of  $N$ . It is seen from this figure that  $N$  is a slowly-varying function of  $y/B$ . For a trapezoidal section, the minimum value of  $N = 2.0$  is obtained for a deep rectangular channel and a maximum value of  $N = 5.33$  is obtained for a triangular channel. It may be noted that if the Chezy formula with  $C = \text{constant}$  is used, values of  $N$  different from the above would result.

**Example 3.17** Obtain the value  $N$  for (a) a wide rectangular channel, and (b) a triangular channel.

**Solution** (a) For a Wide Rectangular Channel  
Considering unit width,  $A = y$

$$R = y$$

$$K^2 = \frac{1}{n^2} y^2 (y^{4/3}) = C_2 y^N$$

By equating the exponents of  $y$  on both sides;  $N = 3.33$

(b) For a Triangular Channel of Side Slope  $m$  Horizontal: 1 Vertical

$$A = my^2, P = 2y\sqrt{m^2 + 1}$$

$$R = \frac{m}{2\sqrt{m^2 + 1}} y$$

$$K^2 = \frac{1}{n^2} (my^2)^2 \left( \frac{m}{2\sqrt{m^2 + 1}} y \right)^{4/3} = C_2 y^N$$

By equating the exponents of  $y$  on both sides,  $N = 5.33$ .

### 3.16 COMPOUND CHANNELS

A compound channel is a channel section composed of a main deep portion and one or two flood plains that carry high-water flows. The main channel carries the dry weather flow and during wet season, the flow may spillover the banks of the main channel to the adjacent flood plains. A majority of natural rivers have compound sections. A compound section is also known as *two-stage channel*. The hydraulic conditions of the main channel and the flood plain differ considerably, especially in the channel geometry and in its roughness. The flood plains generally have considerably larger and varied roughness elements. (Fig. 3.21).

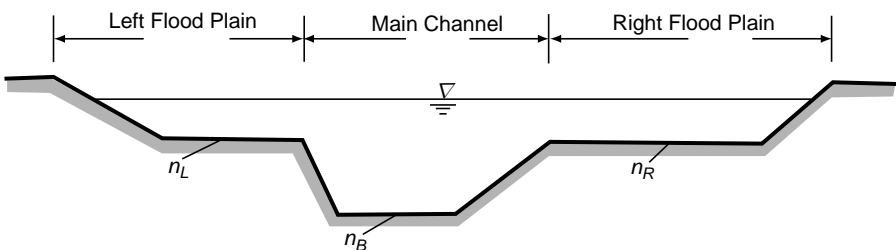


Fig. 3.21 Schematic sketch of a compound channel

The flow in the compound channel when the water is flowing in both the main and flood plains is indeed complicated. The velocity of flow in the flood plain is lower than in the main channel due to relative smaller water depth and higher bed roughness. The main channel flow will have interaction with the flow in the flood plains leading to severe momentum exchange at the interface. Further, there will be complicated interaction with the boundaries at the junction which give rise to



several sets of vortices leading to turbulence generation. The interactions of the main channel flow and the flood plain flows are indeed very complex. Figure 3.22, due to Knight and Shinno<sup>17</sup>, shows a conceptual model of this interaction scenario. Various prominent flow features at the junction of the main and flood bank flows are depicted in this figure. The following salient features are significant:

- At the junction of the main channel with the flood plain a set of vortex structures having vertical axis extending up to the water surface exist. This vortex set is believed to be responsible for momentum exchange between the main and shallow water flows.
- Presence of helical secondary flows in the longitudinal stream direction at various corners of the channel section as shown in Fig. 3.22. These secondary flows have different directions at different corners and have influence in modifying the boundary shear stress.

Field observations have indicated that in the overbank flow situation, the mean velocity of flow for the whole cross section decreases as the depth of flow increases, reaches a minimum and then onwards begins to increase with the depth.

In one-dimensional analysis, Manning's formula is applied to the compound channel by considering a common conveyance  $K$  and a common energy slope  $S_f$  for

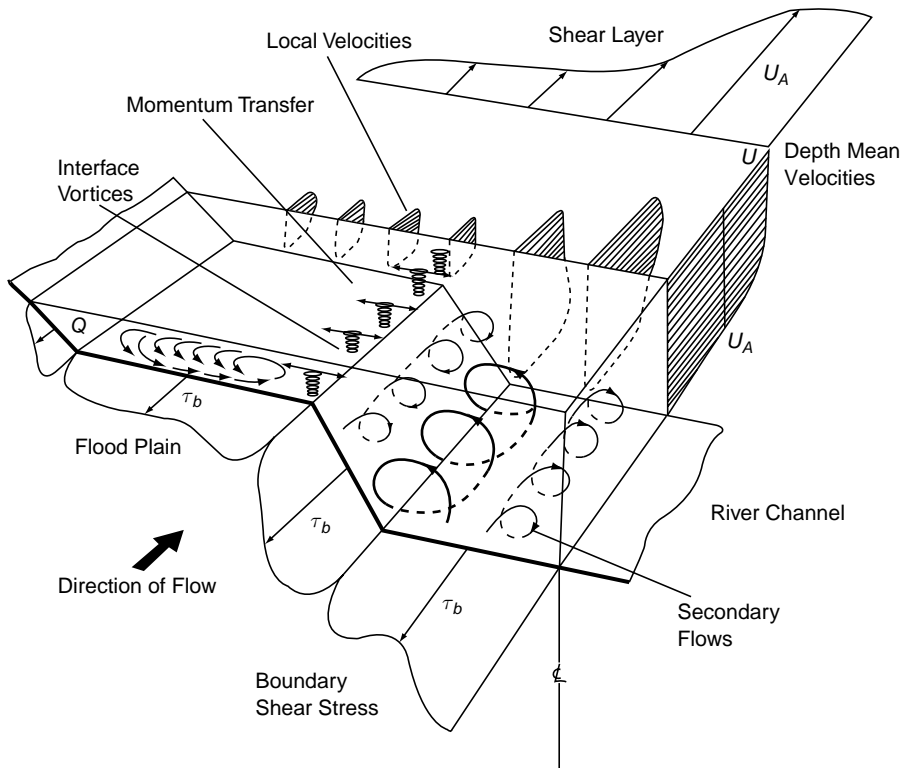


Fig. 3.22 Conceptual model of interaction of flows in flood bank and main channel (Ref. 17)

the entire section to obtain the discharge as  $Q = K \sqrt{S_f}$ . However, to account for the different hydraulic conditions of the main and flood plain sections, the channel is considered to be divided into subsections with each subsection having its own conveyance,  $K_i$ . The sum of the conveyances will give the total channel conveyance ( $\sum K_i = K$ ) for use in discharge computation. Various methods for defining the boundaries of the sub-sections are proposed by different researchers leading to a host of proposed methods. However, the overall method of considering the channel as a composite of sub sections is well accepted and the method is known as *Divided Channel method* (DCM). Currently DCM is widely used and many well-known software packages, including HEC-RAS (2006), adopt this method in dealing with compound channels.

### 3.16.1 Divided Channel Method (DCM)

A large number of methods of defining the sub-sections in the divided channel method are available in literature. These include vertical interface, diagonal interface; horizontal interface, curved interface and variable interface to divide the sub-sections. However, the following two methods are popular, been well studied and have been found to give reasonably good results:

**1. Vertical Interface Method** In this method the flood banks are separated from the main channel by means of vertical interface, (as shown in Fig. 3.24). This interface is considered as a surface of zero shear where in no transfer of momentum takes place. As such, the length of the vertical interface is not included in the calculation of the wetted perimeter of either the over bank flow or the main channel flow.

**2. Diagonal Interface Method** In this method, a diagonal interface (as in Fig. 3.23) is considered from the top of the main channel bank to the centerline of the water surface. This interface is considered to be a surface of zero shear stress and as such the length of the diagonal interfaces are not included in the calculation of the wetted perimeters of the over bank and main channel flows. If the over bank portion has significant roughness discontinuities equivalent roughness (as indicated Sec. 3.10) for over bank region can be adopted.

While there is no general agreement to choose a particular method, it is generally believed that the vertical interface method or the diagonal interface method seem to give the best results. HEC-RAS uses vertical interface procedure. In the procedure adopted by HEC-RAS, the flow in the over bank areas are subdivided using the *n-values break points* (locations where *n-values* change significantly) as the basis. Main channel is not normally subdivided. Conveyance is calculated for each sub division by considering vertical interface. It is known the DCM over estimates the discharge to some extent and due to extreme complexity of the hydraulics of the problem, a high degree of accuracy in the discharge estimation should not be expected in any of the procedures connected with compound channels. Example 3.18 illustrates the use of these two DCM procedures.

An improvement of the DCM is the *Weighted Divided Channel Method* (WDCM) due to Lambert and Myers. In this method, improved mean velocities in the main channel and flood plain areas are obtained by using a defined weighing factor to the velocities in the stream sections predicted by vertical interface method and horizontal interface method. In horizontal interface method the channel is considered to be divided in to two parts by a horizontal interface at the level of the banks of the main channel. The top portion is considered as shallow overland flow and the bottom deep portion is the main channel the depth of flow being only up to the top of the banks as restricted by the horizontal interface. This interface is considered as a surface of zero shear and as such, the length of the horizontal interface is not included in the calculation of the wetted perimeter of either the over bank flow or the main channel flow.

### 3.16.2 Other Methods

In addition to the DCM, there have been many other approaches to the study of compound channel discharge distribution problem. Ref. (18, 19.) contain brief reviews of these methods and also results of important studies. Briefly, salient approaches other than DCM are:

**Empirical Methods** Several empirical methods have been developed for estimating the discharge division between the main channel and the flood channel. Out of these methods the *Coherence method* of Ackers (1993) and the  $\phi$ -*index method* of Wormleaton and Merrit (1990) are prominent.

**Numerical Methods** Computation procedures of solving governing equations by using various turbulence models have been used by various researchers.

**Exchange Discharge Model(EDM)** This model proposed by Bousmar and Zech(1999) focuses on exchange of discharges and momentum transfers through a computation procedures.

**Example 3.18** | A compound channel is symmetrical in cross section and has the following geometric properties.

*Main channel: Trapezoidal cross section, Bottom width = 15.0 m, Side slopes = 1.5 H : 1V, Bank full depth = 3.0 m, Manning's coefficient = 0.03, Longitudinal slope = 0.0009 Flood plains: Width = 75 m, Side slope = 1.5 H : 1V, Manning's coefficient = 0.05, Longitudinal slope = 0.0009. Compute the uniform flow discharge for a flow with total depth of 4.2 m by using DCM with (i) diagonal interface, and (ii) vertical interface procedures.*

**Solution** The schematic representation of the channel is shown in Fig. 3.23. Figure 3.24 and 3.25 are the definition sketches of diagonal interface and vertical interface methods, respectively.

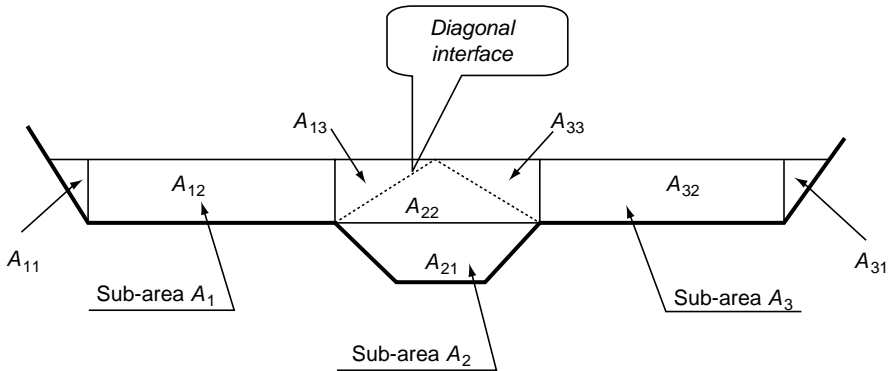


Fig. 3.23 Channel cross-sectional area division for diagonal interface procedure-Example-3.18

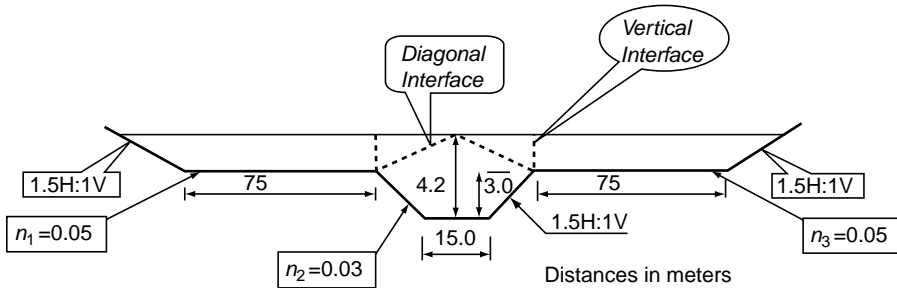


Fig. 3.24 Schematic representation of compound channel of Example-3.18

(i) **Diagonal Interface Procedure** The channel section is considered divided into three subsections  $A_1$ ,  $A_2$  and  $A_3$ , by means of two diagonal interface as shown in Fig. 3.23. The calculation of area and wetted perimeters of each of the three sub-areas is given below:

By symmetry, Sub-area  $A_1 = \text{Sub-area } A_3$ . The diagonal interfaces are as indicated in Fig. 3.23. As per the rules of this computation procedure, the interfaces are treated as

Table of Computation of Geometrical Properties – Diagonal Interfaces:

Sub-area	Area Element	Area ( $m^2$ )	Wetted Perimeter (m)		Hyd. Radius (m)
$A_1$	$A_{11}$	$[0.5 \times 1.2 \times (1.5 \times 1.2)]$	1.08	$1.2 \times (1+1.5)^2)^{0.5}$	2.163
	$A_{12}$	$75 \times 1.2$	90	75	75
	$A_{13}$	$[(0.5 \times 15) + (1.5 \times 3)] \times 0.5 \times 1.2$	7.2	0	0
	<b>Totals</b>		<b>98.28</b>		<b>77.16</b>
$A_2$	$A_{21}$	$[15 + (1.5 \times 3.0)] \times 3.0$	58.5	$15 + 2 \times 3.0 \times [1+(1.5)^2]^{0.5}$	25.82
	$A_{22}$	$[15 + (2 \times 1.5 \times 3)] \times 0.5 \times 1.2$	14.4	0	0
	<b>Totals</b>		<b>72.9</b>		<b>25.82</b>

surfaces of zero shear stress and hence are not included in the calculation of the wetted perimeter.

Discharge by Manning's formula:

$$\text{Sub-Area } A_1 \quad Q_1 = \frac{1}{0.05} \times 98.28 \times (1.274)^{2/3} \times (0.0009)^{1/2} = 69.287 \text{ m}^3/\text{s}$$

$$\text{Sub-Area } A_2 \quad Q_2 = \frac{1}{0.03} \times 72.90 \times (2.824)^{2/3} \times (0.0009)^{1/2} = 145.640 \text{ m}^3/\text{s}$$

$$\text{Sub-Area } A_3 \quad Q_3 = Q_1 = \frac{1}{0.05} \times 98.28 \times (1.274)^{2/3} \times (0.0009)^{1/2} = 69.287 \text{ m}^3/\text{s}$$

$$\text{Total discharge } Q = Q_1 + Q_2 + Q_3 = 284.21 \text{ m}^3/\text{s}$$

**(ii) Vertical Interface Procedure** The channel section is considered divided into three subsections,  $A_1$ ,  $A_2$ , and  $A_3$ , by means of two vertical interfaces which start at the intersection of the flood plains and the main channel as shown in Fig. 3.25. The calculation of area wetted perimeters of each of the three sub-areas is given below:

By symmetry, sub-area  $A_1 =$  sub-area  $A_3$ . The vertical interfaces are as indicated in Fig. 3.25. As per the rules of this computation procedure, the interfaces are treated as surfaces of zero shear stress and hence are not included in the calculation of the wetted perimeter.

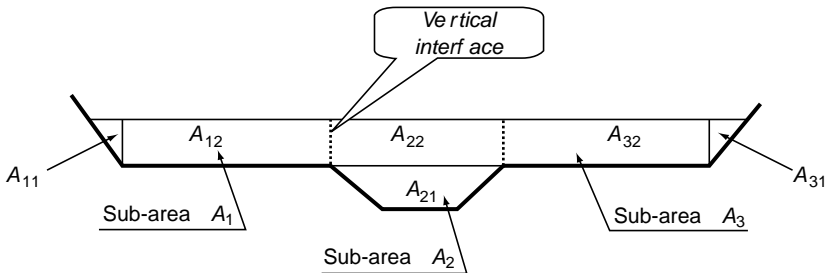


Fig. 3.25 Channel cross-sectional area division for vertical interface procedure — Example-3.18

Table of Computation of Geometrical properties  $M$  – Vertical Interfaces

Sub-area	Area Element	Area ( $\text{m}^2$ )		Wetted Perimeter ( $\text{m}$ )		Hyd. Radius ( $\text{m}$ )
$A_1$	$A_{11}$	$[0.5 \times 1.2 \times (1.5 \times 1.2)]$	1.08	$1.2 \times (1 + (1.5)^2)^{0.5}$	2.163	<b>1.180</b>
	$A_{12}$	$75 \times 1.2$	90	75	75	
	<b>Totals</b>		<b>91.08</b>		<b>77.163</b>	
$A_2$	$A_{21}$	$[15 + (1.5 \times 3.0)] \times 3.0$	58.5	$15 + 2 \times 3.0 \times [1 + (1.5)^2]^{0.5}$	25.817	<b>3.382</b>
	$A_{22}$	$[15 + (2 \times 1.5 \times 3)] \times 1.2$	28.8	0	0	
	<b>Totals</b>		<b>87.3</b>		<b>25.817</b>	

Discharge by Manning's formula:

$$\text{Sub-Area } A_1 \quad Q_1 = \frac{1}{0.05} \times 91.08 \times (1.180)^{2/3} \times (0.0009)^{1/2} = 61.035 \text{ m}^3/\text{s}$$

$$\text{Sub-Area } A_2 \quad Q_2 = \frac{1}{0.03} \times 87.3 \times (3.382)^{2/3} \times (0.0009)^{1/2} = 196.697 \text{ m}^3/\text{s}$$

$$\text{Sub-Area } A_3 \quad Q_3 = Q_1 = \frac{1}{0.05} \times 91.08 \times (1.180)^{2/3} \times (0.0009)^{1/2} = 61.035 \text{ m}^3/\text{s}$$

$$\text{Total discharge } Q = Q_1 + Q_2 + Q_3 = 318.77 \text{ m}^3/\text{s}$$

### 3.17 CRITICAL SLOPE

Critical slope is the slope of a specified channel necessary to have uniform flow of a given discharge with critical depth as the normal depth. Thus the normal discharge formula

$$Q = \frac{1}{n} AR^{2/3} S^{1/2} \text{ would become}$$

$$Q = \frac{1}{n} A_c R_c^{2/3} S_c^{1/2} \quad (3.61)$$

Where  $A_c$  = area of the channel at critical depth  $y_c$

$R_c$  = hydraulic radius of the channel at critical depth  $y_c$  and

$S_c$  = critical slope

$$\text{From Eq. 3.61} \quad S_c = \left( \frac{n^2 Q^2}{A_c^2 R_c^{4/3}} \right) \quad (3.62)$$

Since the critical depth is a function of the channel geometry and the discharge, the critical slope  $S_c$  for a give channel is a function of the discharge. If the critical slope  $S_c$  is larger than the channel slope  $S_0$  the normal depth of flow will be larger than the critical depth and the flow is subcritical and the channel is called *mild slope channel*. Similarly, if the critical slope  $S_c$  is smaller than the channel slope  $S_0$  the normal depth of flow will be smaller than the critical depth and the flow is supercritical and the channel is called *steep slope channel*. Further, if the critical slope  $S_c$  is equal to the channel slope  $S_0$  the normal depth of flow is equal to the critical depth and the flow is critical and the channel is called as *Critical slope channel*. Further details about the channel classification are given in Chapter 4. Thus the critical slope of a channel is a conceptual slope value which depends on the discharge in the channel. Its relative value with respect to the actual slope of the channel determines the nature of flow of the discharge in the channel.

Consider a wide rectangular channel. The expression for the critical slope  $S_c$  given in Eq. 3.62 becomes,

$$S_c = \frac{n^2}{g y_c^{1/3}} \quad (3.62a)$$

Substituting the value of critical depth as  $y_c = (q^2 / g)^{1/3}$ ,

$$S_c = \left( \frac{n^2 g^{10/9}}{q^{2/9}} \right) \quad (3.63)$$

This Eq. 3.63 indicates that  $S_c$  decreases with increase in  $q$  and asymptotically reaches a value of zero for  $q \rightarrow \infty$ . However for a rectangular channel of finite aspect ratio, the behavior is slightly different, the wide rectangular channel being the limiting case.

### 3.17.1 Critical Depth for Rectangular Channel of Finite Aspect Ratio

Consider a rectangular channel of width  $B$ . By Eq. 3.62

$$S_c = \left( \frac{n^2 Q^2}{A_c^2 R_c^{4/3}} \right)$$

For critical flow condition in the channel,  $\frac{Q^2}{g} = \frac{A_c^3}{T_c}$ . Also  $R_c = \frac{B y_c}{(B + 2 y_c)}$ .

Substituting for  $A_c$  and  $R_c$  in Eq. 3.62 and after simplifying

$$S_c = \frac{g n^2}{B^{1/3}} \left[ \frac{\left( 1 + \frac{2 y_c}{B} \right)^{4/3}}{\frac{y_c}{B}} \right]$$

$$S_{*c} = \frac{S_c B^{1/3}}{g n^2} = \frac{(1 + 2\eta)^{4/3}}{\eta^{1/3}} \quad (3.64)$$

where  $\eta = y_c/B$ .

The variation of the non-dimensional term  $S_{*c} = \frac{S_c B^{1/3}}{g n^2}$  with  $\eta$  is shown in Fig. 3.26.

It is seen that the parameter  $S_{*c}$  and hence  $S_c$  has a minimum value at a value of  $\eta = \eta_{\min}$  and increase on either side of this  $\eta_{\min}$  value. Thus there is a minimum value of critical slope for a rectangular channel. The minimum value of critical slope is known as *Limit slope* and is designated as  $S_L$ . By differentiating Eq. 3.64 with respect to  $\eta$  and equating the derivative to zero, the minimum value of  $\eta = \eta_{\min} = y_c/B$  is found to be 1/6. The corresponding value of minimum  $S_{*c}$  is 8/3. Hence for a rectangular channel the limit slope is described by

$$S_L = \frac{8}{3} \left( \frac{g n^2}{B^{1/3}} \right) \quad (3.65)$$

and this slope occurs at  $\eta_{\min} = y_c/B = 1/6$ .

From Fig. 3.26 it can be observed that the channel slope is mild for all areas lying to the left of the critical slope curve and it is steep for all areas lying to the right of the critical slope curve. From Eq. 3.65 it can be observed that the limit slope decreases with increase in the value of  $B$  and as such for very large values of  $B$ , the limit slope  $S_L \approx 0$ . Non-existence of limit slope for a wide rectangular channel is also seen from the behavior of critical slope for such channels as given by Eq. 3.63. The ratio  $S_c/S_L$  is given by

$$S_c / S_L = \frac{3(1+2\eta)^{4/3}}{8\eta^{1/3}} = \left[ \frac{3}{8} S_{*c} \right] \tag{3.65a}$$

Thus the abscissa of Fig. 3.26 also represents  $S_c/S_L$ ; a unit of  $x$ -axis being 2.667 units of  $S_c/S_L$ . If the actual bed slope of the channel  $S_0$  is less than  $S_L$ , the channel slope remains mild for all values of depth. However, for any  $S_0 > S_L$ , there is a range of depths  $y_{c1}$  and  $y_{c2}$  between which the slope will be steep and outside this range the slope will behave as mild. Further, for a given depth, there is only one critical slope and for a given slope greater than  $S_L$  there will be two depths at which the slope will behave as critical slope.

These aspects of critical slope and limit slope are made clear in the following Example 3.19.

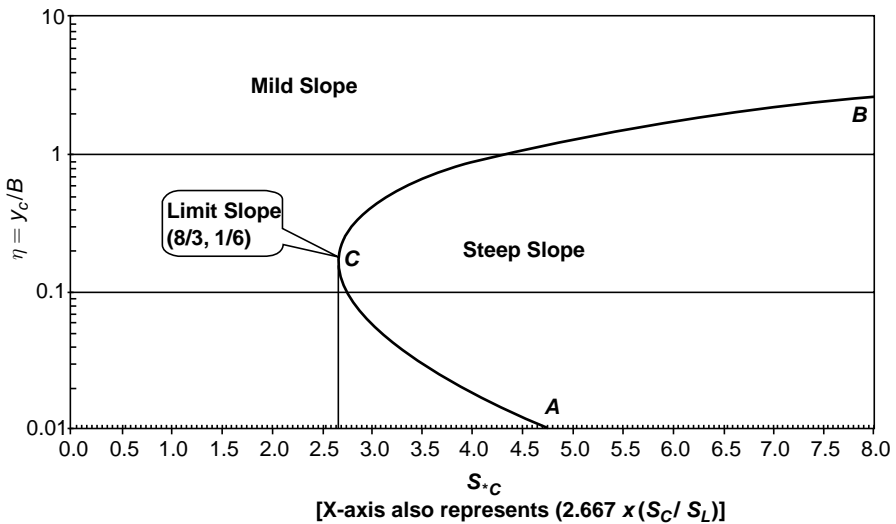


Fig. 3.26 Variation of critical slope in rectangular channels

**Example 3.19** | A concrete lined ( $n = 0.013$ ) rectangular channel of bottom width 2.5 m is laid on a slope of 0.006. (i) For this channel, estimate the critical slope which will have a normal depth of flow of 1.50 m. What will be the discharge at this state? (ii) What is the limit slope of this channel? (iii) Identify the regions of steep and mild slopes, if any, for variation of normal depth from 0.50 m to 6.0 m in this channel.



Solution (i)  $\eta = y_c/B = 1.5/2.5 = 0.60$

$$S_{*c} = \frac{S_c B^{1/3}}{gn^2} = \frac{(1+2\eta)^{4/3}}{\eta^{1/3}}$$

$$S_c \times \frac{(2.5)^{1/3}}{9.81 \times (0.013)^2} = \frac{(1+2 \times 0.60)^{4/3}}{(0.60)^{1/3}}$$

$$818.635 S_c = 3.3924$$

$$S_c = 0.004144$$

Since the normal depth  $= y_c =$  critical depth,

$$\text{Discharge } Q = B\sqrt{gy_c^3} = 2.5 \times \sqrt{9.81 \times (1.5)^3} = 14.385 \text{ m}^3/\text{s}$$

(ii) Limit slope  $S_L = \frac{8}{3} \left( \frac{gn^2}{B^{1/3}} \right) = \frac{8}{3} \times \frac{9.81 \times (0.013)^2}{(2.5)^{1/3}} = 0.00325745$

(iii) The actual slope of the channel  $S_0 = 0.006$ . Since  $S_0 > S_L$ , flow in both steep and mild slope categories is possible. From Fig. 3.26 it is seen that there will be two depths  $y_{c1}$  and  $y_{c2}$ , at which the flow will be critical. Further, within the range of  $y_{c1}$  and  $y_{c2}$ , the channel slope will be steep. Outside the range of these two depths, the channel slope will be mild. Setting  $S_c = 0.006$ ,

$$S_{*c} = \frac{S_c B^{1/3}}{gn^2} = \frac{0.006 \times (2.5)^{1/3}}{9.81 \times (0.013)^2} = 4.9118$$

And by Eq. (3.60),  $\frac{(1+2\eta)^{4/3}}{\eta^{1/3}} = 4.9118$

There are two positive roots of  $\eta$  and the values of these have to be determined by trial and error. Fig. 3.26, which is drawn to scale, affords a first trial. By trial and error, the two values of  $\eta$  are found to be as below:

$$\eta_1 = y_{c1}/B = 0.03823 \text{ given } y_{c1} = 2.5 \times 0.03823 = 0.9558 \text{ m}$$

$$\eta_2 = y_{c2}/B = 0.5464 \text{ giving } y_{c2} = 2.5 \times 0.5464 = 1.366 \text{ m}$$

Hence, for any normal depth  $y_0$ , the regions with mild and steep slopes are as follows:

- (i) For  $y_0 < 0.9558$  m, the channel slope is mild,
- (ii) For  $1.366 \text{ m} > y_0 > 0.9558$  m, the channel slope is steep, and
- (iii) For  $y_0 > 1.366$  m, the channel slope is mild.

### 3.18 GENERALISED FLOW RELATION

Since the Froude number of the flow in a channel if  $F = \frac{V}{\sqrt{gA/T}}$

$$\frac{Q^2}{g} = \frac{F^2 A^3}{T} \tag{3.66}$$

If the discharge  $Q$  occurs as a uniform flow, the slope  $S_0$  required to sustain this discharge is, by Manning's formula,

$$S_0 = \frac{Q^2 n^2}{A^2 R^{4/3}} \quad (3.67)$$

Substituting Eq. 3.66 in Eq. 3.67 and simplifying

$$S_0 = \frac{F^2 g n^2 P^{4/3}}{TA^{1/3}}$$

or

$$\frac{S_0}{F^2 g n^2} = \frac{P^{4/3}}{TA^{1/3}} = f(y) \quad (3.68)$$

For a trapezoidal channel of side slope  $m$ ,

$$\frac{S_0}{F^2 g n^2} = \frac{(B + 2\sqrt{m^2 + 1} y)^{4/3}}{(B + 2my_0)[(B + my_0)y_0]^{1/3}} \quad (3.69)$$

Non-dimensionalising both sides, through multiplication by  $B^{1/3}$ ,

$$S_* = \left( \frac{S_0 B^{1/3}}{F^2 g n^2} \right) = \frac{(1 + 2\sqrt{m^2 + 1} \eta)^{4/3}}{(1 + 2m\eta)(1 + m\eta)^{1/3} (\eta)^{1/3}} \quad (3.70)$$

in which  $\eta = y_0/B$ . Designating  $\left( \frac{S_0 B^{1/3}}{F^2 g n^2} \right) = S_* =$  generalized slope

$$S_* = f(m, \eta) \quad (3.71)$$

Equation 3.70 represents the relationship between the various elements of uniform flow in a trapezoidal channel in a generalised manner. The functional relationship of Eq. 3.70 is plotted in Fig. 3.26. This figure can be used to find, for a given trapezoidal channel, (a) the bed slope required to carry a uniform flow at a known depth and Froude number and (b) the depth of flow necessary for generating a uniform flow of a given Froude number in a channel of known bed slope.

For a rectangular channel,  $m = 0$  and hence Eq. (3.70) becomes

$$S_* = \frac{(1 + 2\eta)^{4/3}}{\eta^{1/3}} \quad (3.72)$$

For a triangular channel,  $B = 0$  and hence Eq. (3.70) cannot be used. However, by redefining the generalised slope for triangular channels, by Eq. 3.69

$$\frac{S_0 y^{1/3}}{F^2 g n^2} = S_{*t} = (2^{1/3}) \left( \frac{1 + m^2}{m^2} \right)^{2/3} \quad (3.73)$$

**Roots and Limit Values of  $S_*$  for Trapezoidal Channels** Equation 3.70 can be written as

$$S_*^3 = \frac{(1 + 2\eta\sqrt{1 + m^2})^4}{(1 + 2m\eta)^3 \eta(1 + m\eta)} \quad (3.74)$$

This is a fifth-degree equation in  $\eta$ , except for  $m = 0$  when it reduces to a fourth-degree equation. Out of its five roots it can be shown that (a) at least one root shall be real and positive and (b) two roots are always imaginary. Thus depending upon the value of  $m$  and  $S_*$ , there may be one, two or three roots. The limiting values of  $S_*$  are obtained by putting,  $\frac{dS_*}{d\eta} = 0$ , which results in

$$8\eta\sqrt{1 + m^2}(1 + m\eta)(1 + 2m\eta) - (1 + 2\eta\sqrt{1 + m^2})(1 + 10m\eta + 10m^2\eta^2) = 0 \quad (3.75)$$

Solving Eq. 3.75 the following significant results are obtained.<sup>20</sup>

1. For rectangular channels ( $m = 0$ ), a single limiting value with  $S_* = 8/3$  and  $\eta_L = 1/6$  is obtained.
2. Between  $m = 0$  and  $m = 0.46635$  there are two limiting values.
3. At  $m = 0.46635$ , the two limit values merge into one at  $S_* = 2.1545$  and  $\eta = 0.7849$ .
4. For  $m > 0.46635$ , there are no limiting points.

For rectangular channels, an interesting extension of result (1) noted above is as follows: At the limiting state, for given  $B$ ,  $S_0$  and  $\eta$ , the Froude number can be considered as the maximum uniform flow Froude number ( $F_{\max}$ ) in the given channel. Thus

$$S_{*L} = \frac{S_0 B^{1/3}}{F_{\max}^2 g n^2} = \frac{8}{3}$$

And by Eq. 3.65 
$$\frac{S_0}{S_L} = F_{\max}^2$$

Thus 
$$S_0 = F_{\max}^2 S_L \quad (3.76)$$

Equation 3.76 represents the channel slope required to have uniform flow Froude number in the given channel which is equal to or less than the pre assigned  $F_{\max}$ , for all discharges. It is interesting to observe in Fig. 3.27 that for  $m = 0.46635$ ,  $S_*$  is essentially constant at a value of 2.15 over a range of values of  $\eta$  extending from 0.5 to 1.5 and  $S_*$  varies very slowly with  $\eta$  in the rest of the plot. Thus a trapezoidal section with  $m = 0.46635$  would give a channel in which the Froude number of the flow is essentially constant over a sufficiently large range of depths.

### 3.18.1 Critical Slope and Limit Slope

The slope of a channel which carries a given discharge as a uniform flow at the critical depth is called the critical slope,  $S_c$ . The condition governing the critical slope in any channel can be easily obtained from Eq. 3.70 by putting  $F = 1.0$ . For trapezoidal

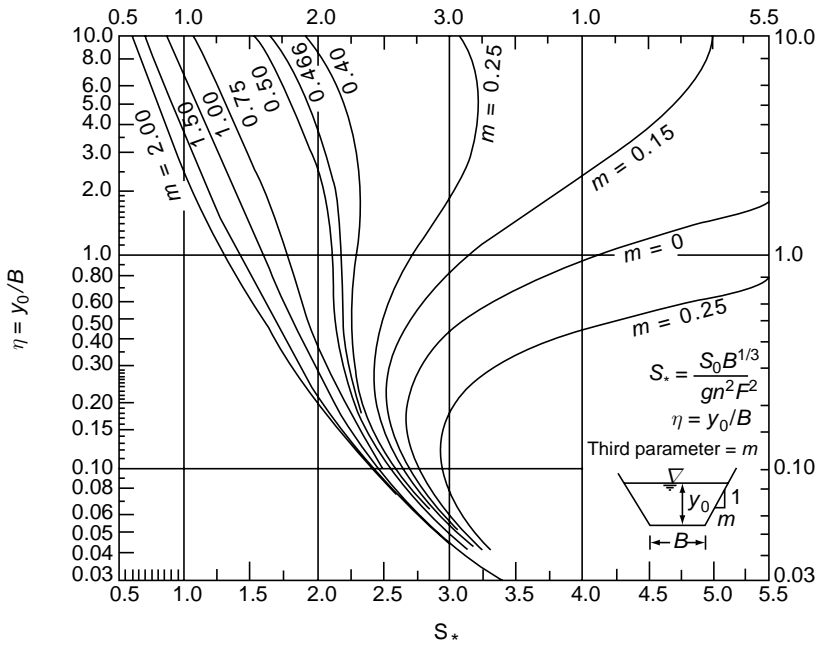


Fig. 3.27 Generalised flow relation [Ref. 20]

channels, by denoting the generalised critical slope,  $\frac{S_c B^{1/3}}{gn^2} = S_{*c}$  and  $\frac{y_c}{B} = \eta_c$ , the behaviour of  $S_{*c}$  can be studied using Fig. 3.27. All the conclusions derived in the pervious section for  $S_*$  will also apply to the  $S_{*c} - \eta_c$  relationship.

For a channel of given shape and roughness  $S_c$  will have a least value under conditions corresponding to a limit value of  $S_{*c}$ . The least value of  $S_c$  is called the limit slope,  $S_{Lc}$ . Keeping the critical slope and limit slope in mind, Fig. 3.27 can be studied to yield the following points:

1. For a trapezoidal channel of given geometry and roughness, a given depth of critical flow can be maintained by one and only one critical slope. However, for a given critical slope there can be more than one critical depth.
2. For channels of the second kind ( $m$  is negative) and for rectangular channels ( $m = 0$ ), only one limit slope exists. Slopes flatter than this cannot be critical and the slopes steeper than this can be critical at two different depths. For a rectangular channel, the limit value of  $S_{*c}$  is  $8/3$  at  $\eta_c = 1/6$ .
3. When  $m \geq 0.46635$ , any slope can be critical and for each slope there will be only one critical depth. There are no limit slopes in this range. For  $m = 0.46635$ , the limit value of  $S_{*c}$  is  $2.15446$  at  $\eta_c = 0.7849$ .
4. For  $0 < m < 0.46635$ , there are two values of limit slopes,  $S_{L1}$  and  $S_{L2}$  with  $S_{L1} < S_{L2}$  (a) For  $S_{L2} > S_c > S_{L1}$ , there are three critical depths for each value of  $S_c$ ; the largest of these, however, may be impracticably large. (b) For  $S_c = S_{L1}$  or  $S_c = S_{L2}$  there are two critical depths. (c) For  $S_c > S_{L2}$  or  $S_c < S_{L1}$ , there is only one critical depth for each value of the slope.

**Example 3.20**

A rectangular channel is 4.0 m wide and has  $n = 0.015$ .

- (a) Determine the bed slope required to maintain uniform flow in this channel with a flow depth of 1.25 m and a uniform flow Froude number of (i) 2.0, (ii) 1.0, and (iii) 0.50. Also, find the limit slope and the corresponding critical discharge.
- (b) Find the longitudinal slope required to ensure that the uniform flow Froude number in this channel is equal to or less than 0.50 for all discharges.

*Solution* (a) Recalling Eq. 3.72,

$$S_* = \frac{S_0 B^{1/3}}{gn^2 F^2} = \frac{(1 + 2\eta)^{4/3}}{n^{1/3}}$$

Substituting  $\eta = \frac{1.25}{4.0} = 0.3125$  in the right-hand side of the above equation,

$$S_* = 2.81528 = \frac{S_0 (4.0)^{1/3}}{(9.81)(0.015)^2 (F)^2}$$

Thus,

- (i) For  $F = 2.0$ ,  $S_0 = 0.015658$
- (ii)  $F = 1.0$ ,  $S_0 = S_c = 0.003915$
- (iii)  $F = 0.5$ ,  $S_0 = 0.0009787$

At the limit slope,  $F = 1.0$ , and limit  $S_{*c} = 8/3$  and  $\eta_c = 1/6$

$$S_L = \frac{2.667 \times (9.81)(0.015)^2}{(4)^{1/3}} = 0.003708$$

$$y_{Lc} = \frac{4.0}{6} = 0.667 \text{ m}$$

- (b) Here  $F = F_{\max} = 0.50$

By Eq. (3.72)  $S_0 = F_{\max}^2 S_L$

and  $S_L = 0.003708$  as calculated in part (a) above.

Hence required  $S_0 = (0.50)^2 \times 0.003708 = 0.000927$

**Example 3.21**

A trapezoidal channel section with  $m = 0.25$ ,  $B = 3.0$  m, and  $n = 0.015$ , has to carry a uniform flow with a Froude number of 0.5.

- (a) If the bed slope of  $S_0 = 0.001052$  is to be used, at what depths would this flow be possible?
- (b) Within what range of  $S_0$  would the above feature of three possible depths be feasible?

*Solution* (a)  $S_* = \frac{S_0 B^{1/3}}{gn^2 F^2} = \frac{(0.001052)(3.0)^{1/3}}{(9.81)(0.015)^2 (0.5)^2} = 2.75$

From Fig. (3.27), for  $m = 0.25$ .

$$\eta_1 = 0.75 \text{ giving } y_1 = 2.25 \text{ m}$$

$$\eta_2 = 1.00 \text{ giving } y_2 = 3.00 \text{ m}$$

and from Eq. (3.70) by trial and error,  $\eta_3 = 18.70$  giving  $y_3 = 56.10 \text{ m}$ .

(b) From Fig. (3.27), the limit values of  $S_*$  are 2.40 and 3.25. As such, the slope  $S_0$  has to lie between  $2.40 \times gn^2/B^{1/3}$  and  $3.25 \times gn^2/B^{1/3}$ , i.e. between  $S_0 = 9.181 \times 10^{-1}$  and  $1.243 \times 10^{-3}$

### 3.19 DESIGN OF IRRIGATION CANALS

For a uniform flow in a canal,

$$Q = \frac{1}{n} AR^{2/3} S_0^{1/2}$$

where  $A$  and  $R$  are in general functions of the geometric elements of the canal. If the canal is of trapezoidal cross-section.

$$Q = f(n, y_0, S_0, B, m) \quad (3.77)$$

Equation 3.77 has six variables out of which one is a dependent variable and the rest five are independent ones. Similarly, for other channel shapes, the number of variables depend upon the channel geometry. In a channel design problem, the independent variables are known either explicitly or implicitly, or as inequalities, mostly in terms of empirical relationships.

In this section the canal-design practice adopted by the Irrigation Engineering profession in India is given. This practice may have application in other fields also. The guidelines given below are meant only for rigid-boundary channels, i.e. for lined and unlined non-erodible channels. The design considerations for unlined alluvial channels follow different principles governed by sediment transport and related aspects. The wide variety of soil and topographical features of the country led different states and agencies, in the past, to adopt their own design practices. Reference 21 indicates the effort of the Central Water Commissions (CWC), India, towards standardisation and general guidelines applicable to the whole country. Relevant Indian standards for irrigation canal design are found in IS: 4745–1968, IS: 7112–1973<sup>12,13</sup>.

**Canal Section** Normally, a trapezoidal section is adopted. Rectangular cross-sections are also in use in special situations, such as in rock cuts, steep chutes and in cross-drainage works.

The side slope, expressed as  $m$  horizontal: 1 vertical, depends on the type of canal, i.e. lined or unlined, nature and type of soil through which the canal is laid. The slopes are designed to withstand seepage forces under critical conditions, such as (i) a canal running full with banks saturated due to rainfall, and (ii) the sudden draw-down of canal supply. Usually the slopes are steeper in cutting than in filling. For lined canals, the slopes roughly correspond to the angle of repose of the natural soil and the values of  $m$  range from 1.0 to 1.5 and rarely up to 2.0. The slopes recommended by CWC<sup>21</sup> for unlined canals in cutting are given in Table 3.5.

**Table 3.5** Side Slopes for Unlined Canals in Cutting

Sl. No.	Type of Soil	<i>m</i>
1	Very light loose sand to average sandy soil	1.5 to 2.0
2	Sandy loam, Black cotton soil	1.0 to 1.5
3	Sandy to gravelly soil	1.0 to 2.0
4	Marum, hard soil	0.75 to 1.5
5	Rock	0.25 to 0.5

**Longitudinal Slope** The longitudinal slope is fixed on the basis of topography to command as much area as possible with the limiting velocities acting as constraints. Usually the slopes are of the order of 0.0001. For lined canals a velocity of about 2.0 m/s is usually recommended.

**Roughness** Procedure for selecting *n* is discussed in Section 3.9. Values on *n* can be taken from Table 3.2.

**Permissible Velocities** Since the cost for a given length of canal depends upon its size, if the available slope permits, it is economical to use highest safe velocities. High velocities may cause scour and erosion of the boundaries. As such, in unlined channels the maximum permissible velocities refer to the velocities that can be safely allowed in the channel without causing scour or erosion of the channel material.

In lined canals, where the material of lining can withstand very high velocities, the maximum permissible velocity is determined by the stability and durability of the lining and also on the erosive action of any abrasive material that may be carried in the stream. The permissible maximum velocities normally adopted for a few soil types and lining materials are indicated in Table 3.6.

**Table 3.6** Permissible Maximum Velocities

Sl. No.	Nature of boundary	Permissible maximum velocity (m/s)
1	Sandy soil	0.30–0.60
2	Black cotton soil	0.60–0.90
3	Muram and Hard soil	0.90–1.10
4	Firm clay and loam	0.90–1.15
5	Gravel	1.20
6	Disintegrated rock	1.50
7	Hard rock	4.0
8	Brick masonry with cement pointing	2.5
9	Brick masonry with cement plaster	4.0
10	Concrete	6.0
11	Steel lining	10.0

In addition to the maximum velocities mentioned above, a minimum velocity in the channel is also an important constraint in the canal design.

Too low a velocity would cause deposition of suspended matter, like silt, which can not only impair the carrying capacity but also increase the maintenance costs. Also, in unlined canals, too low a velocity may encourage weed growth. The minimum velocity in irrigation channels is of the order of 0.30 m/s.

**Free Board** Free board for lined canals is the vertical distance between the full supply level to the top of the lining (Fig. 3.28). For unlined canals, it is the vertical distance from the full supply level to the level of the top of the bank.

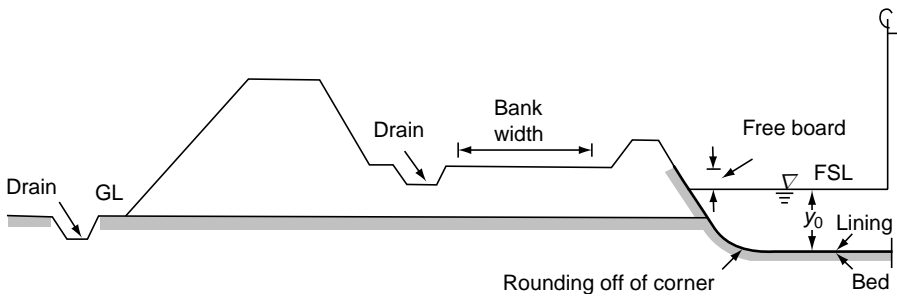


Fig. 3.28 Typical section of a lined irrigation canal

This distance should be sufficient to prevent over-topping of the canal lining or banks due to waves. The amount of free board provided depends on the canal size, location, velocity and depth of flow. The relevant Indian standards<sup>12,13</sup> suggest the minimum free board to be as below:

	Discharge	Free board (m)	
	(m <sup>3</sup> /s)	Unlined	Lined
(a)	$Q < 10.0$	0.50	0.60
(b)	$Q < 10.0$	0.75	0.75

However, the current practice of providing free board seems to be as follows:

$Q(m^3/s)$	< 0.15	0.15–0.75	0.75–1.50	1.50–9.00	> 9.00
Free board (m)	0.30	0.45	0.60	0.75	0.09

**Width-to-Depth Ratio** The relationship between width and depth varies widely depending upon the design practice. If the hydraulically most-efficient channel section is adopted (Section 3.14),  $m = \frac{1}{\sqrt{3}}$ ,  $B = \frac{2y_0}{3} = 1.155y_0$ , i.e.  $\frac{B}{y_0} = 1.1547$ . If any other value of  $m$  is used, the corresponding value of  $B/y_0$  for the efficient section would be, from Eq. 3.54

$$\frac{B}{y_0} = 2\left(\sqrt{1+m^2} - m\right)$$



However, in practice it is usual to adopt a shallower section, i.e. a value of  $B/y_0$  larger than that suggested by Eq. 3.54. The CWC recommendation<sup>21</sup> for  $B/y_0$  as a function of discharge is as follows:

$Q(m^3/s)$	0.30	3.0	14.0	28.0	140	285
$B/y_0$	2.0	4.0	6.0	7.5	14.0	18.0

In large canals it is necessary to limit the depth to avoid dangers of bank failure. Usually depths higher than about 4.0 m are adopted only when it is absolutely necessary.

For selection of width and depth, the usual procedure is to adopt a recommended value of  $B/y_0$  and to find the corresponding  $\frac{Qn}{\sqrt{S_0} B^{8/3}}$  using Table 3A.1. Knowing  $Q$ ,  $n$  and  $S_0$ , the values of  $B$  and  $y_0$  are found. The bottom width is usually adopted to the nearest 25 cm or 10 cm and the depth adjusted accordingly. The resulting velocity is then checked to see that permissible velocity constraints are not exceeded. The typical cross-section of a lined irrigation canal is shown in Fig. 3.28.

**Super elevation** The free board normally provided in design of channels of straight alignment does not account for super elevation of water surface in curved channel alignments. Flow around a curve causes water surface to be higher at the outer curved edge than the normal water surface of straight alignment. This would necessitate extra free board and additional lining height to guard against overtopping and erosion respectively. In subcritical flow, the following formulae by SCS are useful in estimating the super elevation requirement.

For rectangular channels: 
$$E = \frac{3V^2 B}{4g r} \tag{3.78}$$

For Trapezoidal channels: 
$$E = \frac{V^2(B + 2my_0)}{2(g r - 2mV^2)} \tag{3.79}$$

- where  $E$  = Maximum height of water surface above the depth of flow  $y_0$
- $y_0$  = Normal depth of flow for straight alignment at entrance to the curve
- $B$  = Bottom width
- $r$  = Radius of channel centerline
- $V$  = Average velocity of flow cross section at entrance to the curve.
- $m$  = Side slope

**Example 3.22** | A trapezoidal channel is to carry a discharge of 50 m<sup>3</sup>/s. The maximum slope that can be used is 0.004. The soil is hard. Design the channel as (a) a lined canal with concrete lining and (b) an unlined non-erodible channel.

*Solution (a) Lined Canal*

Adopt side slope of 1 : 1, i.e.,  $m = 1.0$  (from Table 3.4)

$n$  for concrete = 0.013 (from Table 3.2)

Recommended  $B/y_0$  for  $Q = 50 \text{ m}^3/\text{s}$  is about 8.0.

For  $B/y_0 = 8.0$  (i.e.  $y_0/B = 0.125$ ), from Table 3A.1

$$\phi = \frac{Qn}{\sqrt{S_0} B^{8/3}} = 0.03108$$

Substituting  $Q = 50.0$ ,  $n = 0.013$ ,  $S_0 = 0.0004$  in the above

$B = 13.5605 \text{ m}$ . Adopt  $B = 13.50 \text{ m}$ . Then actual

$$\phi = \frac{50 \times 0.013}{\sqrt{0.0004} \times (13.5)^{8/3}} = 0.03145$$

Corresponding  $y_0/B = 0.12588$  giving  $y_0 = 1.700 \text{ m}$

$$A = (13.5 + 1.700) \times 1.700 = 25.840$$

$$V = 1.935 \text{ m/s}$$

This value is greater than the minimum velocity of 0.3 m/s; is of the order of 2.0 m/s; and further is less than the maximum permissible velocity of 6.0 m/s for concrete. Hence the selection of  $B$  and  $y_0$  are all right. The recommended geometric parameters of the canal are therefore

$$B = 13.50 \text{ m}, m = 1.0, S_0 = 0.0004$$

Adopt a free board of 0.75 m. The normal depth for  $n = 0.013$  will be 1.70 m.

*(b) Unlined Canal*

From Table 3.4, a side slope of 1 : 1 is adopted. From Table 3.2, take  $n$  for hard soil surface as 0.020.

Recommended  $B/y_0$  for  $Q = 50 \text{ m}^3/\text{s}$  is about 8.0. From Table 3A.1.

$$\text{For } \frac{B}{y_0} = 8.0, \phi = \frac{Qn}{\sqrt{S_0} B^{8/3}} = 0.03108$$

Substituting  $Q = 50.0$ ,  $n = 0.020$  and  $S_0 = 0.0004$  in the above,  $B = 15.998 \text{ m}$ , hence adopt  $B = 16.00 \text{ m}$ . Actual  $\phi = 0.030760$  and the corresponding  $y_0/B = 0.12422$ . Then  $y_0 = 0.12422 \times 16 = 1.988 \text{ m}$ .

$$A = (16.00 + 1.988) \times 1.988 = 35.76 \text{ m}^2$$

$$V = 50/35.76 = 1.398 \text{ m/s}$$

But this velocity is larger than the permissible velocity of 0.90–1.10 m/s for hard soil (Table 3.5). In this case, therefore, the maximum permissible velocity will control the channel dimensions.

Adopt  $V = 1.10 \text{ m/s}$

$$A = \frac{50.0}{1.10} = 45.455 \text{ m}^2 = \left(1 + \frac{my_0}{B}\right) \frac{y_0}{B} B^2$$

For  $B/y_0 = 8.0$ ,  $B = 17.978 \text{ m}$

Adopt  $B = 18.0 \text{ m}$

## 144 Flow in Open Channels

From  $A = (B + my_0) y_0$ , substituting  $A = 45.455$   
 $B = 18.0$ ,  $m = 1.0$ ,  $y_0 = 2.245$  m

$$P = 18.0 + 2\sqrt{1+1} \times 2.245 = 24.35 \text{ m}$$

$$R = A/P = .867 \text{ m}$$

Substituting in the general discharge equation

$$50 = \frac{1}{0.02} \times 45.455 \times (1.867)^{2/3} S_0^{1/2}$$

$$S_0 = 0.0002106$$

Hence, the recommended parameters of the canal are  $B = 18.0$  m,  $m = 1.0$  and  $S_0 = 0.0002106$ . Adopt a free board of 0.75 m. The normal depth for  $n = 0.020$  will be 2.245 m.



## REFERENCES

1. Daily, J W and Harleman, D R F *Fluid Dynamics*, Addison – Wesley, New York, 1966.
2. White, F M, *Fluid Mechanics*, 3/e, McGraw – Hill Book Co., New York, 1994.
3. Jain, A K, 'An Accurate Explicit Equation for Friction Factor,' *Jour. Of Hyd. Div.*, Proc. ASCE, Tech. Note., May 1976, pp 634–677.
4. Nezu, I and Nakagawa, *Turbulence in Open Channels*, IAHR Monograph, A A Balkhema, Rotterdam, 1993.
5. Preston, J H, The Determination of Turbulent Skin Friction by means of Pitot tubes, *Jour. of Royal Aero. Soc.*, London, Vol. 58, 1954, pp. 109–121.
6. Rjaratnam, N and Ahmadi, R. 'Hydraulics of Channels with Flood Plains', *Jour. of Hyd. Research*, IAHR, Vol. 19, No. 11, 1981.
7. Holden, A P and James, C S 'Boundary Shear Distribution on Flood Plains', *Jour. of Hyd. Research*, IAHR, Vol. 27, No. 1, 1989.
8. Issacs, L T and Macintosh, J C 'Boundary Shear Measurements in Open Channels,' *Research Report No. CE 45*, Dept. of Civil Engg., Univ. of Queensland, Australia, Feb. 1985.
9. Lane, E, 'Design of Stable Channels', *Trans ASCE*, Vol. 120, 1955.
10. Chow, V T, *Open Channel Hydraulics*, McGraw – Hill, New York, 1959.
11. Barnes, H H, 'Roughness Characteristics of Natural Channels', *U S Geol. Water Supply Paper No. 1849*, US Govt. Press, Washington, USA, 1967.
12. IS: 4745–1968, *Code of Practice for the Design of Cross Section of Lined Canals in Alluvial Soil*, Indian Standards Institution, New Delhi, 1968.
13. IS: 7112–1973, *Code for Design of Cross Section for Unlined Canals*, Indian Standards Institution, New Delhi, 1974.
14. Arcement, G J, and Schneider, V R *Guide for Selecting Manning's Roughness Coefficients for Natural Channels and Flood Plains*, Reports No. FHWA-TS-84-204, Federal Highway Administration, US Dept. of Transportation, NTIS, Springfield, VA, 1984. [<http://www.fhpa.dot.gov/bridge/wsp2339.pdf>].
15. Cowan, W L, *Estimating Hydraulic Roughness Coefficients*, Agricultural Engg., Vol. 37, No. 7, 1956, pp 473–475.
16. Ben Chie Yen, 'Open Channel Flow Resistance', *Jour. of Hyd. Eng.*, ASCE, Vol. 128, No. 1, Jan 2002, pp. 20–39.

17. Knight, D W and Shiono, K, 'Flood Plain Processes', Chapter 5 in *River Channel and Flood Plain Hydraulics*, Ed. Anderson, M G. et al. John Wiley & Sons, Ltd., 1996.
18. Sturm, T W, *Open channel Hydraulics* McGraw-Hill Higher Education, International ed., Singapore, 2001.
19. Cao, Z., 'Flow Resistance and Momentum Flux in Compound Open Channels', *Jour. of Hyd. Engg.*, ASCE, Vol. 132, No. 12, Dec. 2006, PP 1272–1282.
20. Jones, L E and Tripathy, B N 'Generalized Critical Slope for Trapezoidal Channels', *Jour. of Hyd. Div.*, Proc. ASCE, Vol. 91, No. Hy1, Jan 1965, pp 85–91.
21. CBIP, 'Current Practice in Canal Design in India', *Tech. Report No. 3*, CBIP (India), New Delhi, June 1968.



## PROBLEMS

### Problem Distribution

Topic	Problems
<i>Darcy–Weisbach friction factor</i>	3.1 – 3.3
<i>Velocity distribution</i>	3.4
<i>Boundary shear stress</i>	3.1, 3.22, 3.24, 3.32
<i>Equivalent roughness</i>	3.5 – 3.8
<i>Uniform flow computation</i>	3.9 – 3.33
<i>Computation of normal depth</i>	3.10, 3.12; 3.26 – 3.28; 3.31, 3.32
<i>Standard lined canal sections</i>	3.28 – 3.33, 3.45
<i>Maximum discharge</i>	3.34 – 3.38
<i>Hydraulically efficient sections</i>	3.39 – 3.50
<i>Second hydraulic exponent, <math>N</math></i>	3.51 – 3.54
<i>Compound sections</i>	3.55 – 3.57
<i>Generalised flow relation</i>	3.58 – 3.60
<i>Critical slope and limit slope</i>	3.61 – 3.69
<i>Design of irrigation canal section</i>	3.70

- 3.1 A trapezoidal channel has a bottom width of 2.50 m and depth of flow of 0.80 m. The side slopes are 1.5 horizontal: 1 vertical. The channel is lined with bricks ( $\epsilon_s = 3.0$  mm). If the longitudinal slope of the channel is 0.0003, estimate (a) the average shear stress, (b) the hydrodynamic nature of the surface, (c) Chezy  $C$  by using  $f$ , (d) Manning's  $n$ , (e) the uniform-flow discharge for cases (c) and (d).
- 3.2 The cross-section of a stream could be approximated to a rectangular section of 6.0-m bottom width. The stream is in a mountainous region and is formed by cobbles ( $d_{90} = 300$  mm). Estimate the discharge if the depth of flow is 1.5 m and the bed slope is 0.001.
- 3.3 Using Moody diagram find the friction factor  $f$ , Manning's  $n$  and Chezy  $C$  for a flow of  $7.0$  m<sup>3</sup>/s in a 3.0-m wide rectangular channel at a depth of 1.75 m. Assume the size of roughness magnitude as 2.0 mm and the temperature of water to be 20°C.
- 3.4 Assuming the velocity defect law in the logarithmic form to be applicable to the entire depth of flow  $y_0$  in a wide channel, show that the average velocity in a vertical occurs at  $0.632 y_0$  below the water surface.

- 3.5 A channel has multiple-roughness types in its perimeter. Assuming that the total discharge in the channel is equal to the sum of discharges in the partial areas, show that the equivalent roughness is given by

$$n = \frac{PR^{5/3}}{\sum_1^N \left( \frac{P_i R_i^{5/3}}{n_i} \right)}$$

- 3.6 A trapezoidal channel of 4.0-m bed-width and side slopes 1.5 horizontal: 1 vertical has a sand bed ( $n_1 = 0.025$ ). At a certain reach, the sides are lined by smooth concrete ( $n_2 = 0.012$ ). Calculate the equivalent roughness of this reach if the depth of flow is 1.50 m. (use Horton's formula).
- 3.7 A 3.6-m wide rectangular channel had badly damaged surfaces and had a Manning's  $n = 0.030$ . As a first phase of repair, its bed was lined with concrete ( $n = 0.015$ ). If the depth of flow remains same at 1.2 m before and after the repair, what is the increase of discharge obtained as a result of repair?
- 3.8 For the channel shown in Fig. 3.24 (Example 3.18) calculate the equivalent roughness by Horton's formula.
- 3.9 Find the discharge in the following channels with a bed slope of 0.0006 and  $n = 0.016$ :
- Rectangular,  $B = 3.0$  m,  $y_0 = 1.20$  m
  - Trapezoidal,  $B = 3.0$  m,  $m = 1.5$  and  $y_0 = 1.10$  m
  - Triangular,  $m = 1.5$ ,  $y_0 = 1.50$  m.
- 3.10 A concrete lined trapezoidal channel ( $\eta = 0.015$ ) is 8.0 m wide and has a side slope of 2H: 1V. The longitudinal slope is 0.006. Estimate the normal depth in this channel for a discharge of 40 m<sup>3</sup>/s.
- 3.11 A trapezoidal channel of 10.0-m bed-width and  $m = 1.5$  carries a discharge of 15.0 m<sup>3</sup>/s at a depth of 1.30 m. Calculate the bed slope required (a) if the channel is lined with smooth concrete and (b) if the channel is an unlined, clean, earthen channel.
- 3.12 A circular channel, 2.50 m in diameter, is made of concrete ( $n = 0.014$ ) and is laid on a slope of 1 in 200.
- Calculate the discharge if the normal depth is 1.50 m.
  - Calculate the depth of flow for a discharge of 15.0 m<sup>3</sup>/s.
- 3.13 Calculate the quantity of water that will be discharged at uniform flow depth of 0.9 m in a 1.2-m diameter pipe which is laid at a slope of 1 in 1000. Manning's coefficient can be assumed to be 0.015.
- 3.14 A rectangular channel is to be laid on a slope of 0.0005. The sides will be of smooth concrete ( $n = 0.013$ ). What width of channel is necessary to carry a discharge of 9.0 m<sup>3</sup>/s with a normal depth of 1.60 m?
- [Note: A trial-and-error method using Table 3A.1 is recommended.]
- 3.15 An old rectangular canal having a width of 5.0 m and a slope of 0.0001 was gauged to determine its roughness coefficient. If a discharge of 18.0 m<sup>3</sup>/s was indicated when the depth of uniform flow was 2.0 m, estimate the value of Manning's  $n$ .
- 3.16 What size of concrete pipe ( $n = 0.015$ ) is required to carry a flow of 2.0 m<sup>3</sup>/s at a depth of 0.9-m diameter, when laid on a slope of 0.0002 ?
- 3.17 A trapezoidal channel of 3.0-m bed width and side slope of 1.5 horizontal: 1 vertical carries a full supply of 10.0 m<sup>3</sup>/s at a depth of 1.50 m. What would be the discharge at half of full supply depth (i.e. at 0.75 m)? What would be the depth at half of full supply discharge?
- 3.18 A trapezoidal channel having a side slope of 1.5 horizontal: 1 vertical carries a discharges of 100 m<sup>3</sup>/s with a depth of flow equal to 0.75 width. If  $S_0 = 0.0006$  and  $n = 0.015$  find the bed width and depth of flow.

- 3.19 A rectangular channel ( $n = 0.020$ ) carries a flow of  $25.0 \text{ m}^3/\text{s}$  with the depth of flow equal to the width of the channel. If  $S_0 = 0.0004$  find the Froude number of the flow.
- 3.20 A concrete storm water drain ( $n = 0.012$ ) is  $0.75 \text{ m}$  in diameter and is to discharge  $0.10 \text{ m}^3/\text{s}$ . What is the minimum slope that has to be employed if the depth of flow should not exceed  $0.8\text{-m}$  diameter?
- 3.21 A triangular channel of apex angle  $90^\circ$  and a rectangular channel of the same material have the same bed slope. If the rectangular channel has the depth of flow equal to the width and the flow areas in both channels are the same, find the ratio of discharges in the rectangular and triangular channels respectively.
- 3.22 A circular channel of diameter =  $2.5 \text{ m}$  carries a uniform flow of  $1.5 \text{ m}^3/\text{s}$  at a depth of  $2.0 \text{ m}$ . If Manning's  $n = 0.014$ , estimate the average boundary shear stress per unit length of this channel.
- 3.23 A flow of  $10.0 \text{ m}^3/\text{s}$  is to be passed in a rectangular channel with the depth of flow equal to one-third the width. The channel is lined with smooth concrete ( $n = 0.014$ ). Calculate the channel dimensions and its longitudinal slope necessary to carry the above discharge with a mean velocity of  $2.5 \text{ m/s}$ .
- 3.24 A  $2.6\text{-m}$  wide rectangular channel is lined with rough concrete ( $n = 0.015$ ). The bed slope of the channel is  $0.0004$ . If the normal depth of flow is  $1.25 \text{ m}$ , calculate the (i) conveyance of the channel, (ii) discharge, (iii) Froude number of the flow, and (iv) the average bed shear stress.
- 3.25 The specific energy in a  $2.0\text{-m}$  wide rectangular channel is not to exceed  $1.2 \text{ m}$ . What maximum discharge can be carried in such a channel? What longitudinal slope is required to sustain such a flow? Assume Manning's  $n = 0.015$ .
- 3.26 A brick-lined ( $n = 0.017$ ) trapezoidal channel has  $B = 6.0 \text{ m}$ ,  $m = 1.5$  and  $S_0 = 0.004$ . Find the normal depth of flow for a discharge of (a)  $10.0 \text{ m}^3/\text{s}$ , (b)  $16.0 \text{ m}^3/\text{s}$ , and (c)  $25.0 \text{ m}^3/\text{s}$ .
- 3.27 Show that the normal depth in a triangular channel of side slopes  $m$  horizontal: 1 vertical, is given by

$$y_0 = 1.1892 \left[ \frac{Qn}{\sqrt{S_0}} \right]^{3/8} \left[ \frac{m^2 + 1}{m^5} \right]^{1/8}$$

- 3.28 Determine the bottom width and full supply depth of a standard lined trapezoidal section (Fig. 3.29) to carry  $180 \text{ m}^3/\text{s}$  of flow with a velocity of  $2.0 \text{ m/s}$  when laid on a slope of 1 in 4500. The side slopes are to be 1.25 horizontal: 1 vertical Manning's  $n$  can be assumed to be  $0.014$ .

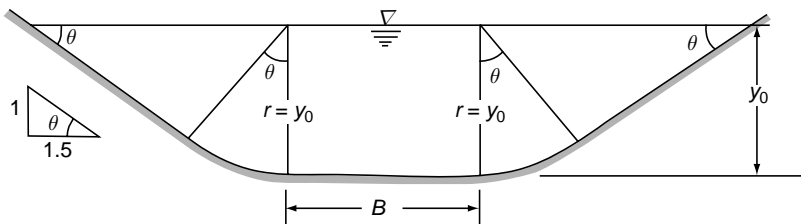


Fig. 3.29 Problem 3.28 and 3.29

- 3.29 A standard lined trapezoidal section (Fig. 3.29) is to carry a discharge of  $100 \text{ m}^3/\text{s}$  at a slope of 1 in 1000. The side slopes are to be 1.5 H : 1 V and the Manning's  $n$  can be taken as  $0.015$ . What bottom width is needed to have a full supply depth of  $2.00 \text{ m}$ ?

- 3.30 Estimate the discharge in a standard lined trapezoidal canal section with  $B = 35$  m,  $S_0 = 1/5000$ , Manning's coefficient  $n = 0.016$ , normal depth  $y_0 = 3.5$  m. The side slopes are 1.5 horizontal : 1 vertical.
- 3.31 A standard lined triangular canal section has a side slope of 1.75 H : 1 V and is laid on a longitudinal slope of 0.0004. The Manning's  $n$  is found to be 0.016. If the channel is designed to convey the fully supply discharge at a velocity of 1.5 m/s, estimate (a) the full supply discharge, and (b) full supply depth.
- 3.32 A standard lined triangular canal section (Fig. 3.30) is to carry a discharge of 25 m<sup>3</sup>/s when laid on a slope of 1 in 1000. The side slopes are 1.25 H : 1 V. Calculate the depth of flow needed. What is the average boundary shear stress in this channel? (Assume  $n = 0.015$ )

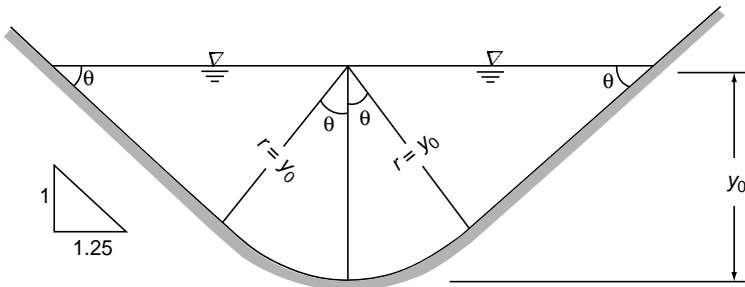


Fig. 3.30 Problem 3.32

- 3.33 A standard lined triangular channel is designed to carry the full supply discharge at a depth of 2.5 m when laid on a slope of 0.0004. The side slope of the channel is 1.25 H : 1 V and Manning's  $n = 0.015$ . Determine the full supply discharge in the canal.
- 3.34 Show that the maximum velocity in a circular channel occurs when  $y/D = 0.81$ .
- 3.35 By using the Chezy formula with constant coefficient  $C$ , show that the condition for maximum discharge in a circular channel occurs when  $y/D = 0.95$ .
- 3.36 A square conduit of side  $s$ , placed with its diagonal vertical, acts as an open channel. Show that the channel carries maximum discharge when  $y = 1.259 s$ .
- 3.37 A triangular duct (Fig. 3.31) resting on a side is carrying water with a free surface. Obtain the condition for maximum discharge when (a)  $m = 0.5$ , (b)  $m = 0.25$  and (c)  $m = 0.10$ .

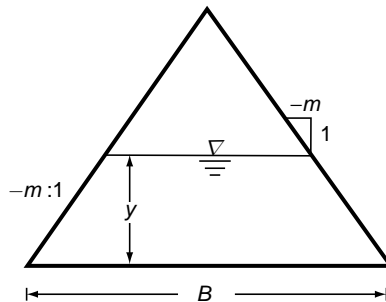


Fig. 3.31 Problem 3.37

- 3.38 Water flows in a channel of the shape of an isosceles triangle of bed width  $a$  and sides making an angle of  $45^\circ$  with the bed. Determine the relation between the depth of flow  $d$

- and the bed width  $a$  for maximum velocity condition and for maximum discharge condition. Use Manning's formula and note that  $d$  is less than  $0.5 a$ .
- 3.39 Determine the dimensions of a concrete-lined ( $n = 0.015$ ) trapezoidal channel of efficient proportions to carry a discharge of  $7.0 \text{ m}^3/\text{s}$ . The bed slope of the channel is  $0.0006$  and  $m = 1.25$ .
- 3.40 A trapezoidal channel is  $5.0\text{-m}$  wide and has a side slope of  $0.5$  horizontal:  $1$  vertical. Find the depth of flow which can make the channel an efficient section. If  $S_0 = 0.0002$  and  $n = 0.02$ , find the corresponding discharge.
- 3.41 A rectangular channel is to carry a certain discharge at critical depth. If the section is to have a minimum perimeter, show that  $y_c = 3B/4$ .
- 3.42 A rectangular channel ( $n = 0.020$ ) is to be  $3.0 \text{ m}$  wide. If a discharge of  $3.00 \text{ m}^3/\text{s}$  is to be passed with the channel having an efficient section, what longitudinal slope is to be provided?
- 3.43 Show that a hydraulically efficient triangular channel section has  $R_e = \frac{y_e}{2\sqrt{2}}$ .
- 3.44 A trapezoidal channel of efficient section is to have an area of  $60.0 \text{ m}^2$ . The side slope is  $1.5$  horizontal:  $1$  vertical. Find the bottom width and depth of flow.
- 3.45 Show that a standard lined triangular canal section is hydraulically efficient for any real side slope  $m$ .
- 3.46 A trapezoidal channel with one side vertical and the other sloping at  $2\text{H} : 1\text{V}$  carries a discharge of  $28 \text{ m}^3/\text{s}$ . Determine the longitudinal slope and cross-sectional dimensions for best hydraulic efficiency if Manning's  $n$   $0.014$ .
- 3.47 A trapezoidal channel has side slopes of  $1\text{H} : 1\text{V}$  and is required to discharge  $14 \text{ m}^3/\text{s}$  with a bed slope of  $1$  in  $1000$ . If unlined the value of Chezy  $C = 45$ . If lined with concrete its value is  $65$ . If the cost of excavation per  $\text{m}^3$  is nine times the cost per  $\text{m}^2$  of lining, determine whether the lined or unlined channel would be cheaper? Assume a free board of  $0.75 \text{ m}$  in both cases. The section can be assumed to be hydraulically efficient.
- 3.48 A lined channel ( $n = 0.014$ ) is of a trapezoidal section with one side vertical and other side on a slope of  $1 \text{ H} : 1\text{V}$ . If the canal has to deliver  $5 \text{ m}^3/\text{s}$  when laid on a slope of  $0.0001$ . Calculate the dimensions of the dimensions of the efficient section which requires minimum of lining.
- 3.49 Show that a hydraulically efficient parabolic section ( $T = K\sqrt{y}$ ) will have the following relationships between the hydraulic radius  $R_e$  top width  $T_e$  and the depth  $y_e$ :  $\left[ \text{Take } P = T + \frac{8}{3}y^2/T \right]$
- $$R_e = \frac{y_e}{2} \quad \text{and} \quad T_e = \sqrt{8}y_e$$
- 3.50 Show that a triangular channel should have a vertex angle of  $78^\circ 77' 47''$  to satisfy simultaneously the conditions of critical state of flow and minimum wetted perimeter.
- 3.51 Show that the second hydraulic exponent  $N$  could be calculated approximately as

$$N = \frac{2y}{3} \left[ 5 \frac{T}{A} - \frac{2}{P} \frac{dP}{dy} \right]$$

- 3.52 Show that for a deep, narrow rectangular channel as  $B/y \rightarrow 0$ ,  $N \rightarrow 2.0$ .



- 3.53 Plot the conveyance  $K = f(y)$  for a trapezoidal channel:  $B = 3.0$  m,  $m = 1.0$ , and  $n = 0.015$ , on a log-log paper. By using this plot find the value of the hydraulic exponent  $N$  in the range  $y = 0.6$  to  $2.3$  m.
- 3.54 Using Fig. 3.20, estimate the value of the second hydraulic exponent  $N$  for the following cases:  
 $m = 1.0$ ,  $y/B = 0.5, 1.0, 2.0$   
 $m = 2.0$ ,  $y/B = 0.5, 1.0, 2.0$
- 3.55 For the compound channel shown below (Fig. 3.32) estimate the discharge for a depth of flow of (i) 1.20 m, and (ii) 1.6 m, by using DCM with vertical interface procedure.

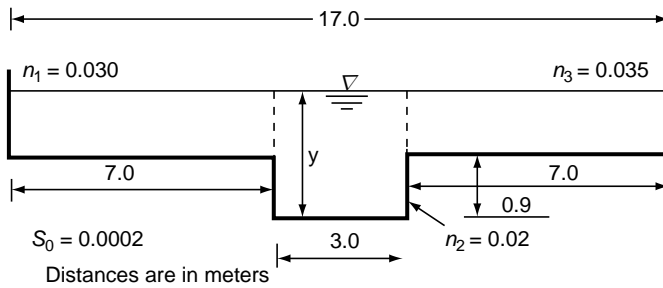


Fig. 3.32 Compound channel of Problem 3.55

- 3.56 Solve Problem (3.55) by using diagonal interfaces,
- 3.57 A compound channel is trapezoidal in cross section and consists of identical flood banks on the left and right of the main channel. The following are the salient geometric properties of the compound section  
*Main channel:* Bottom width = 5.0 m, Side slopes = 1.5 H : 1 V, Bank full depth = 2.0 m, Manning's coefficient = 0.025, Longitudinal slope = 0.001  
*Flood plains:* Width = 25 m, Side slope = 2.0 H : 1 V, Manning's coefficient = 0.06, Longitudinal slope = 0.001. Compute the uniform flow discharge for a flow with total depth of 2.5 m by using DCM with (i) diagonal interface, and (ii) vertical interface procedures.
- 3.58 Develop the generalised flow relation (similar to Eq. (3.64)) relating the generalised slope and depth in a trapezoidal channel by using the Chezy formula with a constant coefficient  $C$ . Show from this expression that, (a) for a triangular channel, the critical slope is independent of depth and (b) for a rectangular channel there is no limit slope.
- 3.59 A 5.0-m wide rectangular channel is laid on a slope of 0.001. If a uniform flow with Froude number = 0.5 is desired, at what depths would this be possible?
- 3.60 A 25.-m wide rectangular channel has Manning's  $n = 0.016$ . If the longitudinal slope of the channel is 0.0004, calculate (a) the maximum uniform flow Froude number possible in this channel and (b) the corresponding discharge.
- 3.61 A brick-lined rectangular channel ( $n = 0.017$ ) of 6.0-m bottom width is laid on a slope of 0.003. (i) For this channel, estimate the critical slope which will have a normal depth of flow of 2.0 m. (ii) Identify the regions of steep and mild slopes, if any, for variation of normal depth from 0.10 m to 4.0 m in this channel
- 3.62 A rectangular channel ( $n = 0.015$ ) has a width of 2.50 m and it is desired to have Froude number at uniform flow to be equal to or less than 0.4 for all discharges in this channel. Determine the channel slope necessary to achieve these criteria.
- 3.63 A triangular channel ( $n = 0.018$ ) has a bed slope of 0.016 and a side slope of 1.5 H : 1 V. Estimate the uniform flow Froude number for a normal depth of 0.5 m.
- 3.64 For a rectangular channel of bottom width  $B$ , bed slope  $S_0$  and Manning's Coefficient  $n$ , show that (i) the maximum uniform flow Froude number occurs at the

normal depth  $y_0 = B/6$ , and (ii) the discharge corresponding to the maximum Froude number is

$$Q = \frac{B^{8/3} \sqrt{S_0}}{24n}$$

- 3.65 For a trapezoidal section  $B = 3.0$  m,  $m = 1.5$  and  $n = 0.02$ , find the (a) bed slope required to have a uniform flow at a Froude number of 0.2 and depth of flow = 2.5 m, (b) critical slope for the same depth of flow of 2.5 m, and (c) depth of flow with a bed slope of 0.0009 to cause a uniform flow Froude number of 0.5.
- 3.66 For a triangular channel with apex angle =  $90^\circ$ , determine the critical slope for a critical depth of 1.35 m. If the channel is laid at this slope, what would be the Froude number of the uniform flow for a depth of flow of 2.0 m? (Assume  $n = 0.02$ ).
- 3.67 A 1.2-m wide rectangular channel is lined with smooth concrete ( $n = 0.013$ ). Determine the limit slope and the corresponding discharge and critical depth.
- 3.68 Obtain an expression for the critical slope in a circular channel as  $S_{c_c} = f(\eta_c)$  where

$$S_{c_c} = \frac{S_c D^{1/3}}{gn^2} \text{ and } \eta_c = y_c/D. \text{ Show that the limit slope occurs at } y_c/D = 0.316.$$

- 3.69 Show that for a parabolic channel  $T = K\sqrt{y}$ , the limit slope is given by  $\frac{S_{Lc} K^{2/3}}{gn^2} = 3.36$

$$\text{and this limit value occurs at } \frac{\sqrt{y_c}}{K} = \frac{1}{2\sqrt{2}}.$$

$$\left[ \text{Assume } P = Ky^{1/2} + \frac{8}{3} \frac{y^{3/2}}{K} \right]$$

- 3.70 Design a trapezoidal channel to carry 75 m<sup>3</sup>/s of flow. The maximum permissible slope is 0.0005. It is proposed to adopt a brick-in-cement mortar lining. The soil is classified as average sandy soil.

## OBJECTIVE QUESTIONS

- 3.1 In a non-prismatic channel
- unsteady flow is not possible
  - the flow is always uniform
  - uniform flow is not possible
  - the flow is not possible
- 3.2 In a uniform open channel flow
- the total energy remains constant along the channel
  - the total energy line either rises or falls along the channel depending on the state of the flow
  - the specific energy decreases along the channel
  - the line representing the total energy is parallel to the bed of the channel
- 3.3 Uniform flow in an open channel exists when the flow is steady and the channel is
- prismatic
  - non-prismatic and the depth of the flow is constant along the channel
  - prismatic and the depth of the flow is constant along the channel
  - frictionless

- 3.4 In *uniform flow* there is a balance between  
 (a) gravity and frictional forces (b) gravity and inertial forces  
 (c) inertial and frictional forces (d) inertial and viscous forces
- 3.5 Uniform flow is not possible if the  
 (a) friction is large (b) fluid is an oil  
 (c)  $S_0 \leq 0$  (d)  $S_0 > 0$
- 3.6 A rectangular channel of longitudinal slope 0.002 has a width of 0.80 m and carries an oil (rel. density = 0.80) at a depth of 0.40 m in uniform flow mode. The average shear stress on the channel boundary in pascals is  
 (a)  $3.14 \times 10^{-3}$  (b)  $6.28 \times 10^{-3}$   
 (c)  $3.93 \times 10^{-3}$  (d) 0.01256
- 3.7 A triangular channel with a side slope of 1.5 horizontal: 1 vertical is laid on slope of 0.005. The shear stress in  $\text{N/m}^2$  on the boundary for a depth of flow of 1.5 m is  
 (a) 3.12 (b) 10.8 (c) 30.6 (d) 548
- 3.8 The dimensions of the Chezy coefficient  $C$  are  
 (a)  $L^2 T^{-1}$  (b)  $LT^{-1/2}$  (c)  $M^0 L^0 T^0$  (d)  $L^{1/2} T^{-1}$
- 3.9 The dimensions of Manning's  $n$  are  
 (a)  $L^{1/6}$  (b)  $L^{1/2} T^{-1}$   
 (c)  $L^{-1/3} T$  (d)  $L^{-1/3} T^{-1}$
- 3.10 The dimensions of the Darcy–Weisbach coefficient  $f$  are  
 (a)  $L^{1/6}$  (b)  $LT^{-1}$  (c)  $L^{1/2} T^{-4}$  (d)  $M^0 L^0 T^0$
- 3.11 A channel flow is found to have a shear Reynolds number  $\frac{u_* \varepsilon_s}{\nu} = 25$ , where  $\varepsilon_s$  = sand grain roughness,  $u_*$  = shear velocity and  $\nu$  = kinematic viscosity. The channel boundary can be classified as hydrodynamically  
 (a) rough (b) in transition regime  
 (c) smooth (d) undular
- 3.12 If the bed particle size  $d_{50}$  of a natural stream is 2.0 mm, then by Strickler formula, the Manning's  $n$  for the channel is about  
 (a) 0.017 (b) 0.023  
 (c) 0.013 (d) 0.044
- 3.13 In using the Moody chart for finding  $f$  for open-channel flows, the pipe diameter  $D$  is to be replaced by  
 (a)  $R$  (b)  $D/2$   
 (c)  $P$  (d)  $4R$
- 3.14 The Manning's  $n$  for a smooth, clean, unlined, sufficiently weathered earthen channel is about  
 (a) 0.012 (b) 0.20  
 (c) 0.02 (d) 0.002
- 3.15 The Manning's  $n$  is related to the equivalent sand grain roughness,  $\varepsilon_s$  as  
 (a)  $n \propto \varepsilon_s^{-1/6}$  (b)  $n \propto \varepsilon_s^{1/6}$  (c)  $n \propto \varepsilon_s^{1/3}$  (d)  $n = \frac{\varepsilon_s}{4R}$
- 3.16 The Darcy–Weisbach  $f$  is related to Manning's  $n$  as  
 (a)  $f = \frac{8g n^2}{R^{1/3}}$  (b)  $f = \frac{8 n^2}{8R^{1/3}}$   
 (c)  $f = \frac{R^{1/3}}{8g n^2}$  (d)  $f = \frac{64ng}{R^{1/3}}$

- 3.17 The Manning's  $n$  for a straight concrete sewer is about  
 (a) 0.025 (b) 0.014 (c) 0.30 (d) 0.14
- 3.18 An open channel carries water with a velocity of 0.605 m/s. If the average bed shear stress is  $1.0 \text{ N/m}^2$ , the Chezy coefficient  $C$  is equal to  
 (a) 500 (b) 60 (c) 6.0 (d) 30
- 3.19 The conveyance of a triangular channel with side slope of 1 horizontal: 1 vertical is expressed as  $K = C y^{8/3}$ ; where  $C$  is equal to  
 (a)  $2^{8/3}$  (b)  $1/n$  (c)  $1/2n$  (d)  $2\sqrt{2}/n$
- 3.20 In a wide rectangular channel if the normal depth is increased by 20 per cent, the discharge would increase by  
 (a) 20% (b) 15.5% (c) 35.5% (d) 41.3%
- 3.21 In a uniform flow taking place in a wide rectangular channel at a depth of 1.2 m, the velocity is found to be 1.5 m/s. If a change in the discharge causes a uniform flow at a depth of 0.88 m in this channel, the corresponding velocity of flow would be  
 (a) 0.89 m/s (b) 1.22 m/s (c) 1.10 m/s (d) 1.50 m/s
- 3.22 It is expected that due to extreme cold weather the entire top surface of a canal carrying water will be covered with ice for some days. If the discharge in the canal were to remain unaltered, this would cause  
 (a) no change in the depth  
 (b) increase in the depth of flow  
 (c) decrease in the depth of flow  
 (d) an undular surface exhibiting increase and decrease in depths
- 3.23 By using Manning's formula the depth of flow corresponding to the condition of maximum discharge in a circular channel of diameter  $D$  is  
 (a)  $0.94 D$  (b)  $0.99 D$  (c)  $0.86 D$  (d)  $0.82 D$
- 3.24 In a circular channel the ratio of the maximum discharge to the pipe full discharge is about  
 (a) 1.50 (b) 0.94 (c) 1.08 (d) 1.00
- 3.25 For a circular channel of diameter  $D$  the maximum depth below which only one normal depth is assured  
 (a)  $0.5 D$  (b)  $0.62 D$  (c)  $0.82 D$  (d)  $0.94 D$
- 3.26 A trapezoidal channel had a 10 per cent increase in the roughness coefficient over years of use. This would represent, corresponding to the same stage as at the beginning, a change in discharge of  
 (a) +10% (b) -10% (c) 11% (d) +9.1 %
- 3.27 For a hydraulically-efficient rectangular section,  $B/y_0$  is equal to  
 (a) 1.0 (b) 2.0 (c) 0.5 (d)  $1/\sqrt{3}$
- 3.28 A triangular section is hydraulically-efficient when the vertex angle  $\theta$  is  
 (a)  $90^\circ$  (b)  $120^\circ$  (c)  $60^\circ$  (d)  $30^\circ$
- 3.29 For a hydraulically efficient triangular channel with a depth of flow  $y$ , the hydraulic radius  $R$  is equal to  
 (a)  $2\sqrt{2}y$  (b)  $y/2$  (c)  $\sqrt{2}y$  (d)  $y/2\sqrt{2}$
- 3.30 A hydraulically-efficient trapezoidal channel has  $m = 2.0$ .  $B/y_0$  for this channel is  
 (a) 1.236 (b) 0.838 (c) 0.472 (d) 2.236
- 3.31 In a hydraulically most efficient trapezoidal channel section the ratio of the bed width to depth is  
 (a) 1.155 (b) 0.867 (c) 0.707 (d) 0.50
- 3.32 In a hydraulically efficient circular channel flow, the ratio of the hydraulic radius to the diameter of the pipe is  
 (a) 1.0 (b) 0.5 (c) 2.0 (d) 0.25

- 3.33 For a wide rectangular channel the value of the first hydraulic exponent  $N$  is  
 (a) 3.0 (b) 4.0 (c) 3.33 (d) 5.33
- 3.34 If the Chezy formula with  $C = \text{constant}$  is used, the value of  $N$  for a wide rectangular channel will be  
 (a) 2.0 (b) 3.0 (c) 3.33 (d) 5.33
- 3.35 For a trapezoidal channel of most-efficient proportions  $\left[ Qn / (B^{8/3} S_0^{1/2}) \right] = \phi =$   
 (a)  $1/\sqrt{3}$  (b) 0.7435 (c) 0.8428 (d) 1.486
- 3.36 In a given rectangular channel the maximum value of uniform-flow Froude number occurs when  
 (a)  $y = B/6$  (b)  $R = y/2$  (c)  $y = B/2$  (d)  $y_0 = y_c$
- 3.37 The limit slope of a rectangular channel 10 m wide and  $n = 0.015$  is  
 (a) 0.000423 (b) 0.00372 (c) 0.00273 (d) 0.0732
- 3.38 In a rectangular channel 10 m wide and  $n = 0.015$ , the critical depth corresponding to the limit slope is  
 (a) 1.333 m (b) 0.667 m (c) 2.667 m (d) 1.667 m
- 3.39 A rectangular channel  $B = 4.0$  m,  $n = 0.015$  is to carry a uniform discharge at a depth of 1.0 m and Froude number = 0.5. The required bottom slope is  
 (a) 0.0035 (b) 0.00505 (c) 0.00095 (d) 0.00045
- 3.40 A trapezoidal channel with  $0 < m < 0.46$  will have  $x$  number of limit slopes where  $x$  is  
 (a) 1 (b) 2 (c) 3 (d) 0



APPENDIX 3A

Table 3A.1 gives the variation of  $\phi = f(\eta_0, m)$  as represented by Eq. (3.32) and provides a convenient aid to determine the normal depth in rectangular and trapezoidal channels. At the normal depth

$$\phi = \frac{nQ}{\sqrt{S_0} B^{8/3}} \quad \text{and} \quad \eta_0 = \frac{y_0}{B}$$

Note that the column  $m = 0$  corresponds to a rectangular channel

Table 3A-1 Values of  $\phi$  for Trapezoidal Channels

$\eta_0$	Value of $\phi$					$\eta_0$	Value of $\phi$				
	$m = 0$	$m = 1.0$	$m = 1.5$	$m = 2.0$	$m = 2.5$		$m = 0$	$m = 1.0$	$m = 1.5$	$m = 2.0$	$m = 2.5$
0.100	0.01908	0.02139	0.02215	0.02282	0.02345	0.155	0.03736	0.04463	0.04713	0.04938	0.05151
0.105	0.02058	0.02321	0.02407	0.02484	0.02556	0.160	0.03919	0.04708	0.04982	0.05227	0.05459
0.110	0.02212	0.02509	0.02607	0.02694	0.02776	0.165	0.04104	0.04960	0.05257	0.05523	0.05777
0.115	0.02369	0.02702	0.02814	0.02912	0.03005	0.170	0.04292	0.05217	0.05539	0.05828	0.06104
0.120	0.02529	0.02902	0.03027	0.03138	0.03243	0.175	0.04482	0.05479	0.05828	0.06141	0.06439
0.125	0.02693	0.03108	0.03247	0.03371	0.03489	0.180	0.04675	0.05747	0.06123	0.06462	0.06785
0.130	0.02860	0.03319	0.03475	0.03613	0.03744	0.185	0.04869	0.06021	0.06426	0.06791	0.07139
0.135	0.03029	0.03537	0.03709	0.03862	0.04007	0.190	0.05066	0.06300	0.06735	0.07128	0.07503
0.140	0.03202	0.03760	0.03949	0.04119	0.04280	0.195	0.05265	0.06584	0.07052	0.07474	0.07876
0.145	0.03377	0.03988	0.04197	0.04384	0.04561	0.200	0.05466	0.06874	0.07375	0.07827	0.08259
0.150	0.03555	0.04223	0.04452	0.04657	0.04852						



Table 3A-1 (Continued)

$\eta_0$	Value of $\phi$					$\eta_0$	Value of $\phi$				
	$m = 0$	$m = 1.0$	$m = 1.5$	$m = 2.0$	$m = 2.5$		$m = 0$	$m = 1.0$	$m = 1.5$	$m = 2.0$	$m = 2.5$
0.910	0.42812	1.07489	1.36067	1.62992	1.89015	1.31	0.66524	2.25468	2.99960	3.70806	4.39526
0.920	0.43394	1.09843	1.39256	1.66974	1.93767	1.32	0.67126	2.29076	3.05072	3.77362	4.47486
0.930	0.43977	1.12226	1.42488	1.71015	1.98592	1.33	0.67728	2.32719	3.10236	3.83988	4.55536
0.940	0.44561	1.14638	1.45764	1.75114	2.03489	1.34	0.68330	2.36395	3.15453	3.90684	4.63673
0.950	0.45145	1.17080	1.49084	1.79271	2.08460	1.35	0.68932	2.40106	3.20723	3.97452	4.71900
0.960	0.45730	1.19550	1.52449	1.83488	2.13503	1.36	0.69535	2.43850	3.26046	4.04292	4.80217
0.970	0.46315	1.22050	1.55859	1.87765	2.18621	1.37	0.70138	2.47629	3.31422	4.11203	4.88623
0.980	0.46901	1.24580	1.59314	1.92101	2.23813	1.38	0.70741	2.51442	3.36851	4.18186	4.97120
0.990	0.47488	1.27140	1.62814	1.96498	2.29080	1.39	0.71345	2.55290	3.42335	4.25242	5.05707
1.000	0.48075	1.29729	1.66359	2.00954	2.34422	1.40	0.71949	2.59173	3.47872	4.32370	5.14385
1.010	0.48663	1.32348	1.69950	2.05472	2.39840	1.41	0.72553	2.63090	3.53463	4.39571	5.23155
1.020	0.49251	1.34997	1.73586	2.10051	2.45333	1.42	0.73158	2.67042	3.59109	4.46845	5.32016
1.030	0.49840	1.37677	1.77269	2.14691	2.50903	1.43	0.73762	2.71029	3.64809	4.54193	5.40970
1.040	0.50430	1.40387	1.80998	2.19393	2.56550	1.44	0.74367	2.75052	3.70563	4.61615	5.50016
1.050	0.51020	1.43127	1.84773	2.24157	2.62274	1.45	0.74973	2.79109	3.76373	4.69111	5.59155
1.060	0.51611	1.45898	1.88596	2.28983	2.68076	1.46	0.75578	2.83202	3.82237	4.76681	5.68387
1.070	0.52202	1.48700	1.92465	2.33872	2.73955	1.47	0.76184	2.87330	3.88157	4.84326	5.77713
1.080	0.52794	1.51533	1.96381	2.38823	2.79913	1.48	0.76790	2.91494	3.94133	4.92045	5.87133
1.090	0.53386	1.54396	2.00345	2.43839	2.85950	1.49	0.77397	2.95694	4.00164	4.99841	5.96647
1.100	0.53979	1.57291	2.04356	2.48917	2.92067	1.50	0.78003	2.99929	4.06251	5.07711	6.06256
1.110	0.54572	1.60216	2.08415	2.54060	2.98262	1.51	0.78610	3.04200	4.12394	5.15657	6.15960
1.120	0.55165	1.63173	2.12522	2.59267	3.04538	1.52	0.79217	3.08508	4.18594	5.23680	6.25760
1.130	0.55760	1.66162	2.16677	2.64538	3.10895	1.53	0.79824	3.12851	4.24850	5.31779	6.35655
1.140	0.56354	1.69182	2.20881	2.69874	3.17332	1.54	0.80432	3.17231	4.31163	5.39954	6.45647
1.150	0.56949	1.72234	2.25133	2.75276	3.23851	1.55	0.81040	3.21647	4.37532	5.48207	6.55736
1.160	0.57545	1.75317	2.29434	2.80743	3.30451	1.56	0.81647	3.26100	4.43959	5.56536	6.65921
1.170	0.58141	1.78433	2.33784	2.86275	3.37133	1.57	0.82256	3.30589	4.50443	5.64944	6.76204
1.180	0.58737	1.81580	2.38184	2.91874	3.43898	1.58	0.82864	3.35115	4.56984	5.73429	6.86584
1.190	0.59334	1.84760	2.42633	2.97539	3.50746	1.59	0.83473	3.39678	4.63584	5.81992	6.97063
1.200	0.59931	1.87972	2.47132	3.03271	3.57677	1.60	0.84081	3.44278	4.70241	5.90633	7.07640
1.21	0.60528	1.91216	2.51681	3.09069	3.64692	1.61	0.84691	3.48914	4.76956	5.99354	7.18316
1.22	0.61126	1.94493	2.56279	3.14935	3.71790	1.62	0.85300	3.53588	4.83729	6.08153	7.29091
1.23	0.61725	1.97802	2.60929	3.20869	3.78973	1.63	0.85909	3.58300	4.90561	6.17031	7.39965
1.24	0.62323	2.01145	2.65628	3.26870	3.86241	1.64	0.86519	3.63048	4.97452	6.25989	7.50940
1.25	0.62922	2.04520	2.70379	3.32940	3.93595	1.65	0.87129	3.67834	5.04402	6.35026	7.62015
1.26	0.63522	2.07928	2.75181	3.39078	4.01033	1.66	0.87739	3.72658	5.11410	6.44144	7.73190
1.27	0.64122	2.11369	2.80033	3.45285	4.08558	1.67	0.88349	3.77520	5.18478	6.53342	7.84466
1.28	0.64722	2.14844	2.84937	3.51561	4.16170	1.68	0.88959	3.82419	5.25605	6.62620	7.95844
1.29	0.65322	2.18351	2.89893	3.57906	4.23868	1.69	0.89570	3.87357	5.32792	6.71980	8.07323
1.30	0.65923	2.21893	2.94901	3.64321	4.31653	1.70	0.90181	3.92332	5.40039	6.81420	8.18905

# Gradually Varied Flow Theory

# 4

## 4.1 INTRODUCTION

A steady non-uniform flow in a prismatic channel with gradual changes in its water surface elevation is termed as *gradually varied flow* (GVF). The backwater produced by a dam or weir across a river and the drawdown produced at a sudden drop in a channel are few typical examples of GVF. In a GVF, the velocity varies along the channel and consequently the bed slope, water surface slope, and energy slope will all differ from each other. Regions of high curvature are excluded in the analysis of this flow.

The two basic assumptions involved in the analysis of GVF are the following:

1. The pressure distribution at any section is assumed to be hydrostatic. This follows from the definition of the flow to have a gradually-varied water surface. As gradual changes in the surface curvature give rise to negligible normal accelerations, the departure from the hydrostatic pressure distribution is negligible. The exclusion of the region of high curvature from the analysis of GVF, as indicated earlier, is only to meet this requirement.
2. The resistance to flow at any depth is assumed to be given by the corresponding uniform flow equation, such as the Manning's formula, with the condition that the slope term to be used in the equation is the energy slope and not the bed slope. Thus, if in a GVF the depth of flow at any section is  $y$ , the energy slope  $S_f$  is given by

$$S_f = \frac{n^2 V^2}{R^{4/3}} \quad (4.1)$$

where  $R$  = hydraulic radius of the section at depth  $y$ .

## 4.2 DIFFERENTIAL EQUATION OF GVF

Consider the total energy  $H$  of a gradually varied flow in a channel of small slope and  $\alpha = 1.0$  as

$$H = Z + E = Z + y + \frac{V^2}{2g} \quad (4.2)$$

where  $E$  = specific energy.



A schematic sketch of a gradually varied flow is shown in Fig. 4.1. Since the water surface, in general, varies in the longitudinal ( $x$ ) direction, the depth of flow and total energy are functions of  $x$ . Differentiating Eq. 4.2 with respect to  $x$

$$\frac{dH}{dx} = \frac{dZ}{dx} + \frac{dE}{dx} \quad (4.3)$$

i.e. 
$$\frac{dH}{dx} = \frac{dZ}{dx} + \frac{dy}{dx} + \frac{d}{dx} \left( \frac{V^2}{2g} \right) \quad (4.4)$$

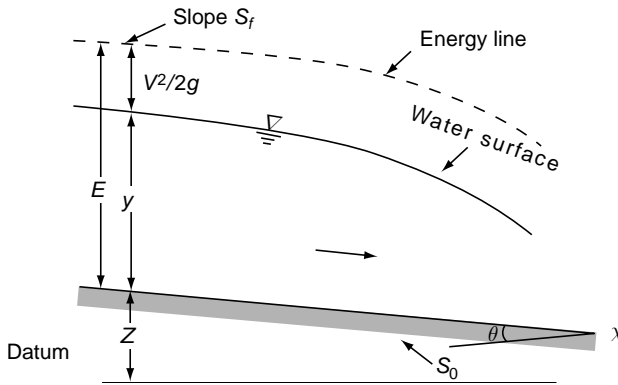


Fig. 4.1 Schematic sketch of GVF

In equation 4.4, the meaning of each term is as follows:

1.  $\frac{dH}{dx}$  represents the energy slope. Since the total energy of the flow always decreases in the direction of motion, it is common to consider the slope of the decreasing energy line as positive. Denoting it by  $S_f$ , we have

$$\frac{dH}{dx} = -S_f \quad (4.5)$$

2.  $\frac{dZ}{dx}$  denotes the bottom slope. It is common to consider the channel slope with bed elevations decreasing in the downstream direction as positive. Denoting it as  $S_0$ , we have

$$\frac{dZ}{dx} = -S_0 \quad (4.6)$$

3.  $\frac{dy}{dx}$  represents the water surface slope relative to the bottom of the channel.

4. 
$$\frac{d}{dx} \left( \frac{V^2}{2g} \right) = \frac{d}{dy} \left( \frac{Q^2}{2gA^2} \right) \frac{dy}{dx}$$

$$= -\frac{Q^2}{gA^3} \frac{dA}{dy} \frac{dy}{dx}$$

Since  $dA/dy = T$ ,

$$\frac{d}{dx} \left( \frac{V^2}{2g} \right) = -\frac{Q^2 T}{gA^3} \frac{dy}{dx} \quad (4.7)$$

Equation 4.4 can now be rewritten as

$$-S_f = -S_0 + \frac{dy}{dx} - \left( \frac{Q^2 T}{gA^3} \right) \frac{dy}{dx}$$

Re-arranging

$$\frac{dy}{dx} = \frac{S_0 - S_f}{1 - \frac{Q^2 T}{gA^3}} \quad (4.8)$$

This forms the basic differential equation of GVF and is also known as the *dynamic equation* of GVF. If a value of the kinetic-energy correction factor  $\alpha$  greater than unity is to be used, Eq. 4.8 would then read as

$$\frac{dy}{dx} = \frac{S_0 - S_f}{1 - \frac{\alpha Q^2 T}{gA^3}} \quad (4.8a)$$

**Other Forms of Eq. 4.8** (a) If  $K$  = conveyance at any depth  $y$  and  $K_0$  = conveyance corresponding to the normal depth  $y_0$ , then

$$K = Q/\sqrt{S_f} \quad (\text{By assumption 2 of GVF}) \quad (4.9)$$

and

$$K_0 = Q/\sqrt{S_0} \quad (\text{Uniform flow})$$

$$S_f/S_0 = K_0^2/K^2 \quad (4.10)$$

Similarly, if  $Z$  = section factor at depth  $y$  and  $Z_c$  = section factor at the critical depth  $y_c$ ,

$$Z^2 = A^3/T$$

and

$$Z_c^2 = \frac{A_c^3}{T_c} = \frac{Q^2}{g}$$

Hence, 
$$\frac{Q^2 T}{g A^3} = \frac{Z_c^2}{Z^2} \quad (4.11)$$

Using Eqs 4.10 and 4.11, Eq. 4.8 can now be written as

$$\begin{aligned} \frac{dy}{dx} &= S_0 \frac{1 - \frac{S_f}{S_0}}{1 - \frac{Q^2 T}{g A^3}} \\ &= S_0 \frac{1 - \left(\frac{K_0}{K}\right)^2}{1 - \left(\frac{Z_c}{Z}\right)^2} \end{aligned} \quad (4.12)$$

This equation is useful in developing direct integration techniques.

(b) If  $Q_n$  represents the normal discharge at a depth  $y$  and  $Q_c$  denotes the critical discharge at the same depth  $y$ ,

$$Q_n = K \sqrt{S_0} \quad (4.13)$$

and

$$Q_c = Z \sqrt{g} \quad (4.14)$$

Using these definitions, Eq. 4.8 can be written as

$$\frac{dy}{dx} = S_0 \frac{1 - (Q/Q_n)^2}{1 - (Q/Q_c)^2} \quad (4.15)$$

(c) Another form of Eq. 4.8 is Eq. 4.3 and can be written as

$$\frac{dE}{dx} = S_0 - S_f \quad (4.16)$$

This equation is called the differential-energy equation of GVF to distinguish it from the GVF differential equations (Eqs (4.8), (4.12) and (4.15)). This energy equation is very useful in developing numerical techniques for the GVF profile computation.

### 4.3 CLASSIFICATION OF FLOW PROFILES

In a given channel,  $y_0$  and  $y_c$  are two fixed depths if  $Q$ ,  $n$  and  $S_0$  are fixed. Also, there are three possible relations between  $y_0$  and  $y_c$  as (i)  $y_0 > y_c$ , (ii)  $y_0 < y_c$  and (iii)  $y_0 = y_c$ . Further, there are two cases where  $y_0$  does not exist, i.e. when (a) the channel bed is horizontal, ( $S_0 = 0$ ), (b) when the channel has an adverse slope,

( $S_0$  is -ve). Based on the above, the channels are classified into five categories as indicated in Table 4.1.

For each of the five categories of channels, lines representing the critical depth and normal depth can be drawn in the longitudinal section. These would divide the whole flow space into three regions as:

- Region 1: Space above the top most line
- Region 2: Space between top line and the next lower line
- Region 3: Space between the second line and the bed

Figure 4.2 shows these regions in the various categories of channels.

**Table 4.1** Classification of Channels

Sl. No	Channel category	Symbol	Characteristic condition	Remark
1	Mild slope	M	$y_0 > y_c$	Subcritical flow at normal depth
2	Steep slope	S	$y_c > y_0$	Supercritical flow at normal depth
3	Critical slope	C	$y_c = y_0$	Critical flow at normal depth
4	Horizontal bed	H	$S_0 = 0$	Cannot sustain uniform flow
5	Adverse slope	A	$S_0 < 0$	Cannot sustain uniform flow

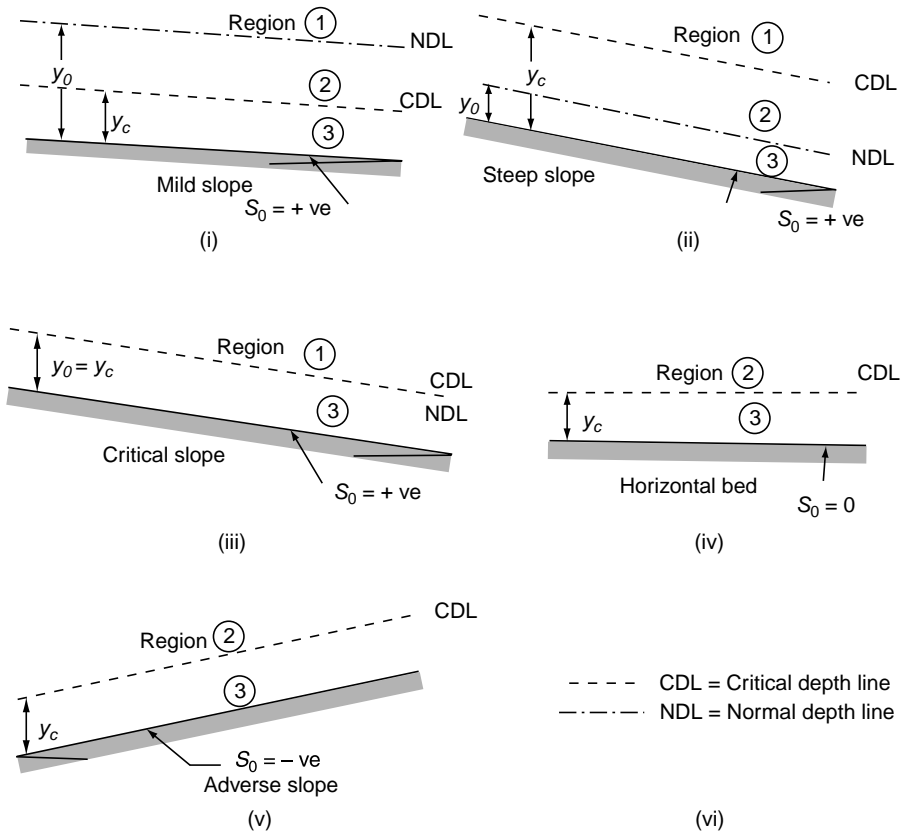


**Fig. 4.2** Regions of flow profiles

Depending upon the channel category and region of flow, the water surface profiles will have characteristic shapes. Whether a given GVF profile will have an increasing or decreasing water depth in the direction of flow will depend upon the term  $dy/dx$  in Eq. 4.8 being positive or negative.

It can be seen from Eq. 4.12 that  $\frac{dy}{dx}$  is positive

- or
- (i) if the numerator  $> 0$  and the denominator  $> 0$
  - (ii) if the numerator  $< 0$  and the denominator  $< 0$ .

i.e.  $\frac{dy}{dx}$  is positive if (i)  $K > K_0$  and  $Z > Z_c$  or

$$(ii) K < K_0 \text{ and } Z > Z_c$$

For channels of the first kind,  $K$  is a single-valued function of  $y$ , and hence

$$\frac{dy}{dx} > 0 \text{ if (i) } y > y_0 \text{ and } y > y_c \text{ or}$$

$$(ii) y < y_0 \text{ and } y < y_c$$

Similarly,  $\frac{dy}{dx} < 0$  if (i)  $y_c > y > y_0$  or

$$(ii) y_0 > y > y_c$$

Further, to assist in the determination of flow profiles in various regions, the behaviour of  $dy/dx$  at certain key depths is noted by studying Eq. 4.8 as follows:

1. As  $y \rightarrow y_0$ ,  $\frac{dy}{dx} \rightarrow 0$ , i.e. the water surface approaches the normal depth line asymptotically.
2. As  $y \rightarrow y_c$ ,  $\frac{dy}{dx} \rightarrow \infty$ , i.e. the water surface meets the critical depth line vertically. This information is useful only as indicative of the trend of the profile. In reality, high curvatures at critical depth zones violate the assumption of gradually-varied nature of the flow and as such the GVF computations have to end or commence a short distance away from the critical-depth location.
3.  $y \rightarrow \infty$ ,  $\frac{dy}{dx} \rightarrow S_0$ , i.e. the water surface meets a very large depth as a horizontal asymptote.

Based on this information, the various possible gradually varied flow profiles are grouped into twelve types (Table 4.2). The characteristic shapes and end conditions of all these profiles are indicated in Fig. 4.3.

In Fig. 4.3, an exaggerated vertical scale is adopted to depict the nature of curvature. In reality the GVF profiles, especially  $M_1$ ,  $M_2$  and  $H_2$  profiles, are very flat. The longitudinal distances are one to two orders of magnitude larger than the depths. It is evident from Fig. 4.3 that all the curves in region 1 have positive slopes; these

Table 4.2 Types of GVF Profiles

Channel	Region	Condition	Type
Mild slope	{ 1	$y > y_0 > y_c$	$M_1$
	{ 2	$y_0 > y > y_c$	$M_2$
	{ 3	$y_0 > y_c > y$	$M_3$
Steep slope	{ 1	$y > y_c > y_0$	$S_1$
	{ 2	$y_c > y > y_0$	$S_2$
	{ 3	$y_c > y_0 > y$	$S_3$
Critical slope	{ 1	$y > y_0 = y_c$	$C_1$
	{ 3	$y < y_0 = y_c$	$C_3$
Horizontal bed	{ 2	$y > y_c$	$H_2$
	{ 3	$y < y_c$	$H_3$
Adverse slope	{ 2	$y > y_c$	$A_2$
	{ 3	$y < y_c$	$A_3$

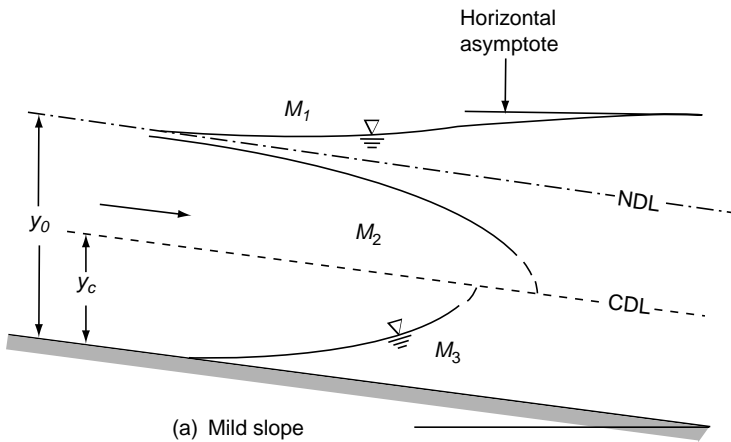


Fig. 4.3 Various GVF Profiles (Contd)

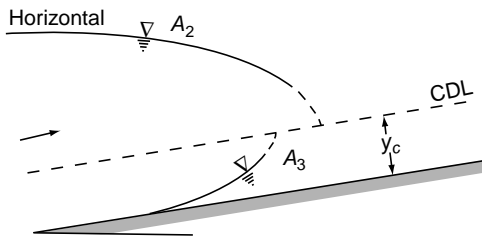
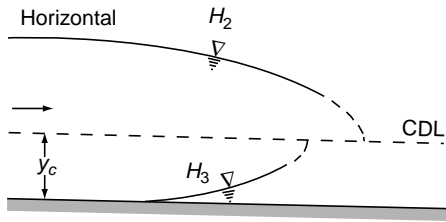
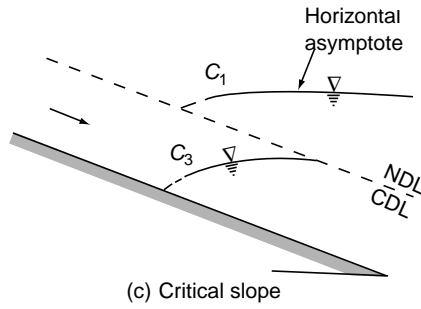
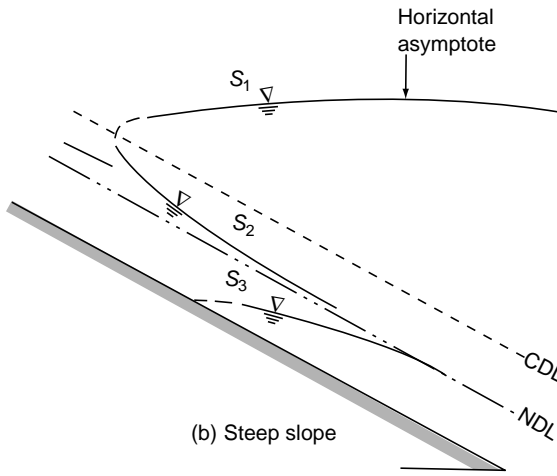


Fig. 4.3 Various GVF profiles

are commonly known as backwater curves. Similarly, all the curves in region 2 have negative slopes and are referred to as drawdown curves. At critical depth the curves are indicated by dashed lines to remind that the GVF equation is strictly not applicable in that neighbourhood.

**Example 4.1** | A rectangular channel with a bottom width of 4.0 m and a bottom slope of 0.0008 has a discharge of 1.50 m<sup>3</sup>/s. In a gradually varied flow in this channel, the depth at a certain location is found to be 0.30 m. Assuming  $n = 0.016$ , determine the type of GVF profile.

*Solution* (a) To find the normal depth  $y_0$

$$\phi = \frac{Qn}{\sqrt{S_0} B^{8/3}} = \frac{1.50 \times 0.016}{\sqrt{0.0008} \times (4.0)^{8/3}} = 0.021046$$

Referring to Table 3A:1, the value of  $y_0/B$  for this value of  $\phi$ , by interpolation, is

$$\frac{y_0}{B} = 0.1065$$

$$y_0 = 0.426 \text{ m}$$

(b) Critical depth  $y_c$

$$q = Q/B = \frac{1.5}{4.0} = 0.375 \text{ m}^3/\text{s}/\text{m}$$

$$y_c = (q^2/g)^{1/3} = \left( \frac{(0.375)^2}{9.81} \right)^{1/3} = 0.243 \text{ m}$$

(c) Type of profile

Since  $y_0 > y_c$ , the channel is a mild-slope channel. Also, given  $y = 0.30$  m is such that

$$y_0 > y > y_c.$$

As such the profile is of the  $M_2$  type (Table 4.2).

#### Alternative method

Instead of calculating normal depth through use of tables, the critical slope is calculated. By using Eq. (3.64).

$$S_{*c} = \frac{S_c B^{1/3}}{gn^2} = \frac{(1+2\eta)^{4/3}}{\eta^{1/3}}$$



$$S_c = \frac{gn^2}{B^{1/3}} \frac{(1+2\eta)^{4/3}}{\eta^{1/3}} \quad (4.17)$$

Here  $\eta = y_c/B = 0.243/4.0 = 0.06075$ . Substituting in Eq. 4.17

$$S_c = \frac{9.81 \times (0.016)^2}{(4.0)^{1/3}} \times \frac{(1+2 \times (0.06075))^{4/3}}{(0.06075)^{1/3}} = 0.004689$$

Since  $S_0$  is less than  $S_c$  the channel slope is mild. Since given depth  $y = 0.30$  m is less than  $y_c = 0.243$  m, it follows that  $y_0 > y > y_c$ . As such the GVF profile is of  $M_2$  type.

#### 4.4 SOME FEATURES OF FLOW PROFILES

(a) **Type-M Profiles** The most common of all GVF profiles is the  $M_1$  type, which is a subcritical flow condition. Obstructions to flow, such as weirs, dams, control structures and natural features, such as bends, produce  $M_1$  backwater curves Fig. 4.4 (a). These extend to several kilometres upstream before merging with the normal depth.

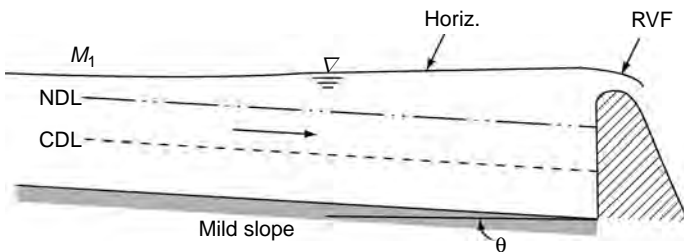


Fig. 4.4 (a)  $M_1$  profile

The  $M_2$  profiles occur at a sudden drop in the bed of the channel, at constriction type of transitions and at the canal outlet into pools Fig. 4.4 (b).

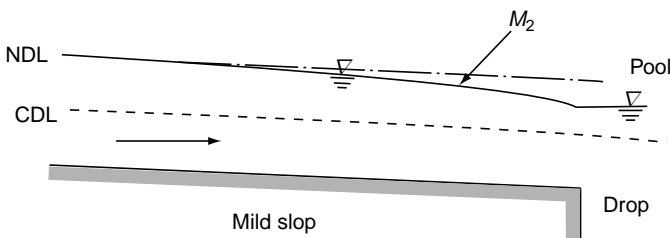


Fig. 4.4 (b)  $M_2$  profile

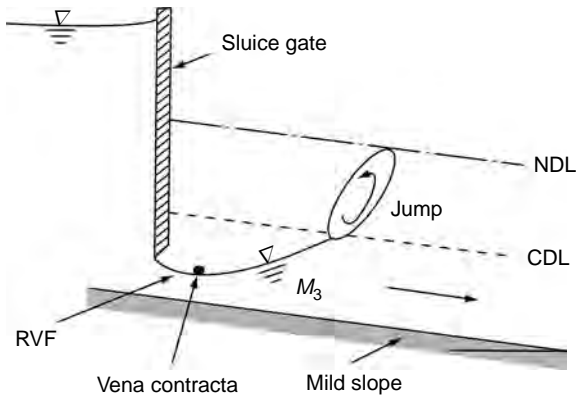


Fig. 4.4 (c)  $M_3$  profile

Where a supercritical stream enters a mild-slope channel, the  $M_3$  type of profile occurs. The flow leading from a spillway or a sluice gate to a mild slope forms a typical example (Fig. 4.4(c)). The beginning of the  $M_3$  curve is usually followed by a small stretch of rapidly-varied flow and the down stream is generally terminated by a hydraulic jump. Compared to  $M_1$  and  $M_2$  profiles,  $M_3$  curves are of relatively short length.

**(b) Type-S Profiles** The  $S_1$  profile is produced when the flow from a steep channel is terminated by a deep pool created by an obstruction, such as a weir or dam (Fig. 4.4 (d)). At the beginning of the curve, the flow changes from the normal depth (supercritical flow) to subcritical flow through a hydraulic jump. The profiles extend downstream with a positive water surface slope to reach a horizontal asymptote at the pool elevation.

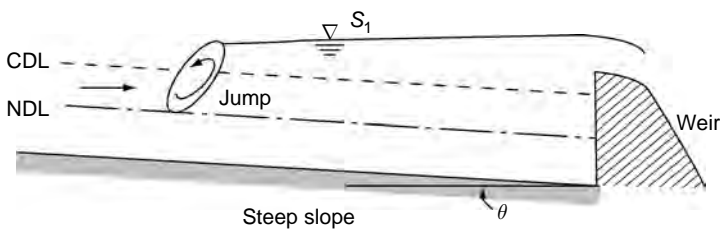


Fig. 4.4(d)  $S_1$  profile

Profiles of the  $S_2$  type occur at the entrance region of a steep channel leading from a reservoir and at a break of grade from mild slopes to steep slope (Fig. 4.4(e)). Generally  $S_2$  profiles are of short length.

Free flow from a sluice gate with a steep slope on its downstream is of the  $S_3$  type (Fig. 4.4(f)). The  $S_3$  curve also results when a flow exists from a steeper slope to a less steep slope (Fig. 4.4(g)).

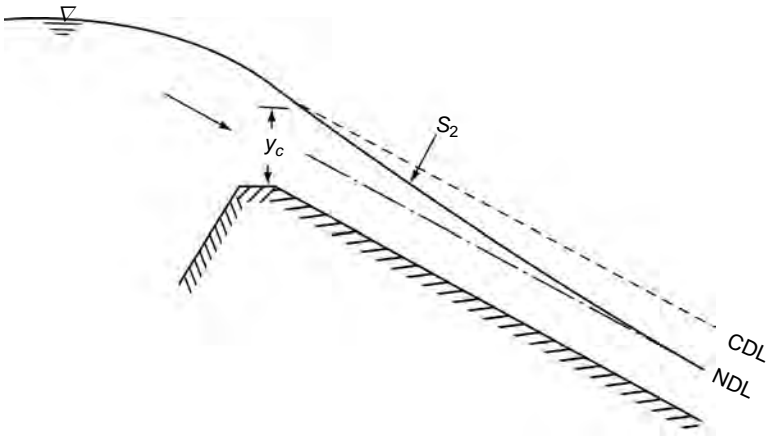


Fig. 4.4(e)  $S_2$  profile

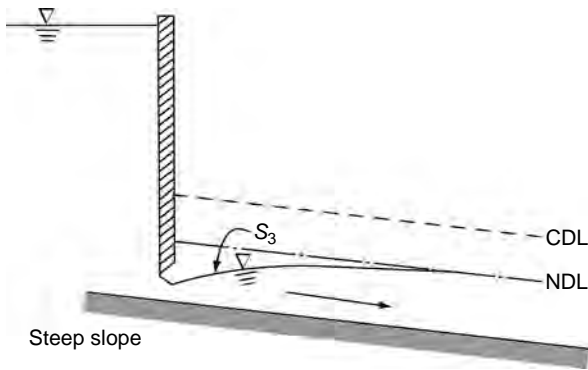


Fig. 4.4(f)  $S_3$  profile

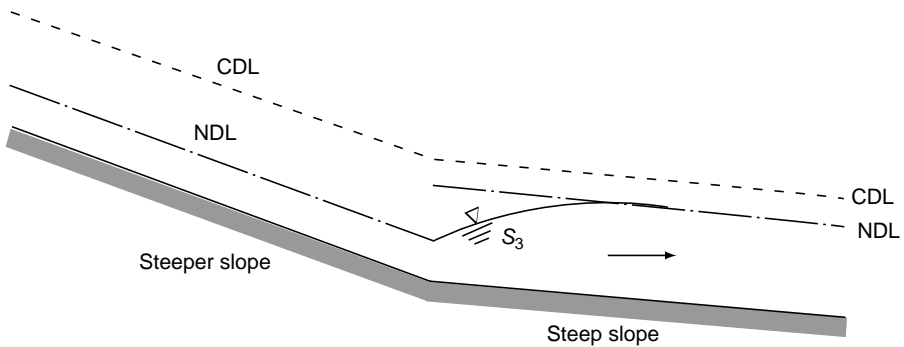


Fig. 4.4(g)  $S_4$  profile

(c) **Type C Profiles**  $C_1$  and  $C_3$  profiles are very rare and are highly unstable.

(d) **Type H Profiles** A horizontal channel can be considered as the lower limit reached by a mild slope as its bed slope becomes flatter. It is obvious that there is no

region 1 for a horizontal channel as  $y_0 = \infty$ . The  $H_2$  and  $H_3$  profiles are similar to  $M_2$  and  $M_3$  profiles respectively [Fig. 4.4(h)]. However, the  $H_2$  curve has a horizontal asymptote.

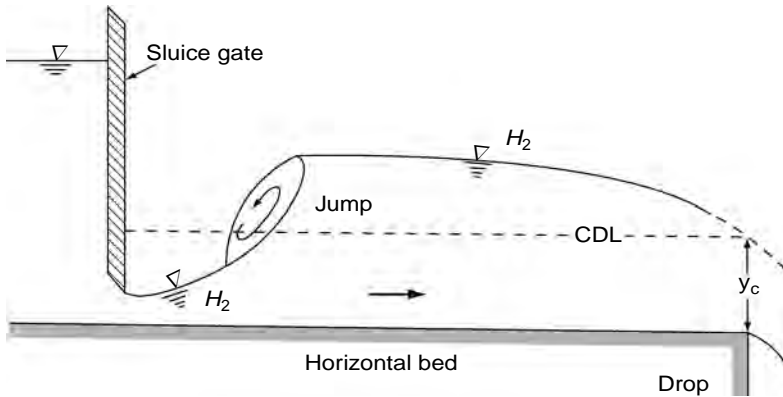


Fig. 4.4(h)  $H_2$  and  $H_3$  profiles

(e) **Type A Profiles** Adverse slopes are rather rare and  $A_2$  and  $A_3$  curves are similar to  $H_2$  and  $H_3$  curves respectively (Fig. 4.4 (i)). These profiles are of very short length.

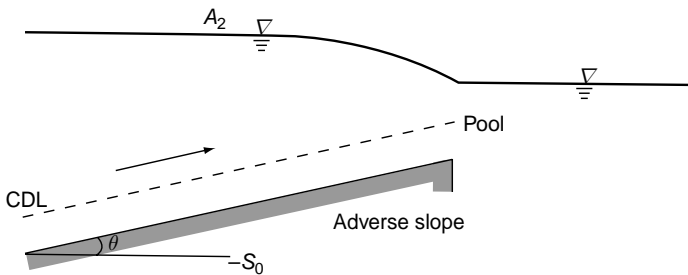


Fig. 4.4(i)  $A_2$  profile

## 4.5 CONTROL SECTIONS

A control section is defined as a section in which a fixed relationship exists between the discharge and depth of flow. Weirs, spillways sluice gates are some typical examples of structures which give rise to control sections. The critical depth is also a control point. However, it is effective in a flow profile which changes from subcritical to supercritical flow. In the reverse case of transition from supercritical flow to subcritical flow, a hydraulic jump is usually formed by passing the critical depth as a control point. Any GVF profile will have at least one control section.

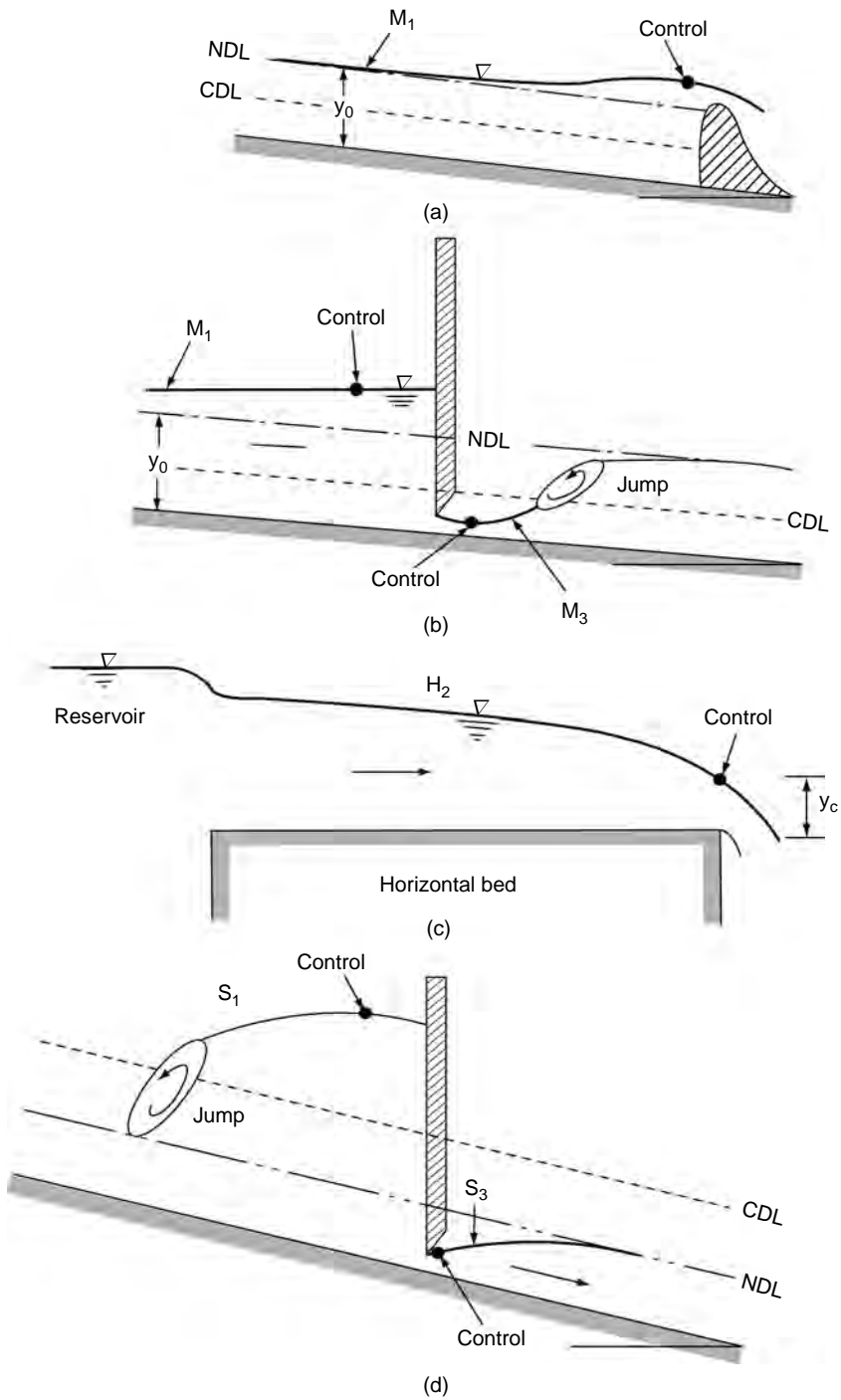


Fig. 4.5 (contd)

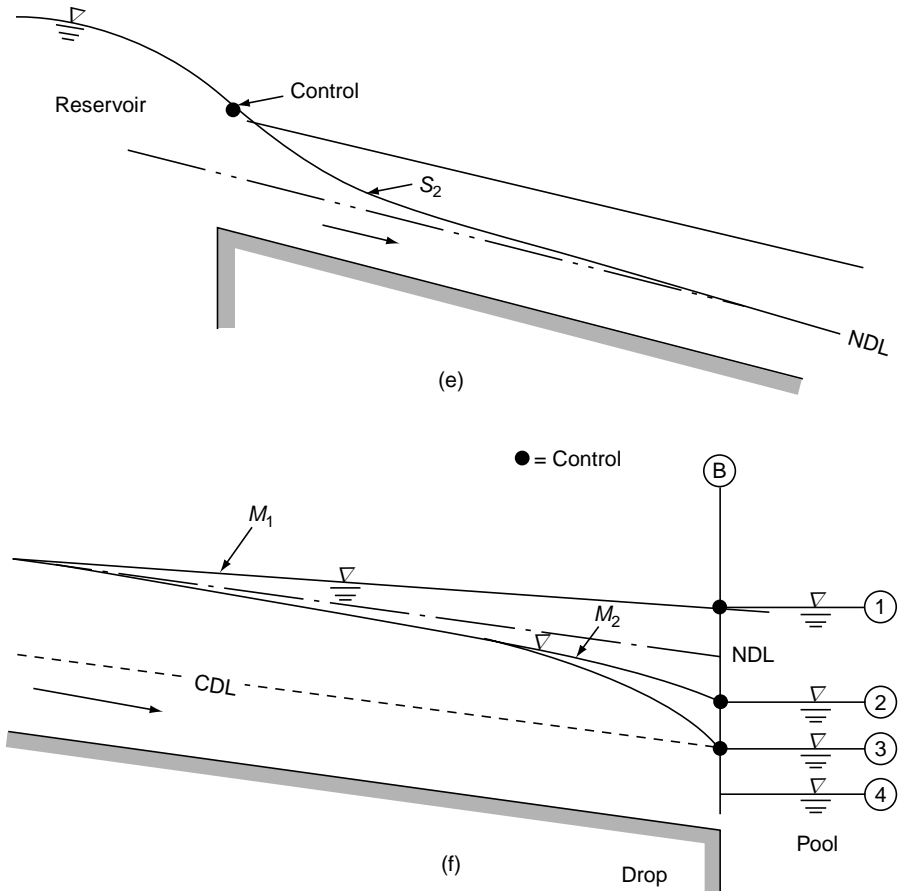


Fig. 4.5 Examples of controls in GVF

In the synthesis of GVF profiles occurring in serially connected channel elements, the control sections provide a key to the identification of proper profile shapes. A few typical control sections are indicated in Fig. 4.5 (a-d). It may be noted that subcritical flows have controls in the downstream end while supercritical flows are governed by control sections existing at the upstream end of the channel section. In Figs 4.5(a) and (b) for the  $M_1$  profile, the control section (indicated by a dark dot in the figures) is just upstream of the spillway and sluice gate respectively. In Figs 4.5(b) and (d) for  $M_3$  and  $S_3$  profiles respectively, the control point is at the vena contracta of the sluice-gate flow. In subcritical-flow reservoir offtakes Fig. 4.5(c), even though the discharge is governed by the reservoir elevation, the channel entry section is not strictly a control section. The water-surface elevation in the channel will be lower than the reservoir elevation by an amount equivalent to  $(1+K)V^2/2g$  where  $K$  is the entrance-loss coefficient. The true control section will be at a downstream location in the channel. For the situation shown in Fig. 4.5(c) the critical depth at the free overflow at the

channel end acts as the downstream control. For a sudden drop (free overflow) due to curvature of the streamlines the critical depth actually occurs at distance of about  $4.0 y_c$  upstream of the drop. This distance, being small compared to GVF lengths, is neglected and it is usual to perform calculations by assuming  $y_c$  to occur at the drop.

For a supercritical canal intake Fig. 4.5(e), the reservoir water surface falls to the critical depth at the head of the canal and then onwards the water surface follows the  $S_2$  curve. The critical depth occurring at the upstream end of the canal is the control for this flow.

A mild-slope channel discharging into a pool of variable surface elevation is indicated in Fig. 4.5(f). Four cases are shown. In case 1, the pool elevation is higher than the elevation of the normal-depth line at  $B$ . This gives rise to a drowning of the channel end. A profile of the  $M_1$  type is produced with the pool level at  $B$  as control. The velocity head of the channel flow is lost in turbulence at the exit and there is no recovery in terms of the change in surface elevation. In case 2, the pool elevation is lower than the elevation of the normal-depth line but higher than the critical-depth line at  $B$ . The pool elevation acts as a control for the  $M_2$  curve. In case 3, the pool elevation has dropped down to that of the critical-depth line at  $B$  and the control is still at the pool elevation. In case 4, the pool elevation has dropped lower than the elevation of the critical-depth line at  $B$ . The water surface cannot pass through a critical depth at any location other than  $B$  and hence a sudden drop in the water surface at  $B$  is observed. The critical depth at  $B$  is the control for this flow.

## 4.6 ANALYSIS OF FLOW PROFILE

The process of identification of possible flow profiles as a prelude to quantitative computations is known as analysis of flow profile. It is essentially a synthesis of the information about the GVF profiles and control sections discussed in the previous section.

A channel carrying a gradually varied flow can in general contain different prismatic-channel sections of varying hydraulic properties. There can be a number of control sections of varying locations. To determine the resulting water-surface profile in a given case, one should be in a position to analyse the effects of various channel sections and controls connected in series. Simple cases are illustrated to provide information and experience to handle more complex cases.

**Break in Grade** Simple situations of a series combination of two channel sections with differing bed slopes are considered. In Fig. 4.6(a), a break in grade from a mild channel to a milder channel is shown. It is necessary to first draw the critical-depth line (CDL) and the normal-depth line (NDL) for both slopes. Since  $y_c$  does not depend upon the slope (as  $Q = \text{constant}$ ), the CDL is at a constant height above the channel bed in both slopes. The normal depth  $y_{01}$  for the mild slope is lower than that of the milder slope ( $y_{02}$ ). In this case,  $y_{02}$  acts as a control, similar to the

weir or spillway case and an  $M_1$  backwater curve is produced in the mild-slope channel.

Various combinations of slopes and the resulting GVF profiles are presented in Fig. 4.6(a-h). It may be noted that in some situations there can be more than one possible profiles. For example, in Fig. 4.6(e), a jump and  $S_1$  profile or an  $M_3$  profile and a jump are possible. The particular curve in this case depends on the channel and its properties.

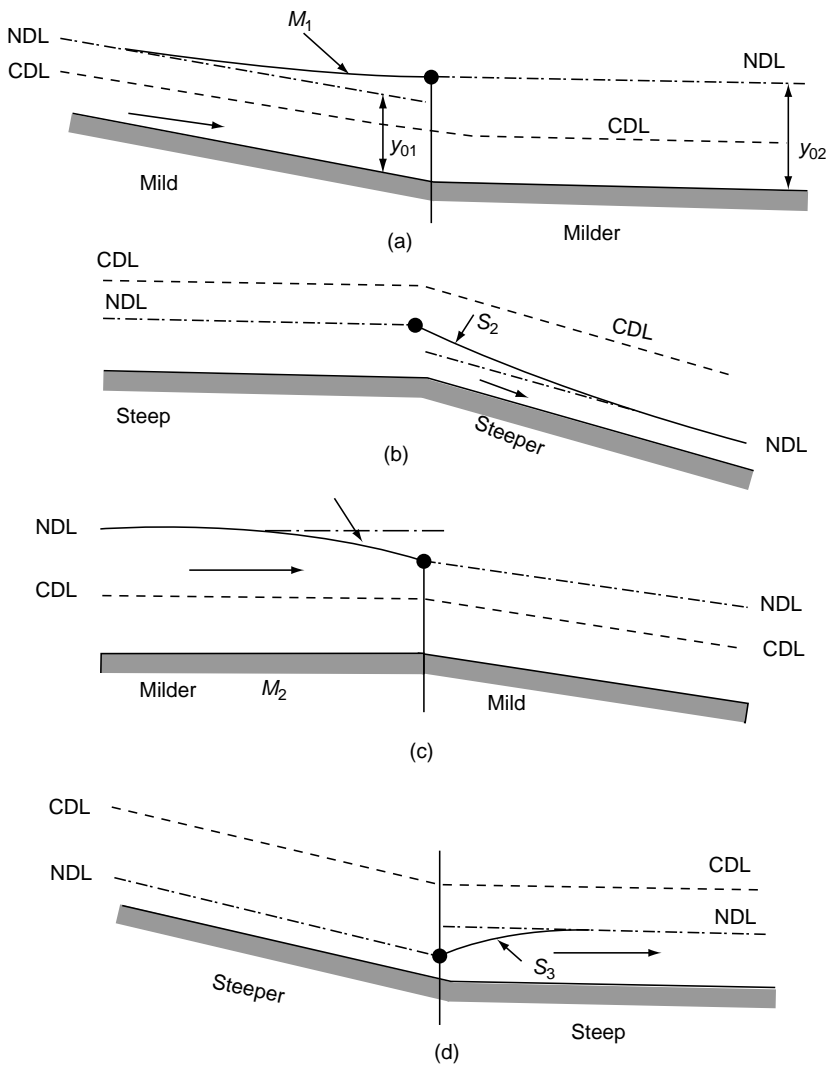


Fig. 4.6 (Contd)



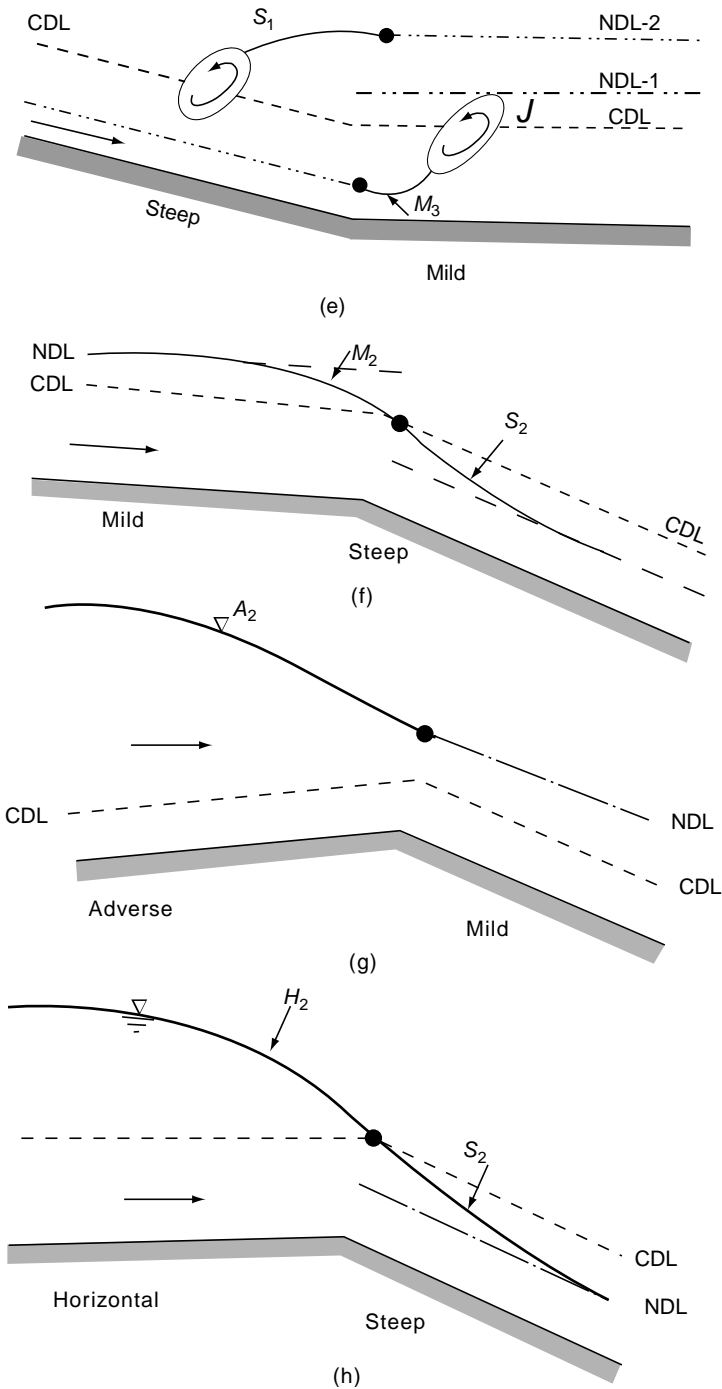


Fig. 4.6 GVT profiles at break in grades

In the examples indicated in Fig. 4.6, the section where the grade changes acts as a control section and this can be classified as a natural control. It should be noted that even though the bed slope is considered as the only variable in the above examples, the same type of analysis would hold good for channel sections in which there is a marked change in the roughness characteristics with or without a change in the bed slope. A long reach of unlined canal followed by a lined reach serves as a typical example for the same. The junction provides a natural control of the kind discussed above. A change in the channel geometry (say, the bed width or side slope) beyond a section while retaining the prismatic nature in each reach also leads to a natural control section.

**Serial Combination of Channel Sections** To analyse a general problem of many channel sections and controls, the following steps are to be adopted:

1. Draw the longitudinal section of the systems.
2. Calculate the critical depth and normal depths of various reaches and mark the CDL and NDL in all the reaches.
3. Mark all the controls—both the imposed as well as natural controls.
4. Identify the possible profiles.

**Example 4.2** | A rectangular channel of 4.0-m width has a Manning’s coefficient of 0.025. For a discharge of 6.0 m<sup>3</sup>/s in this channel, identify the possible GVF profiles produced in the following break in grades.

- a)  $S_{01} = 0.0004$  to  $S_{02} = 0.015$   
 b)  $S_{01} = 0.005$  to  $S_{02} = 0.0004$

*Solution*  $q = 6.0 / 4.0 = 1.50 \text{ m}^3/\text{s/m}$

$$y_c = \left( \frac{q^2}{g} \right)^{\frac{1}{3}} = \left[ \frac{(1.5)^2}{9.81} \right]^{1/3} = 0.612 \text{ m.}$$

For normal depth calculation:  $\phi = \frac{Qn}{\sqrt{S_0} \times B^{8/3}} = \frac{6.0 \times 0.025}{\sqrt{S_0} \times (4.0)^{8/3}} = \frac{0.00372}{\sqrt{S_0}}$

Using this relation, the normal depth for various cases are calculated as below.

$S_0$	$\phi$	$y_0/B$ from Table 3A-1	$y_0$ (m)
0.0004	0.1860	0.4764	1.906
0.015	0.0303	0.1350	0.540
0.005	0.0526	0.1950	0.780

Depending upon the relative values of  $y_{01}$ ,  $y_c$  and  $y_{02}$ , the type of grade changes are identified as below:

Case	$y_{01}$ (m)	$y_{02}$ (m)	$y_c$ (m)	Type of grade change	Possible Types of Profiles
a)	1.906	0.540	0.612	Mild to Steep	$M_2$ and $S_2$
b)	0.780	1.906	0.612	Mild to Milder mild	$M_1$

Various possible GVF profiles in these two cases are shown in Fig. 4.7 (a) and 4.7(b).

**(Alternative method)**

Instead of calculating normal depth through use of tables, the critical slope is calculated. By using Eq. (3.64).

$$S_{*c} = \frac{S_c B^{1/3}}{gn^2} = \frac{(1 + 2\eta)^{4/3}}{\eta^{1/3}}$$

$$S_c = \frac{gn^2}{B^{1/3}} \frac{(1 + 2\eta)^{4/3}}{\eta^{1/3}} \tag{4.17}$$

Here,  $\eta = y_c / B = 0.612 / 4.0 = 0.153$ . Substituting in Eq. 4.17

$$S_c = \frac{9.81 \times (0.025)^2}{(4.0)^{1/3}} \times \frac{(1 + 2 \times (0.153))^{4/3}}{(0.153)^{1/3}} = 0.0103$$

Classification of Channels based on value of slope relative to  $S_c = 0.013$

Case	$S_{01}$	Type	$S_{02}$	Type	Type of grade change
a)	0.0004	Mild	0.015	Steep	Mild to Steep
b)	0.005	Mild	0.0004	Mild	Mild to Milder mild

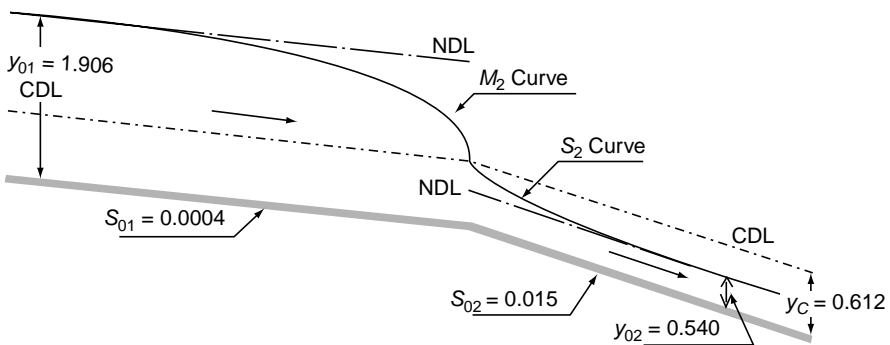


Fig. 4.7(a)  $M_2$  and  $S_2$  curves-Example 4.2 (a)

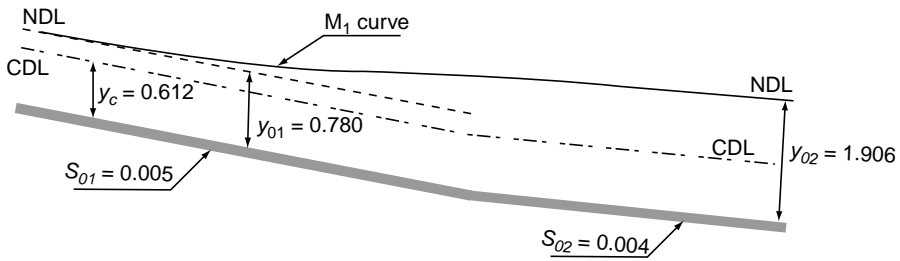


Fig 4.7(b)  $M_1$  curve – Example 4.2 (b)

**Example 4.3** Identify and sketch the GVF profiles in three mild slopes which could be described as mild, steeper mild and milder. The three slopes are in series. The last slope has a sluice gate in the middle of the reach and the downstream end of the channel has a free overfall.

**Solution** The longitudinal section of the channel, critical-depth line and normal-depth lines for the various reaches are shown in Fig. 4.8. The free overfall at *E* is obviously a control. The vena contracta downstream of the sluice gate at *D* is another control. Since for subcritical flow the control is at the downstream end of the channel, the higher of the two normal depths at *C* acts as a control for the reach *CB*, giving rise to an  $M_1$  profile over *CB*. At *B*, the normal depth of the channel *CB* acts as a control giving rise to an  $M_2$  profile over *AB*. The controls are marked distinctly in Fig. 4.8. With these controls the possible flow profiles are: an  $M_2$  profile on channel *AB*,  $M_1$  profile on channel *BC*,  $M_3$  profile and  $M_2$  profile connected through a jump on the stretch *DC*. All these possible types are marked in Fig. 4.8. The details of computation of the various profiles and the location of the jump is discussed in the next chapter.

**Example 4.4** A trapezoidal channel has three reaches *A*, *B* and *C* connected in series with the following properties:

Reach	Bed width <i>B</i>	Side slope <i>m</i>	Bed slope $S_0$	<i>n</i>
<i>A</i>	4.0 m	1.0	0.0004	0.015
<i>B</i>	4.0 m	1.0	0.009	0.012
<i>C</i>	4.0 m	1.0	0.004	0.015

**Solution** For a discharge of 22.5 m<sup>3</sup>/s through this channel, sketch the resulting water-surface profiles. The length of the reaches can be assumed to be sufficiently long for the GVF profiles to develop fully.

The normal depth and critical depths in the reaches *AB* and *BC* are calculated by using Tables 3A.2 and 2A.2. respectively as follows:

Reach	$\phi = \frac{Qn}{\sqrt{S_0}B^{8/3}}$	$\frac{y_0}{B}$	$y_0$ (m)	$\frac{Qm^{1.5}}{\sqrt{g}B^{2.5}}$	$\frac{my_c}{B}$	$y_c$ (m)	Classification of the reach
A	0.4186	0.566	2.264	0.2245	0.329	1.316	Mild slope
B	0.0706	0.203	0.812	0.2245	0.329	1.316	Steep slope
C	0.1324	0.296	1.172	0.2245 <td 0.329	1.316	Steep slope	

Reach A is a mild-slope channel as  $y_0 > y_c$  and reaches B and C are steep slope channels. Reach B is steeper than reach C. The various reaches are schematically shown in Fig. 4.9. The CDL is drawn at a height of 1.316 m above the bed level and the NDLS are drawn at the appropriate  $y_0$  values.

The controls are marked in the figure. Reach A will have an  $M_2$  drawdown curve, reach B and  $S_2$  drawdown curve and reach C and  $S_3$  rising curve as shown in the figure. It may be noted that the resulting profile as above is a serial combination of Fig. 4.6(d) and (f).

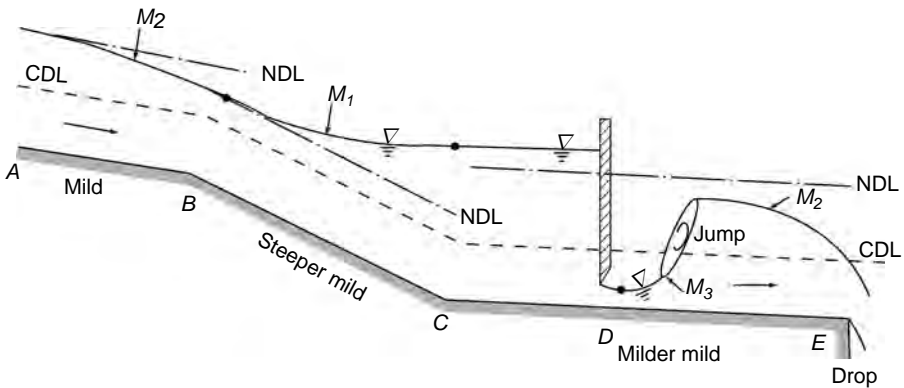


Fig. 4.8 GVF profile for Example 4.3

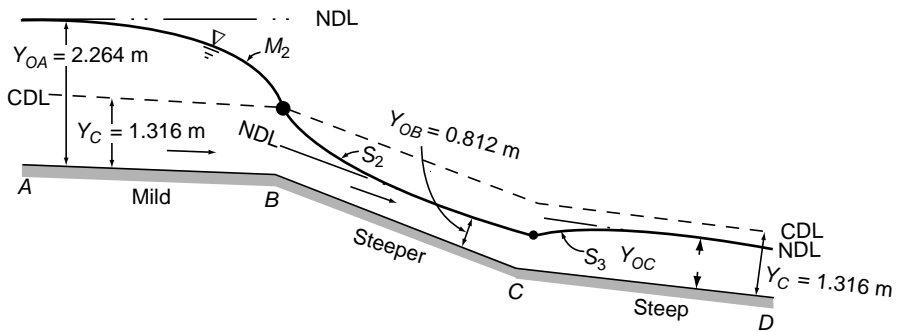


Fig. 4.9 GVF profile for Example 4.4

**Example 4.5** In a rectangular channel, two reaches *M* and *N* are in series, with reach *M* being upstream of reach *N*. These channel reaches have the following characteristics:

Reach	Width (m)	Discharge (m <sup>3</sup> /s)	Slope	<i>n</i>
<i>M</i>	5.0	15.0	0.0004	0.025
<i>N</i>	4.0	15.0	0.0003	0.015

Sketch the resulting GVF profile due to the change in the channel characteristics as above.

Solution  $q_m = 15.0 / 5.0 = 3.00 \text{ m}^3/\text{s/m}$   $y_{c_m} = \left(\frac{q^2}{g}\right)^{1/3} = \left[\frac{(3.0)^2}{9.81}\right]^{1/3} = 0.9717 \text{ m}$

$q_n = 15.0 / 4.0 = 3.75 \text{ m}^3/\text{s/m}$   $y_{c_n} = \left(\frac{q^2}{g}\right)^{1/3} = \left[\frac{(3.75)^2}{9.81}\right]^{1/3} = 1.1275 \text{ m}$

Normal depth calculations:

Reach	$\phi = \frac{nQ}{\sqrt{S_0} B^{8/3}}$	$\eta$ from Table 3A.1	Normal depth $y_0$ (m)
<i>M</i>	0.256496	0.6071	3.036 m
<i>N</i>	0.32220	0.7254	2.902 m

Reach	$y_0$ (m)	$y_c$ (m)	Slop classification	Nature of break in grade	Nature of GVF due to break in grade
<i>M</i>	3.3036	0.9717	Mild	Mild to	$M_2$ curve in Reach
<i>N</i>	2.902	1.1275	Mild	Steeper mild	<i>M</i>

The channel slope changes from Mild Slope to Steeper mild slope and an  $M_2$  curve is formed in the reach *M*. The curve has the upstream asymptote of  $y_{0m} = 3.3036 \text{ m}$  and ends at a depth of 2.902 m at the junction of the two reaches. The nature of the GVF profile is shown schematically in Fig. 4.10.

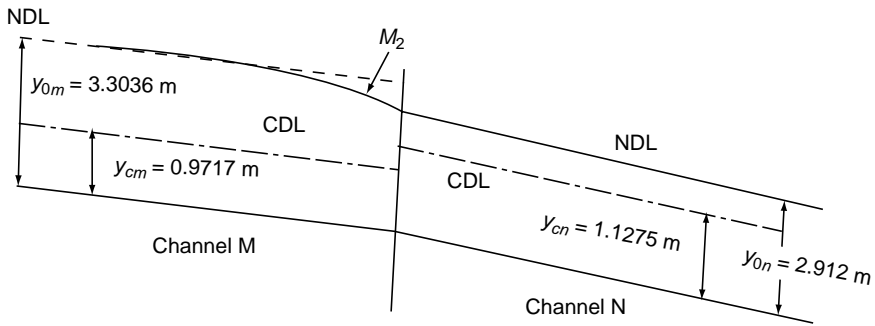


Fig. 4.10 GVF profile of Example 4.5

### 4.7 TRANSITIONAL DEPTH

The transitional depth is defined as the depth at which the normal discharge  $Q_n$  is equal to the critical discharge  $Q_c$  and the slope of the gradually varied flow profile is horizontal. For such a situation,

$$\frac{dy}{dx} = S_0 \quad (4.18)$$

Since in a GVF from Eq. (4.15)

$$\frac{dy}{dx} = S_0 \frac{1 - (Q/Q_n)^2}{1 - (Q/Q_c)^2}$$

at the transitional depth

$$\frac{Q}{Q_n} = \frac{Q}{Q_c} \text{ or } \frac{K_0}{K} = \frac{Z_c}{Z} \quad (4.19)$$

i.e

$$\frac{Q/\sqrt{S_0}}{\frac{1}{n}AR^{2/3}} = \frac{Q/\sqrt{g}}{A\sqrt{A/T}}$$

or

$$\frac{S_0}{n^2 g} = \frac{A}{T} \frac{1}{R^{4/3}} = \frac{P^{4/3}}{TA^{1/3}} \quad (4.20)$$

Equation 4.20 is the same as the generalized-flow relation (Eq. (3.69)) with  $F = 1.0$ . For a trapezoidal channel, the non-dimensionalised form of Eq. 4.20 will be

$$S_{*0c} = \frac{S_0 B^{1/3}}{n^2 g} = \frac{(1 + 2\eta_r \sqrt{m^2 + 1})^{4/3}}{(1 + 2m\eta_r)(1 + m\eta_r)^{1/3} \eta_r^{1/3}} \quad (4.21)$$

where  $\eta_t = y_t =$  transitional depth. It may be noted that  $S_{*0c}$  is similar to  $S_{*c}$  (Section 3.16) but with the bed slope  $S_0$  being used in place of  $S_c$ .

In a given problem, normally  $S_0, B, n$  are fixed and the value of  $\eta_t$  is required. It is important to note that in the gradually-varied flow calculations,  $Q_n$  and  $Q_c$  are fictitious discharges and are different from the actual discharge  $Q$ . As such, at a transitional depth  $y_t$ , the actual flow Froude number is not unity (Example 4.4). Since Eq. (4.20) is the same as Eq. (3.50) of the generalized-flow relationship, the behaviour of the transitional depth in trapezoidal, rectangular and triangular channels is exactly the same as the behaviour of the critical depth with critical slope (discussed in Section 3.16). The generalised-flow diagram (Fig. 3.11) can be used for the solution of Eq. (4.21) to determine the transitional depth.

It may be seen from Eq. (4.20) that the transitional depth depends only on the channel geometry, roughness and slope and is independent of the actual discharge. In general, there can be one, two or three transitional depths depending upon the flow and channel geometry. However, situations with more than one transitional depth in a profile are rare. In gradually varied flow computations, the transitional depth is useful to locate sections where the water surface may have a point of inflexion with respect to the horizontal. In spatially-varied flows, the transitional depth provides a very effective way of determining the control points.

**Example 4.5** | A 2.0-m wide rectangular channel ( $n = 0.015$ ), carries a discharge of  $4.0 \text{ m}^3/\text{s}$ . The channel is laid on slope of 0.0162. A downstream sluice gate raises the water surface to 7.0 m immediately behind it. Find the transitional depth.

*Solution* From Section 3.17, the limit value of  $S_{*c} = \frac{S_{Lc} B^{1/3}}{gn^2} = 2.667$

$$\text{Limit slope} \quad S_{Lc} = \frac{2.667(9.81)(0.015)^2}{(2.0)^{1/3}} = 0.004672$$

Since the actual slope  $S_0 > S_{Lc}$ , transitional depth is possible.

The normal depth  $y_0$ , for given  $S_0, n, B$  and  $Q$  is found by using Table 3A.1.

$$\phi = \frac{4.0 \times 0.015}{\sqrt{0.0162 \times (2.0)^{8/3}}} = 0.07424$$

$$y_0 / B = 0.2466, y_0 = 0.493 \text{ m}$$

$$\text{Critical depth } y_c = \left( \frac{16}{4 \times 9.81} \right)^{1/3} = 0.742 \text{ m}$$



Since  $y_0 < y_c < y$ , the channel is a steep-slope channel and the GVF profile is an  $S_1$  curve. At the transitional depth, from Eq. (4.21),

$$S_{*0c} = \frac{S_0 B^{1/3}}{gn^2} = \frac{0.0162 \times (2.0)^{1/3}}{(9.81) \times (0.015)^2} = 9.247$$

$$= \frac{(1 + 2\eta_t)^{4/3}}{\eta_t^{1/3}}$$

By using trial-and-error method the two transitional depths are found as

$$\eta_{t1} = 2.985, \quad y_{t1} = 5.970 \text{ m}$$

$$\eta_{t2} = 0.00125, \quad y_{t2} = 0.0025 \text{ m}$$

The second transitional depth,  $y_{t2}$  is not of any significance in this problem.

The  $S_1$  curve starting after a jump from the normal depth will continue to rise till  $y = y_t = 5.970 \text{ m}$  at which point it will become horizontal. Beyond  $y_t$ , The Froude number at  $y = y_t$  is

$$F_t = \frac{4.0 / (2.0 \times 5.97)}{\sqrt{9.81 \times 5.97}} = 0.0438$$

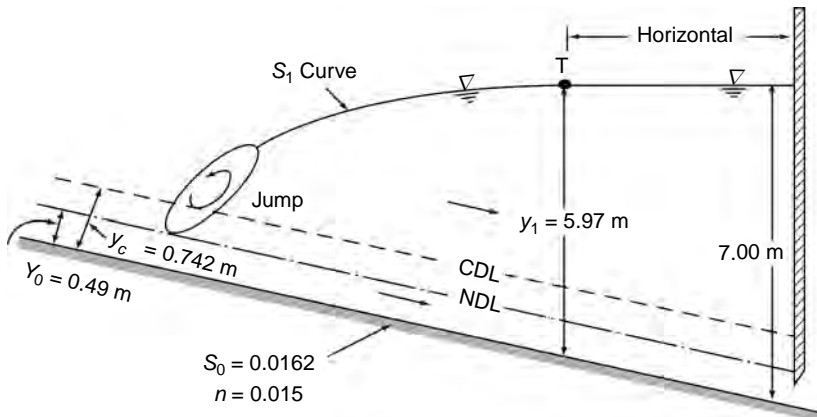


Fig. 4.11 Example 4.6

## PROBLEMS

*Problem Distribution*

<i>Topic</i>	<i>Problems</i>
<i>GVF equation</i>	4.1, 4.2
<i>Classification of GVF profiles</i>	4.3, 4.5–4.7
<i>Water surface slope</i>	4.4
<i>GVF profiles at break in grade</i>	4.8, 4.11
<i>Profile analysis</i>	4.9, 4.10, 4.12 – 4.15

- 4.1 (i) Show that the differential equation of gradually varied flow in a rectangular channel of variable width  $B$  can be expressed as

$$\frac{dy}{dx} = \frac{S_0 - S_f + \left( \frac{Q^2 y}{gA^3} \frac{dB}{dx} \right)}{1 - \frac{Q^2 B}{gA^3}}$$

- (ii) Further, show that for horizontal, frictionless rectangular channel of varying width  $B$ , the above relation reduces to

$$(1 - F^2) \frac{dy}{dx} - F^2 \left( \frac{y}{B} \right) \frac{dB}{dx} = 0$$

where  $F$  = Froude number.

- 4.2 Using the basic differential equation of GVF, show that  $dy/dx$  is positive for  $S_1$ ,  $M_3$  and  $S_3$  profiles
- 4.3 Show that for a wide rectangular channel the slope is mild or steep according to  $S_0$  being less than or greater than

$$\left( \frac{n^2 g^{10/9}}{q^{2/9}} \right)$$

- 4.4 A 3.0-m wide rectangular channel has a longitudinal slope of 150 mm/kmh and Manning's  $n = 0.02$ . When the discharge in the channel is  $0.85 \text{ m}^3/\text{s}$ , estimate the slope of the water surface in the channel (relative to the horizontal) at a point where the depth of flow is 0.75 m.
- 4.5 In a very long, wide rectangular channel the discharge intensity is  $3.0 \text{ m}^3/\text{s}/\text{metre width}$ . The bed slope of the channel is 0.004 and Manning's  $n = 0.015$ . At a certain section in this channel, the depth of flow is observed to be 0.90 m. What type of GVF profile occurs in the neighbourhood of this section?
- 4.6 In a 4.0-m wide rectangular channel ( $n = 0.017$ ) the bed slope is 0.0006. When the channel is conveying  $10.0 \text{ m}^3/\text{s}$  of flow, estimate the nature of GVF profiles at two far away sections  $P$  and  $R$  in this channel where the depth of flow is measure as 1.6 m and 2.1 m respectively.

- 4.7 A circular channel having a 2.0-m diameter ( $n = 0.015$ ) is laid on a slope of 0.005. When a certain discharge is flowing in this channel at a normal depth of 1.0 m, GVF was found to occur at a certain reach of channel. If a depth of 0.70 m was observed at a section in this GVF reach, what type of GVF profile was occurring in the neighborhood of this section?
- 4.8 In a very long trapezoidal channel with bed width  $B = 3.0$  m, side slope  $m = 1.5$ , Manning's  $n = 0.016$ , Longitudinal slope  $S_0 = 0.0004$ , the normal depth is measured as 1.20 m. Determine the type of GVF profile existing at a section  $X$  in this channel when the depth of flow at  $X$  is (i) 0.5 m, (ii) 0.8 m and (iii) 1.50 m.
- 4.9 A long and wide rectangular channel ( $n = 0.016$ ) has a discharge intensity of 4.0 m<sup>3</sup>/s per metre width. If the bed slope changes from 0.008 to 0.012 at a section, sketch the possible GVF profiles due to this break in grade.
- 4.10 Analyse the flow profile in a 4.0-m wide rectangular channel ( $n = 0.015$ ), carrying a discharge of 15.0 m<sup>3</sup>/s. The bed slope of the channel is 0.02 and a 1.5 m high weir ( $C_d = 0.70$ ) is built on the downstream end of the channel.
- 4.11 At a certain section in a rectangular channel, a constriction of the channel produces a choking condition. Sketch the GVF profile produced on the upstream as a result of this, if the channel is on (a) mild slope and (b) steep slope.
- 4.12 A 4.0-m wide rectangular channel has a Manning's coefficient of 0.025. For a discharge of 6.0 m<sup>3</sup>/s, identify the possible types of GVF profiles produced in the following break in grades:

$$(a) S_{01} = 0.0004 \quad \text{to} \quad S_{02} = 0.005$$

$$(b) S_{01} = 0.015 \quad \text{to} \quad S_{02} = 0.0004$$

- 4.13 Sketch the possible GVF profiles in the following serial arrangement of channels and control. The flow is from left to right:
- (a) steep – horizontal – mild slope
  - (b) mild – sluice gate – steep – horizontal – sudden drop
  - (c) steep – steeper – mild – milder slope
  - (d) free intake – steep – sluice gate – mild slope
  - (e) steep – mild – sluice gate – mild – sudden drop
  - (f) sluice gate – adverse – horizontal – steep slope
- 4.14 Sketch the GVF profiles produced on the upstream and downstream of a sluice gate introduced in a
- (a) steep slope, (b) mild slope, and (c) horizontal-bed channel.
- 4.15 A rectangular channel has two reaches  $A$  and  $B$  in series with characteristics as below:

Reach	Width(m)	Discharge(m <sup>3</sup> /s)	Slope	$n$
$A$	4.80	7.40	0.0005	0.015
$B$	4.80	5.00	0.0005	0.015

The decrease in discharge at  $B$  is due to the withdrawal of some flow at the junction and can be considered to be a local phenomenon. Sketch the GVF profiles produced in the channels if (a) the channel is continuous and without any obstruction at the junction, and (b) a sluice gate is provided at the junction.

- 4.16 In a rectangular channel two reaches  $A$  and  $B$  in series, with reach  $A$  being upstream of Reach  $B$ , have the following characteristics:

Reach	Width (m)	Discharge (m <sup>3</sup> /s)	Slope	n
A	3.5	10.0	0.0004	0.020
B	3.0	10.0	0.0160	0.015

Sketch the resulting GVF profiles due to change in the channel characteristics as above.

- 4.17 For the channel arrangement shown in Fig 4.11, sketch and label the possible types of GVF profiles.

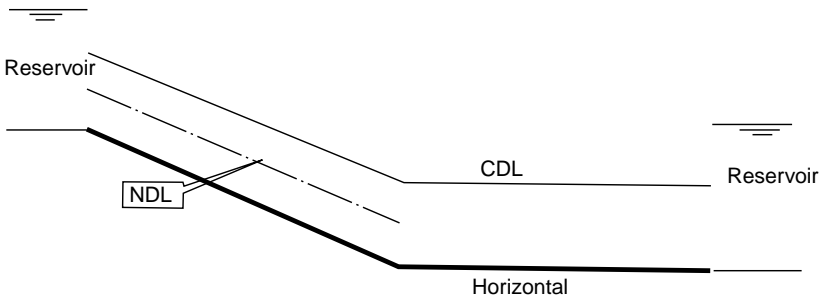


Fig. 4.11 Problem 4.17

- 4.18 For the channel arrangement shown in Fig. 4.12, sketch and label the possible types of GVF profiles.

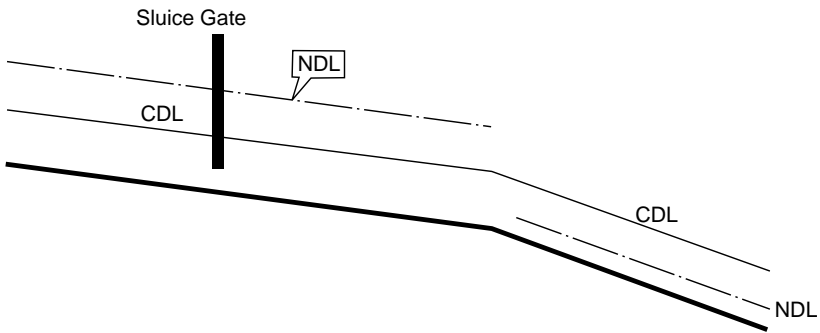


Fig. 4.12 Problem 4.18

## OBJECTIVE QUESTIONS

- 4.1 In terms of conveyances and section factors, the basic differential equation of GVF can be written as  $dy/dx =$

(a)  $S_0 \frac{1 - (K_0/K)^2}{1 - (Z/Z_c)^2}$

(b)  $S_0 \frac{1 - (K/K_0)^2}{1 - (Z_c/Z)^2}$

(c)  $S_0 \frac{1 - (K_0/K)^2}{1 - (Z_c/Z)^2}$

(d)  $S_0 \frac{1 - (K/K_0)^2}{1 - (Z/Z_c)^2}$

186 Flow in Open Channels

4.2 In GVF profiles as the depth  $y \rightarrow y_c$ ,

(a)  $\frac{dy}{dx} \rightarrow 0$

(b)  $\frac{dy}{dx} \rightarrow \infty$

(c)  $\frac{dy}{dx} \rightarrow S_0$

(d)  $\frac{dy}{dx} \rightarrow$  a finite value

4.3 For a wide rectangular channel, if the Manning's formula is used, the differential equation of GVF becomes  $dy/dx =$

(a)  $S_0 \frac{1 - (y_0 / y)^{3.33}}{1 - (y_c / y)^{3.33}}$

(b)  $S_0 \frac{1 - (y_0 / y)^{3.33}}{1 - (y_c / y)^3}$

(c)  $S_0 \frac{1 - (y / y_0)^{3.33}}{1 - (y / y_c)^3}$

(d)  $S_0 \frac{1 - (y / y_0)^3}{1 - (y_c / y_0)^{3.33}}$

4.4 For a very wide rectangular channel, if Chezy formula is used, the differential equation of GVF is given by  $dy/dx =$

(a)  $S_0 \frac{1 - (y_0 / y)^{3.33}}{1 - (y_c / y)^{3.33}}$

(b)  $S_0 \frac{1 - (y_0 / y)^3}{1 - (y_c / y)^3}$

(c)  $S_0 \frac{1 - (y_0 / y)^3}{1 - (y_c / y)^{3.33}}$

(d)  $S_0 \frac{1 - (y_0 / y)^{3.33}}{1 - (y_c / y)^3}$

4.5 Uniform flow is taking place in a rectangular channel having a longitudinal slope of 0.004 and Manning's  $n = 0.013$ . The discharge per unit width in the channel is measured as  $1.2 \text{ m}^3/\text{s}/\text{m}$ . The slope of the channel is classified in GVF analysis as

(a) mild

(b) critical

(c) steep

(d) very steep

4.6 In a GVF,  $dy/dx$  is positive if

(a)  $K > K_0$  and  $Z > Z_c$

(b)  $K > K_0$  and  $Z < Z_c$

(c)  $K_0 > K_c$  and  $Z_0 > Z_c$

(d)  $Z > K$  and  $Z_c > K_0$

4.7 A 2.0-m wide rectangular channel has normal depth of 1.25 m when the discharge is  $8.75 \text{ m}^3/\text{s}$ . The slope of the channel is classified as

(a) steep

(b) mild

(c) critical

(d) essentially horizontal

4.8 Identify the *incorrect* statement:

The possible GVF profiles in

(a) mild slope channels are  $M_1$ ,  $M_2$  and  $M_3$

(b) adverse slope channels are  $A_2$  and  $A_3$

(c) horizontal channels are  $H_1$  and  $H_3$

(d) critical slope channels are  $C_1$  and  $C_3$

4.9 The following types of GVF profiles do not exist:

(a)  $C_2$ ,  $H_2$ ,  $A_1$

(b)  $A_2$ ,  $H_1$ ,  $C_2$

(c)  $H_1$ ,  $A_1$ ,  $C_2$

(d)  $C_1$ ,  $A_1$ ,  $H_1$

- 4.10 The total number of possible types of GVF profiles are  
 (a) 9 (b) 11  
 (c) 12 (d) 15
- 4.11  $dy/dx$  is negative in the following GVF profiles:  
 (a)  $M_1, S_2, A_2$  (b)  $M_2, A_2, S_3$   
 (c)  $A_3, A_2, M_2$  (d)  $M_2, A_2, H_2, A_2$
- 4.12 If in a GVF  $dy/dx$  is positive, then  $dE/dx$  is:  
 (a) always positive (b) negative for an adverse slope  
 (c) negative if  $y > y_c$  (d) positive if  $y > y_c$
- 4.13 In a channel the gradient of the specific energy  $dE/dx$  is equal to  
 (a)  $S_0 - S_f$  (b)  $S_f - S_0$   
 (c)  $S_0 - S_f - \frac{dy}{dx}$  (d)  $S_0(1 - F^2)$
- 4.14 In a wide river the depth of flow at a section is 3.0 m,  $S_0 = 1$  in 5000 and  $q = 3.0$  m<sup>3</sup>/s per metre width. If the Chezy formula with  $C = 70$  is used, the water surface slope relative to the bed at the section is  
 (a)  $-2.732 \times 10^{-4}$  (b)  $1.366 \times 10^{-4}$   
 (c)  $1.211 \times 10^{-5}$  (d)  $-6.234 \times 10^{-4}$
- 4.15 The  $M_3$  profile is indicated by the following inequality between the various depths:  
 (a)  $y_0 > y_c > y$  (b)  $y > y_0 > y_c$   
 (c)  $y_c > y_0 > y$  (d)  $y > y_c > y_0$
- 4.16 A long prismatic channel ends in an abrupt drop. If the flow in the channel far upstream of the drop is subcritical, the resulting GVF profile  
 (a) starts from the critical depth at the drop and joins the normal depth asymptotically  
 (b) lies wholly below the critical depth line  
 (c) lies wholly above the normal depth line  
 (d) lies partly below and partly above the critical depth line
- 4.17 When there is a break in grade due to a mild slope  $A$  changing into a milder slope  $B$ , the GVF profile produced is  
 (a)  $M_3$  curve on  $B$  (b)  $M_2$  curve on  $B$   
 (c)  $M_1$  curve on  $B$  (d)  $M_1$  curve on  $A$
- 4.18 In a channel the bed slope changes from a mild slope to a steep slope. The resulting GVF profiles are  
 (a)  $(M_1, S_2)$  (b)  $(M_1, S_3)$   
 (c)  $(M_2, S_2)$  (d)  $(M_2, S_1)$
- 4.19 A rectangular channel has  $B = 20$  m,  $n = 0.020$  and  $S_0 = 0.0004$ . If the normal depth is 1.0 m, a depth of 0.8m in a GVF in this channel is a part of  
 (a)  $M_1$  (b)  $M_2$   
 (c)  $M_3$  (d)  $S_2$
- 4.20 A rectangular channel has uniform flow at a normal depth of 0.50 m. The discharge intensity in the channel is estimated as 1.40 m<sup>3</sup>/s/m. If an abrupt drop is provided at the downstream end of this channel, it will cause  
 (a)  $M_2$  type of GVF profile  
 (b)  $S_2$  type of GVF profile  
 (c) No GVF profile upstream of the drop  
 (d)  $M_1$  type of profile
- 4.21 The flow will be in the supercritical state in the following types of GVF profiles:  
 (a) All  $S$  curves (b)  $M_2$   
 (c)  $A_3, M_3, S_2$  (d)  $S_2, M_2, S_3$

4.22 At the transitional depth

- (a)  $\frac{dy}{dx} = \infty$
- (b) the slope of the GVF profile is zero
- (c)  $dy/dx = -S_0$
- (d) the slope of GVF profile is horizontal

# Gradually Varied Flow Computations

# 5

## 5.1 INTRODUCTION

Almost all major hydraulic-engineering activities in free-surface flow involve the computation of GVF profiles. Considerable computational effort is involved in the analysis of problems, such as (a) determination of the effect of a hydraulic structure on the flow pattern in the channels, (b) inundation of lands due to a dam or weir construction, and (c) estimation of the flood zone. Because of its practical importance the computation of GVF has been a topic of continued interest to hydraulic engineers for the last 150 years. Dupuit (1848) was perhaps the first to attempt the integration of the differential equation of GVF [Eq. (4.8)]. In the early periods the effort was to integrate [Eq. (4.8)] through the use of a simple resistance equation (such a Chezy equation with constant  $C$ ) and through other simplifications in the channel geometry (wide rectangular channel, parabolic channel, etc.). Bakhmeteff<sup>1</sup> developed a fairly satisfactory method involving the use of varied-flow functions applicable to a wide range of channels. This method has undergone successive refinements, through various corrections, from time to time by subsequent research workers in this field and finally in 1955 Chow<sup>2</sup> evolved a fairly comprehensive method using only one varied-flow function.

Simultaneously, with the development of direct integration as above, to meet the practical needs, various solution procedures involving graphical and numerical methods were evolved for use by professional engineers. The advent of high-speed computers has given rise to general programmes utilizing sophisticated numerical techniques for solving GVF in natural channels. The various available procedures for computing GVF profiles can be classified as:

1. Direct integration
2. Numerical method
3. Graphical method

Out of these the graphical method is practically obsolete and is seldom used. Further, the numerical method is the most extensively used technique. In the form of a host of available comprehensive softwares, it is the only method available to solve practical problems in natural channels. The direct integration technique is essentially of academic interest. This chapter describes the theory of GVF computations and a few well established procedures and specific methods which have possibilities of wider applications.



## 5.2 DIRECT INTEGRATION OF GVF DIFFERENTIAL EQUATION

The differential equation of GVF for the prismatic channel, from Eq. 4.12, given by

$$\frac{dy}{dx} = S_0 \frac{1 - (K_0^2 / K^2)}{1 - (Z_c^2 / Z^2)} = F(y)$$

is a non-linear, first order, ordinary differential equation. This can be integrated by analytical methods to get closed form solutions only under certain very restricted conditions. A method due to Chow<sup>2</sup>, which is based on certain assumptions but applicable with a fair degree of accuracy to a wide range of field conditions, is presented here.

Let it be required to find  $y = f(x)$  in the depth range  $y_1$  to  $y_2$ . The following two assumptions are made:

1. The conveyance at any depth  $y$  is given by

$$K^2 = C_2 y^N \quad (5.1)$$

and at the depth  $y_0$  by

$$K_0^2 = C_2 y_0^N \quad (5.2)$$

This implies that in the depth range which includes  $y_1$ ,  $y_2$  and  $y_0$ , the coefficient  $C_2$  and the second hydraulic exponent  $N$  are constants.

2. The section factor  $Z$  at any depth  $y$  is given by

$$Z = C_1 y^M \quad (5.3)$$

and at the critical depth  $y_0$  by

$$Z_c^2 = C_1 y_c^M \quad (5.4)$$

implying that in the depth range which includes  $y_1$ ,  $y_2$  and  $y_c$ , the coefficient  $C_1$  and the first hydraulic exponent  $M$  are constants.

Substituting the relationships given by Eqs 5.1 through 5.4 in Eq. 4.12,

$$\frac{dy}{dx} = S_0 \frac{1 - (y_0 / y)^N}{1 - (y_c / y)^M} \quad (5.5)$$

Putting  $u = y/y_0$ ,  $dy = y_0 du$  and Eq. 5.5 simplifies to

$$\frac{du}{dx} = \frac{S_0}{y_0} \left[ \frac{1 - 1/u^N}{1 - (y_c^M / y_0^M) \frac{1}{u^M}} \right]$$

i.e. 
$$dx = \frac{y_0}{S_0} \left[ 1 - \frac{1}{1-u^N} + \left( \frac{y_c}{y_0} \right)^M \frac{u^{N-M}}{1-u^N} \right] du$$

Integrating

$$x = \frac{y_0}{S_0} \left[ u - \int_0^u \frac{du}{1-u^N} + \left( \frac{y_c}{y_0} \right)^M \int_0^u \frac{u^{N-M}}{1-u^N} du \right] + \text{Const.} \quad (5.6)$$

Calling 
$$\int_0^u \frac{du}{1-u^N} = F(u, N)$$

the second integral can be simplified as follows:

Put 
$$v = u^{N/J} \text{ where } J = \frac{N}{(N-M+1)}$$

to get 
$$dv = \frac{N}{J} u^{\frac{N}{J}-1} du$$
  

$$= (N-M+1) u^{N-M} du$$

$$\therefore \int_0^u \frac{u^{N-M}}{1-u^N} du = \frac{1}{(N-M+1)} \int_0^v \frac{dv}{1-v^J}$$
  

$$= \frac{J}{N} F(v, J) \quad (5.8)$$

It may be noted that  $F(v, J)$  is the same function as  $F(u, N)$  with  $u$  and  $N$  replaced by  $v$  and  $J$  respectively.

Eq. 5.6 can now be written as

$$x = \frac{y_0}{S_0} \left[ u - F(u, N) + \left( \frac{y_c}{y_0} \right)^M \frac{J}{N} F(v, J) \right] \quad (5.9)$$

Using Eq. 5.9 between two sections  $(x_1, y_1)$  and  $(x_2, y_2)$  yields

$$(x_2 - x_1) = \frac{y_0}{S_0} \left[ (u_2 - u_1) - \{F(u_2, N) - F(u_1, N)\} \right. \\ \left. + \left( \frac{y_c}{y_0} \right)^M \frac{J}{M} \{F(v_2, J) - F(v_1, J)\} \right] \quad (5.10)$$

The function  $F(u, N)$  is known as the *varied-flow function*. Extensive tables of  $F(u, N)$  are readily available<sup>1,2,3</sup> and a table showing  $F(u, N)$  for a few values of  $N$  is presented in Table 5A.1 in Appendix 5A at the end of this chapter.

A method of obtaining the exact analytical solutions of  $\int_0^u \frac{du}{1-u^N}$  for integral and non-integral values of  $N$  is given by Gill<sup>4</sup>. Numerical integration of  $\int_0^u \frac{du}{1-u^N}$

can be performed easily on a computer to obtain tables of varied-flow functions. Bakhmeteff gives a procedure for this in the appendix of his treatise<sup>1</sup>.

In practical applications, since the exponents  $N$  and  $M$  are likely to depend on the depth of flow, though to a smaller extent, average values of the exponents applicable to the ranges of values of depths involved must be selected. Thus the appropriate range of depths for  $N$  includes  $y_1$ ,  $y_2$ , and  $y_0$ ; and for  $M$  it includes  $y_1$ ,  $y_2$ , and  $y_0$ . In computing water-surface profiles that approach their limits asymptotically (e.g.  $y \rightarrow y_0$ ), the computations are usually terminated at  $y$  values which are within 1 per cent of their limit values.

**Example 5.1** | A trapezoidal channel has a bed width  $B = 5.0$  m,  $S_0 = 0.0004$ , side slope  $m = 2$  horizontal : 1 vertical and  $n = 0.02$ . The normal depth of flow  $y_0 = 3.0$  m. If the channel empties into a pool at the downstream end and the pool elevation is 1.25 m higher than the canal bed elevation at the downstream end, calculate and plot the resulting GVF profile. Assume  $\alpha = 1.0$ .

**Solution** For uniform flow:  $y_0 = 3.0$  m

$$A_0 = (5 + 2 \times 3.0) \times 3.0 = 33.0 \text{ m}^2$$

$$P_0 = 5 + 2\sqrt{1 + 2^2} \times 3.0 = 18.41 \text{ m}$$

$$R_0 = 33.0 / 18.41 = 1.793 \text{ m}$$

$$Q = Q_0 = \frac{1}{0.02} \times (33.0)(1.793)^{2/3} \sqrt{0.0004} = 48.70 \text{ m}^3/\text{s}$$

For critical-depth calculation:

$$\phi = \frac{m^{1.5} Q}{\sqrt{g \cdot B^{2.5}}} = \frac{(2.0)^{1.5} \times 48.70}{\sqrt{9.81 \times (5.0)^{2.5}}} = 0.7867$$

From Table 2A.2.

$$\zeta_c = \frac{m y_c}{B} = 0.676$$

Critical depth  $y_c = 1.690$  m.

Since  $y_0 > y_c$ , the channel slope is mild. Also, since the downstream pool elevation is 1.25 m above the channel bed while  $y_c = 1.69$  m, the downstream control will be the critical depth. The water-surface profile will be an  $M_2$  curve extending from  $y_c = 1.69$  m at the downstream end to  $y \rightarrow y_0 = 3.0$  m at the upstream end.

In the flow profile the following ranges of parameters are involved:

depth  $y = 3.00$  m to 1.69 m

$y/B = 0.60$  to 0.338

$N = 4.17$  to 3.88 (From Fig. 3.8)

$M = 3.94$  to 3.60 (From Fig. 2.8)

For computation purposes, average constant values of  $N = 4.0$  and  $M = 3.75$  are selected.

For use in Eq. 5.9,

$$u = y/3.00, \quad \text{and} \quad J = \frac{N}{N - M + 1} = \frac{4.0}{1.25} = 3.2$$

$$\frac{y_0}{S_0} = 7500$$

$$v = u^{N/J} = u^{1.25}, \quad \left(\frac{y_c}{y_0}\right)^M \frac{J}{N} = \left(\frac{1.69}{3.00}\right)^{3.75} \left(\frac{3.2}{4.0}\right) = 0.093$$

Equation 5.9 for calculation of the distance  $x$  reduces to

$$x = 7500 [u - F(u, 4.0) + 0.093 F(v, 3.2)] + \text{Const.}$$

The calculations are performed in the manner shown in Table 5.1.

The calculations commence from the downstream control depth of  $y_c = 1.69$  m and are terminated at  $y = 2.97$  m, i.e. at a value of depth which is 1 per cent less than  $y_0$ .

**Table 5.1** Computation of GVF Profile: Example 5.1

$N = 4.0$		$M = 3.75$		$J = 3.2$		$u = y/3.0$		$v = u^{1.25}$
$y(m)$	$u$	$v$	$F(u, 4.0)$		$F(v, 3.2)$	$x$ (m)	$\Delta x$ (m)	$L$ (m)
1.69	0.563	0.488	0.575		0.501	259	0	0
1.80	0.600	0.528	0.617		0.547	254	5	5
1.89	0.630	0.561	0.652		0.585	243	11	16
2.01	0.670	0.606	0.701		0.639	213	30	46
2.13	0.710	0.652	0.752		0.699	173	40	86
2.25	0.750	0.698	0.808		0.763	97	76	162
2.37	0.790	0.745	0.870		0.836	-17	114	276
2.49	0.830	0.792	0.940		0.918	-185	168	444
2.61	0.870	0.840	1.025		1.019	-452	267	711
2.73	0.910	0.889	1.133		1.152	-869	417	1128
2.82	0.940	0.926	1.246		1.293	-1393	524	1652
2.91	0.970	0.967	1.431		1.562	-2368	975	2627
2.94	0.980	0.975	1.536		1.649	-3020	652	3279
2.97	0.990	0.988	1.714		1.889	-4112	1092	4371

In nominating the depths in the first column, it is advantageous if  $u$  values are fixed at values which do not involve interpolation in the use of tables of varied-flow functions and the corresponding  $y$  values entered in the first column. If the value of  $u$  or  $v$  is not explicitly given in the varied-flow function tables, it will have to be interpolated between two appropriate neighbouring values, e.g. to find  $F(v, J) = F(0.698, 3.2)$ , Table 5A.1 is used to give  $F(0.69, 3.2) = 0.751$  and  $F(0.70, 3.2) = 0.766$ . By linear interpolation between these two values,  $F(0.698, 3.2)$  is taken as 0.763.

The last column indicates the distance from the downstream end to the various sections. It can easily be appreciated that the necessary interpolations in the use of the varied-flow function table not only make the calculations laborious but are also sources of possible errors. Another source of error is the fixing of constant values of  $N$  and  $M$  for the whole reach. The computed profile is plotted in Fig. 5.1 (note the highly-exaggerated vertical scale to show details).

If the distance between two sections of known depth is required, the evaluation of the varied-flow functions at intermediate steps is not needed.

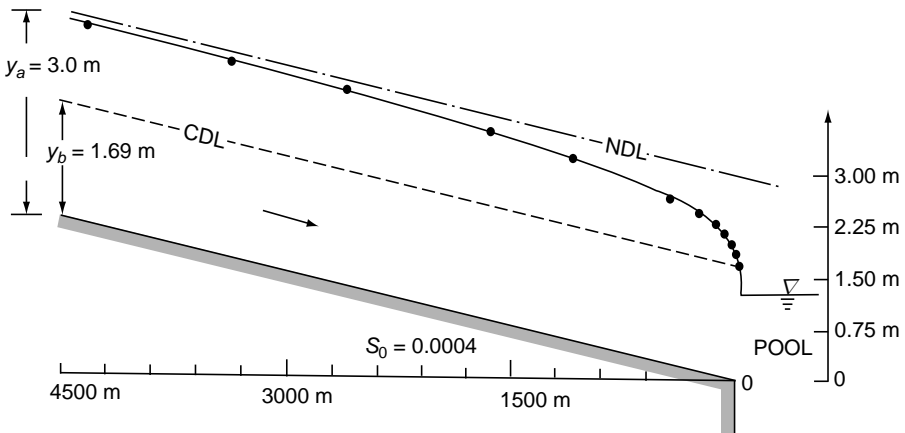


Fig. 5.1 GVF profile for Example 5.1

**Example 5.2**

Find the distance between two Sections A and B of Example 5.1, given  $y_A = 1.80$  m and  $y_B = 2.25$  m.

**Solution** Referring to the basic calculations performed in Example 5.1, the following  $u$ ,  $v$  and  $F$  values are evaluated:

Section	$y$ (m)	$u$	$v$	$F(u, 4)$	$F(v, 3.2)$
A	1.80	0.60	0.528	0.617	0.547
B	2.25	0.75	0.698	0.808	0.763
Difference		0.15		0.191	0.216

The distance between *A* and *B* is calculated by using Eq. (5.10) as

$$L = x_B - x_A = 7500 (0.15 - 0.191 + 0.093 (0.216)) = 157 \text{ m} \quad (\text{the } -\text{ve sign is not significant})$$

If it is required to find the depth  $y_2$  at a section distance  $\Delta x$  from a given section where the depth is  $y_1$ , one has to calculate the distances to a few selected depths and determine the required depth by interpolation.

**Example 5.3** Given  $y_1 = 2.25 \text{ m}$  in Example 5.1, find the depth at a distance of 1300 m upstream of this section.

*Solution* At  $y_1 = 2.25 \text{ m}$ ,  $u_1 = 0.75$ . Select a set of two  $u$  values (and hence two depths) as a trial. The calculations are as follows:

Section	$y$ (m)	$u$	$v$	$F(u, 4.0)$	$F(v, 3.2)$	$x$ (m)	$\Delta x$ (m)	$L$ (m)
1	2.25	0.75	0.698	0.808	0.763	97	0	0
2	2.73	0.91	0.889	1.133	1.152	-869	966	966
3	2.82	0.94	0.926	1.246	1.293	-1393	524	1490

By interpolation between Sections 2 and 3, the depth at a distance of 1300 m from the Section 1 is

$$y = 2.73 + \left[ \frac{(2.82 - 2.73)}{(1490 - 966)} \times (1300 - 966) \right] = 2.787 \text{ m}$$

### 5.3 BRESSE'S SOLUTION

For a wide rectangular channel, if the Chezy formula with  $C = \text{constant}$  is used the hydraulic exponents take the value  $M = 3.0$  and  $N = 3.0$ . By putting these values of  $M = 3.0$  and  $N = 3.0$  in Eq. (5.9) the GVF profile would be

$$x = \frac{y_0}{S_0} \left[ u - \left( 1 - \left( \frac{y_c}{y_0} \right)^3 \right) F(u, 3) \right] + \text{a constant} \quad (5.11)$$

And from Eq. (5.7)

$$F(u, 3) = \int_0^u \frac{du}{1-u^3}$$

The function  $F(u, 3)$  was first evaluated by Bresse in 1860 in a closed form as

$$F(u, 3) = \frac{1}{6} \ln \left[ \frac{u^2 + u + 1}{(u-1)^2} \right] - \frac{1}{\sqrt{3}} \arctan \left[ \frac{\sqrt{3}}{2u+1} \right] + \text{a constant} \quad (5.12)$$

$F(u, 3)$  is known as Bresse's function. Apart from historical interest, values of Bresse's function being based on an exact solution are useful in comparing the relative accuracies of various numerical schemes of computation.

[Note: Table 5A-1 has a constant of value 0.6042 added to all values of  $F(u, N)$ .

Bresse's solution is useful in estimating approximately the length of GVF profiles between two known depths. The length of  $M_1$  profile from 150% of normal depth downstream to 101% of normal depth upstream can be shown to be given by

$$\frac{LS_0}{y_0} = 1.654 - 1.164F^2 \quad (5.13)$$

where  $F$  is the Froude number of the normal flow in the channel.

In general the length of the GVF profile between two feasible depths are given by

$$\frac{LS_0}{y_0} = A + BF^2 \quad (5.14)$$

where values of  $A$  and  $B$  for some ranges are as given below:

Value of $A$	Value of $B$	Range of percentage of $y/y_0$ values	Typical case
0.599	-0.869	97% to 70%	$M_2$ curve
0.074	-0.474	70% to 30%	$M_2$ curve
1.654	-1.164	101% to 150%	$M_1$ curve
1.173	-0.173	150% to 250%	$M_1$ curve
-1.654	1.164	150% to 101%	$S_2$ curve

**Example 5.4**

A 50-m wide river has an average bed slope of 1 in 10000. Compute the backwater curve produced by a weir which raises the water surface immediately upstream of it by 3.0 m when the discharge over the weir is 62.5 m<sup>3</sup>/s. What will be the raise in water level at a point that is 35 km upstream of the weir? Use Chezy's resistance equation with  $C = 45$  and use Bresse's backwater functions.

**Solution** Here,  $Q = 62.5$  m<sup>3</sup>/s and  $q = 62.5/50 = 1.25$  m<sup>3</sup>/s/m width

By Chezy formula

$$q = Cy_0^{3/2} \sqrt{S_0}$$

$$1.25 = 45 \times y_0^{3/2} \sqrt{0.0001}$$

$$y_0 = 1.976 \text{ m}$$

Critical depth  $y_c$  is given by  $y_c = \left(\frac{q^2}{g}\right)^{1/3} = \left(\frac{(1.25)^2}{9.81}\right)^{1/3} = 0.542 \text{ m}$

$$\frac{y_c}{y_0} = 0.274, \frac{y_0}{S_0} = 19760 \text{ and } u = y/1.976$$

Bresse’s backwater equation for wide rectangular channels is

$$\begin{aligned} x &= \frac{y_0}{S_0} \left[ u - \left\{ 1 - \left( \frac{y_c}{y_0} \right)^3 \right\} \right] F(u, 3) + \text{Constant} \\ &= 19760 \left[ u - \{ 1 - 0.9794 \} \right] \times F(u, 3) + \text{Constant} \\ x &= 19760 \left[ u - \{ 1 - 0.9794 \} \right] \times F(u, 3) + \text{Constant} \end{aligned} \tag{5.15}$$

Using this equation the backwater curve is calculated as in the following Table. The calculations are continued up to 1.01 times the normal depth.

$$y_1 = 3.0 + 1.976 = 4.976 \text{ m}$$

**Table 5.2** GVF Profile Computations – Example 5.4

Depth <i>y</i> (m)	<i>u</i>	<i>F</i> ( <i>u</i> ,3)	<i>x</i> from Eq (i)	<i>x</i> (m)	Distance from The weir <i>L</i> (m)
4.976	2.518	0.082	48173.1		0
4.347	2.200	0.017	43143	5030	5030
3.952	2.000	0.132	36965.5	6178	11208
3.557	1.800	0.166	32355.5	4610	15818
3.162	1.600	0.218	27397.2	4958	20776
2.766	1.400	0.304	21780.9	5616	26392
2.371	1.200	0.48	14422.9	7358	33750
2.075	1.050	0.802	5227.53	9195	42946
2.016	1.020	1.191	-2893.29	8121	51066
1.996	1.010	1.419	-7503.19	4610	55676

By linear interpolation between sections at distances 33750 and 42946 m the depth at the section that is 35 km upstream of the weir is 2.331 m.

Rise in the water level at this section = 2.331 – 1.976 = 0.355 m.

**Example 5.5** (a) Integrate the differential equation of GVF for a horizontal channel to get the profile equation as

$$x = \frac{y_c}{S_c} \left[ \frac{(y/y_c)^{N-M+1}}{N-M+1} - \frac{(y/y_c)^{N+1}}{N+1} \right] + \text{constant}$$

where  $S_c$  = critical slope.



(b) Using the result of part (a) above develop an equation for GVF profile in a wide, rectangular, horizontal channel.

Solution 
$$\frac{dy}{dx} = \frac{S_0 - S_f}{1 - \frac{Q^2 T}{gA^3}} \quad (5.16)$$

For a horizontal channel  $S_0 = 0$

Also, 
$$S_f = \frac{Q^2}{K^2} = \frac{K_c^2 S_c}{K^2} = \left(\frac{y_c}{y}\right)^N S_c$$

Further, 
$$\frac{Q^2}{g} = Z_c^2 \text{ and } \frac{A^3}{T} = Z^2$$

Thus 
$$\frac{Q^2 T}{gA^3} = \left(\frac{y_c}{y}\right)^M$$

Equation 5.16 is now written as 
$$\frac{dy}{dx} = \frac{-\left(\frac{y_c}{y}\right)^N S_c}{1 - \left(\frac{y_c}{y}\right)^M}$$

$$-dx \cdot S_c = \left[1 - (y_c/y)^M\right] \frac{1}{(y_c/y)^N} dy$$

$$= \left[\left(\frac{y}{y_c}\right)^N - \left(\frac{y}{y_c}\right)^{N-M}\right] dy$$

$$\therefore -S_c x = y_c \left[ \frac{(y/y_c)^{N+1}}{N+1} - \frac{(y/y_c)^{N-M+1}}{N-M+1} \right] + \text{Constant}$$

$$\therefore x = \frac{y_c}{S_c} \left[ \frac{(y/y_c)^{N-M+1}}{N-M+1} - \frac{(y/y_c)^{N+1}}{N+1} \right] + \text{Constant}$$

(b) For a wide rectangular channel, by Eq. 3.62 (a)  $S_c = \frac{n^2 g}{y_c^{1/3}}$ ,

Noting that  $N = 10/3$  and  $M = 3$ ,

Substituting for  $S_c$ ,  $N$  and  $M$  in the result of Part (a), viz., that for a horizontal rectangular channel,

$$\therefore x = \frac{y_c}{S_c} \left[ \frac{(y/y_c)^{N-M+1}}{N-M+1} - \frac{(y/y_c)^{N+1}}{N+1} \right] + \text{Constant},$$

we get for a wide rectangular, horizontal channel, the GVF profile as

$$\therefore x = \frac{y_c^{4/3}}{n^2 g} \left[ \frac{3}{4} (y/y_c)^{4/3} - \frac{3}{13} (y/y_c)^{13/3} \right] + \text{constant}$$

### 5.4 CHANNELS WITH CONSIDERABLE VARIATION IN HYDRAULIC EXPONENTS

There are many channel shapes which have appreciable variation of the hydraulic exponents with the depth of flow. A circular channel is a typical example of such channels with the variation of the hydraulic exponents with  $y/D$  being as shown in Fig. 5.2. In such channels

$$K^2 = C_2 y^N \quad \text{and} \quad K_0^2 = C_{20} y^{N_0} \tag{5.17}$$

where the suffix '0' refers to normal-depth conditions. Similarly,

$$Z^2 = C_1 y^M \quad \text{and} \quad Z_c^2 = C_{1c} y^{M_c} \tag{5.18}$$

in which the suffix 'c' refers to critical-flow conditions. Substituting Eqs 5.17 and 5.18 in the differential equation of GVF [Eq. (4.12)]

$$\frac{dy}{dx} = S_0 \frac{1 - \left( \frac{C_{20}}{C_2} \right) \left( \frac{y_0^{N_0}}{y^N} \right)}{1 - \left( \frac{C_{1c}}{C_1} \right) \left( \frac{y_c^{M_c}}{y^M} \right)} \tag{5.19}$$

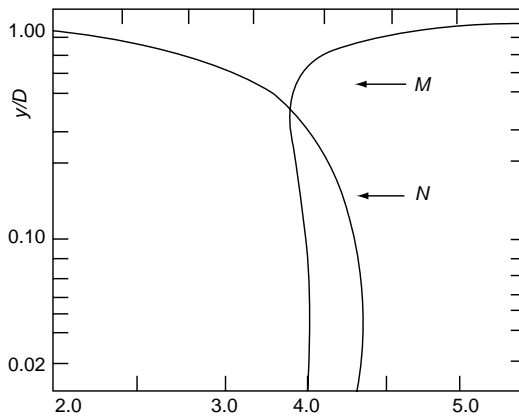


Fig. 5.2 Variation of  $N$  and  $M$  for a circular channel [6]

When there is considerable variation in the values of hydraulic exponents with the depth,

$$N \neq N_0, M \neq M_c \quad \text{and as such} \quad C_{20} \neq C_2 \quad \text{and} \quad C_{1c} \neq C_1.$$

Obviously, Eq. (5.9) cannot be used as a solution of Eq. 5.19

Assuming  $C_{20} = C_2$  and  $C_{1c} = C_1$  Chow<sup>3</sup> has obtained the solution of Eq. 5.19 as

$$x = \frac{y_0^{N_0/N}}{S_0} \left[ u - F(u, N) + \left( \frac{y_c^{Mc/M}}{y_0^{N_0/N}} \right)^M \left( \frac{J}{N} \right) F(v, J) \right] \text{ a constant} \quad (5.20)$$

In which  $u = y/y_0^{N_0/N}$ . However, it has been shown<sup>6</sup> that this assumption is not valid and Eq. 5.20 may give considerable errors. A generalised procedure for direct integration of Eq. 5.19 using the varied-flow function is given by Subramanya and Ramamurthy<sup>5</sup>.

## 5.5 DIRECT INTEGRATION FOR CIRCULAR CHANNELS

### 5.5.1 Keifer and Chu's method

The direct integration of the differential equation of GVF by Chow's method is very inconvenient to use in the computation of GVF profiles in circular channels.

A different approach of integration of the differential equation of GVF for circular channels, developed by Keifer and Chu<sup>6</sup>, simplifies the calculation procedure considerably.

Let  $Q$  be the actual discharge in a circular channel of diameter  $D$  and bed slope  $S_0$ . Then

$$Q = K\sqrt{S_f} \quad (5.21)$$

and

$$Q = K_0\sqrt{S_0} \quad (5.22)$$

where  $K$  and  $K_0$  are the conveyance at depths  $y$  and  $y_0$  respectively,  $y_0$  = normal depth,  $S_f$  = energy slope at depth  $y$ . Let  $Q_D$  = a hypothetical discharge corresponding to uniform flow with the channel flowing full.

Then

$$Q_D = K_D\sqrt{S_0} \quad (5.23)$$

where  $K_D$  = conveyance at depth  $D$ .

i.e.

$$K_D = \frac{1}{n} \left( \pi D^2/4 \right) (D/4)^{2/3}$$

$$\left( \frac{K_0}{K} \right)^2 = \left( \frac{K_0}{K_D} \right)^2 \left( \frac{K_D}{K} \right)^2$$

But

$$\left( \frac{K_D}{K} \right)^2 = \left[ \frac{\left( \pi D^2/4 \right) (D/4)^{2/3}}{AR^{2/3}} \right] = f_1(y/D)$$

and 
$$\left(\frac{K_0}{K_D}\right)^2 = \left(\frac{Q}{Q_D}\right)^2 = (Q_r)^2 \tag{5.24}$$

∴ 
$$\left(\frac{K_0}{K}\right)^2 = Q_r^2 f_1(y/D) \tag{5.25}$$

The differential equation of GVF, Eq. 4.12, becomes

$$\frac{dy}{dx} = S_0 \frac{1 - Q_r^2 f_1(y/D)}{1 - Q^2 T/gA^3}$$

Noting that 
$$\frac{Q^2 T}{gA^3} = \frac{Q^2}{g} \frac{1}{D^5} \frac{T/D}{(A^3/D^6)} = \frac{Q^2}{gD^5} f_2(y/D) \tag{5.26}$$

and putting  $y/D = \eta$

$$\frac{d\eta}{dx} = \frac{S_0}{D} \left[ \frac{1 - Q_r^2 f_1(\eta)}{1 - \frac{Q^2}{gD^5} f_2(\eta)} \right]$$

$$dx = \frac{D}{S_0} \left[ \frac{d\eta}{1 - Q_r^2 f_1(\eta)} - \frac{Q^2}{gD^5} \frac{f_2(\eta) d\eta}{1 - Q_r^2 f_1(\eta)} \right]$$

Integrating,

$$x = \frac{D}{S_0} \left[ \int_0^\eta \frac{d\eta}{1 - Q_r^2 f_1(\eta)} - \frac{Q^2}{gD^5} \int_0^\eta \frac{f_2(\eta) d\eta}{1 - Q_r^2 f_1(\eta)} \right] + \text{Const.} \tag{5.27}$$

∴ 
$$x = \frac{D}{S_0} \left[ I_1 - \frac{Q^2}{gD^5} I_2 \right] + \text{Const.} \tag{5.28}$$

where 
$$I_1 = \int_0^\eta \frac{d\eta}{1 - Q_r^2 f_1(\eta)} = I_1(Q_r, \eta)$$

and 
$$I_2 = \int_0^\eta \frac{f_2(\eta) d\eta}{1 - Q_r^2 f_1(\eta)} = I_2(Q_r, \eta)$$

Functions  $I_1$  and  $I_2$  are known as *Keifer and Chu functions* and are available in slightly different forms in References 3, 6 and 7. The computation of GVF profiles in circular channels is considerably simplified by the use of these functions. Since  $y/D = \eta = 1/2(1 - \cos \theta) = f(\theta)$  where  $2\theta =$  angle subtended by the water surface at the centre of the section the functions  $I_1$  and  $I_2$  can also be represented as  $I_1(Q_r, \theta)$ , and  $I_2(Q_r, \theta)$ . Tables 5A.2(a) and 5A.2(b) in Appendix 5A show the functions  $I_1$  and

$I_2$  respectively, expressed as functions of  $Q_r$  and  $\theta/\pi$ . Reference 7 gives details of evaluating the integrals to get  $I_1$  and  $I_2$ . Example 5.6 illustrates the use of Keifer and Chu method [Eq. 5.28] for circular channels.

It may be noted that the functions  $I_1$  and  $I_2$  are applicable to circular channels only. However, a similar procedure of non-dimensionalising can be adopted to any other channel geometry, e.g. oval and elliptic shapes, and functions similar to  $I_1$  and  $I_2$  can be developed. Applications of the above procedure for use in rectangular channels is available in literature<sup>8</sup>.

**Example 5.6** | A 2.0-m diameter circular concrete drainage pipe ( $n = 0.015$ ) is laid on a slope of 0.001 and carries a discharge of 3.0 m<sup>3</sup>/s. If the channel ends in a free overfall, compute the resulting GVF profile.

*Solution*  $Q = 3.0 \text{ m}^3/\text{s}$

$$Q_D = \frac{1}{0.015} \times \left( \frac{\pi}{4} \times 2^2 \right) \times \left( \frac{2.0}{4} \right)^{2/3} \times \sqrt{0.001} = 4.17 \text{ m}^3/\text{s}$$

For normal depth,  $\frac{Qn}{\sqrt{S_0} D^{8/3}} = 0.2241$ , and

from Table 2.A1,  $y_0 / D = 0.628$ , giving  $y_0 = 1.256 \text{ m}$ , and  $(2\theta / 2\pi)_0 = 0.582$ .

For critical depth,  $\frac{Q}{\sqrt{g}} \frac{1}{D^{2.5}} = 0.1693$  and

from Table 2A.1,  $y_c / D = 0.411$ , giving  $y_c = 0.822 \text{ m}$ , and  $(2\theta / 2\pi)_c = 0.443$ .

$$Q_r = Q/Q_D = 0.719$$

$$Q^2/gD^5 = 0.0287$$

Since  $y_0 > y_c$ , the channel is on a mild slope. The downstream control will be the critical depth  $y_c = 0.822 \text{ m}$ . The GVF profile is an  $M_2$  curve extending from the critical depth upwards to the normal depth.

The calculations are performed by using the Keifer and Chu method. Equation 5.28 reduces to

$$x = 2000 [I_1 - 0.0287 I_2] + \text{Const.}$$

Values of  $(2\theta/2\pi)$  in the range 0.443 to 0.582 are selected and by referring to Tables 5A.2(a) and 5A.2(b), values of  $I_1$  and  $I_2$  corresponding to a known  $\theta$  and  $Q_r = 0.719$  are found by interpolation. For a given value of  $(2\theta / 2\pi)$  the value of  $y/D$  is found by the relation  $y/D = \frac{1}{2} (1 - \cos \theta)$ . The values of  $x$  and  $\Delta x$  between

two successive values of  $y$  are found by using Eq. (5.28). The calculations are performed in the following tabular form:

**Table 5.3** GVF Profile Computation – Example 5.6

$Q_r = 0.719$		$D = 2.0 \text{ m}$ $x = 2000(I_1 - 0.0287 I_2) + \text{Const.}$					
$\left(\frac{2\theta}{2\pi}\right)$	$y/D$	$y \text{ (m)}$	$I_1$	$I_2$	$x \text{ (m)}$	$\Delta x \text{ (m)}$	$L \text{ (m)}$
0.443	0.411	0.822	0.0245	3.4470	-149	0	0
0.460	0.437	0.875	0.0346	3.7551	-146	3	3
0.500	0.500	1.000	0.0762	4.6263	-113	33	36
0.530	0.547	1.094	0.1418	5.5188	-33	80	116
0.550	0.578	1.156	0.2296	6.4334	+90	123	329
0.570	0.609	1.218	0.4983	8.6787	+498	408	647

A plot of  $y$  vs  $L$  gives the requisite profile.

Some errors in the interpolation of  $I_1$  and  $I_2$  functions are usually involved in the use of the tables. For greater accuracy, detailed tables of  $I_1$  and  $I_2$  at closer intervals of  $Q_r$  and  $\theta/\pi$  have to be generated and used.

## 5.6 SIMPLE NUMERICAL SOLUTIONS OF GVF PROBLEMS

The numerical solution procedures to solve GVF problems can be broadly classified into two categories as:

**(a) Simple Numerical Methods** These were developed primarily for hand computation. They usually attempt to solve the energy equation either in the form of the differential energy equation of GVF or in the form of the Bernoulli equation.

**(b) Advanced Numerical Methods** These are normally suitable for use in digital computers as they involve a large number of repeated calculations. They attempt to solve the differential equation of GVF [Eq. (4.8)].

The above classification is a broad one as the general availability of personal computers (PCs) have made many methods under category (b) available for desk-top calculations. Two commonly used simple numerical methods to solve GVF problems, viz. (i) *Direct-step method* and (ii) *Standard-step method* are described in this section.

### 5.6.1 Direct-Step Method

This method is possibly the simplest and is suitable for use in prismatic channels. Consider the differential-energy equation of GVF [Eq. (4.16)].

$$\frac{dE}{dx} = S_0 - S_f$$

Writing this in the finite-difference form

$$\frac{\Delta E}{\Delta x} = S_0 - \bar{S}_f \tag{5.29}$$

Where  $\bar{S}_f$  = average-friction slope in the reach  $\Delta x$

$$\therefore \Delta x = \frac{\Delta E}{S_0 - \bar{S}_f} \tag{5.30}$$

and between two Sections 1 and 2

$$(x_2 - x_1) = \Delta x = \frac{(E_2 - E_1)}{S_0 - \frac{1}{2}(S_{f1} + S_{f2})} \tag{5.31}$$

Equation (5.30) is used as indicated below to calculate the GVF profile.

**Procedure** Referring to Fig. 5.3, let it be required to find the water-surface profile between two Sections 1 and  $(N + 1)$  where the depths are  $y_1$  and  $y_{N+1}$  respectively. The channel reach is now divided into  $N$  parts of known depths, i.e., values of  $y_i$   $i = 1, N$  are known. It is required to find the distance  $\Delta x_i$  between  $y_i$  and  $y_{i+1}$ . Now, between the two Sections  $i$  and  $i + 1$ ,

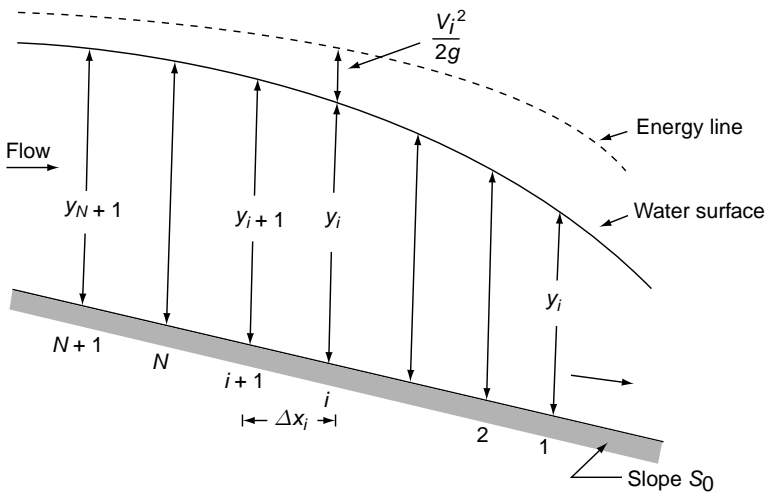


Fig. 5.3 Direct step method

$$\Delta E = \Delta \left( y + \frac{V^2}{2g} \right) = \Delta \left( y + \frac{Q^2}{2gA^2} \right)$$

$$\Delta E = E_{i+1} - E_i = \left[ y_{i+1} + \frac{Q^2}{2gA_{i+1}^2} \right] - \left[ y_i + \frac{Q^2}{2gA_i^2} \right] \quad (5.32)$$

and

$$\bar{S}_f = \frac{1}{2} (\bar{S}_{f_{i+1}} + S_{f_i}) = \frac{n^2 Q^2}{2} \left[ \frac{1}{A_{i+1}^2 R_{i+1}^{4/3}} + \frac{1}{A_i^2 R_i^{4/3}} \right] \quad (5.33)$$

From Eq. (5.30),  $\Delta x_i = \frac{E_{i+1} - E_i}{\bar{S}_0 - \bar{S}_f}$ . Using Eqs (5.32) and (5.33),  $\Delta x_i$  can be evaluated in the above expression. The sequential evaluation of  $\Delta x_i$  starting from  $i = 1$  to  $N$ , will give the distances between the  $N$  sections and thus the GVF profile. The process is explicit and is best done in a tabular manner if hand computations are used. Use of spread sheet such as MS Excel is extremely convenient.

**Example 5.7** For the channel section and flow conditions indicated in Example 5.1, (a) calculate the GVF profile from the section having critical depth up to a section having a depth of 2.96 m by direct step method. (b) Further, calculate the distance between two sections having depths of 2.30 m and 2.80 m respectively.

**Solution** The flow profile is an  $M_2$  curve with  $y_c = 1.69$  m as the control at the downstream end. The calculations start at the control and are carried in the upstream direction. The depth range is from 1.60 m to 2.69 m and this is divided in to 17 reaches. Calculations are performed on a spread sheet and Table 5.4 shows the details. Note that non uniform depth increments are adopted; the depth increment in a reach is larger if the reach is part of the profile where the curvature is high and smaller depth increments are adopted where the curve is flatter. This is a procedure commonly adopted in hand computation and there is no apparent benefit while computations are carried through the use of a spread sheet.

Col. 2 has the normal depth. Cols. 3 through 7 have the area  $A$ , wetted perimeter  $P$ , hydraulic radius  $R$ , velocity  $V$  and specific energy  $E$  respectively. Col.8 has the difference in specific energy  $\Delta E$  of two successive values of  $E$ . The friction slope  $S_f = \frac{n^2 V^2}{R^{4/3}}$  and is indicated in Col.9. The average of two successive  $S_f$  values is  $\bar{S}_f$  and is entered in Col. 10. Col. 12 contains  $\Delta x$  calculated by using Eq. (5.30), i.e.,  $\frac{\text{Col.8}}{\text{Col.11}}$ . The last column contains cumulative distances from the starting point.

The negative sign of  $x$  does not have any significance other than the location of the origin and hence not considered in the last column.



**Table 5.4** Computation of Flow Profile by Direct Step Method (Example 5.7) (Through Use of Spread Sheet)

$B = 5.0 \text{ m}$		$m = 2.0$		$S_0 = 0.0004$		$Q = 48.70 \text{ m}^3/\text{s}$			$n = 0.02$			
1	2	3	4	5	6	7	8	9	10	11	12	13
Sl. No	$y \text{ (m)}$	$A \text{ (m}^2\text{)}$	$P \text{ (m)}$	$R \text{ (m)}$	$V \text{ (m/s)}$	$E \text{ (m)}$	$\Delta E \text{ (m)}$	$S_f$	$\bar{S}_f$	$S_0 - \bar{S}_f$	$\Delta x \text{ (m)}$	$x \text{ (m)}$
1	1.69	14.162	12.558	1.12775	3.439	2.293		0.00403				0.0
2	1.80	15.480	13.050	1.18622	3.146	2.304	0.0118	0.00315	0.00359	-0.00319	-3.7	3.7
3	2.00	18.000	13.944	1.29085	2.706	2.373	0.0686	0.00208	0.00262	-0.00222	-30.9	34.6
4	2.10	19.320	14.391	1.34246	2.521	2.424	0.0508	0.00172	0.00190	-0.00150	-33.8	68.5
5	2.20	20.680	14.839	1.39365	2.355	2.483	0.0588	0.00142	0.00142	-0.00102	-57.4	126
6	2.30	22.080	15.286	1.44447	2.206	2.548	0.0653	0.00119	0.00131	-0.00091	-71.9	198
7	2.40	23.520	15.733	1.49493	2.071	2.619	0.0706	0.00100	0.00110	-0.00070	-101.2	299
8	2.50	25.000	16.180	1.54508	1.948	2.693	0.0749	0.00085	0.00093	-0.00053	-142.2	441
9	2.60	26.520	16.628	1.59494	1.836	2.772	0.0785	0.00072	0.00079	-0.00039	-202.9	644
10	2.65	27.295	16.851	1.61977	1.784	2.812	0.0404	0.00067	0.00070	-0.00030	-136.1	780
11	2.70	28.080	17.075	1.64453	1.734	2.853	0.0411	0.00062	0.00064	-0.00024	-167.8	948
12	2.75	28.875	17.298	1.66923	1.687	2.895	0.0417	0.00057	0.00060	-0.00020	-211.3	1159
13	2.80	29.680	17.522	1.69387	1.641	2.937	0.0422	0.00053	0.00055	-0.00015	-274.3	1434
14	2.85	30.495	17.746	1.71846	1.597	2.980	0.0428	0.00050	0.00051	-0.00011	-373.5	1807
15	2.88	30.989	17.880	1.73318	1.572	3.006	0.0259	0.00047	0.00049	-0.00009	-304.4	2111
16	2.91	31.486	18.014	1.74788	1.547	3.032	0.0261	0.00045	0.00046	-0.00006	-403.9	2515
17	2.94	31.987	18.148	1.76257	1.522	3.058	0.0262	0.00044	0.00044	-0.00004	-582.6	3098
18	2.96	32.323	18.238	1.77235	1.507	3.076	0.0176	0.00042	0.00043	-0.00003	-596.9	3695

(b) From Table 5.4 distance between two sections having depths of 2.30 m and 2.80 m respectively is  $\Delta x = 1433.6 - 197.7 = 1235.9 \text{ m}$

**Useful hints**

- The calculations must proceed upstream in sub-critical flow and downstream in supercritical flow to keep the errors minimum.
- The steps need not have the same increment in depth. The calculations are terminated at  $y = (1 \pm 0.01) y_0$
- The accuracy would depend upon the number of steps chosen and also upon the distribution of step sizes.
- When calculations are done through use of a hand calculator, care must be taken in evaluating  $\Delta E$  which is a small difference of two large numbers.

**Example 5.8** A river 100 m wide and 3.0 m deep has an average bed slope of 0.0005. Estimate the length of GVF profile produced by a low dam which raises the water surface just upstream if it by 1.50 m. Assume  $n = 0.035$ .

**Solution** Considering the river as a wide rectangular channel, the discharge per unit width is

$$q = \frac{1}{n} y_0^{5/3} S_0^{1/2} = \frac{1}{0.035} (3.0)^{5/3} (0.0005)^{1/2}$$

$$= 3.987 \text{ m}^3/\text{s/m}$$

The critical depth  $y_c = \left(\frac{q^2}{g}\right)^{1/3} = \left(\frac{(3.987)^2}{9.81}\right)^{1/3} = 1.175 \text{ m}$

Since  $y > y_0 > y_c$ , the GVF profile is an  $M_1$  curve with depth of  $y = 4.50 \text{ m}$  at the low dam as the control. The direct step method with 10 steps is used to estimate the length of the backwater profile. The calculations are performed through use of a spread sheet and the details are shown in Table 5.5. The calculations are terminated at 3.03 m. The length of the profile is found to be 8644 m.

**Table 5.5** Computation of Flow Profile by Direct Step Method (Example 5.8)

Wide Rectangular Channel $S_0 = 0.0005$ $n = 0.035$ $q = 3.987 \text{ m}^3/\text{s/m}$									
1	2	3	4	5	6	7	8	9	10
Sl. No.	$y \text{ (m)}$	$V \text{ (m/s)}$	$E \text{ (m)}$	$\Delta E \text{ (m)}$	$S_f$	$\bar{S}_f$	$S_0 - \bar{S}_f$	$\Delta x \text{ (m)}$	$x \text{ (m)}$
1	4.5	0.886	4.5400		0.0001294				0
2	4.3	0.927	4.3438	-0.196192	0.0001506	0.0001400	0.000360	-545.015	545
3	4.1	0.972	4.1482	-0.195621	0.0001765	0.0001636	0.000336	-581.464	1126
4	3.9	1.078	3.7592	-0.194930	0.0002086	0.0001925	0.000307	-634.001	2475
5	3.7	1.022	3.9533	-0.194086	0.0002486	0.0002286	0.000271	-715.005	2475
6	3.5	1.139	3.5661	-0.193043	0.0002991	0.0002738	0.000226	-853.589	3329
7	3.3	1.208	3.3744	-0.191740	0.0003640	0.0003315	0.000168	-1138.23	4467
8	3.2	1.246	3.2791	-0.095277	0.0004033	0.0003836	0.000116	-818.624	5286
9	3.1	1.286	3.1843	-0.094813	0.0004483	0.0004258	7.42E-05	-1277.43	6563
10	3.05	1.307	3.1371	-0.047213	0.0004733	0.0004608	3.92E-05	-1203.54	7767
11	3.03	1.316	3.1182	-0.018846	0.0004837	0.0004785	2.15E-05	-876.666	8644

### 5.6.2 Standard-step Method

While the direct-step method is suitable for use in prismatic channels, and hence applicable to artificial channels, there are some basic difficulties in applying it to natural channels. As already indicated, in natural channels the cross-sectional

shapes are likely to vary from section to section and also the cross-section information is known only at a few locations along the channel. Thus, the problem of computation of the GVF profile for a natural channel can be stated as: Given the cross-sectional information at two adjacent sections and the discharge and stage at one section, it is required to determine the stage at the other section. The sequential determination of the stage as a solution of the above problem will lead to the GVF profile.

The solution of the above problem is obtained by a trial-and-error solution of the basic-energy equation. Consider Fig. 5.4 which shows two Sections 1 and 2 in a natural channel. Section 1 is downstream of Section 2 at a distance  $\Delta x$ . Calculation are assumed to proceed upstream. Equating the total energies at Sections 1 and 2,

$$Z_2 + y_2 + \alpha_2 \frac{V_2^2}{2g} = Z_1 + y_1 + \alpha_1 \frac{V_1^2}{2g} + h_f + h_e \quad (5.34)$$

where  $h_f$  = friction loss and  $h_e$  = eddy loss. The frictional loss  $h_f$  can be estimated as

$$h_f = \bar{S}_f \Delta x = \frac{1}{2}(S_{f1} + S_{f2})$$

where

$$S_f = \frac{n^2 V^2}{R^{4/3}} = \frac{n^2 Q^2}{A^2 R^{4/3}} \quad (5.35)$$

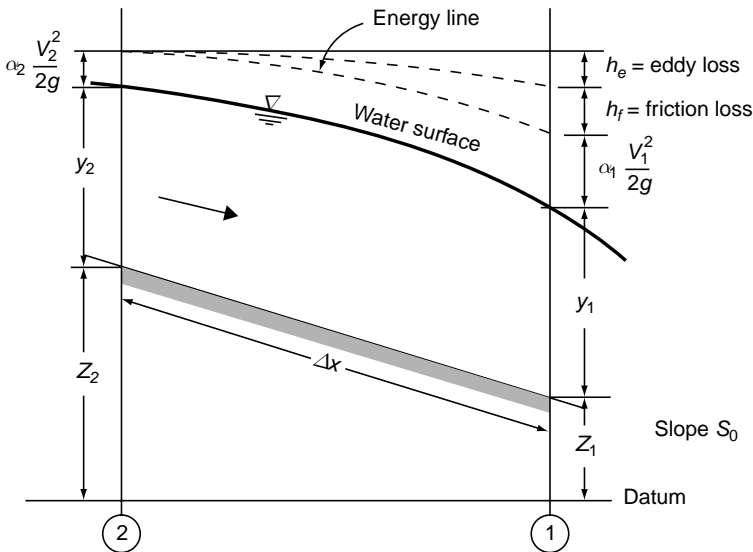


Fig. 5.4 Definition sketch for the Standard-Step method

There is no rational method for estimating the eddy loss but it is usually expressed as,

$$h_e = C_e \left| \frac{\alpha_1 V_1^2 - \alpha_2 V_2^2}{2g} \right| \tag{5.36}$$

where  $C_e$  is a coefficient having the values as below<sup>9</sup>.

Nature of Transition	Value of Coefficient C	
	Expansion	Contraction
1. No transition (Prismatic channel)	0.0	0.0
2. Gradual transition	0.3	0.1
3. Abrupt transition	0.8	0.6

An alternative practice of accounting for eddy losses is to increase the Manning’s  $n$  by a suitable small amount. This procedure simplifies calculations in some cases.

Denoting the stage =  $Z + y = h$  and the total energy by  $H$ , and using the suffixes 1 and 2 to refer the parameters to appropriate sections,

$$H = h + \alpha \frac{V^2}{2g} \quad \text{and Eq. (5.34) becomes}$$

$$H_2 = H_1 + h_f + h_e \tag{5.37}$$

The problem can now be stated as: Knowing  $H_1$  and the geometry of the channel at Sections 1 and 2 it is required to find  $h_2$ . This is achieved in the standard-step method by the trial-and-error procedure outlined below.

**Procedure** Select a trial value of  $h_2$  and calculated  $H_2$ ,  $h_f$  and  $h_e$  and check whether Eq. (5.37) is satisfied. If there is a difference, improve the assumed value of  $h_2$  and repeat calculations till the two sides of Eq. (5.37) match to an acceptable degree of tolerance.

On the basis of the  $i$  th trial, the  $(i + 1)$  th trial value of  $h_2$  can be found by the following procedure suggested by Henderson<sup>11</sup>. Let  $H_E$  be the difference between the left-hand side and right-hand side of Eq. (5.37) in the  $i$  th trial, i.e.

$$H_E = \left[ H_2 - (H_1 + h_f + h_e) \right] \text{ in the } i \text{ th trial.}$$

The object is to make  $H_E$  vanish by changing the depth  $y_2$ .

$$\begin{aligned} \text{Hence} \quad \frac{dH_E}{dy_2} &= \frac{d}{dy_2} \left[ y_2 + Z_2 + \alpha_2 \frac{V_2^2}{2g} - Z_1 - y_1 - \alpha_1 \frac{V_1^2}{2g} \right] \\ &= \frac{1}{2} \Delta x (S_{f1} + S_{f2}) - C_e \left[ \frac{\alpha_1 V_1^2}{2g} - \frac{\alpha_2 V_2^2}{2g} \right] \end{aligned}$$

210 Flow in Open Channels

Since  $y_1, Z_1, Z_2$  and  $V_1$  are constants,

$$\begin{aligned} \frac{dH_E}{dy_2} &= \frac{d}{dy_2} \left[ y_2 + (1 + C_e) \frac{\alpha_2 V_2^2}{2g} - \frac{1}{2} \Delta x S_{f2} \right] \\ &= 1 - (1 + C_e) F_2^2 - \frac{1}{2} \Delta x \cdot \frac{dS_{f2}}{dy_2} \end{aligned} \quad (5.38)$$

Where 
$$F_2^2 = \frac{\alpha_2 Q^2 T_2}{g A_2^3}$$

For a wide rectangular channel,

$$\frac{dS_f}{dy} = \frac{d}{dy} \left( \frac{n^2 q^2}{y^{10/3}} \right) = 3.33 S_f / y$$

Hence 
$$\frac{dS_{f2}}{dy_2} \approx - \frac{3.33 S_{f2}}{y_2} = - \frac{3.33 S_{f2}}{R_2}, \quad \text{leading to}$$

$$\frac{dH_E}{dy_2} = \left[ 1 - (1 - C_e) F_2^2 + \frac{1.67 S_{f2} \cdot \Delta x}{R_2} \right]$$

If  $\frac{dH_E}{dy_2} = \frac{\Delta H_E}{\Delta y_2}$  and  $\Delta y_2$  is chosen such that  $\Delta H_E = H_E$ ,

$$\Delta y_2 = - H_E / \left[ 1 - (1 + C_e) F_2^2 + \frac{1.67 S_{f2} \Delta x}{R_2} \right] \quad (5.39)$$

The negative sign denotes that  $\Delta y_2$  is of opposite sign to that of  $H_E$ . It may be noted that if the calculations are performed in the downward direction, as in supercritical flow, the third term in the denominator will be negative. The procedure is illustrated in the following example. Spread sheets, such as MS Excel, are extremely convenient to calculate GVF profile through the use of the standard step method.

**Example 5.9** | A small stream has a cross section which can be approximated by a trapezoid. The cross-sectional properties at three sections are as follows:

Section	Distance up the River (km)	Bed Elevation (m)	Bed Width (m)	Side Slope
A	100.00	100.000	14.0	1.5 : 1
B	102.00	100.800	12.5	1.5 : 1
C	103.50	101.400	10.0	1.5 : 1

Section A is the downstream-most section. For a discharge of  $100.0 \text{ m}^3/\text{s}$  in the stream, water surface elevation at A was  $104.500 \text{ m}$ . Estimate the water-surface elevation at the upstream Sections B and C. Assume  $n = 0.02$  and  $\alpha = 1.0$  at all sections.

**Solution** The calculations are performed in Table 5.6. In this

Total head  $H$  (Column 7) = Column 4 + Column 6

$h_f$  (Column 12) =  $\bar{S}_f \times L = (\text{Column 10}) \times (\text{Column 11})$

$$h_e = \left[ C_e \Delta \frac{v^2}{2g} \right] \text{ with } C_e = 0 \text{ for expansion.}$$

The first row in the table is based on known information. The second row is based on an assumed stage of  $105.200 \text{ m}$  (i.e. a depth of  $4.400 \text{ m}$ ) at Section B. Column 14 is obtained as  $\{(\text{Column 7 of previous section}) + (\text{Column 12} + \text{Column 13}) \text{ of the present section}\}$ . It represents the right-hand side of the Eq. (5.35), while column 7 represents the left-hand side of the same equation. It is seen that the first trial is not successful as  $\text{Column 7} \neq \text{Column 14}$ . For this trial,  $H_E = 105.272 - 104.797 = 0.475 \text{ m}$ . Substituting in Eq. (5.39) with  $C_e = 0.3$ ,

$F_2^2 \approx \frac{v^2}{gy} \Big|_2 \approx \frac{2 \times 0.072}{4.40} = 0.0327$ ,  $S_{f2} = 1.3308 \times 10^{-4}$ ,  $\Delta x = 2000 \text{ m}$ ,  $R_2 = 2.963$ , leads to  $\Delta y_2 = -0.429 \text{ m}$ .

The next trial stage is therefore taken as  $= 105.200 - 0.429 = 104.771 \text{ m}$ , with a depth of flow of  $3.971 \text{ m}$ .

It may, be seen from the third row in Table 5.6 that in the second trial of the stage  $B = 104.771 \text{ m}$ , Column 7 and Column 14 agree. It is usual to score out the unsuccessful trials after a better one has been obtained to avoid confusion.

The procedure is repeated for Section C, by applying the energy equation between Sections B and C. In the first trial for C,  $H_E = -0.293 \text{ m}$ . The correction  $\Delta y_2$  by Eq. (5.39) is  $+ 0.244 \text{ m}$ . It may be seen that two trials are needed in this section to get the correct water-surface elevation.

### 5.6.3 Standard-step Method for Compound Sections

A majority of natural channels are compound channels (Fig. 5.5). Since the flow in floodbanks (areas 2 and 3 in Fig. 5.5) is normally at a lower velocity than in the main channel, the energy lines corresponding to various sub-areas will be at different elevations above the water surface. A convenient method of handling this situation is to consider a mean velocity  $\bar{V}$  for the entire section and to assume the energy line

to be at a height  $\alpha \frac{\bar{V}^2}{2g}$  above the water surface. Also, a common friction slope  $S_f$  is assumed.

The kinetic-energy correction factor  $\alpha$  for the whole section is obtained as below:



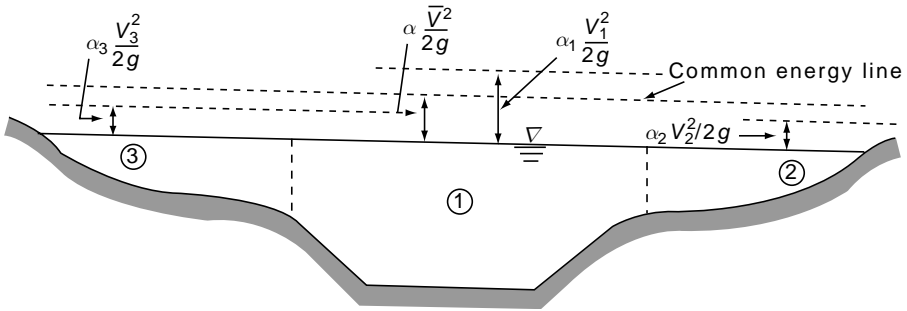


Fig. 5.5 Flow in compound sections

If there are  $N$  partial areas such that

$$\sum_1^N A_i = A = \text{total area,}$$

$$\alpha = \frac{\sum_1^N (V_i^3 A_i)}{\bar{V}^3 \sum_1^N A_i} = \frac{\sum_1^N (Q_i^3 / A_i^2)}{\left( \sum_1^N Q_i \right)^3 / (\sum_1^N A_i)^2} \quad (5.40)$$

Since a common friction slope  $S_f$  is assumed, if  $K_i =$  conveyance of the  $i$ th sub-area

$$Q_i = K_i \sqrt{S_f} \text{ and } Q = \sum_1^N Q_i = \left( \sum_1^N K_i \right) \sqrt{S_f}$$

giving

$$S_f = \frac{Q^2}{\left( \sum_1^N K_i \right)^2} \quad (5.41)$$

Replacing  $Q_i$  in Eq. (5.40) by  $K_i \sqrt{S_f}$ ,

$$\alpha = \frac{\sum_1^N (K_i^3 / A_i^2)}{\left( \sum_1^N K_i \right)^3 / A^2} \quad (5.42)$$

If  $\alpha_i$  are the kinetic-energy correction factors for the partial areas  $A_i$ , Eq. (5.42) becomes

$$\alpha = \frac{\sum_1^N (\alpha_i K_i^3 / A_i^2)}{\left( \sum_1^N K_i \right)^3 / A^2} \quad (5.42-a)$$



Knowing  $S_f$  and  $\alpha$  from Eqs (5.41) and (5.43), the standard-step method can now be used.

In calculating the geometrical parameters of the sub-areas, the interface between two sub-areas can be considered either as a vertical interface (as indicated by dotted lines in Fig. 5.5) or as a diagonal interface or by any other appropriate method indicated in Sec. 3.16.

For a given compound channel section, the value of the kinetic energy correction factor  $\alpha$  as calculated by Eq. (5.42) varies quite rapidly in the region immediately above the overbank level. Fig. 5.6 shows the variation of  $\alpha$  with depth  $y$  for symmetrical compound section. Note the large values of the gradient  $d\alpha/dy$  in a small region of the depth. This gradient  $d\alpha/dy$  has serious implications on the definition and computation of critical depth in compound channels as discussed below.

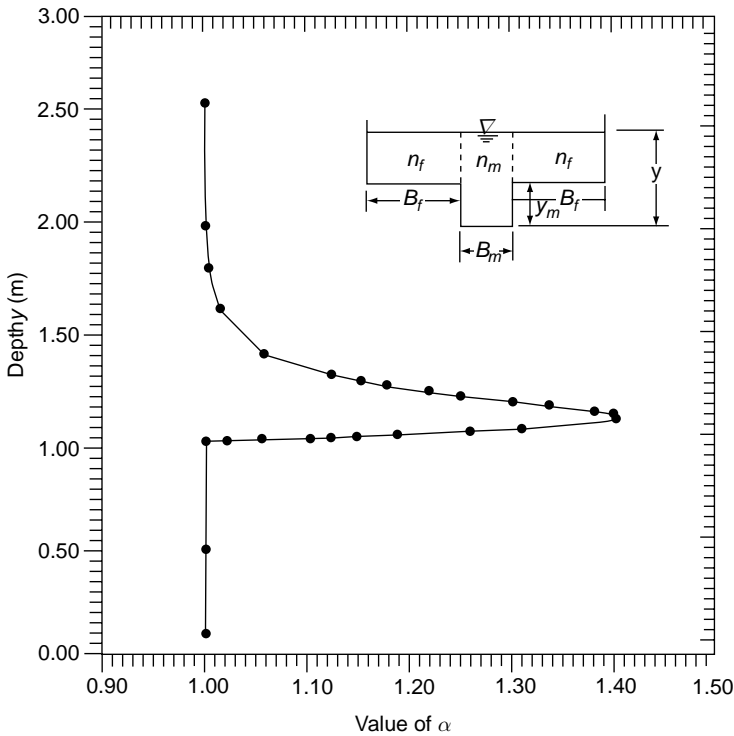


Fig. 5.6 Variation of  $\alpha$  with depth in a symmetric compound channel  
 [ $B_m = 1.0$  m,  $B_f = 3.0$  m,  $y_m = 1.0$  m,  $n_m = 0.013$  and  $n_f = 0.0144$ ].

**Critical Depth in Compound Channels** When a channel has a compound section the discharge is usually computed by the method of partial areas using one of the two methods outlined in the above section. The kinetic energy correction factor  $\alpha$  is calculated by Eq. (5.42). The specific energy  $E = y + \alpha \frac{V^2}{2g}$  may have more than one local minima or maxima under some combination of discharge and geometry. In

such cases the Froude number needs to be properly defined so that the condition of minimum specific energy would correspond to the critical depth.

Several investigators<sup>12, 13, 14</sup> have analytically confirmed the existence of more than one critical depth for compound sections. Blalock and Sturm<sup>11</sup> have analytically and experimentally demonstrated the existence of more than one critical depth in a compound channel. Proper identification of these depths is necessary in steady and unsteady GVF computations, as the critical depth is an important control point. Further, numerical instabilities can be expected in neighbourhood of the critical depth.

Figure 5.7 shows a typical plot of the specific energy  $E$  for the compound channel section shown in Fig. 5.8. Three possible types of  $E$  vs  $y$  plots, shown as Cases 1, 2 and 3 in Fig. 5.7, depending upon the discharge are possible. In Case 2, the specific energy has two minima and local maxima.

Blalock and Sturm<sup>11</sup> have shown that the Froude number must be defined for a compound channel to take care of the variation of the kinetic energy correction factor  $\alpha$ , estimated by Eq. (5.42), with depth adequately so that the Froude number will be unity at the local minima or maxima of the specific energy,  $E$ . Thus as

$$E = y + \alpha \frac{Q^2}{2gA^2}$$

at a local minima or maxima of  $E$ ,

$$\frac{dE}{dy} = 1 - \frac{\alpha Q^2}{gA^2} \frac{dA}{dy} + \frac{Q^2}{2gA^2} \frac{d\alpha}{dy} = 0 \tag{5.43}$$

Noting that  $dA/dy = T$

$$\frac{\alpha Q^2 T}{gA^3} - \frac{Q^2}{2gA^2} \frac{d\alpha}{dy} = 1$$

or 
$$\frac{Q^2 T}{gA^3} \left[ \alpha - \frac{A}{2T} \frac{d\alpha}{dy} \right] = 1 \tag{5.44}$$

The Froude number  $F_c$  for a compound channel section is now defined as

$$F_c = \left[ \frac{\alpha Q^2 T}{gA^3} - \frac{Q^2}{2gA^2} \frac{d\alpha}{dy} \right]^{1/2} \tag{5.45}$$

The term  $\frac{d\alpha}{dy}$  in Eq. (5.44) is determined as

$$\frac{d\alpha}{dy} = \frac{A^2 \sigma_1}{K^3} + \sigma_2 \left( \frac{2AT}{K^3} - \frac{A^2}{K^4} \sigma_3 \right) \tag{5.46}$$

in which 
$$\sigma_1 = \sum_i \left[ \left( \frac{K_i}{A_i} \right)^3 \left( 3T_i - 2R_i \frac{dP_i}{dy} \right) \right] \quad (5.47)$$

$$\sigma_2 = \sum_i \left( \frac{K_i^3}{A_i^2} \right) \quad (5.48)$$

$$\sigma_3 = \sum_i \left[ \left( \frac{K_i}{A_i} \right) \left( 5T_i - 2R_i \frac{dP_i}{dy} \right) \right] \quad (5.49)$$

$R_i = A_i/P_i =$  hydraulic radius of the  $i$  th sub-section.

$T_i =$  top width of  $i$  th sub-section.

Using the above expression for  $d\alpha/dy$ , the Eq. (5.45) for  $F_c$  can be simplified as

$$F_c = \left[ \frac{Q^2}{2gK^3} \left( \frac{\sigma_2\sigma_3}{K} - \sigma_1 \right) \right]^{1/2} \quad (5.50)$$

The term  $dP_i/dy$  in Eqs (5.47) and (5.49) for each sub-section is to be evaluated by considering the appropriate boundaries of the sub-section.

The depth which products  $F_c = 1$  is taken as the critical depth. For a compound channel section as in Fig. 5.8, if  $y_m =$  depth of overbank level above the main channel bed, usually one critical depth [point  $C_1$  in Fig. 5.7] occurs at a depth less than  $y_m$ , i.e.  $y_{c1} < y_m$ . Another critical depth [point  $C_3$  in Fig. (5.7)] occurs at a depth larger than  $y_m$ , i.e.  $y_{c3} > y_m$ . Between these two depths  $y_{c1}$  and  $y_{c3}$  between points  $C_1$  and  $C_3$  in Fig. 5.7, the specific energy reaches a local maxima [point  $C_2$  in Fig. 5.7]. The depth at this condition,  $y_{c2}$ , could also be considered as a kind of critical depth. Usually  $y_{c2}$  is slightly larger than  $y_m$ .

For a symmetrical compound channel as in Fig. 5.8 depending upon the magnitude of discharge three distinct cases of occurrence of critical depths can be identified.

**Case 1.** Only  $y_{c1}$  exists. The corresponding  $E - y$  plot is shown in Fig. (5.7 – Case 1) : Let the discharge be called  $Q_1$ .

**Case 2.** Only  $y_{c3}$  exists. Also  $y_{c3} > y_m$ , Fig (5.7– Case 3 ) shows the corresponding  $E - y$  plot. Let the discharge be called  $Q_3$ .

**Case 3.** All the three critical depths  $y_{c1}$ ,  $y_{c2}$  and  $y_{c3}$  exist. Also,  $y_{c1} < y_{c2} < y_{c3}$ .

The discharge  $Q_2$  for Case 2 will be such that  $Q_1 < Q_2 < Q_3$ .

As an example, for the symmetrical compound channel section of Fig. 5.8 with  $B_m = 1.0$  m,  $B_f = 3.0$  m,  $y_m = 1.0$  m,  $n_f = 0.0144$  and  $n_m = 0.0130$ , a discharge  $Q_2 = 2.5$  m<sup>3</sup>/s belongs to Case 2 with  $y_{c1} = 0.860$  m,  $y_{c2} = 1.003$  m and  $y_{c3} = 1.130$  m. Further, discharge  $Q = 1.60$  m<sup>3</sup>/s and  $3.5$  m<sup>3</sup>/s in the same channel would give Case 1 and Case

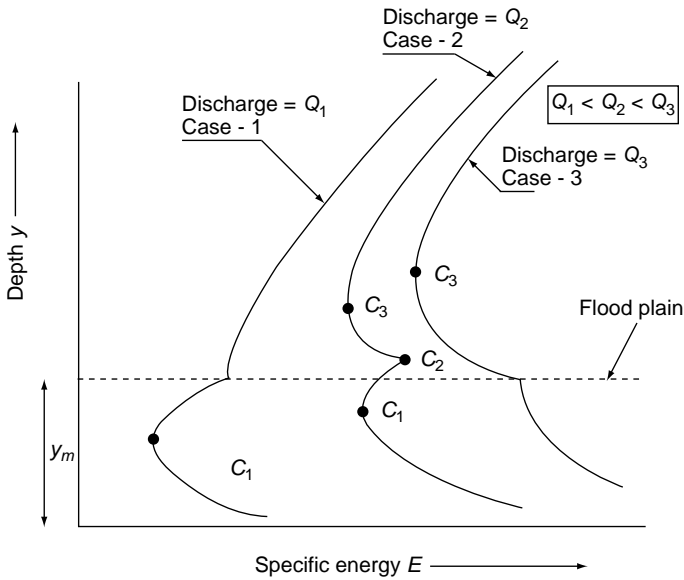


Fig. 5.7 Schematic variation of specific energy with depth in a symmetric compound section of Fig. 5.8

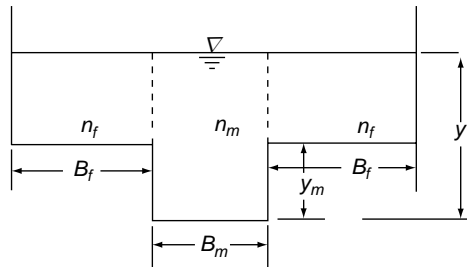


Fig. 5.8 Symmetrical compound section

3 respectively. The range of discharges  $Q_2$  within which the Case 2 occurs, depends upon the geometry of the channel.

Choudhary and Murthy Bhallamudi<sup>13</sup> used a one-dimensional momentum equation and continuity equation for unsteady flows (St. Venant's equations) to derive the Froude number in terms of the momentum correction factor  $\beta$  as

$$F_{cm} = \frac{\beta V}{\sqrt{g \frac{A}{T} + V^2 \left( \beta^2 - \beta - \frac{A}{T} \frac{d\beta}{dy} \right)}} \quad (5.51)$$

The condition at critical flow is obtained by putting  $F_{cm} = 1$  as

$$\frac{g}{Q^2} = \left\{ \frac{\beta T - A \frac{d\beta}{dy}}{A^3} \right\} \quad (5.52)$$

where

$$\beta = \frac{\sum_i (K_i^2 / A_i)}{K^2 / A} \quad (5.53)$$

It appears that for GVF flows in compound channel sections Eq. 5.50 which uses the specific energy criteria and for unsteady flows Eq. 5.52 which is based on the momentum criteria are appropriate choices for the definition of Froude number and hence in the calculation of the critical depths. Usually, the values of the critical depths calculated by using the two methods do not differ appreciably.

It should be noted that the existence of multiple critical depths would be noticed only when the compound section is considered to be made up of sub-areas and the total discharge is calculated as the sum of the partial area discharges. If the compound section is treated as one whole unit for discharge calculation the occurrence of multiple critical depths does not arise.

#### 5.6.4 Backwater Curves in Natural channels

**Methodology** Computation of Backwater curves due to construction of dams, barges and weirs across natural channels is one of the basic procedures in the planning and design of these structures. The basic issues are to know the extent of flooding, areal as well as length of the reach affected by the construction of the structure. For large dams the computations are done for various flood frequencies such as 25, 50, 100, 1000 years and for PMF. In addition to computation of the GVF profile, the sedimentation aspects of the dam and river complex for various time horizons are also computed. The GVF profiles are computed for pre-dam and post dam scenarios. In the post dam situation GVF without siltation and with siltation are estimated.

The basic methodology used is the Standard – Step method. The computations are carried out using well tried out softwares like HEC-RAS and MIKE 21. HEC-RAS has been developed by US Army Corps of Engineers and replaces the widely used HEC-2 of the same organization. HEC-RAS has been developed to perform one dimensional hydraulic analysis for natural as well as man-made channel networks. It is a very versatile program capable of handling very large varieties of water surface computation problems in rigid bed as well as in mobile bed environment. HEC-RAS is available along with user's manual (<http://www.hec.usace.army.mill/software/hec-1>) for download by individuals free of charge. MIKE-11 is a commercial software of the company DHI and is an industry standard for simulating flow and water levels, water quality and sediment transport in rivers, flood plains, irrigation canals, reservoirs and other inland water bodies. Details of MIKE-11 are available in the web site (<http://www.dhigroup.com/Software/WaterResources/MIKE11.aspx>).

**Basic Assumptions of GVF Computations** Before embarking on the computations of GVF profiles of a natural channel, it is advisable to recollect the basic assumptions involved in the computation procedure and to ensure that the field data used in the computations do not violate these constraints: The basic assumptions of the standard step method are:

1. Steady flow
2. Gradually varied water surface (Hydrostatic pressure distribution)
3. One-dimensional analysis
4. Small channel slope
5. Rigid boundary
6. Constant (averaged) friction slope between adjacent sections

### **Basic Data requirement**

- (i) Complete cross-sectional properties at the cross sections under study including the stage discharge information at the sections. The number of sections and intervals between the sections depend upon the site conditions and the purpose of the study. Concurrent water surface elevations (and hence discharges) at a set of stations at various discharges (preferably at high flows) are necessary for calibration and validation of the model.
- (ii) Various discharges selected for the study, viz., 5-year flood, 25-year flood, 100-year flood and PMF etc. obtained by appropriate hydrologic studies.
- (iii) Channel roughness coefficient: These have to be carefully selected on the basis of field survey, study of the photographs and all other relevant details. It has been found that smaller the value of Manning's  $n$  the longer will be the profile and vice versa<sup>3</sup>. Hence the smallest possible  $n$  value should be selected when the longest length of backwater curve, as in the case of submergence studies related to construction of reservoirs, is needed.
- (iv) (a) The accuracy of computations, especially in standard-step method, will have to be pre-decided. HEC-RAS adopts an accuracy of 0.003 m for the elevation as default
  - (b) *The termination depth of the computations:* Since the GVF profiles approach the normal depth asymptotically, the estimation of the backwater curve will have to be terminated at a finite depth to achieve meaningful accuracy. This is usually done up to a depth 1% excess/short of the normal depth, depending upon the nature of the profile. Thus  $M_1$  curves are assumed to stop at a depth of 1.01 times normal depth and  $M_2$  curves are assumed to start from a depth of 0.99 times normal depth. In studies related to backwater effect of a dam, the place where the incremental rise in water surface begins to cause damage is defined as the *end-point* of a backwater curve<sup>3</sup>. For practical purposes, this end point is taken as the termination depth referred above, namely 1.01 times the normal depth.

### **Procedure**

- (i) *Division of Sub-sections* The cross-sectional data has to be analyzed to establish the method of analysis, i.e., whether single channel method or divided channel

method (DCM) of analysis is to be adopted. Compound sections are very common in natural rivers. HEC-RAS adopts the DCM with vertical sections to accommodate the flood plain effect. The composite roughness is calculated by Horton's method. The following procedure is adopted by HEC-RAS to identify regions for adopting composite roughness and divided channel sections:

- (a) Normally, the main channel is not sub divided, except when there is a perceptible change in the roughness coefficient along the perimeter of the main channel
- (b) If the main channel portion side slopes are steeper than 5H:1V and the main channel has more than one  $n$ -value, a composite roughness  $n_c$  (calculated by Horton's method) is adopted for the main channel. Otherwise, for flat side slope cases the main channel also has to be sub-divided appropriately
- (c) The composite roughness is calculated separately for the left and right flood banks.

(ii) *Calibration and Validation* When all the necessary data for the computation of backwater curves in a natural channel has been assembled, the controls identified and the software to be adopted is selected and other details finalised, the next step is to do the calibration of the model.

Model calibration and validation provides an assessment of the model's ability to accurately reproduce known results. Calibration is performed by running the model at the high flow rate with the estimated  $n$ -values. A set of stations where concurrent water surface elevations (and hence discharges) are known are selected. Water surface elevations at these sections are computed for a given set of data. The computed water surface profile covering this set of stations is compared to the measured profile and optimization parameters  $P$  and  $D$  are determined; where

$$P = \left( \sum_{i=1,N} (E_i - E_{ci})^2 \right)^{1/2} \quad (5.54)$$

and

$$D = \left( \sum_{i=1,N} \frac{(E_i - E_{ci})^2}{N} \right)^{1/2} \quad (5.55)$$

in which  $E$  is the measured water surface elevation,  $E_c$  is the computed water surface elevation at each cross-section  $i$  and  $N$  is the total number of sections. It may be noted that  $D$  represents the root mean square of the deviation of the water surface and provides a measure of the accuracy of the model.

The standard calibration procedure is to adjust the value of roughness factor  $n$  such that  $P$  and  $D$  are minimized. The program is then reproducing the known results to its best capability and can be expected to reproduce the other ranges also to the same degree of accuracy. Before application to the data points of the problem, the calibrated program (with calibrated values of  $n$ ) is run on another set of data with known concurrent water surface elevations to verify that the program would indeed

reproduce known results within acceptable degree of error. The data used in the verification stage should be different from the data set used in calibration stage.

The model is now ready for the computation of the desired GVF profiles.

## 5.7 ADVANCED NUMERICAL METHODS

The basic differential equation of GVF [Eq. (4.8)] can be expressed as

$$\frac{dy}{dx} = F(y) \quad (5.56)$$

in which  $F(y) = \frac{S_0 - S_f}{1 - (Q^2 T / g A^3)}$  and is a function of  $y$  only for a given  $S_0$ ,  $n$ ,  $Q$  and channel geometry. Equation 5.56 is non-linear and a class of methods which is particularly suitable for numerical solution of the above equation is the *Runge–Kutta* method. There are different types of Runge–Kutta methods and all of them evaluate  $y$  at  $(x + \Delta x)$  given  $y$  at  $x$ . Using the notation  $y_i = y(x_i)$  and  $x_i + \Delta x = x_{i+1}$  and hence  $y_{i+1} = y(x_{i+1})$ , the various numerical methods for the solution of Eq. 5.56 are as follows:

### (a) Standard Fourth Order Runge–Kutta Methods (SRK)

$$y_{i+1} = y_i + \frac{1}{6}(K_1 + 2K_2 + 2K_3 + K_4) \quad (5.57)$$

where

$$K_1 = \Delta x F(y_i)$$

$$K_2 = \Delta x F\left(y_i + \frac{K_1}{2}\right)$$

$$K_3 = \Delta x F\left(y_i + \frac{K_2}{2}\right)$$

$$K_4 = \Delta x F(y_i + K_3)$$

### (b) Kutta–Merson Method (KM)<sup>15</sup>

$$y_{i+1} = y_i + \frac{1}{2}(K_1 + 4K_4 + K_5) \quad (5.58)$$

where

$$K_1 = \frac{1}{3} \Delta x F(y_i)$$

$$K_2 = \frac{1}{3} \Delta x F(y_i + K_1)$$

$$K_3 = \frac{1}{3} \Delta x F\left(y_i + \frac{K_1}{2} + \frac{K_2}{2}\right)$$



$$K_4 = \frac{1}{3} \Delta x F \left( y_i + \frac{3}{8} K_1 + \frac{9}{8} K_3 \right)$$

$$K_5 = \frac{1}{3} \Delta x F \left( y_i + \frac{3}{2} K_1 - \frac{9}{2} K_3 + 6K_4 \right)$$

An estimate of the truncation error in Eq. 5.58 is given by

$$\varepsilon = 0.2K_1 - 0.9K_3 + 0.8K_4 - 0.1K_5 \quad (5.59)$$

In using the above methods, the channel is divided into  $N$  parts of known length interval  $\Delta x$ . Starting from the known depth, the depths at other sections are systematically evaluated. For a known  $y_i$  and  $\Delta x$ , the coefficients  $K_1, K_2, \dots$ , etc. are determined by repeated calculations and then by substitution in the appropriate main equation [Eq. 5.57 or Eq. 5.58], the value of  $y_{i+1}$  is found. The SRK method involves the determination of  $F(y)$  four times while the KM method involves  $F(y)$  to be evaluated five times for each depth determination. These two methods are direct methods and no iteration is involved. The KM method possesses an important advantage in the direct estimate of its truncation error, which can be used to provide automatic interval and accuracy control in the computations<sup>17</sup>.

**(c) Trapezoidal Method (TRAP)** This is an iteration procedure with

$$y_{i+1} = y_i + \frac{1}{2} \Delta x \{F(y_i) + F(y_{i+1})\} \quad (5.60)$$

The calculation starts with the assumption of  $F(y_{i+1}) = F(y_i)$  in the right hand side of Eq. 5.60. The value of  $y_{i+1}$  is evaluated from Eq. 5.60 and substituted in Eq. 5.56 to get  $F(y_{i+1})$ . This revised  $F(y_{i+1})$  is then substituted in Eq. 5.60. The process is repeated. Thus the  $r$ th iteration will have

$$y_{i+1}^{(r)} = y_i + \frac{1}{2} \Delta x \{F(y_i) + F(y_{i+1})^{(r-1)}\} \quad (5.61)$$

The iteration proceeds till two successive values of  $F(y_{i+1})$  or  $y_{i+1}$  agree to a desirable tolerance.

**Comparison of Various Methods** Studies have been reported by Apelt<sup>15</sup> and Humpridge and Moss<sup>16</sup> on the SRK method; by Apelt<sup>17</sup> on the KM and TRAP methods and by Prasad<sup>17</sup> on the TRAP method. It has been found that all these three methods are capable of direct determination of the GVF profile in both upstream and downstream directions irrespective of the nature of flow, i.e., whether the flow is subcritical or supercritical. Apelt<sup>17</sup> in his comparative study of the three methods has observed that the SRK and KM methods possess better stability characteristics and require less computational effort than the TRAP method. Also, while the SRK method is slightly more efficient than the KM method, the possibility of providing automatic control of the step size and accuracy in the KM process makes it a strong contender for any choice.

All the three methods are well-suited for computer applications and can easily be adopted to GVF calculations in natural channels. In these three methods when the calculations involve critical depth, care should be taken to avoid  $dy/dx = \infty$  at  $y = y_c$  by terminating the calculations at a depth slightly different from  $y_c$ .

5.8 FLOW PROFILES IN DIVIDED CHANNELS

Divided channels, also known as *island-type* flow, occur when the discharge is divided into two or more separate channels as it flows round one or more islands. Typical simple island type and multi-island type flows are shown in Figs 5.9 and 5.10 respectively. While the divided channels occur frequently in natural channels they can also occur in storm water systems. In analysing the divided flow, it is advantageous to represent the flow situation by net work of nodes and links, e.g., Fig. 5.11 is such a representation of Fig. 5.9

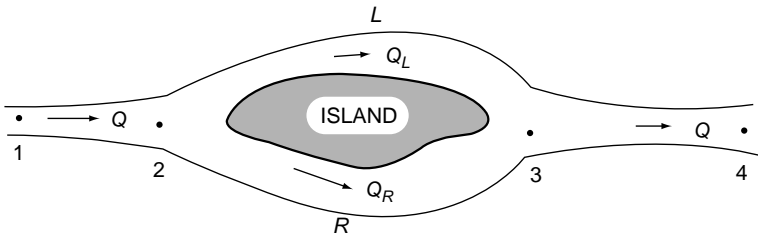


Fig. 5.9 Simple-island-type flow

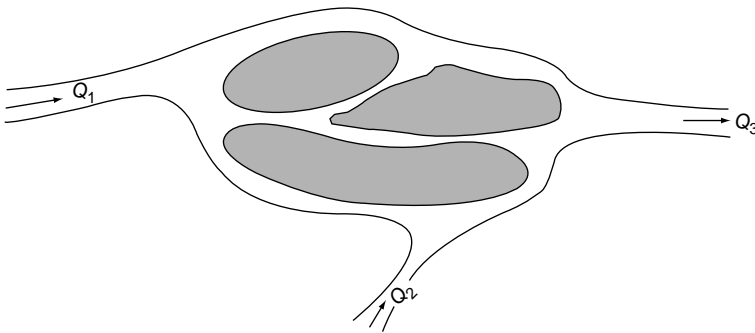


Fig. 5.10 Multi-island-type flow

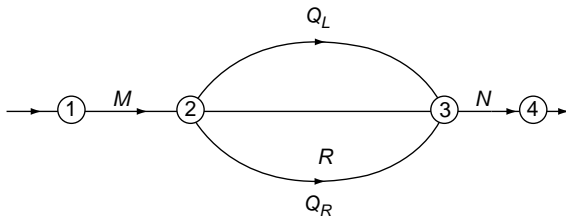


Fig. 5.11 Schematic representation of Fig. 5.9

**Simple-island-Type Flow** The usual problem in this category is the determination of the division of discharge  $Q$  for a given downstream water-surface elevation. Referring to Fig. 5.9 and 5.11, the geometry of the main channel as well as the channels  $L$  and  $R$  are known. For a Known stage at Section 4, it is required to find the division of the discharge  $Q$  into  $Q_L$  and  $Q_R$  in the channels  $L$  and  $R$  respectively. The flow is assumed to be subcritical, as it is the most usual case. In the solution of this problem the continuity equation at each node and the energy equation for various paths are employed. Thus in Fig. 5.11, the total discharge  $Q$  is divided into  $Q_L$  and  $Q_R$  at node 2 and is recombined at node 3. By the energy equation, the drop of the total energy between nodes 2 and 3 in path  $L$  must be the same as the drop between these nodes in the path  $R$ .

The solution to the problem is achieved through a trial-and-error procedure. First a trial division of  $Q_L$  and  $Q_R$  is assumed such that  $Q_L + Q_R = Q$ . Starting from a known stage at 4, the water-surface elevations at the various nodes are calculated by GVF computations as below:

Step	From-to	Path	Find Elevation	Discharge at Node Used
(a)	4-3	$N$	3	$Q$
(b)	3-2	$L$	2	$Q_L$
(c)	3-2	$R$	2	$Q_R$

The elevation at Node 2 calculated in steps (b) and (c) must be the same for a correct division of flow. However, since an arbitrary division was assumed, the two values would differ by an amount  $\Delta H$ . If the calculations are repeated for different assumed values of  $Q_L$ , in the successive iterations the experience of the previous calculations are used to guide better selections of  $Q_L$  values. If  $\Delta H = \{\text{elevation at 2 by step (b)} - \text{Elevation at 2 by step (c)}\}$ , the correct value of  $Q_L$  to give zero value of  $\Delta H$  is obtained by interpolation (Fig. 5.12).

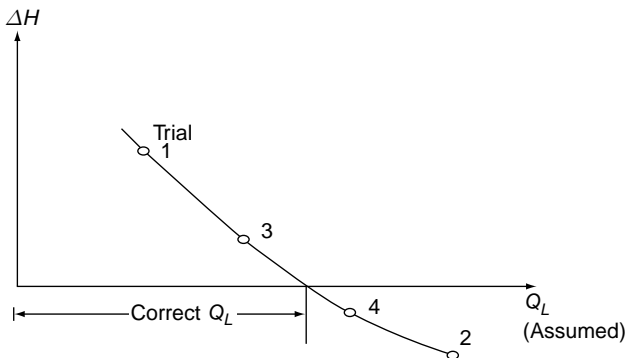


Fig. 5.12 Interpolations of  $\Delta H$  to get  $Q$

**Multi-island-Type Flows** The trial-and-error type of solution, used in the simple-island type flow, will become extremely tedious if it is to be successfully applied to multi-island type flows. Considering the problem as analogous to that of the pipe network problem, Wylie<sup>18</sup> and Vreugdenhil<sup>19</sup> have developed iterative numerical procedures for solving the general multi-island system. An efficient algorithm for the solution of parallel channel network is available in Ref. (20).

### 5.9 ROLE OF END CONDITIONS

The channel end conditions, being the boundary conditions for GVF computations play a very important role. Some common end conditions and few cases of interaction of end conditions on the flow are discussed in this section.

**Outlet** An ideal outflow of a canal into a lake is shown in Fig. 5.13(a). The kinetic energy of the stream is recovered as potential energy and as such the lake water is higher than the channel water surface at the outlet by an amount  $\Delta h = \frac{\alpha V^2}{2g}$ . In reality, there will be energy losses at the outflow and one can safely assume that all the kinetic energy of the outflow is lost in shear. Hence, the outflow situation for mild slope channels is adopted as follows:

If  $y_L$  = depth of water in the lake and  $y_d$  = depth of flow in the canal at the outlet, both measured above the channel bed

- |                     |             |                 |
|---------------------|-------------|-----------------|
| 1. If $y_L > y_c$ , | $y_d = y_L$ | [Fig. 5.13 (b)] |
| 2. If $y_L = y_c$ , | $y_d = y_c$ | [Fig. 5.13 (c)] |
| 3. If $y_L < y_c$ , | $y_d = y_c$ | [Fig. 5.13 (d)] |

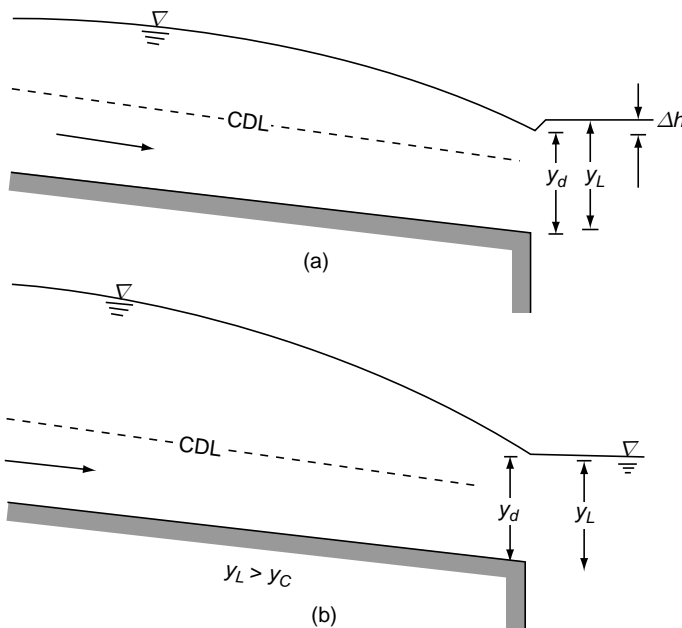


Fig. 5.13 (Contd)

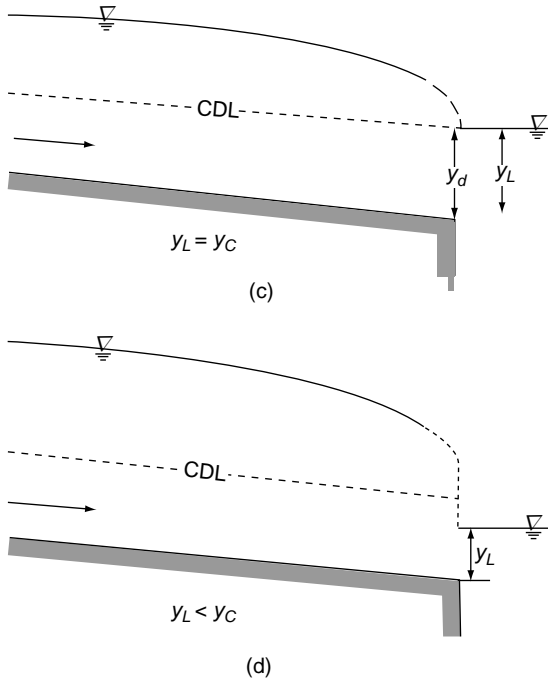


Fig. 5.13 End conditions

In supercritical flow the control is on the upstream of the channel and as such  $y_d = y_L$ .

**Inlet** Figure 5.14 shows a free inlet from a reservoir to a mild-slope channel. There will be a certain amount of energy loss at the entrance. Initially the flow will be non-uniform which soon adjusts to uniform flow. At the end of the entrance zone, for uniform flow,

$$H + \Delta Z = y_0 + \alpha \frac{V_0^2}{2g} + h_f + \Delta H_L \tag{5.62}$$

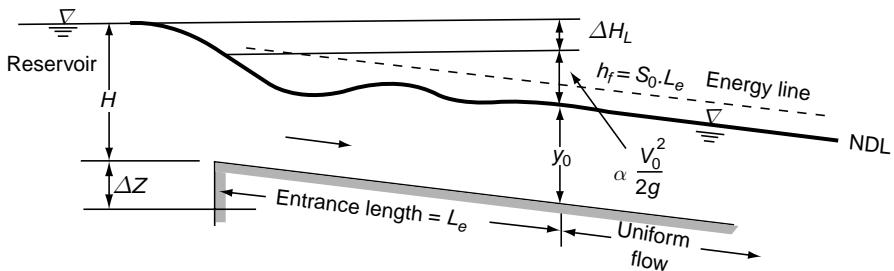


Fig. 5.14 Mild-slope channel inlet

where  $h_f = \Delta Z =$  head loss due to friction at the rate of  $S_0$  and  $\Delta H_L =$  entrance loss  $= K \frac{V_0^2}{2g}$  in which  $K =$  a coefficient whose value may range from 0.1 to 0.25 for a well-rounded entrance. Thus at the lake entrance for a mild channel

$$H = y_0 + (\alpha + K) \frac{V_0^2}{2g} \tag{5.63}$$

If the channel has a steep slope, the critical depth control exists at the channel inlet and the flow will be established through an  $S_2$  curve [Fig. 4.5(e)].

**Interaction of Exit and Inlet Conditions** Consider the case of a canal connecting two lakes. Let us assume the canal to be of short length so that both the reservoirs are spanned by the GVF profile generated. Let the inlet depth  $y_1$  be constant and the outlet-pool depth  $y_L$  be a variable (Fig. 5.15). The interaction of the downstream pool elevation with the upstream lake, through a GVF profile, is reflected by the change in the discharge of the canal. The discharge carried by a canal under conditions of varied flow was termed by Bakhmeteff<sup>1</sup> as *delivery* of a canal.

**Delivery in Mild Channels Under Varying Downstream Pool Elevation**

Referring to Fig. 5.15,  $y_L =$  downstream-pool depth measured from the channel bottom at the outlet. The value of  $y_2$  is assumed to vary while  $y_1$  is assumed to remain constant. Let  $L =$  length of the channel and  $S_0 =$  bed slope. When  $y_L = y_{Lm} = y_1 + LS_0$ , i.e. when  $am$  is a horizontal line, the discharge in the channel is zero. If  $y_L = y_0$ , i.e. when the water surface  $ap$  is parallel to the bed and uniform flow prevails, the uniform-flow discharge is  $Q_0$ . For any  $y_{Lm} > y_L > y_0$ , the discharge  $Q$  will be less than  $Q_0$ , the resulting GVF profile will be of  $M_1$  type. The decrease in the discharge ( $Q < Q_0$ ) takes place because of the interaction of the  $M_1$  curve causing a drowning effect at the inlet. The variation of the discharge  $Q$  with  $y_L$  in this zone is shown in Fig. 5.15.

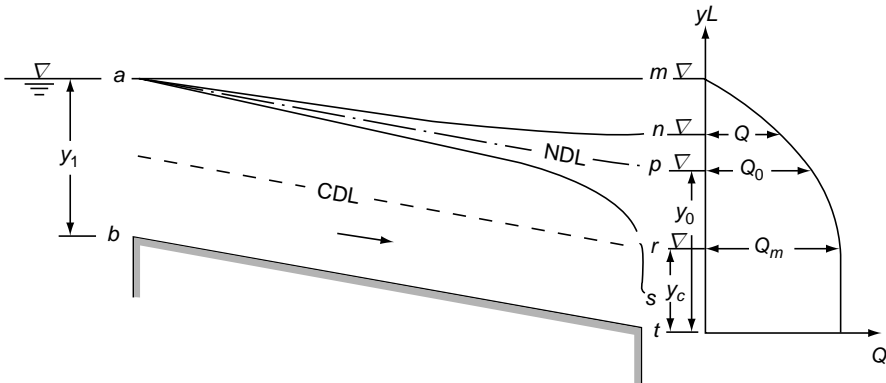


Fig. 5.15 Delivery in a mild-slope channel

When  $y_c < y_L < y_0$ , the  $M_2$  profile occurs and causes a drawdown effect at the inlet resulting in an enhanced discharge  $Q > Q_0$ . The maximum value of  $Q = Q_m$  occurs at  $y_L = y_c$ . Further decrease in the value of  $y_L$  does not cause any change in  $M_2$  profile, excepting for a hydraulic drop to occur ( $rs$  in Fig. 5.15).

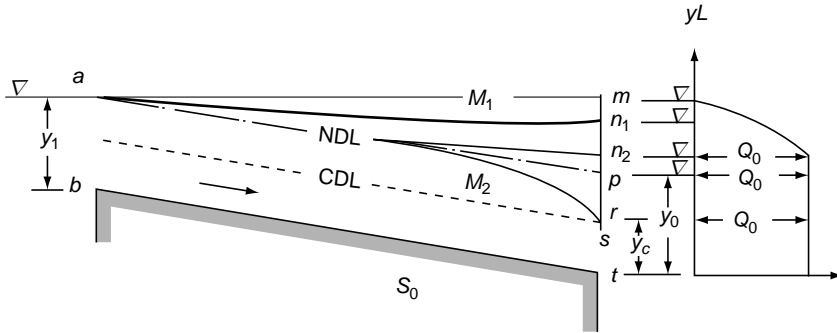


Fig. 5.16 Delivery in a long channel

A channel of this kind, where  $Q_m > Q_0$ , i.e. where the GVF curves reach up to the intake and affect the discharge is called a *short* channel. Conversely, a *long* channel is one where the intake is so far away from the outlet that none of the  $M_2$  curves reach the intake. In a long channel some  $M_1$  curves may also not reach the intake. Figure 5.16 indicates the delivery in a long channel. It may be noted that in a long channel,  $Q_m = Q_0$  and  $Q_0$  can also occur for  $y_L > y_0$ .

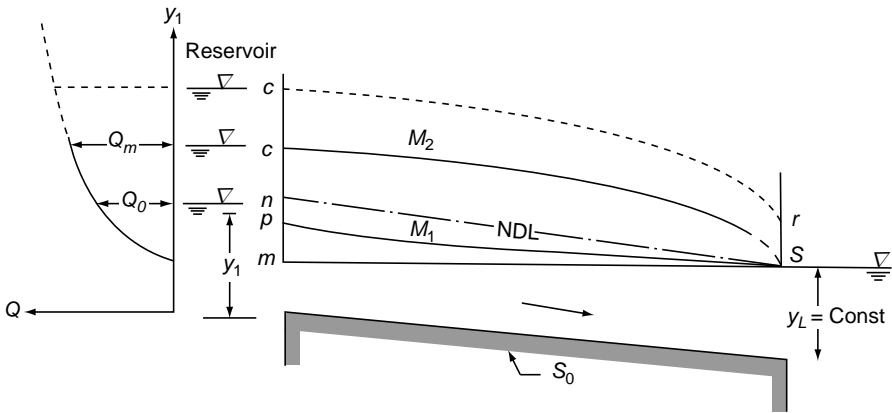


Fig. 5.17 Delivery under varying upstream reservoir level

**Delivery in Mild Channels Under Varying Upstream Reservoir Elevations**

In this case the downstream pool elevation is kept constant and the upstream reservoir depth  $y_1$  is varied (Fig. 5.17). The length of the channel is  $L$  and  $S_0$  is its bed slope. When  $y_1 = y_{lm} = (y_L - LS_0)$ , i.e. line  $ms$  is horizontal, there is no flow in the canal. When  $y_1 < (y_L - LS_0)$ , the flow is to the reservoir, i.e. in the negative direction and is not considered here.

Uniform flow takes place when  $y_1 = y_{1n}$ , i.e. line  $ns$  is parallel to the bed and the delivery is  $Q_0$ . For  $y_{1n} < y_1 < y_{1m}$ , the discharge is less than  $Q_0$  and the water surface profile is an  $M_1$  curve. For values of  $y_1 > y_{1n}$ , the water surface profile is an  $M_2$  curve and the delivery is  $Q > Q_0$ . The maximum discharge  $Q_m$  compatible with  $y_L = \text{constant}$  occurs when the depth  $y_L = \text{critical depth}$  (line  $cs$  in Fig. 5.17). Any further increase in the upstream depth  $y_1$  would no doubt increase the delivery  $Q$ , but the downstream water depth will be a critical depth  $y_c > y_L$  followed by a *hydraulic drop* (lined  $cr$  in Fig. 5.17), Which is strictly not compatible with the condition  $y_L = \text{constant}$ .

An extensive analysis of delivery problems is reported in literature<sup>1</sup>.

**Example 5.10** | A wide rectangular channel of slope 0.0004 and  $n = 0.02$  connects two reservoirs 1.5 km apart. The upstream reservoir level is constant at an elevation of 104.00 m and the elevation of the canal invert at the intake is 101.00 m. The intake is free and the loss of energy at the intake can be neglected. (a) What should be the downstream reservoir level to cause uniform flow in the entire length of the channel? (b) If the downstream reservoir level is 103.40 m, will it affect the uniform flow discharge?

**Solution** (a) Refer to Fig. 5.18(a). Neglecting losses at the entry

$$H = y_0 + \frac{V_0^2}{2g}$$

As the channel is wide 
$$V_0 = \frac{1}{n} y_0^{2/3} S_0^{1/2}$$

$$y_0 = H - \frac{1}{2g} \left[ \frac{1}{n} y_0^{2/3} S_0^{1/2} \right]^2$$

$$y_0 = 3.0 - \frac{1}{2 \times 9.81} \left[ \frac{1}{(0.02)^2} y_0^{4/3} \times 0.0004 \right]$$

Solving by trial and error,  $y_0 = 2.80$  m

Bed level at downstream end of the channel, i.e., at the Section B

$$= 101.00 - (0.0004 \times 1500) = 100.40 \text{ m}$$

Downstream pool elevation =  $100.40 + 2.80 = 103.20$  m

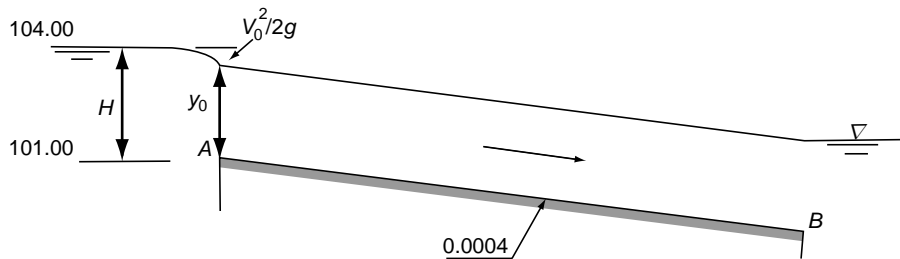


Fig. 5.18(a) Definition sketch of Example 5.10(a)



230 Flow in Open Channels

(b) Flow when the downstream pool elevation is at 103.40 m:  
 Assume the flow at the inlet is not affected by the downstream lake elevation.

$$y_0 = 2.80 \text{ m}$$

$$q_0 = \text{normal discharge} = \frac{1}{0.02} (2.80)^{5/3} (0.0004)^{1/2} = 5.547 \text{ m}^3/\text{s/m}$$

$$\text{Critical depth } y_c \text{ for this discharge} = \left(\frac{q^2}{g}\right)^{1/3} = \left(\frac{(5.547)^2}{9.81}\right)^{1/3} = 1.464 \text{ m} < y_0$$

The flow is thus subcritical, the channel is a mild slope channel and an  $M_1$  curve will result with downstream lake elevation at 103.40 m. (See Fig. 5.18(b)).

- (i) If this curve, calculated with discharge =  $q_0$ , extends beyond the inlet A, then the inlet is drowned and the discharge in the channel will be less than  $q_0$ .
- (ii) If the length of this  $M_1$  curve is less than 1500 m, the inlet is free and uniform flow will prevail in the upper reaches of the channel unaffected by backwater of downstream lake. The canal discharge will therefore be  $q_0$ .

The  $M_1$  profile is calculated by Direct step method starting from the downstream end B. The calculations are shown in Table 5.6. It is seen that the  $M_1$  curve for  $q_0 = 5.547 \text{ m}^3/\text{s/m}$  extends beyond the inlet A. Hence the uniform flow discharge is affected by the downstream pool elevation of 103.40 m.

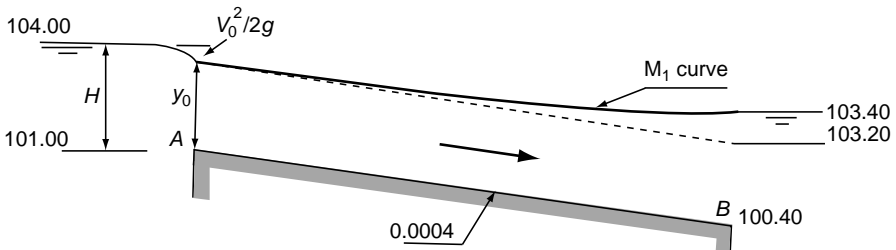


Fig. 5.18(b) Definition sketch of Example 5.10(b)

Table 5.6 Computation of Flow Profile by Direct Step Method (Example 5.10)

Wide Rectangular channel					$n = 0.02$	$S_0 = 0.0004$	$q = 5.547 \text{ m}^3/\text{s/m}$		
Sl. No.	$y \text{ (m)}$	$V \text{ (m/s)}$	$E \text{ (m)}$	$\Delta E \text{ (m)}$	$S_f$	$\bar{S}_f$	$S_0 - \bar{S}_f$	$\Delta x \text{ (m)}$	$x \text{ (m)}$
1	3.00	1.849	3.174		0.000316				0
2	2.95	1.880	3.130	-0.0440	0.000334	0.000325	7.48E-05	-589	589
3	2.90	1.913	3.086	-0.0437	0.000354	0.000344	5.59E-05	-782	1371
4	2.85	1.946	3.043	-0.0434	0.000375	0.000364	3.56E-05	-1220	2591

**Example 5.11** A rectangular channel,  $B = 3.0$  m and  $n = 0.015$ , takes off from a reservoir. The channel slope is  $0.017$ . At the intake the bed of the channel is at an elevation of  $100.00$  m. If the reservoir water surface is at  $102.00$  m and the entrance losses are equal to  $0.2$  times the velocity head at the intake, calculate the discharge in the channel. At what distance from the intake would the uniform flow commence?

**Solution** First it is necessary to find whether the slope is mild or steep. By Eq. (3.65)

limit slope  $S_L = \frac{8}{3} \frac{gn^2}{B^{1/3}}$ . Here,  $B = 3.0$  m,  $S_0 = 0.017$  and  $n = 0.015$

$$S_L = \frac{8}{3} \times \frac{(9.81) \times (0.015)^2}{(3.0)^{1/3}} = 0.004$$

Since  $S_0 > S_L$ , the channel slope is steep. An  $S_2$  curve is formed at the inlet to reach the normal depth asymptotically, (Fig 5.19). Here  $H = 102.00 - 100.00 = 2.00$  m.

At the inlet,  $y_c + \frac{V_c^2}{2g} + 0.2 \frac{V_c^2}{2g} = 2.0$ . Since in a rectangular channel  $\frac{V_c^2}{2g} = 0.5y_c$

$$1.5y_c + 0.1y_c = 2.0$$

$$\text{Hence } y_c = 1.25 \text{ m and } \frac{V_c^2}{2g} = 0.625 \text{ m.}$$

$V_c = 3.502$  m/s,  $q = (3.502 \times 1.25) = 4.377$  m<sup>3</sup>/s/m and  $Q = 4.377 \times 3.0 = 13.13$  m<sup>3</sup>/s.

To find normal depth:  $\phi = \frac{13.13 \times 0.015}{(3)^{8/3} \times \sqrt{0.017}} = 0.0807$  From Table 3A.1,  $\frac{y_0}{B} = 0.260$  and  $y_0 = 0.780$  m. The  $S_2$  profile at the inlet is calculated by direct step method and details shown in Table 5.7. it is seen from this table that the normal depth would occur at a distance of about 127 m from the inlet.

**Table 5.7** Computation of Flow Profile by Direct Step Method (Example 5.11)

Rectangular Channel, $B = 3.0$ m			$S_0 = 0.017$	$n = 0.015$	$q = 4.377$ m <sup>3</sup> /s/m					
1	2	3	4	5	6	7	8	9	10	11
Sl. No.	$y$ (m)	$V$ (m/s)	$E$ (m)	$\Delta E$ (m)	$R$ (m)	$S_f$	$\bar{S}_f$	$S_0 - \bar{S}_f$	$\Delta x$ (m)	$x$ (m)
1	1.25	3.502	1.875		0.682	0.00460				0
2	1.10	3.979	1.907	0.0321	0.635	0.00653	0.00556	0.01144	2.8	3
3	0.95	4.607	2.032	0.1250	0.582	0.00984	0.00818	0.00882	14.2	17
4	0.85	5.149	2.202	0.1696	0.543	0.01348	0.01166	0.00534	31.8	49
5	0.79	5.541	2.355	0.1531	0.517	0.01663	0.01505	0.00195	78.7	127

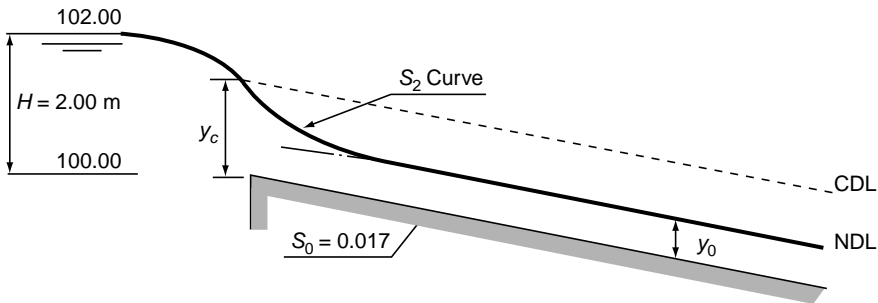


Fig. 5.19 Definition sketch of Example 5.11

## REFERENCES

1. Bakhmeteff, B A, *Hydraulics of Open Channels*, McGraw – Hill, New York, 1932.
2. Chow, V T, 'Integrating the Equation of Gradually Varied Flow', *Proc. ASCE*, Vol. 81, Nov. 1955, pp 1–32.
3. Chow, V T, *Open channel Hydraulics*, McGraw – Hill, New York, 1959.
4. Gill, M A, 'Exact Solutions of Gradually Varied Flow', *J. of Hyd. Div., Proc. ASCE*, Sept. 1976, pp 1353–1364.
5. Subramanya, K and Ramamurthy, A S, 'Flow Profile Computation by Direct Integration', Tech. Note, *J. of Hyd. Div., Proc. ASCE*, Sept. 1974, pp 1306–1311.
6. Keifer, C J and Chu, H H, 'Backwater Function by Numerical Integration', *Trans. ASCE*, Vol. 120, No. 2748, 1955, pp 429–448.
7. Nalluri, C and Tomlinson J H, 'Varied Flow Function for Circular Channels', *J. of Hyd. Div., Proc. ASCE*, July. 1978, pp 983–1000.
8. Subramanya, K, 'Backwater Curves in Rectangular Channels', *Water Power (London)*, Vol. 23, No. 7, July 1971, pp 264.
9. Hydrologic Centre, 'HEC -2 – Water Surface Profile User's Manual', *Hydrologic Centre, US Army Corps of Engrs.*, Oct. 1973.
10. Henderson, F M, *Open Channel Flow*, Macmillan, New York, 1966.
11. Blalock, M E and T M Sturm, 'Minimum Specific Energy in Compound Channels', *J. of Hyd. Div., Proc. ASCE*, Vol. 107, 1981, pp 699–717.
12. Chaudhry, M H and Murthy Bhallamudi S, 'Computation of Critical Depth in Symmetrical Compound Channels', *IAHR, J. of Hyd. Resch.*, Vol. 26, No. 4, 1988, pp 377–395.
13. Petryk, S and Grant E U, 'Critical Flow in rivers in Flood Plains' *J. of Hyd. Div., Proc. ASCE*, Vol. 104, 1978, pp 583–594.
14. Konneman, N, Discussion of Ref. 11, *J. of Hyd. Div., Proc. ASCE*, Vol. 108, 1982, pp 462–464.
15. Apelt, C J, 'Numerical Integration of the Equation of Gradually Varied and Spatially Varied Flow', *Fourth Australasian Conf. on Hydraulics and Fluid Mechanics.*, Nov. 1971, pp 146–153.
16. Humridge, H B and Moss, W D, 'The Development of a Comprehensive Computer Program for the Calculation of Flow in Open Channels', *Proc. Inst. Of Engrs. (London)*, Paper No. 7406, 1972, pp 49–64.
17. Prasad, R, 'Numerical Method of Computing Water Surface Profiles', *J. of Hyd. Div., Proc. ASCE*, Jan. 1970, pp 75–86.
18. Wyile, E B, 'Water Surface Profile in Divided Channels', *IAHR, J. of Hyd. Resch.*, Vol. 10, No. 3, 1972, pp 325–341.

19. Vreugndhil, C B, 'Computation Methods for Channel Flow', Chap. III. *Proc. Of Tech. Meeting 26 Hydraulic Research for Water Management*, Pub. No. 100, The Delft Hyd. Lab., Delft, 1973, pp 38–77.
20. Chaudhry, M H, *Open Channel Flow*, Prentice–Hall, Englewood Cliffs, New Jersey, USA, 1993.

## ? PROBLEMS

### Problem Distribution

Sl. No.	Topic	Problems
1.	Direct integration of GVF – Special cases	5.1 to 5.4
2.	Computation of GVF	
	-by Varied Flow Function	5.5
	-by Bresse's function	5.11, 5.12, 5.12
	-by Keifer and Chu method	5.15
	-Direct step method	5.6, 5.9, 5.13, 5.17, 5.20, 5.22
	-Standard step method	5.16
3.	Simple island flow	5.14
4.	Flow at free inlet	5.22 to 5.66

5.1 Prove that the GVF profile for a horizontal channel can be expressed as

$$x = \left[ -\frac{C_1}{Q^2(N+1)} y^{N+1} + \frac{C_2 y^{N-M+1}}{gC_1(N-M+1)} \right] + \text{Constant}$$

Where  $C_1$  and  $C_2$  are coefficients associated with the hydraulic exponents  $M$  and  $N$  respectively.

5.2 Show that for a horizontal channel, by assuming Chezy  $C = \text{constant}$ , the GVF profile is given by

$$x = \frac{C^2}{g} \left[ y - \frac{y^4}{4y_c^3} \right] + \text{Constant}$$

5.3 Establish that the GVF profile in a frictionless rectangular channel is given by

$$x = \frac{y_0}{S_0} \left[ 1 + \frac{1}{2} \left( \frac{y_c}{y} \right)^3 \right] + \text{Constant}$$

5.4 Show that in a wide rectangular critical slope channel the gradually varied flow profiles calculated by using Chezy formula with  $C = \text{constant}$  are horizontal lines.

- 5.5 A trapezoidal channel having  $B = 6.0$  m, side slope  $m = 2.0$ ,  $S_0 = 0.0016$ , Manning's  $n = 0.02$  carries a discharge of  $12.0$  m<sup>3</sup>/s. Compute and plot the backwater produced due to operation of a sluice gate at a downstream section which backs up the water to a depth of  $4.0$  m immediately behind it. Use Varied flow functions.
- 5.6 Calculate the backwater curve of Problem 5.5 by direct-step method.
- 5.7 A trapezoidal channel  $B = 5.0$  m and  $m = 2.0$  is laid on a slope of  $0.0004$ . If the normal depth of flow is  $3.10$  m, compute: (a) the profile of an  $M_1$  curve in this channel lying between depths of  $5.0$  m and  $3.15$  m, and (b) the profile of an  $M_3$  curve lying between depths of  $0.5$  m and  $1.2$  m. Assume Manning's  $n = 0.02$ .
- 5.8 A rectangular brick-lined channel ( $n = 0.016$ ) of  $4.0$ -m width is laid on a bottom slope of  $0.0009$ . It carries a discharge of  $15$  m<sup>3</sup>/s and the flow is non-uniform. If the depth at a Section A is  $2.6$  m, calculate the depth at section B,  $500$  m downstream of A, by using (a) only one step, and (b) two steps.
- 5.9 A sluice gate discharges a stream of  $0.59$  m depth with a velocity of  $15$  m/s in a wide rectangular channel. The channel is laid on an adverse slope of  $S_0 = -0.002$  and ends with an abrupt drop at a distance of  $100$  m from the gate. Assuming  $n = 0.02$ , calculate and plot the resulting GVF profile.
- 5.10 Figure 5.5 shows the section of a stream with flow in the flood plain. Idealise the section as shown in the figure into three parts with side slopes of  $2 : 1$  and bottom width and depth for parts 1, 2 and 3 as  $15.0$  m,  $5.0$  m;  $10.0$  m,  $1.50$  m;  $15.0$  m and  $2.5$  m respectively. Determine the value of the overall kinetic-energy correction factors  $\alpha$  and the friction slope for a discharge of  $200$  m<sup>3</sup>/s. The values of the kinetic-energy correction factors for the three subsections can be assumed as  $\alpha_1 = 1.20$ ,  $\alpha_2 = 1.05$  and  $\alpha_3 = 1.15$ . Assume  $n = 0.035$  for all the boundaries.
- 5.11 A stream which could be considered as a wide rectangular channel has a slope of  $0.0003$  and Chezy  $C = 40$ . Calculate the backwater profile produced by a weir on the stream which raises the water surface immediately upstream of it by  $4.0$  m when the discharge over the weir is  $3.0$  m<sup>3</sup>/s/m. Use Bresse's back water functions.
- 5.12 Derive Equation (5.13) and verify the values of the coefficients given in the table accompanying the equation.
- 5.13 A  $3$ -m wide rectangular channel laid on a slope of  $0.005$  carries a flow at a normal depth of  $1.20$  m. A sharp-crested rectangular suppressed weir ( $C_d = 0.62$ ) is located with its crest at  $2.0$  m above the channel bottom at the downstream end of the channel. Compute and plot the water surface profile. Assume  $n = 0.02$ .

Path	Width	Slope	Length	$N$
Left	$15.0$ m	$0.0009$	$2000$ m	$0.025$
Right	$10.0$ m	$0.0010$	$1800$ m	$0.030$

- 5.14 A small stream is of rectangular cross section. At a certain section it divides itself, encloses an island and then rejoins to form a single channel again. The properties of the two paths past the island are as follows:  
 At a short distance downstream of the confluence the discharge is found to be  $160$  m<sup>3</sup>/s and depth of flow of  $4.0$  m. Find the discharge in each channel and the depth of flow at the point of division. Neglect the energy loss at the division and at the confluence.
- 5.15 A concrete circular channel ( $n = 0.015$ ) of diameter =  $2.0$  m is laid on a slope of  $0.05$ . This channel is used for emptying a pond. The flow enters the channel as a free inlet from the pond. Compute and plot the water-surface profile for a discharge of  $8.00$  m<sup>3</sup>/s.

Station	Distance up the Stream	Elevation of the Stream Bed (m)	Cross-section
1	50.0 m	100.0	trapezoid: $B = 15.0$ m $m = 1.5$
2	52.0 km	101.0	trapezoid: $B = 14.0$ m $m = 1.5$
3	54.0 km	102.0	trapezoid: $B = 14.00$ m $m = 1.25$
4	56.0 km	103.0	trapezoid: $B = 13.00$ m $m = 1.25$

- 5.16 A stream has the following cross-sectional data:  
For a discharge of  $150 \text{ m}^3/\text{s}$ , the depth of flow of the downstream-most Section 1 is 5.10 m. Assume  $n = 0.025$ . Using the standard-step method, compute the water-surface elevations at Sections 2, 3 and 4. (Assume gradual transition).
- 5.17 A trapezoidal channel,  $B = 4.5$  m,  $m = 0.5$  and  $n = 0.020$ , has  $S_0 = 0.01$ . There is a break in grade to the horizontal at a section. The depth of flow at the junction is 3.0 m when the discharge is  $30.0 \text{ m}^3/\text{s}$ . Sketch the resulting water-surface profile on the sloping channel.
- 5.18 A rectangular channel of 6.0 m width carries a discharge of  $8.40 \text{ m}^3/\text{s}$ . The channel slope is 0.0004 and the Manning's  $n = 0.015$ . At the head of the channel the flow emanates from the sluice gate. The depth of flow at the vena contracta is 0.15 m. If the hydraulic jump is formed at a depth of 0.25 m, find the distance between the toe of the jump and the vena contracta.
- 5.19 A trapezoidal channel  $B = 4.50$  m,  $m = 1.0$ ,  $n = 0.03$  has a bed slope of  $S_0 = 0.003$ . The channel ends in a sudden drop. Calculate the GVF profile for a discharge of  $25.0 \text{ m}^3/\text{s}$ .
- 5.20 A trapezoidal channel  $B = 7.5$  m,  $m = 1.5$  and  $n = 0.025$  is laid on a slope of 0.0004. When the discharge is  $20.0 \text{ m}^3/\text{s}$ , a low weir at a downstream location creates a pool of depth 3.00 m just upstream of it. Calculate the length of the backwater and also the depth at a section 1.0 km upstream of the weir.
- 5.21 A wide rectangular channel of slope 0.0005 connects two reservoirs 20 km apart. The upstream reservoir level can be considered to be constant and the downstream reservoir elevation is variable. The elevation of the canal invert at the intake is 200.00 m. The intake is free and the normal depth and the uniform flow discharge intensity in the canal are 2.00 m and  $4.0 \text{ m}^3/\text{s}/\text{m}$  width respectively. If the downstream reservoir level reaches 192.40 m, will it affect the uniform flow discharge in the channel? (Use Bresse's function).
- 5.22 A wide rectangular channel with a bed slope of 0.015 takes off from a reservoir. The inlet to the channel is free and the discharge intensity is  $3.00 \text{ m}^3/\text{s}/\text{m}$ . Calculate the GVF profile from the inlet to the section where the depth is 1% excess of the normal depth. Assume Manning's coefficient  $n = 0.015$ .
- 5.23 A rectangular channel,  $B = 4.0$  m and  $n = 0.015$ , is laid on a slope of 0.0004. The channel is 500-m long and connects two reservoirs. The bed of the channel at the intake is at an elevation of 120.0 m. The intake is free and has a loss coefficient of 0.2 (a). If uniform flow takes place at a depth of 2.0 m, what are the elevations of the upstream and downstream reservoirs? (b) If the elevation of the upstream reservoir is held constant and the downstream reservoir elevation is lowered by 1.0 m, what is the delivery of the channel?
- 5.24 A 6.0-m wide rectangular channel has  $n = 0.012$  and  $S_0 = 0.006$ . The canal takes off from a reservoir through an uncontrolled smooth inlet. If the elevation of the water surface is 2.10 m above the channel bed, estimate the discharge in the channel and the minimum

distance from the inlet at which the flow can be considered to be uniform. Neglect energy losses at the entrance to the channel.

- 5.25 Write an algorithm for computing the discharge in a trapezoidal channel taking off from a reservoir, given  $S_0$ ,  $n$ ,  $B$ ,  $m$  and  $H$ , where  $H$  = reservoir elevation above the channel invert at the upstream end. The channel-entrance losses can be neglected.
- 5.26 A trapezoidal channel  $B = 3.0$  m,  $m = 1.50$ ,  $n = 0.025$  and  $S_0 = 0.00050$  takes off from a reservoir with free inlet. The reservoir elevation is 7.0 m above the channel bed at the inlet. Calculate the discharge in the channel by neglecting entrance losses.

## OBJECTIVE QUESTIONS

- 5.1 Bresse's backwater function corresponds to the indicated set of  $(M, N)$  values:
- (a) (3,2) (b)  $\left(3\frac{1}{3}, 3\frac{1}{3}\right)$   
 (c)  $\left(3, 3\frac{1}{3}\right)$  (d) (3,3)
- 5.2 The solution of the differential equation of GVF by Chow's method, involves the use of varied flow function  $F(u, N) =$
- (a)  $\int_0^u \frac{du}{1+u^N}$  (b)  $\int_0^u (1-u^N) du$   
 (c)  $\int_0^u \frac{udu}{1-u^N}$  (d)  $\int_0^u \frac{du}{1-u^N}$
- 5.3 The Keifer and Chu varied-flow functions are useful for GVF computations in
- (a) all types of channels (b) channels with closing top  
 (c) circular channels only (d) rectangular channels only
- 5.4 The Kutta-Merson method of solving the GVF differential equation involves
- (a) evaluation of the function four times for each step  
 (b) evaluation of the function five times for each step  
 (c) three evaluations of the function per step  
 (d) iteration procedure
- 5.5 The standard-step method aims to solve
- (a) the differential equation of GVF  
 (b) the differential-energy equation of GVF  
 (c) the Bernoulli equation  
 (d) the momentum equation
- 5.6 The trapezoidal method (TRAP) of numerical integration of GVF involves
- (a) direct solution involving evaluation of the function four times  
 (b) iterative procedure  
 (c) Simpson's rule  
 (d) Graphical procedure
- 5.7 Bresse's backwater function is applicable to
- (a) Circular channels  
 (b) Trapezoidal channels  
 (c) Any shape of channel  
 (d) Wide rectangular channel
- 5.8 The direct-step method of calculating the GVF profile uses the relation
- (a)  $\Delta E = \Delta x (S_0 - S_f)$  (b)  $\Delta x = \Delta E / (S_0 - S_f)$   
 (c)  $\Delta x = \Delta E (S_0 - S_f)$  (d)  $\Delta y = \Delta x (S_0 - S_f) / (1 - F^2)$

- 5.9 In the direct-step method and standard-step methods, the calculations
- must proceed upstream in subcritical flow
  - must end on a control section
  - must always proceed upstream
  - must proceed upstream in supercritical flow
- 5.10 The direct-step method
- is best-suited for natural channels
  - is accurate for all step sizes
  - is most accurate for calculating supercritical flow profiles
  - is none of these
- 5.11 The standard-step method is
- an unguided trial-and-error method
  - a rapidly-converging iterative procedure
  - not applicable to natural channels
  - not applicable to artificial channels
- 5.11 In a compound section the slope of the common energy line  $S_f$  is
- |   |   |
|---|---|
| (a) $\frac{Q^2}{\sum K_i^2 / A^2}$        | (b) $\frac{Q^2}{(\sum K_i)^2}$                        |
| (c) $\frac{\sum Q_i^2}{\sum K_i^2 / A^2}$ | (d) $\frac{\sum (K_i^3 / A_i^2)}{(\sum K_i)^3 / A^2}$ |
- 5.12 The standard Runge-Kutta method for solving GVF profiles is
- an iterative procedure
  - not rapidly converging
  - dependent on the nature of the profile
  - independent of the direction of computation
- 5.14 In a simple island-type divided channel of rectangular cross-section, the discharge division
- is judged by common sense
  - is inversely proportional to Manning's  $n$
  - is to be found by iterative GVF calculations
  - has no fixed value
- 5.15 For an uncontrolled canal inlet at a reservoir, the discharge drawn
- is fixed by the critical depth that occurs at the inlet
  - is determined by a control on the downstream end
  - depends on whether the channel is steep or otherwise
  - is a constant
- 5.16 A mild channel connecting two reservoirs is called a *short channel* if
- the discharge varies with the downstream-pool elevation
  - the channel is on a steep slope
  - the channel is frictionless
  - some  $M_2$  curves extend all the way up to the reservoir
- 5.17 A mild slope channel enters a lake with a sudden drop in its bed. If the depth of water in the lake measured above the channel bed at its outlet  $y_L$  is greater than the critical depth, then the depth of flow in the canal at the outlet  $y_d$
- |                                   |             |
|-----------------------------------|-------------|
| (a) $= y_L$                       | (b) $= y_c$ |
| (c) $= \text{normal depth} = y_0$ | (d) $< y_0$ |
- 5.18 A compound section as in Fig. 5.19 may have a maximum of
- one critical depth
  - two critical depths
  - three critical depths
  - four critical depths



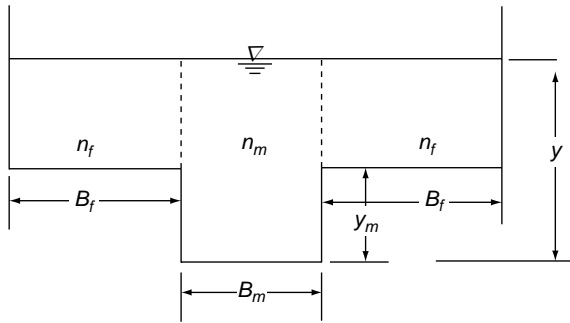


Fig. 5.19 Symmetrical compound section



## APPENDIX 5A

This appendix contains the varied-flow functions and the Keifer and Chu functions.

1. Tables 5A.1 contains the varied-flow functions  $F(u, N) = \int_0^u \frac{du}{1-u^N}$  for a few values of  $N$ .

This table is reproduced by permission of the American Society of Civil Engineers and contains material from Chow, V T, 'Integrating the equations of gradually varied-flow' *Proc. ASCE*, Vol. 81, Paper No. 838, pp. 1-32, Nov. 1955.

2. Tables 5A.2(a) and 5A.2(b) contain the Keifer and Chu functions  $I_1(Q_r, \theta/\pi)$  and  $I_2(Q_r, \theta/\pi)$  respectively. These functions are for the use of GVF computations in circular channels through the use of Eq. (5.28). In these tables  $2\theta =$  angle subtended by the water surface at the centre of the channel and  $\theta$  is related to the depth  $y$  by the relation

$$y/D = \frac{1}{2}(1 - \cos \theta)$$

Values of  $2\theta$  for different  $y/D$  values are available in Table 2A.1.

$Q_r$  is the discharge ratio given by Eq. (5.24). Tables 5A.2(a) and 5A.2(b) are the adopted versions of original tables supplied to the author for publication through the courtesy of Dr Chandra Nalluri, University of New Castle-upon-Tyne, New Castle-upon Tyne, England. The step lines in the tables indicate the barriers for interpolation representing the location of normal depth.

Appendix – 5A

Table 5A.1 Varied Flow Function  $F(u, N)$

$u/N$	2.6	2.8	3.0	3.2	3.4	3.6	3.8	4.0	4.2	4.6	5.0
0.00	0.000	0.000	0.000	0.000	0.000	0.000	0.000	0.000	0.000	0.000	0.000
0.02	0.020	0.020	0.020	0.020	0.020	0.020	0.020	0.020	0.020	0.020	0.020
0.04	0.040	0.040	0.040	0.040	0.040	0.040	0.040	0.040	0.040	0.040	0.040
0.06	0.060	0.060	0.060	0.060	0.060	0.060	0.060	0.060	0.060	0.060	0.060
0.08	0.080	0.080	0.080	0.080	0.080	0.080	0.080	0.080	0.080	0.080	0.080
0.10	0.100	0.100	0.100	0.100	0.100	0.100	0.100	0.100	0.100	0.100	0.100
0.12	0.120	0.120	0.120	0.120	0.120	0.120	0.120	0.120	0.120	0.120	0.120
0.14	0.140	0.140	0.140	0.140	0.140	0.140	0.140	0.140	0.140	0.140	0.140
0.16	0.160	0.160	0.160	0.160	0.160	0.160	0.160	0.160	0.160	0.160	0.160
0.18	0.181	0.180	0.180	0.180	0.180	0.180	0.180	0.180	0.180	0.180	0.180
0.20	0.201	0.200	0.200	0.201	0.200	0.200	0.200	0.200	0.200	0.200	0.200
0.22	0.221	0.221	0.221	0.220	0.220	0.220	0.220	0.220	0.220	0.220	0.220
0.24	0.242	0.241	0.240	0.240	0.240	0.240	0.240	0.240	0.240	0.240	0.240
0.26	0.262	0.262	0.261	0.261	0.261	0.260	0.260	0.260	0.260	0.260	0.260
0.28	0.283	0.282	0.282	0.281	0.281	0.281	0.280	0.280	0.280	0.280	0.280
0.30	0.304	0.303	0.302	0.302	0.301	0.301	0.300	0.300	0.300	0.300	0.300
0.32	0.325	0.324	0.323	0.322	0.322	0.321	0.321	0.321	0.321	0.320	0.320
0.34	0.346	0.344	0.343	0.343	0.342	0.342	0.341	0.341	0.341	0.340	0.340
0.36	0.367	0.366	0.364	0.363	0.363	0.362	0.362	0.361	0.361	0.361	0.360
0.38	0.389	0.387	0.385	0.384	0.383	0.383	0.382	0.382	0.381	0.381	0.381
0.40	0.411	0.408	0.407	0.405	0.404	0.403	0.403	0.402	0.402	0.401	0.401
0.42	0.433	0.430	0.428	0.426	0.425	0.424	0.423	0.423	0.422	0.421	0.421
0.44	0.456	0.452	0.450	0.448	0.446	0.445	0.444	0.443	0.443	0.442	0.441
0.46	0.479	0.475	0.472	0.470	0.468	0.466	0.465	0.464	0.463	0.462	0.462
0.48	0.502	0.497	0.494	0.492	0.489	0.488	0.486	0.485	0.484	0.483	0.482
0.50	0.525	0.521	0.517	0.514	0.511	0.509	0.508	0.506	0.505	0.504	0.503
0.52	0.550	0.544	0.540	0.536	0.534	0.531	0.529	0.528	0.527	0.525	0.523
0.54	0.574	0.568	0.563	0.559	0.556	0.554	0.551	0.550	0.548	0.546	0.544
0.56	0.599	0.593	0.587	0.583	0.579	0.576	0.574	0.572	0.570	0.567	0.565
0.58	0.626	0.618	0.612	0.607	0.603	0.599	0.596	0.594	0.592	0.589	0.587
0.60	0.653	0.644	0.637	0.631	0.627	0.623	0.620	0.617	0.614	0.611	0.608
0.61	0.667	0.657	0.650	0.644	0.639	0.635	0.631	0.628	0.626	0.622	0.619
0.62	0.680	0.671	0.663	0.657	0.651	0.647	0.643	0.640	0.637	0.633	0.630
0.63	0.694	0.684	0.676	0.669	0.664	0.659	0.655	0.652	0.649	0.644	0.641
0.64	0.709	0.693	0.690	0.683	0.677	0.672	0.667	0.664	0.661	0.656	0.652
0.65	0.724	0.712	0.703	0.696	0.689	0.684	0.680	0.676	0.673	0.667	0.663
0.66	0.738	0.727	0.717	0.709	0.703	0.697	0.692	0.688	0.685	0.679	0.675
0.67	0.754	0.742	0.731	0.723	0.716	0.710	0.705	0.701	0.697	0.691	0.686
0.68	0.769	0.757	0.746	0.737	0.729	0.723	0.718	0.713	0.709	0.703	0.698
0.69	0.785	0.772	0.761	0.751	0.743	0.737	0.731	0.726	0.722	0.715	0.710
0.70	0.802	0.787	0.776	0.766	0.757	0.750	0.744	0.739	0.735	0.727	0.722
0.71	0.819	0.804	0.791	0.781	0.772	0.764	0.758	0.752	0.748	0.740	0.734
0.72	0.836	0.820	0.807	0.796	0.786	0.779	0.772	0.766	0.761	0.752	0.746
0.73	0.854	0.837	0.823	0.811	0.802	0.793	0.786	0.780	0.774	0.765	0.759
0.74	0.868	0.854	0.840	0.827	0.817	0.808	0.800	0.794	0.788	0.779	0.771

(Continued)



Table 5A.1 Varied Flow Function  $F(u, N)$

$u/N$	2.6	2.8	3.0	3.2	3.4	3.6	3.8	4.0	4.2	4.6	5.0
1.18	0.694	0.591	0.509	0.443	0.388	0.343	0.305	0.272	0.244	0.199	0.165
1.19	0.676	0.574	0.494	0.429	0.375	0.331	0.294	0.262	0.235	0.191	0.157
1.20	0.659	0.559	0.480	0.416	0.363	0.320	0.283	0.252	0.226	0.183	0.150
1.22	0.628	0.531	0.454	0.392	0.341	0.299	0.264	0.235	0.209	0.168	0.138
1.24	0.600	0.505	0.431	0.371	0.322	0.281	0.248	0.219	0.195	0.156	0.127
1.26	0.574	0.482	0.410	0.351	0.304	0.265	0.233	0.205	0.182	0.145	0.117
1.28	0.551	0.461	0.391	0.334	0.288	0.250	0.219	0.193	0.170	0.135	0.108
1.30	0.530	0.442	0.373	0.318	0.274	0.237	0.207	0.181	0.160	0.126	0.100
1.32	0.510	0.424	0.357	0.304	0.260	0.225	0.196	0.171	0.150	0.118	0.093
1.34	0.492	0.408	0.342	0.290	0.248	0.214	0.185	0.162	0.142	0.110	0.087
1.36	0.475	0.393	0.329	0.278	0.237	0.204	0.176	0.153	0.134	0.103	0.081
1.38	0.459	0.378	0.316	0.266	0.226	0.194	0.167	0.145	0.127	0.097	0.076
1.40	0.444	0.365	0.304	0.256	0.217	0.185	0.159	0.138	0.120	0.092	0.071
1.42	0.431	0.353	0.293	0.246	0.208	0.177	0.152	0.131	0.114	0.087	0.067
1.44	0.417	0.341	0.282	0.236	0.199	0.169	0.145	0.125	0.108	0.082	0.063
1.46	0.405	0.330	0.273	0.227	0.191	0.162	0.139	0.119	0.103	0.077	0.059
1.48	0.394	0.320	0.263	0.219	0.184	0.156	0.133	0.113	0.098	0.073	0.056
1.50	0.383	0.310	0.255	0.211	0.177	0.149	0.127	0.108	0.093	0.069	0.053
1.55	0.358	0.288	0.235	0.194	0.161	0.135	0.114	0.097	0.083	0.061	0.046
1.60	0.335	0.269	0.218	0.179	0.148	0.123	0.103	0.087	0.074	0.054	0.040
1.65	0.316	0.251	0.203	0.165	0.136	0.113	0.094	0.079	0.067	0.048	0.035
1.70	0.298	0.236	0.189	0.153	0.125	0.103	0.086	0.072	0.060	0.043	0.031
1.75	0.282	0.222	0.177	0.143	0.116	0.095	0.079	0.065	0.054	0.038	0.027
1.80	0.267	0.209	0.166	0.133	0.108	0.088	0.072	0.060	0.049	0.034	0.024
1.85	0.254	0.198	0.156	0.125	0.100	0.082	0.067	0.055	0.045	0.031	0.022
1.90	0.242	0.188	0.147	0.117	0.094	0.076	0.062	0.050	0.041	0.028	0.020
1.95	0.231	0.178	0.139	0.110	0.088	0.070	0.057	0.046	0.038	0.026	0.018
2.00	0.221	0.169	0.132	0.104	0.082	0.066	0.053	0.043	0.035	0.023	0.016
2.10	0.202	0.154	0.119	0.092	0.073	0.058	0.046	0.037	0.030	0.019	0.013
2.20	0.186	0.141	0.107	0.083	0.065	0.051	0.040	0.032	0.025	0.016	0.011
2.3	0.173	0.129	0.098	0.075	0.058	0.045	0.035	0.028	0.022	0.014	0.009
2.4	0.160	0.119	0.089	0.068	0.052	0.040	0.031	0.024	0.019	0.012	0.008
2.5	0.150	0.110	0.082	0.062	0.047	0.036	0.028	0.022	0.017	0.010	0.006
2.6	0.140	0.102	0.076	0.057	0.043	0.033	0.025	0.019	0.015	0.009	0.005
2.7	0.131	0.095	0.070	0.052	0.039	0.029	0.022	0.017	0.013	0.008	0.005
2.8	0.124	0.089	0.065	0.048	0.036	0.027	0.020	0.015	0.012	0.007	0.004
2.9	0.117	0.083	0.060	0.044	0.033	0.024	0.018	0.014	0.010	0.006	0.004
3.0	0.110	0.078	0.056	0.041	0.030	0.022	0.017	0.012	0.009	0.005	0.003
3.5	0.085	0.059	0.041	0.029	0.021	0.015	0.011	0.008	0.006	0.003	0.002
4.0	0.069	0.046	0.031	0.022	0.015	0.010	0.007	0.005	0.004	0.002	0.001
4.5	0.057	0.037	0.025	0.017	0.011	0.008	0.005	0.004	0.003	0.001	0.001
5.0	0.048	0.031	0.020	0.013	0.009	0.006	0.004	0.003	0.002	0.001	0.000
6.0	0.036	0.022	0.014	0.009	0.006	0.004	0.002	0.002	0.001	0.000	0.000
7.0	0.028	0.017	0.010	0.006	0.004	0.002	0.002	0.001	0.001	0.000	0.000
8.0	0.022	0.013	0.008	0.005	0.003	0.002	0.001	0.001	0.000	0.000	0.000
9.0	0.019	0.011	0.006	0.004	0.002	0.001	0.001	0.000	0.000	0.000	0.000
10.0	0.016	0.009	0.005	0.003	0.002	0.001	0.001	0.000	0.000	0.000	0.000
20.0	0.011	0.006	0.002	0.001	0.001	0.000	0.000	0.000	0.000	0.000	0.000



**Table 5A. 2(a)** (Continued) **Keifer and Chu Function  $I_e$**

$\theta/\pi Q$	1.00	1.07	1.10	1.20	1.30	1.40	1.50	1.60
0.69	0.6146	0.3772	0.3263	0.2251	0.1702	0.1353	0.1111	0.0933
0.68	0.6146	0.3772	0.3263	0.2251	0.1702	0.1353	0.1111	0.0933
0.67	0.6146	0.3772	0.3263	0.2251	0.1702	0.1353	0.1111	0.0933
0.66	0.6146	0.3772	0.3263	0.2251	0.1702	0.1353	0.1111	0.0933
0.65	0.6146	0.3772	0.3263	0.2251	0.1702	0.1353	0.1111	0.0933
0.64	0.6146	0.3772	0.3263	0.2251	0.1702	0.1353	0.1111	0.0933
0.63	0.6146	0.3772	0.3263	0.2251	0.1702	0.1353	0.1111	0.0933
0.62	0.6146	0.3772	0.3263	0.2251	0.1702	0.1353	0.1111	0.0933
0.61	0.6146	0.3772	0.3263	0.2251	0.1702	0.1353	0.1111	0.0933
0.60	0.6146	0.3772	0.3263	0.2251	0.1702	0.1353	0.1111	0.0933
0.59	0.6146	0.3772	0.3263	0.2251	0.1702	0.1353	0.1111	0.0933
0.58	0.6146	0.3772	0.3263	0.2251	0.1702	0.1353	0.1111	0.0933
0.57	0.6146	0.3772	0.3263	0.2251	0.1702	0.1353	0.1111	0.0933
0.56	0.6146	0.3772	0.3263	0.2251	0.1702	0.1353	0.1111	0.0933
0.55	0.6146	0.3772	0.3263	0.2251	0.1702	0.1353	0.1111	0.0933
0.54	0.6146	0.3772	0.3263	0.2251	0.1702	0.1353	0.1111	0.0933
0.53	0.6146	0.3772	0.3263	0.2251	0.1702	0.1353	0.1111	0.0933
0.52	0.6146	0.3772	0.3263	0.2251	0.1702	0.1353	0.1111	0.0933
0.51	0.6146	0.3772	0.3263	0.2251	0.1702	0.1353	0.1111	0.0933
0.50	0.6146	0.3772	0.3263	0.2251	0.1702	0.1353	0.1111	0.0933
0.49	0.6146	0.3772	0.3263	0.2251	0.1702	0.1353	0.1111	0.0933
0.48	0.6146	0.3772	0.3263	0.2251	0.1702	0.1353	0.1111	0.0933
0.47	0.6146	0.3772	0.3263	0.2251	0.1702	0.1353	0.1111	0.0933
0.46	0.6146	0.3772	0.3263	0.2251	0.1702	0.1353	0.1111	0.0933
0.45	0.6146	0.3772	0.3263	0.2251	0.1702	0.1353	0.1111	0.0933
0.44	0.6146	0.3772	0.3263	0.2251	0.1702	0.1353	0.1111	0.0933
0.43	0.6146	0.3772	0.3263	0.2251	0.1702	0.1353	0.1111	0.0933
0.42	0.6146	0.3772	0.3263	0.2251	0.1702	0.1353	0.1111	0.0933
0.41	0.6146	0.3772	0.3263	0.2251	0.1702	0.1353	0.1111	0.0933
0.40	0.6146	0.3772	0.3263	0.2251	0.1702	0.1353	0.1111	0.0933
0.39	0.6146	0.3772	0.3263	0.2251	0.1702	0.1353	0.1111	0.0933
0.38	0.6146	0.3772	0.3263	0.2251	0.1702	0.1353	0.1111	0.0933

(Continued)







**Table 5A. 2(b) (Continued)** **Keifer and Chu Function  $I_2$**

$\theta/\pi \leq I_1$	0.10	0.20	0.30	0.40	0.50	0.60	0.70	0.80	0.90	1.00	1.07	1.10	1.20	1.30	1.40	1.50	1.60
0.69	0.3456	0.3584	0.3712	0.4096	0.4480	0.5248	0.6528	0.8960	1.6384	4.9408	3.6992	3.3664	2.6112	2.1248	1.7664	1.5104	1.3056
0.68	0.3840	0.3968	0.4224	0.4480	0.5120	0.5888	0.7296	1.0368	2.0608	4.6080	3.5584	3.2640	2.5472	2.0736	1.7408	1.4848	1.2800
0.67	0.4352	0.4480	0.4736	0.5120	0.5632	0.6656	0.8320	1.2032	2.8416	4.3392	3.4304	3.1488	2.4832	2.0352	1.7024	1.4584	1.2544
0.66	0.4736	0.4992	0.5248	0.5632	0.6400	0.7552	0.9472	1.4208	1.10976	4.1216	3.3024	3.0464	2.4192	1.9840	1.6640	1.4208	1.2288
0.65	0.5336	0.5504	0.5760	0.6272	0.7168	0.8448	1.0880	1.6896	6.4256	3.9296	3.1872	2.9568	2.3552	1.9456	1.6384	1.3952	1.2160
0.64	0.5888	0.6144	0.6400	0.7040	0.7936	0.9600	1.2544	2.0736	5.6320	3.7504	3.0848	2.8544	2.2912	1.8944	1.6000	1.3606	1.1904
0.63	0.6528	0.6784	0.7168	0.7808	0.8960	1.0752	1.4592	2.6752	5.1584	3.5968	2.9824	2.7648	2.2272	1.8432	1.5616	1.3440	1.1648
0.62	0.7296	0.7552	0.7936	0.8704	0.9984	1.2288	1.7024	4.0448	4.8000	3.4432	2.8800	2.6752	2.1760	1.8048	1.5232	1.3056	1.1392
0.61	0.8064	0.8320	0.8832	0.9728	1.1264	1.3952	2.0224	8.1792	4.5056	3.3152	2.7776	2.5984	2.1120	1.7536	1.4848	1.2900	1.1136
0.60	0.8832	0.9216	0.9856	1.0880	1.2672	1.6128	2.4832	6.6944	4.2624	3.1872	2.6880	2.5088	2.0480	1.7152	1.4464	1.2544	1.0880
0.59	0.9856	1.0240	1.0880	1.2160	1.4336	1.8688	3.2000	5.9904	4.0576	3.0592	2.5984	2.4320	1.9840	1.6640	1.4080	1.2160	1.0624
0.58	1.0880	1.1264	1.2160	1.3696	1.6256	2.1888	4.8000	8.6656	3.8656	2.9440	2.5088	2.3552	1.9328	1.6128	1.3824	1.1904	1.0368
0.57	1.2032	1.2544	1.3568	1.5360	1.8688	2.6112	9.5104	5.1328	3.6864	2.8416	2.4192	2.2784	1.8688	1.5744	1.3440	1.1520	1.0112
0.56	1.3312	1.3952	1.5104	1.7280	2.1376	3.2256	7.7184	4.8256	3.5328	2.7392	2.3424	2.2016	1.8176	1.5232	1.3056	1.1264	0.9856
0.55	1.4720	1.5488	1.6896	1.9584	2.4832	4.2368	6.8736	4.5568	3.3792	2.6368	2.2656	2.1248	1.7536	1.4720	1.2672	1.0880	0.9600
0.54	1.6256	1.7152	1.8944	2.2144	2.9312	7.1424	6.2976	4.3264	3.2384	2.5344	2.1888	2.0484	1.7024	1.4336	1.2288	1.0624	0.9216
0.53	1.8048	1.9200	2.1248	2.5344	3.5328	10.6624	5.8496	4.1088	3.0976	2.4448	2.0992	1.9840	1.6384	1.3824	1.1904	1.0240	0.8960
0.52	2.0096	2.1376	2.3936	2.9184	4.4160	8.9344	5.4784	3.9168	2.9696	2.3552	2.0352	1.9072	1.5872	1.3440	1.1520	0.9084	0.8704
0.51	2.2400	2.3936	2.7136	3.4048	6.0032	7.9872	5.1584	3.7248	2.8554	2.2656	1.9584	1.8432	1.5360	1.2928	1.1136	0.9600	0.8448
0.50	2.4832	2.6752	3.0848	4.0320	399.6288	7.3088	4.8768	3.5584	2.7392	2.1760	1.8816	1.7792	1.4720	1.2544	1.0752	0.9344	0.8192
0.49	2.7776	3.0080	3.5328	4.8896	12.5056	6.7840	4.6080	3.3920	2.6240	2.0864	1.8048	1.7024	1.4208	1.2032	1.0368	0.8960	0.7808
0.48	3.0976	3.3920	4.0704	6.1824	10.7136	6.3360	4.3776	3.2384	2.5088	2.0096	1.7408	1.6384	1.3696	1.1648	1.0084	0.8704	0.7552
0.47	3.4816	3.8400	4.7488	8.6528	9.6128	5.9392	4.1600	3.0976	2.4064	1.9200	1.6640	1.5744	1.3184	1.1136	0.9600	0.8320	0.7296
0.46	3.9040	4.3776	5.6820	23.4496	8.7936	5.9392	3.9424	2.9568	2.3040	1.8432	1.6000	1.5104	1.2672	1.0752	0.9216	0.8064	0.7040
0.45	4.4032	3.0048	8.2224	16.0256	8.1408	5.2736	3.7504	2.8160	2.2016	1.7664	1.5360	1.4464	1.2160	1.0240	0.8832	0.7680	0.6784
0.44	4.9664	5.7728	8.6016	13.7856	7.5776	4.9920	3.5584	2.6880	2.0992	1.6896	1.4720	1.3824	1.1648	0.9856	0.8448	0.7424	0.6528
0.43	5.6320	6.7072	11.8016	12.3520	7.0912	4.7104	3.3792	2.5600	1.9968	1.6128	1.3952	1.3184	1.1136	0.9472	0.8064	0.7040	0.6144
0.42	6.4128	7.9104	15.61984	11.2768	6.6432	4.4544	3.2128	2.4320	1.9072	1.5360	1.3312	1.2672	1.0624	0.8960	0.7808	0.6784	0.5888
0.41	7.3344	9.4720	23.9232	10.3936	6.2336	4.2112	3.0464	2.3040	1.8176	1.4592	1.2672	1.2032	1.0112	0.8576	0.7424	0.6400	0.5632
0.40	8.4352	11.6352	20.1600	9.6256	5.8624	3.9808	2.8800	2.1888	1.7152	1.3824	1.2160	1.1392	0.9600	0.8192	0.7040	0.6144	0.5376
0.39	9.7536	14.9376	17.8688	8.9600	5.5040	3.7504	2.7264	2.0736	1.6256	1.1520	1.1520	1.0880	0.9088	0.7808	0.6656	0.5760	0.5210
0.38	11.3792	21.2224	16.1536	8.3456	5.1712	3.5456	2.5728	1.9584	1.5488	1.2416	1.0880	1.0240	0.8576	0.7296	0.6272	0.5504	0.4864
0.37	13.3760	61.7856	14.7584	7.7824	4.8640	3.3280	2.4320	1.8560	1.4592	1.1776	1.0240	0.9728	0.8192	0.6912	0.6016	0.5248	0.4608
0.36	15.9104	39.1680	13.5680	7.2704	4.5568	3.1360	2.2912	1.7408	1.3696	1.1136	0.9728	0.9216	0.7680	0.6528	0.5632	0.4864	0.4352
0.35	19.2256	33.0112	12.5184	6.7840	4.2752	2.9440	2.1504	1.6384	1.2928	1.0496	0.9088	0.8704	0.7296	0.6144	0.5376	0.4608	0.4096

(Continued)



# Rapidly Varied Flow-1 —Hydraulic Jump

## 6

### 6.1 INTRODUCTION

Hydraulic jump is one subject which has extensively been studied in the field of hydraulic engineering. It is an intriguing and interesting phenomenon that has caught the imagination of many research workers since its first description by Leonardo da Vinci. The Italian engineer Bidone (1818) is credited with the first experimental investigation of this phenomenon. Since then considerable research effort has gone into the study of this subject. The literature on this topic is vast and ever-expanding. The main reason for such continued interest in this topic is its immense practical utility in hydraulic engineering and allied fields. A hydraulic jump primarily serves as an energy dissipator to dissipate the excess energy of flowing water downstream of hydraulic structures, such as spillways and sluice gates. Some of the other uses are: (a) efficient operation of flow-measurement flumes, (b) mixing of chemicals, (c) to aid intense mixing and gas transfer in chemical processes, (d) in the desalination of sea water, and (e) in the aeration of streams which are polluted by bio-degradable wastes.

A hydraulic jump occurs when a supercritical stream meets a subcritical stream of sufficient depth. The supercritical stream jumps up to meet its alternate depth. While doing so it generates considerable disturbances in the form of large-scale eddies and a reverse flow roller with the result that the jump falls short of its alternate depth. Figure 6.1 is a schematic sketch of a typical hydraulic jump in a horizontal channel. Section 1, where the incoming supercritical stream undergoes an abrupt rise in the depth forming the commencement of the jump, is called the toe of the jump. The jump proper consists of a steep change in the water-surface elevation with a reverse flow roller on the major part. The roller entrains considerable quantity of air and the surface has white, frothy and choppy appearance. The jump, while essentially steady, will normally oscillate about a mean position in the longitudinal direction and the surface will be uneven. Section 2, which lies beyond the roller and with an essentially level water surface is called the end of the jump and the distance between Sections 1 and 2 is the length of the jump,  $L_j$ . The initial depth of the supercritical stream is  $y_1$  and  $y_2$  is the final depth, after the jump, of the subcritical stream. As indicated earlier,  $y_2$  will be smaller than the depth alternate to  $y_1$ . The two depths  $y_1$  and  $y_2$  at the ends of the jump are called *sequent depths*. Due to high turbulence and shear action of the roller, there is considerable loss of energy in the jump between Sections 1 and 2. In view of the high energy loss, the nature of which is difficult to estimate,

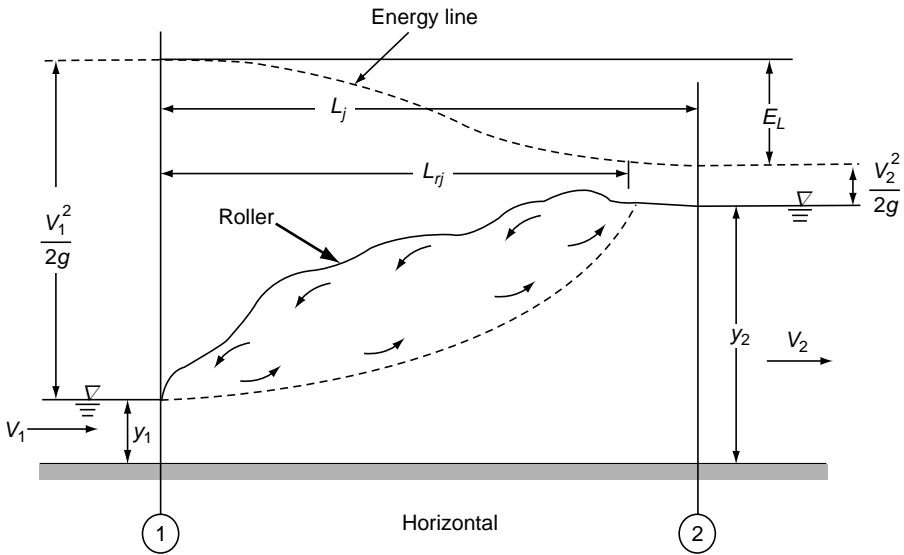


Fig. 6.1 Definition sketch of a hydraulic jump

the energy equation cannot be applied to Sections 1 and 2 to relate the various flow parameters. In such situations, the use of the momentum equation with suitable assumptions is advocated. In fact, the hydraulic jump is a typical example where a judicious use of the momentum equation yields meaningful results.

## 6.2 THE MOMENTUM EQUATION FORMULATION FOR THE JUMP

The definition sketch of a hydraulic jump in a prismatic channel of arbitrary shape is presented in Fig. 6.2. The channel is inclined to the horizontal at an angle  $\theta$ . Sections 1 and 2 refer to the beginning and end of the jump respectively.

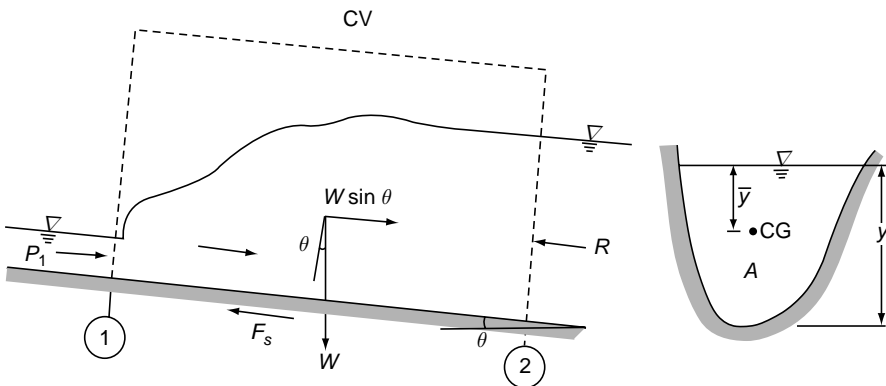


Fig. 6.2 Definition sketch for the general momentum equation

A control volume enclosing the jump as shown by dashed lines in the figure, is selected. The flow is considered to be steady.

Applying the linear momentum equation in the longitudinal direction to the control volume,

$$P_1 - P_2 - F_s + W \sin \theta = M_2 - M_1 \quad (6.1)$$

where  $P_1$  = pressure force at the control surface at Section 1 =  $\gamma A_1 \bar{y}_1 \cos \theta$  by assuming hydrostatic pressure distribution, where  $\bar{y}_1$  = depth of the centroid of the area below the water surface.

$P_2$  = pressure force at the control surface at Section 2 =  $\gamma A_2 \bar{y}_2 \cos \theta$  if hydrostatic pressure distribution is assumed.

(Note that  $P \approx \gamma A \bar{y}$  if  $\theta$  is small.)

$F_s$  = shear force on the control surface adjacent to the channel boundary.

$W \sin \theta$  = longitudinal component of the weight of water contained in the control volume.

$M_2$  = momentum flux in the longitudinal direction going out through the control surface =  $\beta_2 \rho Q V_2$ .

$M_1$  = momentum flux in the longitudinal direction going in through the control surface =  $\beta_1 \rho Q V_1$ .

The hydraulic jump is a rapidly-varied flow phenomenon and the length of the jump is relatively small compared to GVF profiles. Thus frictional force  $F_s$  is usually neglected as it is of secondary importance. Alternatively, for smaller values of  $\theta$ , ( $W \sin \theta - F_s$ ) can be considered to be very small and hence is neglected.

For a horizontal channel,  $\theta = 0$  and  $W \sin \theta = 0$ .

### 6.3 HYDRAULIC JUMP IN A HORIZONTAL RECTANGULAR CHANNEL

(a) *Sequent Depth Ratio* Consider a horizontal, frictionless and rectangular channel. Considering unit width of the channel, the momentum equation, Eq. 6.1, can be written in the form

$$\frac{1}{2} \gamma y_1^2 - \frac{1}{2} \gamma y_2^2 = \beta_2 \rho q V_2 - \beta_1 \rho q V_1 \quad (6.2)$$

Taking  $\beta_2 = \beta_1 = 1.0$  and noting that by continuity

$$q = \text{discharge per unit width} = V_1 y_1 = V_2 y_2$$

$$(y_2^2 - y_1^2) = \frac{2q^2}{g} \left( \frac{1}{y_1} - \frac{1}{y_2} \right)$$

i.e., 
$$y_1 y_2 (y_1 + y_2) = \frac{2q^2}{g} = 2y_c^3 \quad (6.3)$$

On non-dimensionalising,

$$\frac{1}{2} \frac{y_2}{y_1} \left( 1 + \frac{y_2}{y_1} \right) = \frac{q^2}{g y_1^3} = F_1^2 \quad (6.3a)$$

where  $F_1$  = Froude number of the approach flow =  $V_1 / \sqrt{g y_1}$   
 Solving for  $(y_2 / y_1)$  yields

$$\frac{y_2}{y_1} = \frac{1}{2} \left( -1 + \sqrt{1 + 8F_1^2} \right) \quad (6.4)$$

This equation which relates the ratio of the sequent depths  $(y_2 / y_1)$  to the initial Froude number  $F_1$  in a horizontal, frictionless, rectangular channel is known as the *Belanger momentum equation*. For high values of  $F_1$ , say  $F_1 > 8.0$ , Eq. 6.4 can be approximated for purposes of quick estimation of the sequent depth ratio as

$$y_2 / y_1 \approx 1.41 F_1 \quad (6.4a)$$

Equation 6.4 can also be expressed in terms of  $F_2 = V_2 / \sqrt{g y_2}$  = the subcritical Froude number on the downstream of the jump as

$$\frac{y_1}{y_2} = \frac{1}{2} \left( -1 + \sqrt{1 + 8F_2^2} \right) \quad (6.5)$$

**(b) Energy Loss** The energy loss  $E_L$  in the jump is obtained by the energy equation applied to Sections 1 and 2 as

$$E_L = E_1 - E_2 \quad (\text{as the channel is horizontal, Fig. 6.1})$$

$$\begin{aligned} &= \left( y_1 + \frac{q^2}{2g y_1^2} \right) - \left( y_2 + \frac{q^2}{2g y_2^2} \right) \\ &= (y_1 - y_2) + \frac{1}{2} \frac{q^2}{g} \left( \frac{y_2^2 - y_1^2}{y_1^2 y_2^2} \right) \end{aligned}$$

Substituting for  $q^2/g$  from Eq. 6.3 and simplifying

$$E_L = \frac{(y_2 - y_1)^3}{4 y_1 y_2} \quad (6.6)$$

or

$$\frac{E_L}{y_1} = \frac{\left( \frac{y_2}{y_1} - 1 \right)^3}{4 \left( \frac{y_2}{y_1} \right)} \quad (6.6a)$$

The relative energy loss  $\frac{E_L}{E_1} = \left( \frac{E_L}{y_1} \right) / \left( \frac{E_1}{y_1} \right)$

But 
$$\frac{E_1}{y_1} = 1 + \frac{F_1^2}{2}$$

$$\frac{E_L}{E_1} = \frac{\left(\frac{y_2}{y_1} - 1\right)^3}{4\left(\frac{y_2}{y_1}\right)\left(1 + \frac{F_1^2}{2}\right)}$$

Substituting for  $(y_2/y_1)$  from Eq. 6.4 and simplifying,

$$\frac{E_L}{E_1} = \frac{\left(-3 + \sqrt{1 + 8F_1^2}\right)^3}{8\left(2 + F_1^2\right)\left(-1 + \sqrt{1 + 8F_1^2}\right)} \quad (6.7)$$

Equation 6.7 gives the fraction of the initial energy lost in the hydraulic jump. The variation of  $E_L/E_1$  with  $F_1$  is shown in Fig. 6.3 which highlights the enormous energy dissipating characteristic of the jump. At  $F_1 = 5$ , about 50 per cent of the initial energy in the supercritical stream is lost and at  $F_1 = 20$ ,  $E_L/E_1$  is about 86 per cent. Figure 6.3 also serves as a yardstick for comparing the efficiencies of other types of jumps and energy-dissipating devices.

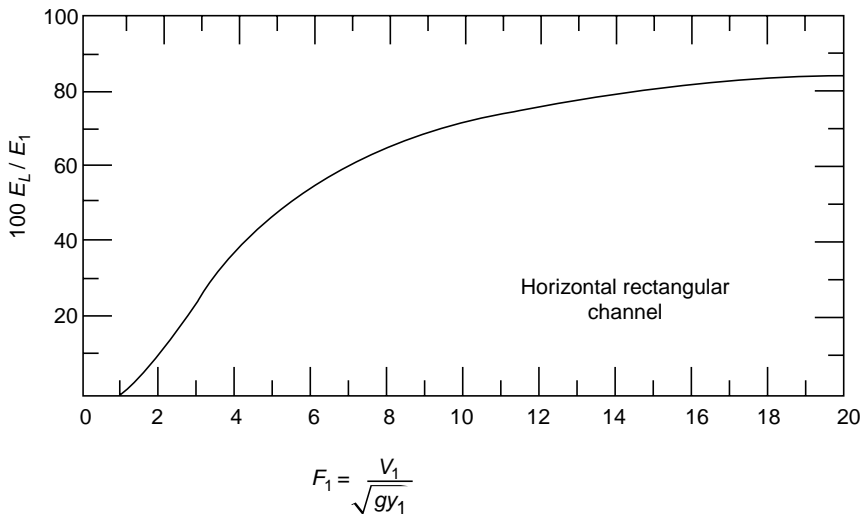


Fig. 6.3 Relative energy loss in a jump

Experimental studies by many research workers and specifically the comprehensive work of Bradley and Peterka<sup>1</sup> which covered a range of Froude numbers

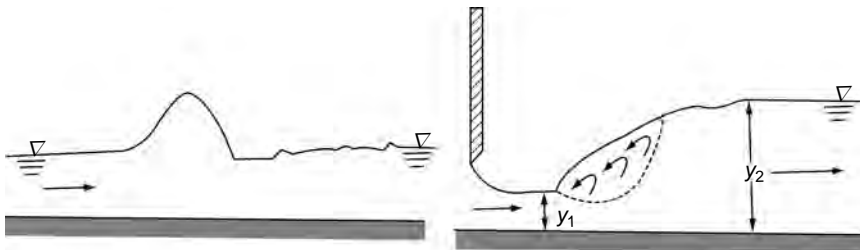
up to 20, have shown that Eqs 6.4 and 6.6 adequately represent the sequent-depth ratio and energy loss respectively in a hydraulic jump formed on a horizontal floor.

**(c) Classification of Jumps** As a result of extensive studies of Bradley and Peterka<sup>1</sup> the hydraulic jumps in horizontal rectangular channels are classified into five categories based on the Froude number  $F_1$  of the supercritical flow, as follows:

(i) *Undular Jump*  $1.0 < F_1 \leq 1.7$  The water surface is undulating with a very small ripple on the surface. The sequent-depth ratio is very small and  $E_L/E_1$  is practically zero. A typical undular jump is shown in Fig. 6.4 (a).

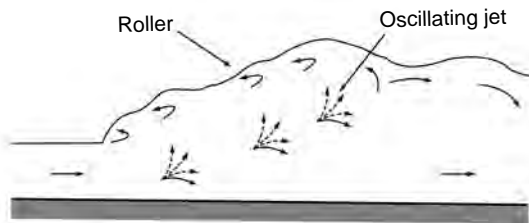
(ii) *Weak Jump*  $1.7 < F_1 \leq 2.5$  The surface roller makes its appearance at  $F_1 \approx 1.7$  and gradually increases in intensity towards the end of this range, i.e.  $F_1 \approx 2.5$ . The energy dissipation is very small, is  $E_L/E_1$  about 5 per cent at  $F_1 = 1.7$  and 18 per cent at  $F_1 = 2.5$ . The water surface is smooth after the jump (Fig. 6.4 (b)).

(iii) *Oscillating Jump*  $2.5 < F_1 \leq 4.5$  This category of jump is characterised by an instability of the high-velocity flow in the jump which oscillates in a random manner between the bed and the surface. These oscillations produce large surface waves that travel considerable distances downstream [Fig. 6.4(c)].



(a) Undular jump,  $1.0 < F_1 \leq 1.7$

(b) Weak jump,  $1.7 < F_1 \leq 2.5$



(c) Oscillating jump,  $2.5 < F_1 \leq 4.5$

**Fig. 6.4 (Continued)**



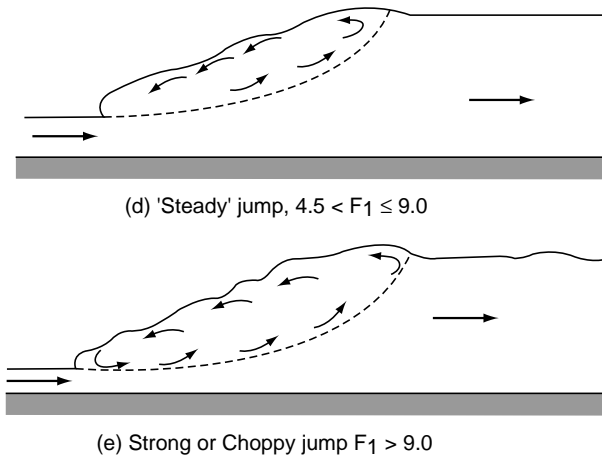


Fig. 6.4 Classification of jumps (1)

Special care is needed to suppress the waves in stilling basins having this kind of jump. Energy dissipation is moderate in this range;  $E_L / E_1 = 45$  per cent at  $F_1 = 4.5$ .

(iv) 'Steady' Jump  $4.5 < F_1 \leq 9.0$  In this range of Froude numbers, the jump is well-established, the roller and jump action is fully developed to cause appreciable energy loss (Fig. 6.4 (d)). The relative energy loss  $E_L / E_1$  ranges from 45 per cent to 70 per cent in this, class of jump. The 'steady jump' is least sensitive in terms of the toe-position to small fluctuations in the tailwater elevation.

(v) Strong or Choppy Jump  $F_1 > 9.0$  In this class of jump the water surface is very rough and choppy. The water surface downstream of the jump is also rough and wavy (Fig. 6.4(e)). The sequent-depth ratio is large and the energy dissipation is very efficient with  $E_L / E_1$  values greater than 70 per cent.

It is of course obvious that the above classification is based on a purely subjective consideration of certain gross physical characteristics. As such, the range of Froude numbers indicated must not be taken too rigidly. Local factors in stilling basin design can cause overlaps in the range of Froude numbers. Figure 6.5 (Plate 1) shows four typical hydraulic jumps in a rectangular laboratory flume.

An interesting and useful relationship involving  $F_1$  and a non-dimensional parameter made up of  $E_L$  and  $q$  is obtained as below:  
Using Eq. (6.6a) and Eq. (6.4)

$$\frac{E_L}{y_1} = \frac{1}{16} \frac{(-3 + \sqrt{1 + 8F_1^2})^3}{(-1 + \sqrt{1 + 8F_1^2})}$$

Since  $F_1^2 = \frac{q^2}{g y_1^3}$ ,  $y_1 = \frac{q^{2/3}}{g^{1/3} F_1^{2/3}}$

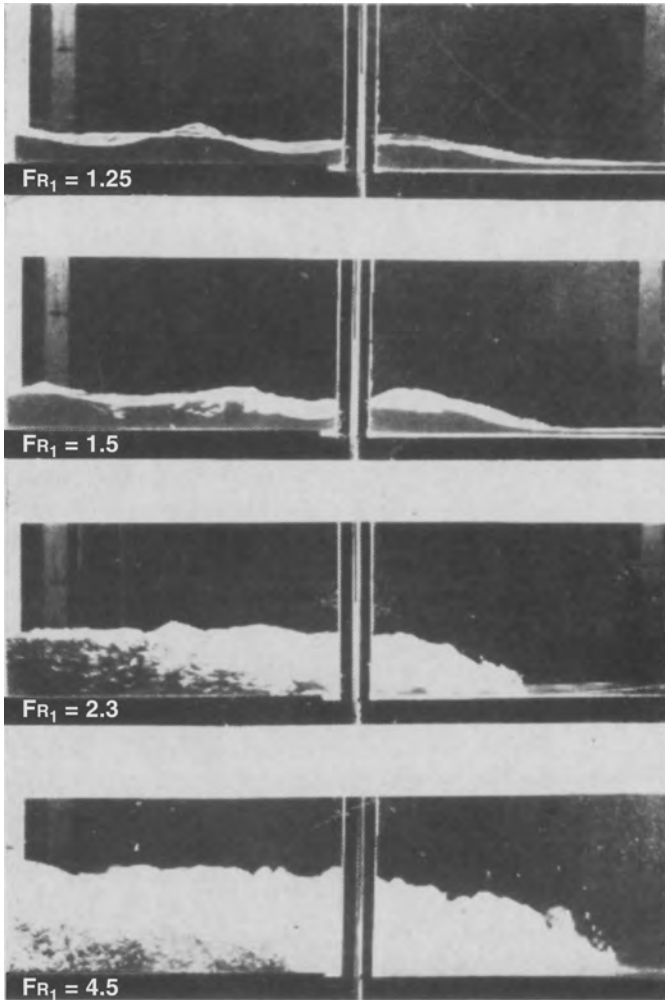


**Fig. 6.5** Hydraulic jumps at different froude numbers (Courtesy: M G Bos)  
[Note: The flow is right to left]

Substituting for  $y_1$  in the expression for  $\frac{E_L}{y_1}$  given above,

$$\frac{16g^{1/3}E_L}{q^{2/3}} = \frac{(-3 + \sqrt{1 + 8F_1^2})^3}{(F_1)^{2/3}(-1 + \sqrt{1 + 8F_1^2})} = f(F_1) \quad (6.8)$$

A common problem encountered in the hydraulic design of stilling basins for barrages is to estimate the elements of the hydraulic jump when discharge intensity ( $q$ ) and energy loss ( $E_L$ ) are the only known parameters of the jump. Equation 6.8 is very

useful in this context. A trial and error solution procedure is used to solve Eq. 6.8 to obtain  $F_1$  for known  $q$  and  $E_L$ . Knowing  $F_1$ , other parameters of the jump are then found by direct use of the relevant equations. Example 6.4 illustrates the above use of Eq. 6.8. A good description of the above problem and an exact solution for determination of sequent depths when  $q$  and  $E_L$  are the only known parameters of the jump is given by Swamee and Rathie<sup>2</sup>.

**(d) Characteristics of Jump in a Rectangular Channel**

(i) *Length of the Jump* The length of the jump  $L_j$  is an important parameter affecting the size of a stilling basin in which the jump is used. There have been many definitions of the length of the jump resulting in some confusion in comparing various studies. It is now usual to take the length of the jump as the horizontal distance between the toe of the jump to a section where the water surface levels off after reaching the maximum depth (Fig. 6.1). Because the water-surface profile is very flat towards the end of the jump, large personal errors are introduced in the determination of the length  $L_j$ .

Experimentally, it is found that  $L_j/y_2 = f(F_1)$ . The variation of  $L_j/y_2$  with  $F_1$  obtained by Bradley and Peterika<sup>1</sup> is shown in Fig. 6.6. This curve is usually recommended for general use. It is evident from Fig. 6.6 that while  $L_j/y_2$  depends on  $F_1$  for small values of the inlet Froude number, at higher values (i.e.  $F_1 > 5.0$ ) the relative jump length  $L_j/y_2$  is practically constant beyond a Froude number value of 6.1. Elevatorski<sup>3</sup> has shown that the data of reference 1 can be expressed as

$$L_j = 6.9 (y_2 - y_1) \tag{6.9}$$

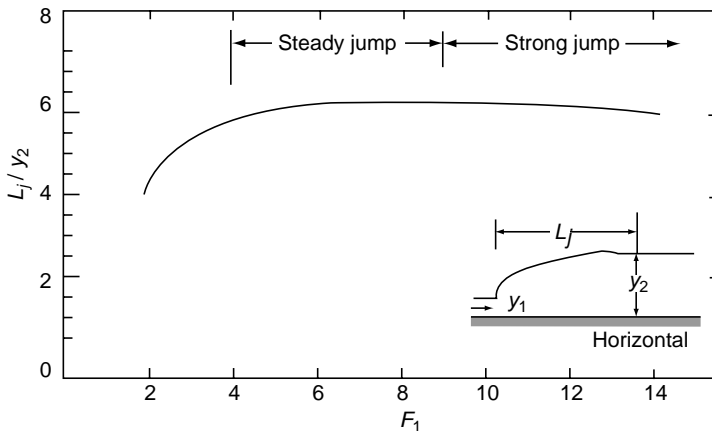


**Fig. 6.6** Length of the hydraulic jump on a horizontal floor

(ii) *Pressure Distribution* The pressures at the toe of the jump and at the end of the jump follow hydrostatic pressure distribution. However, inside the body of the jump, the strong curvatures of the streamlines cause the pressures to deviate from the hydrostatic distribution. Observations by Rajaratnam<sup>4</sup> have shown that in the initial portions of the jump the pressures in the jump body will be less than the hydrostatic pressure. The deficit from the hydrostatic pressure increases with an increase in the initial Froude number  $F_1$ . However, at the bottom of the channel and in a narrow region close to the bed, the pressures are essentially hydrostatic. Thus the pressure-head profile on the bed is the same as the mean water-surface profile.

(iii) *Water-Surface Profile* A knowledge of the surface profile of the jump is useful in the efficient design of side walls and the floor of a stilling basin. Consider the coordinate system shown in Fig. 6.7. The coordinates of the profile are  $(x, h)$  with the boundary condition that at  $x = 0, h = 0$ , and at  $x = L_j, h = (y_2 - y_1)$ . In general,  $h = f(x, F_1)$ .

Based on an analysis of a large number of jump profiles and bed-pressure profiles obtained by various investigators, Subramanya<sup>5</sup> and Rajaratnam and Subramanya<sup>6</sup> have shown that the jump profile can be expressed in a non-dimensional manner as

$$\eta = f(\lambda) \tag{6.10}$$

in which

$$\eta = \frac{h}{0.75(y_2 - y_1)}$$

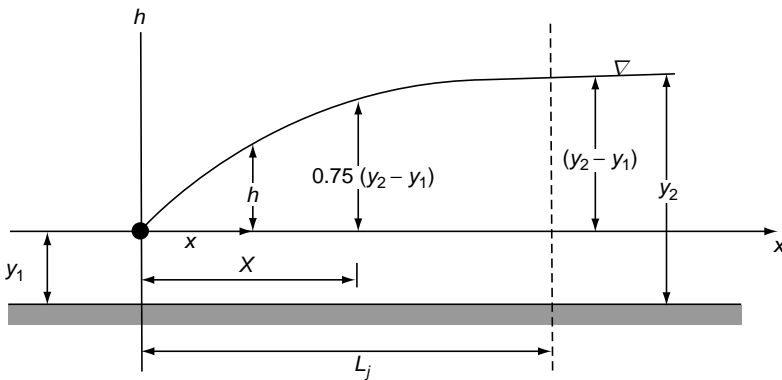


Fig. 6.7 Definition sketch for the jump profile (6)

and  $\lambda = x / X$ , where  $X$  = a length scale defined as the value of  $x$  at which  $h = 0.75(y_2 - y_1)$ . The variation of  $\eta$  with  $\lambda$  is given in Table 6.1.

**Table 6.1** Coordinates of the Non-dimensional Jump Profile.<sup>5,6</sup>

$\lambda$	$\eta$	$\lambda$	$\eta$	$\lambda$	$\eta$
0.00	0.000	0.60	0.655	1.30	1.140
0.05	0.185	0.70	0.736	1.40	1.180
0.10	0.245	0.80	0.820	1.50	1.215
0.15	0.280	0.90	0.920	1.60	1.245
0.20	0.320	1.00	1.000	1.80	1.290
0.30	0.405	1.10	1.060	2.00	1.320
0.40	0.485	1.20	1.105	2.20	1.333
0.50	0.570			2.40	1.333

It may be noted that in the  $\eta - \lambda$  relationship the Froude number does not appear explicitly. In Eq. 6.10,  $X$  is the length scale and is given by<sup>5,6</sup>

$$\frac{X}{y_1} = 5.08 F_1 - 7.82 \tag{6.11}$$

Equation 6.11 together with Table 6.1 enables one to adequately predict the jump profile.

Since the profile approaches  $h = (y_2 - y_1)$  at  $x = L_j$  asymptotically, the coordinates calculated from Table 6.1 may not exactly match the requirement of the end of the jump. For practical purposes it is suggested that the coordinates  $(\eta, \lambda)$  be used to plot the profile up to  $\lambda \approx 1.80$  and then to smoothly finish the curve by joining the profile to the end of the jump at  $x = L_j$ .

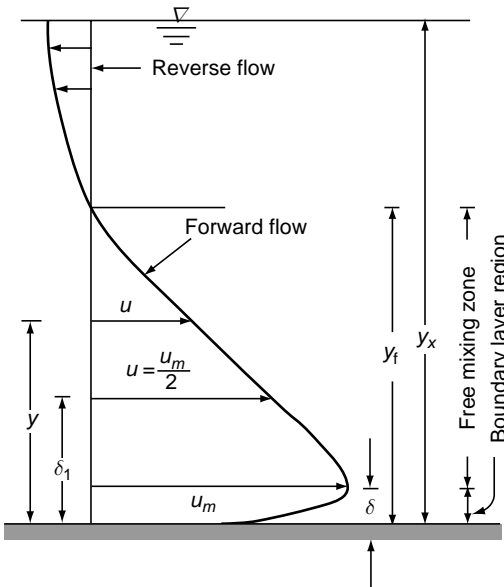


**Fig. 6.8** Velocity distribution in a jump

(iv) *Velocity profile* When the supercritical stream at the toe enters the jump body, it undergoes shearing action at the top as well as at the solid boundaries. The top surface of the high-velocity flow will have high relative velocities with respect to the fluid mass that overlays it. The intense shear at the surface generates a free shear layer which entrains the fluid from the overlying mass of fluid. The boundary shear at the bed causes a retardation of the velocity in a boundary layer. As a result of these actions the velocity distribution in a section at a distance  $x$  from the toe will be as shown in Fig. 6.8. It is seen that the velocity profile has two distinct

portions—a forward flow in the lower main body and a negative velocity region at the top. In the forward flow, the total volumetric rate of flow will be in excess of the discharge  $Q$  entering the jump at the toe. This is due to the flow entrainment at the shear layer. To maintain continuity, i.e. to account for the excess forward flow, a reverse flow exists at the top. This situation results in the formation of the roller.

The forward velocity profile has zero velocity at the bed, maximum velocity at a distance  $\delta$  and then gradually decreases to zero at a height  $y_f$  above the bed. The region  $0 < y < \delta$  can be called the boundary layer part and the region  $\delta < y < y_f$  the free-mixing zone. This velocity configuration indicates that the motion of the forward flow is similar to a wall jet except that the pressure gradient is adverse. The velocity profile and shear stress can be studied by following the methods of analysis similar to those used in the study of wall jets.

The velocity  $u$  at a distance  $y$  from the bed in the boundary layer portion ( $0 < y < \delta$ ) can be expressed by a velocity-defect law

$$\frac{u - u_m}{u_*} = f(y/\delta) \quad (6.12)$$

where  $u_* = \sqrt{\tau_0/\rho}$  = shear velocity and  $u_m$  = maximum velocity at  $y = \delta$ . In the free-mixing zone the velocity profile is found to be self-similar and can be expressed as<sup>3</sup>

$$\frac{u}{u_m} = f(y/\delta_1) \quad \left( \text{for } \frac{y}{\delta_1} > 0.16 \right) \quad (6.13)$$

where  $\delta_1$  = value of  $y$  at which  $u = \frac{u_m}{2}$ . The maximum velocity  $u_m$  occurs at  $y = \delta \approx 0.16\delta_1$ . It may be noted that the non-dimensionalised velocity profile is explicitly independent of  $F_1$  and  $x$ . The scales of the above relationship are  $u_m$  and  $\delta_1$  which are given by

$$\frac{u_m}{V_1} = f(x/y_1) \quad (6.14)$$

and 
$$\frac{\delta_1}{y_1} = f(x/y_1) \quad (6.15)$$

Both Eq. 6.14 and Eq. 6.15 are found<sup>4</sup> to be independent of the initial Froude number  $F_1$ .

(v) *Other Characteristics* In addition to characteristics mentioned above, information about shear stress and turbulent characteristics enhance one's understanding of the jump phenomenon. It has been found that the initial boundary-layer thickness and relative roughness of the bed play a major role in these aspects. Useful information on these topics are available in literature<sup>4,7</sup>.

(e) *Computations* Computations related to hydraulic jumps in rectangular channels are relatively simple. While most of the problem types are amenable to direct solution, a few types require trial and error solution procedure. The available relations are

- (i) Continuity equation
- (ii) Momentum equation for sequent depths and
- (iii) Energy equation for energy loss in the jump.

The basic variables can be discharge intensity  $q$ ; sequent depths  $y_1$  and  $y_2$ ; and energy loss  $E_L$ . There can be many other derived variables and corresponding relationships. Based on the above there can be a variety of problem types and a few common ones are illustrated in the following examples.

**Example 6.1** In a hydraulic jump occurring in a rectangular channel of 3.0-m width, the discharge is  $7.8 \text{ m}^3/\text{s}$  and the depth before the jump is 0.28 m. Estimate (i) sequent depth, and (ii) the energy loss in the jump.

*Solution* (i)  $V_1 = \frac{7.8}{(3 \times 0.28)} = 9.286 \text{ m/s}$

$$F_1 = \frac{V_1}{\sqrt{g y_1}} = \frac{9.286}{\sqrt{9.81 \times 0.28}} = 5.603$$

The sequent depth ratio is given by Eq. (6.4) as

$$\frac{y_2}{y_1} = \frac{1}{2} \left[ -1 + \sqrt{1 + 8F_1^2} \right] = \frac{1}{2} \left[ -1 + \sqrt{1 + 8 \times (5.603)^2} \right] = 7.424$$

Sequent depth =  $y_2 = 0.28 \times 7.424 = 2.08 \text{ m}$

(ii) The energy loss  $E_L$  is given by Eq. 6.6 as

$$E_L = \frac{(y_2 - y_1)^3}{4 y_1 y_2} = \frac{(2.08 - 0.28)^3}{4 \times 0.28 \times 2.08} = 2.503 \text{ m}$$

**Example 6.2** A rectangular channel carrying a supercritical stream is to be provided with a hydraulic jump type of energy dissipater. It is desired to have an energy loss of 5.0 m in the hydraulic jump when the inlet Froude number is 8.5. What are the sequent depths of this jump?

*Solution* Given  $F_1 = 8.5$  and  $E_L = 5.0 \text{ m}$

By Eq. 6.4  $\frac{y_2}{y_1} = \frac{1}{2} \left[ -1 + \sqrt{1 + 8F_1^2} \right] = \frac{1}{2} \left[ -1 + \sqrt{1 + 8 \times (8.5)^2} \right] = 11.53$

By Eq. 6.7  $\frac{E_L}{y_1} = \frac{\left( \frac{y_2}{y_1} - 1 \right)^3}{4 \left( \frac{y_2}{y_1} \right)}$

$$\frac{5.0}{y_1} = \frac{(11.53-1)^3}{4 \times 11.53} = 25.32$$

$$y_1 = 5.0/25.32 = 0.198 \text{ m}$$

and  $y_2 = 0.198 \times 11.53 = 2.277 \text{ m}$

**Example 6.3** | A hydraulic jump takes place in a rectangular channel with sequent depths of 0.25 m and 1.50 m at the beginning and end of the jump respectively. Estimate the (i) discharge per unit width of the channel and (ii) energy loss.

**Solution** (i) By Eq. 6.4  $\frac{y_2}{y_1} = \frac{1}{2}[-1 + \sqrt{1 + 8F_1^2}]$

$$\frac{1.50}{0.25} = \frac{1}{2}[-1 + \sqrt{1 + 8F_1^2}]$$

Thus,  $F_1^2 = 21$  and  $F_1 = 4.583$  m.

$$V_1 = 4.583 \times \sqrt{9.81 \times 0.25} = 7.177 \text{ m/s}$$

Discharge per unit width =  $q = V_1 y_1 = 7.177 \times 0.25 = 1.794 \text{ m}^3/\text{s/m}$  width

(ii) The energy loss  $E_L$  is given by Eq. 6.6 as

$$E_L = \frac{(y_2 - y_1)^3}{4y_1 y_2} = \frac{(1.50 - 0.25)^3}{4 \times 0.25 \times 1.50} = 1.302 \text{ m}$$

**Example 6.4** | In a hydraulic jump taking place in a horizontal apron below an Ogee shaped weir the discharge per unit width is  $0.25 \text{ m}^3/\text{s/m}$  and the energy loss is 2.75 m. Estimate the depths at the toe and heel of the jump.

**Solution** This kind of problem needs a trial and error solution procedure. Eq. 6.8 is used for easy trial and error solution.

Here  $q = 0.25 \text{ m}^3/\text{s/m}$  and  $E_L = 2.75 \text{ m}$ .

$$\frac{16g^{1/3} E_L}{q^{2/3}} = \frac{16 \times (9.81)^{1/3} \times 2.75}{(0.25)^{2/3}} = 51.135$$

By Eq. 6.8, 
$$f(F_1) = \frac{(-3 + \sqrt{1 + 8F_1^2})^3}{(F_1)^{2/3} (-1 + \sqrt{1 + 8F_1^2})} = 51.135 \quad (6.16)$$



Equation 6.16 is solved for  $F_1$  by a trial and error procedure. Table E-6.4 given below indicates the various trials in a typical solution procedure: Use of Spread sheet (such as MS Excel) greatly facilitates the procedure.

**Table E-6.4** Trial and Error Procedure – Example 6.4

Trial	Assumed $F_1$ Value	Numerator of $f(F_1)$	Denominator of $f(F_1)$	$f(F_1)$	Remarks
1	5.0	1396.46	38.53	36.24	Increase the value of $F_1$ in the next trial
2	6.0	2744.00	52.83	51.94	Decrease $F_1$ by a small amount
3	5.9	2581.31	51.32	50.30	Increase $F_1$ by a very small amount
4	5.95	2661.82	52.07	52.12	Value of $F_1$ can be accepted

Hence,  $F_1=5.95$ . Using Eq. 6.4

$$\frac{y_2}{y_1} = \frac{1}{2} \left( -1 + \sqrt{1 + 8F_1^2} \right) = \frac{1}{2} \left( -1 + \sqrt{1 + 8 \times (5.95)^2} \right) = 7.929$$

By Eq. 6.6a 
$$\frac{E_L}{y_1} = \frac{\left( \frac{y_2}{y_1} - 1 \right)^3}{4 \left( \frac{y_2}{y_1} \right)} = \frac{(7.929 - 1)^3}{4(7.929)} = 10.490$$

$$y_1 = 2.75 / (10.49) = 0.262 \text{ m}$$

$$y_2 = 0.262 \times 7.929 = 2.079 \text{ m}$$

**Example 6.5** An overflow spillway (Fig. 6.9) is 40.0 m high. At the design energy head of 2.5 m over the spillway find the sequent depths and energy loss in a hydraulic jump formed on a horizontal apron at the toe of the spillway. Neglect energy loss due to flow over the spillway face. (Assume  $C_d = 0.738$ ).

**Solution** The discharge per meter width of the spillway is

$$\begin{aligned} q &= \frac{2}{3} C_d \sqrt{2g} H_d^{3/2} \\ &= \frac{2}{3} \times 0.738 \times \sqrt{2 \times 9.81} \times (2.5)^{3/2} \\ &= 8.614 \text{ m}^3/\text{s/m} \end{aligned}$$

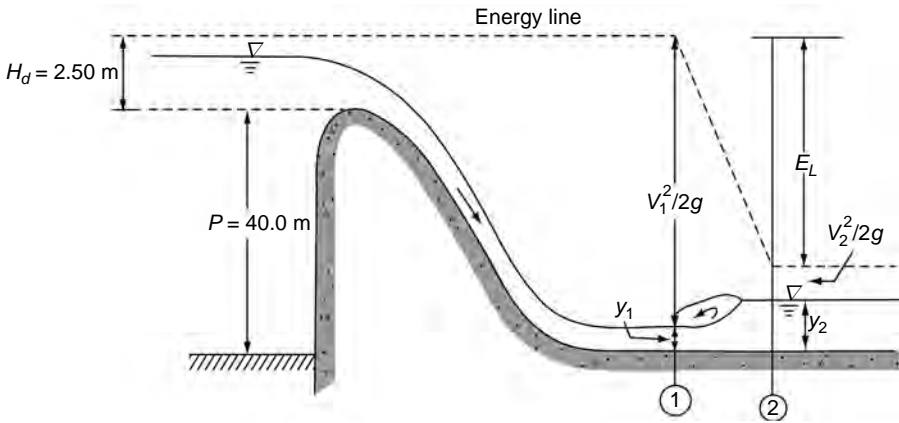


Fig. 6.9 Example 6.5

By the energy equation

$$P + H_d = y_1 + \frac{V_1^2}{2g}$$

(Energy loss over the spillway is neglected)

$$y_1 + \frac{(8.614)^2}{2g y_1^2} = 42.5$$

By trial-and-error

$$y_1 = 0.30 \text{ m}$$

$$V_1 = \frac{q}{y_1} = \frac{8.614}{0.3} = 28.71 \text{ m/s}$$

$$F_1 = V_1 / \sqrt{g y_1} = 28.71 / \sqrt{9.81 \times 0.3} = 16.74$$

By Eq. 6.4,

$$\frac{y_2}{0.30} = \frac{1}{2} \left[ -1 + \sqrt{1 + 8(16.74)^2} \right] = 23.18$$

$$y_2 = 6.954 \text{ m}$$

Energy loss

$$E_L = \frac{(y_2 - y_1)^3}{4 y_1 y_2} \tag{6.6}$$

$$= \frac{(6.954 - 0.3)^3}{4 \times 0.30 \times 6.954} = 35.30 \text{ m}$$

$$E_1 = \text{Energy at Section 1} = 42.5 \text{ m}$$

$$\text{Percentage of initial energy lost} = \frac{E_L}{E_1} \times 100 = 83.0\%$$

**Example 6.6** | A spillway discharges a flood flow at a rate of 7.75 m<sup>3</sup>/s per metre width. At the downstream horizontal apron the depth of flow was found to be 0.50 m. What tailwater depth is needed to form a hydraulic jump? If a jump is formed, find its (a) type, (b) length, (c) head loss, (d) energy loss as a percentage of the initial energy, and (e) profile.

*Solution*  $q = 7.75 \text{ m}^3/\text{s/m}$ , and  $y_1 = 0.50 \text{ m}$

$$V_1 = \frac{7.75}{0.50} = 15.50 \text{ m/s}$$

$$F_1 = \frac{15.50}{\sqrt{9.81 \times 0.50}} = 7.0$$

*Sequent-depth* By Eq. (6.4)

$$\frac{y_2}{y_1} = \frac{1}{2} \left( -1 + \sqrt{1 + 8 \times (7)^2} \right) = 9.41$$

$$y_2 = 4.71 \text{ m} = \text{required tailwater depth.}$$

(a) *Type* Since  $F_1 = 7.0$ , a 'steady' jump will be formed

(b) Since  $F_1 > 5.0$ ,  $L_j = 6.1 y_2$

$$L_j = \text{length of the jump} = 6.1 \times 4.71 = 28.7 \text{ m}$$

$$\begin{aligned} \text{(c) } E_L = \text{head loss} &= \frac{(y_2 - y_1)^3}{4 y_1 y_2} = \frac{(4.71 - 0.50)^3}{4 \times 0.5 \times 4.71} \\ &= 7.92 \text{ m} \end{aligned}$$

$$\text{(d) } E_1 = y_1 + \frac{V_1^2}{2g} = 0.5 + \frac{(15.50)^2}{2 \times 9.81} = 12.75 \text{ m}$$

$$\frac{E_L}{E_1} = 62.1\%$$

(e) *Profile* By Eq. (6.11)

$$\frac{X}{y_1} = 5.08(7.0) - 7.82 = 27.74$$

$$X = 13.87 \text{ m}$$

$$0.75(y_2 - y_1) = 3.16 \text{ m}$$

$$\therefore \lambda = \frac{x}{13.87} \text{ and } \eta = \frac{h}{3.16}$$

Substituting these for the values of  $\lambda$  and  $\eta$  given in Table 6.1 a relation between  $x$  and  $h$  is obtained. As suggested in Section 6.4(c), the profile is calculated up to  $\lambda \approx 1.80$ , i.e. up to  $x = 25.0$  m and then is joined by a smooth curve to the end of the jump at  $x = L_j = 28.7$  m. The change in the depth in this range would be  $0.0433 \times 3.16 = 0.14$  m. This being a flat curve, i.e., a change of 0.14 m in 3.70 m, the procedure as above is adequate.

#### 6.4 JUMPS IN HORIZONTAL NON-RECTANGULAR CHANNELS

If the side walls of a channel are not vertical, e.g. in the case of a trapezoidal channel, the flow in a jump will involve lateral expansion of the stream in addition to increase in depth. The cross-sectional areas are not linear functions of the depth of flow. This aspect introduces not only computational difficulties in the calculation of the sequent-depth ratio but also structural changes in the jump. A brief introduction to this wide field of jumps, in non-rectangular channel, is given in this section.

**(a) Basic Equations** Consider a horizontal frictionless channel of any arbitrary shape, such as in Fig. 6.2. For a hydraulic jump in this channel, the general momentum (Eq. 6.1) with the assumption of  $\beta_2 = \beta_1 = 1.0$  reduces to:

$$P_1 - P_2 = M_2 - M_1 \tag{6.17}$$

i.e. 
$$\gamma A_1 \bar{y}_1 - \gamma A_2 \bar{y}_2 = \rho Q_2 V_2 - \rho Q_1 V_1$$

$$= \frac{\rho Q_2^2}{A_2} - \frac{\rho Q_1^2}{A_1} \tag{6.18}$$

where  $A$  = area of cross-section any  $\bar{y}$  = depth of the centre of gravity of the area from the water surface.

Rearranging Eq. 6.17

$$P_1 + M_1 = P_2 + M_2$$

i.e. 
$$P + M = \gamma \left( A \bar{y} + \frac{Q^2}{gA} \right) = \text{Const.} \tag{6.19}$$

i.e. 
$$\frac{P + M}{\gamma} = P_s = A \bar{y} + \frac{Q^2}{gA} = \text{Const.} \tag{6.19a}$$

The term  $P_s \left( = \frac{P + M}{\gamma} \right)$  is the specific force (Section 1.11 (c)).

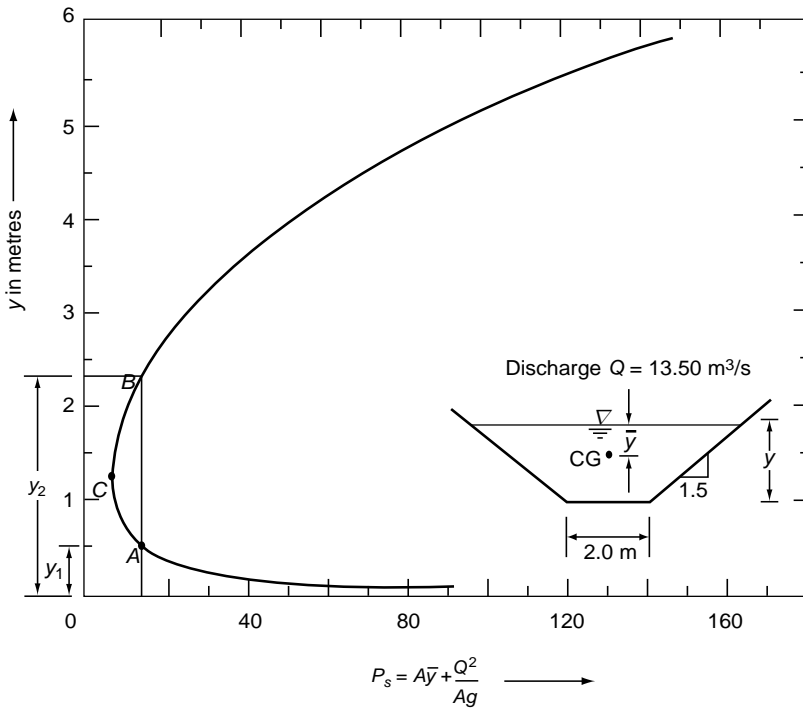


Fig. 6.10 Specific-force diagram for Example 6.7

The specific force  $P_s$  is a function of the depth of flow, channel geometry and discharge. A parabolic curve with two distinct limbs resembling the specific-energy curve is obtained for plots of  $P_s$  vs  $y$  for a given  $Q$  in a given channel (Fig. 6.10). The lower limb represents the supercritical flow and the upper limb the subcritical flow. An ordinate drawn at a given  $P_s$  cuts the curve at two points  $A$  and  $B$  where the respective depths represent the sequent depths for the given discharge. The point  $C$  corresponding to the merger of these two depths is obviously the critical depth for the given flow  $Q$ .

The specific-force diagram provides a convenient means of finding sequent depths for a given discharge in a given horizontal channel. If suitably non-dimensionalised, it can provide a quick graphical solution aid in cases involving a large number of calculations. For small and isolated calculations, Eq. 6.19a is solved by a trial-and-error procedure to obtain the sequent depths.

The energy loss  $E_L$  due to a jump in a non-rectangular horizontal channel is

$$E_L = E_1 - E_2 = (y_1 - y_2) + \frac{Q^2}{2g} \left( \frac{1}{A_1^2} - \frac{1}{A_2^2} \right) \quad (6.20)$$

**Example 6.7** A trapezoidal channel is 2.0 m wide at the bottom and has side slope of 1.5 horizontal: 1 vertical. Construct the specific-force diagram for a discharge of 13.5 m<sup>3</sup>/s in this channel. For this discharge find the depth sequent to the supercritical depth of 0.5 m.

**Solution** The channel cross section is shown as an inset in Fig. 6.10.

$$A_1 = (2.0 + 1.5 \times 0.5) \times 0.5 = 1.375 \text{ m}^2$$

$$T_1 = 2.0 + 2 \times 1.5 \times 0.5 = 3.5 \text{ m}$$

$$\frac{A_1}{T_1} = 0.393 \text{ m}$$

$$V_1 = \frac{13.5}{1.375} = 9.818 \text{ m/s}$$

$$F_1 = \frac{9.818}{\sqrt{9.81 \times 0.393}} = 5.00$$

For a trapezoidal section

$$\begin{aligned} A\bar{y} &= \left[ \left( By \frac{y}{2} \right) + my^2 \frac{y}{3} \right] \\ &= \frac{y^2}{6} (3B + 2my) \end{aligned}$$

Specific force

$$P_s = \frac{Q^2}{Ag} + A\bar{y}$$

$$= \frac{(13.5)^2}{9.81A} + A\bar{y}$$

$$P_s = \frac{18.578}{(2.0 + 1.5y)y} + \frac{y^2}{6} (6 + 3y)$$

Values of  $P_s$  were computed using this equation for different  $y$  values, ranging from  $y = 0.1$  m to  $y = 6.0$  m and is shown plotted in Fig. 6.10.

From Fig. 6.10, the depth sequent to  $y_1 = 0.5$  m is  $y_2 = 2.38$  m (point  $B$ ).

**(b) Sequent-depth Ratios** Expressions for sequent-depth ratios in channels of regular shapes can be obtained by re-arranging the terms in Eq. 6.19a to get equality of specific forces as

$$\frac{Q^2}{gA_1} + A_1\bar{y}_1 = \frac{Q^2}{gA_2} + A_2\bar{y}_2$$

$$A_2\bar{y}_2 - A_1\bar{y}_1 = \frac{Q^2}{g} \left( \frac{1}{A_1} - \frac{1}{A_2} \right)$$

$$A_1\bar{y}_1 \left( \frac{A_2\bar{y}_2}{A_1\bar{y}_1} - 1 \right) = \frac{Q^2}{g} \left( \frac{A_2 - A_1}{A_1A_2} \right)$$

Noting that  $F_1^2 = \frac{Q^2T_1}{gA_1^3}$ , and on re-arranging

$$\left( \frac{A_2}{A_1} \frac{\bar{y}_2}{\bar{y}_1} - 1 \right) = F_1^2 \left( \frac{A_1/T_1}{\bar{y}_1} \right) \left( 1 - \frac{A_1}{A_2} \right) \tag{6.21}$$

Substituting the expression for  $A$ ,  $T$  and  $\bar{y}$  pertinent to the given geometry will lead to an equation relating the sequent-depth ratio to the inlet Froude number and other geometric parameters of the channel. In most non-rectangular channels Eq. 6.21 contains the sequent-depth ratio  $y_2 / y_1$  in such a form that it needs a trial-and-error procedure to evaluate it. Reference 8 gives useful information of hydraulic jumps in all shapes of channels.

**(c) Jumps in Exponential Channels** Exponential channels represent a class of geometric shapes with the area related to the depth as  $A = k_1y^a$  in which  $k_1$  and  $a$  are characteristic constants. For example, values of 1.0, 1.5 and 2.0 for  $a$  represent rectangular, parabolic and triangular channels respectively.

In the case of an exponential channel (Fig. 6.11),

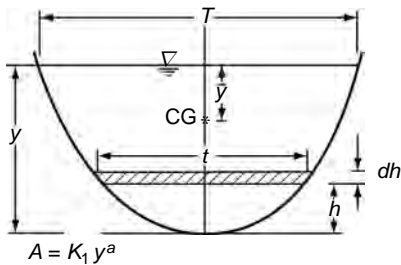


Fig. 6.11 Exponential channel

Top width

$$T = \frac{dA}{dy} = k_1 a y^{a-1} \tag{6.22}$$

$$\frac{A}{T} = (y/a) \tag{6.23}$$

$$\bar{y} = \frac{1}{A} \int_0^y t(y-h)dh,$$

where  $t$  = top width at any height  $h$ .

$$= \frac{1}{A} \int_0^y k_1 a h^{a-1} (y-h)dh$$

Simplifying  $\bar{y} = y / (a + 1)$

Substituting for  $T$ ,  $(A / T)$  and  $y$  in Eq. 6.21

$$\left( \frac{y_2^a}{y_1^a} \cdot \frac{y_2}{y_1} - 1 \right) = F_1^2 \left( \frac{y_1 / a}{y_1 / (a + 1)} \right) \left( 1 - \frac{y_1^a}{y_2^a} \right) \quad (6.24)$$

i.e. 
$$\left( \frac{y_2}{y_1} \right)^{a+1} - 1 = F_1^2 \left( \frac{a+1}{a} \right) \left( 1 - \left( \frac{y_1}{y_2} \right)^a \right) \quad (6.25)$$

Using this equation the ratio  $y_2 / y_1$  can be evaluated as a function of  $F_1$  and  $a$ .

The energy loss  $E_L$  due to a jump in a horizontal exponential channel can be expressed by using Eq. 6.20 as

$$\frac{E_L}{E_1} = \frac{2a \left( 1 - \frac{y_2}{y_1} \right) + F_1^2 \left( 1 - \left( \frac{y_1}{y_2} \right)^{2a} \right)}{(2a + F_1^2)} \quad (6.26)$$

Experimental studies by Argyropoulos on hydraulic jumps in parabolic channels<sup>9</sup> and triangular channels<sup>10</sup> have shown that the sequent-depth ratios calculated by Eq. 6.25 agree closely with the experimental data.

**Example 6.8** | A hydraulic jump takes place in a horizontal triangular channel having side slopes of 1.5 H : 1 V. The depths before and after the jump are 0.30 m and 1.20 m respectively. Estimate the (i) flow rate, (ii) Froude number at the beginning and end of the jump, and (iii) energy loss in the jump.

*Solution*

$$P = \gamma A \bar{y} = \gamma (m y^2) \frac{y}{3}$$

$$M = \frac{\rho Q^2}{A} = \frac{\rho Q^2}{m y^2}$$

By Eq. (6.19) 
$$P + M = \frac{\gamma m y^3}{3} + \frac{\rho Q^2}{m y^2} = \text{Const.}$$

$$\frac{g m y_1^3}{3} + \frac{Q^2}{m y_1^2} = \frac{g m y_2^3}{3} + \frac{Q^2}{m y_2^2}$$

$$\frac{Q^2}{m} \left[ \frac{1}{y_1^2} - \frac{1}{y_2^2} \right] = \frac{g m}{3} (y_2^3 - y_1^3)$$



$$Q^2/g = \frac{m^2}{3} \frac{(y_2^3 - y_1^3)}{\left[ \frac{(y_2^2 - y_1^2)}{y_1^2 y_2^2} \right]}$$

$$Q^2/g = \frac{m^2}{3} \frac{y_1^3 (\eta^3 - 1) \eta^2 y_1^4}{(\eta^2 - 1) y_1^2}$$

where  $\eta = y_2/y_1$

$$Q^2/g = \frac{m^2}{3} y_1^5 \frac{(\eta^3 - 1) \eta^2}{(\eta^2 - 1)}$$

Here  $m = 1.5, y_1 = 0.3, \eta = \frac{y_2}{y_1} = \frac{1.20}{0.3} = 4.0$

$$Q^2/g = \frac{(1.5)^2}{3} (0.3)^5 \frac{[4^3 - 1](4)^2}{[4^2 - 1]} = 0.12247$$

$$Q = 1.096 \text{ m}^3/\text{s}$$

For a triangular channel, Froude number  $F = \frac{Q}{A\sqrt{g A/T}}$

$$F^2 = \frac{Q^2 T}{g A^3} = \frac{Q^2 2my}{g m^3 y^6} = \frac{2Q^2}{g m^2 y^5}$$

$$F_1^2 = \frac{2 \times (1.096)^2}{9.81 \times (1.5)^2 \times (0.3)^5} = 44.88; \quad F_1 = 6.693$$

$$F_2^2 = \frac{2 \times (1.096)^2}{9.81 \times (1.5)^2 \times (1.2)^5} = 0.04375; \quad F_2 = 0.209$$

Energy loss:  $E_L = E_1 - E_2$

$$= \left( y_1 + \frac{V_1^2}{2g} \right) - \left( y_2 + \frac{V_2^2}{2g} \right)$$

$$A_1 = 1.5 \times (0.3)^2 = 0.135 \text{ m}^2; \quad V_1 = \frac{1.096}{0.135} = 8.119 \text{ m}$$

$$A_2 = 1.5 \times (1.2)^2 = 2.160 \text{ m}^2; \quad V_2 = \frac{1.096}{0.16} = 0.507 \text{ m}$$

$$E_L = \left( 0.3 + \frac{(8.119)^2}{2 \times 9.81} \right) - \left( 1.2 + \frac{(0.507)^2}{2 \times 9.81} \right)$$

$$= 3.66 - 1.213 = 2.447 \text{ m}$$

**Example 6.9** | A circular culvert of 2.0-m diameter carries a discharge of 3.0 m<sup>3</sup>/s. If the supercritical depth in a hydraulic jump occurring in this channel is 0.55 m determine the sequent depth. Assume horizontal frictionless channel.

*Solution*  $y_1 = 0.55 \text{ m}$   $y_1/D = 0.55/2 = 0.275$

From Table 2A.1 for  $y_1/D = 0.275$ ,  $A_1/D^2 = 0.17555$

Thus  $A_1 = 0.17555 \times (2.0)^2 = 0.7022 \text{ m}^2$ .

For a circular channel section flowing part full, the distance of the centre of gravity from the centre of the circular section ( $\hat{z}$  in Fig. 6.12) is given by

$$\hat{z} = -\frac{2(r^2 - z^2)^{3/2}}{3A}$$

Also, from Fig. 6.12 the depth of the centre of gravity from the water surface of the flow section  $\bar{y} = y - (r + \hat{z})$

In the present case,  $z = r - y = 1.0 - 0.55 = 0.45 \text{ m}$

$$\hat{z}_1 = -\frac{2 \left[ (1.0)^2 - (0.45)^2 \right]^{3/2}}{3 \times 0.7022} = -0.6762 \text{ m}$$

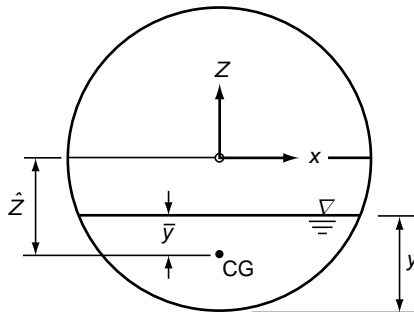


Fig. 6.12 Definition sketch – Example 6.9

Trial	$y_2(m)$	$y_2/D$	$A_2/D^2$ from Table 2A-1	$A_2(m^2)$	$Z_2$	$\hat{z}_2$	$\bar{y}_2$	$P_{s2}$	Remarks
1	1.50	0.7500	0.63185	2.52740	0.500	0.1713	0.6713	2.0597	Reduce $y_2$ slightly
2	1.20	0.6000	0.49203	1.96812	0.200	0.3186	0.5186	1.4868	Reduce $y_2$ slightly
3	1.18	0.5900	0.48221	1.92884	0.180	0.3290	0.5090	1.4574	Give very small increment to $y_2$
4	1.185	0.5925	0.48467	1.93866	0.185	0.3264	0.5114	1.4646	Accept

$$\bar{y}_1 = 0.55 - 1.00 + 0.6762 = 0.2262 \text{ m}$$

$$\begin{aligned} \text{Specific force at Section 1} &= P_{s1} = \frac{Q^2}{gA_1} + A_1\bar{y}_1 \\ &= \frac{(3.0)^2}{9.81 \times 0.7022} + (0.7022 \times 0.2262) = 1.4654 \end{aligned}$$

Equating the specific forces before and after the jump,  $P_{s1} = P_{s2} = 1.4654$

$$\text{Further } P_{s2} = \frac{Q^2}{gA_2} + A_2\bar{y}_2 = 1.4654 \quad (6.27)$$

The value of  $y_2$  satisfying this equation is obtained by trial and error.

Trial and error solution of Eq. 6.27

The sequent depth  $y_2 = 1.185 \text{ m}$

*Note:* For hydraulic jumps occurring in horizontal, frictionless circular channels several empirical equations are available for facilitating quick calculations. Following are two such equations:

(1) Straub(1978):

$$(i) \text{ For } 0.02 < \frac{y_c}{D} \leq 0.85, y_c = \frac{1.01}{(D)^{0.265}} \left[ \frac{Q}{\sqrt{g}} \right]^{0.506} \quad (6.28)$$

$$(ii) F_1 = \left( \frac{y_c}{y_1} \right)^{1.93} \quad (6.29)$$

(iii) (a) For  $F_1 < 1.7$ ,  $\frac{y_1}{y_2} = (y_c)^2$  (6.30)

(b) For  $F_1 \geq 1.7$  (in SI Units)

$$\frac{y_2}{y_1} = 1.087(y_c)^{0.07} \left( \frac{y_c}{y_1} \right)^{1.73}$$

(2) K. Subramanya(1996):

$$\frac{y_2}{y_1} = -0.01F_1^2 + 0.8644F_1 + 0.3354$$
 (6.31)

**Alternative Methods to Example 6.9**

**(1) By using Straub’s Equations**

$$y_c = \frac{1.01}{(D)^{0.265}} \left[ \frac{Q}{\sqrt{g}} \right]^{0.506}$$

$$y_c = \frac{1.01}{(2.0)^{0.265}} \left[ \frac{3.0}{\sqrt{9.81}} \right]^{0.506} = 0.823 \text{ m}$$

$$y_c / D = 0.823 / 2.0 = 0.412$$

Hence calculation of  $y_c$  is OK and  $\frac{y_2}{y_1} = 1.087(y_c)^{0.07} \left( \frac{y_c}{y_1} \right)^{1.73} = 2.1534$

Sequent depth  $y_2 = 1.1844 \text{ m}$ .

**(2) Alternative Method-2**

$y_1 = 0.55 \text{ m}$   $y_1/D = 0.55 / 2 = 0.275$   
 From Table 2A.1 for  $y_1/D = 0.275$ ,  $A_1/D^2 = 0.17556$  and  $T_1/D = 0.89296$   
 Thus  $A_1 = 0.17556 \times (2.0)^2 = 0.7022 \text{ m}^2$ .  
 and  $T_1 = 0.89296 \times 2.0 = 1.78596 \text{ m}$

For using Eq. 6.31  $V_1 = \frac{Q}{A_1} = \frac{3.0}{0.7022} = 4.272 \text{ m/s}$

$$F_1 = \frac{V_1}{\sqrt{g \frac{A_1}{T_1}}} = \frac{4.272}{\sqrt{9.81 \times \frac{0.7022}{1.78596}}} = 2.1752$$

By Eq. 6.31  $\frac{y_2}{y_1} = -0.01F_1^2 + 0.8644F_1 + 0.3354$

$$\frac{y_2}{y_1} = -0.01(2.175)^2 + 0.8644(2.175) + 0.3354$$

$$= -0.04731 + 1.8803 + 0.3354 = 2.1683$$

Sequent depth  $y_2 = 2.168 \times 0.55 = 1.193$  m

(It may be noted that this method is easier and the error is less than 1%)

### 6.5 JUMPS ON A SLOPING FLOOR

When a hydraulic jump occurs in a channel with a sloping floor, the situation is described by the general momentum equation, Eq. 6.1. There are too many unknown terms relative to the number of available equations and unless additional information is provided the solution of the momentum equation is not possible. Even if the simplified situation of a rectangular frictionless channel is considered, the term  $W \sin \theta$  representing the longitudinal component of weight of the water in the jump poses a problem as an unknown quantity. This is because  $W \sin \theta$  involves the length and profile of the jump, information about which can be obtained only through experimental observations. As such, even though many attempts have been made to obtain the sequent-depth ratio through the momentum equation, no satisfactory general solution is available so far. An example of a typical simplification of Eq. 6.1 to obtain the sequent-depth ratio in a jump on a sloping floor is given below.

The definition sketch of a jump on a sloping floor in a rectangular frictionless channel is indicated in Fig. 6.13. The momentum correction factors  $\beta_1$  and  $\beta_2$  are assumed equal to unity. A unit width of the channel is considered with  $q =$  discharge per unit width,  $y_1 =$  depth before the jump and  $y_2 =$  depth at the end of the jump. Consider a control volume as shown by dashed lines and the momentum equation in the longitudinal direction would be, from Eq. 6.1

$$P_1 - P_2 + W \sin \theta = M_2 - M_1 \tag{6.32}$$

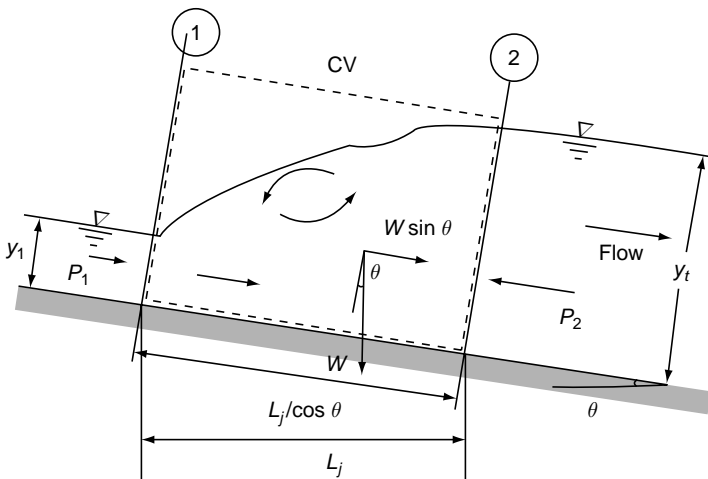


Fig. 6.13 Definition sketch for a jump on a sloping floor

Assuming hydrostatic pressure distribution at Section 1 and 2,

$$P_1 = \frac{1}{2} \gamma y_1^2 \cos \theta$$

and

$$P_2 = \frac{1}{2} \gamma y_t^2 \cos \theta$$

If the water surface were a straight line joining  $y_1$  and  $y_t$ , then the area of the jump  $= \frac{1}{2} (y_1 + y_t) \frac{L_j}{\cos \theta}$ .

(Note that the length of the jump  $L_j$  is defined as a horizontal distance between  $y_1$  and  $y_t$ ). Introducing a coefficient to account for the curvature of the jump profile and  $\cos \theta$  term,

$$W = \frac{1}{2} K \gamma L_j (y_1 + y_t) \tag{6.33}$$

The momentum flux  $M_1 = \rho q^2 / y_1$  and  $M_2 = \rho q^2 / y_t$ . Equation 6.32 can now be re-written as

$$\frac{1}{2} \gamma [y_1^2 \cos \theta - y_t^2 \cos \theta + K L_j (y_1 + y_t) \sin \theta] = \rho q^2 \left( \frac{1}{y_t} - \frac{1}{y_1} \right)$$

Re-arranging

$$\left( \frac{y_t}{y_1} \right)^2 - 1 - \frac{K L_j \tan \theta}{y_1} \left( 1 + \frac{y_t}{y_1} \right) = \frac{2 F_1^2}{\cos \theta} \left( \frac{y_t / y_1 - 1}{y_t / y_1} \right)$$

where  $F_1 = V_1 / \sqrt{g y_1}$ .

[Note that  $F_1$  is not the exact Froude number of the inclined channel flow at Section 1 =  $F_{1s}$  but is only a convenient non-dimensional parameter. The Froude number of flow in channels with large  $\theta$  is given by Eq. 2.8a. Hence for  $\alpha = 1.0$ ,  $F_{1s} = V_1 \sqrt{g \cos \theta} \cdot A / T$ .]

$$\text{i.e.} \quad \left( \frac{y_t}{y_1} \right)^3 - \frac{K L_j \tan \theta}{y_1} \left( \frac{y_t}{y_1} \right)^2 - \left( 1 + \frac{K L_j \tan \theta}{y_1} + \frac{2 F_1^2}{\cos \theta} \right) \left( \frac{y_t}{y_1} \right) + \frac{2 F_1^2}{\cos \theta} = 0 \tag{6.34}$$

Equation (6.34) can be used to estimate the sequent-depth ratio by a trial-and-error procedure if the term  $(K L_j)$  is known. In general,  $(K L_j)$  can be expected to be a function of  $F_1$  and  $\theta$  and its variation can be obtained only through experimental study.

### 6.5.1 Characteristics of Jumps on a Sloping Floor

Extensive experiments have been conducted by the U.S. Bureau of Reclamation resulting in useful information on jumps on a sloping floor<sup>11</sup>. Based on the USBR study, the following significant characteristics of sloping-floor jumps can be noted.

(a) **Sequent Depth  $y_t$**  Defining  $y_2 =$  equivalent depth corresponding to  $y_1$  in a horizontal floor jump  $= \frac{y_1}{2} \left( -1 + \sqrt{1 + 8F_1^2} \right)$ , the sequent depth  $y_t$  is found to be related to  $y_2$  as

$$\frac{y_t}{y_2} = f(\theta)$$

The variation of  $\left( \frac{y_t}{y_2} \right)$  with  $\tan \theta$  is shown in Fig. 6.14. By definition  $\frac{y_t}{y_2} = 1.0$  when  $\tan \theta = 0$  and it is seen from Fig. 6.13 that  $y_t/y_2$  increases with the slope of the channel having typical values of 1.4 and 2.7 at  $\tan \theta = 0.10$  and 0.30 respectively. Thus the sloping-floor jumps require more tailwater depths than the corresponding horizontal-floor jumps.

The best fit line for the variation of  $y_t / y_2$  with  $\tan \theta$  shown in Fig. 6.14, can be expressed as

$$y_t / y_2 = 1.0071 \exp (3.2386 \tan \theta) \tag{6.35}$$

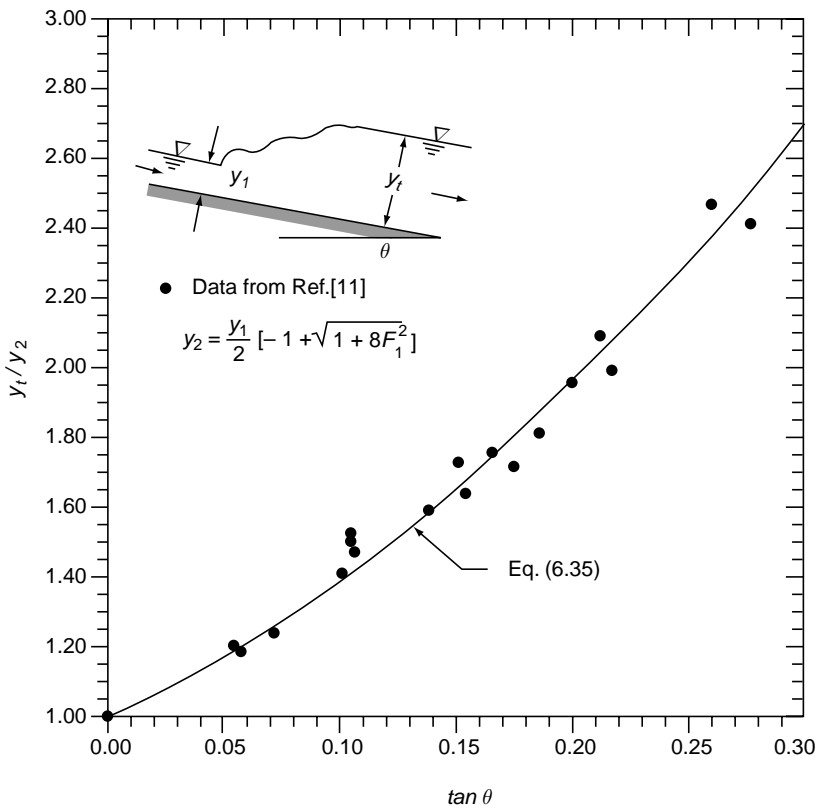


Fig. 6.14 Variation of  $y_t/y_2$  in jumps on a sloping floor

(b) **Length of the Jump  $L_j$**  The length of the jump  $L_j$  was defined in the USBR study as the horizontal distance between the commencement of the jump and a point on the subcritical flow region where the streamlines separate from the floor or to a point on the level water surface immediately downstream of the roller, whichever is longer.

The length of the jump on a sloping floor is longer than the corresponding  $L_j$  of a jump on a horizontal floor. The variation of  $L_j/y_2$  with  $F_1$  for any  $\theta$  is similar to the variation for  $\theta = 0$  case shown in Fig. 6.6. In the range of  $4.0 < F_1 < 13$ ,  $L_j/y_2$  is essentially independent of  $F_1$  and is a function of  $\theta$  only. The variation can be approximately expressed as<sup>12</sup>

$$L_j/y_2 = 6.1 + 4.0 \tan \theta \tag{6.36}$$

in the range of  $4.5 < F_1 < 13.0$ .

Elevatorski's<sup>3</sup> analysis of the USBR data indicates that the jump length can be expressed as

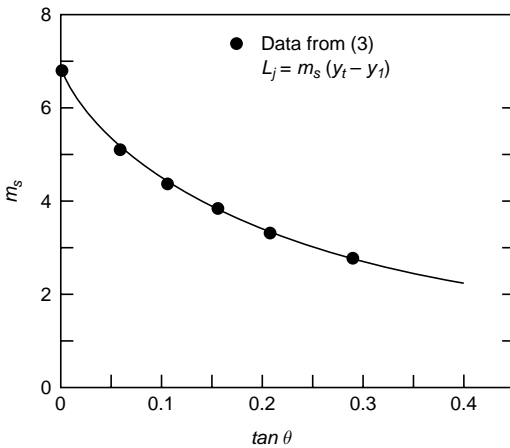


Fig. 6.15 Length of jumps on sloping floor

$$L_j = m_s(y_t - y_1) \tag{6.37}$$

in which  $m_s = f(\theta)$ . The variation of  $m_s$  with  $\tan \theta$  is shown in Fig. 6.15. It may be seen that  $m_s = 6.9$  for  $\tan \theta = 0$  and decreases with an increase in the value of the channel slope. Equation 6.37 is based on a wider range of values for  $F_1$  than in Eq. 6.37.

(c) **Energy Loss  $E_L$**  Knowing the sequent depths  $y_t$  and  $y_1$  and the length of the jump, the energy loss  $E_L$  can be calculated as

$$E_L = H_1 - H_2$$

where

$H$  = total energy at a section

$$E_L = (E_1 + L_j \tan \theta) - E_2$$

$$= y_1 \cos \theta + \frac{V_t^2}{2g} + L_j \tan \theta - y_1 \cos \theta - \frac{V_1^2}{2g} \tag{6.38}$$

where  $y_t$  = sequent depth in a sloping channel at Section 2. It is found that the relative energy loss  $E_L/H_1$  decreases with an increase in the value of  $\theta$ , being highest at  $\tan \theta = 0$ . The absolute value of  $E_L$  is a function of  $\theta$ , being least when  $\theta = 0$ .



**Example 6.10** A rectangular channel is laid on a slope of 1 horizontal:0.15 vertical. When a discharge of 11.0 m<sup>3</sup>/s/metre width is passed down the channel at a depth of 0.7 m, a hydraulic jump is known to occur at a section. Calculate the sequent depth, length of the jump and energy loss in the jump. What would be the energy loss if the slope was zero?

*Solution*  $q = 11.00 \text{ m}^3/\text{s}/\text{m}$

At inlet  $V_1 = \frac{11.00}{0.70} = 15.714 \text{ m/s}$

$$F_1 = \frac{15.714}{\sqrt{9.81 \times 0.7}} = 6.0$$

$y_2 =$  equivalent sequent depth in a horizontal floor jump

$$= \frac{y_1}{2} \left[ -1 + \sqrt{1 + 8F_1^2} \right] = \frac{0.70}{2} \left[ -1 + \sqrt{1 + 8 \times (6)^2} \right]$$

$$= 5.6 \text{ m}$$

*Sequent depth* From Eq. 6.35 or from Fig. 6.13, corresponding to a value of  $\tan \theta = 0.15$

$$\frac{y_t}{y_2} = 1.63$$

$$y_t = \text{sequent depth in the inclined floor jump}$$

$$= 1.63 \times 5.6 = 9.13 \text{ m}$$

*Length of the jump*

From Fig. 6.14, corresponding to  $\tan \theta = 0.15$ ,  $m_s = 3.8$

By Eq. 6.37  $L_j = 3.8 (9.13 - 0.70) = 32.03 \text{ m}$

By Eq. 6.36  $L_j = 5.6(6.1 + 4.0 \times 0.15) = 37.52 \text{ m}$

An average value of  $L_j = 34.5 \text{ m}$  could be taken as the jump length.

*Energy loss*

Initial specific energy  $E_1 = y_1 \cos \theta + \frac{V_1^2}{2g}$

$$\cos \theta = 0.98893$$

$$E_1 = (0.7 \times 0.98893) + \frac{(15.714)^2}{2 \times 9.81} = 13.278 \text{ m}$$

(Note the small effect of the  $\cos \theta$  term on the energy.)

$$L_j \tan \theta = 34.5 \times 0.15 = 5.175 \text{ m}$$

$H_1 =$  total energy at Section 1 with the bed level at 2 as datum

$$= E_1 + L_j \tan \theta = 13.278 + 5.175 = 18.453 \text{ m}$$

$$H_2 = E_2 = y_2 \cos \theta + \frac{V_2^2}{2g}$$

$$H_2 = (9.24 \times 0.98893) + \frac{(11.0/9.24)^2}{2 \times 9.81}$$

$$= 9.210 \text{ m}$$

The energy loss

i.e.

$$\begin{aligned} E_L &= H_1 - H_2 \\ E_L &= (E_1 + L_j \tan \theta) - (E_2) \\ &= 18.453 - 9.210 = 9.243. \end{aligned}$$

Also

$$E_L / H_1 = \frac{9.243}{18.453} = 0.501 = 50.1\%$$

For a horizontal floor jump:

$$y_2 = 5.26 \text{ m}, y_1 = 0.70 \text{ m}$$

$$E_L = \frac{(y_2 - y_1)^3}{4y_1y_2} = \frac{(5.26 - 0.70)^3}{4 \times 0.7 \times 5.6} = 7.503 \text{ m}$$

$$E_1 = y_1 + V_1^2 / 2g = 13.286 \text{ m}$$

$$E_L / E_1 = \frac{7.503}{13.286} \times 100 = 56.48\%$$

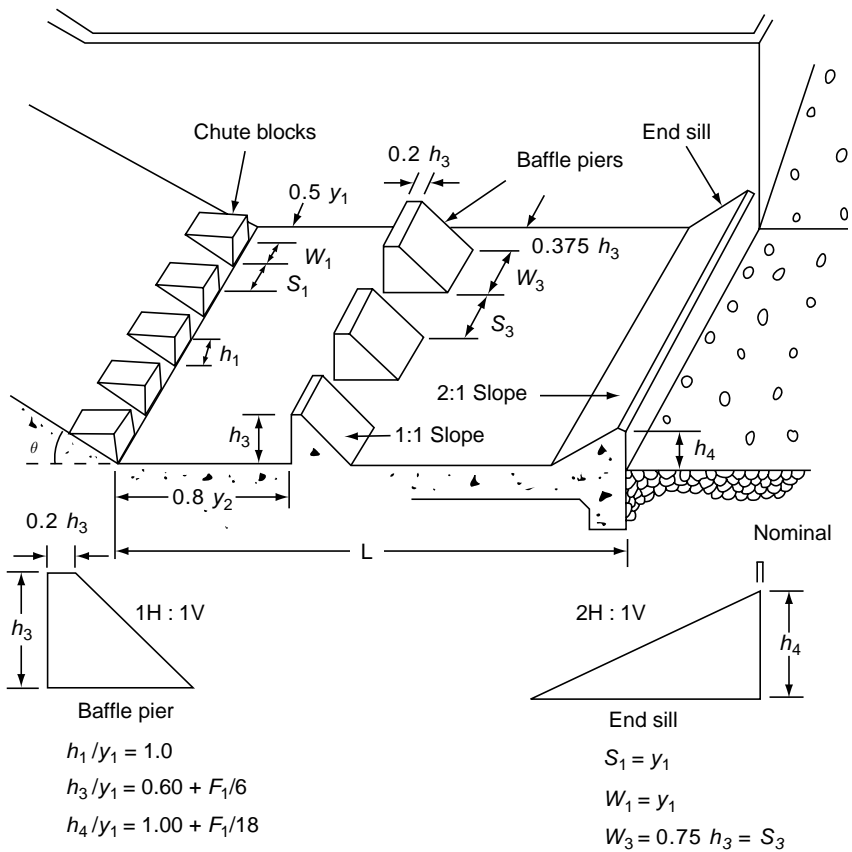
(Note that the relative energy loss in the sloping floor jump is referred to the total energy  $H_1$ .)

## 6.6 USE OF THE JUMP AS AN ENERGY DISSIPATOR

The high energy loss that occurs in a hydraulic jump has led to its adoption as a part of the energy-dissipator system below a hydraulic structure. The downstream portion of the hydraulic structure where the energy dissipation is deliberately allowed to occur so that the outgoing stream can safely be conducted to the channel below is known as a stilling basin. It is a fully-paved channel section and may have additional appurtenances, such as baffle blocks and sills to aid in the efficient performance over a wide range of operating conditions. Stilling basins are so designed that not only a good jump with high energy-dissipation characteristics is formed within the basin but it is also stable. For economic considerations the basin must be as small as practicable.

Designing a stilling basin for a given hydraulic structure involves considerations of parameters peculiar to the location of the structure in addition to the mechanics of flow. This feature makes the engineering design rely rather heavily on the experience of the designer. Model studies are usually resorted to arrive at an efficient design. To assist in the preliminary design, type designs are available.

The US Bureau of Reclamation has developed a series of type designs<sup>13</sup> and Fig. 6.16 shows details of one such design. This stilling basin is recommended for  $F_1 > 4.5$  and  $V_1 < 18$  m/s. Note the chute blocks to assist in splitting and aerating of flow; baffle blocks which offer additional resistance to flow; and the end sill which helps the outgoing stream to be lifted up into a trajectory so that the basin end is not subjected to scouring action. The effect of these appurtenances is to shorten the stilling basin length to  $2.7 y_2$  as against  $6.1 y_2$  required for a free unaided hydraulic jump. Also, the minimum tailwater depth required is  $0.83 y_2$  as against  $y_2$  for an unaided jump. Further details on energy dissipators are available in References 13 and 3.



Tailwater depth =  $0.83 y_2$  (min)

=  $1.00 y_2$  (recommended)

$$y_2/y_1 = \frac{1}{2} \left( -1 + \sqrt{1 + 8 F_1^2} \right)$$

$F_1 \geq 4.5$  and  $V_1 < 18.0$  m/s

Fig. 6.16 USBR-type III stilling basin (after Bradley and Peterka, paper no. 1403, Reference 13)

### 6.7 LOCATION OF THE JUMP

A hydraulic jump is formed whenever the momentum equation (Eq. 6.1) is satisfied between the supercritical and subcritical parts of a stream. In connection with GVF calculations it has already been indicated that the control for supercritical flows is at the upstream end and for subcritical flows the control is at the downstream end. Thus if a jump exists in a stretch of a channel, its location will satisfy three requirements, viz. (a) the inlet depth  $y_1$  is part of the upstream GVF profile, (b) the sequent depth  $y_2$  is part of the downstream GVF profile, and (c) the depths  $y_1$  and  $y_2$  satisfy the momentum equation and are separated by a distance  $L_j$ . The procedure for locating the jump by satisfying the above requirements is illustrated with the help of an example.

Consider a sluice gate acting as an upstream control (point  $A$ ) and the pool elevation (point  $P$ ) acting as a downstream control in a mild-slope channel (Fig. 6.17). The algorithm for the location of the jump by graphical or numerical computation procedure is as follows:

1. Starting from point  $A$ , compute the GVF profile  $ABC$ . Point  $C$  is the critical depth.
2. Calculate the sequent-depth  $CB'A'$  in which every point  $B'$  is sequent to a point  $B$  vertically below it on the curve  $ABC$ . This curve is obtained by using the appropriate form of the general momentum equation (Eq. (6.1)). For a rectangular channel of very small slope, if depth at  $B = y_1$ , depth at  $B' = y_2 = (y_1 / 2) \left[ -1 + \sqrt{1 + 8F_1^2} \right]$ .
3. Noting that  $L_j / y_2 = f(F_1)$ , compute  $L_j$  for each point on the curve  $CB'A'$  and shift the curve by displacing each point in the downstream direction by respective  $L_j$  values. The resulting curve is  $CDE$ .
4. Starting from  $P$ , compute the  $M_2$  profile, curve  $PDQ$ .
5. The intersection of the curve  $PDQ$  with  $CDE$  (point  $D$ ) gives the downstream end of the jump. The toe of the jump, point  $B$ , is located by drawing a horizontal line from  $D$  to cut  $CB'A'$  at  $B'$  and then a vertical from  $B'$  to cut the curve  $ABC$  at  $B$ .

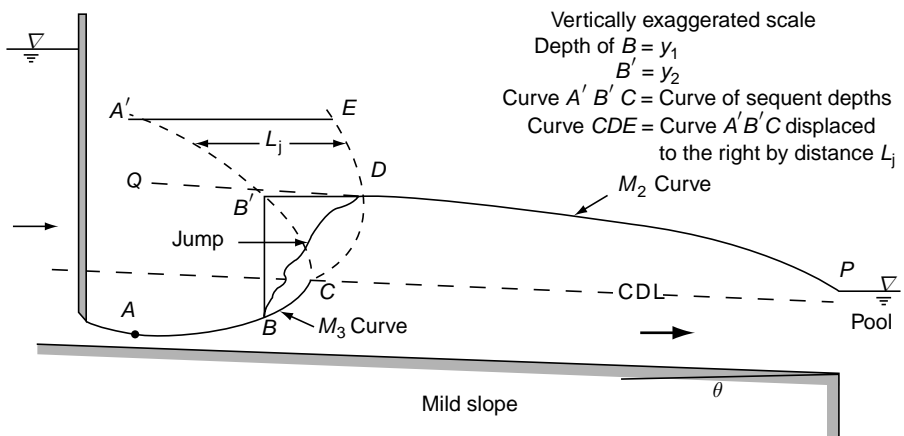


Fig. 6.17 Location of a hydraulic jump

In numerical computations the same principle as above can easily be incorporated. Note that this procedure gives direct determination of the end points of a jump and the method is general and can be applied in a wide variety of jump situations.

In the example described above, the subcritical water surface profile  $M_2$  was a particular GVF profile which depended upon the downstream control. Depending on the control, it could be an  $M_1$  profile also. If instead of a local control, a very long channel would have given a friction control which would ensure uniform flow with the normal depth being controlled by the friction of the channel. The depth downstream of a hydraulic structure, such as a sluice gate, controlled by the downstream channel or local control is known as *tailwater depth*.

Tailwater level plays a significant role in the formation of the jump at a particular location. Consider a flow from a sluice gate of opening  $a$  [Fig. 6.18(a)]. The depth at the vena contracta is  $y_a$ . Let the depth sequent to  $y_a$  be  $y_2$ . Let the tailwater level be  $y_t$ . Depending upon the relative values of  $y_2$  and  $y_t$  two basic types of jumps can be identified.

When  $y_t = y_2$ , a hydraulic jump will form at the vena contracta. Also if  $y_t < y_2$ , the jump is repelled downstream of the vena contracta through an  $M_3$  curve. The depth at the toe of the jump  $y_1$  will be larger than  $y_a$  and the sequent depth  $y_{12} = y_1$  [Fig. 6.18(b)]. Such a jump is known as *repelled jump*. Jumps with sequent depth equal to or less than  $y_2$  are known as *free jumps*, indicating that the supercritical stream before the jump is not affected by tailwater. The procedure indicated at the beginning of this section can be used to locate the position of a free jump.

If however the tailwater is larger than  $y_2$  [Fig. 6.18(c)] the supercritical stream is submerged and the resulting jump is called *submerged* or *drowned* jump. The ratio,  $\frac{y_t - y_2}{y_2} = S$  is called *submergence factor* and influences the characteristics of submerged jump considerably<sup>3</sup>. Generally, the energy dissipation in a submerged jump is smaller than that in a corresponding free jump.

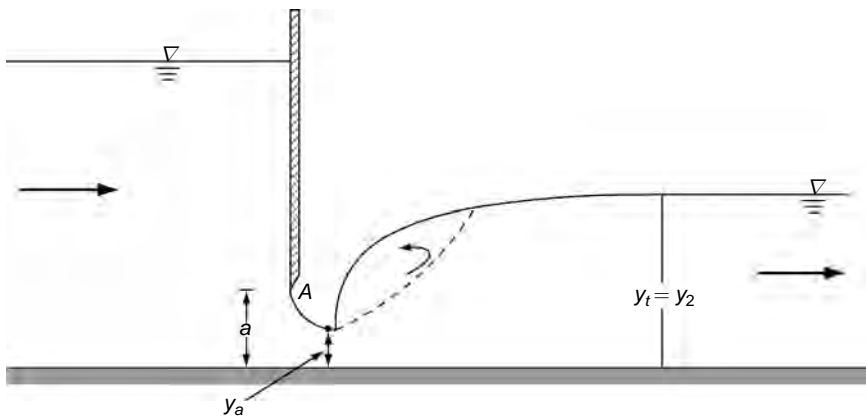


Fig. 6.18 (a) Free jump at vena contracta, ( $y_t = y_2$ )

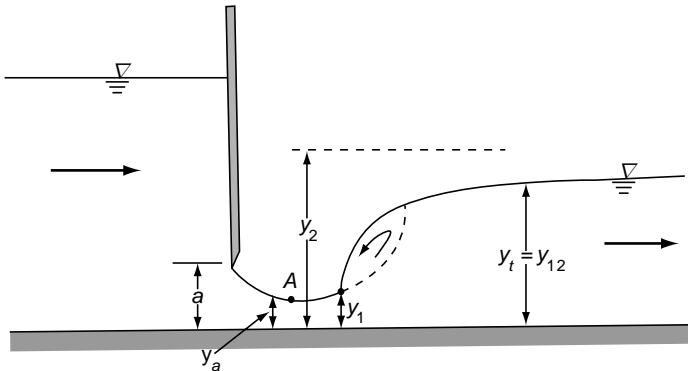


Fig. 6.18 (b) Free repelled jump, ( $y_t < y_2$ )

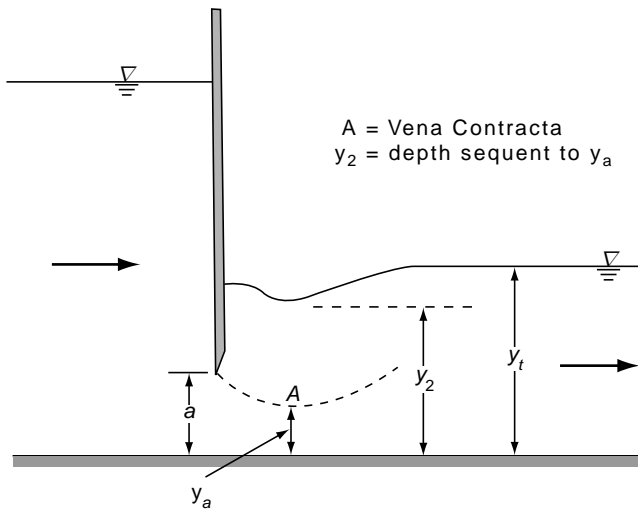


Fig. 6.18 (c) Submerged jump, ( $y_t < y_2$ )

**Example 6.11** A sluice gate in a 3.0-m wide rectangular, horizontal channel releases a discharge of  $18.0 \text{ m}^3/\text{s}$ . The gate opening is 0.67 m and the coefficient of contraction can be assumed to be 0.6. Examine the type of hydraulic jump formed when the tailwater is (i) 3.60 m (ii) 5.00 m, and (iii) 4.09 m.

**Solution** Let A be the section of vena contracta (Fig. 6.17).

$$y_a = \text{depth at vena contracta} = 0.67 \times 0.6 = 0.40 \text{ m}$$

$$V_a = 18.0 / (3.0 \times 0.4) = 15.0 \text{ m/s}$$

$$F_a = \text{Froude number at vena contracta} = \frac{V}{\sqrt{g y_a}}$$

$$F_a = \frac{15.0}{\sqrt{9.81 \times 0.4}} = 7.573$$

If  $y_2$  = Sequent depth required for a jump at vena contracta

$$\begin{aligned} \frac{y_2}{y_a} &= \frac{1}{2} \left[ -1 + \sqrt{1 + 8F_a^2} \right] \\ &= \frac{1}{2} \left[ -1 + \sqrt{1 + 8 \times (7.573)^2} \right] = 10.22 \\ y_2 &= 10.22 \times 0.40 = 4.09 \text{ m} \end{aligned}$$

1. When the tailwater depth  $y_t = 3.60$  m,  
Since  $y_t < y_2$ , a free, *repelled jump* will form.

$$V_t = \frac{18.0}{3.0 \times 3.60} = 1.667 \text{ m/s}$$

$$F_t = \frac{1.667}{\sqrt{9.81 \times 3.60}} = 0.281$$

The depth at the toe of this repelled jump  $y_1$  is given by

$$\begin{aligned} \frac{y_1}{y_t} &= \frac{1}{2} \left[ -1 + \sqrt{1 + 8F_t^2} \right] \\ \frac{y_1}{3.60} &= \frac{1}{2} \left[ -1 + \sqrt{1 + 8 \times (0.281)^2} \right] = 0.1387 \\ y_1 &= 0.50 \text{ m} \end{aligned}$$

An  $M_3$  curve will extend from Section A ( $y_a = 0.40$  m) to Section 1 ( $y_1 = 0.50$  m).

2. When the tailwater depth  $y_t = 5.0$  m.  
Since  $y_t > y_2$ , a submerged jump will occur.
3. When  $y_t = 4.09$ ,  $y_t = y_2$  and a free jump will occur at Section 1 with  $y_t = y_a = 0.40$  m.

**Example 6.12** | The flow in a wide rectangular channel of bed slope  $S_0 = 0.0005$  and  $n = 0.020$  is controlled at the upstream end by a sluice gate. At a certain time the sluice gate was adjusted to discharge  $7.0 \text{ m}^3/\text{s}$  per metre width of the channel with a depth of  $0.40$  m at the vena contracta. Find the location of the jump and the sequent depth.

**Solution** Refer to Fig. 6.19. Sequent depth after the jump =  $y_2$  = tailwater depth.

$$y_0 = \left( \frac{qn}{\sqrt{S_0}} \right)^{3/5} = \left( \frac{7.0 \times 0.020}{\sqrt{0.0005}} \right)^{3/5} = 3.00 \text{ m}$$

$$y_0 = y_2 = 3.00 \text{ m}$$

$$F_2 = \frac{q}{y_2 \sqrt{g y_2}} = \frac{7.0}{3.0 \sqrt{9.81 \times 3.0}} = 0.429$$

$$\frac{y_1}{y_2} = \frac{1}{2} \left( -1 + \sqrt{1 + 8F_2^2} \right) = \frac{1}{2} \left( -1 + \sqrt{1 + 8 \times (0.429)^2} \right) = 0.286 \text{ m}$$

$$y_1 = 0.286 \times 3.0 = 0.86 \text{ m}$$

Length of the jump =  $L_j = 6.1 \times 3.00 = 18.00 \text{ m}$

There will be an  $M_3$ -type GVF profile from the vena contracta to the toe of the jump and this is evaluated by the direct step method.

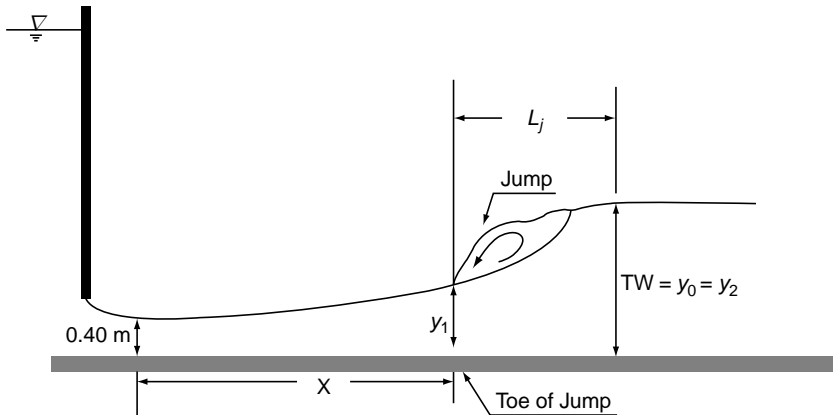


Fig. 6.19 Schematic sketch of Example 6.12

Computation of Flow Profile by Direct Step Method—Example 6.12

Wide Rectangular Channel				$S_0 = 0.0005$	$n = 0.020$	$q = 7.0 \text{ m}^3/\text{s}/\text{m}$				
Sl. No.	Depth $y$ (m)	Velocity $V$ (m/s)	$V^2/2g$	Specific Energy $E$ (m)	$\Delta E$ (m)	$S_f$	$\bar{S}_f$	$\bar{S}_f - S_0$	$\Delta x$ (m)	$x$ (m)
1	0.40	17.50	15.610	16.01		0.4156				0.0
2	0.50	14.00	9.990	10.49	-5.52	0.1976	0.30660	-0.3061	18.0	18.0
3	0.60	11.67	6.937	7.54	-2.95	0.1076	0.15257	-0.1521	19.4	37.4
4	0.70	10.00	5.097	5.80	-1.74	0.0644	0.08597	-0.0855	20.4	57.8
5	0.80	8.75	3.902	4.70	-1.09	0.0412	0.05280	-0.0523	20.9	78.7
6	0.86	8.14	3.377	4.24	-0.47	0.0324	0.03682	-0.0363	12.8	91.6

The toe of the jump is at a distance of 91.6 m from the vena contracta of the jet issuing from the sluice gate.





## REFERENCES

1. Bradley, J N and Peterka, A J 'The Hydraulic Design of Stilling Basins, Hydraulic Jumps on a Horizontal Apion', *J. of Hyd. Div., Proc. ASCE*, Paper No. 1401, October 1957, pp 1401–1–25.
2. Swamee, P K and Rathie, P N, 'Exact Solutions of Sequent Depth Problems', *J. of Irr. and Drainage Engg.*, Vol. 130, No. 6, Nov.-Dec. 2004, pp. 520–522.
3. Elevatorski, E A, *Hydraulic Energy Dissipators*, McGraw-Hill, New York, 1959.
4. Rajaratnam, N, 'Hydraulic Jumps', Chapter in *Advances in Hydrosience*, ed. Chow, V T Vol. 4, Academic Press, New York, 1967, pp 198–280.
5. Subramanya, K, 'Some Studies on Turbulent Wall Jets in Hydraulic Engineering', *Ph. D. thesis*, Univ. of Alberta, Edmonton, Canada, Oct. 1967.
6. Rajaratnam, N and Subramanya, K, 'Profile of the Hydraulic Jump', *J. of Hyd. Div., Proc. ASCE*, Paper No. 5931, May 1968, pp 663–673.
7. Leutheusser, H J and Kartha, V C 'Effects of Inflow Condition on Hydraulic Jump', *J. of Hyd. Div., Proc. ASCE*, Paper No. 9088, Aug 1972, pp 1367–1385.
8. Silvester, R, 'Hydraulic Jumps in all Shapes of Horizontal Channels', *J. of Hyd. Div., Proc. ASCE*, Jan. 1964, pp 23–55.
9. Argyropoulos, P A, 'Theoretical and Experimental Analysis of the Hydraulic Jump in a Sloping Parabolic Flume', *Proc. IAHR*, Lisbon, Vol. 2, 1957, pp D. 12–1–20.
10. Argyropoulos, P A, 'The Hydraulic Jump and the Effect of Turbulence on Hydraulic Structures', *Proc. IAHR*, Durbrovnik, Yugoslavia, 1961, pp 173–183.
11. Bradley, J N and Peterka, A J 'Hydraulic Design of Stilling Basin: Stilling Basin with Sloping Apron (Basin, V)', *J. of Hyd. Div., Proc. ASCE*, Paper No. 1405, Oct. 1957, pp 1405–1–32.
12. Henderson, F M *Open Channel Flow*, Macmillan, New York, 1966.
13. Bradley, J N and Peterka, A J 'Hydraulic Design of Stilling Basins' in Symposium on Stilling Basins and Energy Dissipators', *ASCE, Proc. Symp. Series No. 5*, Paper Nos. 1401 to 1406, June 1961, pp 1401–1 to 1406–17 (also in *J. of Hyd. Div., Proc. ASCE*, Vol. 83, No. HY 5, Oct. 1957).
14. Forster, J W and Skrinde, R A 'Control of the Hydraulic Jump by Sills', *Trans. ASCE*, Vol. 115, 1950, pp 973–1022.
15. Hsu, E Y, 'Discussion on: Control of the Hydraulic Jump by Sills', *Trans. ASCE*, Vol. 115, 1950, pp 988–991.
16. Moore, W L, and Morgan, C W 'Hydraulic Jump at an Abrupt Drop'. *Trans. ASCE*, Vol. 124, 1959, pp 507–524.
17. Harleman, D R F, 'Effect of Baffle Piers on Stilling Basin Performance', *J. of Boston Soc. of Civil Engineers*, Vol. 42, 1955, pp 84–89.
18. Koloseus, H J and Ahmad, D 'Circular Hydraulic Jump', *J. of Hyd. Div., Proc. ASCE*, Jan. 1969, pp 409–422.
19. Arbbabhirama, A and Wan, W C 'Characteristics of a Circular Jump in a Radial Wall Jet' *J. of Hyd. Res., IAHR*, Vol. 13, No. 3, 1973, pp 239–262.
20. Lewson, J D and Phillips, B C 'Circular Hydraulic Jump', *J. of Hyd. Engg., ASCE*, Vol. 109, No. 4, April, 1983, pp 505–518.
21. Arbbabhirama, A and Abella, U 'Hydraulic Jump with a Gradually Expanding Channel', *J. of Hyd. Div., Proc ASCE*, Jan. 1971, pp 31–42.
22. Khalifa, A M and McCorquodale, J A 'Radial Hydraulic Jump', *J. of Hyd. Div., Proc, ASCE*, Sept. 1979, pp 1065–1078.

## PROBLEMS

Problem Distribution

Topic	Problems
1. Elements of jump in a rectangular channel	6.1–6.10
2. Jump below a sluice gate	6.11, 6.23, 6.24, 6.31, 6.32
3. Jump below an overflow spillway	6.12–6.14
4. Jump at an abrupt rise	6.15, 6.30
5. Jump at a sudden drop	6.16
6. Jump on a sloping floor	6.17, 6.25, 6.27
7. Jump in non-rectangular channels	6.18–6.22, 6.26
8. Location of the jump	6.23, 6.24
9. Forced hydraulic jump	6.28
10. Circular hydraulic jump	6.29
11. Repelled jump	6.31, 6.32

(Unless otherwise stated the channel is assumed to be frictionless for purposes of hydraulic jump calculations.)

- 6.1 A hydraulic jump occurs in a horizontal rectangular channel with sequent depths of 0.70 m and 4.2 m. Calculate the rate of flow per unit width, energy loss and the initial Froude number.
- 6.2 A hydraulic jump occurs in a horizontal rectangular channel at an initial Froude number of 10.0. What percentage of initial energy is lost in this jump?
- 6.3 The following table gives some of the possible types of problems associated with a hydraulic jump occurring in a rectangular channel. Complete the following table.  
(Note that Problem 6.3(c) requires a trial-and-error approach. Assume  $F_1$ , find  $y_1$ ,  $y_2$  and check  $E_L$ . Repeat till satisfactory values are obtained.)

Prob. No.	$V_1$ (m/s)	$y_1$ (m)	$q$ (m <sup>2</sup> /s/m)	$F_1$	$y_2$ (m)	$V_2$ (m/s)	$F_2$	$E_L$ (m)	$E_L/E_1$ (%)
a		0.170			1.84				
b				9.00				2.90	
c			2.00					1.75	
d					1.60	0.90			
e	13.50	0.350							
f							0.15	8.00	

- 6.4 A hydraulic jump in a rectangular channel has the Froude number at the beginning of the jump  $F_1 = 5$ . Find the Froude number  $F_2$  at the end of the jump.
- 6.5 Show that the Froude numbers  $F_1$  and  $F_2$  in a hydraulic jump occurring in a rectangular channel are related by

$$(a) F_2^2 = \frac{8F_1^2}{(-1 + \sqrt{1 + 8F_1^2})^3} \quad (b) F_1^2 = \frac{8F_2^2}{(-1 + \sqrt{1 + 8F_2^2})^3}$$

- 6.6 A rectangular channel carrying a supercritical stream is to be provided with a hydraulic jump type of energy dissipator. If it is desired to have an energy loss of 5 m in the jump when the inlet Froude number is 8.5, determine the sequent depths.
- 6.7 Show that in a hydraulic jump formed in a horizontal, frictionless, rectangular channel the energy loss  $E_L$  relative to the critical depth  $y_c$  can be expressed as

$$\left(\frac{E_L}{y_c}\right)^3 = \frac{(a-1)^9}{32(a+1)a^4}$$

where  $a = \text{sequent-depth ratio} = y_2/y_1$ .

- 6.8 In a hydraulic jump occurring in a horizontal, rectangular channel it is desired to have an energy head loss equal to 6 times the supercritical flow depth. Calculate the Froude number of the flow necessary to have this jump.
- 6.9 In a hydraulic jump taking place in a horizontal, rectangular channel a sequent-depth ratio of 10 is desired. What initial Froude number would produce this ratio? What would be the Froude number after the jump?
- 6.10 In a hydraulic jump taking place in a horizontal rectangular channel the discharge intensity and head loss are found to be  $4.7 \text{ m}^3/\text{s}/\text{m}$  and  $6.0 \text{ m}$  respectively. Determine the sequent depths of the jump.
- 6.11 Water from a low dam is released through a sluice gate on a horizontal rectangular channel. The depth of water upstream of the sluice gate is  $16.0 \text{ m}$  above the channel bed and the gate opening is  $1.5 \text{ m}$ . The sluice gate can be assumed to be sharp-edged. If a free hydraulic jump is formed just downstream of the gate, find the sequent depths and the percentage of the initial energy lost in the jump.
- 6.12 An overflow spillway has its crest at elevation  $125.40 \text{ m}$  and a horizontal apron at an elevation of  $95.00 \text{ m}$  on the downstream side. Find the tailwater elevation required to form a hydraulic jump when the elevation of the energy line is  $127.90 \text{ m}$ . The  $C_d$  for the flow can be assumed as  $0.735$ . The energy loss for the flow over the spillway face can be neglected.
- 6.13 In Problem 6.12 if the tailwater elevation is  $102.40 \text{ m}$ , what should be the elevation of the apron floor to cause the jump?
- 6.14 At the bottom of a spillway the velocity and depth of flow are  $12.0 \text{ m/s}$  and  $1.5 \text{ m}$  respectively. If the tailwater depth is  $5.5 \text{ m}$  find the location of the jump with respect to the toe of the spillway. What should be the length of the apron to contain this jump? Assume the apron to be horizontal and Manning's  $n = 0.015$ .
- 6.15 A hydraulic jump is formed in a stilling basin created by a step of height  $\Delta Z$  in a rectangular horizontal channel as in Fig. 6.20. Assuming hydrostatic pressure distribution at Sections 1, 2 and 3, and normal hydraulic jump operation between Sections 1 and 2, show that

$$\left(\frac{y_3}{y_1}\right)^2 = 1 + 2F_1^2 \left(1 - \frac{y_1}{y_3}\right) + \frac{\Delta Z}{y_1} \left[\frac{\Delta Z}{y_1} + 1 - \sqrt{1 + 8F_1^2}\right]$$

(Note: Reference 14 gives details of this aspect of control of hydraulic jumps.)

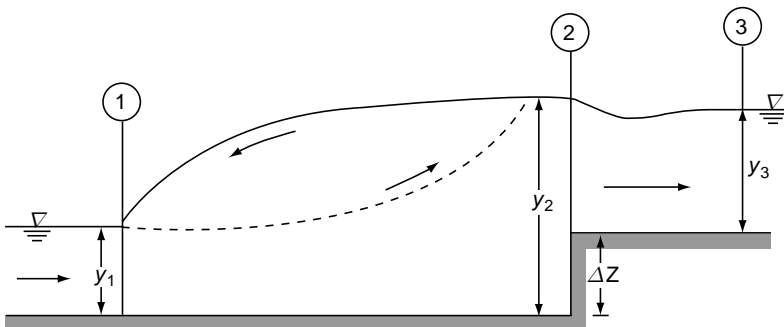


Fig. 6.20 Jump at an abrupt rise—Problem 6.15

6.16 When a hydraulic jump occurs at an abrupt drop in a rectangular channel, depending upon the relative step height  $\Delta Z/y_1$ , two distinct situations are possible as shown in Figs 6.21 and 6.22. Considering the reaction of the step as shown in Figs 6.21 and 6.22 show that, for the case A:

$$F_1^2 = \frac{\left(\frac{y_2}{y_1} - \frac{\Delta Z}{y_1}\right)^2 - 1}{2\left(1 - \frac{y_1}{y_2}\right)}$$

and for the case B:

$$F_1^2 = \frac{\left(\frac{y_2}{y_1}\right)^2 - \left(1 + \frac{\Delta Z}{y_1}\right)^2}{2\left(1 - \frac{y_1}{y_2}\right)}$$

(Note: This situation has been studied in detail by Hsu<sup>15</sup>, and Moore and Morgan<sup>16</sup>.)

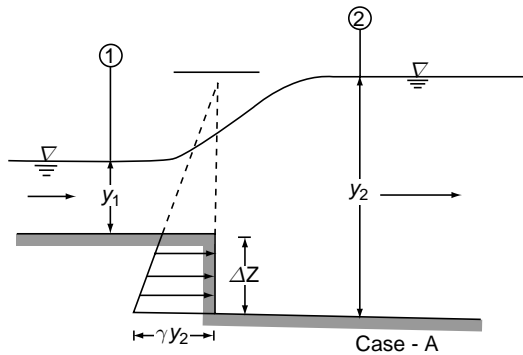


Fig. 6.21 Jump at a sudden drop—Problem 6.16, (Case A)

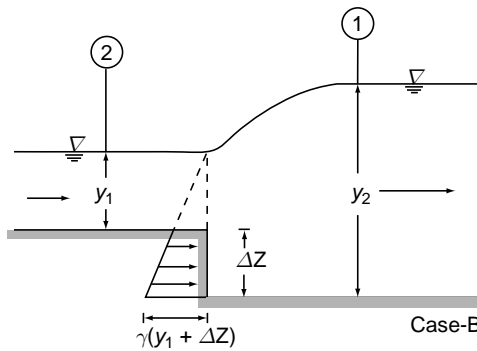


Fig. 6.22 Jump at a sudden drop—Problem 6.16, (Case B)

- 6.17 The Rihand dam in U.P., India, has a sloping apron stilling basin with a slope of 0.077. If the depth for a flood flow of 64.0 m<sup>3</sup>/s per metre width is 1.93 m, estimate the sequent depth, length of the jump and energy loss in the hydraulic jump.
- 6.18 A hydraulic jump occurs in a horizontal 90° triangular channel. If the sequent depths in this jump are 0.60 m and 1.20 m, estimate the flow rate and the Froude numbers at the beginning and end of the jump.
- 6.19 For a hydraulic jump taking place in a horizontal, frictionless, triangular channel show that the sequent depths  $y_1$  and  $y_2$  are related to the pre-jump Froude number  $F_1$  as

$$F_1^2 = \frac{2\eta^2(\eta^3 - 1)}{3(\eta^2 - 1)}$$

where  $\eta = y_2 / y_1$ .

- 6.20 A horizontal trapezoidal channel of 2.0-m bed width and side slopes 2 horizontal : 1 vertical carries a discharge of 6.225 m<sup>3</sup>/s at a depth of 0.20 m. If a hydraulic jump takes place in this channel, calculate the sequent depth and energy loss.
- 6.21 A trapezoidal channel of 7.0-m bottom width and side slope 1 horizontal : 1 vertical carries a discharge of 20 m<sup>3</sup>/s. Prepare the specific energy and specific-force diagrams for this channel. If the depth after a jump on a horizontal floor in this channel for the given discharge is known to be 2.25 m, find the sequent depth and energy loss. What are the limitations of the plots prepared by you? Can you think of a non-dimensional representation of the specific-force and specific-energy diagrams so that they can be used for jump computations in trapezoidal channels having a wide range of geometrical parameters and discharges?
- 6.22 A circular culvert of 1.5-m diameter carries a discharge of 1.0 m<sup>3</sup>/s. The channel can be assumed to be horizontal and frictionless. If the depth at the beginning of a hydraulic jump occurring in this channel is 0.30 m, determine sequent depth.
- 6.23 A sluice gate discharges 10.0 m<sup>3</sup>/s per meter width in to a wide rectangular channel of  $n = 0.025$  and bottom slope  $S_0 = 0.0002$ . The depth of flow at the vena contracta is 0.40 m. If the channel ends in a sudden drop at a distance of 1300 m downstream of the gate, locate the position of the jump.
- 6.24 The flow in a wide rectangular channel of bed slope  $S_0 = 0.0008$  and  $n = 0.025$  is controlled at the upstream end by a sluice gate. The sluice gate is adjusted to discharge 8.0 m<sup>3</sup>/s per meter width of the channel, with a depth of 0.50m at the vena contracta Find the location of the jump and the sequent depth
- 6.25 A wide rectangular steep channel ( $\tan \theta = 0.20$ ) has a horizontal apron. Find the maximum tailwater depth that will have a jump completely in a horizontal apron when a discharge of 2.47 m<sup>3</sup>/s per metre width passes down the steep channel at a depth of 0.30 m. What tailwater depth will cause the jump to occur completely on the sloping channel?
- 6.26 Prepare a plot of  $E_L / E_1$  vs  $F_1$  for rectangular, parabolic and triangular horizontal channels using Eqs (6.23) and (6.24). Observe that the highest relative energy loss occurs in a triangular channel.
- 6.27 (a) Show that the relative energy loss in a hydraulic jump occurring on a sloping rectangular channel is

$$\frac{E_L}{H_1} = \frac{\cos \theta \left( 1 - \frac{y_t}{y_1} \right) + \frac{F_1^2}{2} \left[ 1 - \left( \frac{y_1}{y_t} \right)^2 \right] + \left( \frac{L}{y_t} \frac{y_t}{y_1} \right) \tan \theta}{\cos \theta + \frac{F_1^2}{2} + \left( \frac{L}{y_t} \frac{y_t}{y_1} \right) \tan \theta} = f(F_1, \theta)$$

where  $H_1 =$  total energy referred to the bed at the end of the jump as datum and  $F_1 = V_1 / \sqrt{gy_1}$ .

(b) Analyse  $E_L$  and show that the magnitude of energy loss is larger in a sloping-channel jump as compared to the loss in a corresponding horizontal-channel case.

6.28 Baffles are provided in stilling basins to introduce an additional drag force on the flow.

(a) Figure 6.23 (a) shows a baffle wall placed in a horizontal rectangular channel jump.

The drag force per unit length of the baffle wall can be expressed as  $P_B = C_D \frac{\rho V_1^2}{2} h$

in which  $C_D =$  drag coefficient. Show that the sequent-depth ratio  $y_2 / y_1$  for this case is related as

$$\left[ 2F_1^2 - \frac{y_2}{y_1} \left( 1 + \frac{y_2}{y_1} \right) \right] = \frac{C_D F_1^2 (h / y_1)}{(1 - y_1 / y_2)}$$

(b) Figure 6.23(b) shows a jump assisted by baffle blocks. Write the momentum equation to this case. (References 17 and 4 contain information on the role of baffles in the stilling-basin performance).

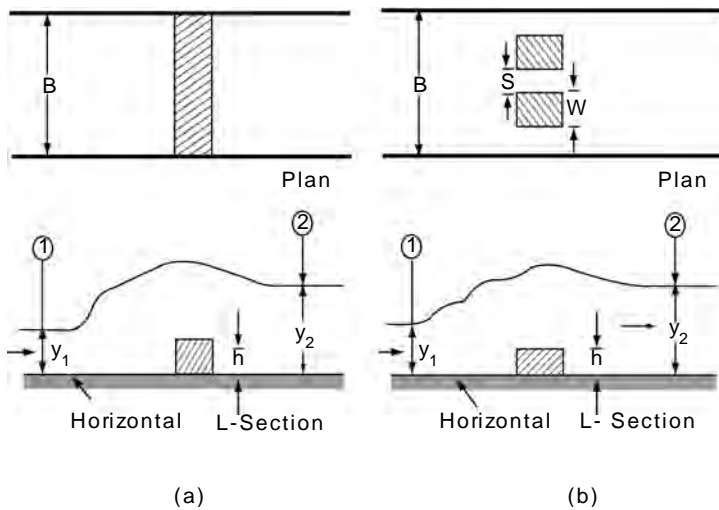


Fig. 6.23 (a) Jump assisted by a baffle wall—Problem 6.28 (a)  
 (b) Jump assisted by baffle blocks—Problem 6.28 (b)

6.29 A vertical jet of water striking a horizontal surface spreads out radially and can form a circular hydraulic jump under proper tailwater conditions. Figure 6.24 is a definition sketch for such a circular jump. Use momentum and continuity equations to get

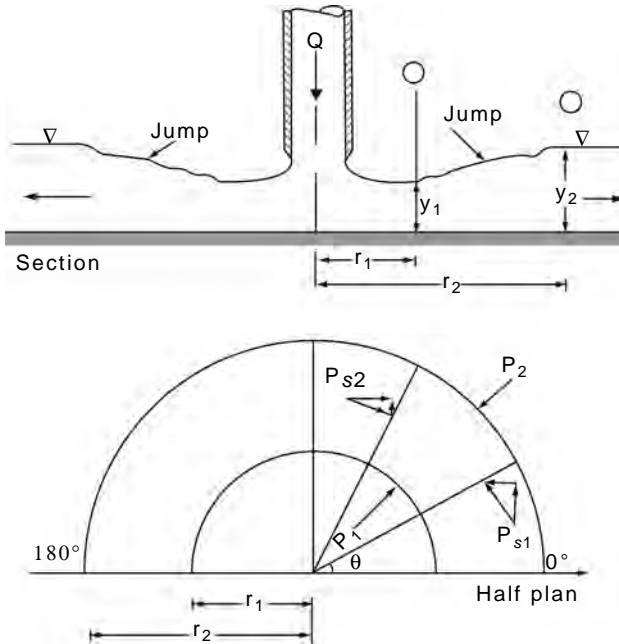


Fig. 6.24 Circular hydraulic jump—Problem 6.29

$$\left[1 - RY^2\right] + \frac{1}{3}(R - Y)(1 + Y + Y^2) = \frac{2F_1^2}{RY}(1 - RY)$$

in which  $R = r_2/r_1$ ,  $F_1^2 = \frac{V_1^2}{gy_1}$  and  $Y = \frac{y_2}{y_1}$

**Hint:** Consider a small element of the jump of angular width  $d\theta$  as in Fig. 6.22 and apply momentum and continuity equations in the  $x$ -direction. The major difference between the jump in a prismatic rectangular channel and the present case of circular jump is that in the present case the hydrostatic forces on the two walls of the element have a net component in the  $x$ -direction. To evaluate this, one requires the profile of the jump. One of the common assumptions is to assume the profile to be linear. In the present case also assume the profile of the jump to be a straight line.

[Note: References 18, 19 and 20 can be consulted for details on circular hydraulic jumps. The same equation applies to a jump in a gradually expanding rectangular channel details of which are available in references 21 and 22.]

- 6.30 A discharge of 6.65 m<sup>3</sup>/s per metre width from a low spillway enters a horizontal apron at a depth of 0.5 m. The tailwater depth is 3.0 m. Determine the depth of depression of the stilling basin below the original stream bed necessary to ensure that a hydraulic jump will form in the stilling basin.
- 6.31 Water flows from under a sluice gate into a wide rectangular channel having a bed slope of 0.0001. The gate opening is such that the discharge rate is 6.0 m<sup>3</sup>/s/metre width. Determine whether a free hydraulic jump can occur and if so determine its sequent depths when the depth at the vena contracta is (i) 0.50 m and (ii) 0.40 m. Assume Manning's  $n = 0.015$ .

- 6.32 An opening of a reservoir is controlled by a sluice gate. The gate opening is 1.30 m. Water surface elevation upstream of the gate is 100.00 m. If the elevation of the bed is 85.00 m and the tailwater elevation is 91.00 m.
- What is the discharge per unit width?
  - What kind of jump is formed? What are the sequent depths?
  - What is the maximum tailwater depth that could be sustained by a free jump? (Assume  $C_c = 0.75$  and  $C_d = 0.71$  for the sluice gate).

## § OBJECTIVE QUESTIONS

- The hydraulic jump is a phenomenon
  - in which the water surface connects the alternate depths
  - which occurs only in frictionless channels
  - which occurs only in rectangular channels
  - none of these
- A hydraulic jump occurs when there is a break in grade from a
  - mild slope to steep slope
  - steep slope to mild slope
  - steep slope to steeper slope
  - mild slope to milder slope
- The sequent-depth ratio in a hydraulic jump formed in a horizontal rectangular channel is 16.48. The Froude number of the supercritical stream is
  - 8.0
  - 4.0
  - 20
  - 12.0
- The Froude number of a subcritical stream at the end of a hydraulic jump in a horizontal rectangular channel is 0.22. The sequent-depth ratio of this jump is.
  - 11.25
  - 15.25
  - 8.35
  - 6.50
- If the Froude number of a hydraulic jump is 5.50, it can be classified as
  - an oscillating jump
  - a weak jump
  - a strong jump
  - a steady jump
- The initial depth of a hydraulic jump in a rectangular channel is 0.2 m and the sequent-depth ratio is 10. The length of the jump is about
  - 4 m
  - 6 m
  - 12 m
  - 20 m
- In a hydraulic jump taking place in a horizontal rectangular channel the sequent depths are 0.30 m and 1.50 m respectively. The energy loss in this jump is
  - 1.92 m
  - 1.50 m
  - 0.96 m
  - 1.20 m
- Seventy per cent of the initial energy is lost in a jump taking place in a horizontal rectangular channel. The Froude number of the flow at the toe is
  - 4.0
  - 9.0
  - 20.0
  - 15.0
- In a hydraulic jump occurring in a horizontal rectangular channel with an initial Froude number of 12, the sequent depth ratio is found to be 13.65. The energy dissipation as a percentage of the initial specific energy is about
  - 62%
  - 50%
  - 87%
  - 73%
- The concept of constancy of specific force at the beginning and the end of a jump
  - assumes horizontal frictionless channel
  - is valid for jumps in a rectangular sloping floor basin
  - is valid for all kinds of channels provided the friction can be assumed to be negligibly small
  - assumes constancy of specific energy



- 6.11 A sluice gate discharges a flow with a depth of  $y_1$  at the vena contracta.  $y_2$  is the sequent depth corresponding to  $y_1$ . If the tailwater depth  $y_t$  is larger than  $y_2$  then
- (a) a repelled jump occurs                      (b) a free jump occurs  
 (c) a submerged jump takes place              (d) no jump takes place
- 6.12 If  $y_2$  = sequent depth for a rectangular channel obtained by assuming horizontal frictionless channel in the momentum equation and  $y_{2a}$  = corresponding actual sequent depth measured in a horizontal rectangular channel having high friction, one should expect
- (a)  $y_2 > y_{2a}$               (b)  $y_2 = y_{2a}$               (c)  $y_2 < y_{2a}$               (d)  $y_2 \leq y_{2a}$
- 6.13 If the length of the jump in a sloping rectangular channel =  $L_{js}$  and the corresponding length of the jump in a horizontal rectangular channel having same  $y_1$  and  $F_1$  is  $L_j$ , then
- (a)  $L_j > L_{js}$               (b)  $L_{js} > L_j$               (c)  $L_j = L_{js}$               (d)  $L_j/L_{js} = 0.80$
- 6.14 If  $E_{LS}$  = energy loss in a jump in a sloping rectangular channel and  $E_{LH}$  = energy loss in a corresponding jump on a horizontal rectangular channel having the same  $y_1$  and  $F_1$ , then
- (a)  $E_{LH} = E_{LS}$               (b)  $E_{LH} > E_{LS}$               (c)  $E_{LH} < E_{LS}$               (d)  $E_{LH}/E_{LS} = 0.80$

# Rapidly Varied Flow-2

# 7

## 7.1 INTRODUCTION

Rapidly varied flows (RVP) are a class of flows which have high curvatures, a consequence of which is the presence of non-hydrostatic pressure distribution zones in a major part of the flow. Further, these flows are essentially local phenomenon in the sense friction plays a minor role. The hydraulic jump studied in Chapter 6 is an important RVF phenomenon. In this chapter a few steady, rapidly varied flow situations are discussed. Since a very wide variety of RVF problems occur in practice, an exhaustive coverage of all situations is not possible in a book of this nature and hence a few basic and important flow types are covered. The RVFs covered in this chapter are due to (i) sharp-crested weirs, (ii) overflow spillways, (iii) broad-crested weirs, (iv) end depths, (v) sluice gates, and (vi) culverts. Many of the RVFs studied here are used for flow measurement purposes.

## 7.2 SHARP-CRESTED WEIR

A weir is a structure built across a channel to raise the level of water, with the water flowing over it. If the water surface, while passing over the weir, separates at the upstream end and the separated surface jumps clear off its thickness, the weir is called a *sharp-crested weir*. It is also known as a *notch* or a *thin plate weir*. Sharp-crested weirs are extensively used as a fairly precise flow-measuring device in laboratories, industries and irrigation practice. The sharp-crested weirs used in practice are usually vertical metal plates with an accurately-machined upstream edge of thickness not exceeding 2.0 mm and a bevel of angle greater than  $45^\circ$  on the downstream face edge. The weirs come in many geometric shapes but the rectangular and triangular ones are the most commonly used.

### 7.2.1 Rectangular Weir

Figure 7.1 shows the definition sketch of flow over a sharp-crested rectangular weir. The water surface of the stream curves rapidly at the upstream of the weir and plunges down in a parabolic trajectory on the downstream. This surface is known as *upper nappe*. At the weir crest, the flow separates to have a free surface which

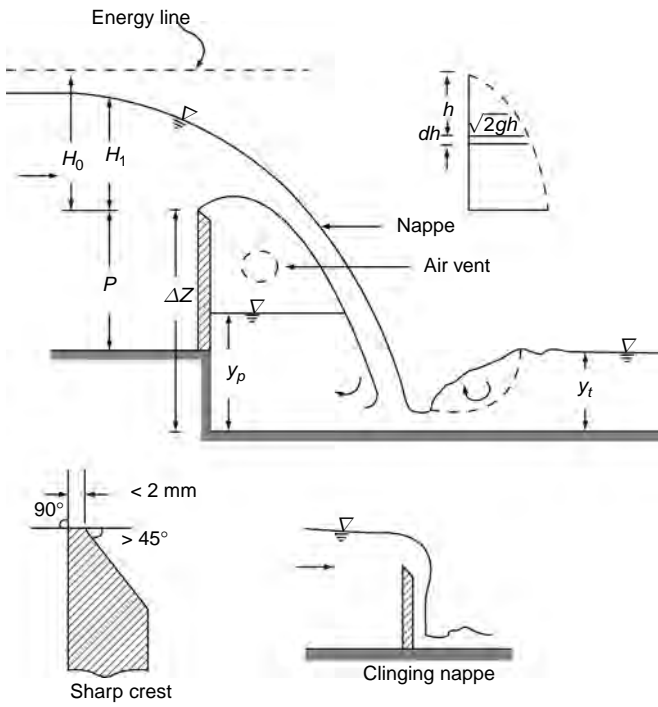


Fig. 7.1 Definition sketch of a sharp-crested weir

initially jumps up to a level higher than the weir crest before plunging down. This surface is known as *lower nappe*. If the weir extends to the full width of the channel, the lower nappe encloses a space having air initially at atmospheric pressure. As the flow proceeds for sometime, some of the air from this pocket is entrained by the moving water surfaces and the pressure in the air pocket falls below the atmospheric pressure. This in turn causes the nappe surfaces to be depressed. This change is a progressive phenomenon. A limiting case of the air pocket completely evacuated is a *clinging nappe* shown in Fig. 7.1. To maintain standardised conditions for flow measurement, the air pocket below the lower nappe should be kept at a constant pressure. The atmospheric pressure in this pocket is achieved through the provision of air vents. The weir flow as above assumes at tailwater level far below the crest and is termed *free flow*. A detailed description of nappe changes and its effects on flow measurement are available in literature<sup>1</sup>. Figures 7.2 and 7.3 show a fully aerated and non-aerated nappe respectively.

### 7.2.2 Discharge Equation

It is usual to derive the discharge equation for free flow over a sharp-crested weir by considering an ideal undeflected jet and to apply a coefficient of contraction to account for the deflection due to the action of gravity.

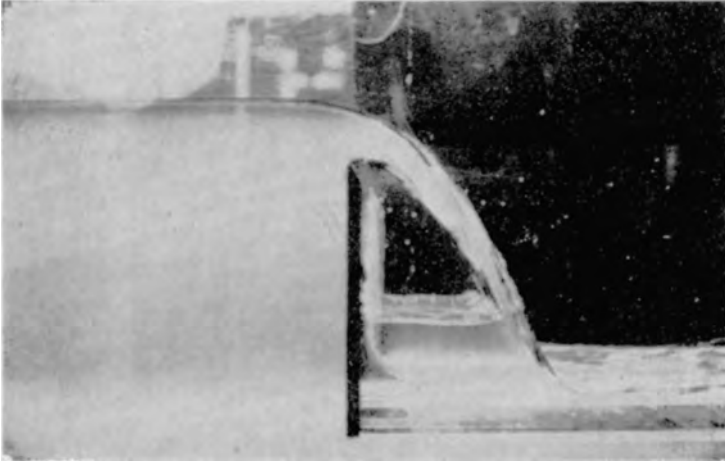


Fig. 7.2 Fully-aerated nappe (Courtesy: M G Bos)

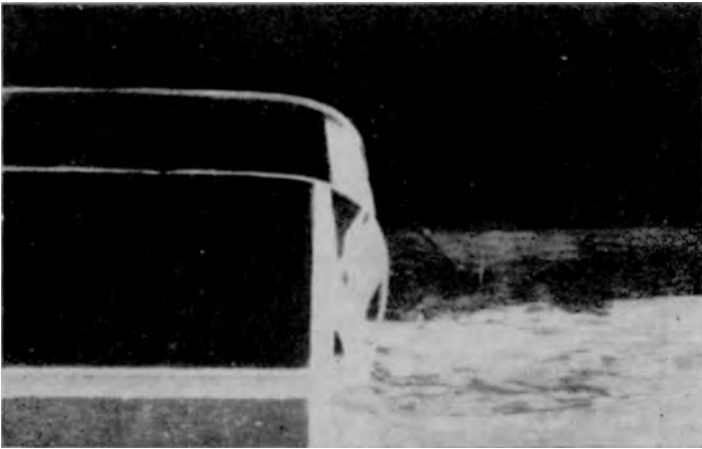


Fig. 7.3 Non-aerated nappe (Courtesy: M G Bos)

Thus for a rectangular weir of length  $L$  spanning the full width  $B$  of a rectangular channel (i.e.,  $L = B$ ), the ideal discharge through an elemental strip of thickness  $dh$  at a depth  $h$  below the energy line (Fig. 7.1), is given by

$$dQ_i = L\sqrt{2gh} \, dh \quad (7.1)$$

Thus the ideal discharge  $Q_i = L\sqrt{2g} \int_{\frac{V_0^2}{2g}}^{H_1 + \frac{V_0^2}{2g}} \sqrt{h} \, dh \quad (7.2)$

and the actual discharge  $Q = C_c Q_i$  (7.3)

in which  $C_c$  = coefficient of contraction.

Thus 
$$Q = \frac{2}{3} C_c \sqrt{2g} L \left[ \left( H_1 + \frac{V_0^2}{2g} \right)^{3/2} - \left( \frac{V_0^2}{2g} \right)^{3/2} \right]$$
 (7.4)

However, since Eq. 7.4 is rather inconvenient to use, the discharge equation is written in terms of  $H_1$ , the depth of flow upstream of the weir measured above the weir crest, as

$$Q = \frac{2}{3} C_d \sqrt{2g} L H_1^{3/2}$$
 (7.5)

where  $C_d$  = coefficient of discharge which takes into account the velocity of approach  $V_0$  and is given by

$$C_d = C_c \left[ \left( 1 + \frac{V_0^2}{2gH_1} \right)^{3/2} - \left( \frac{V_0^2}{2gH_1} \right)^{3/2} \right]$$
 (7.6)

In ideal fluid flow  $C_d = f(H_1/P)$  and this variation has been studied by Stretkoff<sup>2</sup>. In real fluid flow  $C_d$  should in general be a function of Reynolds number and Weber number, in addition to the weir height factor  $H_1/P$ . If Reynolds number is sufficiently large and if the head  $H_1$  is sufficiently high to make the surface tension effects negligible, the coefficient of discharge

$$C_d = f(H_1/P)$$

The variation of  $C_d$  for rectangular sharp-crested weirs is given by the well-known *Rehbock formula*

$$C_d = 0.611 + 0.08 \frac{H_1}{P}$$
 (7.7)

which is valid for  $H_1/P \leq 5.0$ .

### 7.2.3 Sills

For very small values of  $P$  relative to  $H_1$ , i.e., for  $\frac{H_1}{P} > 20$ , the weir acts as a sill placed at the end of a horizontal channel and as such is termed *sill*. Assuming that the critical depth  $y_c$  occurs at the sill

$$H_1 + P = y_c = \left( \frac{Q^2}{gB^2} \right)^{1/3}$$
 (7.8)

i.e. 
$$Q = B\sqrt{g} (H_1 + P)^{3/2} = \frac{2}{3} C_d \sqrt{2g} L H_1^{3/2} \quad (7.9)$$

and  $L = B$ ,  
the value of  $C_d$  from Eq. (7.9) works out to be

$$C_d = 1.06 \left( 1 + \frac{P}{H_1} \right)^{3/2} \quad (7.10)$$

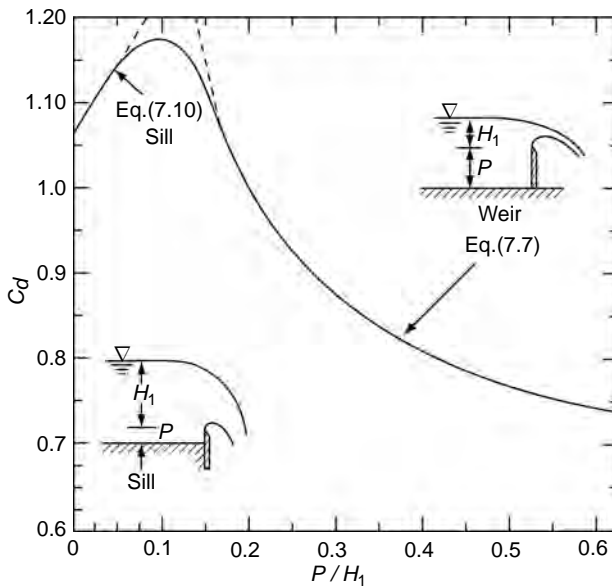


Fig. 7.4 Variation of  $C_d$  for weirs and sills

This relationship for  $C_d$  has been verified experimentally by Kandaswamy and Rouse<sup>3</sup>. The variation of  $C_d$  given by Eq. 7.7 for weirs and by Eq. 7.10 for sills is shown in Fig. 7.4.

In the intermediate region of weirs and sills (i.e.  $20 > H_1/P > 5$ ) the  $C_d$  values are expected to have a smooth transition from Eq. 7.7 to Eq. 7.10 as shown in Fig. 7.4.

A review of the effect of liquid properties on  $C_d$  is available in Ref. 1. Generally, excepting at very low heads, i.e.  $H_1 \lesssim 2.0$  cm, for the flow of water in rectangular channels, the effects of Reynolds number and Weber number on the value of  $C_d$  are insignificant. Thus for practical purposes, Eq. 7.7 and Eq. 7.10 can be used for the estimation of discharges. The head  $H_1$  is to be measured upstream of

the weir surface at a distance of about  $4.0 H_1$  from the weir crest. If weirs are installed for metering purposes, the relevant standard specifications (e.g. International Standards: ISO: 1438, 1979, Thin-plate weirs) must be followed in weir settings.

### 7.2.4 Submergence

In free flow it was mentioned that the tailwater level is far below the crest to affect the free plunging of the nappe. If the tailwater level is above the weir crest, the flow pattern would be much different from the free-flow case (Fig. 7.5). Such a flow is called *submerged flow*. The ratio  $H_2/H_1$  where  $H_2$  = downstream water-surface elevation above the weir crest, is called *submergence ratio*. In submerged flow, the discharge over the weir  $Q_s$  depends upon the submergence ratio. An estimation of  $Q_s$  can be made by use of Villemonte formula<sup>1,4</sup>

$$Q_s = Q_1 \left[ 1 - \left( \frac{H_2}{H_1} \right)^n \right]^{0.385} \quad (7.11)$$

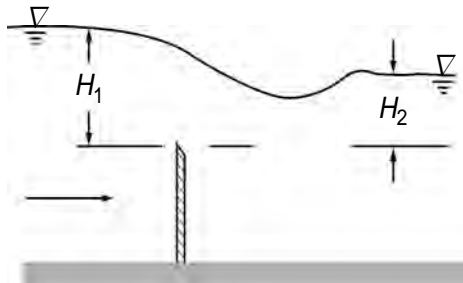


Fig. 7.5 Submerged sharp-crested weir

where  $Q_1$  = free-flow discharge under head  $H_1$ ,  $n$  = exponent of head in the head-discharge relationship  $Q = KH^n$ . For a rectangular weir,  $n = 1.5$ .

The minimum value of  $H_2/H_1$  at which the discharge under a given head  $H_1$  deviates by 1 per cent from the value determined by the free-flow equation is termed *modular limit* or *submergence limit*. In sharp-crested rectangular weirs the modular limit is negative, i.e. the submergence effect is felt even before the tailwater reaches the crest elevation. Thus to ensure free-flow it is usual to specify the tailwater surface to be at least 8 cm below the weir crest for small weirs. This minimum distance will have to be larger for large weirs to account for fluctuations of the water level immediately downstream of the weir due to any wave action.

### 7.2.5 Aeration Need of Rectangular Weir

The need for aeration of rectangular weirs spanning the full width of a channel was indicated in Sec. 7.2.1. The rate of air supply ( $Q_a$  in  $\text{m}^3/\text{s}$ ) required to completely meet the aeration need is given by<sup>5</sup>

$$\frac{Q_a}{Q} = \frac{0.1}{(y_p / H_1)^{3/2}} \quad (7.12)$$

in which  $Q$  = water discharge and  $y_p$  = water-pool depth on the downstream of the weir plate (Fig. 7.1). If a submerged hydraulic jump takes place,  $y_p$  can be estimated by the tailwater depth. On the other hand, for the case of a free jump occurring on the downstream,  $y_p$  can be estimated by the following empirical equation<sup>5</sup>

$$y_p = \Delta Z \left[ \frac{Q_2}{L^2 g (\Delta Z)^3} \right]^{0.22} \quad (7.13)$$

where  $\Delta Z$  = difference in elevation between the weir crest and the downstream floor (Fig. 7.1).

To cause air flow into the air pocket through an air vent, a pressure difference between the ambient atmosphere and the air pocket is needed. Assuming a maximum permissible negative pressure in the pocket (say 2 cm of water column), the size of the air vent can be designed by using the usual Darcy-Weisbach pipe flow equation.

**Example 7.1** | A 2.0-m wide rectangular channel has a discharge of  $0.350 \text{ m}^3/\text{s}$ . Find the height of a rectangular weir spanning the full width of the channel that can be used to pass this discharge while maintaining an upstream depth of 0.850 m.

*Solution* A trial-and-error procedure is required to solve for  $P$ . Assuming  $C_d = 0.640$ , by Eq. 7.5

$$H_1^{3/2} = 0.350 / \left( \frac{2}{3} \times 0.640 \times \sqrt{19.62} \times 2.0 \right) = 0.0926$$

$$H_1 = 0.205 \text{ m and } P = 0.850 - 0.205 = 0.645 \text{ m}$$

$$H_1/P = 0.318 \text{ m and } C_d = 0.611 + (0.08 \times 0.318) = 0.636$$

2nd iteration: Using the above value of  $C_d$

$$H_1^{3/2} = \frac{0.0926}{0.636} \times 0.640 = 0.09318$$

$$H_1 = 0.206 \text{ m, } P = 0.644 \text{ m, } H_1/P = 0.320$$

and  $C_d = 0.637$



Accepting the value of  $C_d$  the final values are  $H_1 = 0.206$  m and  $P = 0.644$  m. The height of the required weir is therefore  $P = 0.644$  m.

**Example 7.2** A 2.5-m wide rectangular channel has a rectangular weir spanning the full width of the channel. The weir height is 0.75 m measured from the bottom of the channel. What discharge is indicated when this weir is working under submerged mode with depths of flow, measured above the bed channel, of 1.75 m and 1.25 m on the upstream and downstream of the weir respectively.

**Solution** Weir height  $P = 0.75$  m,

$$H_1 = 1.75 - 0.75 = 1.00 \text{ m and } H_2 = 1.25 - 0.75 = 0.5 \text{ m}$$

$$H_1 / P = 1.0 / 0.75 = 1.333 \text{ and } H_2 / H_1 = 0.5 / 1.0 = 0.50$$

$$C_d = 0.611 + 0.08 (1.333) = 0.718$$

$$Q_f = \frac{2}{3} C_d \sqrt{2g} L (H_1)^{3/2} = \frac{2}{3} \times 0.718 \times \sqrt{19.62} \times 2.5 \times (1.0)^{3/2} = 5.30 \text{ m}^3/\text{s}$$

By Villemonte equation for submerged weir flow, and noting that for rectangular weir flow  $n = 1.5$

$$Q_s = Q_f \left[ 1 - \left( \frac{H_2}{H_1} \right)^{1.5} \right]^{0.385} = 4.24 \times \left[ 1 - (0.5)^{1.5} \right]^{0.385} = 4.48 \text{ m}^3/\text{s}.$$

### 7.2.6 Contracted Weir

The discharge Eqs 7.4 and 7.5 have been derived for a weir which spans the full width of the channel. In such weirs there will be no contraction of the streamlines at the ends and as such they are termed *uncontracted* or *suppressed weirs*. However, if the length of the weir  $L$  is smaller than the width of the channel, such weirs are known as *contracted weirs* (Fig. 7.6). In contracted weirs, the flow issuing out of the weir opening will undergo contraction at the sides in addition to the contraction caused by upper and lower nappes. As a result, the effective width of the weir is reduced.

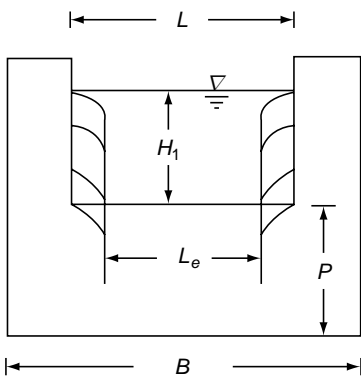


Fig. 7.6 Weir with end contractions

As a result, the effective width of the weir is reduced.

The discharge from contracted weir can be obtained by using the effective length  $L_e$  in the Eq. 7.4. The well-known *Francis formula* gives

$$L_e = L - 0.1nH_1 \quad (7.14)$$

where  $n =$  number of end contractions. For the weir shown in Fig.7.6,  $n = 2$ , and if  $m$  number of piers are introduced on a weir crest,  $n = 2m + 2$ . The discharge equation for the contracted weir is written as

$$Q = \frac{2}{3} C_c \sqrt{2g} (L - 0.1nH_1) \left[ \left( H_1 + \frac{V_0^2}{2g} \right)^{3/2} - \left( \frac{V_0^2}{2g} \right)^{3/2} \right] \quad (7.15)$$

For  $L > 3H_1$  and  $H_1 / P < 1.0$ , the value of  $C_c$  is taken as  $C_c = 0.622$ .

For contracted sharp-crested weirs, Kindsvater and Carter <sup>6</sup> have given a modified version of Eq. 7.15, based on their extensive experimental investigation covering a wide range of variables, as

$$Q = \frac{2}{3} C_{dc} \sqrt{2g} L_e H_{1e}^{3/2} \quad (7.16)$$

where  $C_{dc}$  = coefficient of discharge for contracted weir,  $L_e$  = effective length and  $H_{1e}$  = effective head. The effective length and head are obtained as

$$L_e = L + K_L \quad (7.16a)$$

and

$$H_{1e} = H_1 + K_H \quad (7.16b)$$

where  $K_H$  and  $K_L$  are additive correction terms to account for several phenomena attributed to viscosity and surface tension. Values of recommended  $K_H$  and  $K_L$  are given in Table 7.1. The discharge coefficient  $C_{dc}$  is a function of  $\frac{L}{B}$  and  $H_1/P$ , expressed as

$$C_{dc} = K_1 + K_2 \left( \frac{H_1}{P} \right) \quad (7.17)$$

The variation of  $K_1$  and  $K_2$  are also shown in Table 7.1.

**Table 7.1** Value s of Parameters for Use in Eq. (7.16)\*<sup>6</sup>

$L/B$	$K_L$ (m)	$K_H$ (m)	$K_1$	$K_2$
1.0	-0.0009	$K_H = 0.001 \text{ m} = \text{Const.}$	0.602	+0.0750
0.9	0.0037		0.599	+0.0640
0.8	0.0043		0.597	+0.0450
0.7	0.0041		0.595	+0.0300
0.6	0.0037		0.593	+0.0180
0.5	0.0030		0.592	+0.0110
0.4	0.0027		0.591	+0.0058
0.3	0.0025		0.590	+0.0020
0.2	0.0024		0.589	-0.0018
0.1	0.0024		0.588	-0.0021

\*Equation (7.16) is subject to the limitations  $H_1/P < 2.0$ ,  $H_1 > 0.03 \text{ m}$ ,  $L > 0.15 \text{ m}$  and  $P > 0.10 \text{ m}$ .

**Example 7.3**

A 2.0-m wide rectangular channel has a contracted rectangular weir of 1.500-m length and 0.60-m height. What would be the depth of flow upstream of the weir when the flow through the channel is 0.350 m<sup>3</sup>/s?

*Solution* In this case  $\frac{L}{B} = \frac{1.50}{2.00} = 0.75$ . From Table 7.1,

$$K_L = 0.0042, K_H = 0.001, K_1 = 0.596 \text{ and } K_2 = 0.0375.$$

$$L_e = L + K_L = 1.50 + 0.0042 = 1.5042 \text{ m}$$

As a trial-and-error procedure is needed to calculate  $H_1$ , assume  $C_{dc} = 0.60$  for the first trial. From Eq. 7.16

$$H_{1e}^{3/2} = 0.350 \left/ \left( \frac{2}{3} \times 0.60 \times \sqrt{19.62} \times 1.5042 \right) \right. = 0.13133$$

$$H_{1e} = 0.2584 \text{ m}, H_1 = 0.2584 - 0.001 = 0.2574 \text{ m}$$

$$H_1 / P = \frac{0.2574}{0.60} = 0.429 \text{ and from Eq. 7.17}$$

$$C_{dc} = 0.596 + (0.0375 \times 0.429) = 0.612$$

*2nd iteration:* Using the above value of  $C_{dc}$

$$H_{1e}^{3/2} = \frac{0.13133}{0.612} \times 0.600 = 0.128755$$

$$H_{1e} = 0.255 \text{ m}, H_1 = 0.254 \text{ m}, H_1/P = 0.4233 \text{ and}$$

$$C_{dc} = 0.612 \text{ which is the same as the assumed value.}$$

Hence the final values are  $H_1 = 0.254 \text{ m}$  and  $C_{dc} = 0.612$ .

Upstream depth  $= H_1 + P = 0.254 + 0.600 = 0.854 \text{ m}$

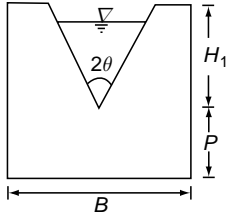
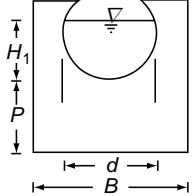
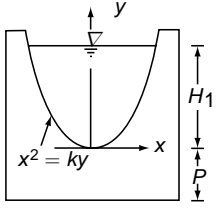
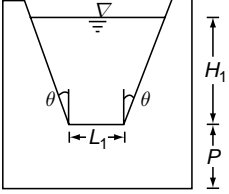
The water surface on the upstream will be at a height of 0.854 m above the bed.

### 7.2.7 Non-Rectangular Weirs

Sharp-crested weirs of various shapes are adopted for meeting specific requirements based on their accuracy, range and head-discharge relationships. The general form of head-discharge relationship for a weir can be expressed as  $Q = KH_1^n$ , where  $K$  and  $n$  are coefficients. The coefficient  $n$  depends upon the weir shape and  $K$  depends upon the weir shape and its setting. The discharge equations for some commonly used weir shapes are given in Table 7.2.

A variety of sharp-crested weir shapes have been designed to give specific head-discharge relationships and are described in literature<sup>1</sup>. A type of weir for which the discharge varies linearly with head, known as *Sutro Weir* finds use in flow measure

**Table 7.2** Discharge Relationships for some Commonly Used Non-Rectangular Thin-Plate Weirs

Shape	Discharge
	$Q = \frac{8}{15} C_d \sqrt{2g} \tan \theta H_1^{5/2}$ $C_d = f_n(\theta)$ <p>For <math>2\theta = 90^\circ, C_d = 0.58</math></p>
	$Q = C_d \phi d^{2.5}, \phi = f(H_1/d), C_d = f(H_1/d)$
	$Q = \frac{1}{4} \pi C_d \sqrt{k} \sqrt{2g} H_1^2$
	$Q = \frac{2}{3} C_d \sqrt{2g} H_1^{3/2} \left( L_1 + \frac{4}{5} H_1 \tan \theta \right)$

ment of small discharges and in automatic control of flow, sampling and dosing through float operated devices.

The details of some special sharp-crested weirs are given in the next section.

## 7.3 SPECIAL SHARP-CRESTED WEIRS

### 7.3.1 Introduction

This section deals with special sharp-crested weirs designed to achieve a desired discharge-head relationship. These are also sometimes called *proportional* weirs

(P-weirs). Since the flow over a P-weir can be controlled easily by float-regulated dosing devices, these are widely used in industry and irrigation.

Given any defined shape of weir, the discharge through it can be easily determined, e.g. in the case of a rectangular weir, the discharge is proportional to  $h^{3/2}$ , and in the case of a triangular weir (V-notch) the discharge is proportional to  $h^{5/2}$ , etc., where  $h$  is the head causing flow. The reverse problem of finding the shape of a weir to have a known head-discharge relationship constitutes the design of proportional weirs. The design of proportional weirs has considerable applications in hydraulic, environmental and chemical engineering.

### 7.3.2 Linear Proportional Weir

The linear proportional weir, with its linear head-discharge characteristic is used as a control for float-regulated dosing devices, as a flow meter and as an outlet for grit chambers (sedimentation tanks). The linear proportional weir was invented by Stout (1897). This weir is only of theoretical interest as its width at base is infinite. This was improved by Sutro (1908) to develop a practical linear P-weir and is well-known as the *Sutro weir*. Referring to Fig. 7.7, the Sutro weir has a rectangular base over which a designed shape is fitted. It is found that for flows above the base weir the discharges are proportional to the heads measured above a reference plane located at one-third the depth of the base weir. Referring to Fig. 7.7.

$$Q = b \left( h + \frac{2}{3}a \right) \tag{7.18}$$

where  $b$  = the proportionality constant.

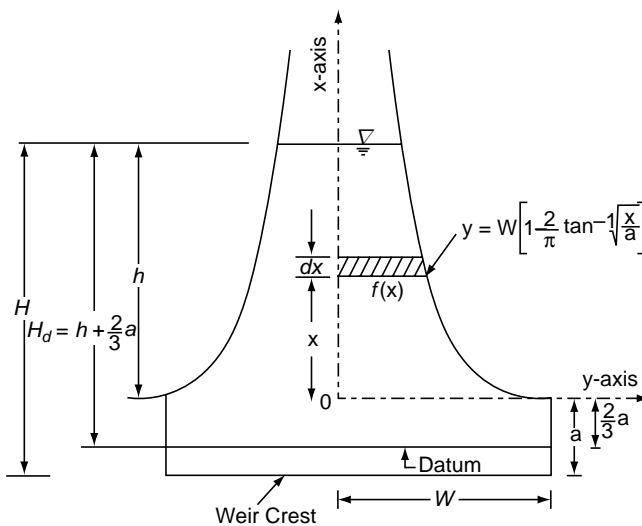


Fig. 7.7 Definition sketch of linear weir proportional weir

### 7.3.3 Shape of the Sutro Weirs

Referring to Fig. 7.7, let the weir have the base on a rectangular weir of width  $2W$  and depth  $a$ . For convenience, the horizontal and vertical axes at the origin  $O$  are chosen as  $y$  and  $x$ -axes respectively. The weir is assumed to be symmetrical about the  $x$ -axis.

The discharge through the rectangular weir when the depth of flow is  $h$  above the origin is

$$q_1 = \frac{4}{3}WC_d\sqrt{2g}[(h+a)^{3/2} - h^{3/2}] \quad (7.19)$$

where  $C_d$  = coefficient of discharge.

The discharge through the upper portion above the origin called the *complimentary weir* is

$$q_2 = 2C_d\sqrt{2g} \int_0^h \sqrt{h-x} f(x)dx \quad (7.19a)$$

The total discharge through the weir is

$$Q = q_1 + q_2$$

We wish this discharge to be proportional to the head measured above the reference plane situated  $\frac{a}{3}$  above the crest of the weir. This reference plane is chosen arbitrarily by Sutro for mathematical convenience. Thus

$$\begin{aligned} Q &= q_1 + q_2 \\ &= \frac{4}{3}WC_d\sqrt{2g}[(h+a)^{3/2} - h^{3/2}] + 2C_d\sqrt{2g} \int_0^h \sqrt{h-x} f(x)dx \\ &= b\left(h + \frac{2a}{3}\right) \quad \text{for } h \geq 0 \end{aligned} \quad (7.20)$$

where  $b$  is the proportionality constant.

As there is no flow above the base weir when  $h = 0$ , we have by substituting  $h = 0$  in Eq. 7.20

$$b = WK a^{1/2} \quad (7.21)$$

where  $K = 2C_d\sqrt{2g}$

Substituting this value of  $b$  in Eq. 7.20

$$\frac{2}{3}W[(h+a)^{3/2} - h^{3/2}] + \int_0^h \sqrt{h-x} f(x) dx = Wa^{1/2}\left(h + \frac{2a}{3}\right) \quad (7.22)$$

Re-arranging,

$$\int_0^h \sqrt{h-x} f(x) dx = Wa^{1/2}\left(h + \frac{2a}{3}\right) - \frac{2}{3}W[(h+a)^{3/2} - h^{3/2}]$$

$$\begin{aligned}
 &= W \left[ \frac{2}{3} a^{3/2} + a^{1/2} h + \frac{2}{3} h^{3/2} - \frac{2}{3} (a+h)^{3/2} \right] \\
 &= \frac{2}{3} W \left[ h^{3/2} - \frac{3}{8} a^{-1/2} h^2 + \frac{1}{16} a^{-3/2} h^3 - \frac{3}{128} a^{-5/2} h^4 + \dots \right] \quad (7.22a)
 \end{aligned}$$

It is required to find the function  $f(x)$  such that Eq. 7.22a is satisfied for all positive values of  $h$ . This is achieved by expressing  $f(x)$  in a series of powers of  $x$  and determining their coefficients. A general term  $x^m$  in  $f(x)$  results in a term

$$\begin{aligned}
 \int_0^h \sqrt{h-x} x^m dx &= \int_0^h x^m \left( h^{1/2} - \frac{1}{2} h^{-1/2} x + \frac{1}{8} h^{-3/2} x^2 - \dots \right) dx \\
 &= \text{Const } (h)^{m+(3/2)} \quad (7.23)
 \end{aligned}$$

so that the first term in Eq. 7.22a can be obtained by a constant term in the series for  $f(x)$  and the other terms by taking  $m$  half an odd integer. Consequently we assume,

$$f(x) = y = A_1 + A_2 x^{1/2} + A_3 x^{3/2} + A_4 x^{5/2} + \dots \quad (7.24)$$

Substituting this in Eq. 7.22a

$$\begin{aligned}
 &\int_0^h (A_1 \sqrt{h-x} + A_2 \sqrt{hx-x^2} + \dots) dx \\
 &= \frac{2A_1}{3} h^{3/2} + \frac{\pi A_2 h^2}{8} + \frac{\pi A_3 h^3}{16} + \frac{5\pi A_4 h^4}{128} + \dots \\
 &= \frac{2}{3} W \left[ h^{3/2} - \frac{3}{8} a^{-1/2} h^2 + \dots \right]
 \end{aligned}$$

This leads to

$$\begin{aligned}
 A_1 &= W \\
 A_2 &= -\frac{2}{\pi} a^{-1/2} W \\
 A_3 &= \frac{2}{3\pi} a^{-3/2} W
 \end{aligned}$$

and so on.

Substituting these coefficients in Eq. 7.24

$$f(x) = W \left[ 1 - \frac{2}{\pi} \left\{ \frac{x^{1/2}}{a^{1/2}} - \frac{x^{3/2}}{a^{3/2}} + \frac{x^{5/2}}{5a^{5/2}} - \dots \right\} \right]$$

$$= W \left[ 1 - \frac{2}{\pi} \tan^{-1} \sqrt{\frac{x}{a}} \right] \quad (7.25)$$

The discharge equation for the Sutro weir can now be summarised as

$$Q = b \left( h + \frac{2}{3} a \right) = b \left( H - \frac{a}{3} \right) = b H_d \quad (7.26)$$

where  $b = WKa^{1/2}$  and  $K = 2C_d \sqrt{2g}$

$H$  = depth of flow in the channel. (It is usual practice to make the crest of the base coincide with the bed of the channel)

$h$  = head measured from the top of the rectangular base weir

$H_d$  = depth of water over the datum.

The sharp edged Sutro weir is found to have an average coefficient of discharge of 0.62.

A simple weir geometry, called *quadrant plate weir*, which has the linear head-discharge relationship is described in Ref. 7. This weir has the advantage of easy fabrication and installation under field conditions. Linear proportional weirs having non-rectangular base weirs are described in Ref. 8 and 9.

**Example 7.4** | A Sutro weir has a rectangular base of 30-cm width and 6-cm height. The depth of water in the channel is 12 cm. Assuming the coefficient of discharge of the weir as 0.62, determine the discharge through the weir. What would be the depth of flow in the channel when the discharge is doubled? (Assume the crest of the base weir to coincide with the bed of the channel).

**Solution** Given  $a = 0.06$  m,  $W = 0.30/2 = 0.15$  m,  $H = 0.12$  m

$$K = 2 C_d \sqrt{2g} = 2 \times 0.62 \times \sqrt{2 \times 9.81} = 5.4925$$

$$b = W K a^{1/2} = 0.15 \times 5.4925 \times (0.06)^{1/2} = 0.2018$$

$$\begin{aligned} \text{From Eq. 7.26} \quad Q &= b \left( H - \frac{a}{3} \right) \\ &= 0.2018 \left( 0.12 - \frac{0.06}{3} \right) = 0.02018 \text{ m}^3/\text{s} \\ &= 20.18 \text{ litres/s} \end{aligned}$$

When the discharge is doubled,  $Q = 2 \times 0.02018 = 0.04036 \text{ m}^3/\text{s}$



From Eq. 7.26,  $0.04036 = 0.2018 \left( H - \frac{0.06}{3} \right)$

$$H = 0.2 + 0.02 = 0.22 \text{ m}$$

$$= 22 \text{ cm}$$

**Example 7.5** Design a Sutro weir for use in a 0.30-m wide rectangular channel to have linear discharge relationship in the discharge range from 0.25 m to 0.60 m<sup>3</sup>/s. The base of the weir will have to span the full width of the channel. Assume  $C_d = 0.62$ .

*Solution* Here  $2W = 0.30 \text{ m}$ , and  $C_d = 0.62$ .

$$K = 2C_d \sqrt{2g} = 2 \times 0.62 \times \sqrt{2 \times 9.81} = 5.49$$

$$Q_{\min} = \frac{2}{3} WK a^{3/2} = 0.25$$

$$\frac{2}{3} \times 0.15 \times 5.49 \times a^{3/2} = 0.25$$

$$a = 0.592 \text{ m}$$

$$b = WK \sqrt{a} = 0.15 \times 5.49 \times \sqrt{0.592} = 0.6337$$

$$Q = b H_d$$

For  $Q = 0.60 \text{ m}^3/\text{s}$ ,  $H_d = \frac{Q}{b} = \frac{0.60}{0.6337} = 0.9468 \text{ m}$

$$= H - \frac{a}{3} = h + \frac{2}{3} a \quad (\text{Refer Fig. 7.7})$$

$H = 1.1444 \text{ m}$  and  $h = 0.0552 \text{ m}$ .

Using Eq.7.25, the profile  $y = f(x)$  is calculated as

$$y = f(x) = 0.15 \left[ 1 - \frac{2}{\pi} \tan^{-1} \sqrt{\frac{x}{0.592}} \right]$$

### 7.3.4 General Equation for the Weir

Cowgill<sup>8</sup> and Banks<sup>9</sup> have shown that the curve describing the weir producing a discharge  $Q = b h^m$  for  $m \geq 1/2$  is given by

$$y = y(x) = \frac{b}{2C_d \sqrt{2g\pi}} \cdot \frac{\Gamma(m+1)}{\Gamma(m-1/2)} \cdot (x)^{(m-3/2)} \quad (7.27)$$

when 
$$Q = \int_0^h 2C_d f(x) \sqrt{2g(h-x)} dx$$

- where  $h$  = head measured above the crest of the weir
- $x, y$  = coordinates along vertical and horizontal axis respectively
- $b$  = a coefficient of proportionality
- $C_d$  = coefficient of discharge of the weir
- $\Gamma$  = gamma function.

The relationship between the exponent  $m$  and the profile of the weir is shown in Fig. 7.7-A.

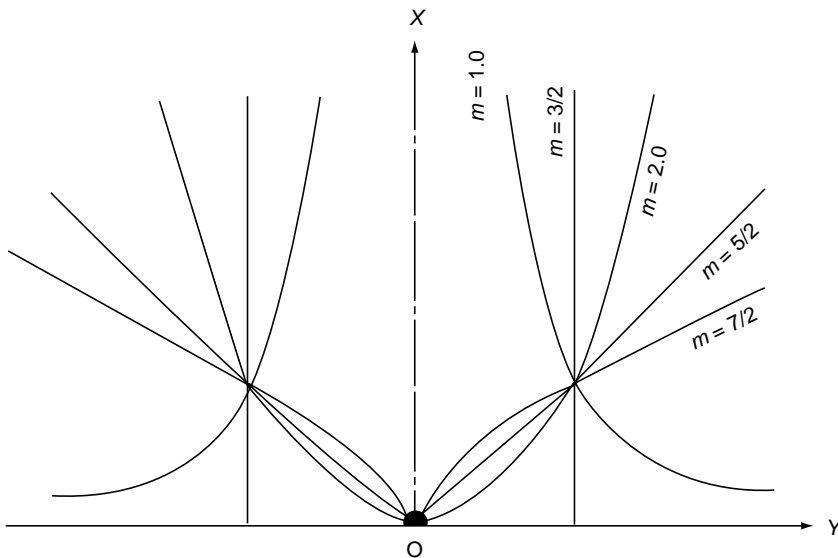


Fig. 7.7A Weir profiles for different values of exponent  $m$

It is clear from Eq. 7.25 that an attempt to design a weir producing a discharge proportional to  $h^m$  for  $m < 3/2$  inevitably leads to a curve which will be asymptotic at the base giving rise to infinite width, which is physically unrealizable. The linear proportional weir ( $m = 1$ ) is one such case. Sutro overcame this defect by the ingenious method of providing a rectangular base. A rational explanation for the selection of the datum was provided by Keshava Murthy<sup>9,12,13</sup> which is enunciated in the theorem of slope discharge continuity.

The slope-discharge-continuity theorem states: 'In any physically realizable weir having a finite number of finite discontinuities in its geometry, the rate of change of discharge is continuous at all points of discontinuity.' Physically this means that the curve describing the discharge versus the head for any compound weir cannot have more than one slope at any point. This is clear as otherwise it would mean, theoretically, there could be more than one value for the discharge in the infinitesimal strip in the neighbourhood of the discontinuity which is physically meaningless. The proof

of this theorem which is based on the use of the theorem of Laplace transforms is beyond the scope of this book.

The P-weir consists of a known base over which a designed complimentary weir is fixed. Each weir is associated with a reference plane or datum which is determined by evaluating a new parameter  $\lambda$  called the *datum constant* by the application of slope discharge-continuity theorem. The problem of design of P-weirs is solved by the technique of solution of integral equations. This is explained by the design of *quadratic weirs* in the following section.

### 7.3.5 Quadratic Weir-notch Orifice

A quadratic weir is a proportional weir in which the discharge  $Q$  is proportional to the square root of the head  $h$ . This weir has applications in bypass flow measurement.

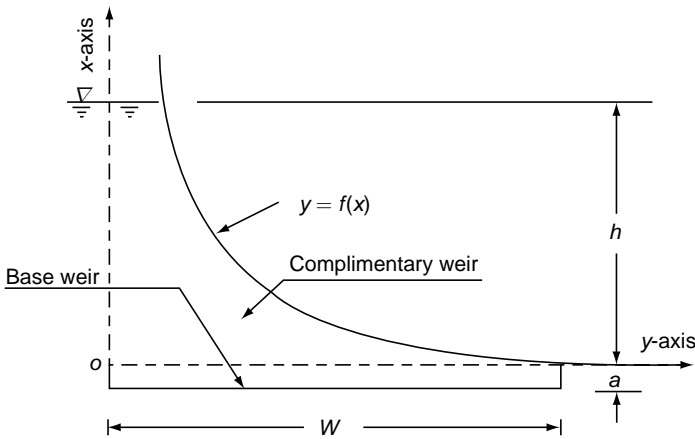


Fig. 7.8 Definition sketch

It is evident from the general Eq. 7.27 that an attempt to design a weir to pass a discharge proportional to  $h^m$ , for  $m < 3/2$  inevitably leads to a curve having infinite width at the bottom which is physically unrealizable. In order to obviate this, the quadratic weir is provided with a base in the form of a rectangular weir of width  $2W$  and depth  $a$ , over which a designed curve is fitted (Fig. 7.8).

Referring to Fig. 7.8 the weir is assumed to be sharp-edged and symmetrical over the  $x$ -axis. When the flow is  $h$  above the base, the discharge through the rectangular weir, below the  $y$ -axis, is

$$q_1 = \frac{2}{3}WK \left[ (h+a)^{3/2} - h^{3/2} \right] \tag{7.28}$$

where  $K = 2C_d \sqrt{2g}$ ,  $C_d$  = the coefficient of discharge. The discharge from the complementary weir above the origin is

$$q_2 = K \int_0^h \sqrt{h-x} f(x) dx \tag{7.28a}$$

Total discharge  $Q = q_1 + q_2$

$$= \frac{2}{3}WK[(h+a)^{3/2} - h^{3/2}] + K \int_0^h \sqrt{h-x} f(x) dx \quad (7.29)$$

We wish to have the discharge  $Q = b\sqrt{h + \lambda a}$ , where  $b$  is the proportionality constant and  $\lambda$  is the datum constant. In other words, the discharge is proportional to the square root of the head measured above a reference plane. The constants  $b$  and  $\lambda$  are to be evaluated. They are determined by the two conditions of continuity of discharge and the requirement of the slope discharge continuity theorem. Rewriting Eq. 7.29

$$Q = \frac{2}{3}WK[(h+a)^{3/2} - h^{3/2}] + K \int_0^h \sqrt{h-x} f(x) dx$$

$$= h\sqrt{h + \lambda a} \quad \text{for } h \geq 0 \quad (7.30)$$

When  $h = 0$ , there is no flow above the base weir. Hence, substituting  $h = 0$  in Eq. 7.30

$$\frac{2}{3}WKa^{3/2} = b\sqrt{\lambda a} \quad (7.31)$$

Differentiating Eq. 7.30 on both sides by using Leibnitz's rule for differentiating under the integral sign, and re-arranging

$$\int_0^h \frac{f(x)}{\sqrt{h-x}} dh = \frac{b}{K\sqrt{h + \lambda a}} - 2W[(h+a)^{1/2} - h^{1/2}] = \phi(h) \quad (7.32)$$

Applying the slope-discharge-continuity theorem, i.e, putting  $h = 0$  in Eq. 7.32. we have

$$\frac{b}{K\sqrt{\lambda a}} = 2Wa^{1/2} \quad (7.33)$$

Solving Equations 7.31 and 7.33

$$\lambda = \frac{1}{3} \text{ and } b = \frac{2}{\sqrt{3}}WKa \quad (7.34)$$

The reference plane for this weir is situated at  $\frac{2a}{3}$  above the crest of the weir. Equation 7.32 is in the Abel's form of integral equation whose solution is<sup>9</sup>:

$$y = f(x) = \frac{1}{\pi} \int_0^h \frac{\phi'(h)}{\sqrt{x-h}} dh$$

Substituting for  $\phi'(h)$

$$y = W \left[ 1 - \frac{2}{\pi} \tan^{-1} \sqrt{\frac{x}{a}} - \frac{6}{\pi} \frac{\sqrt{x/a}}{\left(1 + \frac{3x}{a}\right)} \right] \quad (7.35)$$

The weir profile drawn to scale is shown in Fig.7.9. Beyond  $\frac{x}{a} = 2.0$ , the weir as an

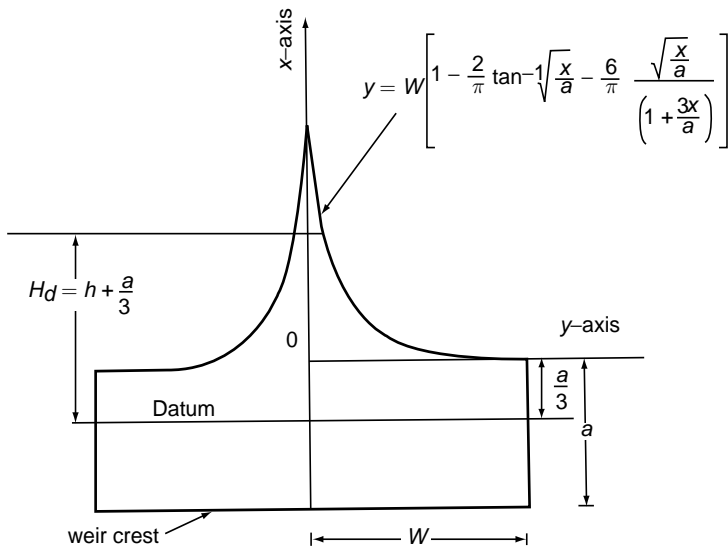


Fig. 7.9 Quadratic weir

orifice for all practical purposes. As this weir gives discharges proportional to the square root of the head (measured above the reference plane), both while acting as a notch as well as an orifice, this device is also called a *notch-orifice*.

The discharge equation for the quadratic weir can now be written as

$$Q = b \sqrt{h + \frac{a}{3}} = b \sqrt{H - \frac{2}{3}a} = b \sqrt{H_d} \quad (7.36)$$

where  $b = \frac{2}{\sqrt{3}} WKa$  and  $K = 2C_d \sqrt{2g}$

and  $h$  = depth of flow above the rectangular base

$H_d$  = head above the reference plane

$H$  = depth of flow

Quadratic weirs having non-rectangular lower portions (base weirs) are described in detail in Ref. 14.

The quadratic weir has an average coefficient of discharge of 0.62. In a quadratic weir the error involved in the discharge calculation for a unit per cent error in head is only 0.5 per cent as against 1.5% in a rectangular weir and 2.5% in a V-notch. Hence this is more sensitive than the rectangular weir and V-notch.

**Example 7.6** *A quadratic weir is designed for installation in a rectangular channel of 30-cm width. The rectangular base of the weir occupies the full width of the channel and is 6 cm in height. The crest of the base weir coincides with the channel bed. (a) Determine the discharge through the weir when the depth of flow in the channel is 15 cm. (b) What would be the depth of flow upstream of the weir when the discharge in the channel is 25 litres/s? [Assume  $C_d = 0.62$ ].*

**Solution** Given:  $a = 0.06$  m,  $W = 0.30/2 = 0.15$  m,  $H = 0.15$  m

$$K = 2 C_d \sqrt{2g} = 2 \times 0.62 \times \sqrt{2 \times 9.81} = 5.4925$$

$$b = \frac{2}{\sqrt{3}} W K a = \frac{2}{\sqrt{3}} \times 0.15 \times 5.4925 \times 0.06 = 0.05708$$

From Eq. (7.36),  $Q = b \sqrt{\left(H - \frac{2a}{3}\right)}$

$$(a) \quad Q = 0.05708 \times \left[0.15 - \left(\frac{2 \times 0.06}{3}\right)\right]^{1/2}$$

$$= 0.0189 \text{ m}^3/\text{s} = 18.93 \text{ litres/s}$$

(b) When the discharge  $Q = 25$  litres/s = 0.025 m<sup>3</sup>/s

$$\text{From Eq. (7.36),} \quad 0.025 = 0.05708 \times \left[H - \left(\frac{2 \times 0.06}{3}\right)\right]^{1/2}$$

$$H = 0.1918 + 0.04 = 0.2318 \text{ m}$$

$$= 23.18 \text{ cm}$$

### 7.3.6 Modelling of Flow Velocity using Special Weirs

In many hydraulic engineering situations, it is desirable to maintain a constant average velocity in a channel for a range of flows. A typical example of this situation is the grit chamber used in waste water treatment. To obtain such a control of the velocity of flow in the channel, proportional weirs can be used at the outlet of the channel. The channel cross-section shape, however, will have to be determined. This, in turn, depends upon the shape of the outlet weir and the relationship between the upstream

head and velocity. Design of such channel shapes controlled by a weir at the outlet is described in references 8 and 15. It is interesting to note that a linear proportional weir, such as a Sutro weir, fixed at the end of a rectangular channel ensures constant average velocity in the channel irrespective of the fluctuations of the discharge.

## 7.4 OGEE SPILLWAY

The ogee spillway, also known as the *overflow spillway*, is a control weir having an ogee (S-shaped) overflow profile. It is probably the most extensively used spillway to safely pass the flood flow out of a reservoir.

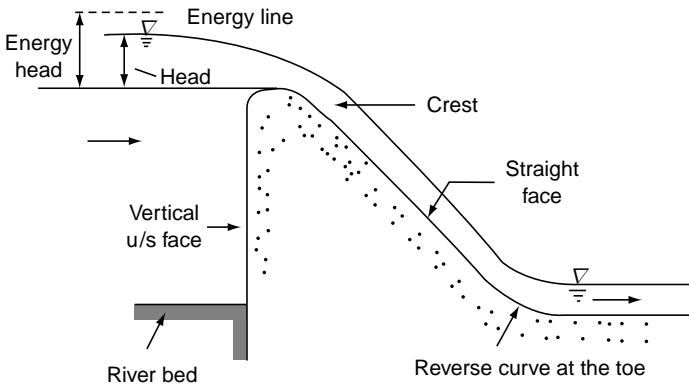


Fig. 7.10 Typical ogee spillway

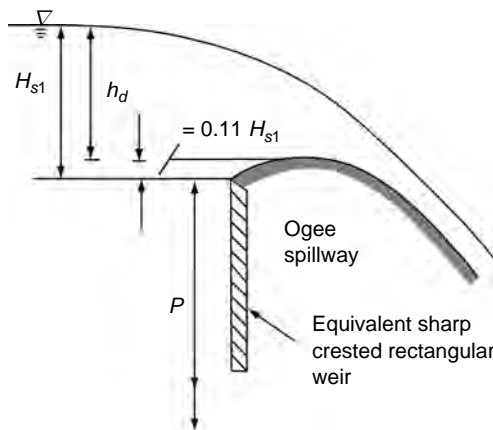


Fig. 7.11 Lower nappe as a spillway profile

A typical ogee spillway is shown in Fig. 7.10. The crest profile of the spillway is so chosen as to provide a high discharge coefficient without causing dangerous cavitation conditions and vibrations. The profile is usually made to conform to the lower nappe emanating from a well-ventilated sharp-crested rectangular weir (Fig. 7.11). This idea is believed to have been proposed by Muller in 1908. Such a profile assures,

for the design head, a high discharge coefficient, and at the same time, atmospheric pressure on the weir. However, heads smaller than the design head cause smaller trajectories and hence result in positive pressures and lower discharge coefficients. Similarly, for heads higher than the design head, the lower nappe trajectory tends to pull away from the spillway surface and hence negative pressure and higher discharge coefficients result.

For a high spillway ( $H_{s1}/P \approx 0$ ), it is found experimentally that the spillway apex is about  $0.11 H_{s1}$  above the equivalent sharp-crested weir crest (Fig. 7.11). The design head for the spillway is then  $h_d = 0.89 H_{s1}$ . Considering the discharge equation with suffix 's' for an equivalent sharp-crested weir

$$q = \frac{2}{3} C_{ds} \sqrt{2g} H_{s1}^{3/2} \quad (\text{for the sharp-crested weir})$$

and 
$$q = \frac{2}{3} C_{d1} \sqrt{2g} h_d^{3/2} \quad (\text{for the overflow spillway})$$

it is easy to see that  $C_{dv} = 1.19 C_{ds}$ , i.e. the ogee spillway discharge coefficients are numerically about 20 per cent higher than the corresponding sharp-crested weir coefficients.

### 7.4.1 Uncontrolled Ogee Crest

If there are no crest gates over them, such spillways are designated as uncontrolled spillways. The crest shapes of uncontrolled ogee spillways have been extensively studied by the US Bureau of Reclamation, and accurate data relating to the nappe profiles, coefficient of discharge and other information pertinent to spillway design are available<sup>16</sup>. Considering a typical overflow spillway crest (Fig. 7.12), the profile of the crest downstream of the apex can be expressed as<sup>16</sup>

$$\frac{y}{H_d} = K \left( \frac{x}{H_d} \right)^n \quad (7.37)$$

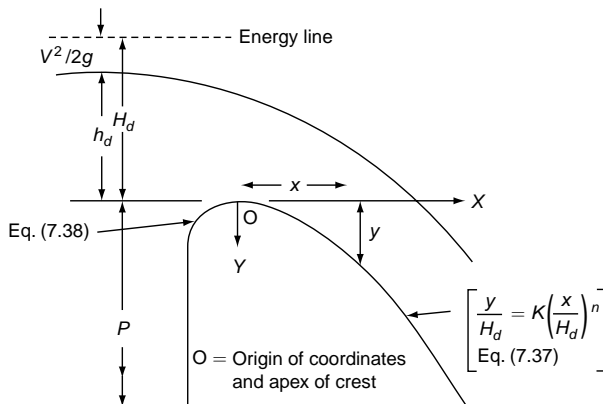


Fig. 7.12 Elements of a spillway crest



in which  $x$  and  $y$  are the coordinates of the downstream curve of the spillway with the origin of coordinates being located on the apex,  $H_d =$  design energy head, i.e. design head measured above the crest to the energy line.  $K$  and  $n$  are constants and their values depend upon the inclination of the upstream face and on the velocity of approach. For low velocities of approach, typical values of  $K$  and  $n$  are

Upstream face	$K$	$n$
Vertical	0.500	1.850
1 Horizontal : 1/3 vertical	0.517	1.836
1 Horizontal : 1 vertical	0.534	1.776

The crest profile upstream of the apex is usually given by a series of compound curves.

Cassidy<sup>17</sup> reported the equation for the upstream portion of a vertical faced spillway as

$$\frac{y}{H_d} = 0.724 \left( \frac{x}{H_d} + 0.270 \right)^{1.85} - 0.432 \left( \frac{x}{H_d} + 0.270 \right)^{0.625} + 0.126 \quad (7.38)$$

This is valid for the region  $0 \geq \frac{x}{H_d} \geq -0.270$  and  $0 \leq \frac{y}{H_d} \leq 0.126$ . The same coordinate system as for the downstream profile (Eq. 7.37) is used for Eq. 7.38 also.

Since the hydraulic characteristics of the approach channel vary from one spillway to another, it is found desirable to allow explicitly for the effect of the velocity of approach in various estimations related to the overflow spillway. With this in view, the expression for the design discharge  $Q_d$  over an ogee spillway at the design head is written as

$$Q_d = \frac{2}{3} C_{d0} \sqrt{2g} L_e H_d^{3/2} \quad (7.39)$$

in which  $H_d =$  design-energy head (i.e., head inclusive of the velocity of approach head),  $C_{d0} =$  coefficient of discharge at the design head and  $L_e =$  effective length of the spillway. If  $H_0 =$  any energy head over the ogee spillway, the corresponding discharge  $Q$  can be expressed as

$$Q = \frac{2}{3} C_0 \sqrt{2g} L_e H_0^{3/2} \quad (7.40)$$

where  $C_0 =$  coefficient of discharge at the head  $H_0$ . In general,  $C_0$  will be different from  $C_{d0}$ . If  $H_0/H_d > 1.0$  then  $C_0/C_{d0} > 1.0$ . If on the other hand,  $H_0/H_d < 1.0$ . then  $C_0/C_{d0} < 1.0$ . By definition, if  $H_0/H_d = 1.0$ ,  $C_0/C_{d0} = 1.0$

The discharge coefficients  $C_0$  and  $C_{d0}$  are both functions of  $P/H_0$  and  $P/H_d$  respectively, and of the slope of the upstream face. For a vertical faced ogee spillway, the variation of  $C_{d0}$  with  $P/H_d$  is shown in Fig. 7.13 (Ref. 18). It is seen that for

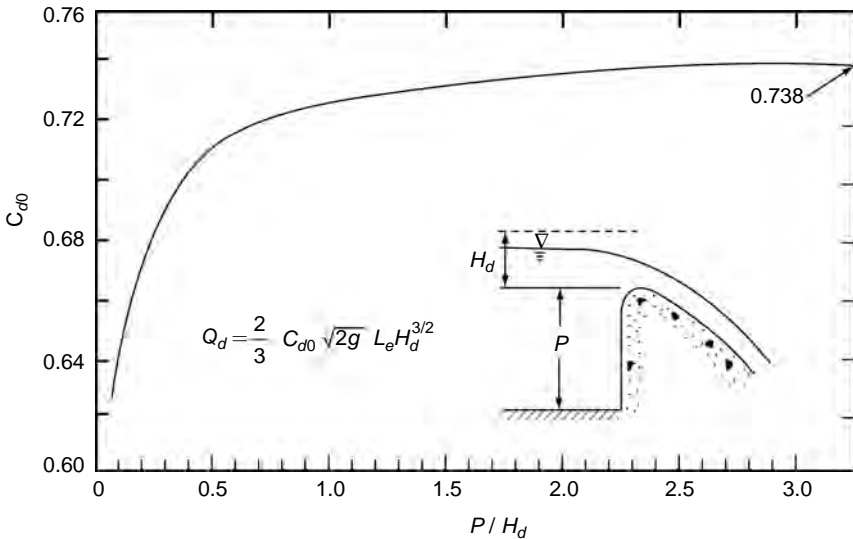


Fig. 7.13 Variation of  $C_{d0}$  with  $P/H_d$

$P/H_d > 2.0$ , i.e. for high overflow spillways, the coefficient  $C_{d0}$  is essentially constant at a value of 0.738. For spillways of small heights and high energy heads, i.e. for  $P/H_d < 1.0$ , the value of  $C_{d0}$  decreases with  $P/H_d$  reaching a value of 0.64 at  $P/H_d = 0.10$ .

The analytical modelling of the spillway flow has been attempted by many investigators. Cassidy<sup>19</sup> has calculated the coefficient of discharge and surface profiles for flow over standard spillway profiles by using the relaxation technique in a complex potential plane. Ikegawa and Washizu<sup>20</sup> have studied the spillway flow through the finite element method (FEM) by making considerable simplification of the basic problem. Diersch et al.<sup>21</sup> have given a generalised FEM solution of gravity flows of ideal fluids and have studied the variation of  $C_0$  with  $H_0/H_d$  for a spillway of  $P/H_d = 4.29$ .

Several experimental data are available on the variation of  $C_0$ . It is found that  $C_0/C_{d0}$  is essentially a function of  $H_0/H_d$  as indicated in Fig. 7.14. It is seen that  $C_0/C_{d0}$  increases continuously with  $H_0/H_d$ . Experiments by Rouse and Reid<sup>17</sup>, Cassidy<sup>17</sup>, Schirmer and Diersch<sup>21</sup> and the FEM studies of Diersch have revealed that the discharge coefficient ratio  $C_0/C_d$  continues to increase with  $H_0/H_d$ , as shown in Fig. 7.14 up to a certain maximum value of head ratio  $(H_0/H_d)_m$ . The increased discharge coefficient at  $(H_0/H_d) > 1.0$  is due to the occurrence of negative pressures on the crest. At sufficiently high negative pressures, separation of the boundary layer from the crest and consequent decrease in the flow efficiency results. Also, if the minimum negative pressures approach the vapour pressure, cavitation can occur. The maximum head ratio  $(H_0/H_d)_m$  thus corresponds to the onset of separation, and its value is known to depend to a small extent on  $P/H_d$ . Experimental studies<sup>17</sup> have shown that there is no possibility of separation and also no pressure fluctuations of any consequence would occur in the overflow spillway operation with  $H_0/H_d \leq 3.0$ , the inception of cavitation is the only problem to be guarded against.

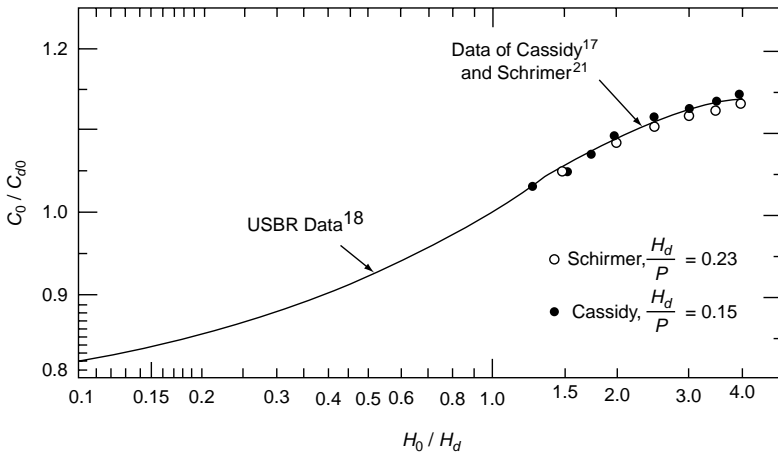


Fig. 7.14 Variation of  $C_0/C_{d0}$  with  $(H_0/H_d)$

It is seen that the overflow spillway, when working at  $1 < H_0/H_d < (H_0/H_d)_m$ , has the desirable feature of higher values of the discharge coefficient  $C_0$ . This feature can be advantageously exploited in the spillway design. As maximum possible flood flow over a spillway is a rare event, the spillway profile can be designed to correspond to a lower value of head such that at the maximum possible flood,  $H_0/H_d > 1.0$ . The other structural features can of course be designed to safely accommodate the flood flow. This ensures that the spillway will be functioning at a higher average efficiency over its operating range. When the maximum flood flow occurs, the spillway will perform at a head more than the design head, and consequently, with an enhanced efficiency. This practice of designing is called *underdesigning of the spillway*.

The use of  $H_0$  and  $H_d$ , the energy heads, in the discharge equation is not very convenient for discharge estimation. Usually, the value of  $V_0^2 / 2g$  is very small relative to the upstream head  $h_0$ , where  $h_0 = (H_0 - V_0^2 / 2g)$ . For spillways with  $h_0 / P < 0.50$ , the velocity of approach can be assumed to be negligibly small and the relevant head over the crest up to the water surface can be used in place of the energy head, i.e.  $h_0$  and  $h_d$  can be used in place of  $H_0$  and  $H_d$  respectively.

To approximately estimate the minimum pressure on the spillway  $P_m$ , for operations higher than the design head, the experimental data of Cassidy<sup>17</sup> in the form

$$\frac{P_m}{\gamma H} = -1.17 \left( \frac{H_0}{H_d} - 1 \right) \tag{7.41}$$

can be used. This equation is valid in the range of  $H_d/P$  from 0.15 to 0.50.

**Example 7.7** | An overflow spillway is to be designed to pass a discharge of 2000 m<sup>3</sup>/s of flood flow at an upstream water-surface elevation of 200.00 m. The crest length is 75.0 m and the elevation of the average stream bed is 165.00 m. Determine the design head and profile of spillway.

*Solution* A trial-and-error method is adopted to determine the crest elevation.

Discharge per unit width  $q_d = \frac{2000}{75} = 26.67 \text{ m}^3/\text{s}/\text{m}$ . Assume  $C_{d0} = 0.736$ .

By Eq. 7.39  $q_d = \frac{2}{3} C_{d0} \sqrt{2g} (H_d)^{3/2}$

$$26.27 = \frac{2}{3} (0.736) \sqrt{19.62} (H_d)^{3/2}$$

$$H_d = 5.32 \text{ m}$$

$$\begin{aligned} \text{Velocity of approach } V_a &= \frac{q}{P + h_0} = \frac{26.67}{(200.00 - 165.00)} \\ &= 0.762 \text{ m/s} \end{aligned}$$

$$h_a = \frac{V_a^2}{2g} = 0.0296 \approx 0.03 \text{ m}$$

Elevation of energy line = 200.03 m

Crest elevation = 200.03 - 5.32 = 195.71 m

$$P = 195.71 - 165.00 = 30.71 \text{ m}$$

$$P/H_d = \frac{30.71}{5.32} = 5.77$$

For this value of  $P/H_d$  from Fig. 7.13,  $C_{d0} = 0.738$ .

*2nd iteration*

$$(H_d)^{3/2} = \frac{26.67}{(2/3)(0.738)\sqrt{19.62}}, \quad H_d = 5.31 \text{ m}$$

$h_a \approx 0.03$ . Elevation of energy line = 200.03 m

Crest elevation = 200.03 - 5.31 = 194.72 m

$$P = 194.72 - 165.00 = 29.72 \text{ m}$$

$P/H_d = 5.60$ . For this  $P/H_d$ , from Fig. 7.13,  $C_{d0} = 0.738$ . Hence no more iterations are required.

Design energy head  $H_d = 5.31 \text{ m}$

and crest elevation = 194.72 m

The downstream profile of the crest is calculated by Eq. 7.37, which for the present case is

$$\frac{y}{5.31} = 0.50 \left( \frac{x}{5.31} \right)^{1.85}$$

The upstream profile is calculated by Eq. 7.38 which, for the range  $0 \leq x \leq 1.434$ , is given as

$$\frac{y}{5.31} = 0.724 \left( \frac{x}{5.31} + 0.270 \right)^{1.85} - 0.432 \left( \frac{x}{5.31} + 0.270 \right)^{0.625} + 0.126$$

The apex of the crest at elevation 194.72 m is the origin of coordinates of the above two profile equations.

**Example 7.8** | In the spillway of Example 7.7 what would be the discharge if the water-surface elevation reaches 202.00 m? What would be the minimum pressure on the spillway crest under this discharge condition?

*Solution*  $h_0 = 202.00 - 194.72 = 7.28 \text{ m}$   
 $h_0 + P = 202.00 - 165.00 = 37.00 \text{ m}$

Assuming the velocity of approach head  $h_a = 0.05 \text{ m}$ , the elevation of the energy line = 202.05 m.

$$H_0 = 202.05 - 194.72 = 7.33 \text{ m}$$

$$\frac{H_0}{H_d} = \frac{7.33}{5.31} = 1.38$$

From Fig. 7.14, corresponding to  $\frac{H_0}{H_d} = 1.38$ ,  $\frac{C_0}{C_{d0}} = 1.04$ .

Since  $C_{d0} = 0.738$

$$C_0 = 0.768$$

$$q = \frac{2}{3} \sqrt{19.62} (0.768)(7.33)^{3/2} = 45.00 \text{ m}^3/\text{s/m}$$

$$V_a = \frac{45.00}{37.00} = 1.216 \text{ m/s}, h_a = \frac{V_a^2}{2g} \approx 0.08 \text{ m}$$

*2nd iteration*

Elevation of the energy line = 202.08

$$H_0 = 202.08 - 194.72 = 7.36 \text{ m}$$

$$\frac{H_0}{H_d} = 1.386 \quad \frac{C_0}{C_{d0}} = 1.04 \text{ from Fig. 7.14,}$$

$$C_0 = 0.768$$

$$q = \frac{2}{3} \sqrt{19.62} (0.768) (7.36)^{3/2} = 45.28 \text{ m}^3/\text{s}/\text{m}$$

$V_a = 1.224 \text{ m}$  and  $h_a \approx 0.08 \text{ m}$  which is the same as the assumed value at the beginning of this iteration.

Hence

$$H_0 = 7.36 \text{ m}, \quad q = 45.28 \text{ m}^3/\text{s}/\text{m}$$

$$Q = 45.28 \times 75 = 3396 \text{ m}^3/\text{s}$$

Minimum pressure

Using Eq. 7.41

$$\begin{aligned} \frac{P_m}{\gamma} &= -1.17(7.36)(1.386 - 1) \\ &= -3.32 \text{ m} \end{aligned}$$

The minimum pressure head over the spillway will be 3.32 m below atmospheric.

### Example 7.9

A spillway with a design height of 30.0 m above the river bed is designed for energy head of 4.25 m. If a minimum pressure head of 4.0 m below atmospheric pressure head is allowed, estimate the allowable discharge intensity over the spillway.

*Solution* By Eq. 7.41

$$\begin{aligned} \frac{P_m}{\gamma H_0} &= -1.17 \left( \frac{H_0}{H_d} - 1 \right) \\ -\frac{4.0}{H_0} &= -1.17 \left( \frac{H_0}{4.25} - 1 \right) \\ H_0^2 - 4.25H_0 - 14.53 &= 0 \end{aligned}$$

$$H_0 = 6.49 \text{ m and } \frac{H_0}{H_d} = 6.49/4.25 = 1.527$$

From Fig. 7.15,  $\frac{C_0}{C_{d0}} = 1.06$  and

$$\frac{P}{H_d} = \frac{6.49}{4.25} = 7.06 > 3.0.$$

Hence  $C_{d0} = 0.738$ . Thus  $C_0 = 1.06 \times 0.738 = 0.782$

Allowable discharge intensity

$$q = \frac{2}{3} \times 0.738 \times \sqrt{19.62} \times (6.49)^{3/2} = 36.0 \text{ m}^3/\text{s}/\text{m}.$$

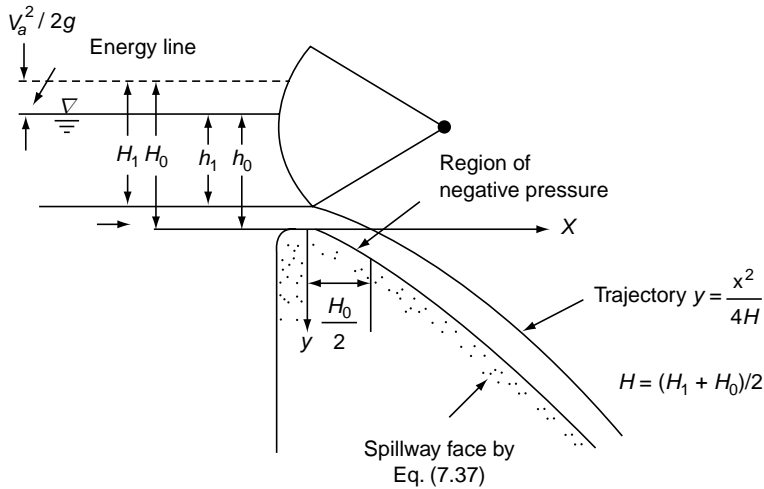


Fig. 7.15 Flow under a crest gate

### 7.4.2 Contractions on the Spillway

Very often an overflow spillway operates with end contractions. These contractions occur due to the presence of abutments and piers on the spillway to carry a bridge. Equation 7.40 is used to calculate the discharge at any head  $H_0$ . The effective length of the spillway  $L_e$  is estimated by

$$L_e = L - 2(NK_p + K_a)H_0 \quad (7.42)$$

in which  $L$  = actual length of the spillway,  $N$  = number of piers,  $K_p$  = pier contraction coefficient and  $K_a$  = abutment contraction coefficient. The values of  $K_p$  and  $K_a$  depend essentially on the geometry of the contraction-causing element in relation to the flow. For preliminary studies, the following values are usually adopted<sup>18</sup>.

Piers:	(i) Square-nosed with rounded corners	$K_p = 0.02$
	(ii) round-nosed	$K_p = 0.01$
	(iii) pointed-nosed	$K_p = 0.00$
Abutments:	(i) Square with sharp corners	$K_a = 0.20$
	(ii) round entry corner	$K_a = 0.10$

### 7.4.3 Spillway with Crest Gates

When spillways are provided with crest gates, they have to operate as uncontrolled spillway under high flood conditions and with partial gate openings at lower flows. At partial gate openings, the water issues out of the gate opening as an orifice flow and the trajectory is a parabola. If the ogee is shaped by Eq. 7.37 the orifice flow, being of a flatter trajectory curve, will cause negative pressures on the spillway crest. These negative pressures can be minimised if the gate sill is placed downstream of the apex of the crest. In this case the orifice flow will be directed downwards at the

initial point itself, causing less difference between the ogee profile and the orifice trajectory.

If the trajectory of the orifice flow with the gate sill located at the apex of the crest is adopted for the spillway profile, the coefficient of discharge at the full-gate opening will be less than that of an equivalent uncontrolled overflow spillway.

The discharge from each bay of a gated ogee spillway is calculated from the following large orifice equation.

$$Q = \frac{2}{3} \sqrt{2g} C_g L_b (H_0^{3/2} - H_1^{3/2}) \quad (7.43)$$

where  $C_g$  = coefficient of the gated spillway,  $L_b$  = effective length of the bay after allowing for two end contractions,  $H_0$  = energy head above the spillway crest and  $H_1$  = energy head above the bottom edge of the gate (Fig. 7.15). The coefficient of discharge  $C_g$  depends upon the geometry of the gate, gate installation, interference of adjacent gates and flow conditions. For radial gates, an approximate value of the coefficient of discharge  $C_g$  can be expressed by using the USBR data<sup>18</sup> as

$$C_g = 0.615 + 0.104 \frac{H_1}{H_0} \text{ for } \frac{H_1}{H_0} < 0.83 \quad (7.44)$$

**Example 7.10** | An overflow spillway with a 15-m crest above the stream bed level has radial gates fitted on the crest. During a certain flow, the gate opening was 1.0 m and the water surface upstream of the gate was observed to be 2.5 m above the crest. Estimate the discharge from a bay of 15-m length by neglecting end contractions

*Solution* Refer to Fig. 7.15.  $h_1 = 1.5$  m and  $h_0 = 2.5$  m.

*First trial:* Assume  $h_0 = H_0$  and  $h_1 = H_1$

$$\text{By Eq. 7.44 } C_g = 0.615 + 0.104 \times \frac{1.5}{2.5} = 0.677$$

$$\text{By Eq. 7.43 } Q = \frac{2}{3} \times 0.677 \times 15 \times \sqrt{19.62} \times \left( (2.5)^{3/2} - (1.5)^{3/2} \right) = 63.445 \text{ m}^3/\text{s}$$

$$\text{Velocity of approach } V_a = \frac{63.445}{(17.5 \times 15)} = 0.2417 \text{ m/s and } \frac{V_a^2}{2g} = 0.003 \text{ m.}$$

$$\text{Second trial: } H_1 = 1.50 + 0.003 = 1.503 \text{ m}$$

$$H_0 = 2.50 + 0.003 = 2.503 \text{ m}$$

$$C_g = 0.615 + 0.104 \times \frac{1.503}{2.503} = 0.677. \text{ No change from the assumed value.}$$



$$Q = \frac{2}{3} \times 0.677 \times 15 \times \sqrt{19.62} \times \left( (2.503)^{3/2} - (1.503)^{3/2} \right) = 63.49 \text{ m}^3/\text{s}$$

In view of the very small change in the value of  $Q$ , no further trials are required.

## 7.5 BROAD-CRESTED WEIR

Weirs with a finite crest width in the direction of flow are called *broad-crested weirs*. They are also termed as *weirs with finite crest width* and find extensive applications as control structures and flow measuring devices. It is practically impossible to generalise their behaviour because a wide variety of crest and cross-sectional shapes of the weir are used in practice. In this section the salient flow characteristics of only a simple, rectangular, horizontal broad-crested weir are presented.

Figure 7.16 is a definition sketch of a free flow over a horizontal broad-crested weir in a rectangular channel. This weir has a sharp upstream corner which causes the flow to separate and then reattach enclosing a separation bubble. If the width  $B_w$  of the weir is sufficiently long, the curvature of the stream lines will be small and the hydrostatic pressure distribution will prevail over most of its width. The weir will act like an inlet with subcritical flow upstream of the weir and supercritical flow over it. A critical-depth control section will occur at the upstream end-probably at a location where the bubble thickness is maximum.

Assuming no loss of energy between Sections 1 and 2 (Fig. 7.16), and further assuming the depth of flow at Section 2 to be critical,

$$H = y_c + \frac{V_c^2}{2g} = \frac{3}{2} y_c$$

$$V_c = \sqrt{gy_c} \quad \text{and} \quad y_c = \frac{2}{3} H$$

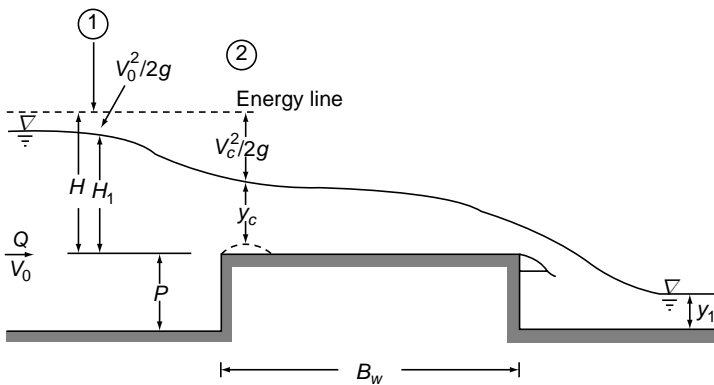


Fig. 7.16 Definition sketch of a broad-crested weir

The ideal discharge per unit width of the weir is

$$q_t = V_c y_c = \frac{2}{3} \sqrt{\left(\frac{2}{3}g\right)} H^{3/2} = 1.705 H^{3/2} \quad (7.45)$$

To account for the energy losses and the depth at Section 2 being not strictly equal to the critical depth, the coefficient of discharge  $C_{d1}$  is introduced in Eq. 7.45 to get an equation for the actual discharge  $q$  as

$$\begin{aligned} q &= C_{d1} q_t \\ &= 1.705 C_{d1} H^{3/2} \end{aligned} \quad (7.46)$$

and  $Q = qL$ , where  $L$  = length of the weir.

It may be noted that in connection with broad-crested weirs,  $L$  = length of the weir measured in a transverse direction to the flow and  $B_w$  = width of the weir measured in the longitudinal direction. Thus  $B_w$  is measured at right angles to  $L$ . In suppressed weirs  $L = B$  = width of the channel. This terminology is apt to be confusing and as such warrants a clear understanding of each of these terms.

Since Eq. 7.46 is rather inconvenient to use as it contains the energy head  $H$ , an alternate form of the discharge equation commonly in use is

$$Q = \frac{2}{3} C_d \sqrt{2g} L H_1^{3/2} \quad (7.47)$$

where  $H_1$  = height of the water-surface elevation above the weir surface measured sufficiently upstream of the weir face and  $C_d$  = the coefficient of discharge.

If the upstream end is rounded, the separation bubble will not exist and instead, a boundary layer will grow over the weir with the critical-depth control point shifting towards this downstream end. The flow over most part of its crest will be subcritical. Considerable flow resistance from the upstream face to the critical flow section exists, influencing the value of  $C_d$ . The round-nosed broad-crested weir is not dealt with in this section and the details on it are available in Ref. 4.

### 7.5.1 Classification

Based on the value of  $H_1/B_w$  the flow over a broad-crested weir with an upstream sharp corner is classified as follows<sup>22, 23</sup>.

1.  $H_1/B_w \lesssim 0.1$ : In this range the critical flow control section is at the downstream end of the weir and the resistance of the weir surface plays an important role in determining the value of  $C_d$  (Fig. 7.17a).  
This kind of weir, termed as *long-crested weir*, finds limited use as a reliable flow-measuring device.
2.  $0.1 \lesssim H_1/B_w \lesssim 0.35$ : The critical depth control occurs near the upstream end of the weir and the discharge coefficient varies slowly with  $H_1/B_w$  in this range (Fig. 7.17b). This kind can be called a *true broad-crested weir*.

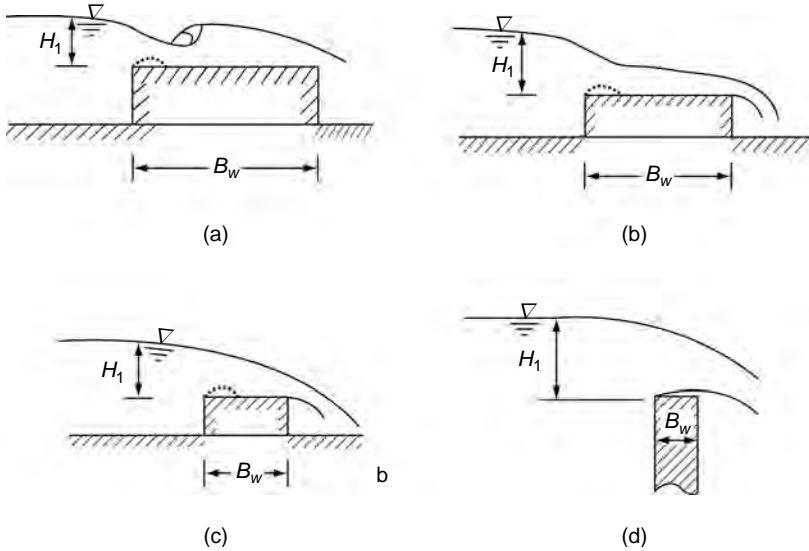


**Fig. 7.17** (a) Long-crested weir ( $H_1/B_w \lesssim 0.1$ )  
 (b) Broad-crested weir ( $0.1 \lesssim H_1/B_w \lesssim 0.35$ )  
 (c) Narrow-crested weir ( $0.35 \lesssim H_1/B_w \lesssim 1.5$ )  
 (d) Sharp-crested weir ( $H_1/B_w \gtrsim 1.5$ )

3.  $0.35 \lesssim H_1/B_w \lesssim$  about 1.5: The water-surface profile will be curvilinear all over the weir. The control section will be at the upstream end (Fig. 7.17c). The weirs of this kind can be termed as *narrow-crested* weirs. The upper limit of this range depends upon the value of  $H_1/P$ .
4.  $H_1/B_w >$  about 1.5: The flow separates at the upstream corner and jumps clear across the weir crest. The flow surface is highly curved (Fig. 7.17d), and the weir can be classified as *sharp-crested*.

### 7.5.2 Discharge Coefficients, $C_d$ and $C_{d1}$

From Eqs 7.47 and 7.46 the discharge coefficients  $C_d$  and  $C_{d1}$  respectively are given as

$$C_d = \frac{Q}{\frac{2}{3}\sqrt{2g} LH_1^{3/2}} \quad \text{and} \quad C_{d1} = \frac{Q}{1.705 LH^{3/2}} \quad (7.48)$$

A formal dimensional analysis of the flow situation will reveal that

$$C_d(\text{or } C_{d1}) = f\left[\frac{H_1}{L}, \frac{H_1}{B_w}, \frac{H_1}{P}, Re, W, \frac{k_s}{H_1}\right] \quad (7.49)$$

in which  $Re$  = Reynolds number,  $W$  = Weber number and  $k_s/H_1$  = relative roughness of the weir surface. In most of the situations of practical interest with broad crested weirs, the parameters  $Re$ ,  $W$ ,  $k_s/H_1$  and  $H_1/L$  have insignificant effect on  $C_d$  (or  $C_{d1}$ ). Hence for practical purposes,

$$C_d \text{ (or } C_{d1}) = f(H_1/B_w \text{ and } H_1/P) \quad (7.50)$$

Considerable experimental investigations have been conducted to study the variation of  $C_d$  (or  $C_{d1}$ ) as indicated by Eq. 7.50. Lakshmana Rao<sup>1</sup> has given a good bibliography on these studies. Govinda Rao and Muralidhar<sup>22</sup> on the basis of extensive studies of the weir of finite crest in the range  $0 \leq H_1/B_w \leq 2.0$  and  $0 \leq H_1/P \leq 1.0$ , have given the following expressions for the variation of  $C_d$ :

1. For long weirs,  $H_1/B_w \leq 0.1$

$$C_d = 0.561 (H_1/B_w)^{0.022} \quad (7.51)$$

2. For broad-crested weirs,  $0.1 \leq H_1/B_w \leq 0.35$

$$C_d = 0.028(H_1/B_w) + 0.521 \quad (7.52)$$

3. For narrow-crested weirs,  $0.45 \lesssim H_1/B_w \lesssim$  about 1.5

$$C_d = 0.120(H_1/B_w) + 0.492 \quad (7.53)$$

The upper limit of  $H_1/B_w$  in Eq 7.53 depends on  $H_1/P$ .

Between cases 2 and 3, there exists a small transition range in which Eq. 7.52 progressively changes into Eq. 7.53. In this transition region Eq. 7.52 can be used up to  $H_1/B_w \leq 0.40$  and Eq. 7.53 for  $H_1/B_w > 0.40$ . It may be noted that Eq. 7.51 through Eq. 7.53 show  $C_d$  as a function of  $H_1/B_w$  only and the parameter  $H_1/P$  has no effect on  $C_d$  in the range of data used in the derivation of these equations. Surya Rao and Shukla<sup>24</sup> have conclusively demonstrated the dependence of  $C_d$  on  $H_1/P$ . As such Equations 7.51, 7.52 and 7.53 are limited to the range  $0 \leq H_1/P \leq 1.0$ .

Singer<sup>23</sup> has studied the variation of  $C_{d1}$  for values of  $H_1/B_w$  up to 1.5 and  $H_1/P$  up to 1.5. For the range  $0.08 \leq H_1/B_w \leq 0.33$  and  $H_1/P < 0.54$ , the value of  $C_{d1}$  is found to remain constant at a value of 0.848. For higher values of  $H_1/B_w$  as well as  $H_1/P$ , the coefficient  $C_{d1}$  is a function of both these parameters.

### 7.5.3 Submerged Flow

If the tailwater surface elevation measured above the weir crest  $H_2 = (y_t - P)$  (Fig. 7.18) is appreciable, the flow over the crest may be entirely subcritical. The discharge in such a case will depend upon both  $H_1$  and  $H_2$ . The submergence (modular) limit depends upon  $H_1/B_w$  and in the broad-crested weir flow range, it is of the order of 65 per cent. At this value, the downstream water surface drowns the critical depth on the crest. For submergences larger than the modular limit, the coefficient of discharge ( $C_d$  or  $C_{d1}$ ) decreases with the submergence ratio  $H_2/H_1$  at a rapid rate. Compared to the sharp-crested weir, the broad-crested weir has very good submergence characteristics.

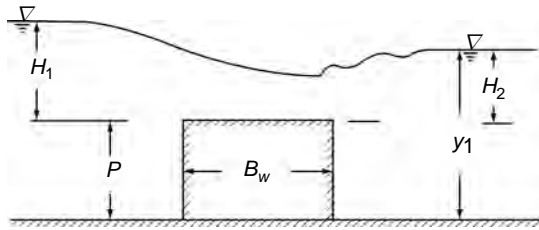


Fig 7.18 Submerged broad-crested weir flow

**Example 7.11** A broad-crested weir with an upstream square corner and spanning the full width of a rectangular canal of 2.0-m width is planned. The proposed crest length is 2.50 m and the crest elevation is 1.20 m above the bed. Calculate the water-surface elevation upstream of the weir when the discharge is (a) 2.0 m<sup>3</sup>/s and (b) 3.50 m<sup>3</sup>/s.

*Solution* (a)  $Q = 2.0 \text{ m}^3/\text{s}$

Assume the weir to function in the broad-crested weir mode and hence assume  $C_d = 0.525$  as a first guess. From Eq. 7.47

$$2.0 = \frac{2}{3} \times 0.525 \times \sqrt{19.62} \times 2.0 \times H_1^{3/2}$$

$$H_1^{3/2} = 0.645 \text{ and } H_1 = 0.747 \text{ m}$$

$$\frac{H_1}{B_w} = 0.299. \text{ The assumption is OK.}$$

By Eq. 7.52  $C_d = 0.028(0.299) + 0.521 = 0.529$

Substituting this  $C_d$  value in Eq. 7.47

$$H^{3/2} = 0.640. H_1 = 0.743 \text{ m and from Eq. 7.52}$$

$$C_d = 0.529$$

Hence the water-surface elevation above the bed = 1.943 m.

(b)  $Q = 3.25 \text{ m}^3/\text{s}$

Since  $Q$  is higher than in case (a), it is likely that  $H_1/B_w > 0.35$ . Hence assuming the weir to function in the narrow-crested weir mode, the calculations are started by assuming  $C_d = 0.55$ .

1st iteration  $C_d = 0.55$

$$\text{From Eq. 7.28, } 3.50 = \frac{2}{3} \times 0.55 \times \sqrt{19.62} \times 2.0 \times H_1^{3/2}$$

$$H_1^{3/2} = 1.077, \quad H_1 = 1.05 \text{ m, } \frac{H_1}{B_w} = 0.42$$

The weir flow is in the transition region between the broad-crested and narrow-crested weir modes. Hence, by Eq. 7.53

$$C_d = 0.120 \times (0.42) + 0.492 = 0.534$$

2nd iteration Using  $C_d = 0.534$  in Eq. 7.47

$$H_1^{3/2} = 1.109, \quad H_1 = 1.071 \text{ m, } \frac{H_1}{B_w} = 0.429$$

From Eq. 7.53,  $C_d = 0.543$

$$\text{3rd iteration } H_1^{3/2} = 1.091, \quad H_1 = 1.060 \text{ m, } \frac{H_1}{B_w} = 0.424$$

$$C_d = 0.543$$

Hence,  $H_1 = 1.060$  and the water-surface elevation above the bed is 2.260 m.

**Example 7.12** Show that for a triangular broad crested weir flowing free the discharge equation can be expressed as

$$Q = \frac{16}{25} C_{d1} \tan \theta \sqrt{\frac{2g}{5}} H^{5/2}$$

where  $H$  = energy head measured from the vertex of the weir,  $\theta$  = semi-apex angle and  $C_{d1}$  = coefficient of discharge.

$$\text{Solution } H = y_c + \frac{V_c^2}{2g} = 1.25y_c$$

$$\text{or } y_c = \frac{4}{5} H$$

$$A = m y_c^2 = \frac{16}{25} \tan \theta H^2 \quad \text{where } \theta = \text{semi vertex angle.}$$

$$F = \frac{V\sqrt{2}}{\sqrt{g}y_c} = 1 \quad \text{or } V = \sqrt{\frac{2g}{5}} H^{1/2}$$

$$Q = C_{d1}VA$$

$$Q = \frac{16}{25} C_{d1} \tan \theta \sqrt{\frac{2g}{5}} H^{5/2}$$

## 7.6 CRITICAL-DEPTH FLUMES

Critical-depth flumes are flow-measuring devices in which a control section is achieved through the creation of a critical-flow section by a predominant width constriction. In practice, these are like broad-crested weirs but with a major change that these are essentially flow-measuring devices and cannot be used for flow-regulation purposes. A typical critical-depth flume consists of a constricted portion called the *throat* and a diverging section. Sometimes a hump is also provided to assist in the formation of critical flow in the throat (Fig. 7.19).

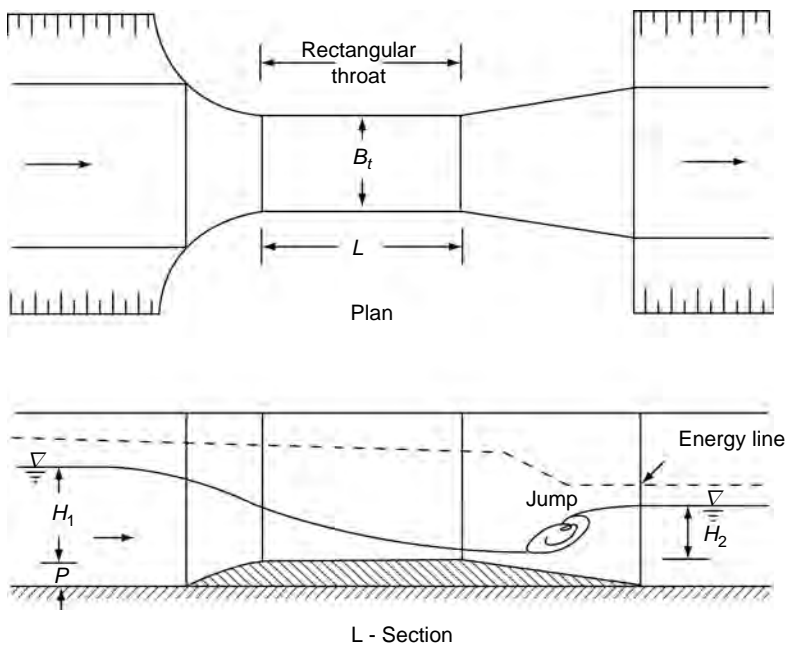


Fig. 7.19 Standing-wave flume

### 7.6.1 Standing-wave Flume

The critical-depth flume shown in Fig. 7.19 is known as a *standing-wave flume* or *throated flume*. This flume can be fitted into any shape of the parent channel. The throat is prismatic and can be of any convenient shape. Thus for a rectangular parent channel, it is convenient to have a rectangular throat, and for a circular sewer, a circular throat is preferable. A hydraulic jump forms on the downstream of the throat and holds back the tailwater. If the throat is submerged by the tailwater, subcritical flow prevails all over the flume. It is usual to operate the flume in the free-flow mode only, i.e. with the throat unsubmerged.

During the operation a critical depth is formed somewhere in the throat and as such its discharge equation is similar to that of a broad-crested weir (Eq. 7.46).

However, it is usual to relate the discharge to the upstream depth  $H_1$  which can be typically recorded by an automated float equipment.

Thus for a rectangular throat section, the discharge is given by

$$Q = C_f B_t H_1^{3/2} \quad (7.54)$$

where  $C_f$  = overall discharge coefficient of the flume =  $f(H_1/L)$ . For a well-designed flume,  $C_f$  is of the order of 1.62. It may be noted that in standing-wave flumes,  $H_1$  is the difference in the water-surface elevation upstream of the inlet and the elevation of the crest at the throat. If the flume is submerged and the subcritical flow prevails all over the flume, Eq. 7.54 is not valid and two depth measurements are needed to estimate the discharge. Constriction flumes operating in the subcritical flow range are called *venturi flumes*.

The modular limit ( $H_2/H_1$ ) of standing wave flumes is high, being of the order of 0.90. It is usual to take it as 0.75 to incorporate a small safety factor and to avoid the region of transition from the free to submerged-flow mode.

Large varieties of standing-wave flumes with different types of modifications of the basic type described above, resulting in different geometric shapes and corresponding flow characteristics are in use<sup>4,5</sup>. However, the basic favourable features of all these throated flumes can be summarised as (i) low energy loss, (ii) rugged construction, (iii) easy passage for floating and suspended material load, and (iv) high modular limit. These features are responsible for extensive use of throated flumes as flow-measuring devices in water-treatment plants and in irrigation practice.

**Example 7.13** (a) A standing-wave flume without a hump is to be provided in a rectangular channel of bottom width = 2.0 m,  $n = 0.015$  and  $S_0 = 0.0004$ . A maximum discharge of  $2.50 \text{ m}^3/\text{s}$  is expected to be passed in this flume. If the modular limit of the flume is 0.75, find the width of the throat. (Assume  $C_f = 1.62$ .)

$$\text{Solution} \quad \phi = \frac{Qn}{\sqrt{S_0} B^{8/3}} = \frac{2.5 \times (0.015)}{\sqrt{0.0004} (2.0)^{8/3}} = 0.29529$$

From Table 3A.1,  $\frac{y_0}{B}$  (corresponding to  $m=0$ ) = 0.656 and normal depth  $y_0 = 1.312$  m. This is the tailwater depth  $H_2$ .

$$\text{For a modular limit of 0.75, } H_1 = \frac{1.312}{0.75} = 1.749 \text{ m}$$

$$\begin{aligned} \text{By Eq. 7.54, } B_t &= \frac{Q}{C_f H_1^{3/2}} = \frac{2.50}{1.62 \times (1.749)^{3/2}} \\ &= 0.667 \text{ m} \end{aligned}$$

**Example 7.14** In the Example 7.12 compare the heading up of water surface (afflux) due to the flume and also due to a suppressed free flowing sharp-crested weir.

**Solution** From Example 7.13 heading up (afflux) due to flume

$$= H_1 - H_2 = 1.749 - 1.312 = 0.47 \text{ m.}$$



*Sharp-crested weir*

For free-flow operation, the crest of the weir should be at least 0.08 m above the tailwater elevation. Hence  $P = 1.312 + 0.080 = 1.392$  m.

1<sup>st</sup> trial: Assume  $C_d = 0.650$

$$\text{By Eq. 7.5 } Q = \frac{2}{3} C_d \sqrt{2g} L h_1^{3/2}$$

$h_1$  = head over the crest

$$h_1^{3/2} = \frac{2.50}{\frac{2}{3} \times 0.65 \times 2.0 \times \sqrt{19.62}} = 0.651, h_1 = 0.751 \text{ m}$$

$$\frac{h_1}{P} = 0.54 \text{ and by Rehbock equation (Eq. 7.7)}$$

$$C_d = 0.611 + 0.08(0.54) = 0.654$$

2<sup>nd</sup> trial Using  $C_d = 0.654$

$$h_1^{3/2} = 0.651 \times \frac{0.650}{0.654} = 0.647, h_1 = 0.748 \text{ m}$$

$$h_1 / P = 0.537 \text{ and } C_d = 0.654$$

Hence,  $h_1 = 0.748$  m

$$\text{Afflux} = 0.748 \text{ m} + 1.392 - 1.312 = 0.828 \text{ m}$$

**7.6.2 Parshall Flume**

The Parshall flume is a type of critical-depth flume popular in the USA. This flume consists of a converging section with a level floor, a throat with a downstream sloping floor and a diverging section with an adverse slope bed (Fig. 7.20). Unlike in the standing-wave flume, the head ( $H_a$ ) is measured at a specified location in the converging section. The discharge in the flume in the free flow mode is given by

$$Q = KH_a^n \quad (7.55)$$

where  $K$  and  $n$  are constants for a given flume. The dimensions of various sizes of Parshall flumes are standardised and further details are available in references 4, 5, 25 and 26.

**7.7 END DEPTH IN A FREE OVERFALL**

A free overfall is a situation in which there is a sudden drop in the bed causing the flow to separate from the stream bed and move down the step with a free nappe. The situation is analogous to the flow over a sharp-crested weir of zero height. A free overfall causes not only a GVF profile in the subcritical flow, but also offers the possibility of being used as a flow measuring device in all flow regimes.

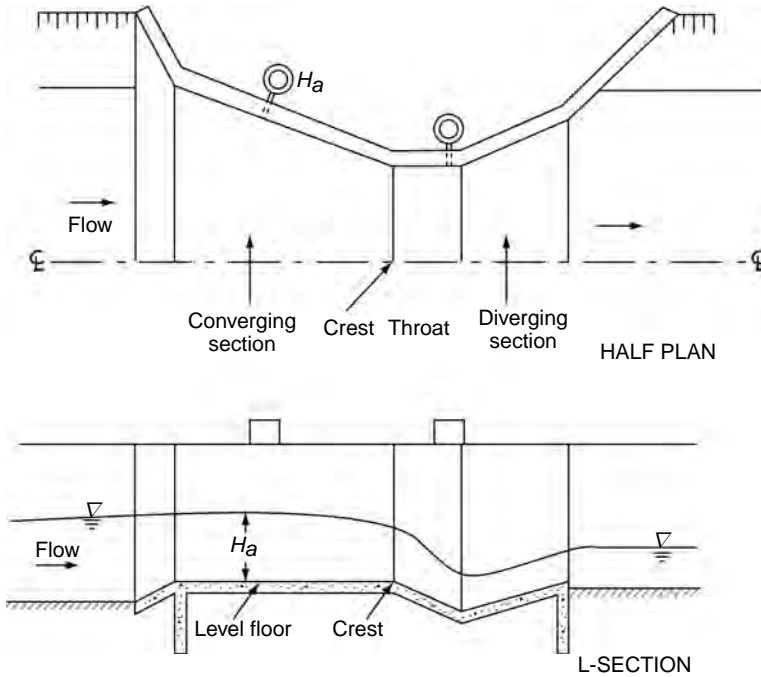


Fig. 7.20 Parshall flume

A typical free overfall is schematically illustrated in Fig. 7.21. The flow in the nappe emerging out of the overfall is obviously affected by gravity. With the atmospheric pressure existing above and below the nappe, the water-surface profile is a parabola. Due to the need for continuity of the water-surface profile, the gravity effect extends a short distance on the water-surface profile behind the edge, causing an acceleration of the flow. Also, at the brink, the pressure should necessarily be atmospheric at points  $F$  and  $F'$ . This causes the pressure distribution at section  $FF'$  to depart from the hydrostatic-pressure distribution and assume a pattern as shown in Fig. 7.21. At sections upstream of the brink, the water-surface curvature gradually decreases and at a section such as 1, at a distance  $x_1$  from  $F$ , the full hydrostatic pressure is re-established. The result of this effect of the free overfall is to cause a reduction in the depth from Section 1 in the down stream direction with the minimum depth  $y_e$  occurring at the brink. This depth  $y_e$  is known as the *end depth* or the *brink depth*.

In subcritical flow a critical section must occur if the flow has to pass over to supercritical state. The critical depth  $y_c$  based on hydrostatic pressure distribution will occur upstream of the brink. In Fig. 7.21 Section 1 can be taken as the critical section with  $y_1 = y_c$ . Then  $x_1 = x_c$ . In supercritical flow,  $y_1$  will be equal to the normal depth,  $y_1 = y_0$ .

### 7.7.1 Experimental Observations

Rouse<sup>27</sup> was probably the first to recognise the interesting feature of the end depth at a free fall. His experiments on the end depth for subcritical flow in a

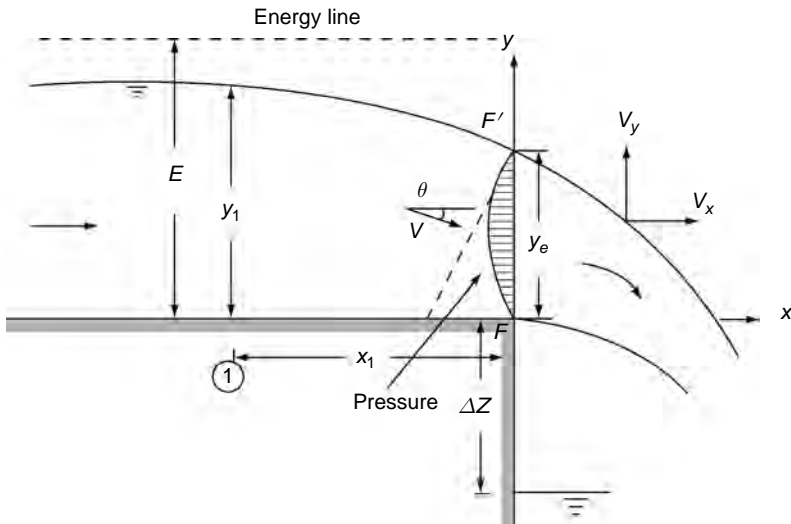


Fig. 7.21 Definition sketch of the end depth

horizontal rectangular channel with side walls continuing downstream on either side of the free nappe with atmospheric pressure existing on the upper and lower sides of the nappe (confined nappe) indicated that  $y_e = 0.715 y_c$ . Since then a large number of experimental studies have been conducted on a variety of channel shapes and boundary conditions. Some of the important studies are summarised in Table 7.3.

Table 7.3 Results of Experimental study on End Depth Ratio in Subcritical Flow in Horizontal Channels

Sl. No	Shape	End depth ratio $\frac{y_e}{y_c}$	Variation (approximate)	Reference
1	Rectangular Channel (Confined Nappe)	0.715	$\pm 2.0\%$	5,27,31
2	Rectangular Channel (Unconfined Nappe)	0.705	$\pm 2.0\%$	28,31
3	Triangular	0.795	$\pm 2.0\%$	28
4	Circular	0.725	$\pm 3.5\%$	29
5	Parabolic	0.772	$\pm 5.0\%$	28

In Table 7.3, the term unconfined nappe means that the side walls terminate at section  $FF'$  and it is seen that this end constraint has the effect of decreasing  $y_e / y_c$  values. For subcritical flow, in horizontal, rectangular channels,  $y_e / y_c = 0.705$  for unconfined nappe as against 0.715 for the confined case. It is interesting to note that the channel-roughness magnitude does not have any significant influence on the value of  $y_e / y_c$  in the subcritical

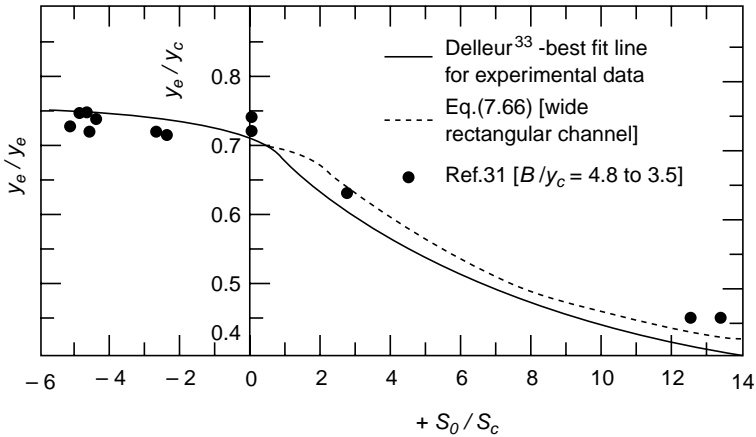


Fig. 7.22 End-depth ratio in rectangular channels

flow range. The possible magnitude of error of the various experimentally determined values of  $y_e/y_c$  is also shown in Table 7.3.

For the supercritical flow cases, Delleur et al.<sup>23</sup> showed that the relative end depth can be expressed as

$$\frac{y_e}{y_c} = f\left(\frac{S_0}{S_c}, \text{channel shape}\right) \tag{7.56}$$

For a given channel, the variation of  $y_e/y_c$  can be expressed as a unique function of  $S_0/S_c$ . The results of some experimental observations on rectangular channels are indicated in Fig. 7.22. Similar variations of  $y_e/y_c$  with  $S_0/S_c$  for triangular, parabolic, circular and trapezoidal channels recorded in various experimental studies are reported in the literature<sup>1</sup>. In experimental studies on large values of  $S_0/S_c$ , considerable scatter of data, of the order  $\pm 10$  per cent, is observed.

Experimental studies<sup>34</sup> have shown that in subcritical flow  $\frac{x_c}{y_c}$  is of the order of 3.0 to 6.0 and is a function of the Froude number of the flow. Further, if the brink flow is not to be affected by the tailwater level, the drop  $\Delta z$  (Fig. 7.21) should be greater than  $0.6 y_c$  (Ref. 5).

### 7.7.2 Analytical Studies

For the prediction of end depth, several analytical attempts have been made by earlier workers. Most of them are based on the application of the momentum equation with various assumptions, especially regarding the velocity and pressure distributions at the brink section. In a typical momentum approach<sup>28,29,32</sup> the pressure force at the brink section is expressed as  $P_e = \gamma A_e \bar{y}_e K_1$ , when  $K_1$  = a pressure-correction factor and  $\bar{y}_e$  = the depth of the centre of gravity below the free surface at the brink section. The success of the momentum equation to predict  $y_e$  depends upon the proper choice of  $K_1$  (the variation of  $K_1$  with the geometry of the problem has to be determined experimentally).

The numerical solution of a two-dimensional ideal fluid-flow at a free overfall has been attempted by some investigators through various finite difference schemes. An excellent review of these studies on potential flow in a free overfall and a theory describing such a flow is presented by Strelkoff et al.<sup>35</sup> While it is possible to solve the end-depth problem in a wide rectangular channel through advanced numerical techniques, such as the finite-element method, the solution of the problem in channels of different shapes have to be tackled by alternative methods.

An elegant method which differs from the above two approaches has been reported by Anderson<sup>34</sup>. Based on Anderson's work, a generalised energy method for the prediction of end-depth in channels of any shape is given by Subramanya<sup>36</sup> and is described below. This method is simple, does not need any coefficient and can predict the end-depths to a remarkable degree of accuracy in a variety of situations.

### 7.7.3 Generalised Energy Method for End Depth Prediction<sup>36</sup>

In a free overfall, the water surface is a continuously falling curve. The water surface profile starts in the channel somewhere upstream of the edge, passes through the brink and ends up as a trajectory of gravity fall. In deriving the general expression for the end-depth, expressions for the curvature of the water surface are separately derived for the channel flow as well as for the free overfall and matched at the brink.

**(a) Curvature of the Channel Flow** Consider a channel of any shape having a free over fall (Fig. 7.21). The water surface curvature is assumed to be relatively small and is assumed to vary linearly from a finite value at the surface to zero value at the channel bottom. The effective piezometric head is then expressed by the Boussinesq equation (Eq. 1-35) The water surface curvature is convex upwards and the specific energy  $E$  at any section is given by Eq. 1.41 as

$$E = h_{ep} + \alpha \frac{V^2}{2g}$$

By using Eq. 1.33 for  $h_{ep}$

$$E = y + \alpha \frac{V^2}{2g} + \frac{1}{3} \frac{V^2 y}{g} \left( \frac{d^2 y}{dx^2} \right) \tag{7.57}$$

i.e. 
$$E = y + \alpha \frac{Q^2}{2gA^2} + \frac{1}{3} \frac{Q^2}{gA^2} y \left( \frac{d^2 y}{dx^2} \right) \tag{7.58}$$

Assume the specific energy  $E$  to be constant in the neighbourhood of the brink and further assume  $\alpha = 1.0$  for simplicity. The conditions at the brink section (denoted by the suffix  $e$ ) is expressed, by non-dimensionalising Eq. 7.58 with respect to the critical depth  $y_c$ , as

$$\frac{E_e}{y_c} = \frac{y_e}{y_c} + \frac{Q^2}{2gA_e^2 y_c} + \frac{1}{3} \frac{Q^2}{gA_e^2 y_c} \frac{y_e}{y_c} \frac{d^2 (y/y_c)}{d(x/y_c)^2} \Big|_{y=y_e} \tag{7.59}$$

Denoting the critical conditions by the suffix  $c$ ,

$$y_e / y_c = \eta; \quad \frac{A_c^3}{A_e^2 T_c y_c} = f(\eta) \text{ and } E_e / y_c = \varepsilon$$

Remembering that  $Q^2 / g = A_c^3 / T_c$  Eq. (7.59) can be simplified as

$$\varepsilon = \eta + \frac{1}{2} f(\eta) + \frac{1}{3} \eta f(\eta) \left. \frac{d^2(y/y_c)}{d(x/y_c)^2} \right|_{y=y_e} \quad (7.60)$$

The expression for the curvature of the channel water surface at the brink is from Eq. 7.60,

$$\left. \frac{d^2(y/y_c)}{d(x/y_c)^2} \right|_{y=y_e} = \frac{3}{\eta f(\eta)} \left[ \varepsilon - \eta - \frac{1}{2} f(\eta) \right] \quad (7.61)$$

**(b) Overflow Trajectory** Referring to Fig. 7.21,  $V_x$  is  $x$  – component of the velocity in the overflow trajectory and is given by

$$V_x = V_e \cos \theta \quad (7.62)$$

where  $V_e$  = mean velocity at the brink inclined at an angle  $\theta$  to the horizontal. For a gravity fall

$$\frac{dV_x}{dt} = 0 \text{ and } \frac{dV_y}{dt} = -g$$

where  $V_y = y$  – component of the velocity in the trajectory.

$$\text{Since } \frac{dy}{dx} = \frac{V_y}{V_x}$$

$$\begin{aligned} \frac{d^2 y}{dx^2} &= -g / V_x^2 = -\frac{g A_e^2}{(V_e A_e)^2 \cos^2 \theta} \\ &= -\frac{g A_e^2}{Q^2 \cos^2 \theta} \end{aligned} \quad (7.63)$$

Noting that  $\frac{Q^2}{g} = \frac{A_c^3}{T_c}$ , Eq. 7.63 can be written as

$$\frac{d^2 y}{dx^2} = -\frac{T_c A_e^2}{A_c^3 \cos^2 \theta} = -\frac{1}{y_c f(\eta) \cos^2 \theta}$$

Thus,

$$\left. \frac{d^2(y/y_c)}{d(x/y_c)^2} \right|_{y=y_e} = -\frac{1}{f(\eta) \cos^2 \theta} \quad (7.64)$$

**(c) General Equation for End Depth Ratio** For a continuous water surface slope at  $(x = 0, y = y_e)$  Eq. 7.61 and Eq. 7.64 must be identical and as such

$$-\frac{1}{f(\eta)\cos^2\theta} = \frac{3}{\eta f(\eta)} \left[ \varepsilon - \eta - \frac{1}{2} f(\eta) \right]$$

Simplifying,

$$6\varepsilon\cos^2\theta - 2\eta(3\cos^2\theta - 1) - 3f(\eta)\cos^2\theta = 0 \quad (7.65)$$

In the usual cases when  $\theta$  is small,  $\cos\theta \approx 1.0$ ,  $\cos^2\theta \approx 1.0$  and Eq. 7.65 simplifies to

$$6\varepsilon - 4\eta - 3f(\eta) = 0 \quad (7.66)$$

This equation is the general equation relating the end-depth ratio  $\eta$  with the non-dimensionalised specific energy at the brink and is based on the assumption of constancy of the specific energy in the neighbourhood of the brink. To illustrate the use of Eq. 7.66, the prediction of end-depth in exponential channels is presented in the following section.

### 7.7.4 End Depth in Exponential Channels

An exponential channel is defined as the one in which the area  $A$  is related to the depth  $y$  as  $A = Ky^a$ , where  $K$  and  $a$  are constants. It is easily seen that  $a = 1.0, 1.5$  and  $2.0$  represents rectangular, parabolic and triangular channels respectively.

For exponential channels,  $T = \frac{dA}{dy} = Ka y^{a-1}$  and  $\frac{A}{T} = \frac{y}{a}$  (7.67)

$$f(\eta) = \frac{A_c^3}{A_e^2 T_c y_c} = \frac{1}{a} (y_c / y_e)^{2a} = \frac{1}{a\eta^{2a}} \quad (7.68)$$

Eq. 7.66 now becomes

$$6\varepsilon - 4\eta - \frac{3}{a} \frac{1}{\eta^{2a}} = 0 \quad (7.69)$$

The solution of Eq. 7.69 is now obtained for subcritical and supercritical channel flows separately.

**(i) Subcritical Flow** If the flow upstream of the brink is subcritical, the critical depth must occur before the end-depth. Assuming constant specific energy  $E$  between the critical section and end section

$$\varepsilon = \frac{E_e}{y_c} = \frac{E_c}{y_c}$$

Since  $E_c = y_c + \frac{Q^2}{2g A_c^2} = y_c + \frac{A_c}{2T_c}$

$$\varepsilon = 1 + \frac{1}{2} \left( \frac{A_c}{T_c} \frac{1}{y_c} \right)$$

By substituting Eq. 7.67 for an exponential channel

$$\varepsilon = 1 + \frac{1}{2a} \tag{7.70}$$

Thus, for a given exponential channel shape (i.e.  $a = \text{constant}$ ),  $\varepsilon$  is constant for subcritical flow.

Eq. 7.69 now becomes

$$6 \left( 1 + \frac{1}{2a} \right) - 4\eta - \frac{3}{a} \frac{1}{\eta^{2a}} = 0$$

and can be solved for a given value of  $a$ . It is seen that for a given value of  $a$ , the end-depth ratio  $\eta$  is a constant in subcritical flow and is independent of the flow parameters like Froude number.

**(ii) Supercritical Flow** If the flow upstream of the brink is supercritical, the normal depth  $y_0$  is less than  $y_c$  and the critical depth does not exist in the profile between  $y_0$  and  $y_c$ . Considering a section between  $y_0$  and  $y_c$  (Fig. 7.23)

$$\varepsilon = \frac{E_g}{y_c} = \frac{E_0}{y_c} = \frac{y_0}{y_c} + \frac{Q^2}{2g A_0^2 y_c}$$

Putting  $\frac{y_0}{y_c} = \delta$  and, noting that  $\frac{Q^2 T_0}{g A_0^3} = F_0^2$

$$\begin{aligned} \varepsilon &= \delta + \frac{F_0^2}{2} \frac{A_0}{T_0 y_0} \\ &= \delta + \frac{F_0^2}{2} f(\delta) \end{aligned} \tag{7.71}$$

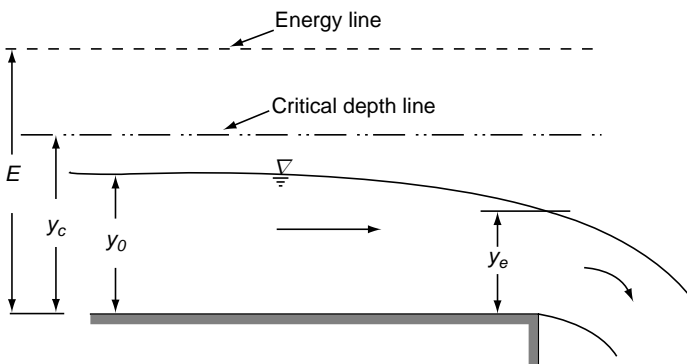


Fig. 7.23 Free overfall in supercritical flow



342 Flow in Open Channels

where  $f(\delta) = \frac{A_0}{T_0 y_c}$

In an exponential channel  $f(\delta) = \delta / a$  (7.72a)

and  $F_0^2 = \frac{A_c^3 T_0}{A_0^3 T_c} = \left(\frac{y_c}{y_0}\right)^{2a+1} = \left(\frac{1}{\delta}\right)^{2a+1}$  (7.72b)

or  $\frac{y_0}{y_c} = \delta = \left[\frac{1}{F_0^{2/(2a+1)}}\right]$  (7.72c)

Thus for an exponential channel having supercritical flow upstream of the brink, by substituting Equations 7.72a, b and c in Eq. 7.71 it is seen that  $\varepsilon$  is a function of the upstream Froude number  $F_0$  given by

$$\varepsilon = \frac{1}{F_0^{2/(2a+1)}} \left(1 + \frac{F_0^2}{2a}\right) \tag{7.73}$$

$$\eta = fn(a, F_0) \tag{7.74}$$

**End-depth ratios in Exponential Channels** Using Eq. 7.69 along with appropriate expression for  $\varepsilon$ , [viz. Eq. 7.70 in subcritical flow and Eq. 7.73 in supercritical flow], the value of the end-depth ratio  $\eta$  can be evaluated for a given flow situation. Table 7.4 gives the values of  $\eta$  for subcritical flows in rectangular, parabolic and triangular channels evaluated by Eq. 7.69 along with the corresponding results obtained experimentally.

**Table 7.4** Comparison of End-Depth Ratios of  $\eta$  Obtained by Eq. (7.69)

Channel shape	$a$	$\eta = \frac{y_e}{y_c}$ by Eq.(7.69)	Mean experimental value ( Table 7.3)	Per cent under estimation
Rectangle	1.0	0.694	0.715 ± 3.5%	2.9
Parabola	1.5	0.734	0.722 ± 5.0%	4.9
Triangle	2.0	0.762	0.795 ± 2.5%	4.2

Generally, the predictions are less by about 5% of the mean experimental values, probably due to the neglect of frictional effects. Considering the nature of scatter of experimental results, the prediction of  $\eta$  by Eq. 7.69 can be taken as satisfactory and adequate.

Figure 7.24 shows the variation of the end-depth ratio  $\eta$  with  $F_0$  for supercritical flows, in rectangular, parabolic and triangular channels, obtained by solving Eq. 7.69. Detailed experimental data are not available to verify these predictions completely. However, available data on triangular channels<sup>27</sup> have shown the prediction

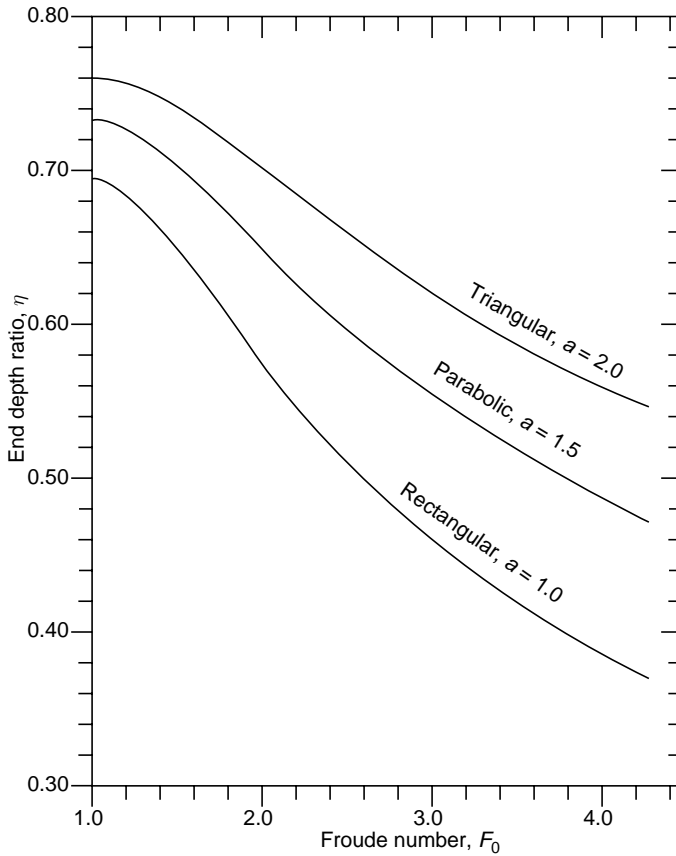


Fig. 7.24 Variation of the end-depth ratio in supercritical flows

to be satisfactory. Satisfactory comparison of available data in rectangular channels is shown in Fig. 7.22.

### 7.7.5 End Depth in Other Channel Shapes

The generalised energy method described in the earlier section is a simple and versatile technique to predict the end-depth ratio  $\eta$  in both subcritical and supercritical flow modes in prismatic channels of any shape. However, Eq. 7.66 and expressions for  $\varepsilon$  and  $f(\eta)$  may not always be simple expressions and may pose some difficulty in the solution for  $\eta$ . Subramanya and Keshavamurthy<sup>37</sup> have used Eq. 7.66 to estimate the end-depth ratio  $\eta$  as a function of  $\frac{my_e}{B}$  for subcritical flows in trapezoidal channels. The available data substantiate the high degree of accuracy of this prediction.

Subramanya and Niraj Kumar<sup>38</sup> have used the generalised energy method (Eq. 7.66) to predict the end-depth in subcritical flows in circular channels as  $\eta = f(y_c/D)$ . It has been shown that  $\eta$  is essentially constant at 0.73 in the entire practical range of  $y_c/D$  viz.  $0 < y_c/D \leq 0.8$ . This compares very well with the value of  $\eta = 0.725 \pm 3.5\%$  obtained by Rajaratnam and Muralidhar<sup>29</sup>. Niraj Kumar<sup>39</sup> has reported extensive use of Eq. 7.66 to predict the end-depth ratio  $\eta$  in a variety of channel shapes including elliptical sections, inverted trapezoidal sections and standard lined triangular canal section.

Numerous applications of the generalized energy method to solve end depth ratio in a variety of channel shapes has been reported in literature. Reference 48 gives a review (as of 2002) of the research work on the topic of end depth in open channels and contains an exhaustive bibliography on the topic

**Example 7.15** | A channel has its area given by  $A = ky^3$  where  $k = a$  constant. For subcritical flow in this channel estimate the ratio of the end-depth to critical depth.

*Solution* This is an exponential channel with  $a = 3.0$ . For subcritical flow by Eq. 7.70

$$\varepsilon = 1 + \frac{1}{2a} = 1.167$$

By Eq. 7.68, 
$$f(\eta) = \frac{1}{a\eta^{2a}} = \frac{1}{3\eta^6}$$

The general equation of end depth Eq. 7.66 is

$$6\varepsilon - 4\eta - 3f(\eta) = 0$$

Substituting for  $\varepsilon$  and  $f(\eta)$ ,  $(6 \times 1.167) - 4\eta - \frac{3}{3\eta^6} = 0$

i.e. 
$$\frac{1}{\eta^6} + 4\eta - 7 = 0$$

Solving by trial and error 
$$\eta = y_e / y_c = 0.80.$$

**Example 7.16** | A rectangular channel carries a supercritical flow with a Froude number of 2.0. Find the end-depth ratio at a free overfall in this channel.

*Solution* In supercritical flow, for an exponential channel,  $\varepsilon = f_n(a, F_0)$

Here  $a = 1.0$

By Eq. 7.53 
$$\varepsilon = \frac{1}{F_0^{2/(2a+1)}} \left( 1 + \frac{F_0^2}{2a} \right)$$

$$= \frac{1}{2^{2/(2+1)}} \left( 1 + \frac{2^2}{(2 \times 1)} \right) = 1.89$$

By Eq. 7.68, 
$$f(\eta) - \frac{1}{a\eta^{2a}} = \frac{1}{\eta^2}$$

The general equation of end-depth, Eq. 7.66 is

$$6\varepsilon - 4\eta - f(\eta) = 0$$

Substituting for  $\varepsilon$  and 
$$f(\eta), 6 \times 1.89 - 4\eta - \frac{3}{\eta^2}$$

i.e. 
$$4\eta^3 - 11.34 + 3 = 0$$

Solving by trial-and-error, 
$$\eta = y_e/y_c = 0.577.$$

### 7.7.6 End Depth as a Flow-Measuring Device

The unique relationship for  $y_e/y_c$  for a given channel at a free overfall has given end depth the status of a flow meter. For flow-measurement purposes, the end section should be truly level in the lateral direction and must be preceded by a channel of length not less than  $15y_c$ . The overfall must be free and where it is confined by side walls, the nappe well ventilated. The accuracy of measurement is better if the slope is flat, i.e. as near to being a horizontal bed as possible. The depth should be measured at the end section on the channel centreline by means of a precision point gauge. In subcritical flows for a given channel shape a constant value of  $y_e/y_c$  as given in Table 7.3 (or as obtained by using the general equation for end depth, Eq. 7.66) is used to estimate the discharge for a given  $y_e$ . The general accuracy of flow-measurement by the end depth method is around 3 per cent in subcritical flows.

International organization for Standards, Geneva, Switzerland has brought out two standards; ISO 3847 (1977) and ISO 4371 (1984) for end depth method of flow measurements in rectangular channels and non-rectangular channels respectively. The website <http://www.lmnoeng.com> contains details of ISO 3847 and 4371 procedures and free softwares for calculation of discharge for a known end depth in rectangular, triangular and circular channels.

In supercritical flows  $y_e/y_c = fn(F_0)$  and as such two depths  $y_e$  and  $y_0$  are needed to estimate the discharge. In view of this, the end-depth method is not advantageous in supercritical flows.

**Example 7.17** | Estimate the discharges corresponding to the following end-depth values in the following horizontal channels. [Assume the flows to be subcritical and use the end depth ratio values given in Table 7.3].

Channel shape	Property	End depth (m)
Rectangular	Bed width = 2.5 m	0.70 m, Confined nappe
Triangular	Side slope = 1.5 H : 1 V	0.55 m
Circular	Diameter = 0.90 m	0.40 m

*Solution* (i) From Table 7.3 for a rectangular channel having a confined nappe at the free fall,

$$y_e / y_c = 0.715$$

$$y_c = 0.70 / 0.715 = 0.979$$

$$q = [g y_c^3]^{1/2} = [9.81 \times (0.979)^3]^{1/2} = 3.034 \text{ m}^3/\text{s/m}$$

$$Q = 2.5 \times 3.034 = 7.585 \text{ m}^3/\text{s}$$

(ii) For a triangular channel from Table 7.3,

$$y_e / y_c = 0.795$$

$$y_c = 0.55 / 0.795 = 0.692$$

$$Q^2 = \frac{g m^2 y_c^5}{2} = \frac{(9.81) \times (1.5)^2 \times (0.692)^5}{2} = 1.751$$

$$Q = 1.323 \text{ m}^3/\text{s}$$

(iii) For a circular channel from Table 7.3,

$$y_e / y_c = 0.725$$

$$y_c = 0.40 / 0.725 = 0.552, y_c / D = 0.552 / 0.90 = 0.613$$

$$\text{From Table 2A-1, } \frac{Q}{\sqrt{g} D^{2.5}} = 0.3637$$

$$Q = 0.875 \text{ m}^3/\text{s}$$

## 7.8 SLUICE-GATE FLOW

Gates in a variety of shapes and with different operational characteristics are used for purposes of flow control. For their design information on the head-discharge relationship, pressure distribution and vibration characteristic is required. In this section the head-discharge characteristic of a vertical sluice gate is dealt with in detail.

### 7.8.1 Sluice Gate

A sluice gate consists of a vertical sliding gate operating within grooves in the sides of the span. An ideal sharp-edged sluice gate in a horizontal rectangular channel is indicated in Fig. 7.25. Note the sharp edge with a bevel in the downstream. This kind of gate is used for idealised studies as in laboratories, since the sharp upstream edge provides a well-defined separation line for the flow. As

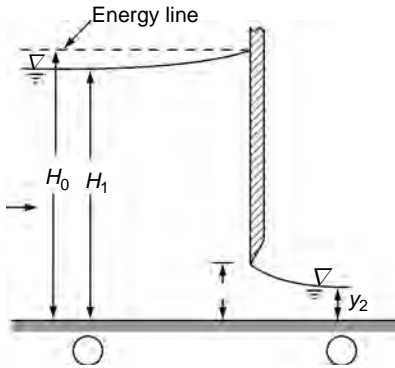


Fig. 7.25 Definition sketch of free sluice gate flow

the water issues out of the gate opening, the free surface converges rapidly till the fast stream attains a minimum depth with flow lines parallel to the bed. This minimum area section, called vena contracta, occurs at a distance of about  $a$  from the plane of the gate, where  $a$  is the height of the gate opening. If the tailwater is not sufficiently high to submerge the vena contracta, the flow, being independent of the tailwater elevation, is designated as free-flow. The flow is subcritical upstream of the gate and is supercritical immediately downstream of the gate when the

gate discharges under free-flow conditions. Referring to the vena contracta as Section 2, the ratio of the depth  $y_2$  to the gate opening  $a$  is called the coefficient of contraction  $C_c$  i.e.,

$$y_2 = C_c a \tag{7.75}$$

Assuming that there is no entry loss between Sections 1 and 2 (Fig. 7.25) and  $\alpha_1 = \alpha_2 = 1.0$ .

$$H_1 + \frac{V_1^2}{2g} = y_2 + \frac{V_2^2}{2g} \tag{7.76}$$

Since the discharge per unit width  $q$  is given by the continuity equation as

$$q = H_1 V_1 = y_2 V_2 = C_c a V_2$$

Equation 7.76 simplifies to

$$q = \frac{C_c}{\sqrt{1 + \left(\frac{a}{H_1}\right) C_c}} a \sqrt{2g H_1}$$

i.e.

$$q = C_{df} a \sqrt{2g H_1} \tag{7.77}$$

where  $C_{df}$  = coefficient of discharge for free-flow given by

$$C_{df} = \frac{C}{\sqrt{1 + \left(\frac{a}{H_1}\right)^2 C_c^2}} \quad (7.78)$$

It may be noted that the term  $\sqrt{2gH_1}$  in Eq. 7.77 which has the dimensions of velocity does not represent any real velocity in the system. Only the overall discharge is properly represented and the terms  $C_{df}$  and  $\sqrt{2gH_1}$  are hypothetical quantities.

Another way of representing the discharge  $q$  is to rearrange Eq. 7.76 to get

$$q = C_d a \sqrt{2g(H_1 - C_c a)} = C_d a \sqrt{2g\Delta H} \quad (7.79)$$

where  $\Delta H$  = difference in the depths of flow at Sections 1 and 2 and  $C_d$  = the coefficient of discharge given by

$$C_d = \frac{C_c}{\sqrt{1 - \left(\frac{C_c a}{H_1}\right)^2}} \quad (7.80)$$

### 7.8.2 Coefficients $C_c$ , $C_{df}$ and $C_d$

The coefficient of contraction  $C_c$  is a function of the geometry of the opening and in sluice-gate flow  $C_c = f(a/H_1)$ . As such, both  $C_{df}$  and  $C_d$  are also functions of  $a/H_1$ . Since the gate has a sharp edge, the separation point is fixed and the Reynolds number of the flow does not have any effect on  $C_c$  and hence on  $C_{df}$  and  $C_d$ .

The value of  $C_c$  is determined by the flow profile from the gate to Section 2. The ideal-fluid flow theory can be used to study the variation of  $C_c$ . However the flow being predominantly gravity-influenced, considerable mathematical difficulties are encountered. Fangmeir and Strelkoff<sup>40</sup> have studied sluice-gate flow by applying the complex-function theory. Solutions obtained with such an approach properly account for the free surfaces upstream and downstream of the gate and are considerable improvements over the earlier works, e.g. Benjamin<sup>41</sup>. Larock<sup>42</sup> has developed a theory which covers sluice gates of arbitrary inclinations as well as radial gates by assuming the upstream free surface to be a fixed horizontal boundary. McCorquodale and Li<sup>43</sup> were probably the first to apply the finite-element method (FEM) to sluice-gate flow. However, they assumed the free surface of the efflux jet to be an ellipse and as such their results are not exact. Isaacs<sup>44</sup> presented a numerical method based on FEM for the analysis of flow from a sluice gate of arbitrary geometry. A generalised FEM approach to two-dimensional and axi-symmetric gravity flows of ideal fluids has been reported by Diersch et al.<sup>21</sup> Their method is applicable to a wide variety of free-surface flow problems, such as sluice-gate flow,

flow over spillways, flow under spillway gates, end-depth problems, etc., and is capable of calculating  $C_c$ , the discharge coefficient and velocity and pressure distributions. Their calculations for the discharge coefficient  $C_{df}$  for a vertical sluice gate gave excellent agreement with earlier experimentally determined values<sup>21</sup> (Fig. 7.26).

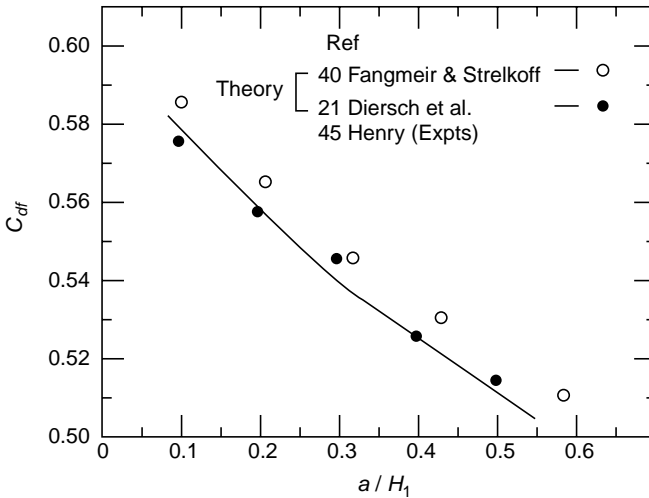


Fig. 7.26 Variation of  $C_{df}$

Experimentally, the variations of  $C_{df}$  and  $C_d$  have been studied by a number of research workers. The results of Henry's experiments<sup>45</sup> are generally recognised to be accurate enough with a possible error of  $\pm 2$  per cent for discharge predictions. The variation of  $C_{df}$  with  $H_1/a$  obtained by Henry with data of Rajaratnam and Subramanya<sup>46</sup> is indicated in Fig. 7.27.

The variation of  $C_d$  with  $a/H_1$ , has been studied by Rajaratnam and Subramanya<sup>46</sup> and Franke and Valentin<sup>47</sup>. The values of  $C_d$  for various values of  $a/H_1$  are indicated in Table 7.5.

Table 7.5 Variation of  $C_d$  with  $a/H_1$  (Rajaratnam and Subramanya)<sup>46</sup>

$a/H_1$	0.00	0.05	0.10	0.20	0.30	0.40	0.50	0.60	0.70
$C_d$	0.61	0.61	0.60	0.605	0.605	0.607	0.620	0.640	0.660

It may be noted that the variation of  $C_d$  in the range of  $a/H_1$  from 0 to 0.30 is very small and one can adopt a constant value of  $a/H_1$  within this range. The  $C_c$  values over the practical ranges of  $a/H_1$ , from Eq. 7.78 are essentially constant at 0.60.



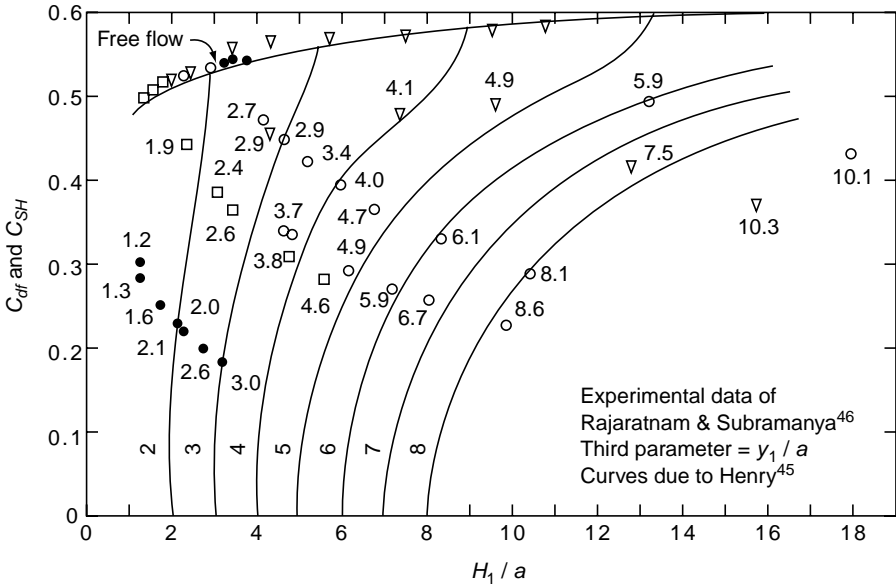


Fig. 7.27 Variation of  $C_{df}$  and  $C_{SH}$  (Henry<sup>45</sup>)

### 7.8.3 Submerged Flow

In free-flow, the tailwater level has no effect on the discharge. If the tailwater level is increased, while keeping the discharge constant, a hydraulic jump that is formed in a downstream section of the canal gradually advances upstream till the toe of the jump is at the vena contracta. Any further increase in the tailwater elevation causes the jump to be submerged. This would cause the depth at Section 2 to be higher than  $C_c a$  and if the discharge is constant, the upstream depth  $H_1$  will have to increase. Such a situation, where the downstream depth  $H_2 > C_c a$ , is designated as *submerged flow* (Fig.7.28). Thus the limit of the free jump is the jump formed at the vena contracta. The tailwater corresponding to this limiting case  $y_{t1}/a$  is known as *modular limit* and represents the maximum relative tailwater depth which would ensure free-flow. Higher values of  $y_1/a$  than the modular limit would cause submerged flow.

In submerged flow the operating head is  $\Delta H = (H_1 - H_2)$  and the discharge is confined in the downstream direction at Section 2 to a depth  $y_v \approx C_c a$ . Above the depth  $y_v$ , at Section 2 there will be a roller in which the upper layers will have negative velocity. By applying the energy equation to Sections 1 and 2 and neglecting the energy losses, it can be shown that

$$q = C_{ds} a \sqrt{2g\Delta H} \tag{7.81}$$

where  $C_{ds}$  = discharge coefficient for submerged flow. It has been experimentally<sup>45</sup> established that  $C_{ds} = C_d = f(a/H_1)$ . For the estimation of discharges in submerged

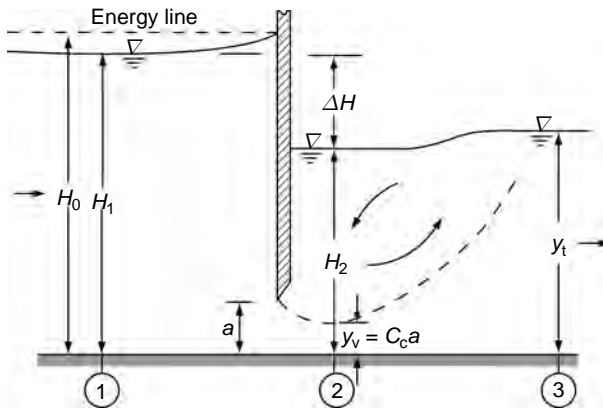


Fig. 7.28 Submerged sluiceway flow

sluice-gate flow, the data in Table 7.5 can be used together with Eq. 7.81. Between Sections 2 and 3 (Fig. 7.28) there exists a submerged hydraulic jump which dissipates some of the energy. If it is desired to find  $H_2$  for a known  $q$  and  $y_t$ , the momentum equation, with due notice that the flux of momentum at Section 2 is confined, to a depth  $y_v$  only, can be used.

If the discharge in the submerged flow is defined in a manner analogous to Eq. 7.77, as

$$q = C_{SH} a \sqrt{2g H_1} \quad (7.82)$$

where  $C_{SH}$  = a discharge coefficient for submerged sluice-gate flow proposed by Henry<sup>45</sup> then by the energy equation between Sections 1 and 2, and by momentum equation between Sections 2 and 3, it can be shown that

$$C_{SH} = f(H_1/a, y_t/a) \quad (7.83)$$

Henry<sup>45</sup> has evaluated  $C_{SH}$ , experimentally and his results along with some experimental data from Raiyaratnam and Subramanya<sup>46</sup> are shown in Fig. 7.27. This curve can be used for the estimates of discharge in submerged flow when  $H_1$ ,  $y_t$  and  $a$  are known. Because of steep gradients of the  $C_{SH}$  curves, considerable errors are likely to arise in the estimation of  $C_{SH}$  from Fig. 7.27 if  $\left(\frac{H_1}{a} - \frac{y_t}{a}\right)$  is small.

### 7.8.4 Practical Gate Lips

In practical applications the bottoms of the vertical-leaf gates are usually made with a bevel on the upstream face, usually with a slope of about  $45^\circ$  and with a narrow seat surface on the bottom. This form of gate has considerably higher discharge coefficients compared to a sharp-edged gate. While the overall functional form of the discharge coefficients can remain essentially the same as for a sharp-edged gate, the actual values which depend on many factors peculiar to the installation have to be determined by model studies.

## 7.9 CULVERT HYDRAULICS

A culvert is a conduit provided to transmit the flow of a stream past an obstacle such as a roadway, railway or any kind of embankment. It entails essentially a constriction of the flow path and consequently the hydraulics of the stream flow undergoes a change in and around this hydraulic structure. While the culverts appear to be simple structures its hydraulics is extremely complex. To appreciate the complexity of flow analysis, consider the following features:

The flow through a culvert

- (i) can be subcritical or supercritical
- (ii) can be a closed conduit flow or an open channel flow or both forms may exist
- (iii) may have an inlet control or an outlet control
- (iv) may be such that the free surface flow in the barrel can have uniform flow or GVF or RVF or any combination of the above
- (v) may be such that either the inlet or the outlet or both inlet and outlet may be submerged or both may be unsubmerged

In view of the many possible flow types in a culvert, the classification of the flow through a culvert has undergone several changes to achieve clarity. Chow<sup>26</sup> (1956) classified the culvert flow in to 6 types based on the submergence or otherwise of the inlet and outlets. USGS (1976)<sup>49</sup> classifies the flow through culvert in to 6 types depending upon the nature of the slope and relative headwater and tailwater elevations. Currently the most widely used classification is that of Federal Highway Administration (FHWA) of US Department of Transport as given in their Hydraulic Design Series-5 (HDS-5) of 2001 (Revised 2005)<sup>50</sup>. The HDS-5 system of classification is described in this section. The following web site of FHWA can be consulted for free download of Ref. (50) as well as for free download of related softwares: <http://www.fhwa.dot.gov/engineering/hydraulics/software.cfm>.

The culvert conduit (also called barrel) can be circular, rectangular, elliptical and other geometrical shapes composed of circular arcs. However, the circular shape is the most commonly adopted shape. Wide choice of materials like concrete, brick and stone masonry, conduits made of sheets of steel and aluminum are available for the construction of the culvert barrel.

Figure 7.29 is a definition sketch of flow through a culvert. In this figure,

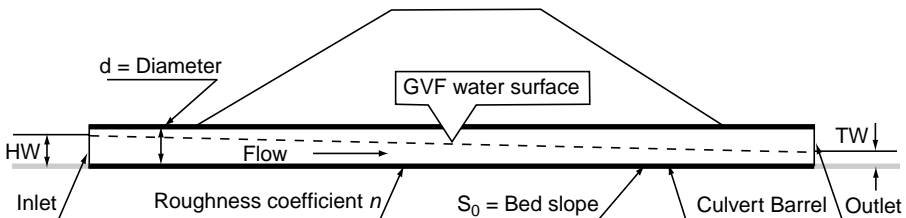


Fig. 7.29 Definition sketch of culvert flow

$HW$  = Headwater = head above the invert of the culvert inlet

$TW$  = Tailwater = depth of water downstream of the culvert measured from the outlet invert

$d$  = Diameter of the culvert conduit

$S_0$  = Slope of the conduit

$n$  = Manning's roughness coefficient of the conduit

This figure shows a type of flow in which both the inlet and the outlet of the culvert are unsubmerged. In this case the flow in to the culvert is in weir flow mode. If the headwater elevation is sufficiently above the top edge of the inlet the flow in to the culvert barrel will be in the orifice flow mode (with discharge proportional to square root of head) and the inlet is said to be submerged. The limit of submergence depends upon the ratio  $\frac{HW}{d}$  and the limiting value is found to be in the range of 1.2 to 1.5.

HDS-5 adopts 1.2 as the minimum  $\frac{HW}{d}$  ratio marking the onset of submerged flow.

Thus for  $\frac{HW}{d} > 1.2$  the inlet is considered to be submerged.

The inlet of a culvert has a very important role in reducing energy losses at the entry, especially in closed conduit flow conditions. The flow entering the culvert barrel undergoes contraction of the flow area at the inlet and a properly designed inlet would increase the coefficient of contraction leading to higher efficiency. Some standard types of culvert inlets popularly used in USA are (i) Projecting barrel, (ii) Cast-in – situ concrete headwall and wing walls, (iii) Pre-cast end sections, and (iv) Culvert end mitered in to the slope. Additional factors like structural stability, aesthetics, erosion control and embankment slope control play a role in the final selection.

The outlet is considered to be submerged for all values of tailwater elevation, measured above the invert of the outlet, which are greater than the diameter of the conduit at the outlet, that is  $\frac{TW}{d} \geq 1.0$ . Considering the control of flow at the inlet and at the outlet, the flow in a culvert is classified by HDS-5 in to four types under inlet control condition and to five types under outlet-control condition. The different types of flows are named alphabetically. For clarity sake, prefixes IC and OC to indicate inlet control and OC outlet control respectively are adopted in this book. Thus Type IC-A indicates inlet control, Type-A flow and OC-C indicates outlet control Type-C flow in the culvert. The details of the classification are given below and also are shown in Figs 7.30 and 7.31.

**Inlet Control (IC)** In this type the flow control is at the inlet, viz., the upstream end of the culvert and four categories of flow are possible as shown in Fig. 7.30 -(i to iv).

*Type IC-A* (Fig.7.31-(i).) Here both the inlet and the outlet are unsubmerged and channel is steep. The inlet acts like a weir and critical depth is formed just downstream of the inlet edge. The free surface flow will be a GVF of  $S_2$  type in the initial

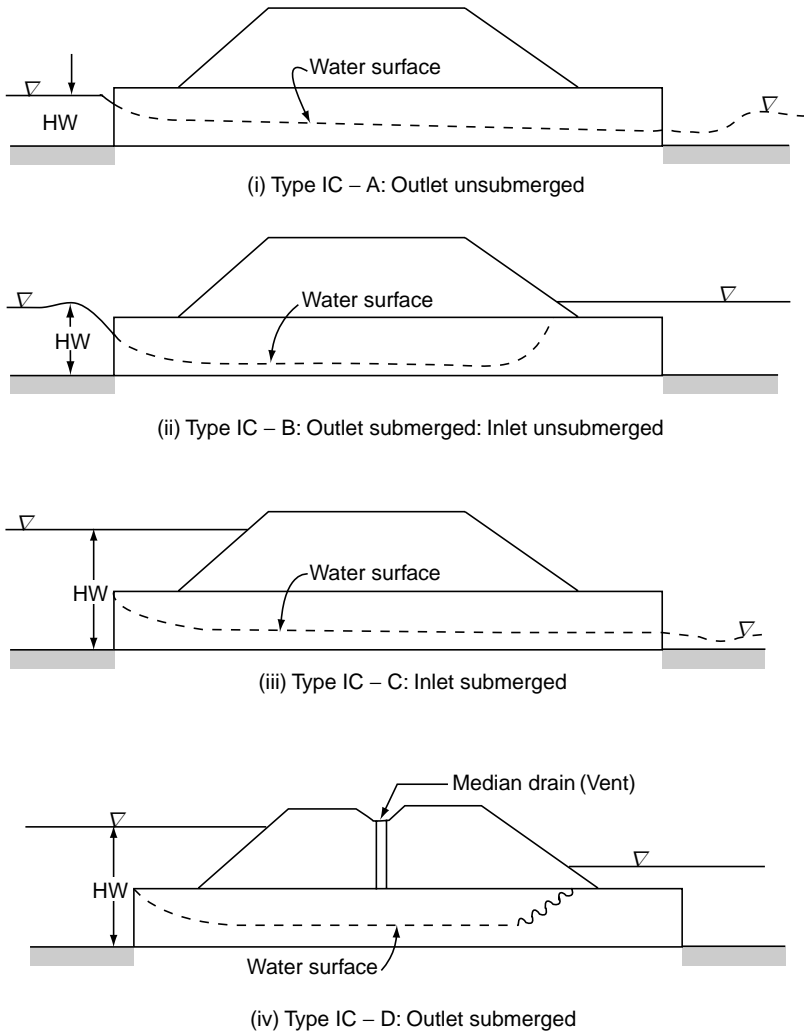


Fig. 7.30 Types of inlet control in culverts (Ref. 50)

portion with the normal depth occurring in the downstream part depending upon the length and other hydraulic characteristics. The tail water level is too low and does not influence the flow at the outlet

*Type IC-B* (Fig. 7.30-(ii).) This type of flow is similar to Type IC-A described earlier but with the additional feature of the tailwater causing the submergence of the outlet. The flow at the inlet is still like a weir with critical depth at the upstream end. The  $S_2$  curve formed will have a hydraulic jump at an appropriate location to cause full conduit pressure flow in the downstream part of the conduit.

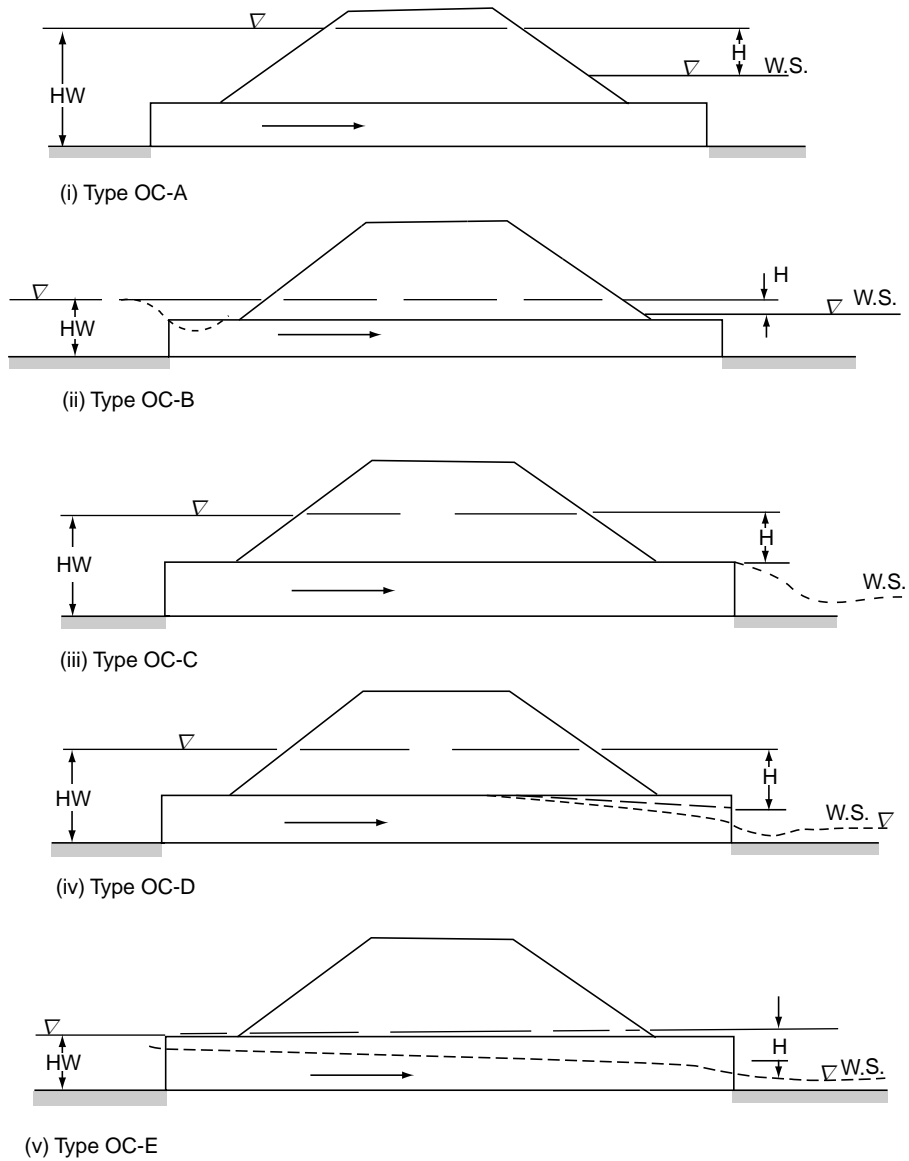


Fig. 7.31 Types of outlet control in culverts (Ref. 50)

*Type IC-C* (Fig.7.30-(iii)) In this type the inlet is submerged with  $HW > 1.2d$ . The tailwater level is too low and a free surface flow takes place as in Type IC-A. Critical depth at the upstream end section,  $S_2$  profile and possibility of occurrence of normal depth at the downstream section are the characteristic features of the water surface profile in the conduit.

*Type IC-D* (Fig. 7.30-(iv).) This type of flow is the equivalent of Type IC-B with inlet being submerged. The tailwater level is high enough to submerge the outlet and a

hydraulic jump is formed inside the barrel. This type of free surface flow inside a barrel with its two ends sealed would require a vent to preserve atmospheric pressure in the air space. The median drain as indicated in the figure would act as the desired vent pipe. The control remains at the inlet and the flow at the inlet is of the orifice type.

**Outlet Control (OC)** In this type the flow control is at the outlet and five categories of flow are possible as shown in Fig. 7.31-(i to v).

*Type OC-A* (Fig. 7.31-i). Here both the inlet and the outlet are submerged. The flow is that of a pure pipe flow (viz. pressure flow) throughout the culvert conduit.

*Type OC-B* (Fig. 7.31-ii). In this type the headwater is low causing the inlet to be un-submerged while the tailwater is high to cause submergence of the outlet. The flow in the culvert conduit is a pressure flow.

*Type OC-C* (Fig. 7.31-iii). This is the limiting case of Type OC-A. The inlet is submerged and the outlet is free. The conduit flows full, with free exit, due to high headwater elevation and consequent high differential head.

*Type OC-D* (Fig. 7.31-iv). Here, the inlet is submerged but the tailwater is low to cause free flow at the outlet. The culvert conduit is full in the initial partial length in the upstream and free surface flow prevails on the downstream portion of the conduit. The channel slope is mild.

*Type OC-E* (Fig. 7.31-v). In this type of flow both the inlet and the outlet of the culvert are un-submerged and the free surface flow prevails over the full length of the conduit. The slope is mild, and as such uniform flow,  $M_2$  and  $M_1$  type of GVF profiles are possible depending upon the hydraulic properties and the tailwater elevation.

### 7.9.1 Factors Affecting Culvert Flow

Based on the details of inlet and outlet control types of flow described above, the factors affecting culvert flow can be listed as in Table 7.6. Inlet control occurs generally in steep, short, culverts with free outlet. Similarly, outlet control can be expected to occur in flat sloped culvert with high tailwater conditions.

**Table 7.6** Factors affecting Culvert Flow

Factor	Inlet control	Outlet control
Head water elevation (HW)	yes	yes
Inlet area	yes	yes
Inlet edge configuration	yes	yes
Inlet shape	yes	yes
Conduit area	No	yes
Conduit shape	No	yes
Conduit length	No	yes
Conduit slope	Yes, to a small extent	yes
Tailwater elevation	No	yes

### 7.9.2 Discharge Equations

Basically the discharge in a culvert is described by the weir flow equation or orifice flow equation or pipe flow equation depending upon the boundary conditions and geometrical configurations. Numerous coefficients to account for friction, entrance losses and other type of losses which depend on the conduit geometry, inlet geometry and conduit characteristics are involved. Based on thorough experimental results FHWA has identified the various equations and appropriate coefficients applicable to different types of flow situations. Reference 50 can be consulted for details regarding discharge estimation in various types of flows.

**Performance Diagram** A plot of the headwater elevation against discharge in a culvert installation is known as the performance curve of the culvert and summarises various head - discharge relationships that may exist for the culvert. This is an important and useful plot in the design process. Further, the performance chart helps in understanding the conditions of flow at the design headwater elevation and also in knowing the sensitivity of the (HW) – Q relation at that point. Thus the performance curve enables one to estimate the consequences of flow rates higher than the design rate at the site and also benefits of inlet improvements.

Figure 7.32 shows the typical performance curve of a culvert. It is seen that two discharges for the selected design flow are possible. For conservative design if  $Q_1$  is

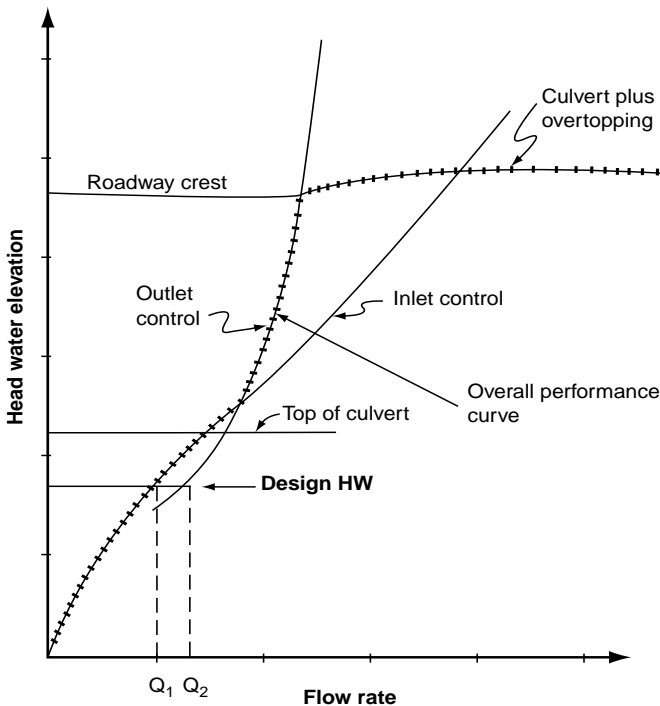


Fig. 7.32 Culvert performance curve with roadway overtopping (Ref. 50)



selected the culvert barrel capacity is higher than what has been designed and this can be utilized by inlet improvement.

It is normal practice in India to design culverts for free surface flow operation. However, in USA the culverts are invariably designed to flow full at design discharge. Another aspect to be considered in the design of culverts is the velocity of flow at the outlet in relation to scour of the bed material of the stream. Generally rip-rap protection is needed at the outlet and in some cases energy dissipaters also have to be provided to prevent serious scours due to high outlet velocities.

### 7.9.3 Design of Culverts

Reference 50 contains valuable information, worked examples and nomographs for the design of culverts under all types of flow conditions. FHWA web site <http://www.fhwa.dot.gov/engineering/hydraulics/software.com> contains complete information on FHWA Hydraulics Engineering Publications and Software for culvert analysis and related topics. Culvert Analysis Program, HY-8 by FHWA is free public domain software. Web site <http://www.imnoeng.com> contains free computation/design facility and valuable information on all aspects of culvert flow. A program for design of culverts under inlet/outlet control and for preparation of performance chart using HDS-5 methodology is available in this web site. A large number of commercial softwares are available for culvert design and details about these can be obtained through the internet search.



## REFERENCES

1. Lakshmana Rao, N S, 'Theory of Weirs', a Chapter in *Advances in Hydrosience*, Vol. 10, 1975, Academic Press, Inc., New York, pp 310–406.
2. Strelkoff, T S, 'Solutions of Highly Curvilinear Gravity Flows', *J. of Engg. Mech. Div., Proc. ASCE*, Vol. 90, June 1964, pp 195–219.
3. Kandaswamy, P K, and Rouse, H, 'Characteristics of Flow Over Terminal Weirs and Sills', *J. of Hyd. Div., Proc. ASCE*, Vol. 83, Paper No. 1345, August 1957, pp 1–13.
4. Ackers, P, *Weirs and Flumes for Flow Measurement*, John Wiley & Sons Ltd., Chichester, U.K., 1978.
5. Bos, M G, (Ed.), *Discharge Measurement Structures*, Int. Inst. for Land Reclamation and Improvement. Wageningen, The Netherlands, Pub. No. 20, 1976.
6. Kindsvater, C E, and Carter, R W, 'Discharge Characteristics of Rectangular Thin Plate Weirs', *J. of Hyd Div., Proc. ASCE*. Vol. 83, Dec. 1957, pp 1–36.
7. Rama Murthy, A S, Subramanya, K and Pani, B, S, 'Quadrant Plate Weirs', *J. of Hyd. Div., ASCE*, Vol. 103, No., HY 12 1977. *Proc. paper 13395*. pp 1431–41.
8. Rao, N S L, 'Theory of Weirs'. Chap., in *Advances in Hydrosience*. Academic Press. New York, USA, Vol. 10, 1975, pp 309–406.
9. Fonck, R M, 'Datum Line Fixation for Linear Proportional Weirs', *J. of App. Mech. Trans ASME*, Vol. 45, Brief Notes, pp 441–442, June 1978.
10. Cowgill, P, 'The Mathematics of Weir Forms' *Quart. Appl. Maths.*, Vol. 2, No. 2, 1944, p. 142.
11. Banks, R B, 'A Note on the Generalised Weir Equation,' North-Western Univ., *Paper HP 0654*, Nov. 1954.

12. Keshava Murthy, K, and Seshagiri, N, 'A generalised mathematical theory and experimental verification of proportional notches,' *J. of Franklin Inst.*, USA. vol 285. No. 5. May 1968. pp 347–363.
13. Keshava Murthy, K, 'On the Design of the Quadratic Weir,' *J. of Franklin Inst.*, USA. Vol. 287, No. 2. 1969, pp 159–174.
14. Keshava Murthy, K, and Pillai, G, 'Some Aspects of Quadratic Weirs' *J. of Hyd. Div.*, ASCE, Vol. 103, No. HY 9, *Proc. paper 13231*, 1977, pp 1059–76.
15. Majcherek, H, 'Modelling of Flow Velocity Using Weirs', *J. of Hyd. Div.*, ASCE, Vol. 111, No. HY 1, *Proc. paper 19415*, 1985, pp 79–92.
16. U.S. Dept. of Interior, *Studies of Crests for Overfall Dams*, U.S. Bureau of Reclamation, Boulder Canyon Final Reports, Bulletin 3, Part VI, 1948.
17. Cassidy, J. J, 'Designing Spillway Crests for High-Head Operation' *J. of Hyd. Div.*, *Proc. ASCE*, March 1970, pp 745–753.
18. U S Dept. of Interior, *Design of Small Dams*, USBR, Oxford and IBH Pub. Co., New Delhi, 1974.
19. Cassidy, J. J, 'Irrotational Flow Over Spillways of Finite Height', *J. of Engg. Mech. Div.*, *Proc. ASCE*, Dec. 1965, pp 153–173.
20. Ikegawa M, and Washizu, K, 'Finite Element Method Applied to Analysis of Flow Over a Spillway Crest', *Int. J. for Num. Methods in Engg.*, Vol. 6, 1973, pp 179–189.
21. Diersch, H J, Schirmer A, and Busch K F, 'Analysis of Flows with Initially Unknown Discharge', *J. of Hyd. Div.*, *Proc. ASCE*, March 1977, pp. 213–232.
22. Govinda Rao, N S, and Muralidhar, D, 'Discharge Characteristics of Weirs of Finite Crest Width', *La Houille Blanche*, August/Sept. No. 5, 1963, pp 537–545.
23. Singer, J. 'Square-edged Broad-crested Weir as a Flow Measuring Device', *Water and Water Engg.*, June 1964, Vol. 68, No. 820, pp 229–235.
24. Surya Rao, S and Shukla, M K 'Characteristics of Flow Over Weirs of Finite Crest Width', *J. of Hyd. Div.*, *Proc. ASCE*, Nov. 1971, pp 1807–1816.
25. Skogerboe, G V, Hyat M L, Englund, I D, and Johnson, J R, 'Design and Calibration of Submerged Open Channel Flow Measurement Structures, Part 2, Parshall Flumes, Utah Water Res. Lab., Utah State Univ., Logan, Utah, Report No. WG 31–3, March 1967.
26. Chow, V T, '*Open Channel Hydraulics*', McGraw-Hill, Book Co. Inc., New York 1959.
27. Rouse, H, 'Discharge Characteristics of the Free Overfall', *Civil Engineering*, ASCE, April 1936, pp 257–260.
28. Rajaratnam, N, and Muralidhar, D. 'End Depth for Exponential Channels', *J. of Irr. and Drain. Div.*, *Proc. ASCE*, March 1964, pp 17–39.
29. Rajaratnam, N, and Muralidhar, D, 'End Depth for Circular Channels', *J. of Hyd. Div.*, *Proc. ASCE*, March 1964, pp 99–119.
30. Rajaratnam, N, and Muralidhar, D, 'The Trapezoidal Free Overfall', *J. of Hyd. Res.*, IAHR, Vol. 8. No. 4, 1970, pp 419–447.
31. Rajaratnam, N, and Muralidhar, D, 'Characteristics of Rectangular Free Overfall' *J. of Hyd. Res.*, IAHR, Vol. 6, No. 3, 1968, pp 233–258.
32. Diskin, M H, 'The End Depth at a Drop in Trapezoidal Channels', *J. of Hyd. Div.*, *Proc. ASCE*, July 1961, pp 11–32.
33. Delleur, J W, Dooge, J C I, and Gent K W, 'Influence of Slope and Roughness on the Free Overfall', *J. of Hyd. Div. Proc. ASCE*, Aug. 1956, pp 30–35.
34. Anderson, M V, 'Non-uniform flow in front of a free overfall', *Acta Polytechnica Scandinavia*, Ci 42, Copenhagen, 1967.
35. Strelkoff, T, and Moayeri, M S, 'Pattern of Potential Flow in a Free Overfall', *J. of Hyd. Div.*, *Proc. ASCE*, April 1970, pp 879–901.

36. Subramanya, K, 'Measurement of Discharge in an Exponential Channel by the End Depth Method'. *Proc. Inst. Conf. on Measuring Techniques*, BHRA, London, England, pp 313–324, April 1986.
37. Subramanya, K, and Keshava Murthy, K, 'End Depth in a Trapezoidal Channel' *J. Inst. Of Engrs. (India)*, Civil Engg. Div., Vol. 67, Part CI 6, pp. 343–46, May 1987.
38. Subramanya, K and Niraj Kumar, 'End Depth in Horizontal Circular Channels', *J. of the Institution of Engineers India*, Civil Engg. Div., Vol. 73 Part CV 6, pp 185–187, March 1993.
39. Niraj Kumar, "Studies on Some Open Channel Discharge-Measuring Devices", *M. Tech. Thesis, Civil Engg. Dept., I.I.T. Kanpur*, Dec. 1989.
40. Fangmeir, D D, and Strelkoff, T, 'Solution for Gravity Flow Under a Sluice Gate', *J. of Engg. Mech. Div., Proc. ASCE*. Vol. 94, Feb. 1968, pp 153–176.
41. Benjamin, T B, 'On the Flow in Channels when Rigid Obstacles are Placed in the Stream', *J. of Fl. Mech.*, Vol. 1, 1955, pp 227–248.
42. Larock, B, E, 'Gravity-affected Flows from Planar Sluice Gates', *J. of Hyd. Div., Proc. ASCE*, July 1969, pp 1211–1226.
43. McCorquodale, J A, and Li, C Y, 'Finite Element Analysis of Sluice Gate Flow', *84th Annual General Meeting*, Engg. Inst. of Canada, Ottawa, Canada, Sept. 1970, pp 1–12+4.
44. Isaacs, L T, 'Numerical Solution for Flow Under Sluice Gates', *J. of Hyd. Div., Proc. ASCE*, May 1977, pp 473–482.
45. Henry, H, 'Discussion on Diffusion of Submerged Jets', *Trans. ASCE*, Vol. 155, 1950, pp 687–697.
46. Rajarathnam, N and K Subramanya, 'Flow Equation for the Sluice Gate', *J. of Irr. and Drain. Div., Proc. ASCE*, Sept. 1967, pp 167–186.
47. Franke, P G, and Valentin, F, 'The Determination of Discharge Below Gates in Case of Variable Tailwater Conditions', *J. of Hyd. Res., IAHR*, Vol. 7, No. 4, 1969 pp 433–447.
48. Dey, S, 'Free Overfall in Open Channels: State-of-the-art review', *Flow Measurements and Instrumentation*. Elsevier, 13, 2002, pp. 247–264.
49. Bodhaine, G L, Measurements of Peak Discharges at Culverts by Indirect Methods, *Techniques of Water Resources Investigations*, Book 3, Chapter A3, US Geological Survey, 1976.
50. Federal Highway Administration, *Hydraulic Design of Culverts*, Report FHWA – NH1-01–020, Hydraulic Design Series 5, (HDS-5), US Department of Transportation, Sept. 2001, (Revised 2005).



## PROBLEMS

### Problem Distribution

SI No	Topic	Problems
1	Rectangular weir	7.1 to 7.3, 7.6, 7.7, 7.19
2	Weirs of various shapes	7.4,
3	Triangular notch	7.5
4	Sutro weir	7.8, 7.10
5	Quadratic weir	7.9, 7.11
6	Ogee spillway	7.12 to 7.16
7	Broad crested weir	7.17, 7.18, 7.19
8	Critical depth flume	7.20, 7.21
9	End depth	7.22 to 7.27
10	Sluice gate	7.28 to 7.32

- 7.1 A rectangular sharp-crested suppressed weir is 2.0 m long and 0.6 m high. Estimate the discharge when the depth of flow upstream of the weir is 0.90 m. If the same discharge was to pass over an alternative contracted weir of 1.5 m length and 0.60 m height at the same location, what would be the change in the water-surface elevation?
- 7.2 A sharp-crested suppressed weir is 1.5 m long. Calculate the height of the weir required to pass a flow of  $0.75 \text{ m}^3/\text{s}$  while maintaining an upstream depth of flow of 1.50 m.
- 7.3 A rectangular sharp-crested suppressed weir is 3.0 m long and 1.2 m high. During a high flow in the channel, the weir was submerged with the depths of flow of 1.93 m and 1.35 m at the upstream and downstream of the weir respectively. Estimate the discharge.
- 7.4 Develop expressions as given in Table 7.2 for the discharge over triangular, circular, parabolic and trapezoidal sharp-crested weirs.
- 7.5 A right angled triangular notch discharges under submerged condition. Estimate the discharge if the heights of water surface measured above the vertex of the notch on the upstream and downstream of the notch plate are 0.30 m and 0.15 m respectively (Assume  $C_d = 0.58$ ).
- 7.6 A 15-m high sharp-crested weir plate is installed at the end of a 2.0-m wide rectangular channel. The channel side walls are 1.0 m high. What maximum discharge can be passed in the channel if the prescribed minimum free board is 20 cm?
- 7.7 A sharp-crested weir of 0.80-m height and 2.0-m length was fitted with a point gauge for recording the head of flow. After some use, the point gauge was found to have a zero error; it was reading heads 2 cm too small. Determine the percentage error in the estimated discharges corresponding to an observed head of 50 cm.
- 7.8 Design a Sutro weir for use in a 0.30-m wide rectangular channel to have linear discharge relationship in the discharge range from  $0.25 \text{ m}^3/\text{s}$  to  $0.60 \text{ m}^3/\text{s}$ . The base of the weir will have to span the full width of the channel. Assume  $C_d = 0.62$ .
- 7.9 Design a quadratic weir spanning the full width of a 0.50 m rectangular channel at the base and capable of passing minimum and maximum discharges of  $0.10 \text{ m}^3/\text{s}$  and  $0.40 \text{ m}^3/\text{s}$  respectively under the desired proportionality relationship. (Assume  $C_d = 0.61$ .)
- 7.10 A Sutro weir with a rectangular base is installed in a rectangular channel of width 60 cm. The base weir spans the full width of the channel, has its crest coinciding with the channel bed; and has a height of 12 cm. (i) Estimate the discharge through the channel when the depth of flow in the channel immediately behind the weir is 25 cm. (ii) What discharge in the channel is indicated when the depth of flow is 33 cm? (iii) What depth of flow in the channel can be expected for a discharge of  $0.20 \text{ m}^3/\text{s}$ ? [Take  $C_d = 0.61$ ].
- 7.11 A quadratic weir with rectangular base of 45 cm width and 9 cm height has a depth of flow of 15 cm in the channel. Estimate (i) the discharge through the weir and (ii) the depth of flow in the channel corresponding to a discharge of 25 litres/s. [Take  $C_d = 0.61$ ].
- 7.12 Find the elevation of the water surface and energy line corresponding to a design discharge of  $500 \text{ m}^3/\text{s}$  passing over a spillway of crest length 42 m and crest height 20 m above the river bed. What would be the energy head and minimum pressure head when the discharge is  $700 \text{ m}^3/\text{s}$ ?
- 7.13 A spillway with a crest height of 25.0 m above the stream bed is designed for an energy head of 3.5 m. If a minimum pressure head of 5.0 m below atmospheric is allowed, what is the allowable discharge intensity over the spillway?
- 7.14 A spillway has a crest height of 30.0 m above the bed and a design energy head of 3.0 m. The crest length of the spillway is 50 m. As a part of remodelling of the dam, a three-span bridge is proposed over the spillway. The piers will be 1.5 m thick and are round-nosed and the abutment corners will be rounded. What will be the change in the water-surface elevation for the design-flood discharge?
- 7.15 An overflow spillway with its crest 10 m above the river bed level has radial gates fitted on the crest. During a certain flow, the water surface upstream of the dam was observed to be 2.5 m above the crest and the gate opening was 1.5 m. Estimate the discharge from a bay of 10.0 m length. (Neglect end contractions.)

- 7.16 An ogee spillway with a vertical face is designed to pass a flood flow of  $250 \text{ m}^3/\text{s}$ . The distance between the abutments of the spillway is  $45.0 \text{ m}$ . A three-span bridge is provided over the spillway. The bridge piers are  $1.20 \text{ m}$  wide and are round nosed. If the crest of the spillway is  $10.0 \text{ m}$  above the river bed level, find the elevations of the water surface and energy line. Using this discharge as the design discharge, calculate the spillway crest profile.
- 7.17 A  $2.5\text{-m}$  wide rectangular channel has a broad-crested weir of height  $1.0 \text{ m}$  and a crest width of  $1.5 \text{ m}$  built at a section. The weir spans the full canal width. If the water-surface elevation above the crest is  $0.5 \text{ m}$ , estimate the discharge passing over the weir. If the same discharge passes over another similar weir, but with a crest width of  $2.5 \text{ m}$ , what would be the water-surface elevation upstream of this second weir?
- 7.18 A broad-crested weir of  $2.0\text{-m}$  height and  $3.0\text{-m}$  width spans the full width of a rectangular channel of width  $4.0 \text{ m}$ . The channel is used as an outlet for excess water from a tank of surface area  $0.5$  hectares at the weir crest level. If the water level in the tank at a certain time is  $0.90 \text{ m}$  above the weir crest, what is the discharge over the weir? Estimate the time taken to lower the water-surface elevation by  $60 \text{ cm}$ . (Assume that there is no inflow into the tank and the surface area of the tank is constant in this range.)
- 7.19 A  $2.0\text{-m}$  wide rectangular channel carrying a discharge of  $2.5 \text{ m}^3/\text{s}$  is to be fitted with a weir at its downstream end to provide a means of flow measurement as well as to cause heading-up of the water surface. Two choices, viz. (i) a sharp-crested weir plate of  $0.80 \text{ m}$  height, and (ii) a broad-crested weir block of  $0.80\text{-m}$  height and  $1.0\text{-m}$  width, both spanning the full width of the channel, are considered. Which of these weirs causes a higher heading-up and to what extent?
- 7.20 A standing wave flume is used to measure the discharge in a  $10.0 \text{ m}$  wide rectangular channel. A  $5\text{-m}$  wide throat section has a hump of  $0.5 \text{ m}$  height. What is the discharge indicated when the upstream depth of flow in the channel at the flume entrance is  $2.10 \text{ m}$ ? Assume an overall coefficient of discharge of  $1.620$  for the flume.
- 7.21 A rectangular throated flume is to be used to measure the discharge in a  $9.0 \text{ m}$  wide channel. It is known that the submergence limit for the flume is  $0.80$  and the overall discharge coefficient is  $1.535$ . A throat width of  $5.0 \text{ m}$  is preferred. What should be the height of the hump if the flume is to be capable of measuring a discharge of  $20.0 \text{ m}^3/\text{s}$  as a free flow with the tailwater depth at  $2.30 \text{ m}$ ?
- 7.22 Obtain the end-depth ratio  $\eta = \frac{y_e}{y_c}$  for a triangular channel having (a) subcritical flow and (b) supercritical flow with a Froude number of  $2.5$ .
- 7.23 Show that for a channel whose area  $A = k y^{2.5}$  the end-depth ratio  $\eta$  for subcritical flow mode is  $0.783$ . Also, determine the variation of  $\eta$  with Froude number  $F_0$  for supercritical flow in the channel.
- 7.24 A parabolic channel with a profile  $x^2 = 4ay$ , where  $y$  axis is in the vertical direction, terminates in a free fall. Show that the end-depth ratio  $\eta = y_e/y_c$  for supercritical flow is given by  $2\eta^4 - 4\eta^3 + 1 = 0$ . Determine the relevant root of this equation and compare it with the experimentally obtained value of  $\eta$ .
- 7.25 Find the end depth at a free overfall in a rectangular channel when the upstream flow is at a Froude number of  $3.0$  with a normal depth of  $0.70 \text{ m}$ .
- 7.26 Estimate the discharges corresponding to the following end-depth values in various channels. The channels are horizontal and the flow is subcritical in all cases.
- (i) Rectangular channel,  $B = 2.0 \text{ m}, y_c = 0.6 \text{ m}$   
(ii) Triangular channels,  $m = 1.0, y_c = 0.5 \text{ m}$   
(iii) Circular channel,  $D = 0.90 \text{ m}, y_c = 0.3 \text{ m}$
- [Hint: Use the value of  $y_e/y_c$  given in Table 7.3.]

- 7.27 Write a general momentum equation to the flow at the end-depth region in an exponential channel ( $A = ky^a$ ). Assuming the channel to be horizontal without any friction and the pressure force at the brink to be  $P_e = \gamma \bar{y}_e A_e K_p$ , show that

$$K_1 = \frac{1}{\varepsilon_r^{a+1}} - \left( \frac{a+1}{a} \right) \frac{(1-\varepsilon_r^a)}{\varepsilon_r^{2a} + 1}$$

where  $\varepsilon_r = y_e / y_c$ .

- 7.28 A 2.0-m wide rectangular channel has its depth backed-up to a height of 1.2 m by a sharp-edged sluice gate. If the gate opening is 0.30 m and the downstream flow is free, estimate the discharge through the gate and the force on the gate.
- 7.29 A 2.0-m wide rectangular channel has to pass a flow of 2.4 m<sup>3</sup>/s through a sluice gate opening of 0.4 m. If the water depth upstream of the gate is 2.0 m, find the depth of water immediately below the gate.
- 7.30 Apply the momentum equation to the submerged sluice gate flow (Fig. 7.28) by making suitable assumptions and estimate the depth  $H_2$  immediately below the sluice gate in terms of  $y_r$ ,  $a$ ,  $C_c$  and  $H_1$ .
- 7.31 Obtain an expression for the force on the sluice gate in submerged flow for the situation in Fig. 7.28.
- 7.32 Show that the modular limit of the free flow in a sluice gate (Fig. 7.28) is given by

$$\frac{y_t}{a} = \frac{C_c}{2} [-1 + \sqrt{1 + 8F_{1c}^1}] \text{ where } F_{1c}^2 = \left( \frac{C_d^2}{C_c^2} \right) \left( \frac{H_1}{a} - C_c \right) \text{ and } y_t = \text{tailwater depth.}$$

## OBJECTIVE QUESTIONS

- 7.1 The head over a 3.0-cm sharp-crested sill is 96 cm. The discharge coefficient  $C_d$  for use in the weir formula is  
 (a) 0.738 (b) 0.848 (c) 0.611 (d) 1.11
- 7.2 A suppressed sharp-crested weir is 0.50 m high and carries a flow with a head of 2.0 m over the weir crest. The discharge coefficient  $C_d$  for the weir is  
 (a) 1.06 (b) 0.931 (c) 0.738 (d) 0.611
- 7.3 The discharge  $Q$  in a triangular weir varies as  
 (a)  $H^{0.5}$  (b)  $H^{1.5}$  (c)  $H^{2.0}$  (d)  $H^{2.5}$
- 7.4 In a triangular notch there is a +2% error in the observation of the head. The error in the computed discharge is  
 (a) +2% (b) +5% (c) -5% (d) +2.5%
- 7.5 A nominal 90° triangular notch was found to have 2% error in the vertex angle. While discharging under a constant head, the error in the estimated discharge is  
 (a)  $\pi\%$  (b)  $\pi/4\%$  (c)  $\pi/2\%$  (d) 2%
- 7.6 In submerged flow over sharp-crested rectangular weirs the Villemonnte equation relates  $Q_s / Q_1$  as equal to

(a) $\left[ 1 - \left( \frac{H_2}{H_1} \right) \right]^{0.385}$	(b) $\left[ 1 - \left( \frac{H_2}{H_1} \right)^{0.385} \right]^{1.5}$
(c) $\left[ 1 - \left( \frac{H_2}{H_1} \right)^{1.5} \right]^{0.385}$	(d) $\left[ 1 - \left( \frac{H_2}{H_1} \right)^{0.385} \right]^{1.5}$

- 7.7 In a triangular notch the tailwater head is 50% of the upstream head, both measured above the vertex of the notch. If the free flow discharge under the same upstream head is  $0.5 \text{ m}^3/\text{s}$ , the submerged flow, in  $\text{m}^3/\text{s}$ , is  
 (a) 0.464 (b) 0.411 (c) 0.500 (d) 0.532
- 7.8 A parabolic sharp-crested weir has a profile given by  $x^2 = ky$ . The discharge in the weir is given by  $Q = KH^n$  where  $n$  is  
 (a) 0.5 (b) 1.5 (c) 2.0 (d) 2.5
- 7.9 A separate arrangement for aeration of the nappe is necessary in a  
 (a) contracted rectangular weir  
 (b) suppressed rectangular weir  
 (c) submerged contracted rectangular weir  
 (d) triangular weir
- 7.10 In a linear proportional weir with a rectangular base of height  $a$ , the discharges are linearly proportional to the head  $h_d$  measured above a datum. The minimum head at which the linear head-discharge relation is observed is  $h_d =$   
 (a)  $a$  (b)  $a/2$  (c)  $a/3$  (d)  $2a/3$
- 7.11 In a quadratic weir the measured head above the datum was found to have an error of 2%. This would mean that the discharges estimated from the weir discharge formula will have an error of  
 (a) 0.5% (b) 1% (c) 2% (d) 4%
- 7.12 Designing of the spillway profile to conform to the shape of the nappe of a sharp crested weir makes  
 (a) the pressures on the spillway crest always positive  
 (b) the pressures to be positive for  $H_0 \geq H_d$   
 (c) the pressures on the spillway always zero  
 (d) the pressure on the crest zero for  $H_0 = H_d$  only
- 7.13 If the head  $H_0$  over an overflow spillway is less than the design head  $H_d$ ,  
 (a) the pressure on the spillway crest will be negative  
 (b) the cavitation phenomenon can occur  
 (c) the separation of the streamlines from the surface can occur  
 (d) the coefficient of discharge  $C_0$  will be less than the design coefficient of discharge  $C_{d0}$
- 7.14 The coefficient of discharge  $C_0$  at any head  $H_0$  of a spillway is a function of  
 (a)  $\left(\frac{H_0}{P}\right)$  only (b)  $\left(\frac{H_0}{H_d}\right)$  only  
 (c)  $\left(\frac{H_0}{P}, \frac{H_0}{H_d}\right)$  only (d)  $\left(\frac{P}{H_d}\right)$  only
- 7.15 A vertical face ogee spillway will have a crest profile downstream of the apex given by  $(y/H_d) =$   
 (a)  $0.5 (x/H_d)^{1.50}$  (b)  $0.5 (x/H_d)^{1.85}$   
 (c)  $1.85 (x/H_d)^{0.517}$  (d)  $2.0 (x/H_d)^{2.0}$
- 7.16 A broad-crested weir with  $H_1/B_w = 0.5$  and  $H_1/P = 1.0$  and a sharp-crested weir with  $H_1/P = 1.0$ , both span the full width of a canal. If the coefficient of discharge  $C_d$  of the weir ( $= C_{dw}$ ) and  $C_d$  of the broad-crested weir ( $= C_{db}$ ) are compared, it will be found that  
 (a)  $C_{dw} > C_{db}$  (b)  $C_{db} > C_{dw}$   
 (c)  $C_{dw} = C_{db}$  (d)  $C_{dw} = C_{db}$  for small  $H_1$  only.
- 7.17 A finite crest width weir with  $H_1/B_w = 0.20$  is classified as a  
 (a) long-crested weir (b) broad crested weir  
 (c) narrow-crested weir (d) sharp-crested weir

- 7.18 The modular limit of a sharp-crested weir ( $M_s$ ), broad-crested weir ( $M_b$ ) and standing wave flume ( $M_f$ ) are compared under equivalent conditions. It will be found that  
 (a)  $M_s > M_b > M_f$  (b)  $M_s < M_b < M_f$   
 (c)  $M_s > M_b < M_f$  (d)  $M_s < M_b > M_f$
- 7.19 The overall coefficient of discharge of a standing wave flume  $C_f = Q / (B_f H_1^{3/2})$  is of the order of  
 (a) 0.61 (b) 0.95 (c) 3.30 (d) 1.62
- 7.20 The discharge equation of a Parshall flume is expressed as  $Q =$   
 (a)  $K\sqrt{H_a}$  (b)  $KH_a$  (c)  $KH_a$  (d)  $K(H_1^{3/2} - H_a^{3/2})$
- 7.21 The end depth ratio  $y_e/y_c$  in a channel carrying subcritical flow is a function of  
 (a) shape of the channel only (b) Shape and Manning's coefficient  
 (c) Normal depth only (d) Shape and Froude number
- 7.22 A 2-m wide horizontal rectangular channel carries a discharge 3.0 m<sup>3</sup>/s. The flow is subcritical. At a free overfall in this channel the end depth in metres is  
 (a) 0.438 (b) 0.612 (c) 0.715 (d) 1.488
- 7.23 A 2.5-m wide rectangular channel is known to be having subcritical flow. If the depth at a free overfall is 0.5 m, the discharge in this channel in, m<sup>3</sup>/s, is  
 (a) 2.56 (b) 4.40 (c) 1.83 (d) 3.50
- 7.24 Two horizontal channels A and B of identical widths and depths have roughness such that  $(K_s)_A = 2(K_s)_B$ . If the discharges observed by the end-depth method in these two channels are denoted as  $Q_A$  and  $Q_B$  respectively, then it would be found that  
 (a)  $Q_A > Q_B$  (b)  $Q_A = \frac{1}{2}Q_B$  (c)  $Q_A = Q_B$  (d)  $Q_A < Q_B$
- 7.25 The effective piezometric head  $h_{ep}$  at the brink of a free overfall could be represented as  
 (a)  $h_{ep} < y_e$  (b)  $h_{ep} > y_e$  (c)  $h_{ep} = y_e$  (d)  $h_{ep} = y_e$
- 7.26 If a rectangular channel carrying a discharge of 1.85 m<sup>3</sup>/s/m width shows a brink depth of 0.35 m at a free overfall, then  
 (a) the discharge measured is wrong  
 (b) the end depth is wrongly measured  
 (c) the flow is subcritical regime  
 (d) the flow is in the supercritical regime
- 7.27 In submerged flow through a sluice gate the coefficient of discharge  $C_{ds} =$   
 (a)  $f\left(\frac{a}{H_1}, \frac{y_1}{a}\right)$  (b)  $C_{SH}$  (c)  $C_{df}$  (d)  $C_d$
- 7.28 The coefficient of discharge  $C_d$  in free sluice gate is related to  $C_c$  as  
 (a)  $C_c = \frac{C_c}{\sqrt{1 + (C_c a / H_1)^2}}$  (b)  $C_d = \frac{C_c a}{H_1 \sqrt{1 - (C_c a / H_1)^2}}$   
 (c)  $C_d = \frac{C_c}{\sqrt{1 - (C_c a / H_1)^2}}$  (d)  $C_d = \frac{C_c}{\sqrt{1 - \left(\frac{a}{H_1}\right) C_c}}$
- 7.29 The discharge coefficient  $C_{SH}$  in submerged sluiceway flow is  
 (a)  $f(a/H_1)$  (b)  $f(y_1/a)$  (c)  $f(a/H_1, y_1/a)$  (d)  $= C_d$
- 7.30 Sluice gates used in field applications have  
 (a) a bevel on the upstream face  
 (b) a bevel on the downstream face  
 (c) bevels on both upstream and downstream faces  
 (d) no bevel.



# Spatially Varied Flow



## 8.1 INTRODUCTION

A steady spatially varied flow represents a gradually-varied flow with non-uniform discharge. The discharge in the channel varies along the length of the channel due to lateral addition or withdrawal. Thus, spatially varied flow (SVF) can be classified into two categories: (i) SVF with increasing discharge and (ii) SVF with decreasing discharge. Since there is considerable amount of difference in the flow and analysis of these two categories, they are dealt with separately in this chapter.

## 8.2 SVF WITH INCREASING DISCHARGE

SVF with increasing discharge finds considerable practical applications. Flows in side-channel spillway, wash-water troughs in filter plants, roof gutters, highway gutters are some of the typical instances. Figure 8.1 shows a typical side-channel spillway causing an SVF in the channel below it. The lateral flow enters the channel normal to the channel-flow direction causing considerable turbulence. It is difficult to assess the net energy imparted to the flow and as such the energy equation is not of much use in developing the equation of motion.

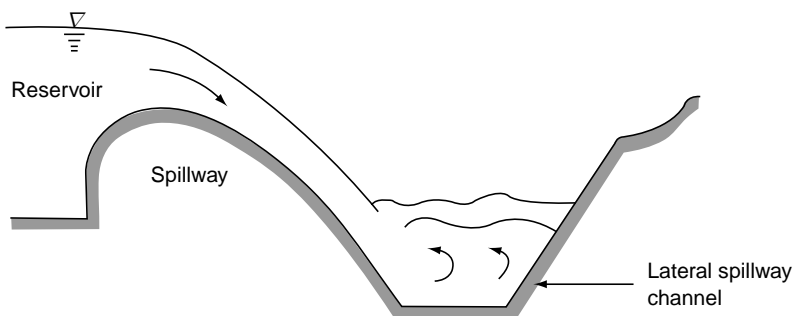


Fig. 8.1 Lateral spillway channel flow

### 8.2.1 Differential Equation of SVF with Increasing Discharges

In applying the momentum equation, the following assumptions are made:

1. The pressure distribution is assumed to be hydrostatic. This amounts to assuming the water-surface curvatures to be moderate. The regions of high curvature, if any, must be delineated and excluded from the analysis.
2. The one-dimensional method of analysis is adopted. The momentum correction factor  $\beta$  is used to adequately represent the effect of non-uniformity of velocity distribution.
3. The frictional losses in SVF are assumed to be adequately represented by a uniform flow resistance equation, such as Manning's formula.
4. The effect of air entrainment on forces involved in the momentum equation is neglected.
5. It is assumed that the lateral flow does not contribute any momentum in the longitudinal direction.
6. The flow is considered to be steady.
7. The channel is prismatic and is of small slope.

Consider a control volume formed by two Sections 1 and 2, distance  $\Delta x$  apart (Fig. 8.2). Applying the momentum equation in the longitudinal  $x$  direction.

$$M_2 - M_1 = P_1 - P_2 + W \sin \theta - F_f \tag{8.1}$$

or

$$\Delta M = -\Delta P + W \sin \theta - F_f \tag{8.1a}$$

in which  $M = \text{momentum flux} = \beta \rho Q^2/A$

$P = \text{pressure force} = \gamma A \bar{y}$

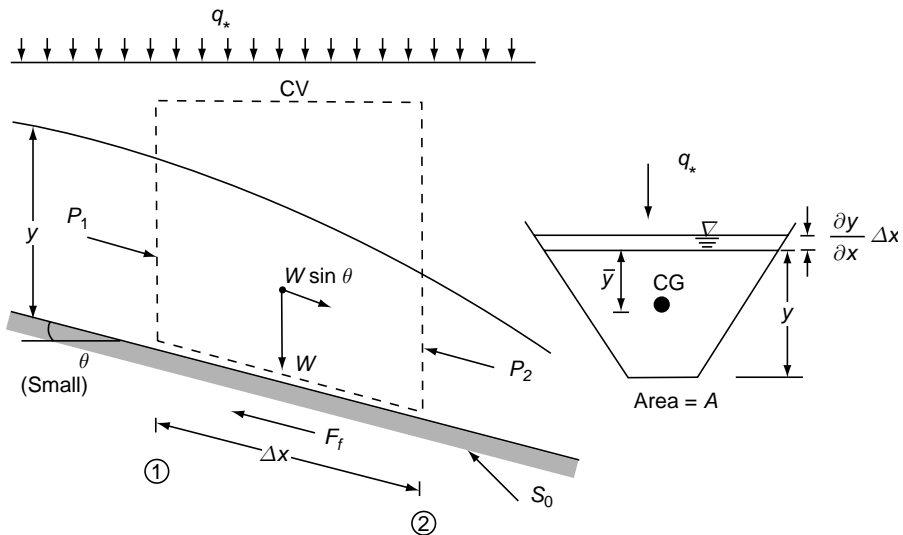


Fig. 8.2 Definition sketch of SVF with lateral inflow

where  $\bar{y}$  = depth of the centre of gravity of the flow cross-section from the water surface,  $W \sin \theta$  = component of the weight of the control volume in the  $x$  direction and  $F_f$  = frictional force =  $\gamma AS_f \Delta x$ .

Dividing Eq. (8.1a) by  $\Delta x$  and taking limits as  $\Delta x \rightarrow 0$ ,

$$\frac{dM}{dx} = -\frac{dP}{dx} + \gamma AS_0 - \gamma AS_f \tag{8.2}$$

In this

$$(i) \quad \frac{dM}{dx} = \rho\beta \left( \frac{2Q}{A} \frac{dQ}{dx} - \frac{Q^2}{A^2} \frac{dA}{dx} \right)$$

$$= \rho\beta \left( \frac{2Q}{A} q_* - \frac{Q^2 T}{A^2} \frac{dA}{dx} \right)$$

where  $q_* = \frac{dQ}{dx}$  = discharge per unit length entering the channel.

$$(ii) \quad \frac{dP}{dx} = \gamma \left( A \frac{d\bar{y}}{dx} + \bar{y} \frac{dA}{dx} \right)$$

By taking moments of the areas about the new water surface after a small change  $dy$  in depth, (Fig. 8.3),

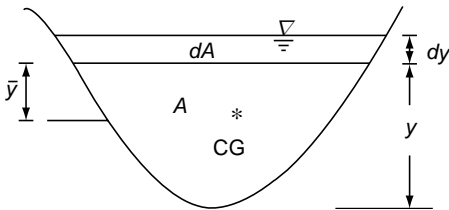


Fig. 8.3 Definition sketch

$$A(\bar{y} + dy) + dA \frac{dy}{2} = (A + dA)(\bar{y} + d\bar{y})$$

$$A dy + \frac{dA dy}{2} = \bar{y} dA + A d\bar{y} + dA d\bar{y}$$

By neglecting second-order small quantities,

$$A d\bar{y} + \bar{y} dA = A dy$$

Thus 
$$\frac{dP}{dx} = \gamma A \frac{dy}{dx}$$

Hence, Eq. (8.2) simplifies to

$$\frac{2\beta Q q_*}{gA^2} - \frac{\beta Q^2 T}{gA^3} \frac{dy}{dx} = -\frac{dy}{dx} + (S_0 - S_f)$$

or 
$$\frac{dy}{dx} = \frac{S_0 - S_f - \left( 2\beta Q q_* / gA^2 \right)}{1 - \beta \frac{Q^2 T}{gA^3}} \tag{8.3}$$

Equation 8.3 is the basic differential equation governing the motion in the SVF with increasing discharge. In general,  $q_*$  is a function of  $x$ . However, in a lateral spillway channel  $q_*$  is constant. In view of the high non-uniform velocity distribution in the channel cross-section, it is necessary to use proper values of the momentum correction factor  $\beta$ . In lateral spillway channels, values of  $\beta$  as high as 1.60 are not

uncommon. It may be noted that if  $\beta = 1.0$  and  $q_* = 0$ , Eq. 8.3 will be the same as that of the differential equation of gradually varied flow (GVF) (Eq. 4.8)

Equation 8.3 is a non-linear equation and is more complex than the GVF equation. Closed-form solutions are not possible except in highly-simplified cases. A numerical solution of the equation is feasible. Starting from a section where the flow properties are known (such as a control section), the water-surface profile can be computed.

### 8.2.2 Control Point

If the flow is subcritical everywhere in the channel, the control of the profile will be located at the downstream end of the channel. However, for all flow situations other than the above, the determination of the control point is a necessity to start the computations.

In an SVF with increasing discharges, the critical depth line is not a straight line parallel to the bed as in GVF but is a curved line. Depending upon the combination of the bottom slope, channel roughness and channel geometry, the critical depth of spatially varied flow can occur at a location somewhere between the ends of the channel, giving rise to a profile which may be subcritical during the first part and supercritical in the subsequent part of the channel. A method of calculation of the critical depth and its location based on the concept of *equivalent critical depth channel* has been proposed by Hinds<sup>1</sup>. An alternative method based on transitional profiles suggested by Smith<sup>2</sup>, which has advantages like simplicity and less tedious calculations compared to Hind's method, is described below:

Consider Eq. 8.3 written as

$$\frac{dy}{dx} = S_0 \frac{1 - \frac{S_f}{S_0} - \frac{2\beta Q q_*}{gA^2 S_0}}{1 - \beta \frac{Q^2 T}{gA^3}} \quad (8.4)$$

Defining  $Q = K\sqrt{S_f}$  = actual discharge

$Q_n = K\sqrt{S_0}$  = normal discharge in the channel at a depth  $y$

$Q_c = \sqrt{\frac{gA^3}{\beta T}}$  = critical discharge modified by  $\beta$ .

Equation 8.4 reduces to

$$\begin{aligned} \frac{dy}{dx} &= S_0 \frac{1 - \frac{K^2 Q^2}{K^2 Q_n^2} - \frac{Q^2 \left( \frac{2\beta K^2 q_*}{gA^2 Q} \right)}{Q_n^2 \left( \frac{gA^2 Q}{gA^2 Q} \right)}}{1 - (Q/Q_c)^2} \\ &= S_0 \frac{1 - \left( \frac{Q}{Q_n} \right)^2 \left( 1 + \frac{2\beta K^2 q_*}{gA^2 Q} \right)}{1 - (Q/Q_c)^2} \end{aligned} \quad (8.5)$$

370 Flow in Open Channels

Redefining  $Q_{n1}$  = modified normal discharge

$$= \frac{Q_n}{\sqrt{1 + \frac{2\beta K^2 q_*}{gA^2 Q}}}$$

Equation 8.5 is simplified as

$$\frac{dy}{dx} = S_0 \frac{1 - \left(\frac{Q}{Q_{n1}}\right)^2}{1 - (Q/Q_c)^2}$$

Equation 8.5a is of the same form as Eq. 4.15, and the location of the transitional profile at a given  $x$  would be determined by the condition  $Q_{n1} = Q_c$ . The intersection of the transitional profile with the critical-depth line will satisfy the condition  $Q = Q_{n1} = Q_c$  and hence would locate the control point; i.e. the section at which the actual flow would pass at critical depth.

At transitional depth,  $Q_{n1} = Q_c$ .

i.e. 
$$\frac{Q_n}{\sqrt{1 + \frac{2\beta K^2 q_*}{gA^2 Q}}} = \sqrt{\frac{gA^3}{\beta T}}$$

or 
$$\frac{2\beta K^2 q_*}{gA^2 Q} = \frac{\beta Q_n^2 T}{A^3 g} - 1 \tag{8.6}$$

Substituting  $Q_n = K \sqrt{S_0}$  and simplifying

$$\frac{q_*}{Q} = \frac{1}{2} \left( \frac{S_0 T}{A} - \frac{gA^2}{\beta K^2} \right) \tag{8.7}$$

which is the equation of the transitional profile for SVF with increasing discharge.

In a general SVF with increasing discharge,

$$Q = Q_i + \int_0^x q_* dx$$

where  $Q_i$  = channel discharge at  $x = 0$ . For the SVF in a lateral spillway channel  $Q_i = 0$ . and  $q_* = \text{Constant}$ , i.e.  $Q = q_* x$  which simplifies Eq. 8.7 to

$$\frac{1}{x_i} = \frac{1}{2} \left( \frac{S_0 T}{A} - \frac{gA^2}{\beta K^2} \right) \tag{8.8}$$

the suffix  $t$  denoting the transitional profile. It is interesting to note that in an SVF due to a side-channel spillway, the transitional profile is independent of the rate of lateral inflow.

To locate the control point, the critical depth line is first calculated and plotted to scale (Fig. 8.4). Note that the critical depth line for SVF with increasing discharge is to be calculated by using the relationship  $Q_c = \sqrt{\frac{gA^3}{\beta T}}$ . The transitional profile is then calculated by Eq. 8.7 and plotted on the same figure and the intersection of the critical-depth line with the transitional profile gives the location of the control section at which the actual flow passes as a critical depth (Fig. 8.4).

This method is of general use and can be easily incorporated into a numerical-method algorithm to compute the SVF profile using a digital computer.

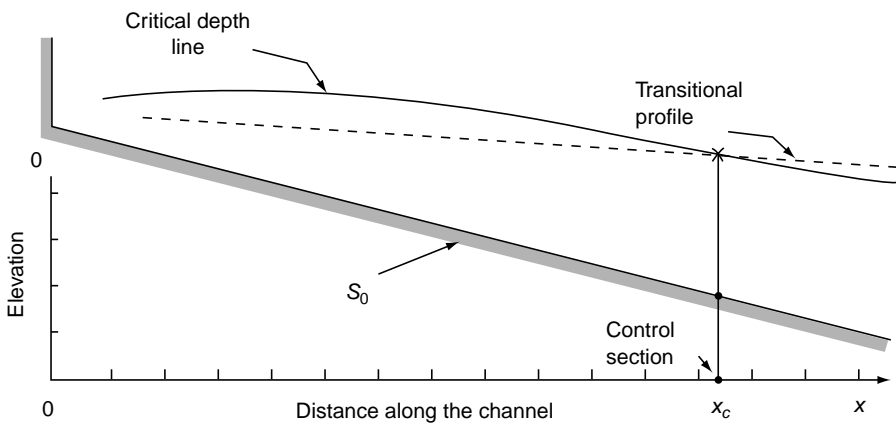


Fig. 8.4 Determination of control section through transitional profile

**Example 8.1** A horizontal, frictionless, rectangular lateral spillway channel of length  $L$  has a free overfall. Show that the equation of the flow profile is

$$\frac{dx^2}{dy} - \frac{x^2}{y} = -\frac{gB^2 y^2}{q_*^2}$$

Show that the solution of the above equation for the condition of critical depth  $y_c$  occurring at the outlet is

$$\left[\frac{x}{L}\right]^2 = \frac{3}{2}\left[\frac{y}{y_c}\right] - \frac{1}{2}\left[\frac{y}{y_c}\right]^3$$

Solution 
$$\frac{dy}{dx} = \frac{S_0 - S_f - \frac{2Qq_*}{gA^2}}{1 - (Q^2T / gA^3)}$$

$S_0 = 0, S_f = 0, A = By, T = B, q_* x = Q$

Hence 
$$\frac{dy}{dx} = -\frac{2q_*^2 x / gB^2 y^2}{1 - (q_*^2 x^2 / gB^2 y^3)}$$

$$\left[1 - \frac{q_*^2 x^2}{gB^2 y^3}\right] dy = -\frac{2q_*^2 x}{gB^2 y^2} dx$$

Put  $t = x^2$ , then  $dt = 2x dx$ . Further, put  $\frac{q_*^2}{gB^2 y^2} = \frac{1}{M}$ . Then

$$\left(1 - \frac{t}{yM}\right) dy = -\frac{1}{M} dt$$

$$\frac{dt}{dy} - \frac{t}{y} = -M \quad \text{that is} \quad \frac{d(x^2)}{dy} - \frac{(x^2)}{y} = -\frac{gB^2 y^2}{q_*^2}$$

The solution is 
$$x^2 = -\frac{gB^2 y^3}{2q_*^2} + C_1 y$$

At the outlet,  $x = L$  and  $y = y_c$

$$L^2 = -\frac{gB^2 y_c^2}{2q_*^2} + C_1 y_c$$

$$C_1 = \frac{1}{y_c} \left( L^2 + \frac{gB^2 y_c^3}{2L^2 q_*^2} \right)$$

$$\frac{x^2}{L^2} = \left[ 1 + \frac{gB^2 y^3}{2L^2 q_*^2} \right] \frac{y}{y_c} - \frac{gB^2 y^3}{2q_*^2 L^2}$$

But  $\frac{gB^2}{L^2 q_*^2} = \frac{gB^2}{Q_L^2}$  and  $\frac{gB^2 y_c^3}{Q_L^2} = 1$

Thus 
$$\left[ \frac{x}{L} \right]^2 = \frac{3}{2} \left[ \frac{y}{y_c} \right] - \frac{1}{2} \left[ \frac{y}{y_c} \right]^3$$

**Example 8.2** | A lateral spillway channel is trapezoidal in section with  $B = 5.0$  m,  $m = 1$  and  $n = 0.015$ . The bed slope is 0.10. Find the location of the control point and the critical depth for a lateral discharge rate of (a)  $q_* = 2.0$  m<sup>3</sup>/s/m, (b)  $q_* = 3.0$  m<sup>3</sup>/s/m. Assume  $\beta = 1.25$ .

**Solution** The computations necessary to plot the critical-depth line and the transitional profile are done in a tabular form as shown in Table 8.1. Various depth values

**Table 8.1** Calculations of Control Point in a Lateral Spillway Channel—Example 8.1

$B = 5.0, m = 1.0, n = 0.015, B = 1.25, S_0 = 0.10, K = \frac{1}{n}AR^{2.3}$										
$y$	$A$	$T$	$Q_c$	$P$	$R = A/P$	$K$	$1/x_i$	$x_i$	$x_c = Q_c/q_*$	
(m)	(m <sup>2</sup> )	(m)	$\frac{\sqrt{gA^3}}{\beta T}$	(m)	(m)		Eq. (8.8)	(m)	$q_* = 3.0 \quad q_* = 2.0$	
1.0	6.00	7.0	15.56	7.828	0.7665	335	0.05707	17.54	5.18	7.78
2.0	14.00	9.0	48.92	10.657	1.3137	1120	0.03153	31.72	16.31	24.46
2.5	18.75	10.0	71.92	12.071	1.5533	1677	0.02618	38.20	23.97	35.96
3.0	24.00	11.0	99.31	13.485	1.7798	2349	0.02251	44.43	33.10	49.66
3.5	29.75	12.0	131.20	14.899	1.9968	3145	0.01982	50.46	43.73	65.60
4.0	36.00	13.0	167.80	16.314	2.2067	4068	0.01775	56.34	55.94	83.90
5.0	50.00	15.0	255.70	19.142	2.6120	6322	0.01475	67.78	85.32	127.85
6.0	66.00	17.0	364.30	21.971	3.0000	9160	0.01268	78.89	121.43	182.15



374 Flow in Open Channels

are assumed and  $x_t$  and  $x_c$ , the longitudinal coordinates of the transitional profile and the critical-depth line respectively, are calculated.  $x_t$  is calculated by using Equation 8.8 and  $x_c = \frac{Q_c}{q_*}$  where  $Q_c = \sqrt{gA^3 / \beta T}$ .

The transitional profile and the critical-depth line for a given  $q_*$  are plotted and the control point is determined by the intersection of these two lines as:

$$q_* = 3.0 \text{ m}^3 / \text{s} / \text{m}, \quad y_c = 4.0 \text{ m}, \quad x_c = 56.0 \text{ m}$$

$$q_* = 2.0 \text{ m}^3 / \text{s} / \text{m}, \quad y_c = 2.65 \text{ m}, \quad x_c = 40.0 \text{ m}$$

**Example 8.3** Obtain an expression to determine the critical depth and its location for a lateral spillway channel of rectangular section. Use the Chezy formula with  $C = \text{constant}$ .

**Solution** In a rectangular section  $B = T$ . Using the Chezy formula.

$$K^2 = A^2 C^2 R$$

The transitional profile for the rectangular channel is obtained by using Eq. 8.8. as

$$\frac{1}{x_t} = \frac{1}{2} \left( \frac{S_0}{y} - \frac{g}{\beta C^2 R} \right)$$

i.e. 
$$x_t = \frac{2\beta C^2 R y}{(\beta C^2 R S_0 - g y)} \tag{8.9}$$

The equation of the critical-depth line is given by

$$Q_c = q_* x_c = \sqrt{(g B^2 y_c^3 / \beta)}$$

i.e. 
$$x_c^2 = g B^2 y_c^3 / \beta q_*^2 \tag{8.10}$$

At the critical-flow section, the critical-depth line and the transitional-depth line intersect. Hence  $x_t = x_c, y = y_c$ .

$$\frac{g B^2 y_c^3}{\beta q_*^2} = \frac{4 \beta^2 C^4 y_c^2 R_c^2}{(\beta C^2 R_c S_0 - g y_c)^2}$$

Simplifying,

$$y_c \left( \beta C^2 S_0 - g \frac{y_c}{R_c} \right)^2 = \frac{4 \beta^3 C^4 q_*^2}{g B^2} \tag{8.11}$$

with suffix  $c$  denoting the critical-depth section. Equation 8.11 is the desired expression for the determination of critical depth. This equation will have to be solved by trial and error to get the critical depth. Substitution of this  $y_c$  in Eq. 8.10, gives the location of the critical-flow section.

### 8.2.3 Classification and Solutions

Unlike GVF, SVF with lateral inflow has not received extensive attention and as such the detailed classification and analysis of a general-flow situation are not available in literature. By assuming zero friction and  $\beta = 1.0$ , Li<sup>3</sup> has made a detailed study and has classified the flow into the following categories:

**Type A** The flow is subcritical throughout the channel and the Froude number increases continuously in the downstream direction.

**Type B** The flow is subcritical throughout but the Froude number will first increase, reach a maximum value less than unity and then decrease.

**Type C** The flow is subcritical initially, passes through a critical section to become supercritical in the downstream portions of the channel and then terminates in a jump due to downstream control such as a submerged outlet.

**Type D** The same as Type C, but the jump is not formed in the channel. The outlet is free.

These four types of flow can be determined by a study of the transitional profile and the critical-depth line along with the downstream end conditions. In general, Type C and D situations can occur in side spillway channel design and Type A and B can occur in washwater-trough and gutter-design problems. Li<sup>3</sup> has classified the above four types of flow in frictionless rectangular channels on the basis of parameters  $F_e$  and  $G = \frac{S_0 L}{y_e}$  where  $F_e$  and  $y_e$  are Froude number and depth of flow at the end of the channel respectively. Solutions to subcritical and supercritical SVFs with increasing discharge in frictionless rectangular channels are also presented by Li<sup>3</sup> as dimensionless graphs.

Gill<sup>4</sup> has given approximate algebraic solutions to SVF with increasing discharges in frictionless rectangular channels based on the method of perturbation. His predictions cover a range of subcritical flow Froude numbers, the supercritical flow, the Type D flow and compare well with Li's work. Gill has extended his analytical method to cover the case of SVF in a wide rectangular channel with the friction effect duly accounted.

In view of the various assumptions with regard to friction, the channel geometry and value of  $\beta$  involved in these studies, one should be cautious in using these results in practical situations.

### 8.2.4 Profile Computation

As already indicated, the basic differential equation of SVF with lateral inflow (Eq. 8.3) is non-linear and no closed-form solutions are available to a general problem. A host of numerical techniques are however, available for its solution. The computations proceed from a control point where the flow properties are known. Regarding the friction formula, in the absence of any other resistance formula exclusively for SVF, a convenient uniform flow formula, such as Manning's formula, is used. There is some evidence that the value of the roughness coefficient is likely to be higher in SVF than in uniform flow. Till conclusive results are available, it is prudent to use uniform flow values. Experimental studies<sup>5,6</sup> have shown that the assumption of  $\beta = 1.0$  is unrealistic and a proper selection of  $\beta$  will greatly enhance the accuracy of prediction of the SVF profile.

**Numerical Methods** The advanced numerical methods (Section 5.8) discussed in connection with GVF computations are all eminently suitable for SVF computations also.

However,  $\frac{dy}{dx}$  in Eq. (8.3) is a function of  $x$  and  $y$ , and can be written as

$$\frac{dy}{dx} = \frac{S_0 - S_f - (2\beta Qq_* / gA^2)}{1 - \beta \frac{Q^2 T}{gA^3}} = F(x, y) \quad (8.3a)$$

The SRK and KM methods (Section 5.8) will take the following forms to suit Eq. 8.3a

(i) *Standard Fourth-Order Runge-Kutta Method (SRK) for SVF*

$$y_{i+1} = y_i + \frac{1}{6}(K_1 + 2K_2 + 2K_3 + K_4) \quad (8.12)$$

in which

$$K_1 = \Delta x \cdot F(x_i, y_i)$$

$$K_2 = \Delta x \cdot F\left(x_i + \frac{1}{2}\Delta x, y_i + \frac{1}{2}K_1\right)$$

$$K_3 = \Delta x \cdot F\left(x_i + \frac{1}{2}\Delta x, y_i + \frac{1}{2}K_2\right)$$

$$K_4 = \Delta x \cdot F(x_i + \Delta x, y_i + K_3)$$

(ii) *Kutta–Merson Method (KM) for SVF*

$$y_{i+1} = y_i + \frac{1}{2}(K_1 + 4K_4 + K_5) \quad (8.13)$$

in which  $K_1 = \frac{1}{3} \Delta x \cdot F(x_i, y_i)$

$$K_2 = \frac{1}{3} \Delta x \cdot F\left(x_i + \frac{1}{3} \Delta x, y_i + K_1\right)$$

$$K_3 = \frac{1}{3} \Delta x \cdot F\left(x_i + \frac{2}{3} \Delta x, y_i + \frac{1}{2} K_1 + \frac{1}{2} K_2\right)$$

$$K_4 = \frac{1}{3} \Delta x \cdot F\left(x_i + \Delta x, y_i + \frac{3}{8} K_1 + \frac{9}{8} K_3\right)$$

$$K_5 = \frac{1}{3} \Delta x \cdot F\left(x_i + \Delta x, y_i + \frac{3}{2} K_1 - \frac{9}{2} K_3 + 6K_4\right)$$

(iii) *Trapezoidal Method (TRAP) for SVF*

$$y_{i+1} = y_i + \frac{1}{2} \Delta x [F(x_i, y_i) + F(x_{i+1}, y_{i+1})] \quad (8.14)$$

The details of these methods, their relative accuracy and advantages are the same as discussed in Section 5.8 in connection with the GVF computations.

### 8.3 SVF WITH DECREASING DISCHARGE

SVF with decreasing discharges occurs in a variety of field situations, typical examples being side weirs, bottom racks and siphon tube irrigation systems. The abstraction of water from a canal by using the above means is normally achieved in such a manner as to cause minimum obstruction and with consequent little energy losses in the parent channel. It is usual to assume that energy loss due to diversion of water is zero and the energy equation is used to derive the basic equation of motion.

#### 8.3.1 Differential Equation for SVF with Decreasing Discharge

The following assumptions are made:

1. The pressure distribution is hydrostatic
2. The one-dimensional method of analysis is used (the energy-correction factor  $\alpha$  is used to adequately represent the non-uniformity of velocity distribution).
3. The friction losses are adequately represented by Manning's formula.
4. Withdrawal of water does not affect the energy content per unit mass of water in the channel
5. The flow is steady
6. The channel is prismatic and is of small slope.

Consider the total energy at a Section  $x$ ,

$$H = Z + y + \alpha \frac{V^2}{2g} \quad (8.15)$$

Differentiating this with respect to  $x$

$$\frac{dH}{dx} = \frac{dZ}{dx} + \frac{dy}{dx} + \frac{d}{dx} \left( \alpha \frac{V^2}{2g} \right) \quad (8.16)$$

But 
$$\frac{dH}{dx} = -S_f \text{ and } \frac{dZ}{dx} = -S_0$$

$$\frac{d}{dx} \left( \alpha \frac{V^2}{2g} \right) = \frac{d}{dx} \left( \alpha \frac{Q^2}{2gA^2} \right) = \frac{\alpha}{2g} \left( \frac{2Q}{A^2} \frac{dQ}{dx} - \frac{2Q^2}{A^3} \frac{dA}{dy} \frac{dy}{dx} \right)$$

$$\frac{dA}{dy} = T \text{ and } \frac{dQ}{dx} = q_*$$

Equation 8.16 simplifies to

$$\frac{dy}{dx} = \frac{S_0 - S_f - \frac{\alpha Q q_*}{gA^2}}{1 - \frac{\alpha Q^2 T}{gA^3}} \quad (8.17)$$

Equation 8.17 is the basic differential equation governing the motion of SVF with decreasing discharges. Note the difference between Eq. 8.17 and Eq. 8.3. When  $q_* = 0$ , Eq. 8.17 will be the same as the differential equation of GVF, Eq. 4.8. Unlike the SVF with increasing discharges, in this case  $q_*$  is not externally controlled but will be implicitly governed by the flow conditions.

### 8.3.2 Computations

The determination of the critical-flow control point in the SVF with decreasing discharges is difficult as  $q_*$  is not explicitly known. Normally, SVF with lateral outflow occurs in a relatively small portion of length of canals and the upstream or downstream depth, depending upon the flow, is known through the characteristics of the outflow structure and main channel. This forms, the starting point for the SVF computations.

It is first necessary to establish a relationship for  $q_*$  as a function of the relevant flow conditions. The SVF profile is then computed by using a numerical procedure, such as SRK, KM or TRAP method discussed in Section 8.2.4. The method of approach depends upon the understanding of the particular flow phenomenon.

A few specific examples of flow situations where SVF with lateral outflow occurs, are described below.

## 8.4 SIDE WEIR

A side weir, also known as a *lateral weir*, is a free-overflow weir set into the side of a channel which allows a part of the liquid to spill over the side when the surface of the flow in the channel rises above the weir crest. Side weirs are extensively used as a means of diverting excess storm waters from urban drainage systems and as water-level control devices in flood-control works. In irrigation engineering, side weirs of broad crest are used as head regulators of distributaries and escapes.

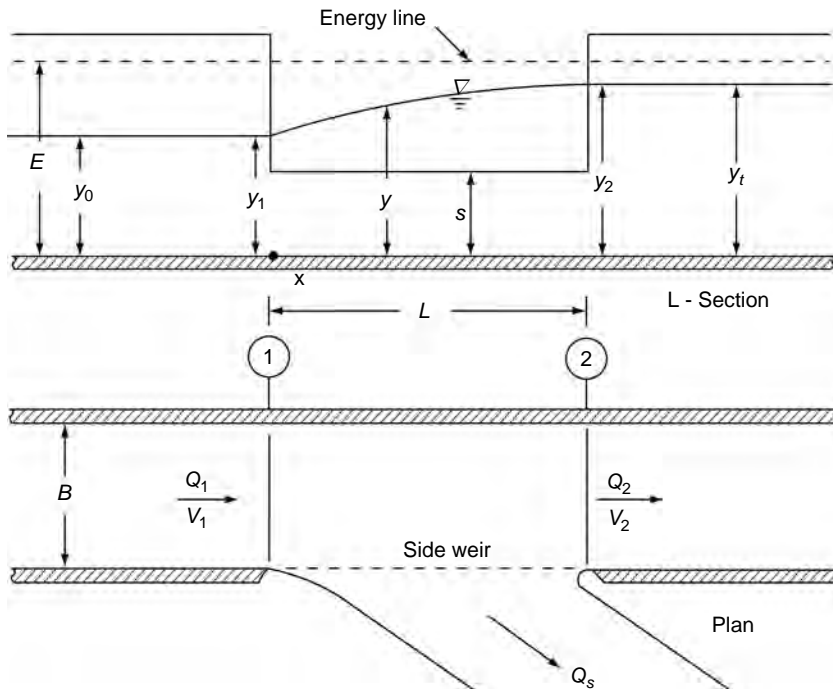


Fig. 8.5 Definition sketch of side weir flow

Figure 8.5 is a definition sketch of the flow over a side weir. Side weirs are usually short structures with  $L/B \leq 3.0$ . It is obvious from specific energy considerations (Section 2.2) that the longitudinal water surface should increase in the downstream direction when the main channel flow is subcritical throughout. Similarly, the water-surface profile would be a decreasing curve for supercritical flow in the channel. The possible flow profiles can be broadly classified into the following three categories:

**Type 1** The channel is on a mild slope and the weir heights  $s > y_{c1}$  where  $y_{c1}$  is the critical depth corresponding to the incoming discharge  $Q_1$  at Section 1, (Fig. 8.6a). At

the downstream end the normal depth corresponding to discharge  $Q_2$  will prevail. Thus  $y_2 = y_t$ , the tailwater depth. At Section 1, the depth  $y_1$  will be such that  $y_{c1} < y_1 < y_0$ , where  $y_0 =$  normal depth for  $Q_0 = Q_1$ . Along the weir the depth increases from  $y_1$  to  $y_2$ . Upstream of Section 1 there will be an  $M_2$  curve from  $y_0$  to  $y_1$ . The control for the SVF will be the downstream depth  $y_2 = y_t$ .

**Type 2** The channel is on mild slope ( $y_0 > y_{c1}$ ) and with  $s < y_{c1}$  (Fig. 8.6b). If the weir is long, flows below critical depth are possible. At the upstream end of the

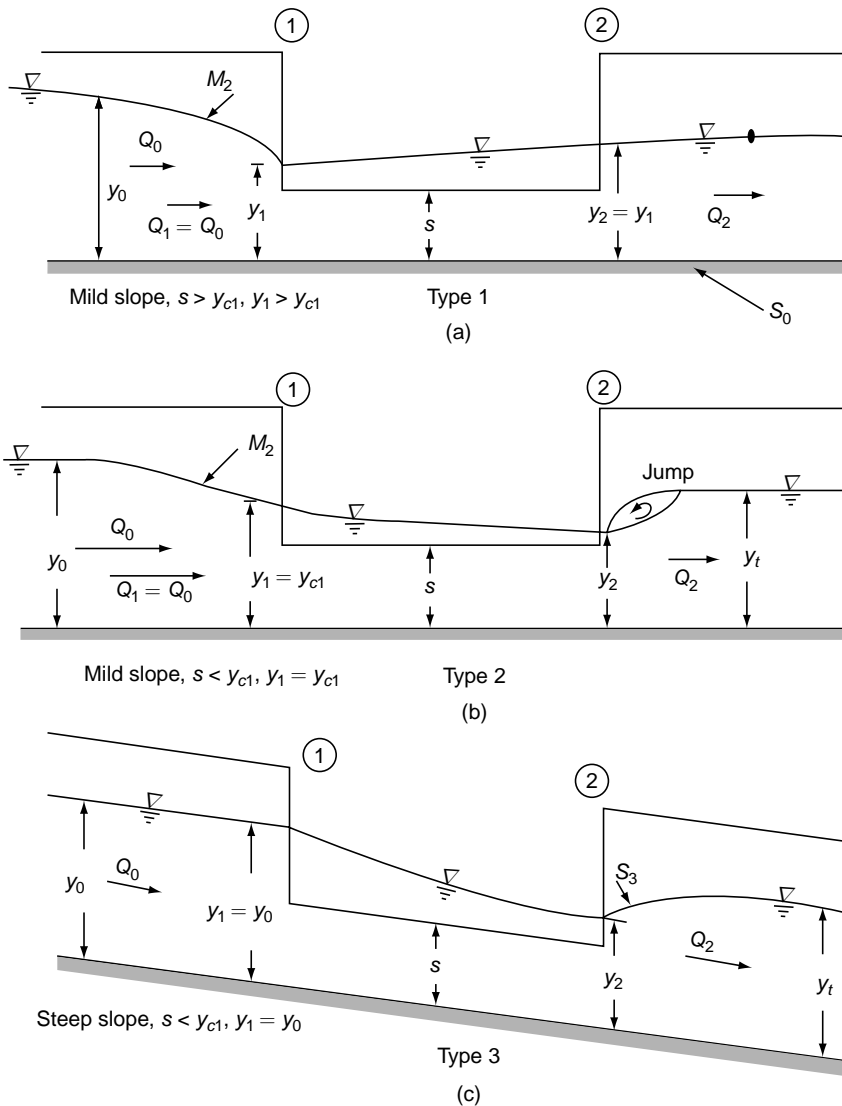


Fig. 8.6 Classification of flow over side weirs

weir, the depth  $y_1$  can be considered to be equal to  $y_{c1}$ . At the downstream end the depth  $y_2$  will rise to the tailwater depth  $y_t$  through a jump. Depending upon the tailwater depth, the jump can also advance into the weir portion. The control for this type 2 profile is at Section 1.

**Type 3** The channel is on a steep slope, ( $y_0 < y_{c1}$ ) and with  $s < y_{c1}$  (Fig. 8.6c). The upstream depth  $y_1 = y_0$  decreasing depth water profile will start from Section 1. At Section 2 the depth reaches a minimum value and in the downstream channel the water surface rises through an  $S_3$  profile to meet the tailwater depth  $y_t$ . The control for this profile is  $y_1 = y_0$  at Section 1.

### 8.4.1 De Marchi Equation for Side Weirs

Referring to the definition sketch (Fig. 8.5), to derive an equation to the sideweir flow, the following assumptions are made:

1. The channel is rectangular and prismatic.
2. The side weir is of short length and the specific energy is taken to be constant between Sections 1 and 2. This is equivalent to assuming  $(S_0 - S_f) = 0$  or  $(S_0 = 0$  and  $S_f = 0)$ . Experimental studies have shown that this is a reasonable assumption.
3. The side weir is assumed to be sharp-edged weir with proper aeration of the nappe and to be discharging freely.
4. Kinetic energy correction factor  $\alpha$  is taken as unity.

The SVF differential equation (Eq. 8.17) with the above assumptions would become

$$\frac{dy}{dx} = \frac{Q \left( -\frac{dQ}{dx} \right) / gB^2 y^2}{1 - \frac{Q^2}{g y^3 B^2}}$$

i.e.

$$\frac{dy}{dx} = \frac{Qy \left( -\frac{dQ}{dx} \right)}{gB^2 y^3 - Q^2} \quad (8.18)$$

The outflow rate = discharge over the side weir per unit length

$$= \left( -\frac{dQ}{dx} \right) = \frac{2}{3} C_M \sqrt{2g} (y - s)^{3/2} \quad (8.19)$$

in which  $C_M$  = a discharge coefficient known as the *De Marchi coefficient*. Also, since the specific energy  $E$  is assumed to be constant, the discharge in the channel at any cross-section is given by

$$Q = By \sqrt{2g(E - y)} \quad (8.20)$$



From Eqs 8.18, 8.19 and 8.20

$$\frac{dy}{dx} = \frac{4}{3} \frac{C_M}{B} \frac{\sqrt{(E-y)(y-s)^3}}{3y-2E} \quad (8.21)$$

Assuming that  $C_M$  is independent of  $x$ , on integration,

$$x = \frac{3B}{2C_M} \cdot \phi_M(y, E, s) + \text{Const.} \quad (8.22)$$

in which

$$\phi_M(y, E, s) = \frac{2E-3s}{E-s} \sqrt{\frac{E-y}{y-s}} - 3 \sin^{-1} \sqrt{\frac{E-y}{E-s}}$$

Equation 8.22 is known as the *De Marchi equation* and the function  $\phi_M(y, E, s)$  is known as the *De Marchi varied flow function*. Applying Eq. 8.22 to Sections 2 and 1,

$$x_2 - x_1 = L = \frac{3}{2} \frac{B}{C_M} (\phi_{M2} - \phi_{M1}) \quad (8.23)$$

knowing  $L$ ,  $s$ , and ( $Q$  and  $y$ ) at either 2 or 1, the discharge over the side weir  $Q_s$  can be computed by Eq. 8.23 and by the continuity equation

$$Q_s = Q_1 - Q_2 \quad (8.24)$$

**De Marchi Coefficient  $C_M$**  Experimental and theoretical studies by Subramanya and Awasthy<sup>7</sup> have shown that in subcritical approaching flow the major flow parameter affecting the De Marchi coefficient is the Froude number of the approaching flow. The functional relationship of  $C_M$  and initial Froude number is shown to be

$$C_M = 0.611 \sqrt{1 - \frac{3F_1^2}{(F_1^2 + 2)}} \quad (8.25)$$

$$\text{where } F_1 = \frac{V_1}{\sqrt{g y_1}}$$

Equation 8.25 can be simplified as

$$C_M = 0.864 \sqrt{\frac{1 - F_1^2}{2 + F_1^2}} \quad (8.26)$$

However, for supercritical approach flow the effect of the approach Froude number is insignificant and the variation of  $C_M$  for  $F_1 > 2.0$  is obtained as

$$C_M = 0.36 - 0.008F_1 \quad (8.27)$$

There have been numerous studies on the side weirs in rectangular channels since last three decades. A majority of these studies are on subcritical approach flow condition as this is the most common situation in practice. Borghi et al.<sup>8</sup> have studied the effect of parameters,  $s/y_1$  and  $L/B$ , and propose the following experimentally derived equation for estimation of the De Marchi coefficient  $C_M$  for subcritical approach flow:

$$C_M = 0.7 - 0.48F_1 - 0.3 \frac{s}{y_1} + 0.06 \frac{L}{B} \quad (8.28)$$

Olivetto et al.<sup>9</sup> have studied the side weir flow in rectangular and circular channels both through theoretical and experimental means. The studies relate to the case of subcritical flow in the approach channel with supercritical flow along the side weirs. Ghodsian<sup>10</sup> has experimentally studied the hydraulic characteristics of sharp crested triangular side weirs. For this flow situation the De Marchi equation has been expressed as

$$C_M = A - BF_1 - C \frac{s}{y_1} \quad (8.29)$$

where  $s$  = height of the vertex of the triangular weir above the bed of the channel. The coefficients  $A$ ,  $B$  and  $C$  are found to be functions of the weir angle  $\theta$ .

Uyumaz<sup>11</sup> has studied the behavior of a rectangular side weir in a triangular channel and has derived the relevant discharge equation. The channel studied had one side vertical and the side weir was located in the vertical side. The coefficient of discharge  $C_M$ , given by Eq. 8.25 and 8.27 was found to be adequate for this case also. However, if the weir is set in the inclined side of the channel, the coefficient  $C_M$  can be expected to be a function of the inclination of the side also.

## 8.4.2 Computations

The design of a side weir or the calculation of the side-weir discharge can be accomplished by use of appropriate Eqs 8.23 through 8.27 along with the selection of the proper control depth. In using the De Marchi equation since it is assumed that  $S_f = S_0 = 0$ , the controls would be  $y_1 = y_0$  for flows of Type 1 and Type 3. However, for Type 2 flows the coefficient  $C_M$  is calculated by taking  $F_1 = F_0$  and for calculations of discharge and depth profile the depth at Section 1 is assumed as  $y_1 = y_{c1}$ . The downstream depth  $y_2$  would, in all types of flows, be determined by the condition of constancy of specific energy, ( $E = \text{constant}$ ).

It is apparent that iterative procedures have to be adopted in the calculation of  $Q_s$  or  $L$ .

**Example 8.4** | A rectangular channel,  $B = 2.0$  m,  $n = 0.014$ , is laid on a slope  $S_0 = 0.001$ . A side weir is required at a section such that it comes into operation when

384 Flow in Open Channels

the discharge is  $0.6 \text{ m}^3/\text{s}$  and diverts  $0.15 \text{ m}^3/\text{s}$  when the canal discharge is  $0.9 \text{ m}^3/\text{s}$ . Design the elements of the side weir.

**Solution** The normal depths at the two discharges are found by referring to Table 3A.1 as:

$Q_0$	$\phi = nQ / \sqrt{S_0} B^{8/3}$	$y_0/B$	$y_0$
0.6	0.0418	0.165	0.33 m
0.9	0.0628	0.220	0.44 m

The height of the weir crest  $s = 0.33 \text{ m}$ .

For a discharge of  $0.9 \text{ m}^3/\text{s}$ :

$$\text{Critical depth } y_{c1} = \left( \left( \frac{0.9}{2.0} \right)^2 / 9.81 \right)^{1/3} = 0.274 \text{ m}$$

Since  $s > y_{c1}$ , and  $y_0 > y_{c1}$ , the flow is of Type 1.

In the use of the De Marchi equation  $y_1 = y_0 = 0.44 \text{ m}$ .

$$V_1 = \frac{0.9}{1 \times 0.44} = 1.023 \text{ m/s}, \quad F_1 = \frac{1.023}{\sqrt{9.81 \times 0.44}} = 0.4924$$

$$\text{Specific energy } E_1 = 0.44 + \frac{(1.023)^2}{2 \times 9.81} = 0.4933 \text{ m} = E_2$$

Discharge over the side weir  $Q_s = 0.15 \text{ m}^3/\text{s}$

Discharge at the end of the weir  $Q_2 = 0.90 - 0.15 = 0.75 \text{ m}^3/\text{s}$

At Section 2,  $E_2 = 0.4933 = E_1$

$$y_2 + \frac{Q_2^2}{(B_2 y_2)^2 2g} = y_2 + \frac{(0.75)^2}{y_2^2 \times 4 \times 2 \times 9.81} = 0.4933$$

By trial-and-error,  $y_2 = 0.46 \text{ m}$

$$F_2 = \sqrt{2 \left( \frac{E}{y_2} - 1 \right)} = 0.38$$

De Marchi varied flow function

$$\phi_M = \left( \frac{2E - 3s}{E - s} \right) \sqrt{\frac{E - y}{y - s}} - 3 \sin^{-1} \sqrt{\frac{E - y}{E - s}}$$

$$\left( \frac{2E - 3s}{E - s} \right) = \frac{(2 \times 0.4933) - (3 \times 0.33)}{0.4933 - 0.33} = -0.02082$$

$$\phi_{M1} = (-0.02082) \sqrt{\frac{0.4933 - 0.44}{0.44 - 0.33}} - 3 \sin^{-1} \sqrt{\frac{0.4933 - 0.44}{0.3493 - 0.33}} = -1.840$$

$$\phi_{M2} = (-0.02082) \sqrt{\frac{0.0333}{0.13}} - 3 \sin^{-1} \sqrt{\frac{0.0333}{0.1633}} = -1.416$$

From Eq. 8.25,

$$C_M = 0.611 \sqrt{1 - \frac{3 \times (0.4924)^2}{2 + (0.4924)^2}} = 0.502$$

From Eq. 8.23,

$$L = \frac{3}{2} \frac{B}{C_M} (\phi_{M2} - \phi_{M1})$$

$$= \frac{3}{2} \times \frac{2.0}{0.502} (-1.416 + 1.840)$$

$$= 2.534 \text{ m}$$

**Example 8.5** In Example 8.3, if the length of the side weir provided is 4.20 m with  $s = 0.33$  m, find the discharge over the side weir and the depth  $y_2$ .

*Solution*  $C_M = 0.502$ ,  $E_1 = E_2 = 0.4933$

$$y_1 = 0.44 \text{ m and } \phi_{M1} = -1.840$$

In Eq. 8.23

$$4.20 = \frac{3}{2} \times \frac{2}{0.502} (\phi_{M2} + 1.840)$$

$$\phi_{M2} = -1.1372.$$

The value of  $y_2$  to satisfy  $\phi_{M2} = -1.1372$  is found by trial-and-error as  $y_2 = 0.471$  m.

$$Q_2 = B y_2 \sqrt{2g(E_2 - y_2)}$$

$$= 2 \times 0.471 \sqrt{2 \times 9.81 \times (0.4933 - 0.471)}$$

$$= 0.623 \text{ m}^3/\text{s}$$

$$\begin{aligned}
 Q_s &= \text{discharge over the side weir} = Q_1 - Q_2 \\
 &= 0.900 - 0.623 = 0.277 \text{ m}^3/\text{s}.
 \end{aligned}$$

### 8.4.3 Uniformly Discharging Side Weirs

In many applications of side weirs, such as in irrigation systems and in the disposal of effluents, it is sometimes necessary to have side weirs in which the discharge rate  $\left(-\frac{dQ}{dx}\right)$  is constant along its length. From Eq. 8.19 it follows that if  $\frac{dQ}{dx} = q_* = \text{constant}$ ,  $(y - s)$  is constant along the weir. If  $s$  is kept constant, the water surface elevation will be constant for such weirs. Further, if specific energy is assumed to be constant, the water surface will be parallel to the energy line; i.e. the velocity of flow will be constant for a uniformly discharging weir. Hence,

$$V_1 = V = V_2$$

By continuity equation,  $Q_1 - q_* x = Q$

i.e.

$$A_1 - \frac{q_* x}{V_1} = A \text{ and } \frac{q_*}{V_1} = \left(\frac{A_1 - A_2}{L}\right)$$

$$A_1 - \left(\frac{A_1 - A_2}{L}\right)x = A \quad (8.30)$$

Thus, the uniformly discharging side weir can be achieved by linear reduction of area of flow. This can be achieved in two ways: (i) by contouring the channel side (Fig. 8.7(a)), and (ii) by contouring the channel bed (Fig. 8.7(b)). Further details on uniformly discharging side weirs are available in literature<sup>12</sup>.

For a uniformly discharging side weir, the lateral outflow  $Q_s$  is therefore,

$$Q_s = \frac{2}{3} C_M \sqrt{2gL} (y - s)^{3/2} \quad (8.31)$$

where  $C_M$  = De Marchi coefficient given by Eq. 8.25 or Eq. 8.27 depending on the nature of the approaching flow. Further, by continuity,

$$Q_1 - Q_2 = Q_s$$

The computations for Type 1, 2 and 3 flows follow the same assumptions as indicated in the previous section.

**Example 8.6** | A 1.5-m wide rectangular channel conveys a discharge of 1.7 m<sup>3</sup>/s at a depth of 0.6 m. A uniformly discharging side weir with crest at 0.42 m above the bed

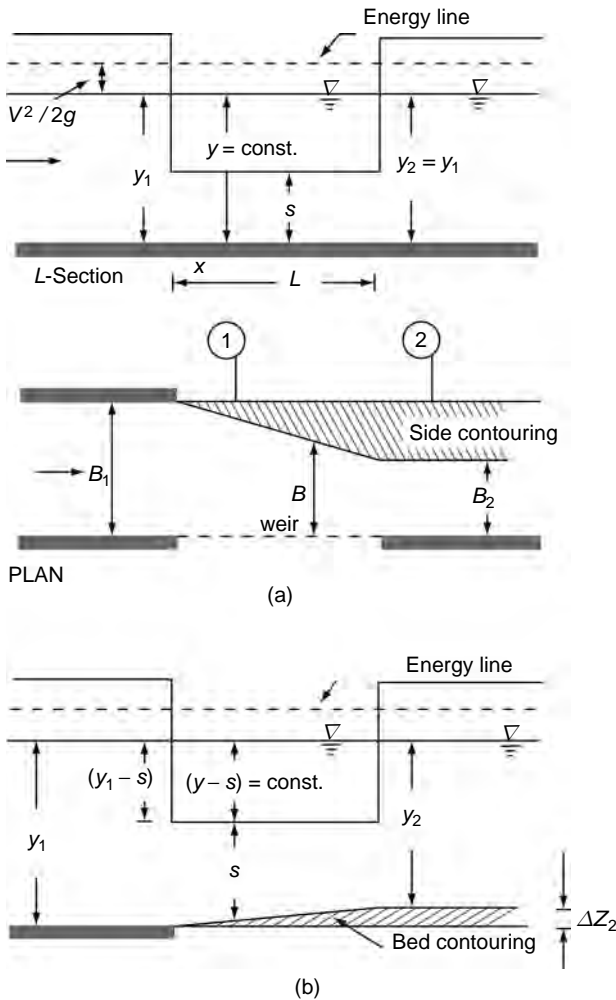


Fig. 8.7 Uniformly discharging side weirs

at the commencement of the side weir is proposed to divert a flow of  $0.30 \text{ m}^3/\text{s}$  laterally. Design the length of the side weir and other geometry of the channel at the weir.

*Solution*  $V_1 = Q_1 / A_1 = (1.17) / (1.5 \times 0.6) = 1.3 \text{ m/s}$

Froude number  $F_1 = V_1 / (gy_1)^{1/2} = 1.3 / (9.81 \times 0.6)^{1/2} = 0.536$

The approach flow is subcritical.

By Eq. 8.25 
$$C_M = 0.611 \sqrt{1 - \frac{3F_1^2}{(F_1^2 + 2)}}$$

$$= 0.611 \sqrt{1 - \frac{3 \times (0.536)^2}{\{(0.536)^2 + 2\}}}$$

$$= 0.482$$

Critical depth at Section 1  $= y_{c1} = (q^2/g)^{1/3} = \left[ \frac{(1.17/1.50)^2}{9.81} \right]^{1/3}$

$$= 0.396 \text{ m}$$

Height of the weir crest  $= s = 0.42 \text{ m}$

Since  $y_{c1} < s$ , Type 1 flow will prevail and  $y_1 = y_0 = 0.60 \text{ m}$ .

Depth of water over the weir  $= (y - s) = (0.60 - 0.42) = 0.18 \text{ m}$ .

Diverted discharge  $Q_s = \frac{2}{3} C_M \sqrt{2g} L(y - s)^{3/2}$

$$0.30 = \frac{2}{3} \times 0.482 \times \sqrt{19.62} \times L \times (0.18)^{3/2}$$

$$= 0.1087 L$$

Length of the side weir  $L = 0.30/0.1087 = 2.76 \text{ m}$

$Q_2 =$  downstream discharge  $= 1.17 - 0.30 = 0.87 \text{ m}^3/\text{s}$

For a uniformly discharging side weir,  $V_1 = V_2 = V$ .

Hence  $V_2 = 1.3 \text{ m/s}$  and  $A_2 = Q_2/V_2 = 0.87/1.3 = 0.6692 \text{ m}^2$ .

(i) *If side contouring is adopted,  $y_1 = y_2 = y$*

Bed width at Section 2  $= B_2 = A_2/y_2 = 0.6692/0.60 = 1.115 \text{ m}$

The bed width varies from 1.50 m at Section 1 to 1.115 m at Section 2, distance 2.76 m downstream of Section 1, linearly.

(ii) *If bed contouring is adopted,  $B_1 = B_2 = B$*

Depth of flow at Section 2  $= y_2 = A_2/B_2 = 0.6692/1.50$   
 $= 0.446 \text{ m}$

$\Delta z_2 =$  change in the elevation of bed at Section 2  
 $= 0.600 - 0.446 = 0.154 \text{ m}$ .

The variation of  $\Delta z$  is linear with a value of zero at Section 1 and 0.154 m at Section 2.

## 8.5 BOTTOM RACKS

A bottom rack is a device provided at the bottom of a channel for purposes of diverting a part of the flow. The device consists essentially of an opening in the channel bottom covered with a metal rack to prevent the transport of unwanted solid material

through the opening. Bottom racks find considerable application in hydraulic engineering as intake structure as for example in *Trench weir* and *kerb outlets*. Trench weirs are used as water intakes in mountain streams and bottom intakes are used in them to prevent gravel entry into the water intake.

Bottom racks can broadly be classified into four categories as:

1. Longitudinal bar bottom racks, in which the bars are laid parallel to the flow direction. This is the most widely used type of rack arrangement.
2. Transverse bar bottom racks, in which the bars are placed transverse to the direction of flow.
3. Perforated bottom plates, in which a plate with a uniformly spaced openings form the rack.
4. Bottom slots, the limiting case of transverse bar bottom rack without any rack.

Further, the above types can either be horizontal or inclined with reference to the approach bed of the canal. The trench weir, which find considerable use as intake structure in mountainous streams, especially for mini and micro hydel projects,

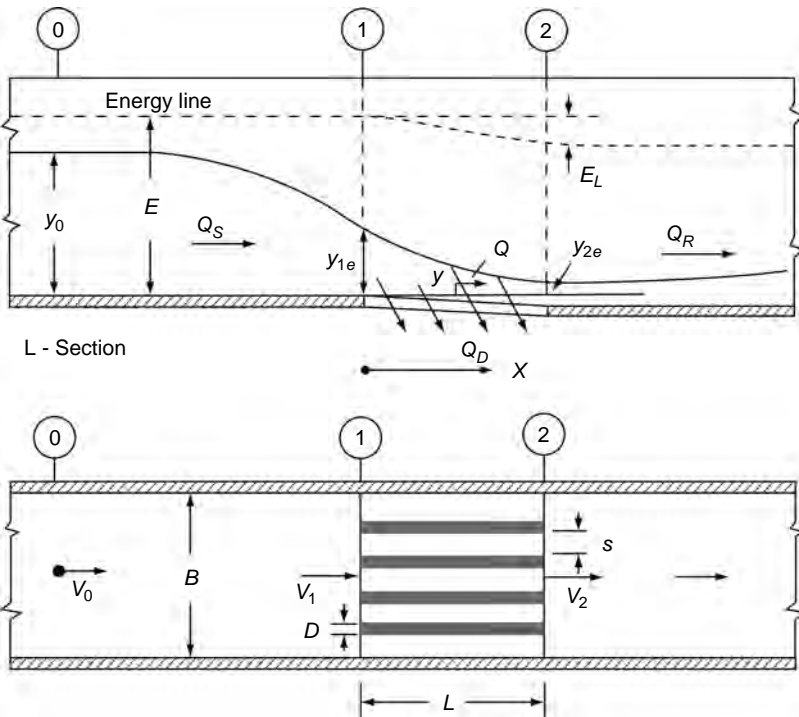


Fig. 8.8 Definition sketch of longitudinal bar bottom rack



contains a sloping longitudinal bar bottom rack made up of round steel bars as its chief component. The inclination of the rack, which is of the order of 1 in 10, is provided to facilitate easy movement of the bed sediment load of the stream over the rack.

Figure 8.8 shows the definition sketch of a longitudinal bar bottom rack. The bars are usually of circular cross-section and are laid along the direction of flow. The flow over the bottom rack can attain a variety of water surface profiles depending upon the nature of the approach flow, state of flow over the rack and tailwater conditions. Subramanya and Shukla<sup>13</sup> have proposed a classification of the flow over bottom racks into five types as below:

**Table 8.2** Types of Flow Over Bottom Racks

Type	Approach	Flow Over the rack	Downstream state
A1	Subcritical	Supercritical	May be a jump
A2	Subcritical	Partially supercritical	Subcritical
A3	Subcritical	Subcritical	Subcritical
B1	Supercritical	Supercritical	May be a jump
B2	Supercritical	Partially supercritical	Subcritical

Figure 8.9 shows the characteristic feature of these five types of flow. Out of the above, Types A1, A3 and B1 are of common occurrence and also are of significance from design considerations.

### 8.5.1 Mostkow Equations for Bottom Racks

Mostkow<sup>12</sup> derived expressions for the water-surface profile for spatially varied flow over bottom racks by making the following assumptions:

1. The channel is rectangular and prismatic.
2. Kinetic energy correction factor  $\alpha = 1.0$ .
3. The specific energy  $E$  is considered constant along the length of the bottom rack.
4. The effective head over the racks causing flow depends upon the type of rack, such as (i) for racks made of parallel bars, the effective head is equal to the specific energy, and (ii) for racks made of circular perforations, the effective head is equal to the depth of flow.

The differential equation of SVF with lateral outflow Eq. 8.17 under the assumptions (1), (2), and (3) would become

$$\frac{dy}{dx} = \frac{Qy \left( -\frac{dQ}{dx} \right)}{gB^2 y^3 - Q^2} \tag{8.32}$$

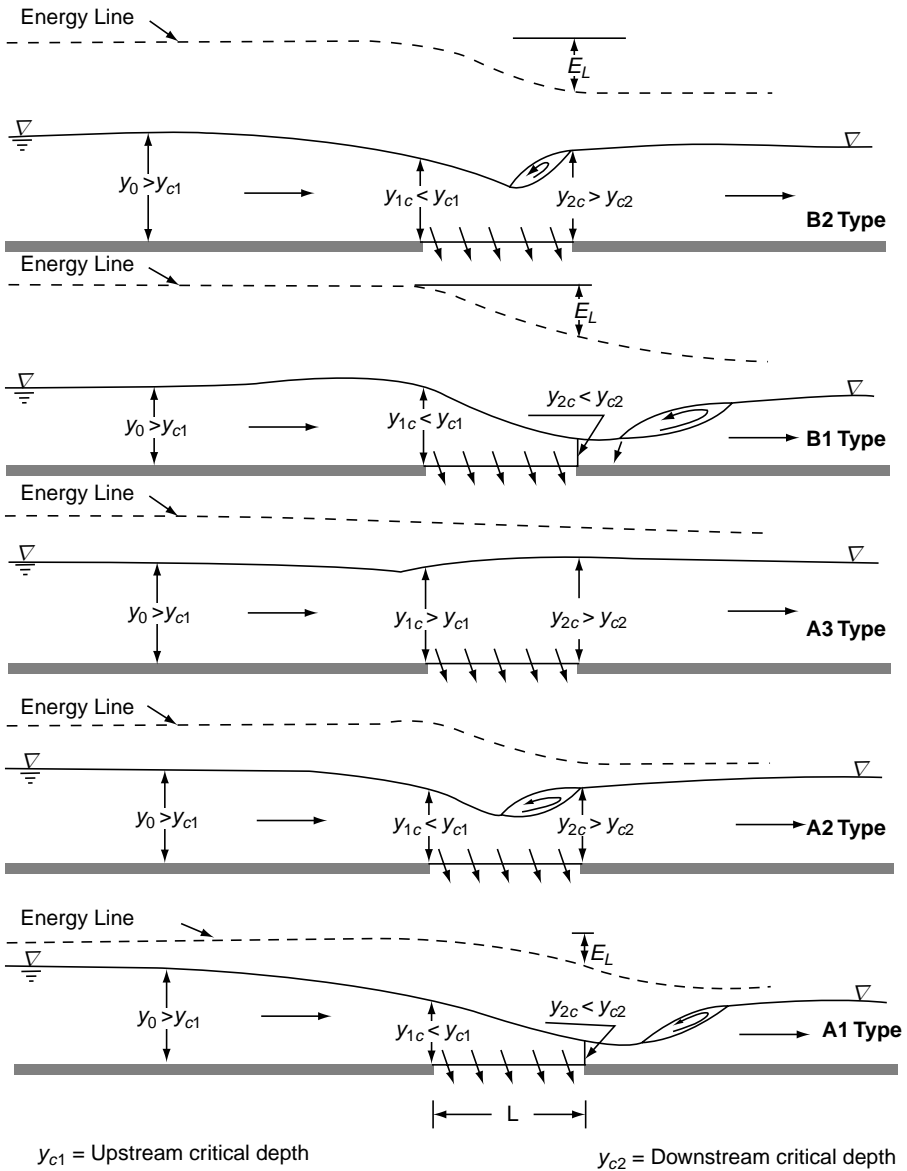


Fig. 8.9 Classification of different types of flows over bottom racks

(a) SVF with Bottom Racks Made of Parallel Bars

Under assumption (4) the outflow per unit length of rack, by considering it as an orifice, is

$$\left(-\frac{dQ}{dx}\right) = C_1 \varepsilon B \sqrt{2gE} \quad (8.33)$$

in which  $C_1$ , = a defined coefficient of discharge and  $\varepsilon$  = void ratio = ratio of the opening area to the total rack area. Since the specific energy  $E$  = constant, the discharge  $Q$  at any section is given by:

$$Q = By\sqrt{2g(E - y)} \quad (8.34)$$

Substituting Eqs 8.33 and 8.34 in Eq. 8.32

$$\frac{dy}{dx} = \frac{2\varepsilon C_1 \sqrt{E(E - y)}}{3y - 2E} \quad (8.35)$$

On integration,

$$x = -\frac{E}{\varepsilon C_1} \frac{y}{E} \sqrt{1 - \frac{y}{E}} + \text{Const.} \quad (8.36)$$

Putting  $y/E = \eta$  and using the boundary condition  $y = y_1$  and  $x = 0$ , gives

$$x = \frac{E}{\varepsilon C_1} (\eta_1 \sqrt{1 - \eta_1} - \eta \sqrt{1 - \eta}) \quad (8.37)$$

which is the equation of the SVF profile. As in the case of the De Marchi equation (Section 8.3.3), the control depths for use in Eq. 8.37 which are compatible with the assumptions are:

- (i)  $y_1 = y_0$  for A3 and B1 type flows and
- (ii)  $y_1 = y_{c1}$  for A1 type flows.

Note that from Eq. 8.37,  $\left(\frac{dQ}{dx}\right)$  is constant along the rack. Hence the total discharge  $Q_s$  diverted out is,

$$Q_s = C_1 \varepsilon BL \sqrt{2gE} \quad (8.38)$$

**(b) SVF Equation for Bottom Racks Made of Perforated Plates**

For perforated plate bottom racks the outflow discharge per unit length, under assumption (4), is

$$\left(-\frac{dQ}{dx}\right) = C_2 \varepsilon B \sqrt{2gy} \quad (8.39)$$

where  $C_2$  = discharge coefficient for perforated plate flow. Substituting Eqs 8.39 and 8.34 in Eq. 8.32, and simplifying

$$\frac{dy}{dx} = \frac{2\varepsilon C_2 \sqrt{y(E - y)}}{3y - 2E} \quad (8.40)$$

Integrating and using the boundary condition  $y = y_i$  at  $x = 0$ , yields the SVF profile for perforated bottom plates as

$$x = \frac{E}{\varepsilon C_2} \left[ \frac{1}{2} \left( \cos^{-1} \sqrt{\eta} - \cos^{-1} \sqrt{\eta_1} \right) + \frac{3}{2} \sqrt{\eta_1(1-\eta_1)} - \sqrt{\eta(1-\eta)} \right] \quad (8.41)$$

in which  $\eta = y/E$  and suffix 1 refers to Section 1.

### 8.5.2 Estimation of Discharge Through a Bottom Rack

**Longitudinal Bar Bottom Rack** For purposes of estimation; the diverted discharge  $Q_d$  is expressed in terms of the specific energy  $E_0$  at the reference approach section, in a manner similar to Eq. 8.38 as

$$Q_d = C_d B L \varepsilon \sqrt{2gE_0} \quad (8.42)$$

where  $C_d$  = coefficient of discharge of the longitudinal bar bottom rack. As a result of experimental studies, Subramanya<sup>15,16</sup> has shown that,

$$C_d = fn [D/s, S_L, \eta_E \text{ and (type of flow)}] \quad (8.43)$$

where  $D$  = diameter of the rack bar;  $s$  = clear spacing of the bars in the rack,

$$S_L = \text{longitudinal slope of the rack and } \eta_E = \text{a flow parameter} = \frac{V_0^2}{2gE_0} = \left( \frac{F_0^2}{2 + F_0^2} \right).$$

The functional relationship for the variation of  $C_d$  in various types of flows are as below:

#### (a) Inclined Racks

$$\text{A1 Type flow : } C_d = 0.53 + 0.4 \log (D/s) - 0.61 S_L \quad (8.44)$$

$$\text{B1 Type flow : } C_d = 0.39 + 0.27 \log (D/s) - 0.8 \eta_E - 0.5 \log S_L \quad (8.45)$$

#### (b) Horizontal Racks

$$\text{A1 Type flow : } C_d = 0.601 + 0.2 \log (D/s) - 0.247 \eta_E \quad (8.46)$$

$$\text{A3 Type flow : } C_d = 0.752 + 0.28 \log (D/s) - 0.565 \eta_E \quad (8.47)$$

$$\text{B1 Type flow : } C_d = 1.115 + 0.36 \log (D/s) - 1.084 \eta_E \quad (8.48)$$

It has been found<sup>15,16</sup> that the energy loss over the rack is significant in Type A1 and Type B1 flows. However, the energy loss over the rack is not significant in Type A3 flows. This implies that Mustkow's water surface profile equation (Eq. 8.41)

could be used only in A3 type flows. In all other cases, the water surface profile is to be computed by using the basic differential equation of SVF (Eq. 8.22) with an estimated value of the energy slope  $S_e$ . Approximate expressions for  $S_e$  in Type A1 and Type B1 flows over longitudinal bottom racks are available in Ref. (15) and (16).

Brunella et al<sup>17</sup> have studied the performance of inclined bottom racks made of circular longitudinal bars. Flow features of the channel below the rack is also studied in detail. Further, this study contains a good review of past studies on bottom racks.

**Transverse Bar Bottom Racks** In these, the rack bars are made of circular bars or rectangular shaped flats and are kept transverse to the direction of flow. Field applications of such racks are rather limited. Detailed information on the variation of a defined coefficient of discharge in flows through and over a bottom rack made of flats of rectangular section are presented by Subramanya and Sengupta<sup>18</sup>.

**Perforated Bottom Plates** Perforated bottom plates find use for diverting bottom layer of a flow in some industrial applications. Hydraulic characteristics of horizontal bottom plates have been studied by Subramanya and Zagade<sup>19</sup>. Figure 8.10 shows the geometry of perforations used in the study. The diverted flow discharge is defined in a manner similar to Mustkow's Eq. 8.39 as

$$Q_d = C_{dp} B L \varepsilon \sqrt{2g y_0} \tag{8.49}$$

where  $C_{dp}$  = defined coefficient of discharge of perforated bottom

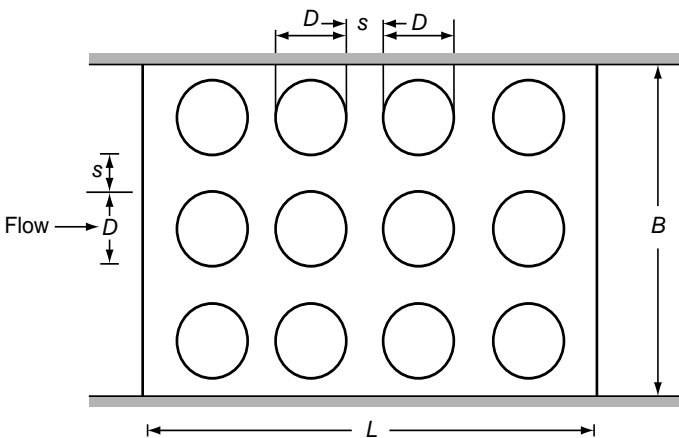


Fig. 8.10 Perforated bottom plate—definition sketch

plate,  $y_0$  = depth of flow at reference approach section. The variation of  $C_{dp}$  for various types of flows are <sup>19</sup>

(a) A1 Type flow:

For  $B/L \geq 2.0$ ,

$$C_{dp} = 0.292 - 0.03 \frac{D}{s} + 0.0083 \frac{D}{t} + 0.058 \frac{B}{L} \quad (8.50)$$

For  $B/L < 1.78$ ,  $C_{dp}$  is essentially independent of  $B/L$  and

$$C_{dp} = 0.41 - 0.03(D/s) + 0.0083(D/t) \quad (8.51)$$

where  $t$  = thickness of the plate, and  $D$  = diameter of the perforation.

(b) B1 Type flows:

$$\frac{C_{dp}}{F_0} = 0.26 - 0.28 \eta_E \quad (8.52)$$

where  $\eta_E$  = a flow parameter =  $\frac{V_0^2}{2gE_0} = \frac{F_0^2}{(2 + F_0^2)}$

As in longitudinal bar bottom racks, here also the energy loss has been found to be significant in A1 and B1 Type flows and as such Mustkow's water surface profile equation (Eq. 8.41) is not valid for these types of flows. Approximate expressions for the estimation of the energy slope  $S_e$  in flows over perforated bottom plates, for use in the basic differential equation of SVF, are available in Ref. (19).

**Bottom Slots** Bottom slots are the limiting cases of transverse bar bottom racks and their practical applications are rather limited. The diverted discharge  $Q_d$  through a slot of length  $L$  and spanning the full width of the channel can be expressed as

$$Q_d = C_{ds} BL \varepsilon \sqrt{2gE_0} \quad (8.53)$$

where  $E_0$  = specific energy of the approach flow, and  $C_{ds}$  = coefficient of discharge of the slot.

The variation of  $C_{ds}$  has been studied by Nasser et al<sup>20</sup> and Ramamurthy et al<sup>21</sup>.



## REFERENCES

1. Hinds, J, 'Side Channel Spillways', *Trans. ASCE*, Vol. 89, 1926, pp 881–927.
2. Smith, K V H, 'Control Point in a Lateral Spillway Channel', *J. of Hyd. Div., Proc. ASCE*, May 1967, pp 27–34.
3. Li, W H, 'Open Channels with Non-uniform Discharge', *Trans. ASCE*, Vol. 120, 1955, pp 255–274.
4. Gill, M A, 'Perturbation Solution of Spatially Varied Flow in Open Channels', *J. of Hyd. Res., IAHR*, Vol.15, No. 4, 1977, pp 337–350.

5. McCool, D K, Gwinn, W R, Ree, W O, and Garton, J E, 'Spatially Varied Flow in Vegetated Channel', *Trans. ASCE*, Vol. 9, No. 3, 1966, pp 440–444.
6. Farney, H S, and Markus, A 'Side-channel Spillway Design', *J. of Hyd. Div., Proc. ASCE*, May 1962, pp 131–154.
7. Subramanya, K, and Awasthy, S C, 'Spatially Varied Flow Over Side-Weirs', *J. of Hyd. Div., Proc. ASCE*, Jan. 1972, pp 1–10.
8. Borghi, S M, et al, 'Discharge Coefficient for Sharp-crested Side Weirs in Sub-critical Flow', *Journal of Hyd. Engg.*, ASCE, Vol. 125, No. 10, 1999, pp. 1051–1056.
9. Olivetto, G, et al, 'Hydraulic Features of Supercritical Flow Along Prismatic Side Weirs', *Journal of Hyd. Research*, IAHR, Vol. 39, No. 1, 2001, pp. 73–82.
10. Ghodsian, M, 'Flow Over Triangular Side Weirs', *Scientia Iranica*, Vol. 11, No. 1 & 2, April 2004, pp. 114–120.
11. Uyumaz, A, 'Side Weir in Triangular Channel', *Journal of Irr. and Drainage Engg.*, ASCE, Vol. 118, No. 6, 1992, pp. 965–970.
12. Ramamurthy, A, S, Subramanya, K, and Caraballada, L, 'Uniformly Discharging Lateral Weirs', *Journal of Irr. and Drainage Div.*, ASCE, Dec. 1978, pp. 399–411.
13. Subramanya, K, and Shukla, S K, 'Discharge Diversion Characteristics of Trench Weirs', *Journal of Civil Engg. Div.*, Inst. Of Engrs. (India), Vol. 69, CI 3, Nov. 1988. pp. 163–168.
14. Mustkow, M A, 'A Theoretical Study of Bottom Type Intakes', *La Houille Blanche*, No. 4, Sept. 1957, pp. 570–580.
15. Subramanya, K, 'Trench Weir Intake for Mini Hydro Projects', *Proc. Hydromech and Water Resources Conf. I.I.Sc.*, Bangaloe, India, 1990, pp. 33–41.
16. Subramanya, K, 'Hydraulic Characteristics of Inclined Bottom Intakes', *Proc. National Symp. On Recent Trends in Design of Hydraulic Structures*, UOR, Roorkee, India, March 1994, pp. 1–9.
17. Brunella, S, et al, 'Hydraulics of Bottom Racks', *Journal of Hyd. Engg.*, Vol. 29, No. 1, Jan. 2003, pp. 2–9.
18. Subramanya, K and Sengupta, D, 'Flow Through Bottom Racks', *Indian Jour. Tech.*, CSIR, Vol. 19, No. 2, Feb. 1981, pp. 64–67.
19. Subramanya, K, and Zagade, S B, 'Flow Over Perforated Bottom Plates', Proc 17<sup>th</sup> Nat. Conf. of FM and FP, REC, Warangal, India, 1990, pp. C-51–C-57.
20. Nasser, M S, et al, 'Flow in Channel with a Slot in a Bed', *Journal of Hyd. Res.*, IAHR, No. 4, 1980, pp. 359–367.
21. Ramamurthy, A S, and Satish, M S, 'Discharge Characteristics of Flow Past a Floor Slot', *Journal if Irr. and Drainage Engg.*, ASCE, Vol. 112, No. 1, 1986, pp. 20–27.

## PROBLEMS

### Problem Distribution

SI. No.	Topic	Problems
1	Lateral spillway channel	8.1 to 8.6
2	Side weir	8.7, 8.8
3	Uniformly discharging side weir	8.9, 8.10
4	Bottom racks	8.11 to 8.13
5	Radial flow	8.34

- 8.1 Show that the following equation is applicable to a control section where critical depth occurs in a frictionless lateral spillway channel:

$$\frac{S_0^2 g A_c T_c}{4 \beta q_*^2} = 1$$

- 8.2 A side channel spillway channel is 100 m long and is rectangular in cross-section with  $B = 5.0$  m,  $n = 0.020$ ,  $\beta = 1.30$  and  $S_0 = 0.15$ . If the lateral inflow rate is  $1.75$  m<sup>3</sup>/s/m, find the critical depth and its location.
- 8.3 A lateral spillway channel is trapezoidal in cross-section with  $B = 10.0$  m, side slope  $m = 0.5$  and Manning's roughness  $n = 0.018$ . The bed slope is  $0.08$ . If the lateral inflow rate is  $2.5$  m<sup>3</sup>/s/m length, find the critical depth and its location. Assume  $\beta = 1.20$ .
- 8.4 Show that for a wide rectangular channel having SVF with a constant in flow rate of  $q_*$ , the critical flow section is given by

$$x_c = \frac{8q_*^2}{g(S_0 - g/C^2)^3}$$

when  $\beta = 1.0$  is assumed and Chezy formula with  $C = \text{constant}$  is used. What would be the corresponding value of  $y_c$ ?

- 8.5 A lateral spillway channel of length  $L$  is rectangular in cross-section. If at the channel exit,  $y_e = \text{depth of flow}$  and  $F_e = \text{Froude number}$ , show by neglecting friction and assuming  $\beta = 1.0$ , that the critical depth  $y_c$  is given by

$$\frac{y_c}{y_e} = 4F_e^2 / G^2 \quad \text{and is located at } x_c, \text{ given by}$$

$$\frac{x_c}{y_e} = \frac{8F_e^2}{G^2 S_0} \quad \text{where } G = \frac{S_0 L}{y_e}$$

- 8.6 A wide rectangular channel of length  $L$  having a uniform lateral inflow rate has a discharge of  $q_e$  per unit width at the channel exit. If the Darcy–Weisbach friction factor  $f$  is used for representing friction effects, show that

$$y_c = \frac{256q_e^2}{gL^2(8S_0 - f)^2}$$

and

$$x_c = \frac{4096q_e^2}{gL^2(8S_0 - f)^3}$$

- 8.7 A 3.0-m wide rectangular channel can carry a discharge of  $3.60$  m<sup>3</sup>/s at a normal depth of  $1.2$  m. Design a side weir so that it will pass all the flow in the canal when the discharge is  $2.00$  m<sup>3</sup>/s and will divert  $0.6$  m<sup>3</sup>/s when the canal discharge is  $3.60$  m<sup>3</sup>/s.



- 8.8 A rectangular canal of 2.0 m width carries a flow with a velocity of 8.75 m/s and depth of 1.25 m. A side weir of height 0.75 m and length 1.20 m is provided in one of its walls. Find the quantity of flow diverted by the side weir.
- 8.9 A rectangular channel is 1.5 m wide and conveys a discharge of 2.0 m<sup>3</sup>/s at a Froude number of 0.3. A uniformly discharging side weir having contouring on the sides only is set at a height of 0.4 m above the bed with its crest horizontal. If the length of the side weir is 1.8 m, estimate the total flow diverted by the side weir.
- 8.10 A rectangular channel is 2.0 m wide and carries a flow of 3.00 m<sup>3</sup>/s at a depth of 0.9 m. At a certain location in this channel a uniformly discharging side weir is proposed to divert 0.30 m<sup>3</sup>/s of flow laterally. The weir crest is horizontal and is placed at a height of 0.65 m above the bed at the commencement of the side weir. Calculate the length of the side weir and other dimensions of the channel geometry to achieve the objective.
- 8.11 Show that, by Mustkow's method of analysis, the minimum length  $L_m$  of a parallel bar bottom rack required to completely divert the initial discharge  $Q_1$  in a channel is given by

$$L_m = \frac{Q_1}{\varepsilon C_1 B \sqrt{2gE}} = \frac{E}{\varepsilon C_1} \left[ \frac{y_1}{E} \sqrt{1 - \frac{y_1}{E}} \right]$$

- 8.12 A mountainous stream is of rectangular cross section and has a width of 10.0 m, depth of flow of 0.25 m and carries a discharge of 6.0 m<sup>3</sup>/s. A trench weir type intake made up of longitudinal parallel bar rack is proposed at a section to divert the flow. The proposed rack has a longitudinal slope of 0.01 and is made of circular bars with diameter to spacing ratio of 1.0. Estimate the minimum length of the rack required to completely divert the flow. The blockage due to debris can be assumed as 50% of rack opening.
- 8.13 A 2.0-m wide rectangular channel carries a discharge of 3.5 m<sup>3</sup>/s at a Froude number of 0.30. A 2.0-m long parallel longitudinal bar bottom rack having a void ratio (ratio of opening to total rack area) of 0.2 is provided at a section. Supercritical flow is known to occur over the rack. Estimate the discharge diverted out.
- 8.14 An axisymmetric radial flow emanates from a source on to a horizontal plane. Show that the basic differential equation of SVF with decreasing discharges can be expressed in this case as

$$\frac{dy}{dx} = \frac{\left( \frac{V^2}{gr} \right) - S_f}{1 - \left( \frac{V^2}{gy} \right)}$$

## OBJECTIVE QUESTIONS

- 8.1 The basic differential equation of SVF with increasing discharge is based on the
- |                         |                        |
|-------------------------|------------------------|
| (a) continuity equation | (c) energy equation    |
| (b) momentum equation   | (d) Manning's equation |
- 8.2 The basic differential equation of SVF with decreasing discharge is based on the
- |                         |                        |
|-------------------------|------------------------|
| (a) continuity equation | (c) energy equation    |
| (b) momentum equation   | (d) Manning's equation |

- 8.3 The differential equation of SVF with decreasing discharge has one extra term in the numerator on the right-hand side when compared to the corresponding GVF equation. This term is
- (a)  $-\frac{2\alpha Qq_*}{gA^2}$                       (b)  $+\frac{2\alpha Qq_*}{gA^2}$   
 (c)  $-\frac{2\beta Qq_*}{gA^2}$                       (d)  $-\frac{\alpha Qq_*}{gA^2}$
- 8.4 The transitional profile in a lateral spillway channel is
- (a) independent of the roughness of the channel  
 (b) independent of rate of lateral flow  
 (c) independent of channel geometry  
 (d) independent of the bottom slope of the channel
- 8.5 The flow profile in a side spillway channel can be determined by using
- (a) Standard step method  
 (b) Standard Runge-Kutta method  
 (c) De Marchi equation  
 (d) Mustokow equation
- 8.6 A lateral spillway channel is rectangular in cross-section with a bottom width of 4.0 m. At a certain flow the critical depth was found to be 0.5 m and occurred at a distance of 5.53 m from the upstream end. The lateral inflow rate in  $\text{m}^3/\text{s}/\text{m}$  is
- (a) 0.20                      (b) 0.40  
 (c) 0.80                      (d) 1.10
- 8.7 The De Marchi varied-flow function is
- (a) used in SVF over bottom racks  
 (b) used in SVF in lateral spillway channels  
 (c) meant for side weirs in frictionless rectangular channels  
 (d) meant for subcritical flows only
- 8.8 The De Marchi coefficient of discharge  $C_M$  for a side weir is
- (a) independent of the Froude number  
 (b) same as that of a normal weir  
 (c) essentially a function of inlet Froude number,  $F_1$   
 (d) approaches unity as  $F_1 \rightarrow 0$
- 8.9 A rectangular channel 2.5 m wide has a discharge of  $2.0 \text{ m}^3/\text{s}$  at a depth of 0.8 m. The coefficient of discharge  $C_M$  of a side weir introduced in a side of this channel with a crest height of 0.2 m above the bed is
- (a) 0.574                      (b) 0.611  
 (c) 0.286                      (d) 0.851
- 8.10 To achieve uniformly discharging side weirs the area of flow  $A$  at any section distance  $x$  from the upstream end of the weir is related as:
- (a)  $A = A_1 - Mx$                       (b)  $A = A_2 - Mx$   
 (c)  $A = Mx$                       (d)  $A = x^{3/2}$
- 8.11 A side weir is provided in the side of channel. If  $E$  = specific energy is assumed constant, at any section within the length of the side weir, the discharge  $Q$  in the channel is given by
- (a)  $Q = \text{constant}$                       (b)  $Q = B\sqrt{(E - y)2g}$   
 (c)  $Q = \frac{By}{\sqrt{2E - y}}$                       (d)  $Q = By\sqrt{2g(E - y)}$

- 8.12 In a uniformly discharging side weir provided in the side of a rectangular channel having subcritical flow, the longitudinal water surface along the weir
- (a) increases in the downstream direction
  - (b) remains parallel to the crest
  - (c) decreases in the downstream direction
  - (d) increases linearly in the downstream direction
- 8.13 In a uniformly discharging side weir in a rectangular channel, if  $x$  is the longitudinal distance from the start of the weir
- (a) the area of the flow cross-section in the canal decreases linearly with  $x$
  - (b) the mean velocity of the flow varies linearly with  $x$
  - (c) the depth of flow above the weir crest varies linearly with  $x$
  - (d) the area of flow cross-section in the canal remains constant
- 8.14 A trench weir type intake has as its main component a
- (a) side weir
  - (b) longitudinal, parallel bar bottom rack
  - (c) transverse, parallel bar bottom rack
  - (d) perforated bottom plate

# Supercritical-Flow Transitions

# 9

## 9.1 INTRODUCTION

The response of a free surface to a small disturbance is markedly different in subcritical and supercritical streams. In supercritical streams, even small boundary changes can cause disturbances which can be felt at considerable distances downstream. The changes in the boundaries required at a supercritical transition are not governed merely by simple energy considerations as in the case of subcritical flows, but the possibilities of surface disturbances make them highly sensitive flow situations requiring very careful attention to the design. This chapter deals with some important aspects of supercritical transitions related to surface disturbances. Much of the basic information relating to supercritical flows was presented at an ASCE symposium by Ippen<sup>1</sup>, Ippen and Dawson<sup>2</sup>, Rouse *et. al.*<sup>3</sup> and Knapp<sup>4</sup>.

## 9.2 RESPONSE TO A DISTURBANCE

Consider a stationary pool of water in which a disturbance, say a solid object, is moving with a velocity  $V$ . Let us assume that the motion of the solid body is transmitted to the water in the form of finite impulses at regular intervals. Each impulse will cause a small wave on the water surface which will travel in all directions at the same relative velocity to the fluid  $C$  from the instantaneous position of the body. It is known that for shallow waves (i.e., waves with large wave lengths compared with the depth) of very small amplitude,  $C = \sqrt{gy}$  and thus the ratio of velocity of movement to  $C$  represents the Froude number of the flow,  $F = V/\sqrt{gy}$ .

The pattern of disturbance when  $V \rightarrow 0$  for a practically stationary disturbance-causing body is a set of concentric circles each moving with a velocity  $C$  [Fig. 9.1(a)]. The radii of the two successive circles differ by  $C\Delta t$ , where  $\Delta t$  is the interval between impulses. The disturbance pattern when  $0 < V/C < 1.0$  is indicated in Fig. 9.1(b). This represents a simple disturbance in a subcritical flow.  $A_1, A_2, A_3$  and  $A_4$  represent the various locations of the body with the circles 1, 2, 3 and 4 denoting various wave fronts, with reference to the present position of the body. Thus, if  $A_0$  is the present position and  $A_1$  the position of the body at time  $(1 \cdot \Delta t)$  prior to the present position, then  $A_0A_1 = V\Delta t$  and radius of circle 1 =  $C\Delta t$ . Similarly,  $A_0A_2 = 2V\Delta t$ ,  $A_0A_3 = 3V\Delta t$  and  $A_0A_4 = 4V\Delta t$ . Also, the radii of circles 2, 3 and 4 are  $2C\Delta t$ ,  $3C\Delta t$  and  $4C\Delta t$  respectively. It is easy to see that the wave fronts are always in front of the

body. The distribution of wave fronts is however not uniform, the waves being crowded in front of the body and sparsely distributed behind it. The crowding of the wave fronts in front of the body will depend on the magnitude of  $V/C$ . When  $V/C = 1.0$ , the waves will all have a common tangent at the nose of the body.

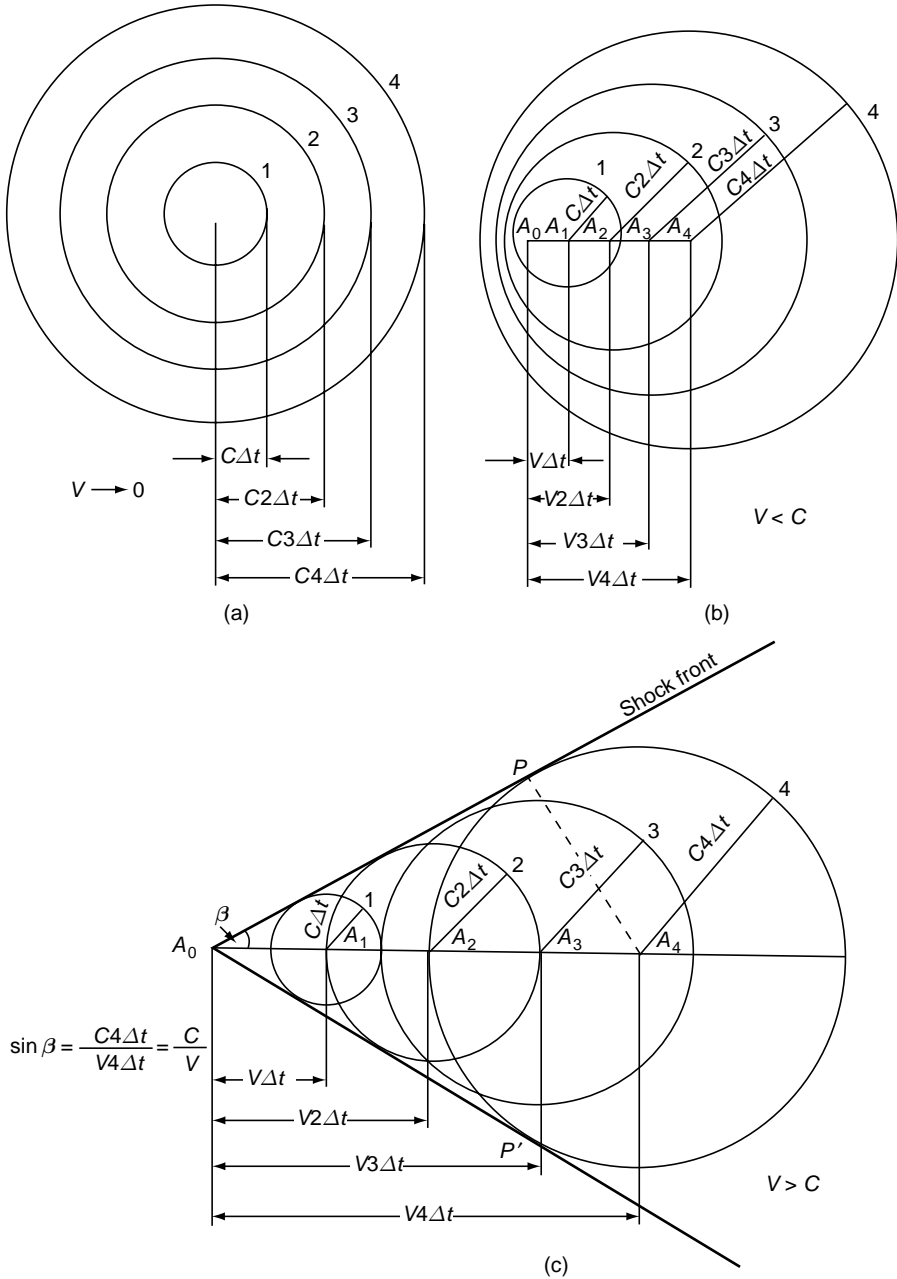


Fig. 9.1 Patterns of disturbance spread: (a) Still water (b) Subcritical flow (c) Supercritical flow

In supercritical flow, i.e., when  $V > C$ , the wave fronts lag behind the body [Fig. 9.1 (c)]. However, a pair of common tangents envelops the various waves and the half angle between these two common tangents is given by

$$\begin{aligned} \sin \beta &= \frac{A_4 P}{A_0 A_4} = \frac{C \Delta t}{V \Delta t} = \frac{C}{V} \\ &= \sqrt{g y} / V = \frac{1}{F} \end{aligned} \tag{9.1}$$

So far, we have considered discrete impulses as the interaction between the solid body and the fluid. On the other hand, if continuous interaction is considered, there will be an infinite number of disturbance circles with the angle  $PA_0P'$ . The lines  $A_0P$  and  $A_0P'$  represent a boundary between two regions, viz. the area within the angle  $PA_0P'$  represent a boundary between two regions, viz. the area within the angle  $PA_0P'$  which is affected by the motion of the solid body and the rest of the area outside the angle  $\beta$  in which the effect of body motion is not felt. The disturbances thus, propagate along the lines  $A_0P$  and  $A_0P'$  which are called *shock fronts* or *shock waves*.

The above situation finds an analogy in the compressible fluid flow in gas dynamics in which case  $C =$  velocity of propagation of sound and  $\sin \beta = \frac{C}{V} = \frac{1}{M}$  where  $M =$  Mach number. The shock waves are also called *Mach lines* or *Mach waves* in compressible fluid flow.

Summing up, it can be concluded that in subcritical velocities of the body ( $0 < V < \sqrt{g y}$ ) the disturbances of any magnitude would be transmitted upstream and downstream. In supercritical velocities ( $V > \sqrt{g y}$ ) the disturbances are confined to an area in the downstream direction bounded by two shock fronts, each aligned at an angle  $\beta$  to the direction of motion.

Now let us consider a situation in which the boundary is stationary and the fluid is moving past it. For a small change in the alignment of the vertical wall of a channel (Fig. 9.2), the disturbance is the change in the momentum

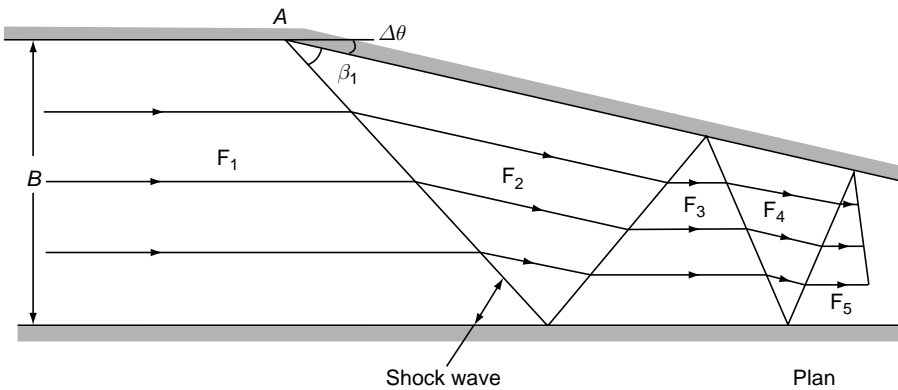


Fig. 9.2 Wave pattern at a change in alignment

caused by the deflection on the boundary by  $\Delta\theta$  at A. In subcritical flow past the boundary, the change in momentum will be reflected by a permanent deformation of the stream surface, upstream and downstream of the point A. In supercritical flow, however, the boundary change at A cannot affect the flow upstream and hence the effect of the disturbance will be confined to a region, downstream of A, bounded by the shock wave emanating from A and the boundary. The effect of the disturbance will be felt as a change of depth in this area. Since the flow is confined between two side boundaries, the shock wave undergoes multiple reflections at the boundaries resulting in a highly disturbed water surface in the downstream.

### 9.3 GRADUAL CHANGE IN THE BOUNDARY

Consider a supercritical flow in a horizontal frictionless rectangular channel (Fig. 9.3) with one of the walls deflected through a small angle  $\Delta\theta$ . The change in the boundary

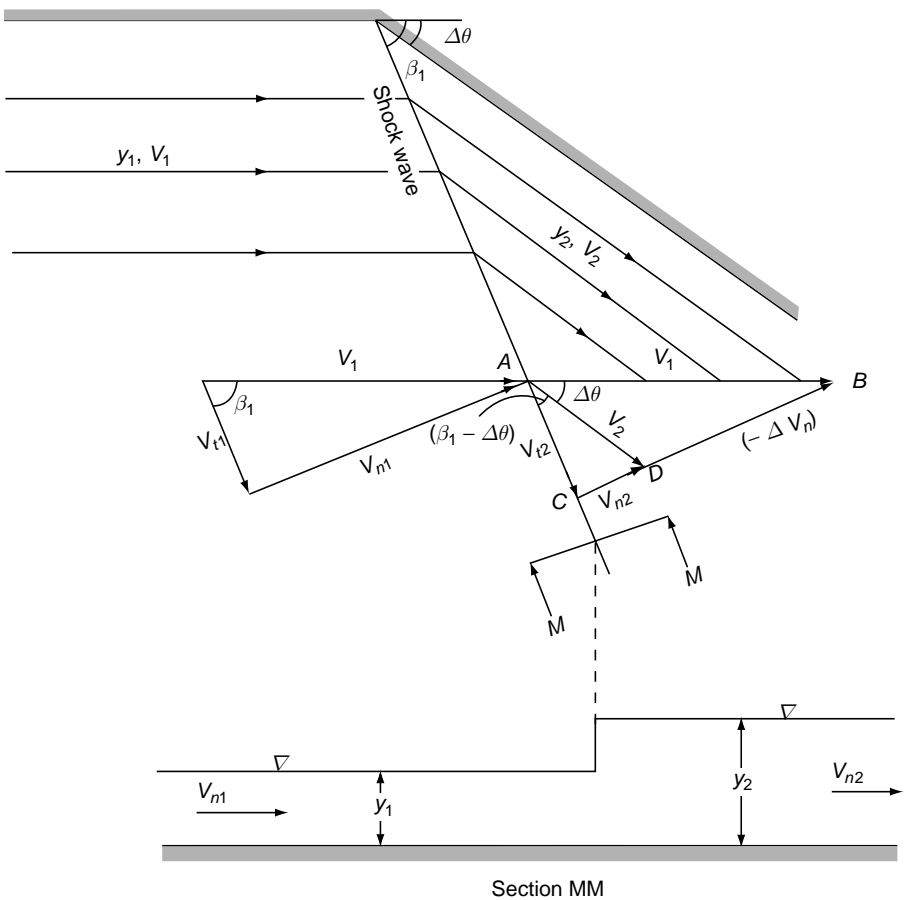


Fig. 9.3 Supercritical flow past a small change in boundary alignment

causes a shock wave at an angle  $\beta_1$ , to the approaching flow. The flow upstream of the shock has a velocity of  $V_1$  and depth  $y_1$  and the flow after the shock has a velocity of  $V_2$  and depth  $y_2$ . From the vector diagram of the velocities,

$$\begin{aligned} V_{n1} &= V_1 \sin \beta_1 \\ V_{t1} &= V_1 \cos \beta_1 \\ V_{n2} &= V_2 \sin (\beta_1 - \Delta \theta) \\ V_{t2} &= V_2 \cos (\beta_1 - \Delta \theta) \end{aligned}$$

where the suffixes  $n$  and  $t$  refer to the normal and tangential directions with respect to the shock front. Considering the unit width of the shock-wave front, the continuity equation can be written as

$$y_1 V_{n1} = y_2 V_{n2} \tag{9.2}$$

In a direction normal to the shock wave, the momentum equation is written as

$$\frac{1}{2} \gamma y_1^2 - \frac{1}{2} \gamma y_2^2 = \rho y_2 V_{n2}^2 - \rho y_1 V_{n1}^2 \tag{9.3}$$

From Eqs 9.2 and 9.3

$$V_{n1} = \sqrt{g y_1} \sqrt{\frac{1}{2} \frac{y_2}{y_1} \left( \frac{y_2}{y_1} + 1 \right)} \tag{9.4}$$

For very small disturbances,  $y_2 \rightarrow y_1$  and hence,

$$\begin{aligned} V_{n1} &= V_1 \sin \beta \rightarrow \sqrt{g y_1}, \text{ and dropping suffixes} \\ V_n &= V \sin \beta = \sqrt{g y} \quad \text{or} \\ \sin \beta &= \frac{\sqrt{g y}}{V} \end{aligned} \tag{9.5}$$

which is the same result as in Eq. 9.1.

From the vector triangle  $ABD$ ,

$$\frac{(-\Delta V_n)}{\sin \Delta \theta} = \frac{V_1}{\sin (90 + \beta_1 - \Delta \theta)}$$

i.e.

$$-\Delta V_n = \frac{V_1 \sin \Delta \theta}{\sin (90 + \beta_1 - \Delta \theta)}$$

As  $\Delta \theta \rightarrow 0$ ,

$$-\frac{dV_n}{d\theta} = \frac{V}{\cos \beta} \tag{9.6}$$



The momentum equation, Eq. 9.3 can be written as

$$P + M = \frac{1}{2} \gamma y^2 + \frac{\gamma}{g} V_n^2 y = \text{Const.}$$

Differentiating,

$$\gamma y dy + \frac{\gamma}{g} (2V_n y dV_n) + \frac{\gamma}{g} (V_n^2 dy) = 0$$

i.e. 
$$\left(1 + \frac{V_n^2}{g y}\right) y dy = -\frac{2V_n}{g} y dV_n$$

For very small angular changes, from Eq. 9.4,  $\frac{V_n^2}{g y} = 1.0$  and hence,

$$\left(-\frac{dy}{dV_n}\right) = \frac{V_n}{g} = \frac{V \sin \beta}{g} \tag{9.7}$$

By Eqs 9.6 and 9.7,

$$\left(-\frac{dV_n}{d\theta}\right) \left(-\frac{dy}{dV_n}\right) = \frac{dy}{d\theta} = \frac{V \sin \beta}{g} \frac{V}{\cos \beta}$$

i.e. 
$$\frac{dy}{d\theta} = \frac{V^2}{g} \tan \beta \tag{9.8}$$

Assume that there is no energy loss, i.e., the specific energy  $E = y + \frac{V^2}{2g} =$  constant. Noting that

$E = y \left(1 + \frac{F^2}{2}\right)$  and  $\sin \beta = \frac{1}{F}$ , Eq. 9.8 can be written as

$$\frac{dy}{d\theta} = \frac{2(E - y)\sqrt{y}}{\sqrt{2E - 3y}} \tag{9.9}$$

The solution of this equation is given as

$$\theta = \sqrt{3} \tan^{-1} \sqrt{\frac{3y}{2E - 3y}} - \tan^{-1} \frac{1}{\sqrt{3}} \sqrt{\frac{3y}{2E - 3y}} - C_1 \tag{9.10}$$

in which  $C_1$  is a constant.

Other forms of Eq. 9.10 are

$$\theta = \sqrt{3} \tan^{-1} \frac{\sqrt{3}}{\sqrt{F^2 - 1}} - \tan^{-1} \frac{1}{\sqrt{F^2 - 1}} - C_1 \tag{9.11}$$

or 
$$\theta = \sqrt{3} \tan^{-1} \frac{\sqrt{F^2 - 1}}{\sqrt{3}} - \tan^{-1} \sqrt{F^2 - 1} - C_2 \tag{9.12}$$

The constants  $C_1$  and  $C_2$  can be evaluated by using the initial condition,  $\theta = 0$  when  $F = F_1$ .

Equation 9.10 or its other forms give the variation of the Froude number at a gradual change in the boundary in a horizontal frictionless channel. Equation 9.12 is in a form which is analogous to the well-known *Prandtl–Meyer function* in supersonic flows. The two constants  $C_1$  and  $C_2$  are related by  $C_1 + C_2 = 65.8846^\circ$ . Figure 9.4 is a plot of Eq. 9.11 in the form of  $(\theta + C_1)$  against  $F$  and is helpful in understanding the interdependence of  $F$  with  $\theta$ . Also, it can be used as an aid in solving problems concerning supercritical flow past curved boundaries.

Engelund and Peterson<sup>5</sup> have shown that Eq. 9.5 relating  $\beta$  with  $F$  is only true for wide rectangular channels. However, for channels with finite aspect ratios, the wave angle  $\beta$  has been shown to be a function of  $F$  and  $B/y$ , where  $B$  = width of the channel. For a single reflecting wave in a channel of width  $B$  (such as in Fig. 9.2) Harrison<sup>6</sup> has shown that

$$\sin \beta = \frac{1}{F} \sqrt{\frac{\tanh(\pi y / B \cos \beta)}{\pi y / B \cos \beta}} \tag{9.13}$$

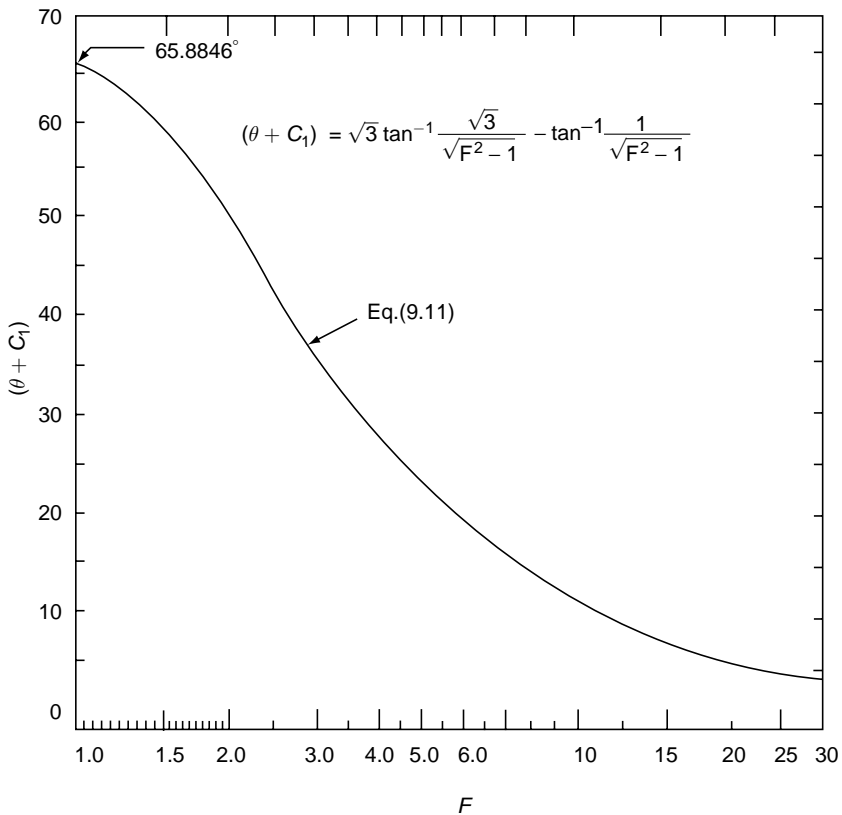


Fig. 9.4 Variation of  $(\theta + C_1)$  with  $F$

Also, Eq. 9.13 can be simplified for small values of  $(\pi y / B \cos \beta) = x$  as

$$\sin \beta = \frac{1}{F} \left( 1 - \frac{x^2}{6} \right) \quad (9.14)$$

The evaluation of Eq. 9.14 indicates that Eq. 9.5 gives values of  $\beta$  within 5 per cent error for  $y/B < 0.15$ . In view of its simple form, Eq. 9.5 is usually used in channels of all aspect ratios to estimate  $\beta$  in preliminary calculations.

Experiments by Ippen and Dawson<sup>2</sup> on a curved wall composed of two reverse circular curves, each with a central angle of  $16^\circ$ , indicated good agreement with Eq. 9.11 in the first half of the curve but showed deviations in the second part, probably due to the neglect of the effects of friction and the aspect ratio in the theory.

**Concave Wall** A curved surface can be considered to be made up of a large number of straight segments, each with a deflection angle  $\Delta\theta$ . For a concave vertical wall surface (Fig. 9.5), at the first break at A, a disturbance line emanates from the boundary at an angle  $\beta_1$  to the flow. Since  $\Delta\theta$  is positive in this case, it will cause a decrease in the Froude number as is evident from Fig. 9.4. Thus  $F_2 < F_1$  and  $y_2 > y_1$ . At the second break in the wall, by similar argument,  $F_3 < F_2$  and  $y_3 > y_2$ . Thus the Froude number decreases and the depth of flow increases in the downstream

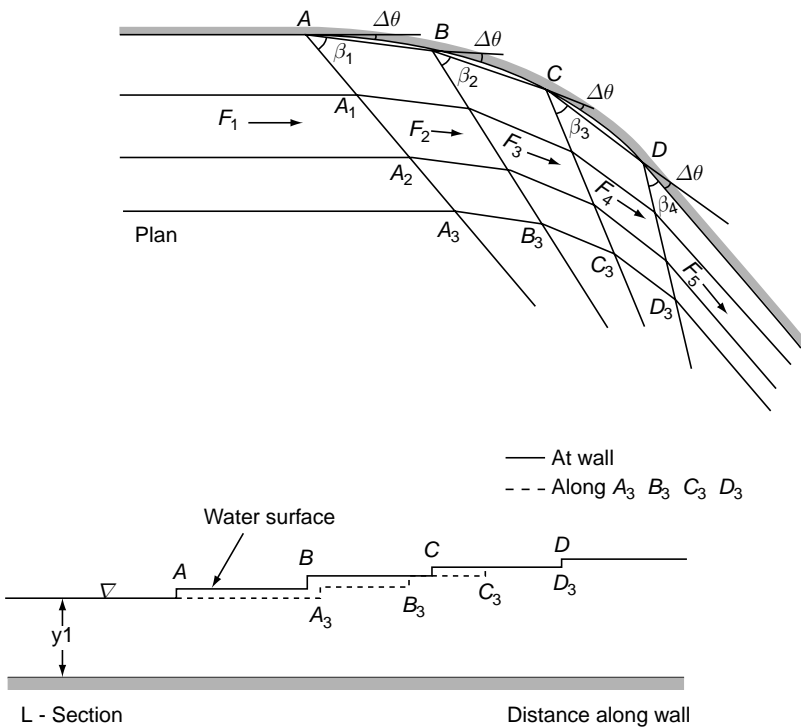


Fig. 9.5 Supercritical flow at a concave wall

direction. Since  $\sin \beta = \frac{1}{F}$ , a decrease in  $F$  causes an increase in the value of  $\beta$ . The water surface profiles will thus have steeper gradients as one moves away from the wall. If these disturbance lines coalesce, a jump will occur. This type of disturbance caused by a concave wall is known as positive disturbance.

**Convex Wall** For a convex vertical wall guiding a supercritical stream as in Fig. 9.6, the wall surface curves away from the direction of flow, and as such  $\Delta \theta$  is negative.

As indicated earlier (Fig. 9.4), a decrease in  $\theta$  causes an increase in the Froude number which, in turn, is responsible for the decrease in depth and also for the reduction in the value of  $\beta$ . Thus, the effect of a convex wall on a supercritical stream is opposite to that of a concave wall. The increase in the value of  $\beta$  causes the disturbance lines to diverge, and consequently, the water-surface profiles are flatter as one moves away from the wall. The disturbance produced by a convex wall is termed as a *negative disturbance*.

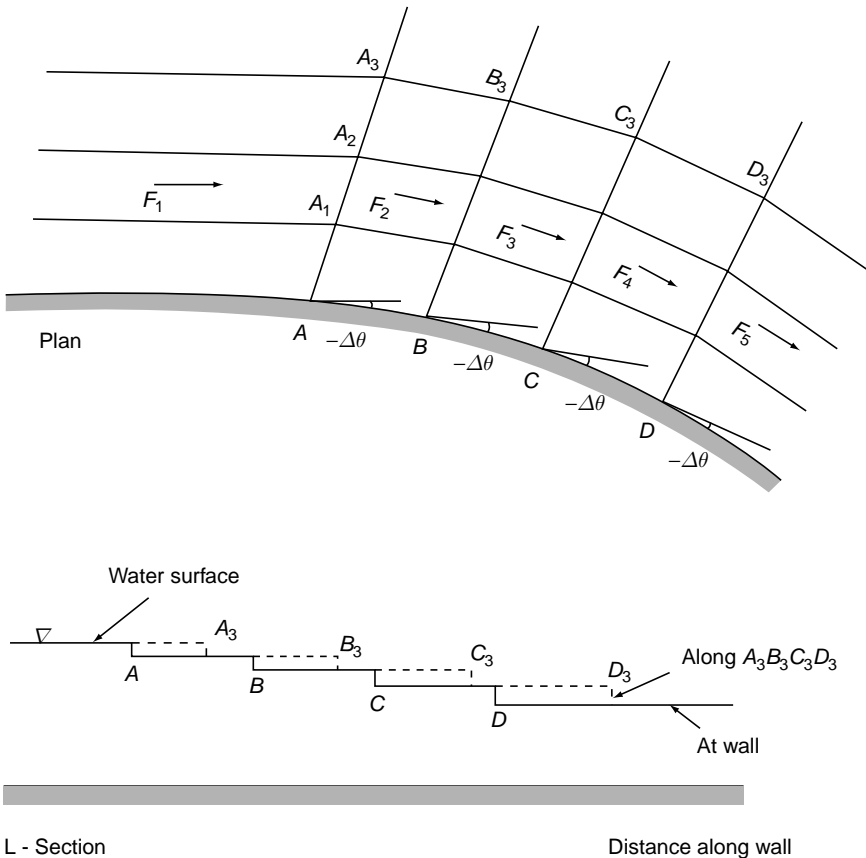


Fig. 9.6 Supercritical flow at a convex curve

**Example 9.1** A supercritical stream with a velocity of 4.34 m/s and a depth of flow of 0.12 m enters a curved boundary of total deflection angle of  $5^\circ$ . Calculate the Froude number, depth of flow and direction of the disturbance line  $\beta$  just after the curve, if the boundary is (a) concave, and (b) convex to the flow. The channel is assumed to be horizontal and frictionless.

$$\text{Solution } F_1 = \frac{4.34}{\sqrt{9.81 \times 0.12}} = 4.0$$

$$\beta_1 = \sin^{-1} \frac{1}{4} = 14.478^\circ$$

Equation 9.11 or Fig. 9.4 can be used to study the effect of the boundary on the flow.

**(a) Concave Wall** For  $F_1 = 4.0$ , from Fig. (9.4),  $(\theta + C_1) = 27.26^\circ$

$$\Delta\theta = +5.0^\circ$$

Hence at the end of the curve,  $(\theta + C_1) = 27.26 + 5.0 = 32.26^\circ$

For this value, from Fig. 9.4,  $F_2 = 3.32$ .

Since the specific energy is assumed to be constant in the derivation of Eq. 9.11,

$$E = y_1 \left( 1 + \frac{F_1^2}{2} \right) = y_2 \left( 1 + \frac{F_2^2}{2} \right)$$

$$y_2 = \frac{0.2 \left( 1 + \frac{4^2}{2} \right)}{\left( 1 + \frac{(3.32)^2}{2} \right)} = 0.166 \text{ m}$$

$$\beta_2 = \sin^{-1} \frac{1}{3.32} = 17.53^\circ$$

**(b) Convex Wall** For  $F_1 = 4.0$ , as found above,  $(\theta + C_1) = 27.26^\circ$

$$\Delta\theta = -5.0^\circ$$

Hence at the end of the curve,  $(\theta + C_1) = 27.26 - 5.0 = 22.26^\circ$

For this value, from Fig. 9.4,  $F_2 = 4.96$

$$y_2 = \frac{0.12 \left( 1 + \frac{16}{2} \right)}{\left[ 1 + \frac{(4.95)^2}{2} \right]} = 0.082 \text{ m}$$

$$\beta_2 = \sin^{-1} \frac{1}{4.95} = 11.655^\circ$$

9.4 FLOW AT A CORNER

In contrast to the gradual change in the boundary through a series of infinitesimally small angular changes, a sudden change in the boundary orientation by a finite angle  $\theta$  is called a corner. The supercritical flow past a convex corner can be analysed in a manner similar to that of a gradual change, while the flow past a concave corner needs a different approach.

9.4.1 Convex Corner

In a convex boundary, the disturbance diverges outward. For a convex corner at A (Fig. 9.7), the deflection angle of  $\theta$  can be considered to be made up of a series of small angles  $\Delta\theta_1, \Delta\theta_2, \dots$ , etc. Let  $AB_1$  be the first disturbance corresponding to  $F_1$  deflected by a small angle  $\Delta\theta_1$ . The inclination of  $AB_1$  to the initial flow direction  $x$  will be  $\beta_1 = \sin^{-1} \frac{1}{F_1}$ . A disturbance line, such as  $AB_1$ , is a characteristic of the incoming flow and is called a *characteristic* or *Froude line*. Across the Froude line  $AB_1$ , the velocity increases from  $V_1$  to  $V_2$  and the streamlines are deflected by an angle  $\Delta\theta_1$ . The next Froude line  $AB_2$  is due to a further change of the boundary direction by  $\Delta\theta_2$ . The inclination of  $AB_2$  is  $\beta_2 = \sin^{-1} \frac{1}{F_2}$  to the flow direction in  $B_1 AB_2$ , i.e., its inclination with  $x$  direction is  $(\beta_2 - \Delta\theta_1)$ . The velocity is now

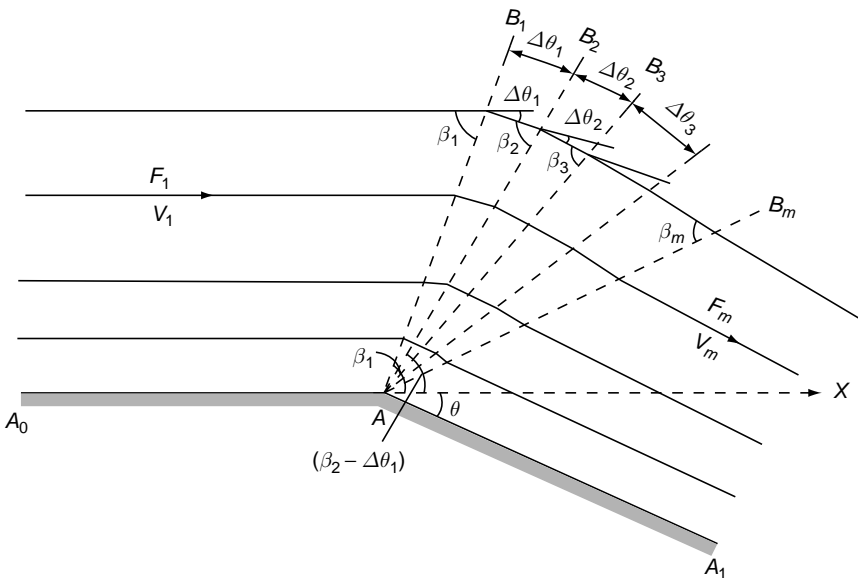


Fig. 9.7 Flow round a convex corner

increased from  $V_2$  to  $V_3$  and the streamlines undergo a further deflection  $\Delta\theta_2$  in their direction. This process continues and the velocity vector gradually changes direction. Since  $\Delta\theta_1$ ,  $\Delta\theta_2$  are arbitrary they can be made infinitesimally small, making the increase in velocity and Froude number gradual. The last Froude line will be  $AB_m$  and its inclination is  $B_m = \sin^{-1} \frac{1}{F_m}$ , where  $F_m$  is the Froude number of the flow past the corner. The streamlines after the Froude line  $AB_m$  will be parallel to the downstream boundary,  $AA_1$ . It may be noted that in this flow, save for friction (which is neglected), there is no change in the energy of the system. Thus in a convex corner, the velocity and depth changes are confined to a fan-shaped region bounded by Froude lines  $F_1$  and  $F_m$  at angles  $\beta_1$ , and  $\beta_m$  respectively. This fan-shaped region is known as the *Prandtl-Meyer fan*. The relationship between  $F$ ,  $\Delta\theta$  and  $\beta$  at any Froude line is governed by Eq. 9.11. The various elements of the flow can be calculated using Fig. 9.4.

**Example 9.2** | A flow with a Froude number of 3.0 passes round a convex corner of deflection angle  $10^\circ$ . If the initial depth of the flow is 0.65 m, find (a) the Froude number after the corner, (b) the depth of flow in the downstream section, and (c) the angular spread of the Prandtl-Meyer fan.

**Solution** Referring to Fig. 9.7,

$$F_1 = 3.0, -\Delta\theta = 10^\circ \text{ and } y_1 = 0.65 \text{ m}$$

$$\beta_1 = \sin^{-1} \frac{1}{F_1} = \sin^{-1} \frac{1}{3} = 19.47^\circ$$

Using Fig. 9.4, for  $F_1 = 3.0$ ,  $\theta + C_1 = 35.0^\circ$ .

For the downstream sections of the corner,

$$(\theta + C_1 - \Delta\theta) = 35.0 - 10.0 = 25^\circ \text{ and corresponding}$$

$$F_m = 4.4$$

$$\beta_m = \sin^{-1} \frac{1}{F_m} = \sin^{-1} \frac{1}{4.4} = 13.14^\circ$$

$$\therefore \text{Width of Prandtl-Meyer fan} = \beta_1 + \theta - \beta_m = 16.33^\circ$$

Since specific energy is assumed to be constant,

$$E = y_1 \left( 1 + \frac{F_1^2}{2} \right) = y_m \left( 1 + \frac{F_m^2}{2} \right)$$

$$\therefore \frac{y_m}{y_1} = \frac{2 + F_1^2}{2 + F_m^2} = \frac{2 + 3^2}{2 + (4.4)^2} = 0.515$$

$$\therefore y_m = 0.515 \times 0.65 = 0.335 \text{ m.}$$

### 9.4.2 Concave Corner and Oblique Shock

If a flow past a concave corner is analysed by a stepwise treatment as in the previous section, it will be found that the first Froude line  $AB_1$  will be downstream of the last Froude line  $AB_m$  (Fig. 9.8). This would require a reverse flow and hence the method is not applicable to the situation. The reason for this anomalous behaviour is that in a concave corner, the various Froude lines intersect and interact causing a rapid change in the water surface and some energy loss. When different Froude lines coalesce, a single shock wave inclined at an angle  $\beta_s$ , to  $x$  direction takes place. Across this shock, there will be a considerable change of depth as in a hydraulic jump. Such a shock wave is called an *oblique shock wave*.

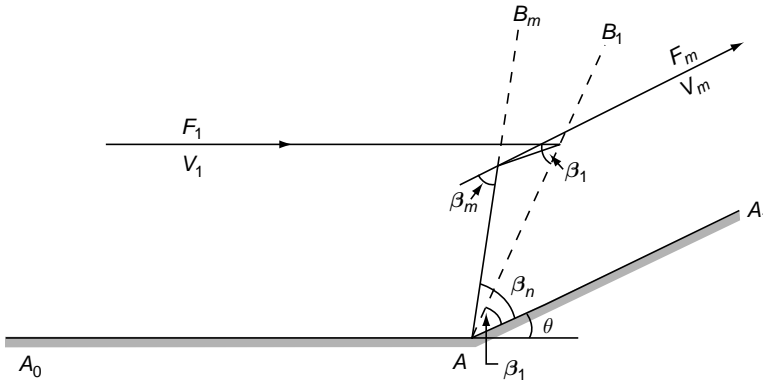


Fig. 9.8 Flow past a concave corner if oblique shock is neglected

Figure 9.9 shows the geometry of an oblique shock.  $\beta_s$  is the inclination of the shock wave to the approaching flow of velocity  $V_1$ , depth  $y_1$  and Froude number  $F_1$ . After the shock, the depth increases to  $y_2$  with the velocity and Froude number decreasing respectively to  $V_2$  and  $F_2$ . The components of the velocity normal and tangential to the shock wave are

$$\begin{aligned} V_{n1} &= V_1 \sin \beta_s & \text{and} & & V_{n2} &= V_2 \sin (\beta_s - \theta) \\ V_{t1} &= V_1 \cos \beta_s & \text{and} & & V_{t2} &= V_2 \cos (\beta_s - \theta) \end{aligned}$$

Consider a control volume of unit width as shown in Fig. 9.9. By the continuity equation

$$y_1 V_1 \sin \beta_s = y_2 V_2 \sin (\beta_s - \theta) \tag{9.15}$$

From the momentum equation in the normal direction to the shock wave, by assuming hydrostatic pressure distribution and neglecting friction.

$$\frac{1}{2} \gamma y_1^2 - \frac{1}{2} \gamma y_2^2 = \rho y_2 V_2^2 \sin^2 (\beta_s - \theta) - \rho y_1 V_1^2 \sin^2 \beta_s \tag{9.16}$$



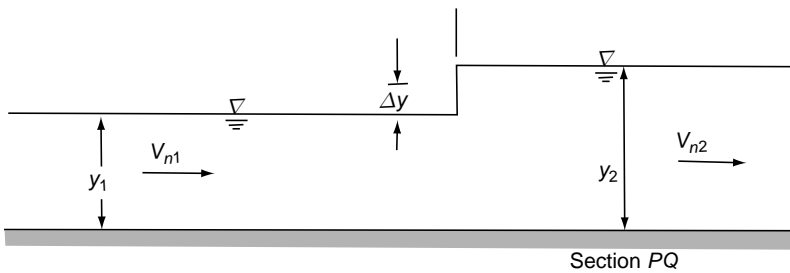
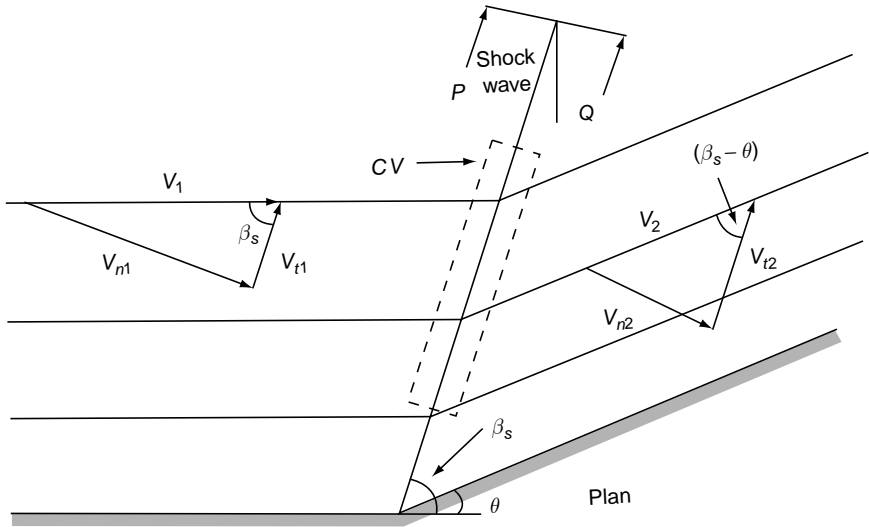


Fig. 9.9 Oblique shock geometry

From the momentum equation in a direction parallel to the shock wave, as there is no net force in that direction, it follows that

$$V_1 \cos \beta_s = V_2 \cos (\beta_s - \theta) \quad (9.17)$$

These three basic relations (Eqs 9.15, 9.16 and 9.17) aid in deriving useful relationships between the various parameters of the oblique shock.

From Eqs 9.15 and 9.16

$$\frac{y_2}{y_1} = \frac{1}{2} \left( -1 + \sqrt{1 + 8F_1^2 \sin^2 \beta_s} \right) \quad (9.18)$$

It may be noted that  $F_1 \sin \beta_s = F_{n1}$  = normal component of the initial Froude number of Eq. 9.18 is of the same form as the familiar hydraulic-jump equation [Eq. (6.4)], in a rectangular channel. Thus the normal components of the velocities satisfy the basic equation of a hydraulic jump and as such an oblique shock wave is called an oblique jump.

From Eqs 9.15 and 9.17

$$\frac{y_2}{y_1} = \frac{\tan \beta_s}{\tan (\beta_s - \theta)} \quad (9.19)$$

Eliminating  $\left(\frac{y_2}{y_1}\right)$  from Eqs 9.18 and 9.19

$$\tan \theta = \frac{\tan \beta_s \left(\sqrt{1 + 8F_1^2 \sin^2 \beta_s} - 3\right)}{2 \tan^2 \beta_s - 1 + \sqrt{1 + 8F_1^2 \sin^2 \beta_s}} \quad (9.20)$$

From Eq. 9.18,

$$F_{n1} = F_1 \sin \beta_s = \sqrt{\frac{1}{2} \left(\frac{y_2}{y_1}\right) \left(\frac{y_2}{y_1} + 1\right)} \quad (9.21)$$

An expression for  $F_2$  in terms of  $F_1$  and  $(y_2 / y_1)$  can be obtained as follows:

$$V_1^2 = V_{n1}^2 + V_{t1}^2$$

and

$$V_2^2 = V_{n2}^2 + V_{t2}^2$$

But by Eq. 9.17,

$$V_{t1} = V_{t2}$$

$$V_2^2 = V_1^2 - V_{n1}^2 + V_{n2}^2$$

From Eq. 9.15,

$$V_{n2} = V_1 \left(\frac{y_1}{y_2}\right) \sin \beta_s$$

$$V_2^2 = V_1^2 \left\{ 1 - \sin^2 \beta_s \left[ 1 - \left(\frac{y_1}{y_2}\right)^2 \right] \right\}$$

i.e.

$$F_2^2 = F_1^2 \left(\frac{y_1}{y_2}\right) - F_{n1}^2 \left(\frac{y_1}{y_2}\right) \left[ 1 - \left(\frac{y_1}{y_2}\right)^2 \right]$$

Substituting for  $F_{n1}$  from Eq. 9.21 and simplifying

$$F_2^2 = \left(\frac{y_1}{y_2}\right) \left[ F_1^2 - \frac{1}{2} \left(\frac{y_1}{y_2}\right) \left(\frac{y_2}{y_2} - 1\right) \left(1 + \frac{y_2}{y_1}\right)^2 \right] \quad (9.22)$$

Equations 9.15 through 9.22 enable the solution of the various elements of the oblique shock wave. Usually a trial-and-error procedure is required for solving oblique-jump problems. Equation 9.20 when plotted as  $\beta_s = f(F_1, \theta)$  (Fig. 9.10), provides a graphical aid which together with relevant equations greatly simplifies the determination of oblique-jump elements. Ippen<sup>1</sup> has given a four quadrant chart for the graphical solution of oblique-jump equations.

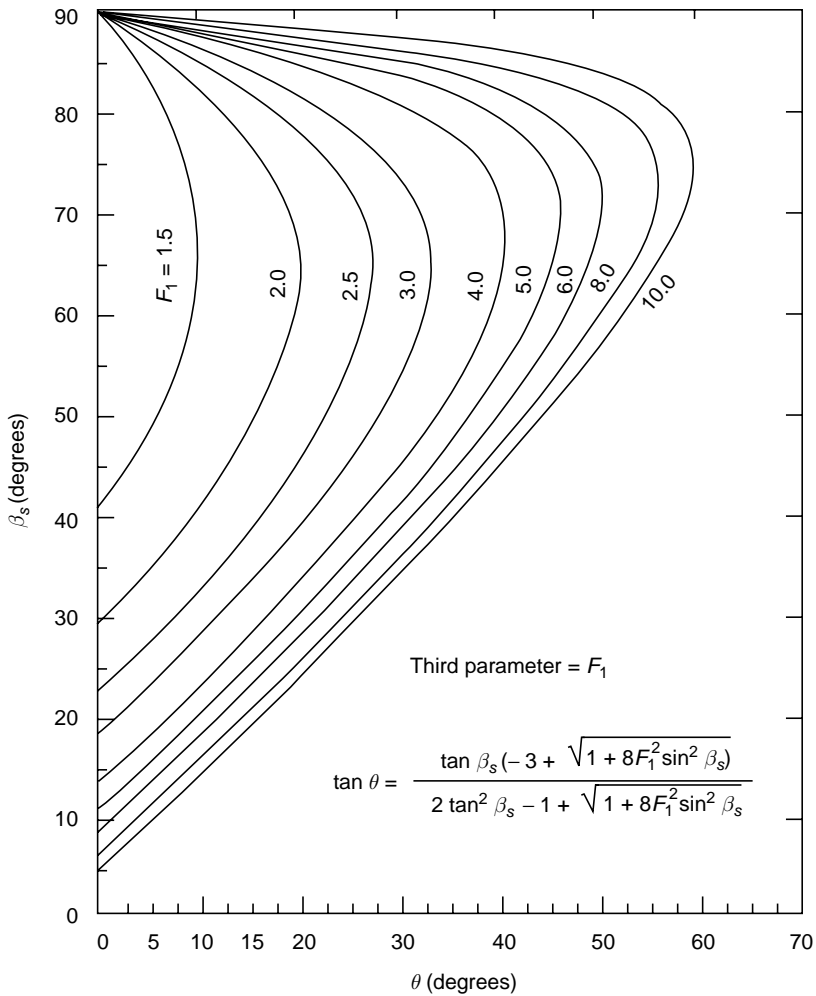


Fig. 9.10 Variation  $\beta_s$  in an oblique shock

In an oblique-jump the energy loss can be estimated by

$$E_{L0} = \left( y_1 + \frac{V_1^2}{2g} \right) - \left( y_2 + \frac{V_2^2}{2g} \right)$$

or

$$\frac{E_{L0}}{y_1} = \left( 1 + \frac{F_1^2}{2} \right) - \left( \frac{y_2}{y_1} \right) \left( 1 + \frac{F_2^2}{2} \right)$$

Substituting for  $F_2^2$  from Eq. 9.22 and simplifying,

$$\frac{E_{L0}}{y_1} = \frac{\left( \frac{y_2}{y_1} - 1 \right)^3}{4(y_2 / y_1)}$$

or

$$E_{L0} = \frac{(y_2 - y_1)^3}{4y_1y_2}$$

which is the same as the energy loss in normal hydraulic-jumps (Eq. 8.6). Usually, the value of  $F_{n1}$  is very small and as such the energy loss in an oblique-jump is relatively small.

**Estimation of  $\beta_s$**  For a given value of  $F_1$  and  $\theta$ , the value of  $\beta_s$  can be estimated by using Fig. 9.10. However, this will only be a rough estimate, because of the scale of the figure and if accurate value is desired the value obtained from Fig. 9.10 can be refined by trial and error through use of Eq. 9.23. For quick and fairly accurate estimation of values of  $\beta_s$  the following correlation equation can be used:

$$\beta_s = (1.4679 - 0.2082 F_1 + 0.0184 F_1^2) \theta + (60.638 F_1^{-1.044}) \quad (9.23)$$

where  $\beta_s$  and  $\theta$  are in degrees. This equation has been derived from Eq. 9.20 for values of  $\theta$  in the range  $1.0^\circ$  to  $11.0^\circ$  and Froude number  $F_1$  in the range 2.0 to 7.5. Equation 9.23 gives results within an error band of  $\pm 2.5\%$ .

**Example 9.3** | A supercritical stream in a wide rectangular channel has a Froude number of 6.0. One of the vertical walls is turned inward at a section with a deflection angle of  $10^\circ$ . Calculate the elements of the oblique-jump formed due to this change in direction if the initial depth of flow is 0.50 m.

**Solution**  $F_1 = 6.0$ ,  $\theta = 10.0^\circ$  and  $y_1 = 0.50$  m

From Fig. 9.10,  $\beta_s = 18.5$

Using Eq. 9.19,

$$\frac{y_2}{y_1} = \frac{\tan \beta_s}{\tan(\beta_s - \theta)} = \frac{\tan 18.5^\circ}{\tan 8.5^\circ} = 2.239$$

$$y_2 = (0.5) \times (2.239) = 1.119 \text{ m}$$

Using Eq. 9.22,

$$F_2^2 = \left( \frac{1}{2.239} \right) \left[ (6.0)^2 - \frac{1}{2} \left( \frac{1}{2.239} \right) (1.239)(3.239)^2 \right]$$

$$= 14.782$$

$$F_2 = 3.84$$

$$F_{n1} = F_1 \sin \beta_s = 1.904$$

$$F_{n2} = F_2 \sin(\theta_2 - \theta) = 0.57$$

(Note the small values of Froude numbers normal to the shock),

Energy loss 
$$E_{L0} = \frac{(y_2 - y_1)^3}{4y_1y_2} = \frac{(1.119 - 0.50)^3}{4(1.119)(0.5)} = 0.106 \text{ m}$$

$$E_1 = y_1 \left( 1 + \frac{F_1^2}{2} \right) = 0.5 \left( 1 + \frac{36}{2} \right) = 9.5 \text{ m}$$

Relative energy loss 
$$\frac{E_{L0}}{E_1} = \frac{0.106}{9.5} = 0.011 = 1.1 \text{ per cent}$$

(Note the very small relative energy loss.)

## 9.5 WAVE INTERACTIONS AND REFLECTIONS

### 9.5.1 Reflection of a Positive Wave

Consider one of the walls of a rectangular channel being deflected inwards by an angle  $\theta$  (Fig. 9.11). An oblique shock wave  $AB$  inclined at an angle  $\beta_A$  to the initial direction emanates from  $A$ , the magnitude of  $\beta_A$  being given by Eq. 9.20. As the wave arrives at  $B$ , the angle of the wall to the flow direction downstream of  $AB$  is the deflection angle causing the next shock wave. In the present example, the wall at  $B$  making an angle  $\theta$  with the flow acts as a concave corner. The approach Froude number is  $F_2$ . An oblique shock  $BC$  making an angle  $\beta_B$  with the flow direction [i.e.,  $(\beta_B - \theta)$  with the wall] will emanate from  $B$ . For known values of  $F_2$  and  $\theta$ ,  $\beta_B$  is obtained from Eq. 9.20 or Fig. 9.10. Since  $F_2 < F_1$ ,  $\beta_B$  will be greater than  $\beta_A$ . The successive reflections are similarly found. It may be

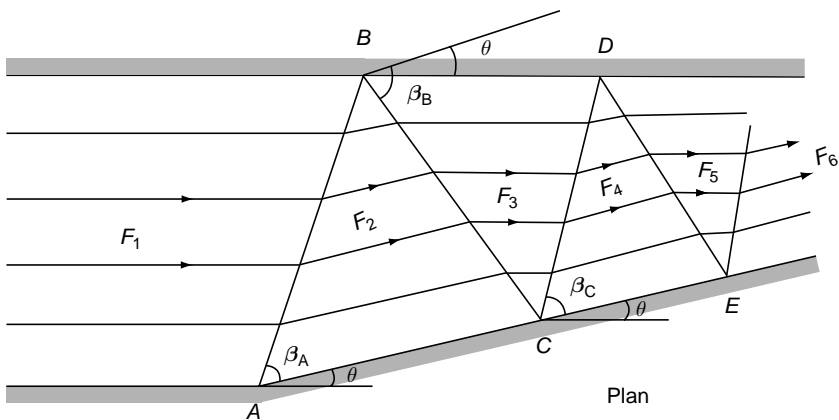


Fig. 9.11 Reflection of a positive wave

noted that after each reflection the value of the Froude number decreases and the  $\beta$  value increases, ultimately reaching  $90^\circ$  when the downstream flow in the channel becomes critical.

### 9.5.2 Interaction of Two Oblique Shocks

Two oblique shocks emanating from either end of an unsymmetrical contraction in a channel are shown in Fig. 9.12(a). The deflection angles are  $\theta_1$  at  $A_1$  and  $\theta_2$  at  $A_2$ . The shock wave  $A_1B$ , is inclined at  $\beta_1$  to the horizontal and  $A_2B$  at  $\beta_2$  to the horizontal. Downstream of  $A_1B_1$  the Froude number is  $F_3$  while downstream of  $A_2B$ , it is  $F_2$ . Downstream of  $BC_1$  and  $BC_2$ , the flow must have the depth and direction same all across the section till it is intercepted by a shock wave. As a first approximation, the flow direction may be taken as inclined at  $(\theta_1 - \theta_2) = \delta$  to the horizontal. Knowing  $\delta$ , the deflection angles of shock waves  $BC_2$  and  $BC_1$  are calculated using the appropriate Froude numbers. Since  $F_2 < F_1$  and  $F_3 < F_1$ ,  $\beta_3 > \beta_2$  and  $\beta_4 > \beta_1$ . It is important to realise that  $A_1BC_2$  (and similarly  $A_2BC_1$ ) is not a single straight line. If the contraction is symmetrical ( $\theta_1 = \theta_2$ ), there will be symmetry about the centreline which acts as a reflection surface and the flow situation is as discussed in Section 9.5.1. A typical cross wave pattern obtained as a result of shock wave interaction in a symmetrical contraction is indicated in Fig. 9.12(b).

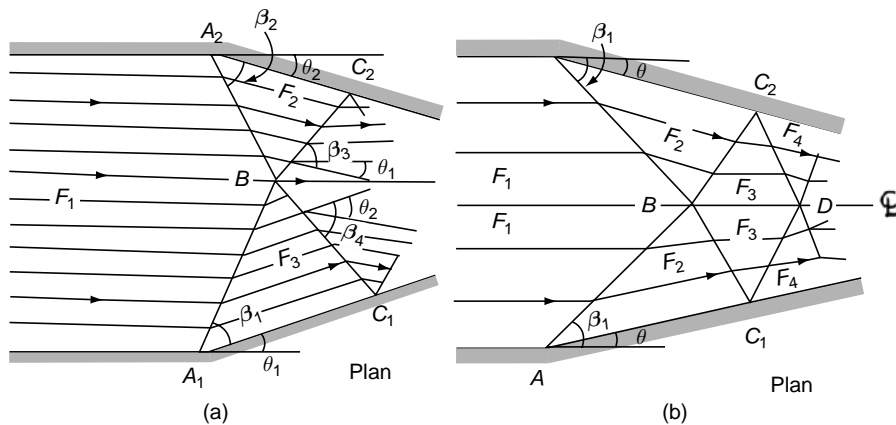


Fig. 9.12 (a) Unsymmetrical contraction (Ref. 1), (b) Symmetrical contraction (Ref. 1)

### 9.5.3 Convergence of Two Oblique Shocks

When two oblique shock waves from two adjacent concave corners coalesce at  $C$  (Fig. 9.13),  $CD$  is a combined shock wave. To calculate the direction  $b_3$  of the shock  $CD$ , the Froude number  $F_1$  and deflection angle  $= (\theta_1 + \theta_2)$  may be used as a good approximation. This is based on the assumption of zero energy loss.

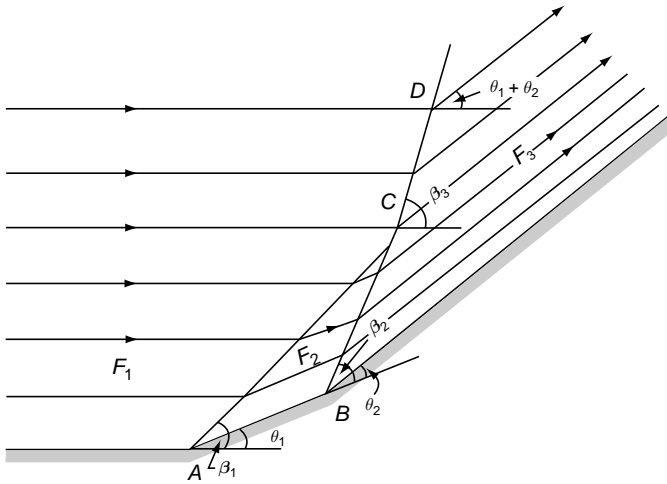


Fig. 9.13 Convergence of two oblique shock waves (Ref. 1)

### 9.5.4 Interaction of a Positive and a Negative Shock

Consider a negative wave (Fig. 9.14) intersecting a positive shock wave from an upstream location A. At B, the Prandtl–Meyer fan is drawn with a large number of Froude lines. The depths at the intersection of these Froude lines with the shock wave are obtained by a simple superposition. The shock wave will be deflected due to a change of the Froude number at the intersection points of the Froude lines.

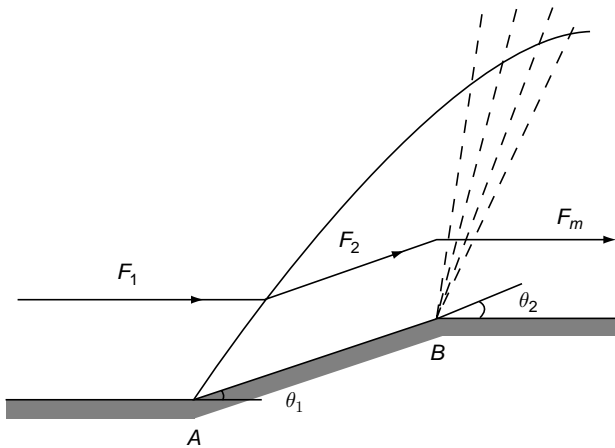


Fig. 9.14 Interaction of two kinds of waves (Ref. 1)

**Example 9.4** For the channel contraction shown in Fig. 9.11, the initial Froude number  $F_1$  is 4.00 and the inward deflection angle  $\theta$  is  $6^\circ$ . Calculate  $F_2$ ,  $F_3$  and  $\beta_A$ ,  $\beta_B$  and  $\beta_C$ .

*Solution* (i) For the first wave,

For  $F_1 = 4.0$  and  $\theta = 6^\circ$ , by using Fig. 9.10,  $\beta_s = \beta_A = 19^\circ$ .

$$\text{From Eq. 9.19, } \frac{y_2}{y_1} = \frac{\tan 19^\circ}{\tan 13^\circ} = 1.491$$

$$\text{From Eq. 9.22, } F_2^2 = \left( \frac{1}{1.491} \right) \left[ 4^2 - \frac{1}{2} \left( \frac{1}{1.491} \right) \times (1.491 - 1) \times (1 + 1.491)^2 \right] = 10.04$$

$$F_2 = 3.169$$

(ii) For the second wave,

For  $F_1 = 3.169$  and  $\theta = 6^\circ$ , by using Fig. 9.10,  $\beta_s = \beta_B = 23.5^\circ$ .

$$\text{From Eq. 9.19, } \frac{y_2}{y_1} = \frac{\tan 23.5^\circ}{\tan 17.5^\circ} = 1.379$$

From Eq. 9.22,

$$F_3^2 = \left( \frac{1}{1.379} \right) \left[ (3.169)^2 - \frac{1}{2} \left( \frac{1}{1.379} \right) \times (1.379 - 1) \times (1 + 1.379)^2 \right] = 6.718$$

$$F_3 = 2.592$$

(iii) For the third wave,

For  $F_1 = 2.592$  and  $\theta = 6^\circ$ , by using Fig. 9.10,  $\beta_s = \beta_C = 26.5^\circ$ .

$$\text{From Eq. 9.19, } \frac{y_2}{y_1} = \frac{\tan 26.5^\circ}{\tan 20.5^\circ} = 1.334$$

From Eq. 9.22,

$$F_4^2 = \left( \frac{1}{1.334} \right) \left[ (2.592)^2 - \frac{1}{2} \left( \frac{1}{1.334} \right) \times (1.334 - 1) \times (1 + 1.334)^2 \right] = 4.525$$

$$F_4 = 2.127$$

## 9.6 CONTRACTIONS

In the contraction of a subcritical flow channel, the main aim is to smoothly guide the flow, and the desirable profile having a short length provides a separation-free streamlined transition with the least energy loss. The curvature of the sides does not



affect the lateral water-surface profile, which remains horizontal. If such a curved contraction is used in a supercritical flow, it is apparent, from the discussion in the earlier sections, that numerous positive and negative waves would be generated at the boundary. These would undergo interactions and multiple reflections to produce a highly undesirable water surface in the downstream channel.

In complete contrast to the streamlining practice adopted in the subcritical flow, it is possible to design an acceptable downstream wave-free supercritical contraction composed of straight-edge boundaries. Figure 9.15 represents a straight-edge contraction in a horizontal frictionless channel. The supercritical flow will meet the concave corners at  $A_1$  and  $A_2$ , each having a deflection angle  $\theta$ . The oblique shock waves formed intersect at  $B$ . Downstream of  $A_1B$  and  $A_2B$  the streamlines will be parallel to the wall and the values of the depth and Froude number attained are  $y_2$  and  $F_2$  respectively. If the length of the contraction is too short, the shock waves  $BC_2$  and  $BC_1$  would reach the boundary beyond the corners  $D_2$  and  $D_1$  respectively as shown in Fig. 9.15. The convex corners  $D_1$  and  $D_2$  will each create a fan of negative waves which also travel downstream, interacting with various positive waves. The result is a highly disturbed downstream water surface due to the presence of cross waves.

If the length of the contraction is too long, the interacted waves  $BC_2$  and  $BC_1$  will hit the sloping walls of the channel, as in Fig. 9.12(b), and even here there will be multiple reflections and cross waves in the downstream channel.

If, however, the contraction length of the channel is so designed that the interacted waves  $BC_2$  and  $BC_1$ , meet the channel walls exactly on the corners  $D_2$  and  $D_1$  respectively (i.e., points  $D$  and  $C$  coincide), the deflecting effect of the shock wave and the wall will cancel each other. The downstream channel will be free from shock waves due to the contraction. The relationship between the various parameters for this ideal contraction are obtained as below.

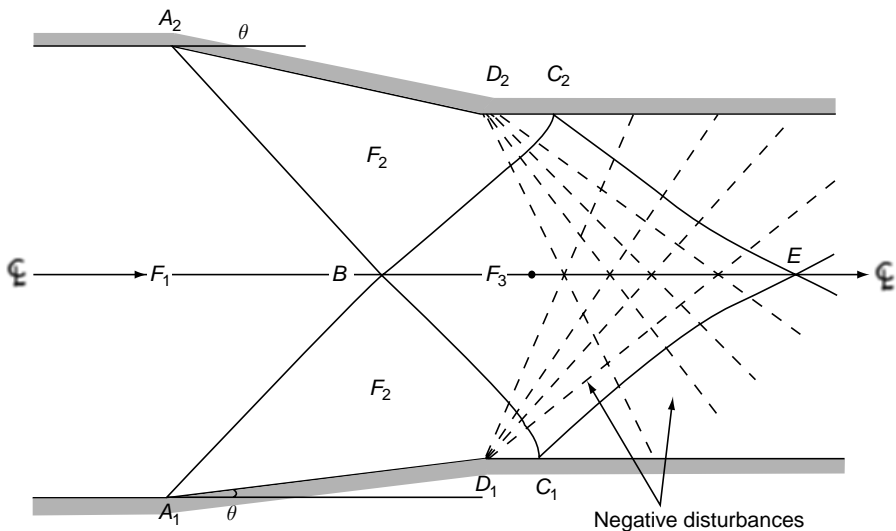


Fig. 9.15 Incorrect contraction

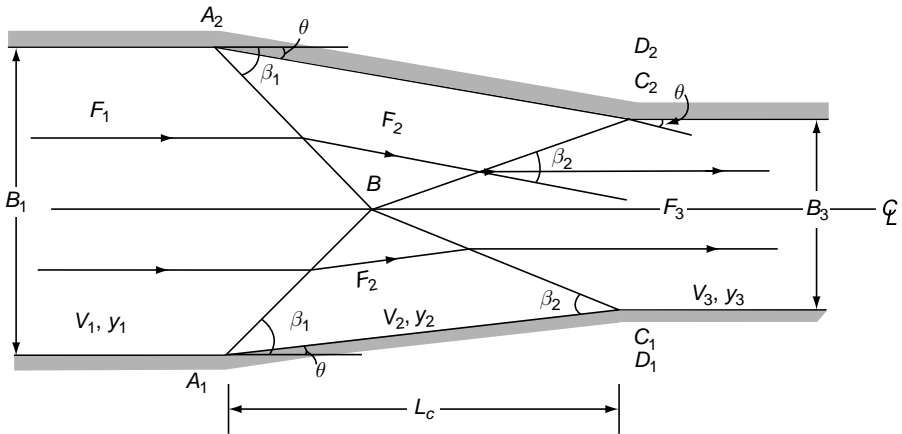


Fig. 9.16 Definition sketch of an ideal contraction

The plan view of an ideal supercritical flow contraction is indicated in Fig. 9.16. The flow is symmetrical about the centreline. Considering the directions normal to the shock fronts  $A_1B$  and  $A_2B$ , the depths  $y_1$  and  $y_2$  can be related by Eq. 9.18 as

$$\frac{y_2}{y_1} = \frac{1}{2} \left( -1 + \sqrt{1 + 8F_1^2 \sin^2 \beta_1} \right) \quad (9.24)$$

in which  $\beta_1 =$  angle the shock waves  $A_1B$  and  $A_2B$  with respect to the initial flow direction. Similarly, for the shock waves  $BC_1$  and  $BC_2$ ,

$$\frac{y_3}{y_2} = \frac{1}{2} \left( -1 + \sqrt{1 + 8F_2^2 \sin^2 \beta_2} \right) \quad (9.25)$$

in which  $\beta_2 =$  angle of the shock waves  $BC$  with respect to the inclined wall. Since there is no change in momentum parallel to a shock front, by Eq. 9.19,

$$\frac{y_2}{y_1} = \frac{\tan \beta_1}{\tan(\beta_1 - \theta)} \quad (9.26)$$

and

$$\frac{y_3}{y_2} = \frac{\tan \beta_2}{\tan(\beta_2 - \theta)} \quad (9.27)$$

Adopting Eq. 9.22,

$$F_2^2 = \left( \frac{y_1}{y_2} \right) \left[ F_1^2 - \frac{1}{2} \left( \frac{y_1}{y_2} \right) \left( \frac{y_2}{y_1} - 1 \right) \left( \frac{y_2}{y_1} + 1 \right) \right] \quad (9.28)$$

and

$$F_3^2 = \left( \frac{y_2}{y_3} \right) \left[ F_2^2 - \frac{1}{2} \left( \frac{y_2}{y_3} \right) \left( \frac{y_3}{y_2} - 1 \right) \left( \frac{y_3}{y_2} + 1 \right) \right] \quad (9.29)$$

where  $F_3 =$  final Froude number.

By the continuity equation,

$$(B_1 y_1) V_1 = (B_3 y_3) V_3$$

i.e. 
$$\left(\frac{B_1}{B_3}\right) = \left(\frac{y_3}{y_1}\right)^{3/2} \frac{F_3}{F_1} \tag{9.30}$$

The length of the ideal contraction is obtained by the geometry of the contraction as

$$L_c = \frac{(B_1 - B_3)}{2 \tan \theta} \tag{9.31}$$

**Design** In the design of supercritical flow contractions usually  $F_1, y_1, B_1$  and  $B_3$  are known and it is required to find the wall deflection angle  $\theta$ . Thus when  $F_1$  and  $\frac{B_3}{B_1}$  are given, there are seven unknowns, namely,  $\theta, \beta_1, \beta_2, F_2, F_3, y_2/y_1$  and  $y_3/y_2$ .

While seven equations, Eqs 9.24 through 9.30, are available, the non-linearity of the equations precludes a closed-form solution of  $\theta$ . Harrison<sup>6</sup> through the use of the Newton-Raphson technique of iteration obtained the design information as

$$\theta = f\left(\frac{B_3}{B_1}, F_1\right) \text{ and } \frac{y_3}{y_1} = f\left(\frac{B_3}{B_1}, F_1\right).$$

Subramanya and Dakshinamoorthy<sup>7</sup>, used Eq. 9.24 through 9.30 to obtain four equations in four unknown  $\theta, F_3, \beta_1$  and  $\beta_2$  and solved them by the least square error minimisation technique. Figure 9.17 is a plot of

$\theta = f\left(\frac{B_3}{B_1}, F_1\right)$  obtained in the study. Figures 9.17 and 9.10 together with the relevant

equations from among equations 9.24 through 9.30 enable the determination of all the elements of a supercritical flow contraction. The curve A in Fig. 9.17 represents the condition of  $F_3 = 1.0$ , and thus the choking condition.

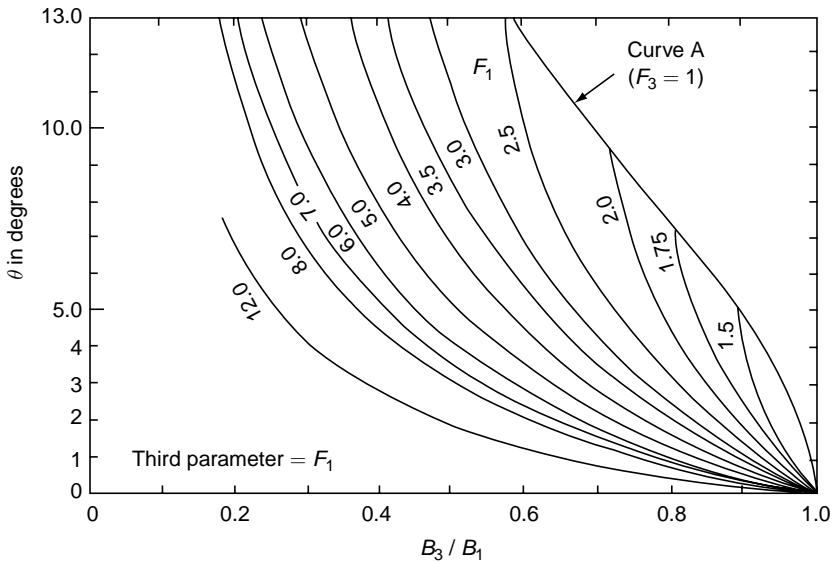


Fig. 9.17 Variation of  $\theta$  in contraction (Ref. 7)

References 1, 2, and 6 contain very useful information pertaining to supercritical flow contractions. The ideal contraction as above is to be used in preliminary designs only and the final design will have to be based on model studies as the friction and slope of the channel not considered in the ideal design can modify the shock-wave geometry. It should be remembered that the straight-edge supercritical contractions are only valid for the design Froude number. For any off-design values of  $F_1$ , the reflected waves do not strike at the corners  $D_1$  and  $D_2$ .

**Example 9.4** | A rectangular channel carries a flow with a Froude number of 6.0 in a 5.0-m wide channel with a depth of 0.75 m. It is required to reduce the width to 2.5 m. Design a contraction and determine all the elements of the transition. Also, determine the energy loss in the transition.

*Solution*  $y_1 = 0.75$  m,  $F_1 = 6.0$  and  $\frac{B_3}{B_1} = 0.5$

From Fig. 9.17,  $\theta = 4.25^\circ$

Referring to Fig. 9.10 or to Eq. 9.23, for  $\theta = 4.25^\circ$  and  $F = 6.0$ ,

$$\beta_1 = 13.0^\circ$$

Using Eq. 9.26, 
$$\frac{y_2}{y_1} = \frac{\tan \beta_1}{\tan(\beta_1 - \theta)} = \frac{\tan 13^\circ}{\tan 8.75^\circ} = 1.50$$

$$y_2 = 1.12 \text{ m}$$

From Eq. 9.28

$$\begin{aligned} F_2^2 &= \left(\frac{1}{1.5}\right) \left[ (6.0)^2 - \left(\frac{1}{1.5}\right) (1.50 - 1)(1.5 + 1)^2 \right] \\ &= 23.305 \\ F_2 &= 4.83 \end{aligned}$$

For the shock waves  $BC_1$  and  $BC_2$ ,  $F_2 = 4.83 =$  initial Froude number and  $\theta = 4.25^\circ$ . Using Fig. (9.10) or Eq. 9.23, with  $\theta = 4.25^\circ$  and  $F = 4.83$ ,

$$\beta_2 = 15.5^\circ$$

From Eq. 9.26,

$$\frac{y_3}{y_2} = \frac{\tan \beta_2}{\tan(\beta_2 - \theta)} = \frac{\tan 15.5^\circ}{\tan 11.25^\circ} = 1.394$$

$$\frac{y_3}{y_1} = \frac{y_3}{y_2} \cdot \frac{y_2}{y_1} = 1.394 \times 1.50 = 2.09$$

$\therefore y_3 = 2.09 \times 0.75 = 1.568$  m

From Eq. 9.29

$$F_3^2 = \left( \frac{1}{1.394} \right) \left[ (4.83)^2 - \frac{1}{2} \left( \frac{1}{1.394} \right) (0.394)(2.394)^2 \right]$$

$$= 16.15$$

$$F_3 = 4.02$$

From Eq. 9.31

$$L_c = \frac{5.0 - 2.5}{2 \tan 4.5^\circ} = 15.883 \text{ m}$$

Check: By Eq. 9.30,  $\frac{F_3}{F_1} = \frac{B_1 / B_3}{(y_3 / y_1)^{3/2}}$

$$F_3 = \frac{6.0 \times 2.0}{(2.09)^{3/2}} = 3.97$$

$\approx 4.02$  with about 1 per cent error.

In view of the possible errors in the use of various plots, this error is acceptable. Thus the elements of the transition can be summed up as

$y_1 = 0.75 \text{ m}$	$\theta = 4.25^\circ$	$L_c = 15.883 \text{ m}$
$B_1 = 5.00 \text{ m}$	$\beta_1 = 13.0^\circ$	$y_2 = 1.125 \text{ m}$
$F_1 = 6.00$	$\beta_2 = 15.5^\circ$	$y_3 = 1.568 \text{ m}$
	$F_2 = 4.83$	$F_3 = 4.02$

Energy loss:

$$E_1 = y_1 \left( 1 + \frac{F_1^2}{2} \right) = 0.75 \left( 1 + \frac{(6.0)^2}{2} \right) = 14.25 \text{ m}$$

$$E_3 = y_3 \left( 1 + \frac{F_3^2}{2} \right) = 1.568 \left( 1 + \frac{(4.02)^2}{2} \right) = 14.238 \text{ m}$$

$$E_L = E_1 - E_3 = 14.250 - 14.238 = 0.012 \text{ m}$$

## 9.7 SUPERCRITICAL EXPANSIONS

### 9.7.1 Introduction

The main aim of a supercritical flow expansion design is to have the desired channel-width expansion and to maintain a downstream water surface which is free

from cross waves. Since a supercritical flow past a convex boundary creates a gradual change in the water surface, an analysis of the flow situation with the help of Eq. 9.11 is feasible. It may be noted that in view of the analogy of these expansions with supersonic nozzles, the advance techniques available for the design of the latter can be advantageously used for the corresponding open-channel flow problems. The basic principles of the supercritical flow expansion design are outlined in the following sections.

### 9.7.2 Design of Expansions

The half plan of an expansion from width  $B_1$  to  $B_2$  in a horizontal rectangular frictionless channel is indicated in Fig. 9.18. The boundary initially expands in a convex curve from  $a$  to  $e$ . In this process the negative disturbances, i.e. Froude lines emanate from the boundary. Five such lines are shown in Fig. 9.18. These lines intersect the corresponding lines from the opposite wall at the centre line which can be treated as a reflecting plain wall. The reflected waves, after interacting with the oncoming lines, finally reach the wall. If the wall is turned through the same angle as a streamline would be turned by the expansion wave, no reflection occurs and the flow is wave-free. The proper wall angles are provided on this basis at points  $a_2, b_2, c_2, d_2, e_2$ . Naturally, a smoother boundary contour can be obtained by considering a large number of Froude lines. It may be noted that the initial curve  $abcde$  is arbitrary and the length and shape of the transition depend upon this curve.

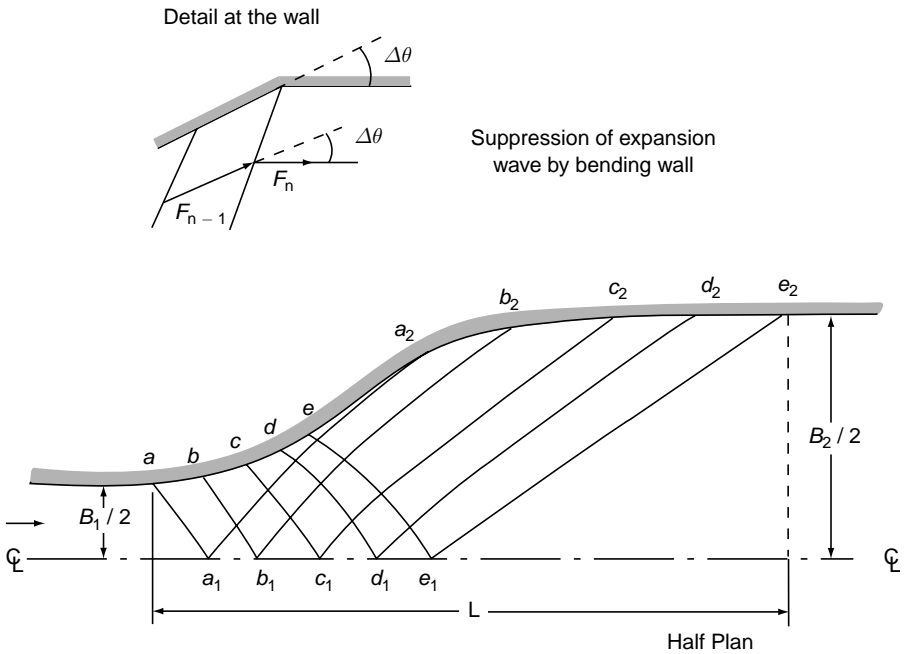


Fig. 9.18 Expansion with reflection free boundary

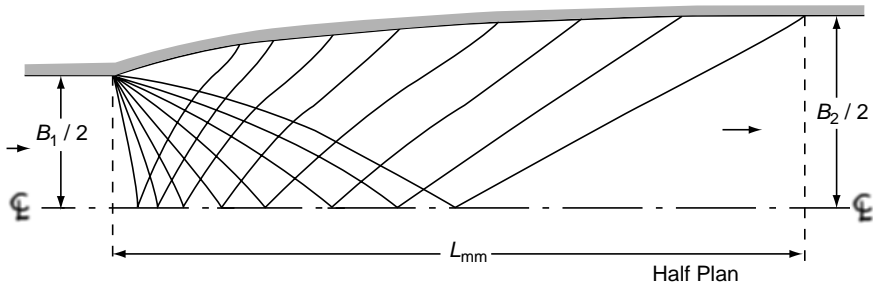


Fig. 9.19 Minimum length expansion

For a minimum length design, the points *a* through *e* will be coincident, i.e. a sharp convex corner at *a* (Fig. 9.19). A Prandtl-Meyer fan will occur at *a* and considering a suitable number of Froude lines, the transition can be designed as before. Figure 9.19 is a typical minimum-length expansion.

Graphical methods of designing the expansion as above are available in Ref. 1. Numerical computation procedures are generally preferred. A FORTRAN program which can easily be converted to the design of supercritical flow expansions is given by Pond and Love<sup>8</sup>.

### 9.7.3 An Empirical Method

Based on an experimental study, Rouse et al.<sup>3</sup> proposed empirical design curves expressed by the equation

$$\frac{B}{B_1} = f \left( \frac{x}{B_1 F_1}, \frac{B_2}{B_1} \right) \quad (9.32)$$

where *B* is the width of channel at any section *x* from the beginning of the expansion, the *B*<sub>1</sub> and *B*<sub>2</sub> are the initial and final widths of the channel respectively. The curves consist of an expansion convex curve followed by reverse curves. The expansion curve is given by<sup>3</sup>

$$\frac{B}{B_1} = \frac{1}{4} \left( \frac{x}{B_1 F_1} \right)^{3/2} + 1.0 \quad (9.33)$$

The coordinates of the reverse curves proposed by Rouse et al.,<sup>3</sup> are summarised in Table 9.1. All the reverse curves are tangential to the expansion curve given by Eq. 9.33.

Equation 9.33 together with the generalised coordinates of Table 9.1 give the boundaries of the supercritical expansion suitable for preliminary studies. Ref. 9 reports experimental study on the Rouse expansion.

### 9.7.4 Inclusion of Resistance

Generally, the bottom slope, friction and channel curvature, if any, affect the performance of a supercritical flow transition and it is the usual practice to test

**Table 9.1** Coordinates of the Reverse Curves in Supercritical Expansions  
Values of  $B/B_1$

$\frac{x}{B_1 F_1}$	$\frac{B_2}{B_1} = 1.5$	2.0	2.5	3.0	3.5	4.0
1.00	1.200					
1.38	1.300	1.400				
1.50	1.350	1.425				
1.75	1.400	1.550	1.550			
2.00	1.450	1.600	1.700			
2.25	1.475	1.650	1.750	1.750		
2.50	1.485	1.775	1.900	1.900	1.925	
2.70	1.500	1.820	2.000	2.100	2.100	2.100
3.00		1.900	2.100	2.200	2.250	2.250
3.50		1.950	2.250	2.400	2.450	2.500
4.00		2.000	2.350	2.550	2.675	2.775
4.50			2.425	2.685	2.825	2.950
5.00			2.500	2.800	3.000	3.150
5.50				2.850	3.150	3.300
6.00				2.925	3.240	3.450
6.50				2.950	3.320	3.550
7.00				3.000	3.400	3.700
7.50					3.425	3.775
8.00					3.475	3.850
8.50					3.485	3.875
9.00					3.500	3.900
9.50						3.930
10.00						3.950
10.50						4.000

the preliminary design through model studies for these effects as well as for the possibility of separation of streamlines at the boundary.

If the supercritical flow in an expansion is considered as a two-dimensional problem, the basic differential equations of motion together with the continuity equation form a system of hyperbolic quasilinear partial-differential equations of the first order. The equations can be solved numerically, e.g. by the method of characteristics. It is possible to include the friction effects as ‘friction slopes’ by using a suitable resistance formula. A generalised problem of an expansion having curved boundaries, with a bottom slope and friction can be analysed through numerical methods. Detailed on this kind of analysis is available in literature.<sup>10,11,12,13</sup>

**Example 9.5** | A 2.5-m wide rectangular channel carrying a flow with a Froude number of 2.5 is to be provided with an expansion to a width of 5.0 m. Obtain the profile of the expansion profile by using Rouse’s curves.



*Solution* Rouse's expansion curve is given by Eq. 9.33 as

$$\frac{B}{B_1} = \frac{1}{4} \left( \frac{x}{B_1 F_1} \right)^{3/2} + 1.0$$

Here  $B_1 = 2.5$  m and  $F_1 = 2.5$ .

$$\begin{aligned} \frac{B}{2.5} &= \frac{1}{4} \left( \frac{x}{2.5 \times 2.5} \right)^{3/2} + 1.0 \\ B &= \frac{x^{3/2}}{25} + 2.5 \end{aligned} \quad (9.34)$$

*Reverse Curve* From Table 9.1, for  $B_2/B_1 = 2.0$ , the reverse curve starts at  $\frac{x}{B_1 F_1} = 1.38$ , i.e., at  $x = 1.38 \times 2.5 \times 2.5 = 8.63$  m. Also from Table 9.1, for  $B_2/B_1 = 2.0$ , the length of transition is given by  $\frac{L}{B_1 F_1} = 4.0$ . Hence  $L = 4.0 \times 2.5 \times 2.5 = 25.0$  m. Coordinates of the reverse curve corresponding to  $B_2/B_1 = 2.0$  are obtained from Table 9.1. Thus for  $0 < x < 8.6$  m,  $B = \frac{x^{3/2}}{25} + 2.5$  and for  $8.6 < x < 25.0$  m values of  $B$  are obtained by using Table 9.1. A smooth curve is drawn through the reverse curve coordinates to merge with the expansion curve (Eq. 9.34) without kinks.

## 9.8 STABILITY OF SUPERCRITICAL FLOWS

A flow is said to be stable if a small perturbation in the flow does not get amplified. From this point of view a subcritical flow is inherently stable. However, in supercritical flows under certain favorable conditions a perturbation can grow until the originally steady flow breaks up in to a train of unsteady surges called *roll waves*. The transformation of a steady supercritical flow in to an unstable unsteady flow situation is analogous to the transition from laminar to turbulent flow. The roll waves are characterized by a series of shock fronts separated by regions of gradually varied flow. The wave speed, height and wavelengths of roll waves generally increase as they move downstream. The onset of roll-waves is an important constraint in the design of channels for supercritical flow.

The stability analysis<sup>14</sup> of the flow leads to the criterion for stable flows as

$$-1 \leq V_e \leq 1 \quad (9.35)$$

In which  $V_e =$  Vendernikov number  $= xF \left( 1 - R \frac{dP}{dA} \right)$

Where  $x = 2/3$  if Manning's formula is used for describing the channel resistance and

$x = 0.5$  if Chezy formula is used for describing the channel resistance

$F =$  Froude number of the flow,

$R$  = hydraulic radius,

$P$  = wetted perimeter, and

$A$  = area of cross section of the flow.

Thus the onset of instability in a channel depends on the channel geometry and the Froude number of the flow. Channels having  $V_e = 0$  will be stable for all values of Froude number and thus constitute channels of absolute stability. Ref. 14 can be consulted for further details on stability.

**Example 9.6** | Derive the conditions for stable supercritical flow in (a) rectangular, and (b) triangular channels. Consider that Manning's formula is used to describe the channel resistance to flow.

*Solution* By Eq. 9.35, for stable supercritical flow  $V_e = \frac{2}{3} F \left( 1 - R \frac{dP}{dA} \right) \leq 1$

(a) *Rectangular channel*  $A = By$  and  $P = B + 2y$

$$\frac{dP}{dA} = \frac{dP}{dy} \frac{dy}{dA} = \frac{2}{B}$$

$$\text{For stable flow, } \frac{2}{3} F \left( 1 - \frac{By}{(B + 2y)} \cdot \frac{2}{B} \right) \leq 1$$

$$\frac{2}{3} F \left( \frac{B}{B + 2y} \right) \leq 1$$

$$\text{i.e., } F \leq \left( \frac{3}{2} + 3 \frac{y}{B} \right)$$

(b) *For triangular channel*  $A = my^2$   $P = 2y\sqrt{1 + m^2}$

$$\frac{dP}{dA} = \frac{dP}{dy} \frac{dy}{dA} = \frac{2\sqrt{1 + m^2}}{2m} = \frac{\sqrt{1 + m^2}}{m}$$

$$\text{For stable flow } \frac{2}{3} F \left( 1 - \left( \frac{my^2}{2y\sqrt{1 + m^2}} \right) \left( \frac{\sqrt{1 + m^2}}{my} \right) \right) \leq 1$$

$$\text{i.e., } \frac{F}{3} \leq 1 \text{ or } F \leq 3$$



## REFERENCES

1. Ippen, A T, 'Mechanics of Supercritical Flow', *Trans. ASCE*, Vol. 116, 1951, p. 268–295.
2. Ippen, A T, and Dawson, J H, 'Design of Supercritical Contractions', *Trans. ASCE*, Vol. 116, 1951, pp 326–346.
3. Rouse, H, Bhoota, B V, and Hsu, E Y, 'Design of Channel Expansions', *Trans. ASCE*, Vol. 116, 1951, pp. 347–363.
4. Knapp, R T, 'Design of Channel Curve for Supercritical Flow', *Trans. ASCE*, Vol. 116, 1951, pp 296–325.
5. Englund, F A, and Munch Peterson, J, 'Steady Flow in Contracted and Expanded Rectangular Channels', *La Houille Blanche*, Vol. 8, No. 4, Aug.-Sept. pp 464–474.
6. Harrison, A J M, 'Design of Channels for Supercritical Flow', *Proc. Inst. of Civil Engrs.* (London), Vol. 35, Nov. 1966, pp 475–490.
7. Subramanya, K, and Dakshinamoorthy, S, 'Design of Supercritical Flow Contractions by Least Square Error Minimisation Technique', *5th Australasian Conf. on Hydr. and Fl. Mech.*, Christchurch, New Zealand, Dec. 1974, pp 57–63.
8. Pond, J E, and Love, J, 'Design of Two-dimensional Sharp-edge-throat Supersonic Nozzle by Digital Computer', *Engg. Expt. Station Series No. 64*, Univ. of Missouri, Columbia, USA, 1967.
9. Mazumdar, S K, and Hager, W H, 'Supercritical Expansion Flow in Rouse Modified and Reverse Transitions', *J. of Hyd. Div., Proc. ASCE*, Vol. 119, No. 2, Feb. 1993, pp 201–219.
10. Ligget, J A, and Vasudev, S U, 'Slope and Friction Effects in Two-dimensional, High – speed Channel Flow', *Proc. 11th Congress of IAHR*, Leningrad, 1965, Vol. 1, pp 1–25.
11. Bagge, G, and Herbich, J B, 'Transitions of Supercritical Open Channel Flow', *J. of Hyd. Div., Proc. ASCE*, Vol. 93, Sept. 1967, pp 23–41.
12. Dakshinamoorthy, S, 'Some Numerical Studies on Supercritical Flow Problems', *Ph. D. Thesis, Indian Institute of Technology*, Kanpur, India, Dec. 1973.
13. Choudhry, M H, *Open Channel Flow*, Prentice-Hall, Englewood Cliffs, New Jersey, 1993.
14. Ligget, J, A, 'Stability', Chap. 6 in *Unsteady Flows in Open Channels*, Vol. I, Ed. by Mahmood, K, and Yevjevich, V, *Water Resources Pub.*, Fort Collins, Colo., USA, pp 259–282



## PROBLEMS

### Problem Distribution

Topic	Problems
<i>Response to a disturbance</i>	9.1 – 9.2
<i>Gradual change in the boundary</i>	9.3 – 9.4
<i>Oblique shock</i>	9.5 – 9.9
<i>Convex corner</i>	9.7 – 9.9
<i>Contractions</i>	9.10 – 9.12 – 9.13
<i>Expansion</i>	9.11 – 9.14 – 9.18
<i>Application of shock principle</i>	9.15 – 9.17
<i>Stability</i>	9.19

- 9.1 A rectangular channel has a velocity of 5 m/s and a depth of 0.60 m. If a thin obstruction such as a vertical pole is present in the midst of the stream, estimate the direction of waves produced.
- 9.2 When a stone was thrown into a pond waves of amplitude 1 cm and velocity 2 m/s were produced. Estimate the depth of water in the pond.
- 9.3 A wide rectangular channel carries a flow with a depth of 0.15 m and a Froude number of 4.5. Calculate and plot the water surface profile next to a side wall which has (i) a concave curve of  $8^\circ$  central angle, and (ii) a convex curve of  $8^\circ$  central angle. The radius of the curved wall is 10 m and the other side wall can be assumed to be too far away to have any interference.
- 9.4 For a gradual change in the boundary of a supercritical stream, an assumption of constant specific energy is made in the derivation of Eq. (9.10). Assuming, instead, a constant velocity, derive an expression for  $\theta$  as  $\theta = \beta + \sin \beta \cos \beta + a$  constant.
- 9.5 A free surface flow with a depth of 0.50 m and initial Froude number of 2.0 approaches a concave corner of deflection angle  $10^\circ$  in one of the walls. Determine the inclination of the shock wave to the original direction of flow and the depth after the shock.
- 9.6 A supercritical stream of velocity 10.0 m/s and depth 0.24 m is deflected by a concave corner having a deflection angle of  $20^\circ$ . Determine the inclination of the shock waves of the original direction of flow, the depth after the shock and the energy loss.
- 9.7 Label the positive and negative shock waves in the cases shown in Fig. 9.20.

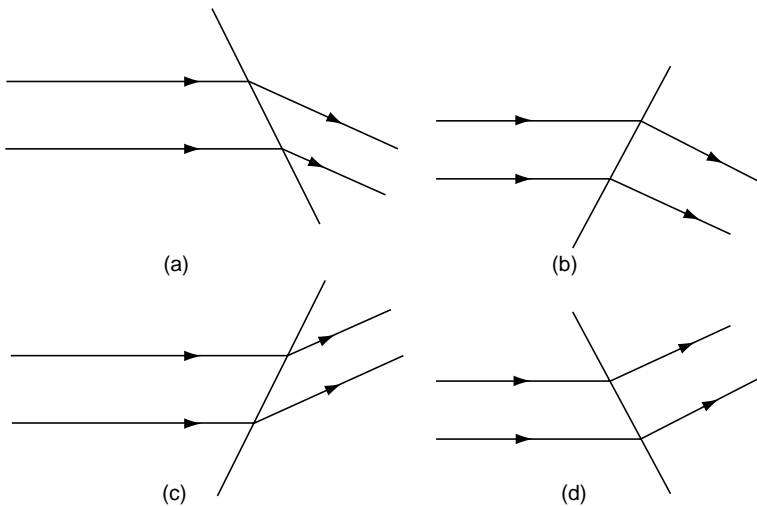


Fig. 9.20 Problem 9.7

- 9.8 If the stream in Problem 9.6 is deflected by a  $9^\circ$  convex corner, determine the downstream flow condition and the angular spread of the Prandtl-Meyer fan.
- 9.9 Sketch the flow past a thin plate kept in a supercritical flow as in Fig. 9.21.
- 9.10 For the channel contraction shown in Fig 9.11, if  $F_1 = 3.5$  and  $\theta = 5^\circ$ , calculate  $F_2$ ,  $F_3$ ,  $\beta_A$ ,  $\beta_B$  and  $\beta_C$ .

434 Flow in Open Channels



Fig. 9.21 Problem 9.9

9.11 A 3.0-m wide horizontal frictionless rectangular channel has an enlarging section as shown in Fig. 9.22. Calculate the expansion waves at 0 for an initial Froude number of 2.0 with a depth of flow of 0.50 m. Sketch a few Froude lines and graphically determine their reflections and interactions.

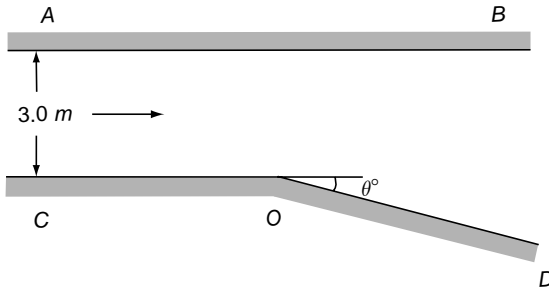


Fig. 9.22 Problem 9.11

9.12 An unsymmetrical contraction, as in Fig. 9.12, has  $F_1 = 4.0$ ,  $\theta_1 = 5^\circ$  and  $\theta_2 = 8^\circ$ . Calculate  $F_2, F_3, \beta_1, \beta_2, \beta_3$  and  $\beta_4$ . Sketch the shock waves and streamlines.

9.13 Design symmetrical contractions for the following sets of data and fill in Table 9.2.

Table 9.2 Problem 9.13

Sl. No.	$F_1$	$y_1$ (m)	$B_1$ (m)	$F_3$	$y_3$ (m)	$B_3$ (m)	$F_2$	$y_2$	$\theta$	$\beta_1$	$\beta_2$
1	5.0	0.70	6.0	—	—	3.0	—	—	—	—	—
2	6.0	0.50	4.0	—	—	—	—	—	$5.0^\circ$	—	—
3	4.0	0.60	—	—	—	2.5	—	—	$6.0^\circ$	—	—
4	—	—	—	—	1.30	2.0	—	—	$7.5^\circ$	$18^\circ$	—

9.14 For values of  $F_1 = 4.0$  and  $B_2/B_1 = 2.0$ , sketch a preliminary design of an expansion.

9.15 If a bridge is to be built across a supercritical stream, from the consideration of mechanics of flow, what factors govern the shape of the bridge piers, span and shape of abutments? Which of these factors will be different in subcritical flow?

- 9.16 The division of supercritical flow at a branch channel or a side weir can be solved by treating the problem as a particular type of channel transition. Considering a simple  $90^\circ$  branch channel, indicate an algorithm for calculating the branch-channel discharge for given main channel flow properties.
- 9.17 Curves are usually used in channels to cause a change in the direction of flow. In supercritical flow it is possible to create a change in direction with wave-free downstream flow by employing sharp corners instead of curves. How can this be achieved and what are the limitations ?
- 9.18 A 3.0-m wide rectangular channel carrying a supercritical flow having a Froude number of 3.0 is to be provided with an expansion to a width of 4.5 m. Obtain the profile of the expansion by using Rouse's curves.
- 9.19 Derive the conditions for stable supercritical flow in (i) rectangular channels, and (ii) triangular channels, if the resistance in the channels is described by Chezy formula.

## OBJECTIVE QUESTIONS

- 9.1 A thin vertical rod placed vertically in a 0.80 m deep channel creates two small disturbance waves each making an angle of  $30^\circ$  with the axis of the channel. The velocity of flow in m/s is  
 (a) 5.60 (b) 2.80  
 (c) 1.40 (d) 0.70
- 9.2 When a stone was thrown into a pond waves of amplitude 0.80 cm and velocity 2.6 m/s were observed. The depth of water in the pond is about  
 (a) 6.9 m (b) 0.69 m  
 (c) 0.83 m (d) 3.13 m
- 9.3 A flow with a Froude number of 6.0 in a wide channel undergoes a change in the direction at a curve. The disturbance at the beginning of the curve makes an angle  $\beta$ .  
 (a) =  $9.59^\circ$   
 (b) =  $6.35^\circ$   
 (c) =  $16^\circ$   
 (d) which depends on whether the curve is convex or concave
- 9.4 When a supercritical flow is guided by a curved convex wall  
 (a) the Froude number decreases  
 (b) the disturbance lines converge  
 (c) the water surface becomes steeper at distances away from the wall  
 (d) the depth decreases along the wall
- 9.5 A flow with  $F_1 = 4.0$  and  $y_1 = 0.9$  m moves past a convex corner and attains  $F_2 = 5.0$  downstream of the corner. The depth  $y_2$  in metres is  
 (a) 1.35 (b) 0.90  
 (c) 0.60 (d) 6.0
- 9.6 If a stream with  $F_1 = 5.0$  flows past a convex corner which produces a Prandtl–Meyer fan of angular spread  $3^\circ 36'$ , the Froude number downstream of the corner is  
 (a) 3.91 (b) 7.24  
 (c) 9.57 (d) 5.02
- 9.7 An oblique jump occurs when  
 (a) a subcritical flow is turned by a convex corner  
 (b) a supercritical flow is turned by a convex corner  
 (c) an obstruction is obliquely placed in a channel  
 (d) when a supercritical flow is deflected by a concave corner

- 9.8 In an oblique hydraulic jump having a deflection angle of  $15^\circ$  with the approaching uniform flow of Froude number 6.0, the sequent depth ratio is
- (a) 1.75 (b) 17.5  
(c) 0.20 (d) 4.0
- 9.9 An oblique hydraulic jump has a deflection angle of  $18.5^\circ$  with the approaching uniform flow. The depths before and after the jump are 0.4 m and 0.90 m respectively. The energy loss head in the jump is
- (a) 0.028 m (b) 0.087 m  
(c) 0.500 m (d) 0.274 m
- 9.10 A supercritical flow past a convex corner produces
- (a) a positive wave  
(b) a Froude line  
(c) a drop in water surface accompanied by considerable energy loss  
(d) a negative disturbance of fixed angular width
- 9.11 In an oblique shock
- (a) the flow after the shock is always subcritical  
(b) the depth of flow downstream of the shock is lower than the upstream depth  
(c) the flow after the shock is always supercritical  
(d) none of these
- 9.12 In a supercritical contraction design
- (a) the length of the transition is constant for all Froude numbers  
(b) the transition is operative for only one depth  
(c) the transition is meant to operate at the design Froude number only  
(d) does not give a unique solution for a given  $F_1$  and  $B_2/B_1$
- 9.13 A streamlined transition unit was designed for the expansion of a subcritical flow in a channel. If this transition unit is introduced in a supercritical flow channel
- (a) it will function efficiently if used as a contraction  
(b) it will function efficiently if used as an expansion  
(c) flow separation occurs if used as a contraction  
(d) cross waves will be produced if used as an expansion

# Unsteady Flows

# 10

## 10.1 INTRODUCTION

For a complete understanding of flow in open channels, in addition to the study of steady flow which has been dealt with in the previous chapters, unsteady flow also deserves attention as it is encountered in one way or other in practice in all open channels. However, the complex nature of unsteady flows together with their diversity in form make the subject matter too difficult and extensive to be treated in a single chapter. As such, only a brief introduction to unsteady open-channel flow problems and the descriptions of a few simple cases are included here. A list of reference for details and for further reading are given at the end of the chapter.

Unsteady flows, also called *transients*, occur in an open channel when the **discharge or depth or both vary with time at a section**. These changes can be due to natural causes, planned action or accidental happenings. Depending upon the curvature of the water surface, the transients can be broadly classified as (i) gradually-varied unsteady flows (GVUF) and (ii) rapidly-varied unsteady flows (RVUF). The chief characteristics of a GVUF are: (i) the small water-surface curvature which enables the pressures to be assumed as hydrostatic and (ii) inclusion of friction in the analysis. Flood flow in a stream is a typical example of this kind of flow. In an RVUF there is appreciable change in the water surface in relatively short distances and the friction plays a minor role in determining the flow characteristics. The formation and travel of a surge due to the sudden closure of a gate is a good example of an RVUF. Some field situations which give rise to transients can be listed as:

1. Heavy rainfall in a catchment, snow melt, breaking of log or ice-jams, etc., which give rise to floods in rivers, streams and surface-drainage systems.
2. Operation of control gates in hydraulic structures and navigation locks; acceptance and rejection of a sudden load by turbines in a hydroelectric installation; sudden starting or tripping of pumps—all leading to the possibility of surges.
3. Tides in estuaries and tidal rivers causing a surge, usually called a *bore*, which is propagated upstream. The bore on the river Severn, near Gloucester, England is a typical example [Fig. 10.1].





Fig. 10.1 The Severn bore (Courtesy: The Citizen, Gloucester, England)

## 10.2 GRADUALLY VARIED UNSTEADY FLOW (GVUF)

As mentioned earlier, the flood flow in a river is a typical GVUF. In view of the importance of floods in various phases of human activity, the problem of determining the modification of flood hydrograph in its passage through a river, known as flood routing, has received considerable attention. Consequently, a large number of solution procedures are available. The basic equations of GVUF relevant to the flood routing are presented in this section.

### 10.2.1 Equation of Continuity

For an unsteady flow in a channel, the continuity equation, as derived in Chapter 1 (Eq. 1.36), is in the form

$$\frac{\partial Q}{\partial x} + T \frac{\partial y}{\partial t} = 0 \quad (10.1)$$

Noting that

$$\frac{\partial Q}{\partial x} = \frac{\partial(AV)}{\partial x} = 0$$

$$A \frac{\partial V}{\partial x} + V \frac{\partial A}{\partial x} + T \frac{\partial y}{\partial t} = 0 \quad (10.2)$$

This equation assumes no lateral inflow or outflow. However, if there is a lateral inflow of  $q$  per unit length of channel, Eq. 10.2 will read as

$$A \frac{\partial V}{\partial x} + V \frac{\partial A}{\partial x} + T \frac{\partial y}{\partial t} - q = 0 \quad (10.3)$$

The cross-sectional area, in general, can be a function of depth and can also vary from section to section, i.e.  $A = A(x, y)$ . The  $x$  derivative of area at constant time is written as

$$\frac{\partial A}{\partial x} = \left( \frac{\partial A}{\partial x} \right)_y + \left( \frac{\partial A}{\partial y} \right)_x \frac{\partial y}{\partial x}$$

in which the suffix denotes the variable to be held constant in addition to time

in taking the derivative. Since  $\left( \frac{\partial A}{\partial y} \right)_x = T$ ,

$$\frac{\partial A}{\partial x} = \left( \frac{\partial A}{\partial x} \right)_y + T \frac{\partial y}{\partial x}$$

The first term  $\left( \frac{\partial A}{\partial x} \right)_y$  represents the rate of change of area with the depth held constant and is the gain in the area due to the width change. The second term  $\left[ T \frac{\partial y}{\partial x} \right]$  represents the gain in the area due to an increase in the depth. The continuity equation in its general form is

$$A \frac{\partial V}{\partial x} + VT \frac{\partial y}{\partial x} + \frac{\partial y}{\partial t} - q + V \left( \frac{\partial A}{\partial x} \right)_y = 0 \quad (10.4)$$

For a prismatic channel,  $\left( \frac{\partial A}{\partial x} \right)_y = 0$ , which simplifies Eq. 10.4 as

$$A \frac{\partial V}{\partial x} + VT \frac{\partial y}{\partial x} + T \frac{\partial y}{\partial t} - q = 0 \quad (10.4a)$$

### 10.2.2 Equation of Motion

The equation of motion for GVUF in a prismatic channel is derived by the application of the momentum equation to a control volume encompassing two sections of the flow as in Fig. 10.2. Since the flow is gradually varied, hydrostatic pressure distribution is assumed. The forces acting on the control volume are:

$F_1 =$  pressure force at the upstream Section 1  $= \gamma A \bar{y}$

$F_2 =$  pressure force at the downstream Section 2

$$= \gamma \left( A + \frac{\partial A}{\partial x} \Delta x \right) \left( \bar{y} + \frac{\partial \bar{y}}{\partial x} \Delta x \right)$$

$F_3 =$  component of the body force in the  $x$  direction

$$= \gamma A \Delta x \sin \theta \text{ and}$$

$F_s =$  shear force on the perimeter  $= P \tau_0 \Delta x$

where  $\bar{y} =$  depth of the centroid of the upstream Section 1 and

$\tau_0 =$  average shear stress acting over the flow boundary.

By neglecting the second order small quantities, the net force in the  $x$  direction is written as

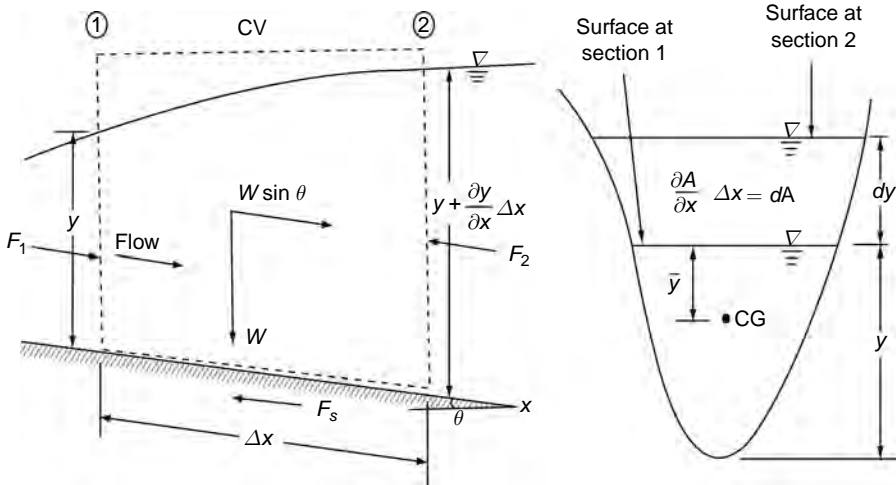


Fig. 10.2 Definition sketch for momentum equation

$$F_{net} = \gamma \left( -A \frac{\partial \bar{y}}{\partial x} - \bar{y} \frac{\partial A}{\partial x} + AS_0 - \frac{P \tau_0}{\gamma} \right) \Delta x$$

By taking the moments of area about the water surface at Section 2 and neglecting the second order small quantities

$$A \frac{\partial \bar{y}}{\partial x} + \bar{y} \frac{\partial A}{\partial x} = A \frac{\partial y}{\partial x} \tag{10.5}$$

Also, 
$$\frac{P \tau_0}{\gamma} = AS_f$$

Hence, 
$$F_{net} = \gamma \left( -A \frac{\partial y}{\partial x} + AS_0 - AS_f \right) \Delta x \quad (10.6)$$

The momentum equation for an unsteady flow states that the net external force on the control volume in a given direction is equal to the net rate of the momentum efflux in that direction plus the time rate of increase of momentum in that direction in the control volume. Assuming  $\beta_1 = \beta_2 = 1.0$  and considering the  $x$  direction:

1. Momentum influx into Section 1 =  $M_1 = \rho AV^2$
2. Momentum efflux from Section 2 =  $M_2 = \rho \left[ AV^2 + \frac{\partial}{\partial x} (AV^2) \Delta x \right]$
3. Time rate of increase of  $x$ -momentum in the control volume

$$M_u = \frac{\partial}{\partial t} (\rho AV \Delta x)$$

By the momentum equation,

$$M_2 - M_1 + M_u = F_{net}$$

i.e. 
$$\frac{\partial}{\partial t} \left( \frac{\gamma}{g} AV \Delta x \right) + \frac{\gamma}{g} \frac{\partial}{\partial x} (AV^2) \Delta x = \gamma A \left( -\frac{\partial y}{\partial x} + S_0 - S_f \right) \Delta x$$

Dividing throughout by  $\frac{\gamma}{g} \Delta x$  and simplifying,

$$\frac{\partial}{\partial t} (AV) + \frac{\partial}{\partial x} (AV^2) + gA \frac{\partial y}{\partial x} = gA (S_0 - S_f)$$

i.e. 
$$\frac{\partial V}{\partial t} + V \frac{\partial V}{\partial x} + g \frac{\partial y}{\partial x} + \frac{V}{A} \left( \frac{\partial A}{\partial t} + V \frac{\partial A}{\partial x} + A \frac{\partial V}{\partial x} \right) = g (S_0 - S_f)$$

By Eq. 10.2, 
$$\frac{\partial A}{\partial t} + V \frac{\partial A}{\partial x} + A \frac{\partial V}{\partial x} = 0$$

and on re-arranging,

$$\frac{\partial y}{\partial x} + \frac{V}{g} \frac{\partial V}{\partial x} + \frac{1}{g} \frac{\partial V}{\partial t} = S_0 - S_f \quad (10.7)$$

If there is a lateral inflow  $q$  per unit length into the control volume with negligible initial momentum in the longitudinal  $x$  direction, the equation of motion will read as

$$\frac{\partial y}{\partial x} + \frac{V}{g} \frac{\partial V}{\partial x} + \frac{1}{g} \frac{\partial V}{\partial t} = (S_0 - S_f) - \frac{qV}{Ag} \quad (10.8)$$

The continuity equation, Eq. 10.2 and the equation of motion (Eq. 10.7) of unsteady open-channel flow are believed to have been first developed by A J C Barré de-Saint Venant in 1871 and are commonly known as *Saint Venant equations*. These are simultaneous, quasi-linear, first order, partial differential equations of hyperbolic type and are not amenable to a general analytical solution.

The St Venant equations are expressed in a number of ways by choosing different dependent variables. Some of the common forms are listed below:

**(i) With flow rate  $Q(x, t)$  and depth  $y(x, t)$  as dependent variables** The velocity  $V$  in Eq. 10.7 is replaced by  $Q/A$  to get St Venant equations as

$$\text{Continuity Equation} \quad \frac{\partial y}{\partial t} + \frac{1}{T} \frac{\partial Q}{\partial x} = 0 \quad (10.9a)$$

$$\text{Momentum Equation} \quad \frac{\partial Q}{\partial t} + \frac{\partial}{\partial x} \left( \frac{Q^2}{A} \right) + gA \frac{\partial y}{\partial x} + gA(S_0 - S_f) = 0 \quad (10.9b)$$

From Eq. 10.5  $A \frac{\partial y}{\partial x} = \frac{\partial}{\partial x} (A\bar{y})$ . Hence Eq. 10.9(b) can be written as

$$\frac{\partial Q}{\partial t} + \frac{\partial}{\partial x} \left( \frac{Q^2}{A} + gA\bar{y} \right) = gA(S_0 - S_f) \quad (10.9c)$$

This equation is known as *momentum equation in conservation form*. This form is particularly useful in handling steep fronts and shocks such as in a surge due to a dam break.

**(ii) With flow rate  $Q(x, t)$  and Stage  $h(x, t)$  as dependent variable** If  $h$  = the elevation of the water surface measured above a datum (i.e. stage), then the water depth  $y = h - h_b$ , where  $h_b$  is the elevation of the bed. Further,

$$\frac{\partial y}{\partial t} = \frac{\partial h}{\partial t} \quad \text{and} \quad \frac{\partial y}{\partial x} = \frac{\partial h}{\partial x} - \frac{\partial h_b}{\partial x} = \frac{\partial h}{\partial x} - S_0$$

The St Venant equations are

$$\text{Continuity Equation} \quad \frac{\partial h}{\partial t} + \frac{1}{T} \frac{\partial Q}{\partial x} = 0 \quad (10.10a)$$

$$\text{Momentum Equation} \quad \frac{\partial Q}{\partial t} + \frac{\partial}{\partial x} \left( \frac{Q^2}{A} \right) + gA \frac{\partial h}{\partial x} + gA S_f = 0 \quad (10.10b)$$

(iii) With flow velocity  $V(x, t)$  and depth  $y(x, t)$  as dependent variables By Eq. 10.4 the continuity equation is:

$$\frac{\partial y}{\partial t} + \frac{A}{T} \frac{\partial V}{\partial x} + V \frac{\partial y}{\partial x} + \frac{V}{T} \left( \frac{\partial A}{\partial x} \right)_y = 0 \quad (10.11a)$$

By Eq. 10.7, the momentum equation is

$$\frac{\partial V}{\partial t} + V \frac{\partial V}{\partial x} + g \frac{\partial y}{\partial x} + g(S_0 - S_f) = 0 \quad (10.11b)$$

Eq. 10.11(b) can be written to reflect the significance of various terms as

$$\left[ \begin{array}{c} S_f = S_0 \\ \leftarrow \text{Steady uniform} \rightarrow \\ \text{Steady Non-uniform [GVF]} \\ \leftarrow \text{Unsteady Non-uniform [GVUF]} \rightarrow \end{array} \right] - \frac{\partial}{\partial x} \left( \frac{V^2}{2g} + y \right) - \frac{1}{g} \frac{\partial V}{\partial t} \quad (10.11c)$$

Simplifications have necessarily to be made in the basic equations to obtain analytical solutions and there are many models under this category of simplified equations. One simple model, viz., the uniformly progressive wave is described here as an example.

**Example 10.1** Show that the momentum equation of St. Venant equations can be written with discharge as the primary variable as

$$\frac{1}{Ag} \frac{\partial Q}{\partial t} + \frac{2Q}{A^2g} \frac{\partial Q}{\partial x} + (1 - F^2) \frac{\partial y}{\partial x} = S_0 - S_f$$

where  $F^2 = \frac{Q^2 T}{gA^3}$

Solution Continuity equation is  $\frac{\partial Q}{\partial x} + \frac{\partial A}{\partial t} = 0$

Equation of motion, is  $\frac{\partial y}{\partial x} + \frac{V}{g} \frac{\partial V}{\partial x} + \frac{1}{g} \frac{\partial V}{\partial t} = (S_0 - S_f) \quad (10.7)$

Putting  $V = Q/A$

$$\begin{aligned} \frac{\partial V}{\partial x} &= \frac{\partial}{\partial x} (Q/A) = \frac{1}{A} \frac{\partial Q}{\partial x} - \frac{Q}{A^2} \frac{\partial A}{\partial x} = \frac{1}{A} \frac{\partial Q}{\partial x} - \frac{QT}{A^2} \frac{\partial y}{\partial x} \\ \therefore \frac{V}{g} \frac{\partial V}{\partial x} &= \frac{Q}{A^2g} \frac{\partial Q}{\partial x} - \frac{Q^2 T}{A^2g} \frac{\partial y}{\partial x} = \frac{Q}{A^2g} \frac{\partial Q}{\partial x} - F^2 \frac{\partial y}{\partial x} \end{aligned} \quad (10.12)$$

$$\frac{\partial V}{\partial t} = \frac{\partial}{\partial t}(Q/A) = \frac{1}{A} \frac{\partial Q}{\partial t} - \frac{Q}{A^2} \frac{\partial A}{\partial t} \quad (10.13)$$

But by continuity equation  $\frac{\partial A}{\partial t} = -\frac{\partial Q}{\partial x}$

Hence Eq. 10.13 becomes  $\frac{1}{g} \frac{\partial V}{\partial t} = \frac{1}{Ag} \frac{\partial Q}{\partial t} + \frac{Q}{A^2 g} \frac{\partial Q}{\partial x}$  (10.14)

Substituting 10.12 and 10.14 in Eq 10.7

$$\frac{1}{Ag} \frac{\partial Q}{\partial t} + \frac{2Q}{A^2 g} \frac{\partial Q}{\partial x} + (1 - F^2) \frac{\partial y}{\partial x} = S_0 - S_f \quad (10.14a)$$

### 10.3 UNIFORMLY PROGRESSIVE WAVE

A highly simplified concept of a flood wave is a uniformly progressive wave in which the wave form is assumed to move with its shape unchanged. A particular case of this type of wave is a *monoclinial wave* consisting of only one limb joining two differing uniform flow water levels upstream and downstream of it. Figure 10.3(a) indicates a typical monoclinial wave which is sometimes approximated to the rising limb of a flood wave. In this the wave front moves with a uniform absolute velocity of  $V_w$ . For an observer who moves along with the wave at a velocity  $V_w$ , the wave appears to be stationary. Hence, this unsteady flow situation can be converted into an equivalent steady-state flow by

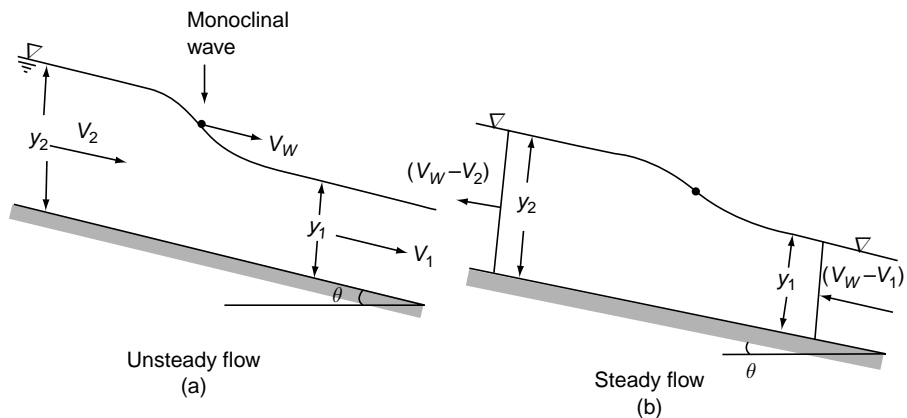


Fig. 10.3 (a) A monoclinial wave (b) Equivalent steady flow

superimposing a velocity  $(-V_w)$  on the system (Fig. 10.3(b)). The continuity equation can then be written as

$$Q_r = A_1 (V_w - V_1) = A_2 (V_w - V_2) = A (V_w - V) \quad (10.15)$$

The quantity  $Q_r$  is termed as *overrun*. Simplifying,

$$V_w = \frac{A_1 V_1 - A_2 V_2}{A_1 - A_2} = \frac{\Delta Q}{\Delta A}$$

From this it may be seen that the maximum value of  $V_w$  is obtained as

$$(V_w)_m = \frac{dQ}{dA} \tag{10.16}$$

Since,  $\frac{dA}{dy} = T$

$$(V_w)_m = \frac{1}{T} \frac{dQ}{dy} \tag{10.17}$$

For a wide rectangular channel, the normal discharge per unit width is

$$q_n = \frac{1}{n} y^{5/3} S_0^{1/2}$$

or,  $\frac{dq_n}{dy} = \frac{5}{3} \frac{1}{n} y^{2/3} S_0^{1/2} = \frac{5}{3} V_n$

where  $V_n = \frac{q_n}{y}$  = normal velocity.

$$\text{Thus } (V_w)_m = k_w V_n \tag{10.18}$$

where  $k_w = 1.67$  for a wide rectangular channel. It can be shown that  $k_w = 1.44$  and  $1.33$  for wide-parabolic ( $R \approx y$ ) and triangular channels respectively. Field observations have indicated that for small rises in the flood stage, the absolute-wave velocities can be roughly estimated by Eq. 10.18.

Considering the equivalent steady-state flow

$$\frac{d}{dt}(V_w - V) = \frac{\partial}{\partial x}(V_w - V) \frac{dx}{dt} + \frac{\partial}{\partial t}(V_w - V) = 0$$

Since  $V_w = \frac{dx}{dt}$  = constant, on simplification,

$$\frac{\partial V}{\partial t} = -V_w \frac{\partial V}{\partial x}$$

Also, since

$$V = V_w - \frac{Q_r}{A}$$

$$\frac{\partial V}{\partial x} = \frac{QT}{A^2} \frac{\partial y}{\partial x}$$



Substituting these in the equation of motion (Eq. 10.7), it can be expressed as

$$\frac{\partial y}{\partial x} + \frac{1}{g}(V - V_w) \frac{\partial V}{\partial x} = S_0 - S_f$$

$$\text{i.e.} \quad \frac{\partial y}{\partial x} = \frac{S_0 - S_f}{1 - \frac{Q_r^2 T}{gA^3}} \quad (10.19)$$

This is the differential equation of a monoclinal rising wave. Note the similarity with the differential equation of GVF (Eq. 4.8). The profile of the wave is obtained by integrating this equation.

Equation 10.19 can be simplified by considering the denominator to be approximately equal to unity for small velocities (i.e. by neglecting the effect of the velocity head) as

$$\frac{\partial y}{\partial x} = S_0 - S_f$$

$$= S_0 \left( 1 - \frac{S_f}{S_0} \right) = S_0 \left( 1 - \frac{Q^2}{Q_n^2} \right)$$

where  $Q_n = K\sqrt{S_0}$  = normal discharge at any depth  $y$  and  $Q$  = actual discharge at that depth. On re-arranging,

$$\frac{Q}{Q_n} = \sqrt{1 - \frac{\partial y / \partial x}{S_0}} \quad (10.20)$$

In a uniformly progressive wave for any point on the wave profile

$$\frac{dy}{dt} = \frac{\partial y}{\partial t} + V_w \frac{\partial y}{\partial x} = 0$$

and hence,

$$\frac{\partial y}{\partial x} = - \frac{\partial y / \partial t}{V_w}$$

Substituting in Eq. 10.20 leads to

$$\frac{Q}{Q_n} = \sqrt{1 + \frac{\partial y / \partial t}{V_w S_0}} \quad (10.21)$$

This equation indicates that during the rising stages in a flood flow, the actual discharge is larger than the discharge read by the normal stage-discharge relationship. Conversely, during the falling stages in a flood flow, the actual discharge is lower than that indicated by the normal stage-discharge curve. Equation 10.21 is used in hydrometry to correct the normal discharges read from a stage-discharge curve when

the depth is changing at a rate  $(\partial y/\partial t)$ . In using this formula for natural channels it is usual to assume  $V_w = 1.4 V_n$ , where  $V_n = Q_n/A$  in cases where  $V_w$  is not known. Also, the energy slope  $S_f$  is used in place of  $S_0$ .

## 10.4 NUMERICAL METHODS

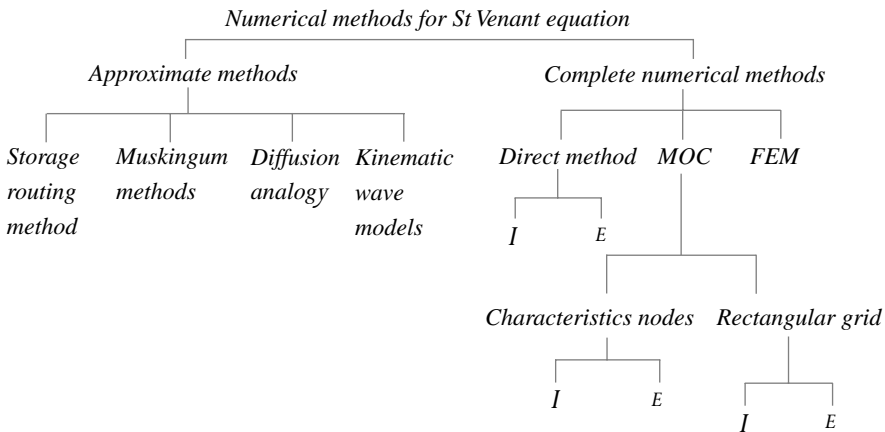
### 10.4.1 Classification

The solution of St Venant equations by analytical methods, as already indicated, has been obtained only for simplified and restricted cases. Graphical solutions are in use since a long time but are seldom preferred these days. The development of modern digital computers during the last three decades has given impetus to the evolution of sophisticated numerical techniques. There are a host of numerical techniques for solving St Venant equations, each claiming certain specific advantages in terms of convergence, stability, accuracy and efficiency. All such techniques can be broadly classified into two categories:

1. Approximate methods which are essentially based on equations of continuity and on a drastically curtailed equation of motion. The storage routing methods popularly adopted by hydrologists, Muskingum method, kinematic wave and diffusion analogy belong to this category.
2. Complete numerical methods which aim to solve the basic St Venant equations through numerical modelling. Several individual methods under this category are available and they can be further classified into sub-classes as in Table 10.1.

In the method of characteristics (MOC), the St Venant equations are converted into a set of two pairs of ordinary differential equations (i.e. characteristic forms)

**Table 10.1** Classification of Numerical Methods for Solving St Venant Equations



*I = Implicit method*

*E = Explicit method*

*MOC = method of characteristics*

*FEM = finite element method*

and then solved by finite-difference methods. In the direct method, the partial derivatives are replaced by finite differences and the resulting algebraic equations are then solved. In the finite-element method (FEM) the system is divided into a number of elements and the partial differential equations are integrated at the nodal points of the elements.

The finite-difference schemes are further classified into explicit and implicit methods. In the explicit method, the finite difference algebraic equations are usually linear and the dependent variables are extracted explicitly at the end of each time step. In the implicit method, the resulting algebraic equations are generally non-linear and the dependent variables occur implicitly. Each of these two methods has different schemes of finite differencing.

To start the solution all methods require an initial condition specifying the values of all the unknowns at an initial time for every computational section along the channel. In the usual subcritical flow, the upstream boundary condition is a hydrograph of the stage or discharge and the downstream boundary condition is normally a stage-discharge relationship. In the absence of a separate resistance formula for unsteady flows, the friction losses are estimated by using a uniform flow resistance equation, typically the Manning's formula is used and in such a case,

$$S_f = \frac{n^2 V^2}{R^{4/3}} = \frac{n^2 Q^2}{A^2 R^{4/3}} = \frac{Q|Q|}{K^2}$$

where  $K$  = conveyance.

### 10.4.2 Method of Characteristics

Consider a unit width of a wide rectangular channel having a GVUF without lateral inflow. Using the celerity of a small wave  $C = \sqrt{gy}$ ,

$$\frac{\partial y}{\partial x} = \frac{2C}{g} \frac{\partial C}{\partial x} \tag{10.22 a}$$

and 
$$\frac{\partial y}{\partial t} = \frac{2C}{g} \frac{\partial C}{\partial t} \tag{10.22 b}$$

Substituting these in the equation of continuity (Eq. 10.2) and noting that for a wide rectangular channel  $T = B = 1.0$  and  $A = y = C^2/g$

$$\frac{2CV}{g} \frac{\partial C}{\partial x} + \frac{C^2}{g} \frac{\partial V}{\partial x} + \frac{2C}{g} \frac{\partial C}{\partial t} = 0 \tag{10.23}$$

The equation of motion (Eq. 10.7) by a similar substitution becomes,

$$\frac{2C}{g} \frac{\partial C}{\partial x} + \frac{V}{g} \frac{\partial V}{\partial x} + \frac{1}{g} \frac{\partial V}{\partial t} = (S_0 - S_f) \tag{10.24}$$

Dividing Eq. 10.23 by  $\pm C$ , adding to Eq. 10.24 and re-arranging,

$$2(C \pm V) \frac{\partial C}{\partial x} \pm 2 \frac{\partial C}{\partial t} + (V \pm C) \frac{\partial V}{\partial x} + \frac{\partial V}{\partial t} = g(S_0 - S_f)$$

On further simplification,

$$\left[ (V \pm C) \frac{\partial}{\partial x} + \frac{\partial}{\partial t} \right] (V \pm 2C) = g(S_0 - S_f) \quad (10.25 \text{ a, b})$$

If 
$$\frac{dy}{dt} = V \pm C, \quad (10.26 \text{ a, b})$$

Eqs 10.26 a,b reduce to

$$\frac{d}{dt} (V \pm 2C) = g(S_0 - S_f) \quad (10.27 \text{ a, b})$$

It may be noted that Eqs 10.27 a, b are satisfied only when Eqs 10.26 a, b are satisfied. Equations 10.26 a, b represent two directions, designated as *characteristics*, namely

1.  $\frac{dx}{dt} = V + C$ , called the positive characteristic: ( $C_+$ ) direction (Eq. 10.26 a).
2.  $\frac{dx}{dt} = V - C$ , called the negative characteristic: ( $C_-$ ) direction (Eq. 10.26 b).

Equations 10.27 a, b represent a pair of ordinary differential equations each valid along the respective characteristic directions and which can be solved by finite difference methods. Similarly, a set of complete equations can be developed for a general prismatic channel.

Considering an  $x-t$  plane, (Fig 10.4), if the depth and velocity are known at two points  $R$  and  $S$ , unknown values of the dependent variables can be found at a point  $P$  which is the intersection of the  $C_+$  characteristic from  $R$  and  $C_-$  characteristic from  $S$ . Thus as a first approximation, from Eq. 10.26 along the  $C_+$  line

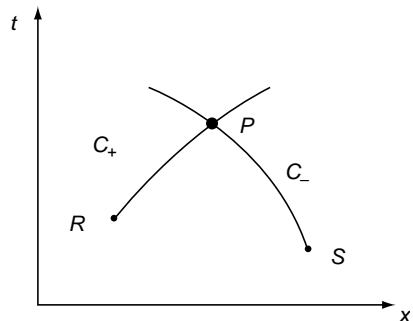


Fig. 10.4 Characteristic lines in the  $x-t$  plane

$$x_P - x_R = (V_R + C_R) (t_P - t_R)$$

and along the  $C_-$  line

$$x_P - x_S = (V_S - C_S) (t_P - t_S)$$

Similarly, from Eq. 10.27,  
for the  $C_+$  line

$$(V_p - V_R) + 2(C_p - C_R) = g(S_0 - S_{fR})(t_p - t_R)$$

and for the  $C_-$  line

$$(V_p - V_S) - 2(C_p - C_S) = g(S_0 - S_{fS})(t_p - t_s)$$

In these four equations there are four unknowns ( $t_p, x_p, V_p$  and  $C_p$ ) which can be

solved. The value of  $y_p$  is calculated from the relation  $y = C^2/g$ . Instead of the above simple finite differencing, other procedures, such as the trapezoidal rule, can be adopted for better accuracy. This procedure of getting  $P$  as the intersection of two characteristics from known points  $R$  and  $S$  is called the *characteristics-grid method*. For a complete numerical solution one boundary condition equation is needed at each end of the channel. A complete solution procedure can be built up on this basis. Let the information along the channel at time  $t$  be known at points 1, 2, 3, ...,  $i$  spaced  $\Delta x_i$  apart (Fig. 10.5). Starting from any three points—say, 2, 3, 4—points  $R$  and  $S$  can be established. Point  $P$  is established by using points  $R$  and  $S$  and the procedure is repeated for the whole  $x-t$  plane. The main advantage of this method is that there is no interpolation but it also has the disadvantage in that the results are obtained at odd  $t$  and  $x$  values.

Another method of solving the characteristic equations is to adopt a rectangular grid work of known spacings in  $t$  and  $x$  axes (Fig. 10.6). The coordinates of  $M, O, N$ , and  $P$  are known. Flow information ( $V$  and  $C$ ) is initially known at  $M, O, N$  and the values of  $V$  and  $C$  at point  $P$  are needed. If  $P$  is the intersection of two characteristics  $C_+$  and  $C_-$ , then  $R$  is the intersections of  $C_+$  characteristic  $PR$  with  $OM$  and  $S$  is the intersection of  $C_-$  characteristic  $PS$  with  $NO$ . Then, as a first approximation

$$\frac{OR}{\Delta t} = V_0 + C_0 \quad \text{and} \quad \frac{SO}{\Delta t} = V_0 - C_0$$

where the suffix '0' denotes the values at point  $O$ . By interpolation between  $O$  and  $M$ , values of  $V_R$  and  $C_R$  are determined. Similarly, by interpolating between  $N$  and  $O$ ,  $V_S$  and  $C_S$  are estimated.

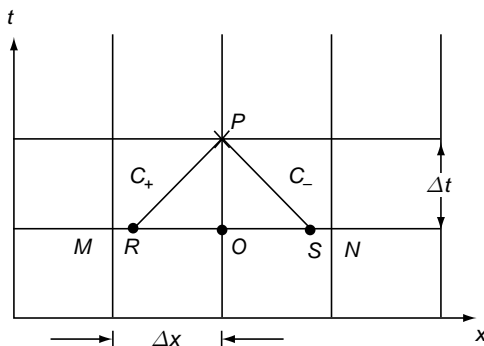


Fig. 10.5 Characteristic grid

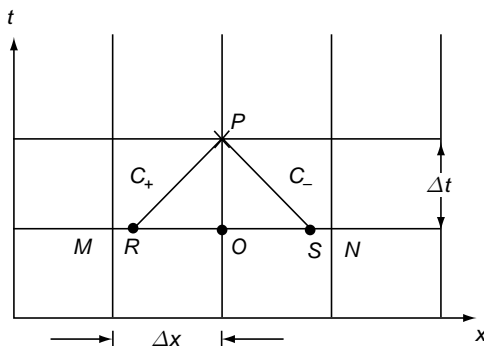


Fig. 10.6 Rectangular grid

where the suffix '0' denotes the values at point  $O$ . By interpolation between  $O$  and  $M$ , values of  $V_R$  and  $C_R$  are determined. Similarly, by interpolating between  $N$  and  $O$ ,  $V_S$  and  $C_S$  are estimated.

Now using a finite-differencing method, the characteristic Eqs 10.25 a, b and 10.27 a, b are solved to obtain  $V_p$  and  $C_p$  at the point  $P$ . The method is repeated for all the nodes of the grid. This method is known as the *rectangular-grid method*.

Basically, four schemes of calculations by MOC are available. These are the *implicit* and *explicit* methods applied to each of the characteristic-grid and rectangular-grid framework (Table 10.1). The details of these various methods and their relative advantages are presented by Wylie<sup>1</sup>. Valuable information on MOC is given by Price<sup>2</sup>, Strelkoff<sup>3</sup> and Choudhry<sup>4</sup>.

The stability of MOC is governed by the *Courant condition*

$$\Delta t \leq \left| \frac{\Delta x}{V \pm C} \right| \tag{10.28}$$

which puts a constraint on the mesh size. Equation 10.28 is automatically satisfied in the characteristics-grid method but a strict adherence to this condition is warranted in the rectangular-grid method. The time steps must be chosen keeping this constraint in mind.

### 10.4.3 Direct Numerical Methods

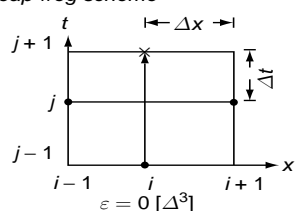
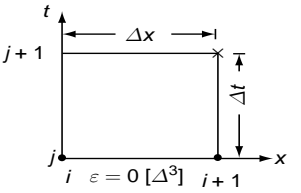
A wide variety of finite-difference schemes exist for solving St Venant equations. A few of these which are in common use are indicated in Table 10.2, in which the finite-difference approximations to the partial derivatives in the  $x-t$  plane and the order of truncation errors, are presented. The substitution of these

**Table 10.2** Finite Difference Schemes for Solving St Venant Equations

$M = f(x, t),$	$\varepsilon = \text{truncation error},$	$X = \text{unknown}$ ● = known
<p>1. Diffusing scheme</p>		
	$\frac{\partial M}{\partial x} = \frac{M_{i+1}^j - M_{i-1}^j}{2\Delta x}$ $\frac{\partial M}{\partial t} = \frac{M_{i+1}^{j+1} - \frac{1}{2}(M_{i+1}^j + M_{i-1}^j)}{\Delta t}$	
<p>2. Upstream differencing scheme</p>		
	$\frac{\partial M}{\partial x} = \frac{M_{i+1}^j - M_i^j}{\Delta x} \quad \text{or} \quad \frac{M_i^j - M_{i-1}^j}{\Delta x}$ $\frac{\partial M}{\partial t} = \frac{M_{i+1}^{j+1} - M_i^j}{\Delta t}$	

(Continued)

Table 10.2 (Continued)

$M = f(x, t),$	$\varepsilon = \text{truncation error},$	$X = \text{unknown}$ • = known
<p>3. Leap-frog scheme</p> 		
		$\frac{\partial M}{\partial x} = \frac{M_{i+1}^j - M_{i-1}^j}{2\Delta x}$
		$\frac{\partial M}{\partial t} = \frac{M_i^{j+1} - M_i^{j-1}}{2\Delta t}$
<p>4. Four point implicit scheme</p> 		
		$\frac{\partial M}{\partial x} = \frac{1}{2\Delta x} (M_{i+1}^j + M_{i+1}^{j+1} - M_i^j - M_i^{j+1})$
		$\frac{\partial M}{\partial t} = \frac{1}{2\Delta t} (M_i^{j+1} + M_{i+1}^{j+1} - M_i^j - M_{i+1}^j)$

approximations to partial derivatives in the St Venant equations result in algebraic equations for the unknowns. In these schemes,  $\Delta t$  and  $\Delta x$  values are fixed to have a rectangular grid in the  $x$ - $t$  plane.

**(a) Explicit Method** In the explicit finite-difference scheme, the St Venant equations are converted into a set of algebraic equations in such a way that the unknown terms ( $V$  and  $y$ ) at the end of a time step are expressed by known terms at the beginning of the time step. Consider, for example, the diffusion scheme. In this scheme (Fig. 10.7), values of  $V$  and  $y$  are known at  $R$  and  $S$  and the values of  $V$  and  $y$  at point

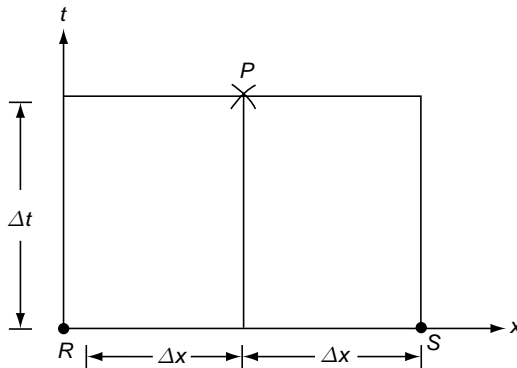


Fig. 10.7 Definition sketch for diffusing scheme

$P$  are desired. This is done by substituting the finite differences for  $\frac{\partial V}{\partial x}$ ,  $\frac{\partial V}{\partial t}$ ,  $\frac{\partial y}{\partial x}$  and  $\frac{\partial y}{\partial t}$  as per the diffusion scheme in Table 10.2, into the St Venant equations. Thus

$$\frac{\partial y}{\partial t} = \frac{y_P - \frac{1}{2}(y_R + y_S)}{\Delta t}$$

$$\frac{\partial y}{\partial x} = \frac{(y_S - y_R)}{2\Delta x}$$

Similar expressions are obtained for  $\frac{\partial V}{\partial t}$  and  $\frac{\partial V}{\partial x}$  also. Further,

$$S_f = \frac{1}{2}(S_{fS} + S_{fR})$$

Substituting these in equations 10.2 and 10.7 and simplifying

$$V_P = \frac{1}{2}(V_R + V_S) + \frac{1}{2} \frac{\Delta t}{\Delta x} \left\{ \frac{1}{2}(V_R^2 - V_S^2) + g(y_R - y_S) \right\} + g\Delta t \left[ S_0 - \frac{1}{2}(S_{fR} + S_{fS}) \right] \quad (10.29)$$

$$y_P = \frac{1}{2}(y_R + y_S) + \frac{\Delta t}{\Delta x} \frac{(Q_R - Q_S)}{(T_R + T_S)} \quad (10.30)$$

From these two equations the two unknowns  $V_P$  and  $y_P$  are solved. The procedure is repeated for all the nodes of the  $x$ - $t$  plane grid. For stability the step sizes  $\Delta t$  and  $\Delta x$  must be so chosen that the Courant condition

$$|C + V| \frac{\Delta t}{\Delta x} \leq 1 \quad (10.31)$$

is satisfied throughout the computation space which in turn puts a limit on the size of time steps. Better accuracy than with the diffusion scheme is obtainable by following other schemes, such as the Leap-Frog or Lax-Wendroff schemes<sup>2</sup>. A variation of Lax-Wendroff scheme, known as McCormack scheme has been widely used in flood routing using explicit scheme<sup>4</sup>.

**(b) Implicit Method** In implicit finite-difference schemes the partial derivatives and the coefficients are replaced in terms of values of the variables at known and unknown time level of the nodes of an elemental cell of size  $\Delta x$  and  $\Delta t$ . The unknown variables therefore appear implicitly in the algebraic equations. The set of



algebraic equations for the entire grid system will have to be solved simultaneously in these methods. Because of the large number of time steps required by an explicit method to route a flood in a channel, implicit methods which can use large time steps without any stability problems are preferred. Several implicit finite-difference schemes have been proposed for the solution of the St Venant equations. Out of these the schemes proposed by Preissmann<sup>4,5</sup>, Amein<sup>6,7</sup>, Strelkoff<sup>3</sup>, Abbot and Ionesq<sup>8</sup>, Beam and Warming<sup>9</sup>, and Liggett and Woolhiser<sup>10</sup> are some of the popular schemes. A few essential details of *Preissmann scheme*, which is by far the most popular of the implicit schemes, are given below.

**Preissmann Scheme** The Preissmann scheme uses a four point weighted method at a point  $P$  as shown in Fig. 10.8. For a given variable  $M$ , such as depth  $y$ , stage  $h$ , or discharge  $Q$ , a weighing coefficient is used to approximate the derivatives and the coefficients are as below:

(i) The time derivatives are

$$\frac{\partial M}{\partial t} \approx \frac{(M_i^{j+1} + M_{i+1}^{j+1}) - (M_i^j + M_{i+1}^j)}{2\Delta t} \quad (10.32)$$

(ii) The space derivatives are

$$\frac{\partial M}{\partial x} \approx \frac{\alpha(M_{i+1}^{j+1} + M_i^{j+1})}{\Delta x} + \frac{(1-\alpha)(M_{i+1}^j - M_i^j)}{\Delta x} \quad (10.33)$$

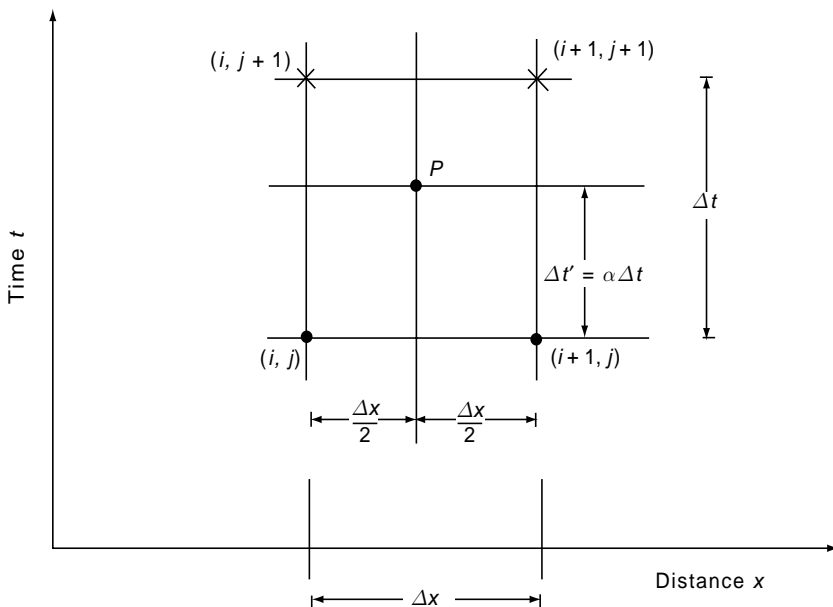


Fig. 10.8 Definition sketch for Preissmann scheme

(iii) The value of  $M$  as a coefficient is

$$M \approx \frac{1}{2}\alpha(M_{i+1}^{j+1} + M_i^{j+1}) + \frac{1}{2}(1-\alpha)(M_{i+1}^j - M_i^j)$$

The value of  $\alpha = \frac{\Delta t'}{\Delta t}$  locates the point  $P$  along the time axis in the finite difference grid.

The Preissmann scheme is unconditionally stable for  $0.50 \leq \alpha \leq 1$ . For typical applications, a value of  $\alpha$  in the range 0.55 to 0.70 is recommended in order to avoid higher order numerical oscillations.

Consider the St. Venant equations in the form of Eqs 10.10a and 10.10b with the discharge  $Q(x, t)$  and stage  $h(x, t)$  as the dependent variables. With

$$S_f = \frac{Q|Q|}{K^2}, \text{ the St Venant equations are}$$

Continuity 
$$\frac{\partial h}{\partial t} + \frac{1}{T} \frac{\partial Q}{\partial x} = 0 \quad (10.10a)$$

Momentum 
$$\frac{\partial Q}{\partial t} + \frac{\partial}{\partial x} \left( \frac{Q^2}{A} \right) + gA \frac{\partial h}{\partial x} + gA \frac{Q|Q|}{K^2} = 0 \quad (10.10c)$$

The application of the Preissmann scheme to the derivatives and the coefficients in the Eqs 10.10a and 10.10c results in

$$\frac{\partial h}{\partial t} \approx \frac{(h_i^{j+1} + h_{i+1}^{j+1}) - (h_i^j + h_{i+1}^j)}{2\Delta t}$$

$$\frac{\partial Q}{\partial t} \approx \frac{(Q_i^{j+1} + Q_{i+1}^{j+1}) - (Q_i^j + Q_{i+1}^j)}{2\Delta t}$$

$$\frac{\partial Q}{\partial x} \approx \frac{\alpha(Q_{i+1}^{j+1} - Q_i^{j+1})}{\Delta x} + \frac{(1-\alpha)(Q_{i+1}^j - Q_i^j)}{\Delta x}$$

$$\frac{\partial}{\partial x} \left( \frac{Q^2}{A} \right) \approx \frac{\alpha}{\Delta x} \left[ \left( \frac{Q^2}{A} \right)_{i+1}^{j+1} - \left( \frac{Q^2}{A} \right)_i^{j+1} \right] + \left[ \frac{(1-\alpha)}{\Delta x} \left[ \frac{Q^2}{A} \right]_{i+1}^j - \left( \frac{Q^2}{A} \right)_i^j \right]$$

$$\frac{\partial h}{\partial x} \approx \frac{\alpha(h_{i+1}^{j+1} - h_i^{j+1})}{\Delta x} + \frac{(1-\alpha)(h_{i+1}^j - h_i^j)}{\Delta x}$$

The coefficients  $A$  and  $T$  are given by —

$$A \approx \frac{1}{2}\alpha(A_{i+1}^{j+1} + A_i^{j+1}) + \frac{1}{2}(1-\alpha)(A_{i+1}^j + A_i^j)$$

$$T \approx \frac{1}{2}\alpha(T_{i+1}^{j+1} + T_i^{j+1}) + \frac{1}{2}(1-\alpha)(T_{i+1}^j + T_i^j)$$

Substituting these expressions in Eq. 10.10a and Eq. 10.10c,

$$\begin{aligned} & \frac{1}{2\Delta t} \left[ (h_i^{j+1} + h_{i+1}^{j+1}) - (h_i^j + h_{i+1}^j) \right] \\ & + \frac{2}{\Delta x} \frac{[\alpha(Q_{i+1}^{j+1} - Q_i^{j+1}) + (1-\alpha)(Q_{i+1}^j - Q_i^j)]}{\alpha(T_{i+1}^{j+1} + T_i^{j+1}) + (1-\alpha)(T_{i+1}^j + T_i^j)} = 0 \end{aligned} \quad (10.34)$$

$$\begin{aligned} & \frac{1}{2\Delta t} \left[ (Q_i^{j+1} + Q_{i+1}^{j+1}) - (Q_i^j + Q_{i+1}^j) \right] \\ & + \frac{\alpha}{\Delta x} \left[ \left( \frac{Q^2}{A} \right)_{i+1}^{j+1} - \left( \frac{Q^2}{A} \right)_i^{j+1} + \frac{(1-\alpha)}{\Delta x} \left( \frac{Q^2}{A} \right)_{i+1}^j - \left( \frac{Q^2}{A} \right)_i^j \right] \\ & + g \left[ \frac{\alpha}{2}(A_{i+1}^{j+1} + A_i^{j+1}) + \frac{(1-\alpha)}{2}(A_{i+1}^j + A_i^j) \right] \left\{ \left[ \frac{\alpha}{\Delta x}(h_{i+1}^{j+1} - h_i^{j+1}) \right. \right. \\ & \left. \left. + \frac{(1-\alpha)}{\Delta x}(h_{i+1}^j - h_i^j) \right] + \frac{1}{2}\alpha \left[ \left( \frac{Q|Q|}{K^2} \right)_{i+1}^{j+1} + \left( \frac{Q|Q|}{K^2} \right)_{i+1}^j \right] \right. \\ & \left. + \frac{(1-\alpha)}{2} \left[ \left( \frac{Q|Q|}{K^2} \right)_{i+1}^j + \left( \frac{Q|Q|}{K^2} \right)_i^j \right] \right\} = 0 \text{ for } 0.5 \leq \alpha \leq 1.0 \end{aligned} \quad (10.35)$$

In these two Eqs 10.34 and 10.35 the terms having superscript  $j$  are known. The unknown terms are those having superscript  $(j + 1)$  and can be expressed in terms of  $Q_i^{j+1}$ ,  $Q_{i+1}^{j+1}$ ,  $h_i^{j+1}$  and  $h_{i+1}^{j+1}$ . As the unknowns are raised to the power other than unity, these equations are non-linear.

If there are a total of  $N$  grid lines at any  $j$  value with the upstream boundary as  $i = 1$  and the downstream boundary as  $i = N$ , there will be  $(N - 1)$  grids at which the above equations are applicable. Thus there are  $(2N - 2)$  equations. Further, there are two unknowns at each of  $N$  grid points, totaling to  $2N$  unknowns. The two additional equations to form the necessary set of equations are supplied by the boundary conditions. In subcritical flows, one boundary condition is applied at the upstream end and another at the downstream boundary. In supercritical flows, however, both the boundary conditions are applied at the upstream end.

The upstream boundary condition is usually a known inflow hydrograph,  $Q_i^{j+1} = f(t^{j+1})$ . The downstream boundary condition is usually a known stage-discharge relationship (i.e. channel rating curve) given as  $Q_N^{j+1} = f(h_N^{j+1})$ . The set of non-linear algebraic equations are solved by adopting an iterative procedure, such as Newton-Raphson method.

It is generally recognized that while an implicit method is more difficult to programme than an explicit method, it has stability, greater accuracy and has economy in computing time. Details on various numerical techniques can be had from Ref. [4, 5]. Extensive bibliography on unsteady flows in open channel flows is available in Ref. [11, 12].

The use of FEM to route floods in channels and natural streams is presented by Cooley and Moin,<sup>13</sup> and King<sup>14</sup>. Szymkiewicz<sup>15</sup> has presented an FEM algorithm to solve St. Venant equations for a channel network. Jie Chen<sup>16</sup> has developed an approximate formulation of St. Venant equations for natural channels which through the use of FEM can be used effectively to simulate dam break problems and flood routing in natural channels.

A large number of software are available, for unsteady flow simulation in general and for flood flow analysis/forecasting and dam break problem in particular. Among these, the HEC-RAS of U.S. Army Corps of Engineers, FLDWAV of U.S. NWS and MIKE-11 of DIH, Denmark are very popular (2007). Among these, HEC-RAS is available along with user's manual (<http://www.hec.usace.army.mill/software/hec-1>) for download by individuals free of charge. Details of MIKE-11 are available at (<http://www.dhigroup.com>). BOSSDAMBRK (<http://www.bossintl.com>), which is commercial software, is an enhanced version of NWS DAMBRK model.

**Example 10.2** Determine the time derivative and space derivative of the flow rate  $Q$  by using Preisman scheme ( $\alpha = 0.65$ ), when the discharges at various  $(x, t)$  values are as given below:

	$x = 1000 \text{ m}$	$x = 1500 \text{ m}$
At $t = 3.0 \text{ h}$	$Q = 125.00 \text{ m}^3/\text{s}$	$Q = 115.00 \text{ m}^3/\text{s}$
At $t = 4.0 \text{ h}$	$Q = 140.00 \text{ m}^3/\text{s}$	$Q = 120.00 \text{ m}^3/\text{s}$

*Solution* Here  $\Delta t = 1.5 \text{ h} = 5400 \text{ s}$  and  $\Delta x = 500 \text{ m}$ .

$$Q_i^j = 125.00 \text{ m}^3/\text{s} \qquad Q_{i+1}^j = 115.00 \text{ m}^3/\text{s}$$

$$Q_i^{j+1} = 140.00 \text{ m}^3/\text{s} \qquad Q_{i+1}^{j+1} = 120.00 \text{ m}^3/\text{s}$$

$$\frac{\partial Q}{\partial t} = \frac{(Q_i^{j+1} + Q_{i+1}^{j+1}) - (Q_{i+1}^j + Q_i^j)}{2\Delta t}$$

$$= \frac{(140.0 + 120.0) - (115.0 + 125.0)}{2 \times 5400} = 0.01852 \text{ m}^3/\text{s/m}$$

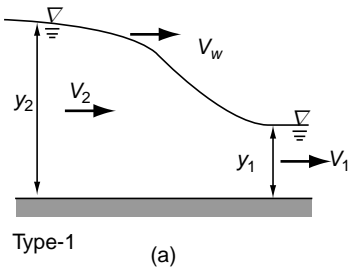
$$\begin{aligned} \frac{\partial Q}{\partial x} &= \alpha \frac{(Q_{i+1}^{j+1} - Q_i^{j+1})}{\Delta x} - \frac{(1-\alpha)}{\Delta x} (Q_{i+1}^j - Q_i^j) \\ &= \frac{0.65 \times (120.0 - 140.0)}{500} - \frac{(1-0.65)}{500} (115.0 - 125.0) = -0.019 \text{ m}^3/\text{s/m} \end{aligned}$$

## 10.5 RAPIDLY VARIED UNSTEADY FLOW – POSITIVE SURGES

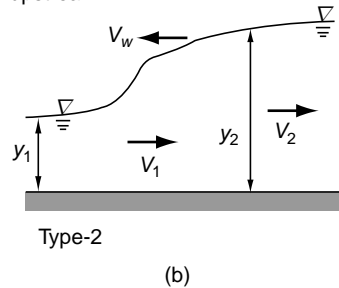
### 10.5.1 Classification

The rapidly-varied transient phenomenon in an open channel, commonly known under the general term surge, occurs wherever there is a sudden change in the discharge or depth or both. Such situations occur, for example, during the sudden closure of a gate. A surge producing an increase in depth is called *positive surge* and the one which causes a decrease in depth is known as *negative surge*. Further,

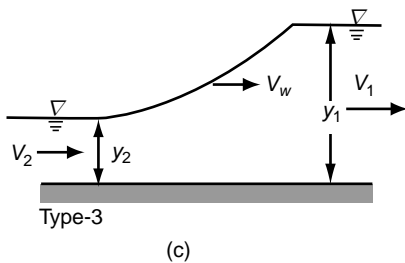
Positive surge moving downstream



Positive surge moving upstream



Negative surge moving downstream



Negative surge moving upstream

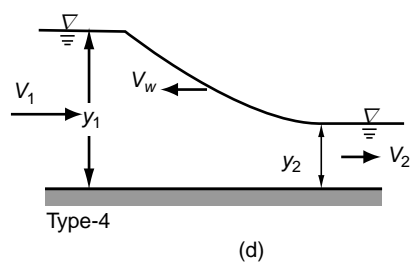


Fig. 10.9 Types of surges

a surge can travel either in the upstream or downstream direction, thus giving rise to four basic types [Fig. 10.9 (a,b,c,d)]. Positive waves generally have steep fronts –sometimes rollers also –and are stable. Consequently they can be considered to be uniformly progressive waves. When the height of a positive surge is small, it can have an undular front. Negative surges, on the hand, are unstable and their form changes with the advance of the surge. Being a rapidly-varied flow phenomenon, friction is usually neglected in the simple analysis of surges.

### 10.5.2 Positive Surge Moving Downstream

Consider a sluice gate in a horizontal frictionless channel suddenly raised to cause a quick change in the depth and hence a positive surge travelling down the channel [Fig. 10.10(a)]. Suffixes 1 and 2 refer to the conditions before and after the passage of the surge, respectively. The absolute velocity  $V_w$  of the surge can be assumed to be constant. The unsteady flow situation is brought to a relative steady state by applying a velocity  $(-V_w)$  to all sections. The resulting flow is indicated in Fig. 10.10(b). In view of the possible loss of energy between Sections 2 and 1 in the equivalent steady

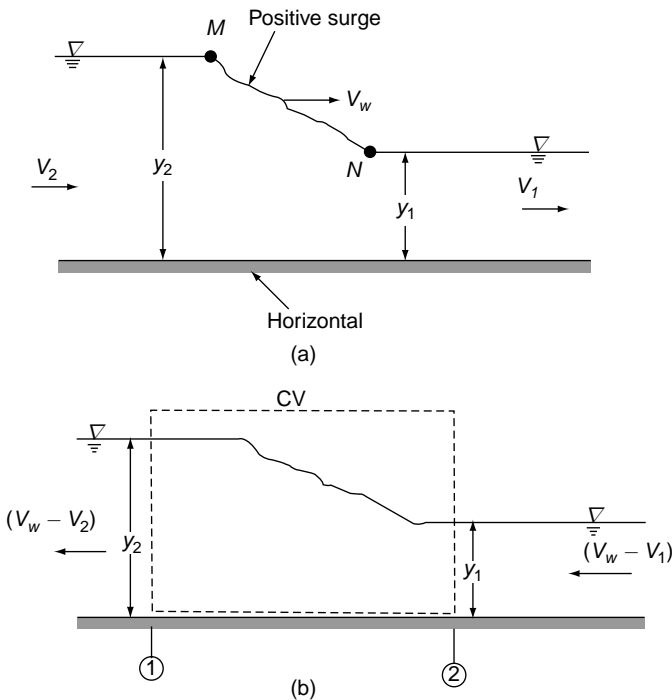


Fig 10.10 (a) Positive surge moving downstream (b) Equivalent steady flow

motion, the linear momentum equation is applied to a control volume enclosing the surge to obtain the equation of motion.

By the continuity equation,

$$A_2(V_w - V_2) = A_1(V_w - V_1) \quad (10.36)$$

The momentum equation, through the assumption of hydrostatic pressure at Sections 1 and 2, yields

$$\gamma A_1 \bar{y}_1 - \gamma A_2 \bar{y}_2 = \frac{\gamma}{g} A_1 (V_w - V_1) [(V_w - V_2) - (V_w - V_1)] \quad (10.37)$$

From Eq. 10.36

$$V_2 = \frac{A_1}{A_2} V_1 + (1 - A_1 / A_2) V_w$$

Substituting this relation in Eq. 10.37,

$$(V_w - V_1)^2 = g \frac{A_2}{A_1 (A_2 - A_1)} (A_2 \bar{y}_2 - A_1 \bar{y}_1) \quad (10.38)$$

$$V_w = V_1 + \sqrt{g (A_2 / A_1) (A_2 \bar{y}_2 - A_1 \bar{y}_1) / (A_2 - A_1)} \quad (10.38a)$$

Since the surge is moving downstream,  $(V_w - V_1)$  is positive and as such only the positive sign of the square root is considered practical.

For a rectangular channel, considering unit width of the channel. The continuity Eq. 10.36 is

$$y_1 (V_w - V_1) = y_2 (V_w - V_2) \quad (10.39)$$

The momentum equation 10.37 is simplified as

$$\frac{1}{2} \gamma y_1^2 - \frac{1}{2} \gamma y_2^2 = \frac{\gamma}{g} y_1 (V_w - V_1) (V_1 - V_2) \quad (10.40)$$

From Eq. 10.39

$$V_2 = \frac{y_1}{y_2} V_1 + \left(1 - \frac{y_1}{y_2}\right) V_w$$

Substituting for  $V_2$  in Eq. 10.40 and on simplifying,

$$\frac{(V_w - V_1)^2}{g y_1} = \frac{1}{2} \frac{y_2}{y_1} \left( \frac{y_2}{y_1} + 1 \right) \quad (10.41)$$

The equation sets 10.36 and 10.38 and 10.39 and 10.41 contain five variables  $y_1$ ,  $y_2$ ,  $V_1$ ,  $V_2$  and  $V_w$ . If three of them are known, the other two can be evaluated. In most of the cases trial and error methods have to be adopted.

**Example 10.3** A 3.0-m wide rectangular channel has a flow of 3.60 m<sup>3</sup>/s with a velocity of 0.8 m/s. If a sudden release of additional flow at the upstream end of the channel causes the depth to rise by 50 per cent, determine the absolute velocity of the resulting surge and the new flow rate.

**Solution** The flow is shown in Fig. 10.11(a). The surge moves in the downstream direction and the absolute velocity of the wave  $V_w$  is positive. By superposing  $(-V_w)$  on the system the equivalent steady flow is obtained (Fig. 10.11 (b)).

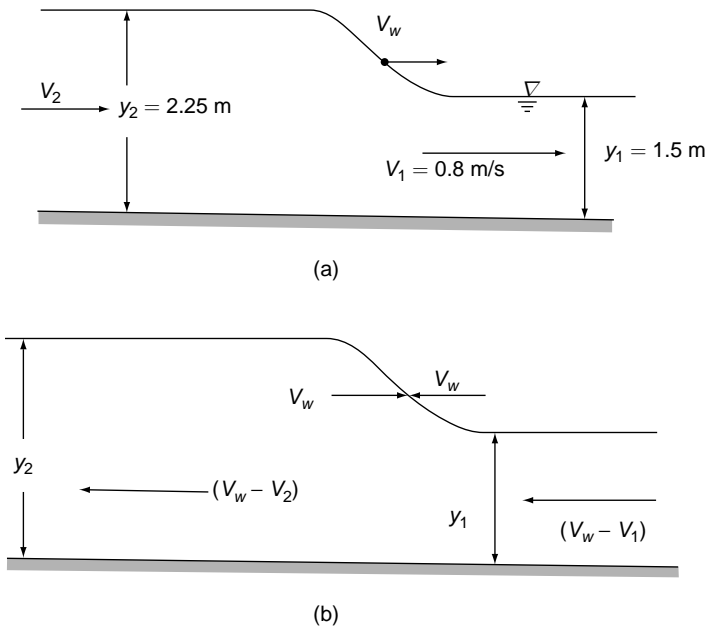


**Fig. 10.11** (a) Positive surge moving downstream (b) Simulated steady flow

$$\text{Here } V_1 = 0.8 \text{ m/s, } y_1 = \frac{3.60}{0.8 \times 3.0} = 1.5 \text{ m, } \frac{y_2}{y_1} = 1.5,$$

$$y_2 = 1.5 \times 1.5 = 2.25 \text{ m} \quad \text{Also } V_2 \text{ is positive.}$$

For a positive surge moving downstream in a rectangular channel, by Eq. 10.41,

$$\frac{(V_w - V_1)^2}{g y_1} = \frac{1}{2} \frac{y_2}{y_1} \left( \frac{y_2}{y_1} + 1 \right)$$

$$\frac{(V_w - 0.8)^2}{9.81 \times 1.5} = \frac{1}{2} \times 1.5 (1.5 + 1)$$



$$(V_w - 0.8)^2 = 27.591 \text{ and by taking the positive root}$$

$$V_w = 6.053 \text{ m/s}$$

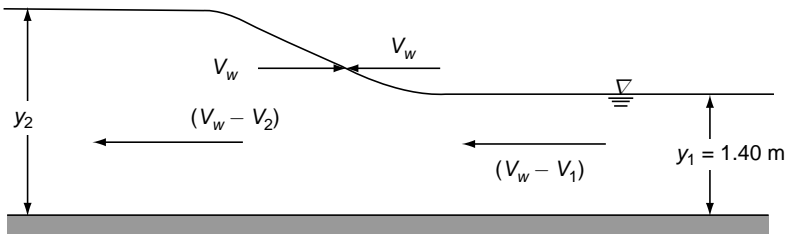
By continuity equation,  $y_1 (V_w - V_1) = y_2 (V_w - V_2)$  and

$$\begin{aligned} V_2 &= \frac{y_1}{y_2} V_1 + \left(1 - \frac{y_1}{y_2}\right) V_w \\ &= \left[\frac{1.5}{2.25} \times 0.8\right] + \left[1 - \frac{1.5}{2.25}\right] \times 6.053 = 2.551 \text{ m/s} \end{aligned}$$

$$\begin{aligned} \text{New flow rate } Q_2 &= B y_2 V_2 = 3.0 \times 2.25 \times 2.551 \\ &= 17.22 \text{ m}^3/\text{s} \end{aligned}$$

**Example 10.4** A rectangular channel carries a flow with a velocity of 0.65 m/s and depth of 1.40 m. If the discharge is abruptly increased threefold by a sudden lifting of a gate on the upstream, estimate the velocity and the height of the resulting surge.

**Solution** The absolute velocity of the surge is  $V_w$  along the downstream direction. By superimposing a velocity  $(-V_w)$  on the system, a steady flow is simulated as shown in Fig. 10.12.



Simulated Steady Flow

Fig. 10.12 Example 10.4

Here  $y_1 = 1.40 \text{ m}$  and  $V_1 = 0.65 \text{ m/s}$ .

$$V_2 y_2 = 3.0 \times 1.40 \times 0.65 = 2.73 \text{ m}^3/\text{s}.$$

By continuity equation,  $y_1 (V_w - V_1) = y_2 (V_w - V_2)$

$$1.40 (V_w - 0.65) = V_w y_2 - 2.73$$

$$V_w (y_2 - 1.40) = 1.82 \quad \text{or} \quad V_w = \frac{1.82}{(y_2 - 1.40)}$$

For a positive surge moving in the downstream direction, by Eq. 10.41

$$\frac{(V_w - V_1)^2}{g y_1} = \frac{1}{2} \frac{y_2}{y_1} \left( \frac{y_2}{y_1} + 1 \right)$$

$$\left[ \frac{1.82}{y_2 - 1.40} - 0.65 \right]^2 = \frac{1}{2} \left( \frac{y_2}{1.40} \right) \left( \frac{y_2}{1.40} + 1 \right)$$

$$\frac{(273 - 0.65y_2)^2}{(y_2 - 1.40)^2} = 3.504 y_2 (1.40 + y_2)$$

By trial and error,  $y_2 = 1.76\text{m}$ .

Height of surge  $\Delta y = y_2 - y_1 = 1.76 - 1.40 = 0.36\text{m}$ .

$$V_w = \frac{1.82}{(1.76 - 1.40)} = 5.06\text{ m/s (in the downstream direction)}.$$

### 10.5.3 Positive Surge Moving Upstream

Figure 10.13(a) shows a positive surge moving upstream. This kind of surge occurs on the upstream of a sluice gate when the gate is closed suddenly and in the phenomenon of tidal bores, (Fig. 10.1). The unsteady flow is converted into an equivalent steady flow by the superposition of a velocity  $V_w$  directed downstream [to the left in Fig. 10.13(a)]. As before, suffixes 1 and 2 refer to conditions at sections of the channel before and after the passage of the surge, respectively.

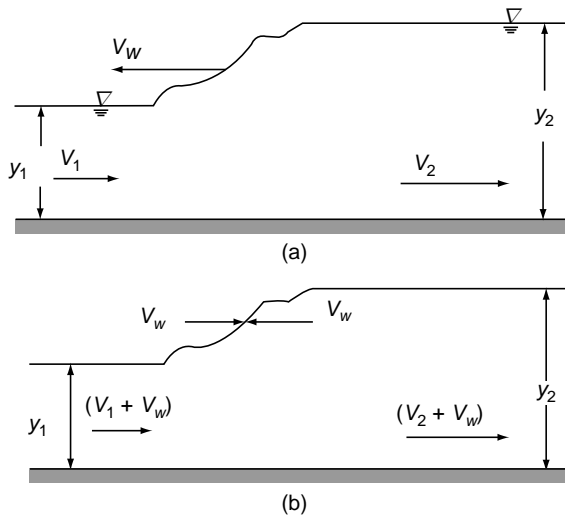


Fig. 10.13 (a) Positive surge moving upstream  
(b) Simulated steady flow

Consider a unit width of a horizontal, frictionless, rectangular channel. Referring to Fig. 10.13(b), the continuity equation is

$$y_1(V_w + V_1) = y_2(V_w + V_2) \tag{10.42}$$

It is seen that the equivalent flow (Fig. 10.13(b)) is similar to a hydraulic jump with initial velocity of  $(V_w + V_1)$  and initial depth of  $y_1$ . The final velocity is  $(V_w + V_2)$  and the depth after the surge is  $y_2$ . By the momentum equation,

$$\begin{aligned} \frac{1}{2} \gamma y_1^2 - \frac{1}{2} \gamma y_2^2 &= \frac{\gamma}{g} y_1 (V_w + V_1) [(V_w + V_2) - (V_w + V_1)] \\ &= \frac{\gamma}{g} y_1 (V_w + V_1) (V_2 - V_1) \end{aligned} \quad (10.43)$$

Using Eq. 10.42, 
$$V_2 = \frac{y_1}{y_2} V_1 - \left(1 - \frac{y_1}{y_2}\right) V_w$$

Substituting this relation, Eq. (10.43) is simplified as

$$\frac{(V_w + V_1)^2}{g y_1} = \frac{1}{2} \frac{y_2}{y_1} \left( \frac{y_2}{y_1} + 1 \right) \quad (10.44)$$

From Eqs 10.44 and 10.42, two of the five variables  $y_1$ ,  $y_2$ ,  $V_1$ ,  $V_2$  and  $V_w$  can be determined if the three other variables are given. It is to be remembered that in real flow  $V_w$  is directed upstream. The velocity  $V_2$  however may be directed upstream or downstream depending on the nature of the bore phenomenon.

### 10.5.4 Moving Hydraulic Jump

The Type-1 and Type-2 surges viz. positive surges moving downstream and moving upstream respectively are often termed *moving hydraulic jumps* in view of their similarity to a steady state hydraulic jump in horizontal channels described in Chapter 6 (Sec. 6.2). This will be clear from a study of the simulated steady flow situations of the above two types of flows as depicted in Fig. 10.10 and Fig. 10.13. This similarity could be used advantageously to develop short cuts to predict some flow parameters of the positive surge phenomenon.

If the velocities relative to the wave velocity  $V_w$  (i.e., the flow situation as would appear to an observer moving along the surge with a velocity  $V_w$ ) are adopted, the relative velocity at Section 1 ( $V_{r1}$ ) can be represented as follows:

1. For Type-1 surge (surge moving downstream)  $V_{r1} = (V_w - V_1)$
2. For Type-2 surge (surge moving upstream)  $V_{r1} = (V_w + V_1)$

With this notation, both Figs 10.10 and 10.13 can be represented by a single Fig. 10.14 which is essentially same as that of a steady flow hydraulic jump.

Further, the Eqs 10.41 and 10.44 obtained by application of momentum equation in Type-1 and Type-2 cases can be expressed by a single equation as below by considering the two surges as a moving hydraulic jump as depicted in Fig. 10.14.

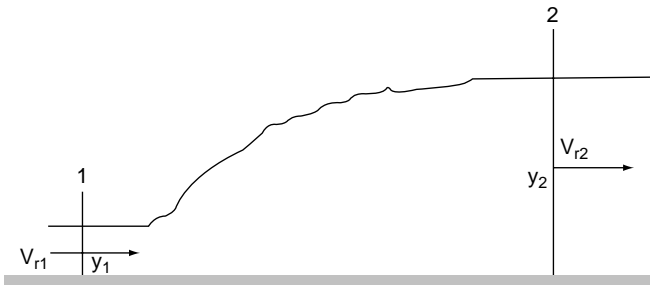


Fig. 10.14 Moving hydraulic jump

$$\frac{V_{r1}^2}{gy_1} = F_{r1}^2 = \frac{1}{2} \frac{y_2}{y_1} \left\{ \frac{y_2}{y_1} + 1 \right\} \tag{10.45}$$

which is of the same form as Eq. 6.3(b) of steady flow hydraulic jump. Using this similarity of form, the ratio  $\frac{y_2}{y_1}$  of the moving hydraulic jump, which is equivalent to the sequent depth ratio of a steady state hydraulic jump, is given by

$$\frac{y_2}{y_1} = \frac{1}{2} \left[ -1 + \sqrt{1 + 8F_{r1}^2} \right] \tag{10.46}$$

The energy loss in the moving hydraulic jump would, by similarity to steady state hydraulic jump, be given by

$$E_L = \frac{(y_2 - y_1)^3}{4y_1y_2} \tag{10.47}$$

which is independent of  $F_{r1}$ . Note that Eqs 10.45 and 10.46 are applicable to both Type-1 and Type-2 surges when the relative velocity  $V_{r1}$  appropriate to the type of surge under study is used. That the concept of treating positive surges as moving hydraulic jump enables the relationships of some parameters to be expressed in a compact form is apparent.

**Example 10.5** | A 4.0-m wide rectangular channel carries a discharge of 12.0 m<sup>3</sup>/s at a depth of 2.0 m. Calculate the height and velocity of a surge produced when the flow is suddenly stopped completely by the full closure of a sluice gate at the downstream end.

**Solution** A positive surge with a velocity ( $-V_w$ ) i.e., travelling upstream, will be generated as a result of the sudden stopping of the flow, (Fig. 10.15(a)). By superimposing a velocity  $V_w$  on the system, a steady flow is simulated as shown in Fig. 10.15(b).

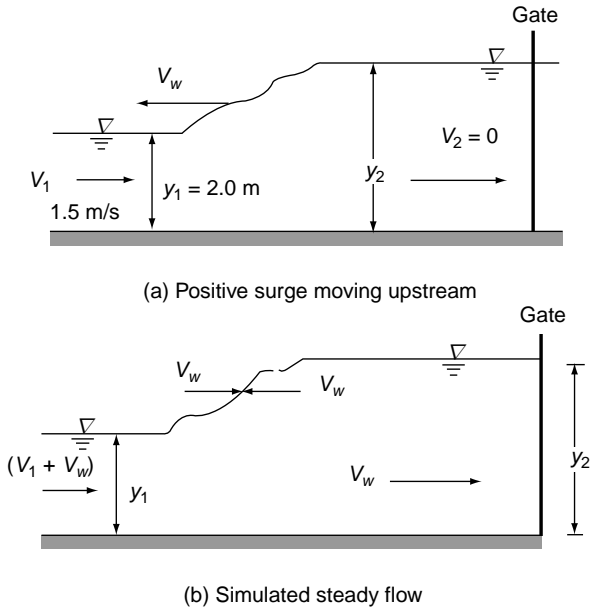


Fig. 10.15 Example 10.5

Here,  $y_1 = 2.0$  m,

$$V_1 = \frac{12.0}{2.0 \times 4.0} = 1.5 \text{ m/s}$$

$$V_2 = 0 \text{ and } y_2 > 2.0$$

By continuity equation, Eq. 10.42,  $y_1(V_w + V_1) = y_2(V_w + V_2)$

$$2.0(1.5 + V_w) = V_w y_2$$

$$V_w = \frac{3.0}{y_2 - 2.0}$$

For a positive surge moving in the upstream direction, by Eq. 10.44

$$\frac{(V_w + V_1)^2}{gy_1} = \frac{1}{2} \frac{y_2}{y_1} \left( \frac{y_2}{y_1} + 1 \right)$$

$$\left[ 1.5 + \left( \frac{3.0}{y_2 - 2.0} \right) \right]^2 = 9.81 \times 2.0 \times \frac{1}{2} \times \frac{y_2}{2.0} \left( \frac{y_2}{2.0} + 1 \right)$$

$$\left[ \frac{1.5y_2}{y_2 - 2.0} \right]^2 = 2.4525 y_2 (y_2 + 2.0)$$

Solving by trial and error,  $y_2 = 2.728$  m.

Height of the surge  $\Delta y = y_2 - y_1 = 0.728$  m.

Velocity of the surge  $V_w = \frac{3.0}{2.728 - 2.0} = 4.121$  m/s in the simulated flow. Hence, the surge is of height 0.728 m and moves upstream with a velocity of 4.121 m/s.

**Example 10.6** In a tidal river the depth and velocity of flow are 0.9 m and 1.25 m/s respectively. Due to tidal action a tidal bore of height 1.2 m is observed to travel upstream. Estimate the height and speed of the bore and the speed of flow after the passage of the bore.

**Solution** Let  $V_w$  (directed downstream) be the velocity of the bore. Superimpose a velocity ( $-V_w$ ) on the system to get simulated flow as shown in Fig. 10.16.

Here  $y_1 = 0.9$  m,  $V_1 = 1.25$  m/s,

$$y_2 = 0.9 + 1.20 = 2.10 \text{ m.}$$

For a positive surge moving in the upstream direction, by Eq. 10.44

$$\frac{(V_w + V_1)^2}{gy_1} = \frac{1}{2} \frac{y_2}{y_1} \left( \frac{y_2}{y_1} + 1 \right)$$

$$(V_w + 1.25)^2 = \frac{9.81 \times 0.9}{2} \times \frac{2.1}{0.9} \times \left( \frac{2.1}{0.9} + 1.0 \right) = 34.335$$

Taking the positive root,  $V_w = 4.61$  m/s

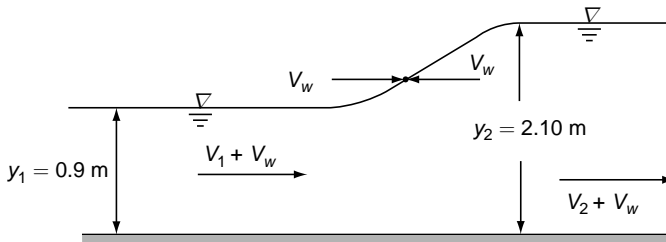


Fig. 10.16 Simulated steady flow

By continuity equation, Eq.10.42,  $y_2(V_w + V_2) = y_1(V_w + V_1)$

$$2.1 (4.61 + V_2) = 0.9 (4.61 + 1.25)$$

$$V_2 = -2.1 \text{ m/s}$$

The bore has a velocity of 4.61 m/s and travels upstream. The river has a velocity of 2.1 m/s directed upstream after the passage of the bore.

## 10.6 RAPIDLY VARIED UNSTEADY FLOW – NEGATIVE SURGES

### 10.6.1 Celerity and Stability of the Surge

The velocity of the surge relative to the initial flow velocity in the canal is known as the celerity of the surge,  $C_s$ . Thus for the surge moving downstream  $C_s = V_w - V_1$  and for the surge moving upstream  $C_s = V_w + V_1$ . From Eqs 10.41 and 10.44 it is seen that in both the cases

$$C_s = \sqrt{\frac{1}{2} g \frac{y_2}{y_1} (y_1 + y_2)} \tag{10.48}$$

For a wave of very small height  $y_2 \rightarrow y_1$  and dropping suffixes,  $C_s = \sqrt{gy}$ , a result which has been used earlier.

Consider a surge moving downstream. If the surge is considered to be made up of a large number of elementary surges of very small height piled one over the other, for each of these  $V_w = V_1 + \sqrt{gy}$ . Consider the top of the surge, (point  $M$  in Fig. 10.10(a)). This point moves faster than the bottom of the surge, (point  $N$  in Fig. 10.10(a)). This causes the top to overtake the lower portions and in this process the flow tumbles down on to the wave front to form a roller of stable shape. Thus the profile of a positive surge is stable and its shape is preserved.

In a negative surge, by a similar argument, a point  $M$  on the top of the surge moves faster than a point on the lower water surface (Fig. 10.17). This results in the stretching of the wave profile. The shape of the negative surge at various time intervals will be different and as such the analysis used in connection with positive surges will not be applicable.

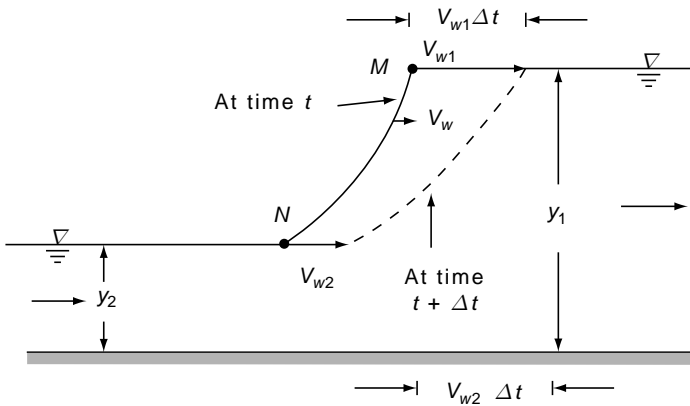


Fig. 10.17 Stretching of a negative surge

For channels of small lengths, the simple analysis of a horizontal frictionless channel gives reasonably good results. However, when the channel length and slope are large, friction and slope effects have to be properly accounted for in a suitable way. Further, changes in the geometry, such as the cross-sectional shape, break in grade and junctions along the channel influence the propagation of surges. A good account of the effect of these factors is available in literature<sup>17,18</sup>.

### 10.6.2 Elementary Negative Wave

Since the shape of a negative surge varies with time due to the stretching of the profile by varying values of  $V_w$  along its height, for purposes of analysis the negative surge is considered to be composed of a series of elementary negative wavelets

of celerity  $\sqrt{gy}$  superimposed on the existing flow. Consider one such elementary negative wave of height  $\delta y$  as in Fig. 10.18(a). The motion is converted to an equivalent steady-state flow by the superimposition of a velocity  $(-V_w)$  on the system. The resulting steady flow is indicated in Fig. 10.18(b). The continuity and momentum equations are applied to a control volume by considering the channel to be rectangular, horizontal and frictionless. The continuity equation is

$$(V_w - V_2) y_2 = (V_w - V_1) y_1$$

Putting  $V_1 = V$ ,  $y_1 = y$  and  $V_2 = V - \delta V$  and  $y_2 = y - \delta y$  and simplifying by neglecting the product of small terms.

$$\delta V y = (V_w - V) \delta y$$

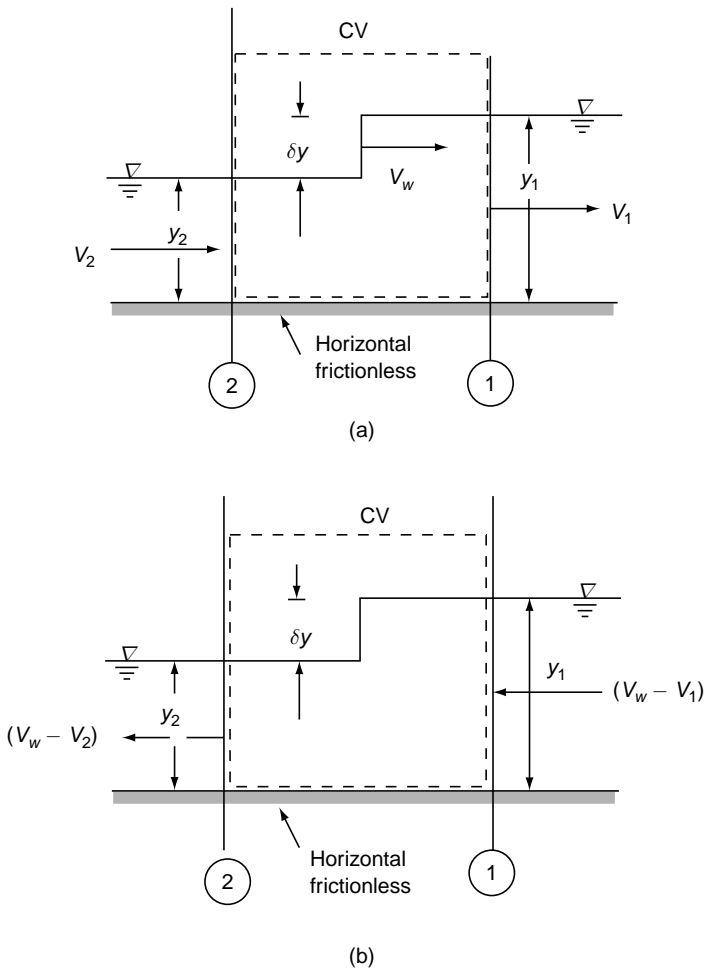


**Fig. 10.18** (a) Elementary negative wave  
(b) Equivalent steady flow



or 
$$\frac{\delta V}{\delta y} = \frac{V_w - V}{y} \quad (10.49)$$

By applying the momentum equation to a control volume enclosing the Sections 1 and 2 in the direction of equivalent steady flow

$$\frac{\gamma}{2} (y_1^2 - y_2^2) = \frac{\gamma}{2} (V_w - V_1) y_1 [(V_w - V_2) - (V_w - V_1)]$$

Introducing the notation as above and neglecting the product of small quantities the momentum equation simplifies to

$$\frac{\delta V}{\delta y} = \frac{g}{(V_w - V)} \quad (10.50)$$

Combining Eqs 10.47 and 10.46

$$(V_w - V)^2 = C^2 = gy$$

or 
$$C = \pm\sqrt{gy} \quad (10.51)$$

in which  $C$  = celerity of the elemental at negative wave.  
Also from Eq. 10.47

$$\frac{\delta V}{\delta y} = \pm\sqrt{g/y}$$

As  $\delta y \rightarrow 0$ , 
$$\frac{dV}{dy} = \pm\sqrt{g/y} \quad (10.52)$$

Equation 10.52 is the basic differential equation governing a simple negative wave which on integration with proper boundary conditions enables the determination of the characteristics of a negative wave.

### 10.6.3 Type 3 Negative Wave Moving Downstream

Consider a sluice gate in a wide rectangular channel passing a flow with a velocity of  $V_1$  and a normal depth of flow of  $y_1$  in the channel downstream of the gate. Consider the sluice gate to partially close instantaneously. Let the new velocity and depth of flow at the gate be  $V_0$  and  $y_0$  respectively. The closure action of the gate would cause a negative wave to form on the downstream channel (Type 3 wave) and the wave would move in the downstream direction as shown in Fig. 10.19. The velocity  $V$  and depth  $y$  at any position  $x$  from the gate is obtained by integrating the basic differential equation of a simple negative wave given by Eq. 10.52.

For the negative wave moving downstream, positive sign in Eq. 10.52 is adopted and the resulting basic differential equation is

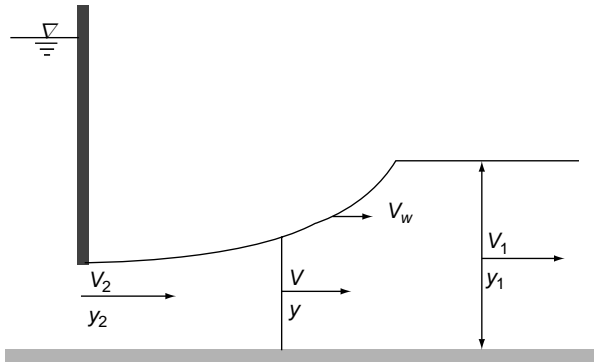


Fig. 10.19 Type-3 negative surge moving downstream

$$\frac{dV}{dy} = \sqrt{gy}$$

On integration  $V = 2\sqrt{gy} + \text{Constant}$

Using the boundary condition  $V = V_1$  at  $y = y_1$

$$V = V_1 + 2\sqrt{gy} - 2\sqrt{gy_1} \tag{10.53}$$

Since the wave travels downstream  $C = V_w - V = \sqrt{gy}$

Hence 
$$V_w = V + \sqrt{gy}$$

$$= V_1 + 3\sqrt{gy} - 2\sqrt{gy_1} \tag{10.53a}$$

If the gate movement is instantaneous at  $t = 0$ , with reference to the co-ordinates shown in Fig. 10.19,  $V_w$  is in the direction of positive  $x$  and hence the profile of the negative wave surface is given by  $V_w = \frac{dx}{dt}$

$$x = V_w t$$

$$x = (V_1 + 3\sqrt{gy} - 2\sqrt{gy_1})t \tag{10.54}$$

Equation 10.54 is the expression for the profile of the negative wave in terms of  $x$ ,  $y$  and  $t$ . This equation is valid for the values of  $y$  between  $y_0$  and  $y_1$ . Substituting in Eq. 10.54, the value of  $\sqrt{gy}$  obtained from Eq. 10.53,

$$x = \left( -\frac{V_1}{2} + \frac{3}{2}V + \sqrt{gy_1} \right) t$$

or

$$V = \left( \frac{2x}{3t} + \frac{V_1}{3} - \frac{2}{3}\sqrt{gy_1} \right) \quad (10.55)$$

Equation 10.55 gives the value of velocity in terms of  $x$  and  $t$ .

Note that the Eqs 10.50, 10.51 and 10.52 can be used for instantaneous complete closure also, in which case  $V_0 = 0$  and  $y_0 = 0$ .

**Example 10.7** | A sluice gate in a wide channel controls the flow of water. When the flow in the downstream channel was at a depth of 2.0 m with a velocity of 4.0 m/s, the sluice gate was partially closed, instantaneously, to reduce the discharge to 25% of its initial value. Estimate the velocity and depth at the gate as well as the surface profile of the negative wave downstream of the gate.

*Solution* Let suffix 1 refers to flow conditions before the gate closure and suffix 2 conditions after the passage of negative wave.

Prior velocity  $V_1 = 4.0$  m/s

New discharge  $q = \frac{4.0 \times 2.0}{4} = 2.0 \text{ m}^3/\text{s} = V_1 y_1$

From Eq. 10.50,  $V = V_1 + 2\sqrt{gy} - 2\sqrt{gy_1}$

$$V_2 = 4.0 + 2\sqrt{9.81y_2} - 2\sqrt{9.81 \times 2.0}$$

$$V_2 = 6.2642\sqrt{y_2} - 4.8589 \quad (10.56)$$

Also  $V_2 y_2 = 2.0 \quad (10.57)$

Solving by trial and error,  $V_2 = 1.781$  m/s and  $y_2 = 1.123$  m

For the profile substituting for  $V_1$  and  $y_1$  in Eq. 10.51

$$\begin{aligned} x &= \left( V_1 + 3\sqrt{gy} - 2\sqrt{gy_1} \right) t \\ &= \left( 4.0 + 3\sqrt{9.81y} - 2\sqrt{9.81 \times 2.0} \right) t \\ x &= \left( 9.396\sqrt{y} - 4.859 \right) t \end{aligned} \quad (10.58)$$

Equation (c) represents a parabola, concave upwards, and holds good for values of  $y$  in the range 1.123 m to 2.0 m.

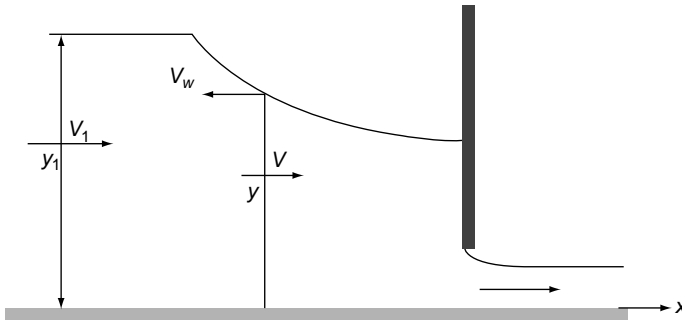


Fig. 10.20 Type – 4 negative surge moving downstream

### 10.6.4 Type 4 – Negative Surge Moving Upstream

Figure 10.20 shows a negative surge produced by instantaneous raising of a sluice gate located at the downstream end of a horizontal, frictionless channel. Type-4 negative wave which starts at the gate is shown moving upstream.

Integrating the basic differential equation, Eq. 10.51, the relationship between the velocity and depth is obtained as

$$V = -2\sqrt{gy} + \text{constant} \tag{10.59}$$

Using suffixes 1 and 2 to denote conditions before and after the passage of the wave respectively, and using the boundary condition  $V = V_1$  at  $y = y_1$

$$V = V_1 + 2\sqrt{gy_1} - 2\sqrt{gy} \tag{10.60}$$

Note that the negative sign of Eq. 10.52 has been used in deriving Eq. 10.59. This is done to obtain positive values of  $V$  for all relevant values of depth  $y$ .

The celerity of the wave  $C$  in this case is

$$C = V_w + V = \sqrt{gy}$$

or

$$\begin{aligned} V_w &= \sqrt{gy} - V \\ &= 3\sqrt{gy} - 2\sqrt{gy_1} - V_1 \end{aligned} \tag{10.61}$$

With reference to the co-ordinate system shown in Fig. 10.20, the wave velocity  $V_w$  is negative in major part of the wave and positive in the lower depths. Considering

$$V_w = -\frac{dx}{dt}$$

the profile of the negative wave is given by

$$(-x) = V_w t = (3\sqrt{gy} - 2\sqrt{gy_1} - V_1)t \tag{10.62}$$

### 10.6.5 Dam Break Problem

A particular case of the above Type-4 negative surge is the situation with  $V_1 = 0$ . This situation models the propagation of a negative wave on the upstream due to instantaneous complete lifting of a control gate at a reservoir. This ideal sudden release of flow from a reservoir simulates the sudden breaking of a dam holding up a reservoir and as such this problem is known as *Dam Break problem*.

Figure 10.21 shows the flow situation due to sudden release of water from an impounding structure. This is a special case of Type-4 wave with  $V_1 = 0$ . The coordinate system used is :  $x = 0$  and  $y = 0$  at the bottom of the gate;  $x$  is positive in the downstream direction from the gate and negative in the upstream direction from the gate;  $y$  is positive vertically upwards. By Eq. 10.61

$$V_w = 3\sqrt{gy} - 2\sqrt{gy_1} \tag{10.63}$$

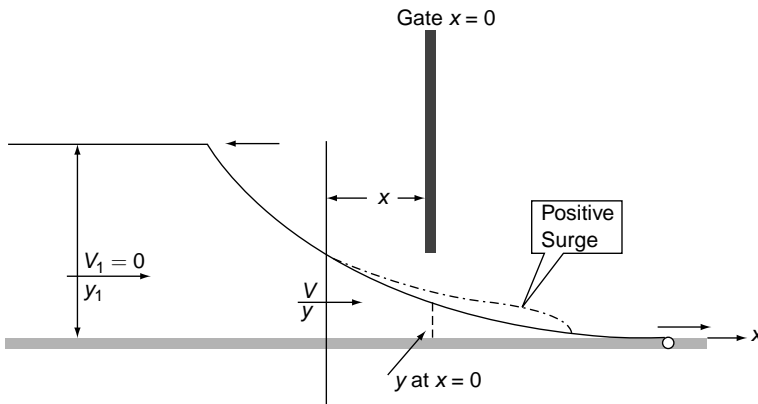


Fig. 10.21 Dam break Problem

and by Eq. 10.60 the velocity at any section is

$$V = 2\sqrt{gy_1} - 2\sqrt{gy} \tag{10.64}$$

The water surface profile of the negative wave is

$$(-x) = (3\sqrt{gy} - 2\sqrt{gy_1})t \tag{10.65}$$

The profile is a concave upwards parabola. The conditions at the gate are interesting. At the gate,  $x = 0$  and using the suffix 0 to indicate the values at the gate, from Eq.10.65

$$\sqrt{y_0} = \frac{2}{3}\sqrt{y_1}$$

i.e., 
$$y_0 = \frac{4}{9} y_1 \tag{10.66}$$

Note that  $y_0$  is independent of time and as such is constant. The salient features of the wave profile are as follows:

$$\begin{aligned} \text{At } y = 0 & \quad x = 2t\sqrt{gy_1} \\ \text{At } y = y_1 & \quad x = -t\sqrt{gy_1} \text{ and} \\ \text{At } x = 0 & \quad y = \frac{4}{9} y_1 \end{aligned}$$

The velocity at the gate  $V_0$  by Eq. 10.64 is

$$V_0 = \frac{2}{3} \sqrt{gy_1} \tag{10.67}$$

The discharge intensity 
$$q = V_0 y_0 = \left( \frac{2}{3} \sqrt{gy_1} \right) \left( \frac{4}{9} y_1 \right) = \frac{8}{27} \sqrt{gy_1^3} \tag{10.68}$$

which is also independent of time  $t$ .

Note that the flow is being analyzed in a horizontal frictionless channel and as such the depth  $y_1$  with  $V_1 = 0$  represents the specific energy,  $E$ . At the gate axis ( $x = 0$ )

$$y_0 = \frac{2}{3} y_1 = \frac{2}{3} E = \text{Critical depth}$$

Also at  $x = 0$ , the Froude number of the flow 
$$F_0 = \frac{V_0}{\sqrt{gy_0}} = \frac{\frac{2}{3} \sqrt{gy_1}}{\sqrt{g \left( \frac{4}{9} y_1 \right)}} = 1.0. \text{ Thus}$$

the flow at the gate axis is critical and the discharge maximum. Further, it is easy to see that upstream of the gate the flow is subcritical and on the downstream of the gate (for positive values of  $x$ ) the flow is supercritical.

This simple ideal analysis of a sudden release from an impounding structure is found to give satisfactory results for a major part of the profile. However, in real situation the downstream end is found to have a rounded positive wave instead of the parabolic profile with its vertex on the  $x$ -axis. In actual dam break the tapered leading edge of the ideal profile is modified due to action of ground friction to cause a positive surge to move downstream. Details about dam break analysis are found in Refs. 4, 19 & 20.

### 10.6.6 Partial lifting of Downstream Gate

A variation of the dam break problem is the case of partial instantaneous lifting of the downstream gate from initial closed position. A simple case of a sluice gate in a rectangular channel of width  $B$  is analyzed as follows.

Consider the sluice gate to be suddenly raised by an amount  $a$  from an initial closed position. If  $a \geq \frac{4}{9} y_1$ , then it amounts to full raised position as indicated in the previous section and the analysis is that of the dam break problem. However, if  $a < \frac{4}{9} y_1$ , then it is partial closure and an analysis for such a case is given below.

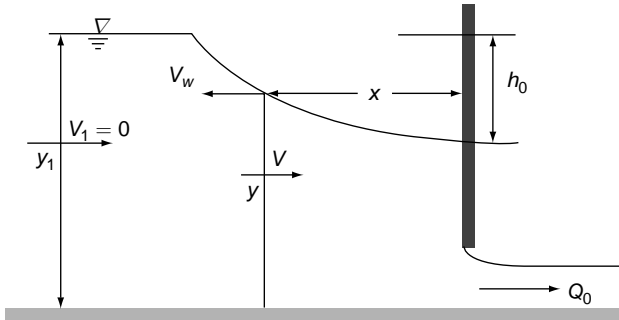


Fig. 10.22 Partial lifting of downstream gate

Refer to Fig. 10.22. Before the operation of the gate, the water upstream of the gate is at rest at a depth  $y_1$ . The gate is lifted instantaneously, and partially, so that  $h_0 =$  drawdown at the gate. A negative wave produced by this action travels upstream with a wave velocity  $V_w$  given by Eq. 10.61 and a forward flow velocity  $V$  is created and is described by Eq. 10.53. Since  $V_1 = 0$ , Eq. 10.61 and 10.60 become,

$$V_w = 3\sqrt{gy} - 2\sqrt{gy_1}$$

$$V = -2\sqrt{gy} + 2\sqrt{gy_1}$$

At  $x = 0$   $y_0 = (y_1 - h_0)$  and velocity  $V = V_0$

Thus 
$$V_0 = 2\sqrt{gy_1} - 2\sqrt{g(y_1 - h_0)} \tag{10.69}$$

The discharge  $Q_0 = By_0 V_0$  which is constant as  $V_0$  and  $y_0$  do not change with time.  $Q_0$  can be expressed in terms of  $h_0$  and  $y_1$  for substituting for  $y_0$  and  $V_0$ , as

$$Q_0 = B (y_1 - h_0) \left( 2\sqrt{gy_1} - 2\sqrt{g(y_1 - h_0)} \right)$$

On simplification, an expression for the discharge can be obtained in non-dimensional form as

$$\frac{Q_0}{By_1\sqrt{gy_1}} = 2 \left( 1 - \frac{h_0}{y_1} \right) \left[ 1 - \sqrt{1 - \frac{h_0}{y_1}} \right] \tag{10.70}$$

Wave Profile: The profile of the negative wave at any time  $t$  is given as

$$(-x) = V_w t = (2\sqrt{gy_1} - 3\sqrt{gy}) t \quad (10.71)$$

where  $y$  = depth of flow at any  $(x, t)$ .

**Example 10.8** | A reservoir having water to a depth of 40 m undergoes an instantaneous, ideal, dam break. Estimate the depth and discharge intensity at the dam site and the water surface profile of the negative wave 3 seconds after the dam break.

*Solution* The water surface profile with positive  $x$  in the downstream of the gate axis, is by Eq. 10.65 is

$$\begin{aligned} (-x) &= (3\sqrt{gy} - 2\sqrt{gy_1})t \\ (-x) &= (3\sqrt{9.81 \times y} - 2\sqrt{9.81 \times 40})t \\ x &= 39.62 t - 9.396 \sqrt{y} \end{aligned}$$

At  $x = 0$ ,  $y = y_0 = (39.62/9.396) = 17.78$  m.

Velocity at  $x = 0$ ,  $V = V_0 = \frac{2}{3}\sqrt{gy_1} = \frac{2}{3}\sqrt{9.81 \times 40} = 13.21$  m/s

Profile after 3 seconds:  $x = 39.62 \times 3 - 9.396 \times 3 \sqrt{y}$

$$: x = 118.86 - 28.188 \sqrt{y}$$

**Example 10.9** | A wide rectangular horizontal channel is passing a discharge of  $1.5 \text{ m}^3/\text{s}/\text{m}$  at a depth of 3.0 m. The flow is controlled by a sluice gate at the downstream end. If the gate is abruptly raised by a certain extent to pass a flow of  $3.0 \text{ m}^3/\text{s}/\text{m}$  to the downstream, estimate (i) the new depth and velocity of flow in the channel at a section when the negative surge has passed it, (ii) the maximum wave velocity of the negative surge, and (iii) profile of the negative surge.

*Solution* This is a case of Type-4 wave, where the negative wave moves upstream. Using the suffix 1 for the conditions before the passage and 2 for conditions after the passage of the negative wave and suffix 0 to the position of the gate,

Velocity at any section

$$\begin{aligned} V &= V_1 + 2\sqrt{gy_1} - 2\sqrt{gy}. \text{ Here } y_1 = 3.0 \text{ m and } V_1 = 1.5/3.0 = 0.5 \text{ m/s.} \\ V &= 0.5 + 2\sqrt{9.81 \times 3.0} - 2\sqrt{9.81 \times y} \\ &= 11.35 - 6.264 \sqrt{y} \end{aligned} \quad (10.72)$$



After the passage of wave,  $V_2 = 3.0/y_2$  and from Eq. 10.72  $V_2 = 11.35 - 6.264\sqrt{y}$

By trial and error,  $y_2 = 2.66$  m and  $V_2 = 1.13$  m/s.

$$\begin{aligned} \text{Velocity of wave, by Eq. 10.61: } V_w &= 3\sqrt{gy} - 2\sqrt{gy_1} - V_1 \\ &= 3\sqrt{gy} - 2\sqrt{9.18 \times 3.0} - 0.5 = 3\sqrt{gy} - 11.35 \end{aligned}$$

$V_w$  is maximum at  $y = y_1$  and hence max.  $V_w = 3\sqrt{9.81 \times 3.0} - 11.35 = 4.925$  m/s

$$\begin{aligned} \text{Wave profile is given by Eq. 10.62 as } (-x) &= (3\sqrt{gy} - 2\sqrt{gy_1} - V_1)t \\ -x &= (3\sqrt{9.81y} - 2\sqrt{9.81 \times 3.0} - 0.5)t \\ x &= (11.35 - 6.264\sqrt{y})t \end{aligned}$$

(The profile is in the negative  $x$  direction.)



## REFERENCES

1. Wylie, E B, 'Unsteady Free Surface Flow Computation', *Jour. of Hyd. Div., Proc. ASCE*, Nov. 1970, pp 2241–2251.
2. Price, R K, 'Comparison of Four Numerical Methods for Flood Routing', *Jour. of Hyd. Div., Proc. ASCE*, July 1974, pp 879–899.
3. Strelkoff, T, 'Numerical Solution of St Venant Equations', *Jour. of Hyd. Div., Proc. ASCE*, Jan. 1970, pp 223–252.
4. Chaudhry, M H, *Open Channel Flow*, Prentice-Hall, New Jersey, USA, 1993.
5. Cunge, J A, Holly, F M, and Verwey, A, *Practical Aspects of Computational River Hydraulics*, Pitman Adv. Pub. Program, Pitman, London, UK, 1980.
6. Amien, M, and Fang, C S, 'Implicit Flood Routing in Natural Channels', *Jour. of Hyd. Div., Proc. ASCE*, Dec. 1970, pp 2481–2500.
7. Amien, M, and Chu, H L, 'Implicit Numerical Modelling of Unsteady Flows', *Jour. of Hyd. Div., Proc. ASCE*, Dec. 1970, pp 717–731.
8. Abbot, M B, and Ionesq, F, 'On the Numerical Computation of Nearly Horizontal Flows', *Jour of Hyd. Res., IAHR*, Vol. 5, No. 2, 1967, pp 96–117.
9. Beam, R M, and Warming, R F, 'An Implicit Finite Difference Algorithm for Hyperbolic Systems in Conservation Law Forms' *Jour. of Comp. Physics*, Vol. 22, 1976, pp. 87–110.
10. Liggett, J A, and Woolhiser, D A, 'Difference Solutions of the Shallow Water Equation', *Jour. of Engg. Mech. Div., Proc. ASCE*, April 1967, pp 39–71.
11. Miller, W A, Jr and Yevjevich, V, (Ed), *Unsteady Flow in Open Channels*. Vol. III-Bibliography., Water Resources Publications, Fort Collins, Colo., USA, 1975.
12. Chow, V T, Maidment, D R, and Mays, L W, *Applied Hydrology*, McGraw-Hill, Singapore, 1988.
13. Cooley, R L, and Moin, S A, 'Finite Element Solution of St. Venant Equations', *Jour. of Hyd. Div., Proc. ASCE*, June 1976, pp 759–775.
14. King, I P, 'Finite element models for unsteady flow through irregular channels', *Proc. First conf. on Finite Elements in Water Resources*, Princeton Univ., USA, July 1976; *Finite Elements in Water Resources*, Pentech Press, 1977, pp 165–184.

15. Szymkiewicz, R, 'Finite element method for the solution of the St Venant equations in an open channel network', *Jour. of Hydrology*, 1991, pp 270–287.
16. Jie Chen, *et al*, "Conservative Formulation for Natural Open Channel and Finite-Element Implementation", *Jour.l of Hyd. Engg.*, Vol. 133, No. 9, Sept. 2007, pp 1064–1073.
17. Jaeger, C, *Engineering Fluid Mechanics*, Blackie and Son Ltd., London, UK, 1956.
18. Chow, V T, *Open Channel Hydraulics*, McGraw – Hill, New York, USA, 1959.
19. Mahmood, K, and Yevdjovich, V, (Ed), *Unsteady Flow in Open Channels*, 3 Vols, Water Resources Publications, Fort Collins, Colo., USA, 1975.
20. French, R H, *Open Channel Hydraulics*, McGraw – Hill Book Co., New York, USA, 1986.

## PROBLEMS

### Problem Distribution

	Topic	Problems
1	Equation of motion of GVUF	10.1–10.2
2	Monoclinal wave	10.3
3	Positive surge	10.4–10.13
4	Negative surge	10.14–10.16

- 10.1 Show that the continuity equation for a GVUF in a non prismatic channel with no lateral in flow is

$$A \frac{\partial V}{\partial x} + VT \frac{\partial y}{\partial x} + \epsilon yV \frac{\partial T}{\partial x} + T \frac{\partial y}{\partial x} = 0$$

where  $\epsilon$  = a coefficient which depends on the nature of the non-prismaticity of the channel with  $\epsilon = 0.5$  and  $1.0$  for triangular and rectangular channels respectively.

- 10.2 Derive the equation of motion for GVUF in a channel having a lateral outflow  $q$  per unit length as

$$\frac{\partial y}{\partial x} + \frac{V}{g} \frac{\partial V}{\partial x} + \frac{1}{g} \frac{\partial V}{\partial t} = S_0 - S_j - D_L$$

where  $D_L = 0$  for bulk lateral outflow as over a side spillway, and  $D_L = \left( \frac{V-u}{Ag} \right) q$  for lateral inflow with  $x$  component of the inflow velocity  $= u$ ;

- 10.3 Show that by using the Chezy formula with  $C = \text{constant}$ , the ratio  $(V_w)_m / V_n$  of a monoclinal wave is  $1.50$  and  $1.25$  for wide rectangular and triangular channels respectively.
- 10.4 Show that the celerity of a positive surge in a prismatic channel can be approximated for small surge heights  $h$  relative to the area  $A$  as

$$C \approx + \sqrt{g \left( \frac{A}{T} + \frac{3}{2}h + \frac{Th^2}{2A} \right)} \approx + \sqrt{g \left( \frac{A}{T} + \frac{3}{2}h \right)}$$

10.5 For a positive surge travelling in a horizontal rectangular channel, fill in the blanks in the following table

Sl. No.	$y_1$ (m)	$V_1$ (m/s)	$y_2$ (m)	$V_2$ (m/s)	$V_H$ (m/s)
a	2.00	1.50	4.00	–	–
b	1.00	1.75	–	–	+5.50
c	1.75	0.70	–	–	–5.00
d	–	3.00	1.50	–	–3.00
e	0.30	–	0.60	–	3.50

- 10.6 At a point in a shallow lake, a boat moving with a speed of 20 km/h is found to create a wave which rises 35 cm above the undisturbed water surface. Find the approximate depth of the lake at this point.
- 10.7 A positive surge is often known as a moving hydraulic jump. Obtain an expression in terms of depths  $y_1$  and  $y_2$  for the energy loss in a moving hydraulic jump in a horizontal rectangular channel. Estimate the energy loss when  $y_1 = 0.9$  m and  $y_2 = 2.10$  m.
- 10.8 A rectangular channel carries a discharge of  $1.50 \text{ m}^3/\text{s}$  per metre width at a depth of 0.75 m. If the sudden operation of a sluice gate at an upstream section causes the discharge to increase by 33 per cent, estimate the height and absolute velocity of the positive surge in the channel.
- 10.9 The depth and velocity of flow in a rectangular channel are 0.9 m/s and 1.5 m/s respectively. If a gate at the downstream end of the channel is abruptly closed, what will be the height and absolute velocity of the resulting surge?
- 10.10 A 2.0 m wide rectangular channel, 2 km long carries a steady flow of  $4.6 \text{ m}^3/\text{s}$  at a depth of 1.15. The sides of the channel are 2.0 m high. If the flow is suddenly stopped by the closure of a gate at the downstream end, will the water spill over the sides of the channel? If there is no spillage, what minimum time interval must elapse before the arrival of the surge at the upstream end?
- 10.11 A trapezoidal canal with  $B = 5.0$  m and side slope 1H : 1V, carries a discharge of  $30.0 \text{ m}^3/\text{s}$  at a depth of 3.0 m. Calculate the speed and height of a positive surge (i) if the flow in the canal is suddenly stopped by the operation of a gate at a downstream section, (ii) if the discharge is suddenly increased to  $45.0 \text{ m}^3/\text{s}$   
(Hint: Use the equation for the celerity given in Problem 10.6 and a trial-and-error procedure).
- 10.12 A wide tidal river has a low water velocity of 1.5 m/s and a depth of flow of 2.5 m. A tide in the sea causes a bore which travels upstream, (a) If the height of the bore is 0.90 m, estimate the speed of the bore and the velocity of flow after its passage, (b) If the bore is observed to cover a distance of 2.5 km in 10 minutes determine its height.
- 10.13 Show that in a positive surge moving down a rectangular channel with absolute velocity  $V_w$ , the depths before the passage of the surge  $y_1$  and after the passage are related by a function of the Froude number of the relative velocity.
- 10.14 A wide rectangular channel carries a discharge of  $10 \text{ m}^3/\text{s}/\text{m}$  at a depth of 3.0 m. Through operation of a gate at its upstream end, the discharge is reduced instantaneously to  $4.0 \text{ m}^3/\text{s}$ . Estimate the height of the negative wave and the velocity of flow in the channel downstream of the gate after the event.
- 10.15 A small dam stores 9 m of water in the reservoir created by it. If a wide section of the dam collapse instantaneously, using the ideal dam break solution, estimate the discharge, depth of flow at the axis of the dam and surface profile 2 s after the dam break.

- 10.16 A negative wave of 0.75-m height is produced in a rectangular channel due to the sudden lifting up of a gate. The initial depth upstream of the gate is 3.0 m. (a) Determine the discharge per unit width through the gate and the profile of the negative wave at 4.0 s after the gate is opened. (b) What will be the discharge if the gate is lifted up by 2.0 m?

## OBJECTIVE QUESTIONS

- 10.1 In a gradually varied unsteady, open-channel flow  $dQ/dx = 0.10$ . If the top width of the channel is 10.0 m,  $\partial A/\partial t$  is  
 (a) 0.1 (b) 0.01 (c) -0.1 (d) -0.01
- 10.2 The equation of motion of GVUF differs from the differential equation of GVF by one essential term. This term is  
 (a)  $\frac{1}{g} \frac{\partial V}{\partial t}$  (b)  $\frac{\partial V}{\partial t}$  (c)  $\frac{1}{g} \frac{\partial V}{\partial t}$  (d)  $\frac{\partial y}{\partial x}$
- 10.3 In a uniformly progressive wave the maximum value of the absolute wave velocity  $V_w$  is equal to  
 (a)  $\frac{\partial Q}{\partial t}$  (b)  $\frac{\partial A}{\partial t}$  (c)  $\frac{\partial Q}{\partial x}$  (d)  $\frac{\partial Q}{\partial x}$
- 10.4 In a flood the water surface at a section in a river was found to increase at a rate of 5.6 cm/h. If the slope of the river is known to be 1/3600 and the velocity of the flood wave is assumed as 2.0 m/s, the normal discharge for the river stage read from the stage discharge curve  $Q_n$  is related to the actual discharge  $Q$  as  $Q/Q_n$  equal to  
 (a) 1.014 (b) 0.96 (c) 0.822 (d) 1.404
- 10.5 The stage discharge relation in a river during the passage of a flood wave is measured. If  $Q_R$  = discharge at a stage when the water surface was rising and  $Q_F$  = discharge at the same stage when the water was falling then  
 (a)  $Q_F = Q_R$  (b)  $Q_R > Q_F$   
 (c)  $Q_R < Q_F$  (d)  $Q_R/Q_F = \text{constant}$  for all stages
- 10.6 In the method of characteristics applied to flood routing, the St Venant equations are converted into  
 (a) four differential equations (c) one ordinary differential equation  
 (b) two ordinary differential equations (d) four partial differential equations
- 10.7 The Courant stability criteria in the method of characteristics requires  $\Delta t/\Delta x$  be  
 (a)  $\leq \left| \frac{1}{V} \right|$  (b)  $> \left| \frac{1}{V \pm C} \right|$   
 (c)  $\leq |V \pm C|$  (d)  $\leq \left| \frac{1}{V \pm C} \right|$
- 10.8 In explicit finite-difference schemes for solving St Venant equations the Courant condition to be satisfied throughout the computational space is  
 (a)  $\frac{\Delta x}{\Delta t} |C + V| \leq 1$  (b)  $\frac{\Delta t}{\Delta x} |C + V| \leq 1$   
 (c)  $\frac{\Delta x}{\Delta t} |C + V| \geq 1$  (d)  $\frac{\Delta t}{\Delta x} |C + V| \geq 1$

- 10.9 In finite-difference schemes for solving St Venant equations
- (a) the explicit schemes are unconditionally stable
  - (b) the implicit schemes require Courant conditions to be satisfied
  - (c) The implicit schemes are stable for values of the weighing coefficient  $\alpha \leq 0.5$ .
  - (d) None of the above statements is correct.
- 10.10 A positive surge of height 0.50 m was found to occur in a rectangular channel with a depth of 2.0 m. The celerity of the surge is in m/s
- (a)  $\pm 4.43$
  - (b)  $\pm 2.25$
  - (c)  $\pm 1.25$
  - (d)  $\pm 5.25$
- 10.11 A trapezoidal channel with  $B = 0.6$  m,  $m = 1.0$  and depth of flow = 2.0 m has a positive surge of height 0.80 m. The celerity of the surge in m/s
- (a)  $\pm 4.43$
  - (b)  $\pm 9.5$
  - (c)  $\pm 3.5$
  - (d) none of these
- 10.12 A stone thrown into a shallow pond produced a wave of amplitude 2 cm and velocity of 1.80 m/s. The depth of the pond in m is
- (a) 1.80
  - (b) 0.33
  - (c) 0.30
  - (d) 0.02
- 10.13 A tidal bore is a phenomenon in which
- (a) a positive surge travels upstream in a tidal river with the incoming tide
  - (b) a positive surge travels downstream in a tidal river with the incoming tide.
  - (c) a positive surge travels downstream in a tidal river with the outgoing tide
  - (d) a negative surge is associated with an incoming tide
- 10.14 In a negative surge
- (a) the wave velocity  $V_w$  is constant
  - (b) the celerity is always negative
  - (c) the water surface is a uniformly progressive wave
  - (d) the celerity varies with depth
- 10.15 A canal has a velocity of 2.5 m/s and a depth of flow 1.63 m. A negative wave formed due to a decrease in the discharge at an upstream control moves at this depth with a celerity of
- (a) + 6.5 m/s
  - (b) - 6.5 m/s
  - (c) + 1.5 m/s
  - (d) - 4.0 m/s

# Hydraulics of Mobile Bed Channels

# 11

## 11.1 INTRODUCTION

The previous chapters considered the characteristics of flows in rigid bed channels. The boundary was considered rigid, the channel slope and geometry fixed and the roughness magnitudes invariant. While these conditions hold good for a wide range of man made channels and to some extent to non-erodible natural channels also, there exists a class of open channel flows in which the boundary is mobile. Unlined channels in alluvium—both man made and natural channels—where the boundaries are deformable and the channel flows carry sediment along with water come under this category. The hydraulics of mobile bed channels, which is basic to successful engineering solution to a host of sediment problems such as erosion, deposition and change in the planform, form the subject matter of the important area of study known as *Sedimentation Engineering* or *Sediment Transport*. Obviously, a vast topic like sediment transport cannot be adequately covered within the confines of a single chapter in a book like this. As such, only a brief introduction to the hydraulics of mobile bed channels with emphasis on the design of stable unlined canals is attempted in this chapter. For further details, the reader should refer to the treatises and other good literature on this, topic [Ref. 1 through 7 and 9].

The *alluvium* or *sediment* refers to the loose, non-cohesive material (such as sand and silt) transported by, suspended in or deposited by water. A channel cut through an alluvium and transports water and also, in general, sediment having the same characteristics as in the boundary of the channel is termed *alluvial channel*. Such channels invariably have extremely complex interaction with the boundary and as such the available knowledge on the subject has a very heavy bias towards experimental observations and empirical correlations.

## 11.1 INITIATION OF MOTION OF SEDIMENT

When the flow of water in a channel having a non-cohesive material (such as sand) is carefully observed, it will be found that in some cases the bed may also become dynamic with the particles of the bed moving in sliding or rolling or jumping mode. Suppose the channel is a laboratory channel where the flow parameters can be controlled. If the motion of the bed particles is observed for a wide range of bed shear stresses  $\tau_0$  ( $= \gamma R S_0$ ), it will be noticed that while for small  $\tau_0$  values there may be

no motion of bed particles at all, the flows with large values of  $\tau_0$  will have definite observable motion. The condition of flow at which the bed particles will just begin to move is known as the condition of *critical motion* or *incipient motion*. The bed shear stress corresponding to incipient motion is known as *critical shear stress* or *critical tractive force* and is designated as  $\tau_c$ . It should be realized that the motion of the bed particles at  $\tau_0 = \tau_c$  is not a step function at  $\tau_c$  but it only implies that in a statistical sense considerable number of bed particles will be set in motion when the critical shear stress is reached.

Considering the sediment, fluid and flow properties at the stage of initiation of motion, Shields<sup>4,5,7,9</sup> proposed two non-dimensional numbers viz. Shear Reynolds

$$\text{number } R_{*c} = \frac{u_{*c} d}{\nu} \text{ and Non-dimensional shear stress } \tau_{*c} = \frac{\tau_c}{(\gamma_s - \gamma) d}$$

where  $d$  = diameter of the bed particle and

$\gamma_s = \rho_s g$  = unit weight of the sediment particle

$\gamma = \rho g$  = unit weight of water

$\tau_c$  = critical shear stress

$u_{*c} = \sqrt{\left(\frac{\tau_c}{\rho}\right)}$  = shear velocity at incipient condition

$\nu$  = kinematic viscosity of water

At the stage of initiation of motion, Shields obtained through experimental study the functional relationship between  $\tau_{*c}$  and  $R_{*c}$  as shown in Fig. 11.1. This curve, known as *Shields curve*, represents the mean line through data points and have been varified by numerous investigators. Shields curve is in some sense similar to Moody diagram representing the variation of the friction factor  $f$ . Here, up to  $R_{*c} = 2$  the flow is similar to the smooth boundary flow, the particles being completely submerged in a laminar sublayer, and  $\tau_c$  is not affected by the particle size. In the range  $2 < R_{*c} < 400$ , the flow is in transition stage where both the particle size  $d$  and fluid viscosity  $\nu$  affect  $\tau_c$ . When  $R_{*c} > 400$ ,  $\tau_{*c}$  is not affected by  $R_{*c}$  as the curve reaches a limiting value of 0.056. At this limiting value the critical shear stress  $\tau_c$  is a function of particle size only. This is an indication of the boundary becoming completely rough and hence the critical stress being independent of the viscosity of the fluid. Some investigators have obtained the constant value of  $\tau_{*c}$  at high  $R_{*c}$  as slightly less than 0.056; It could be as low as 0.045, (Ref. 4, 11, 16)

It is to be noted that the minimum value of  $\tau_{*c}$  is 0.03 and is obtained at  $R_{*c} = 10$ . Thus for  $\tau_* < (\tau_{*c})_{min}$  no motion should ever occur. If in a channel flow  $\tau_0 > \tau_c$  the bed will be in motion and if  $\tau_0 < \tau_c$  the bed could be taken to be not in motion and hence stable. Since in nature the sediments have non-uniform size distribution, it is usual to take the median size ( $d_{50}$ ) as a representative size for the sediments.

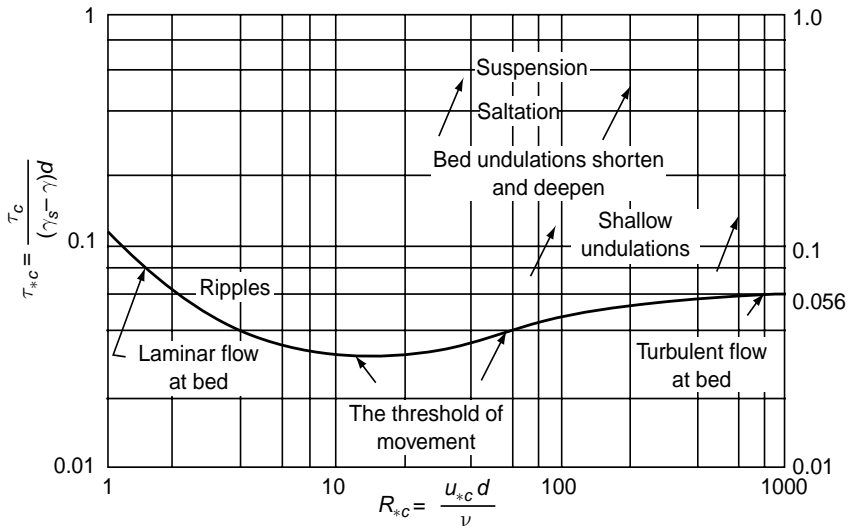


Fig. 11.1 Shield's diagram

For a sediment of relative density 2.65 and water at 20°C in the channel ( $\nu = 1 \times 10^{-6} \text{ m}^2/\text{s}$ )

$$\tau_{*c} = 0.056 \text{ corresponds to } u_{*c}^2 = \frac{\tau_c}{\rho} = 0.056 g \left( \frac{\gamma_s}{\gamma} - 1 \right) d$$

i.e. 
$$u_{*c} = 0.952 d^{1/2}$$

Further  $R_{*c} = 400$  corresponds to

$$\left( u_{*c} \frac{d}{\nu} \right) = (0.952 d^{1/2} d) / (1 \times 10^{-6}) = 400$$

i.e. 
$$d = 0.0056 \text{ m} = 5.6 \text{ mm}; \text{ say } 6 \text{ mm}$$

Designating the particle size in mm as  $d_{mm}$ , for  $d_{mm} > 6.0 \text{ mm}$ , the critical shear stress could be estimated as

$$\tau_c = 0.056 (\gamma_s - \gamma) d \tag{11.1}$$

$$\begin{aligned} \tau_c &= 0.056 \times 1.65 \times 9790 \times d_{mm} / 1000 \tag{11.2} \\ &= 0.905 d_{mm} \end{aligned}$$

Thus in a general way for sediments in water,  $d_{mm} > 6.0 \text{ mm}$  would correspond to rough boundary with critical shear stress given by  $\tau_c = 0.905 d_{mm}$ .

To use the Shields' curve to estimate the critical shear stress for a given particle size  $d_{mm} < 6 \text{ mm}$  one has to adopt a trial and error procedure. This is due to the fact



that  $\tau_c$  occurs in both the non-dimensional parameters of the curve. Swamee and Mittal<sup>8</sup> have expressed the Shields' curve results in an explicit relationship between  $\tau_c$  and  $d$  by an empirical non-dimensional formula. For the specific case of water at  $20^\circ\text{C}$  ( $\nu = 1 \times 10^{-6} \text{ m}^2/\text{s}$ ) and sediment of relative density 2.65, the empirical relationship of Swamee and Mittal<sup>9</sup> reduces to

$$\tau_c = 0.155 + \frac{0.409 d_{mm}^2}{[1 + 0.177 d_{mm}^2]^{1/2}} \quad (11.3)$$

where  $d_{mm}$  is the particle size in mm and  $\tau_c$  is in  $\text{N}/\text{m}^2$ .

This equation is based on the limiting value of the Shields curve as 0.06 and is very convenient in calculating to an accuracy of about 5% error the values of  $\tau_c$  of particle sizes up to about 5.5 mm. For higher sized particles Eq.11.2 is of course more convenient to use.

Consider an alluvial channel with  $R_{*c} > 400$  (i.e. having sediment particles of size greater than 6.0 mm). Then from Fig. 11.1 for this range

$$\frac{\tau_c}{(\gamma_s - \gamma)d} = 0.056$$

If  $d_c$  = size of a particle that will just remain at rest in a channel of bed shear stress  $\tau_0$  then

$$d_c = \frac{\tau_0}{0.056(\gamma_s - \gamma)}$$

But for a uniform channel flow of hydraulic radius  $R$  and bed slope  $S_0$

$$\tau_0 = \gamma R S_0$$

Thus, 
$$d_c = \frac{\gamma R S_0}{0.056(\gamma_s - \gamma)} \quad (11.4)$$

Taking relative density  $\gamma_s / \gamma = 2.65$

$$d_c = 10.82 R S_0 \approx 11 R S_0 \quad (11.5)$$

Equation 11.5 valid for  $d_{mm} \geq 6.0 \text{ mm}$  provides a quick method for estimating the size of a sediment particle that will not be removed from the bed of a channel.

**Example 11.1** | A wide rectangle channel in alluvium of 3.0-mm median size (Relative density = 2.65) has a longitudinal slope of 0.0003. Estimate the depth of flow in this channel which will cause incipient motion.

**Solution** Substituting  $d_{mm} = 3.0$  in Eq. (11.3)

$$\tau_c = 0.155 + \frac{0.409d_{mm}^2}{[1 + 0.177d_{mm}^2]^{1/2}}$$

$$\tau_c = 0.155 + \frac{0.409(3)^2}{[1 + 0.177(3)^2]^{1/2}} = 2.44 \text{ Pa}$$

For flow in a wide rectangular channel at depth  $D$ ,  $\tau_0 = \gamma D S_0$  and at incipient motion  $\tau_0 = \tau_c$ .

Hence,  $9790 \times D \times 0.0003 = 2.44$   
 Depth  $D = 0.831 \text{ m}$ .

**Example 11.2** Estimate the minimum size of gravel that will not move in the bed of a trapezoidal channel of base width = 3.0 m, side slope = 1.5 H: 1V, longitudinal slope = 0.004 and having a depth of flow of 1.30 m.

*Solution*  $R =$  hydraulic radius  $= \frac{(3.0 + 1.5 \times 1.30) \times 1.30}{[3.0 + 2 \times 1.30 \times \sqrt{(1.5)^2 + 1}]}$   
 $= 0.837 \text{ m}$

From Eq. (11.5),  $d_c = 11R S_0$   
 $= 11 \times 0.837 \times 0.004 = 0.0368 \text{ m}$   
 $d_c = 3.7 \text{ cm}$

### 11.3 BED FORMS

When the shear stress on the bed of an alluvial channel due to flow of water is larger than the critical shear stress  $\tau_c$  the bed will become dynamic and will have a strong interaction with the flow. Depending upon the flow, sediment and fluid characteristics, the bed will undergo different levels of deformation and motion. As a result of careful observations the following characteristic bed features are recognized:

1. Plane bed with no sediment motion
2. Ripples and dunes
3. Transition (a) Plane bed with sediment motion and  
(b) Standing wave
4. Antidunes

These bed features are called *bed forms* or *bed irregularities*. Schematically, these bed forms are shown in Fig. 11.2.

The sequence of formation of these bed forms are best understood by considering a hypothetical laboratory channel with sediment bed where the slope and discharge in the channel can be changed at will. Consider an initial plane bed and a very low

velocity of flow being admitted into the channel. The following sequence of bed forms can be expected in the channel.

**(1) Plane Bed with no Sediment Motion** This situation corresponds to the case when the actual shear stress  $\tau_0$  is less than the critical shear stress  $\tau_c$ . There will be no motion of the sediment and the bed will remain plane. The friction offered to the flow is due to the resistance of the grains only.

### **(2) Ripples and Dunes**

**(a) Ripples** If the shear stress in the channel is increased (by increasing either discharge or slope) so that  $\tau_0$  is moderately greater than  $\tau_c$ , the grains in the bed will begin to move and very soon the bed will be covered by a saw tooth type of ripple pattern (Fig. 11.2). The height of the ripples will be considerably smaller than their length. The sediment motion will be essentially in the form of rolling and sliding of the particles on the ripple bed. The water surface will remain essentially calm and plane. An interesting feature of the ripples is that they are not formed if the sediment size is greater than about 0.60 mm.

**(b) Dunes** As the shear stress on the bed is gradually increased in our hypothetical channel, the ripples gradually grow into larger sizes. Then a different bed form known as *dunes* appear with ripples riding over them. At higher shear stress values the ripples disappear leaving behind only the dunes pattern on the bed.

Dunes are larger in size than the ripples with small height to length ratios. The water surface will be wavy and out of phase with the dunes, (Fig. 11.2). The sediment transport will be larger than in ripples and the dunes advance downstream though with a velocity much smaller than that of the water flow. The flow will be in subcritical range.

The flow in a channel with ripples and dunes in the bed is characterised by separation of the flow on the lee side of the bed form. This in turn causes large energy losses and particularly so in duned beds. The shedding of the vortices from the separation region of the dunes cause ruffling of the free water surface. In both the ripples and dunes, the bed form gets eroded on the upstream side and some of this material gets deposited on the lee side of the bed form in a continuous manner causing the crest of the bed wave pattern to move downstream.

While the distinction between the ripples and dunes is clear in a general qualitative sense, it has not been possible to differentiate between them in terms of specific quantifiable parameters. As such, it is usual to consider the ripples and dunes as one class and to distinguish this class of bed form from others.

### **(3) Transition**

**(a) Plane bed with sediment motion** Further increase of the shear stress after the dune bed pattern phase will lead to a transition phase where the bed undulations get washed away progressively to achieve ultimately an essentially plane bed surface (Fig. 11.2). The sediment transport rate would be considerably larger than in dune

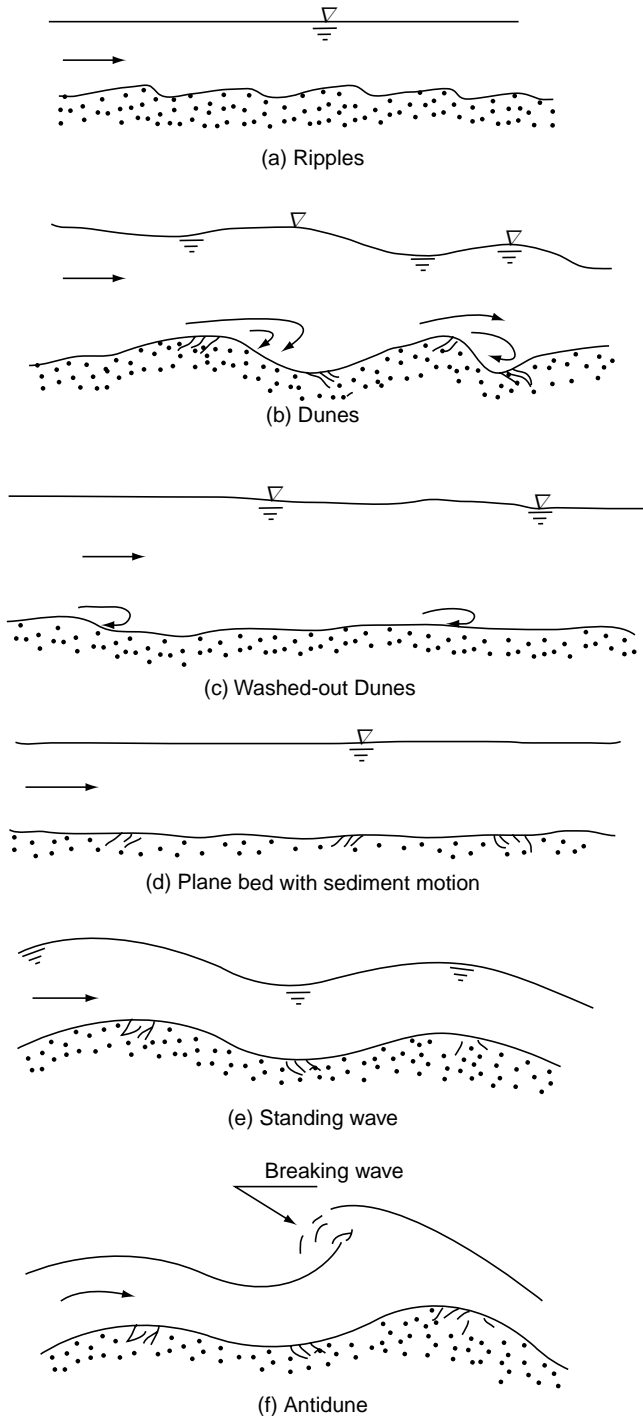


Fig. 11.2 Bed forms in alluvial channels

phase. The flow, however, will be in subcritical range with the Froude number of the flow being nearer unity.

(b) *Standing wave* Further increase in the shear stress beyond the plane bed stage bringing the Froude number nearer unity and beyond it, would lead to the formation of symmetrical sand waves with associated water surface standing wave, (Fig. 11.2). The water surface undulations will be in phase with the sand waves.

The above two bed features viz. plane bed with sediment motion and the standing wave stage, are clubbed into one class called transition. The transition phase of bed form is very unstable.

(4) *Antidunes* If the shear stress in our hypothetical channel is further increased beyond transition phase, the symmetrical sediment wave and the associated standing wave slowly start moving upstream. The waves gradually grow steeper and then break. The bed form at this stage is called *antidunes*. A characteristic feature of the standing wave and antidune type of bed forms is that there is no separation of the flow at these bed forms. As such, the energy loss is mainly due to grain boundary roughness.

It should be noted that while the sand waves move upstream it does so in a relative sense due to a rapid exchange of sediment in the bed profile. The sediment in the lee side of the wave gets eroded and some of it gets deposited on the upstream side of the bed form to cause the wave crest to move upstream. The general flow of water and sediment transport will be in the downstream direction. Further, the antidunes appear only in water-sediment interface in alluvial channels and have not been noticed in air-sediment interface in desert environment. The flow at antidune bed form stage will be supercritical and the sediment transport rate will be very high.

**Bed Form and Resistance** In alluvial channels the different bed forms that can occur have a marked impact on the total resistance to flow. In a mobile bed channel the total resistance to flow could be considered to be made up of the resistance due to the grains composing the bed and the drag resistance offered by the bed form shapes. Thus it is obvious that the same channel may exhibit different resistances depending on the bed form present. Figure 11.3 shows schematically the variation

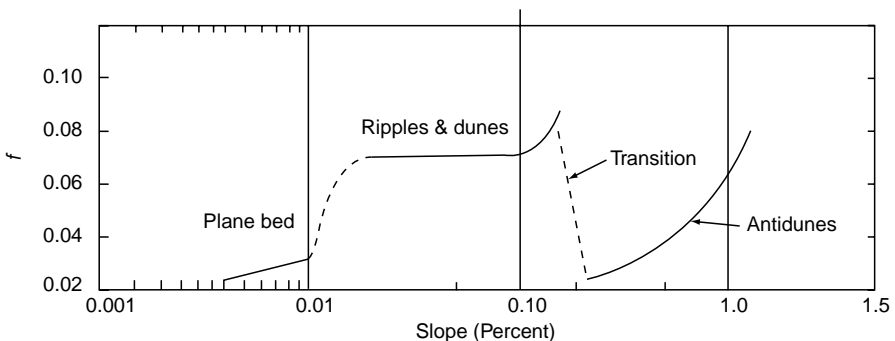


Fig. 11.3 Schematic variation of friction factor  $f$  with bed forms [Based on data on  $d = 0.28$  mm, Ref. 7]

of the Darcy-Weisbach friction factor  $f$  with bed forms. This figure is based on laboratory data of Simons<sup>6</sup> for a sand of  $d = 0.28$  mm and is meant only to illustrate qualitatively the behaviour of  $f$  with bed forms. It can be seen that the friction factor  $f$  has a sudden increase at the onset of ripples, then onwards the increase is gradual in ripples stage and rapid in dunes stage. At the transition phase there is a sudden drop in the value of  $f$ . In the antidune stage the increase is fairly rapid.

Typical orders of magnitude of Manning’s coefficient  $n$ , friction factor  $f$  and non-dimensional Chezy coefficient  $C/\sqrt{g}$  at various bed forms are given Table 11.1. This table highlights the impact of the bed forms on the channel resistance and the need for proper identification of appropriate bed forms in studies connected with the hydraulics of mobile bed channels.

To estimate the resistances due to the grains  $\tau_0'$  and due to bed forms  $\tau_0''$  it is usual to consider the total shear stress  $\tau_0$  to be made up of the two components such that

$$\tau_0 = \tau_0' + \tau_0'' \tag{11.6}$$

**Table 11.1** Range of Resistance Factors—Manning’s coefficient  $n$ , Friction factor  $f$  and Chezy coefficient  $C/\sqrt{g}$ —at Various Bed Forms

Ref. [7]

[Note:  $C/\sqrt{g} = \sqrt{8/f}$ ]

Bed Form	Darcy-Weisbach Friction Factor	Manning’s Coefficient	Non-dimensional Darcy Coefficient
Plane bed without sediment motion	0.020–0.036	0.012–0.016	15–20
Ripples	0.056–0.163	0.018–0.030	7–12
Dunes	0.047–0.163	0.020–0.040	7–13
Plane bed with sediment motion	0.020–0.040	0.010–0.013	16–20
Antidunes (Breaking)	0.040–0.065	0.012–0.018	11–16

Assuming the energy slope  $S_0$  to be the same for both the components and the total hydraulic radius of the channel  $R$  to be made up of two parts  $R'$  and  $R''$

$$\gamma RS_0 = \gamma R' S_0 + \gamma R'' S_0$$

Hence, 
$$R = R' + R'' \tag{11.7}$$

where  $R'$  = hydraulic radius associate with grain roughness and  $R''$  = hydraulic radius associated with bed forms. Further, Manning’s formula is used to represent the channel resistance. If  $n$  = Manning’s roughness coefficient of the channel flow and  $n_s$  = Manning’s roughness coefficient corresponding to the grain roughness only, then the mean velocity in the channel is

$$V = \frac{1}{n} R^{2/3} S_0^{1/2} \tag{11.8a}$$

Also, 
$$V = \frac{1}{n_s} (R')^{2/3} S_0^{1/2} \tag{11.8b}$$

From Eqs 11.8a and b 
$$R' = \left( \frac{n_s}{n} \right)^{3/2} \tag{11.9}$$

Strickler's Equation (Eq. 3.22) is used to estimate  $n_s$  as

$$n_s = \frac{d^{1/6}}{21.1}$$

The shear stress due to the grains, which forms an important parameter in the study of sediment transport mechanics is given by

$$\tau'_0 = \gamma R' S_0 = \left( \frac{n_s}{n} \right)^{3/2} \gamma R S_0 \tag{11.10}$$

**Prediction of Bed Forms** There have been numerous attempts<sup>4,5,6,9</sup> to predict the bed forms in terms of flow and sediment parameters. Whether analytical or empirical, all these attempts are at best partially successful. A typical classification due to Garde and Rangaraju<sup>4</sup> (Fig.11.4) considers the parameters  $S^* = \frac{S_0}{[(\gamma_s - \gamma)/\gamma]}$  and  $R/d$

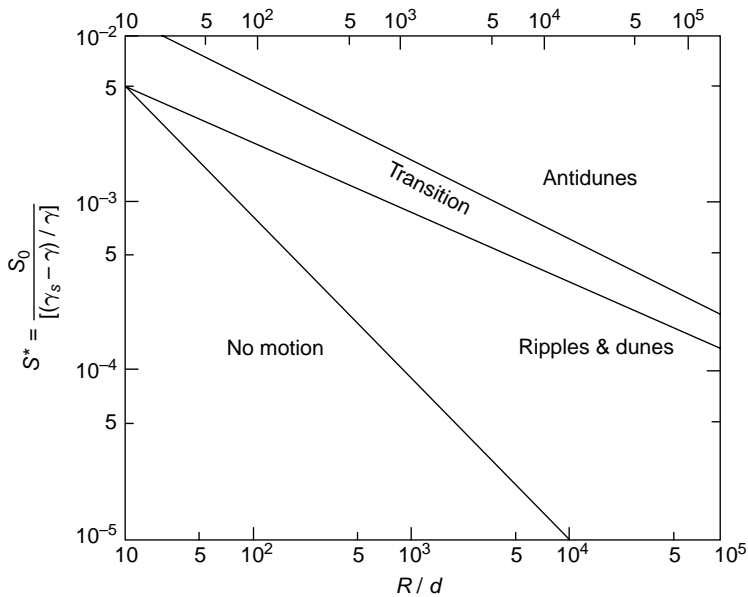


Fig. 11.4 Prediction of bed forms

as significant parameters. The lines demarcating the various bed form phases can be expressed as:

$$\text{For plane bed with no motion} \quad S^* \leq 0.05 (R/d)^{-1} \quad (11.11a)$$

$$\text{For ripples and dunes} \quad 0.05 (R/d)^{-1} \leq S^* \leq 0.014 (R/d)^{-0.46} \quad (11.11b)$$

$$\text{For transition} \quad 0.014 (R/d)^{-0.46} \leq S^* \leq 0.059 (R/d)^{-0.54} \quad (11.11c)$$

$$\text{For antidunes} \quad S^* \geq 0.059 (R/d)^{-0.54} \quad (11.11d)$$

where  $S^* = \frac{S_0}{[(\gamma_s - \gamma) / \gamma]} = S_0 / 1.65$  for sediments with relative density of 2.65.

Fig.11.4 or its equivalent equations 11.11a, b, c, d are useful in the determination of bed forms in a given flow situation.

**Example 11.3** | An unlined irrigation channel in an alluvium of median size 0.30 mm is of trapezoidal section with bed width = 3.0 m, side slope = 1.5 H: 1 V, and longitudinal slope = 0.00035. If this channel carries a discharge of 1.5 m<sup>3</sup>/s at a depth of 0.8 m, estimate the (i) nature of the bed form, (ii) shear stress due to the grain roughness, and (iii) shear stress due to bed forms.

*Solution* Area  $A = [3.0 + (1.5 \times 0.8)] \times 0.8 = 3.36 \text{ m}^2$

Perimeter  $P = \left[ 3.0 + 2 \times 0.8 \times \sqrt{(1.5)^2 + 1} \right] = 5.884 \text{ m}$

$$R = A/P = 3.36/5.884 = 0.571 \text{ m}$$

$$R/d = 0.571/(0.0003) = 1903$$

$$0.05 (R/d)^{-1} = 0.05 (1903)^{-1} = 2.63 \times 10^{-5}$$

$$0.014 (R/d)^{-0.46} = 0.014 (1903)^{-0.46} = 4.34 \times 10^{-4}$$

$$S^* = \frac{S_0}{[(\gamma_s - \gamma) / \gamma]} = S_0 / 1.65 = 0.00035 / 1.65 = 2.12 \times 10^{-4}$$

Since  $0.05 (R/d)^{-1} \leq S^* \leq 0.014 (R/d)^{-0.46}$ , by Eq. 11.11b the bed form is of ripples and dunes category.

Manning's coefficient due to grains by Eq.3.22 is

$$n_s = (0.0003)^{1/6} / 21.1 = 0.0122$$

By Manning's formula,

$$Q = \frac{1}{n} AR^{2/3} S_0^{1/2}$$



$$1.5 = \frac{1}{n} (3.36)(0.571)^{2/3} (0.00035)^{1/2} = \frac{0.0433}{n}$$

$n$  = Manning's coefficient for the whole channel = 0.0288

By Eq. 11.10, the shear stress due to the grains

$$\begin{aligned} \tau'_0 &= \left( \frac{n_s}{n} \right)^{3/2} \gamma R S_0 = \left( \frac{0.0122}{0.0288} \right)^{3/2} \times 9790 \times 0.571 \times 0.00035 \\ &= 0.539 \text{ Pa} \end{aligned}$$

$$\tau_0 = \text{Average bed shear stress due to flow.} = \gamma R S_0$$

$$= 9790 \times 0.571 \times 0.00035 = 1.957 \text{ Pa}$$

$$\tau_0'' = \text{shear stress due to bed forms} = \tau_0 - \tau'_0$$

$$= 1.957 - 0.539 = 1.418 \text{ Pa}$$

## 11.4 SEDIMENT LOAD

In an alluvial channel the sediment particles in the bed will start moving when the bed shear stress  $\tau_0$  exceeds the critical shear stress  $\tau_c$ . At small values of excess bed shear stress ( $\tau_0 - \tau_c$ ) the particles may roll or slide on the bed. Sediment transported in this manner is called *contact load*. Sometimes the sediment particles may leave the boundary to execute a small jump (or hop) to come in contact with the bed again. This mode of sediment transport through a large number of small jumps is known as *saltation load*. The saltation of sediment particles in water flow takes place essentially in a thin layer, of the order of two grain diameters, next to the bed. In view of this, both the contact load and saltation load are considered under one class as *bed load*. Thus all the sediment that will be transported in a thin layer of the order of two grain diameters next to the bed is classified as *bed load*.

At higher shear rates, the fluid turbulence may pick up the displaced particles and keep them in suspension. The sediment transported in suspension mode is known as *suspended load*. Whether a particle will travel as bed load or suspended load depends upon the parameter  $\omega/u_*$  where  $\omega$  = fall velocity of the particle and  $u_* = \sqrt{\tau_0/\rho}$  = shear velocity of the flow. The particles of fall velocity  $\omega$  move in suspension mode when  $\omega/u_* \leq 2.0$ .

The sum of the suspended load and bed load is *total load*. It should be noted that the total load is made up of material emanating from the boundary of the channel and as such it is also sometimes called as *total bed material load*. Sometimes, the suspended material may contain very fine material like clay not found in the boundary of the channel. This material would have come to a stream, and thence to a channel, as a product of erosion during a runoff process. Such suspended material which does not form part of the bed material is known as *wash*

load and its transport characteristics are different from that of bed material suspended load. Unless otherwise specifically mentioned as significant, the wash load is usually ignored in alluvial geometry design. The term suspended load is understood to refer to bed material only.

**Bed Load** The transport rate of sediments in the bed load ( $q_B$ ) is usually referred to in units of weight per second per unit width (N/s/m). A very large number of empirical and semi-analytical expressions are available to estimate the bed load  $q_B$  in terms of sediment, fluid and flow parameters. Duboys (1879) was the first to propose an expression for  $q_B$  as a function of excess of shear stress  $\tau_0$  over the critical shear stress  $\tau_0$ , viz.

$$q_B = \alpha (\tau_0 - \tau_c) \tag{11.12}$$

Since then a very large number of empirical formulae involving the parameter  $(\tau_0 - \tau_c)$  have been proposed by various investigators. Probably the most widely used empirical equation for  $q_B$  is due to Meyer-Peter and Muller<sup>4,5</sup> which relates  $q_B$  in a dimensionless manner as

$$\phi_B = 8 (\tau'_* - 0.047)^{3/2} \tag{11.13}$$

where

$$\begin{aligned} \phi_B &= \text{bed load function} \\ &= \frac{q_B}{\gamma_s (gd^3)^{1/2}} \cdot \frac{1}{\left[ \frac{\gamma_s}{\gamma} - 1 \right]^{1/2}} \end{aligned} \tag{11.14}$$

and

$$\begin{aligned} \tau'_* &= \text{dimensionless grain shear stress} \\ &= \frac{\gamma R S_0}{(\gamma_s - \gamma)d} = \left[ \frac{n_s}{n} \right]^{3/2} \frac{\gamma R S_0}{(\gamma_s - \gamma)d} \end{aligned} \tag{11.15}$$

- in which  $q_B$  = bed load in N/s/m
- $d$  = mean size of sediment
- $R$  = hydraulic radius of the channel
- $\gamma$  = unit weight of water
- $\gamma_s$  = unit weight of sediment particles
- $n$  = Manning's coefficient for the whole channel
- $n_s$  = Manning's coefficient of particle roughness
- $R'$  = hydraulic radius corresponding to grain roughness
- $S_0$  = longitudinal slope of the channel.

In Eq. 11.13 the term 0.047 corresponds to the asymptotic value in the shields diagram.

Other commonly used methods of bed load estimation are due to Einstein<sup>7</sup> and Bagnold<sup>5</sup>, the details of which are available in reference 4, 5, 6, 7 and 9.

**Suspended Load** Consider a steady channel flow of depth  $D$  carrying sediment in suspension. The sediment particles which are lifted up from the bed are kept in suspension due to turbulence while the particles try to settle down due to their weight. This results in a concentration profile  $C = f_n(y)$  with sediment concentration  $C$  being distributed in a vertical in a manner to achieve equilibrium of the forces acting on the particles, (Fig. 11.5).

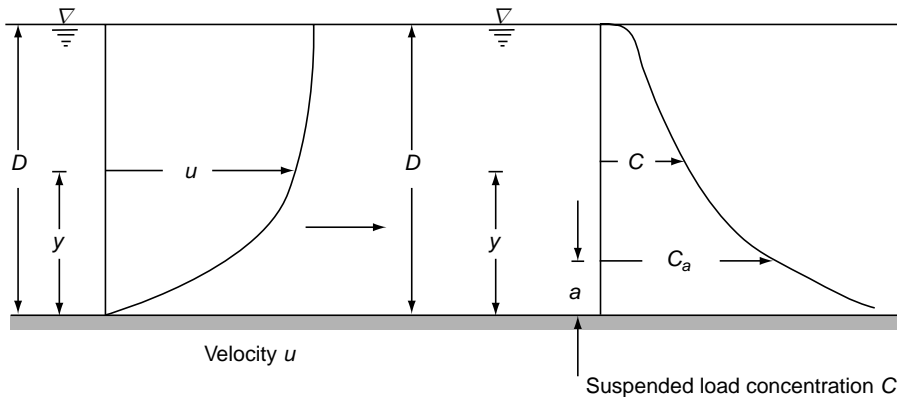


Fig. 11.5 Suspended load concentration and velocity profile in a channel

In a steady flow, the upward diffusion of the sediment is balanced by the settling of the sediment particles and the basic differential equation governing this action is given by

$$C\omega + \varepsilon_s \frac{dC}{dy} = 0 \quad (11.16)$$

where

$C$  = concentration of sediment, by weight

$\omega$  = fall velocity of the sediment particles

$\varepsilon_s$  = mass diffusion coefficient, generally a function of  $y$ .

At any height  $y$  above the bed, the shear stress

$$\tau_y = \tau_0 \left( \frac{D-y}{D} \right) \quad (11.17)$$

By Prandtl's mixing length theory  $\tau_y$  can also be written as

$$\tau_y = \rho \varepsilon_m \frac{du}{dy} \quad (11.18)$$

where  $\varepsilon_m =$  diffusion coefficient for momentum.

By considering the logarithmic form of velocity distribution in the channel.

$$\frac{du}{dy} = \frac{u_*}{ky} \quad (11.19)$$

where  $k =$  Karman's constant ( $\approx 0.4$ ).

Assuming  $\varepsilon_s = \varepsilon_m$ , from Eqs 11.17, 11.18 and 11.19

$$\varepsilon_s = ku_* \frac{y}{D} (D - y) \quad (11.20)$$

Substituting in Eq. 11.16 yields

$$C\omega + ku_* \frac{y}{D} (D - y) \frac{dC}{dy} = 0$$

$$\frac{dC}{C} = - \frac{\omega D}{ku_* y (D - y)} dy \quad (11.21)$$

Assuming  $\frac{\omega}{k u_*} = Z =$  constant, integration of Eq. 11.21 between  $y = a$  and  $y$  yields

$$\int_a^y \frac{dC}{C} = \int_a^y \frac{ZD}{y(D - y)} dy$$

$$\frac{C}{C_a} = \left[ \left( \frac{D - y}{y} \right) \left( \frac{a}{D - a} \right) \right]^Z \quad (11.22)$$

where  $C_a =$  concentration at any height  $a$  above the bed. Equation 11.22 which gives the ratio concentration  $C$  of suspended material at any height  $y$  above the bed to the concentration  $C_a$  at any reference level  $a$  is known as *Rouse equation*. Figure (11.6) shows the variation of  $C/C_a$  with  $(y - a)/(D - a)$  for  $a/D = 0.05$  with  $Z$  as the third parameter. It can be seen that the concentration profile becomes more uniform as the parameter  $Z$  becomes smaller.

Since  $Z$  is proportional to  $\omega$ , for a given shear stress  $\tau_0$ , the smaller the particle size, the more uniform would be the sediment concentration profile. Conversely, for large particle sizes (i.e. large  $\omega$ ), the concentration profile will have high concentrations at the bottom layers.

In the parameter  $Z$ , the Karman coefficient  $k$  is of the order of 0.4. Some experimental observations<sup>4,9</sup> have shown that  $k$  decreases at high concentrations of sediment.

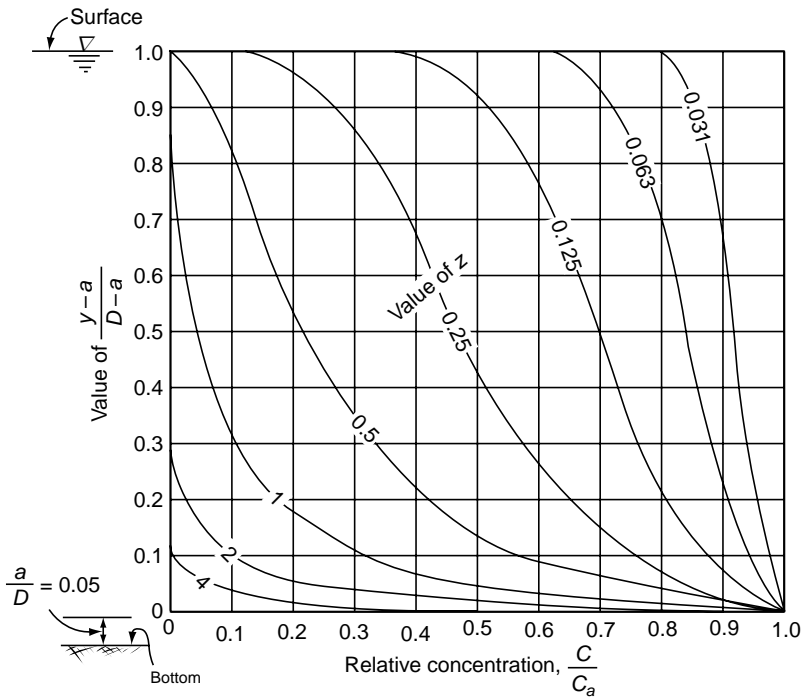


Fig. 11.6 Rouse's equation for  $C/C_a$

Knowing the concentrations profile and the velocity profile in a vertical, (Fig. 11.5), the suspended sediment load  $q_s$  per unit width of channel in a vertical can be estimated as

$$q_s = \int_{a_1}^D C u dy$$

where  $a_1$  = level corresponding to the edge of the bed load layer  $\approx 2d$ . This method requires estimation of  $C_{a1}$  by an alternative means. Details of estimating  $q_s$  are available in Ref. 5

**Example 11.4** In a wide alluvial stream, a suspended load sample taken at a height of 0.30 m above the bed indicated a concentration of 1000 ppm of sediment by weight. The stream is 5.0 m deep and has a bed slope of 1/4000. The bed material can be assumed to be of uniform size with a fall velocity of 2.0 cm/s. Estimate the concentration of sediment at mid depth.

**Solution** By Eq. 11.22

$$\frac{C}{C_a} = \left[ \left( \frac{D-y}{y} \right) \left( \frac{a}{D-a} \right) \right]^z$$

Here  $a = 0.3$  m,  $D = 5.0$  m,  $y = D/2 = 2.5$  m,  $C_a = 1000$ ,  $\omega = 0.02$  m/s.

$$Z = \frac{\omega}{u_* k}$$

Since the channel is wide,  $R = D$  and  $u_* = \sqrt{gDS_0}$ ,  $Z = \frac{\omega}{k\sqrt{gDS_0}}$

Assuming  $k = 0.4$ ,

$$Z = \frac{0.02}{0.4 \times \sqrt{9.81 \times 5 \times 1/4000}} = 0.4515$$

By Eq. 11.22

$$C/1000 = \left[ \frac{(5.0 - 2.5)}{2.5} \times \frac{0.3}{(5.0 - 0.3)} \right]^{0.4515} = 0.2887$$

$C = 2887$  ppm by weight.

**Total Bed Material Load** The sum of the bed load and suspended load form the *total bed material load*. Using expressions derived for estimation of bed load and suspended load elaborate procedures for estimation of total bed material load are given by Einstein, Colby et al, and Bishop et al, [Ref. 5,7,9]. Numerous empirical equations for the estimation of total bed material load have been proposed. One of these, a commonly used equation due to Englund and Hansen<sup>2,4</sup> which expresses the total bed material load per unit width  $q_T$  in terms of easily determinable parameters, is given below:

$$\phi_T f = 0.4 \tau_*^{5/2} \tag{11.23}$$

where

$\phi_T =$  total load function and

$$\phi_T = \frac{q_T}{\gamma_s (gd^3)^{1/2}} \frac{1}{\left[ \frac{\gamma_s}{\gamma} - 1 \right]^{1/2}} \tag{11.24}$$

where  $\tau_* =$  non-dimensional shear

$$= \frac{\tau_0}{[\gamma_s - \gamma]d} \tag{11.25}$$

$f =$  Darcy – Weisbach friction factor

$$= \frac{8gRS_0}{V^2} \tag{11.26}$$

$q_T =$  total bed material load per unit width of channel in N/s/m

$V =$  mean velocity in the channel

and other parameters are same as in Eq. 11.13.

Equation (11.23) is based on data pertaining to a wide range of bed forms and grain sizes and therefore could be relied on to predict the total load fairly adequately.

**Example 11.5** | A wide alluvial channel has a bed material of median size 0.8 mm. The channel has a longitudinal slope of  $5 \times 10^{-4}$ . The depth and velocity in the channel were measured as 1.6 m and 0.90 m/s respectively. Estimate the (a) bed load, (b) total load, and (c) suspended load per metre width of this channel.

*Solution* (a) Bed load,  $q_B$ :

Since the channels is wide  $R = y_0 = 1.60$  m.

By Manning's formula  $V = \frac{1}{n} y_0^{2/3} S_0^{1/2}$

$$0.90 = \frac{1}{n} (1.6)^{2/3} (5 \times 10^{-4})^{1/2}$$

$$n = 0.034$$

By Eq. 3.17,  $n_s = \frac{d^{1/6}}{21.1} = \frac{(0.0008)^{1/6}}{21.1} = 0.0144$

By Eq. 11.9, shear stress due to gain  $\tau_0' = \left(\frac{n_s}{n}\right)^{3/2} \gamma y_0 S_0$

$$\tau_0' = \left[\frac{0.0144}{0.0340}\right]^{3/2} \gamma y_0 S_0 = 0.2756 \gamma y_0 S_0$$

$$\begin{aligned} \tau_0' &= \frac{\tau_0}{(\gamma_s - \gamma)d} = \frac{0.2756 \gamma y_0 S_0}{(\gamma_s - \gamma)d} \\ &= \frac{0.2756 \times 1.6 \times 5 \times 10^{-4}}{1.65 \times 0.0008} = 0.167 \end{aligned}$$

By Eq. 11.4  $\phi_B = \frac{q_B}{\gamma_s (gd^3)^{1/2} \left[\frac{\gamma_s - \gamma}{\gamma}\right]^{1/2}}$

$$\begin{aligned} \phi_B &= \frac{q_B}{2.65 \times 9790 \times [9.81(0.0008)^3]^{1/2}} \times \frac{1}{(1.65)^{1/2}} \\ &= 0.4234 q_B \end{aligned}$$

By Meyer–Peter formula 11.13

$$\phi_B = 8 (\tau_*' - 0.047)^{3/2}$$

$$0.4234 q_B = 8(0.167 - 0.047)^{3/2}$$

$$q_B = 0.785 \text{ N/s per metre width.}$$

(b) Total load,  $q_T$

By Eq. 11.24

$$\phi_T = \frac{q_T}{\gamma_s (gd^3)^{1/2} \left[ \frac{\gamma_s - \gamma}{\gamma} \right]^{1/2}}$$

$$\begin{aligned} \phi_T &= \frac{q_T}{2.65 \times 9790 \times [9.81(0.0008)^3]^{1/2}} \times \frac{1}{(1.65)^{1/2}} \\ &= 0.4234 q_T \end{aligned}$$

The Darcy–Weisbach friction factor  $f$ , by Eq. 11.26 is

$$f = \frac{8gRS_0}{V^2} = \frac{8 \times 9.81 \times 1.6 \times 5 \times 10^{-4}}{(0.9)^2} = 0.0777$$

$$\tau_* = \frac{\gamma y_0 S_0}{(\gamma_s - \gamma)d} = \frac{1.6 \times 5 \times 10^{-4}}{1.65 \times 0.008} = 0.6061$$

By Eq. 11.23

$$\phi_T \cdot f = 0.4 \tau_*^{5/2}$$

$$0.4234 q_T \times 0.0775 = 0.4 \times (0.6061)^{5/2}$$

$$\text{Total load} = q_T = 3.486 \text{ N/s per metre width}$$

(c) Suspended load,  $q_s$

$$q_T = q_s + q_B$$

$$q_s = \text{suspended load} = 3.486 - 0.785$$

$$= 2.701 \text{ N/s per metre width}$$

#### 11.4.1 Measurement and Estimation of Sediment Load

A stream flowing in a watershed transports not only the runoff that is produced in the catchment but also the erosion products out of the watershed by means of its flow. The total sediment load is transported out the catchment by the stream in three components depending upon their origin as *wash load*, *suspended load* and *bed load*.

In connection with the measurement, the following essential properties of different types of sediment loads in a stream are worth noting:

- Wash load is generally composed of fine grained soils of very small fall velocity.
- The suspended load particles move considerably long distances before settling on the bed and sides and any measurement of suspended load also includes wash load.



- Bed load is the relatively coarse bed material and is moved at the bed surface through sliding, rolling, and saltation. In a general sense, bed load forms a small part of total load (usually < 25%) and wash load forms comparatively very small part of the total load.

Bed load measurement in field is extremely difficult. While a large number of devices are available for measuring bed load for experimental / special investigations, no practical device for routine field measurement of bed load is currently in use. For planning and design purposes the bed load of a stream is usually estimated either by use of a bed load equation such as those due to Meyer–Peter and Muller (Eq. 11.13), Einstein<sup>7</sup> and Bagnold<sup>5</sup> or is taken as a certain percentage of the measured suspended load.

The suspended load of a stream is measured by taking the samples of sediment laden stream water. The collection of samples is through specially designed samplers that do not alter the flow configuration in front of the sampler and get representative samples of the stream water. A variety of samplers from the simple ones (for example an ordinary bottle) to highly sophisticated ones are available. The sediment from the collected sample of sediment laden water is removed by filtering and its dry weight determined. It is usual to express suspended load as parts per million (ppm) on weight basis as

$$C_s = \left[ \frac{\text{Weight of sediment in sample}}{\text{weight of (sediment + water) of the sample}} \right] \times 10^6$$

Thus the sediment transport rate in a stream of discharge  $Q \text{ m}^3/\text{s}$  is

$$Q_s = (Q \times C_s \times 60 \times 60 \times 24) / 10^6 = 0.086 QC \text{ Tonnes/day}$$

Routine observations of suspended load are being done at many stream gauging stations in the country. At these stations in addition to stream flow discharge  $Q$  the suspended sediment concentration and hence the suspended sediment load  $Q_s$  is also noted. The relation between  $Q_s$  (tonnes/day) and stream discharge  $Q$  ( $\text{m}^3/\text{s}$ ) is usually represented in a log–log plot known as *sediment rating curve*. The relationship between  $Q_s$  and  $Q$  can be represented as

$$Q_s = KQ^n$$

where the exponent is usually around 2.0.

The sediment rating curve in conjunction with the stream flow hydrograph can be used to estimate the suspended sediment load transport in the stream in a specified time interval. A method of estimating the annual sediment yield of a watershed by using the sediment rating curve in conjunction with flow duration curve is described in Ref. 10. For details regarding Sediment problems and relevant measurement techniques Ref.6 and 11 can be consulted.

### 11.5 DESIGN OF STABLE CHANNELS CARRYING CLEAR WATER [CRITICAL TRACTIVE FORCE APPROACH]

There are two basic types of design procedures used in the design of alluvial channels. These are

1. Critical tractive force method
2. Regime channel method

The first one, viz., the critical tractive force approach attempts to restrict the shear stress anywhere in the channel to a value less than the critical shear stress of the bed material. If the channel carries clear water there will be no deposition problem and hence the channel will be of stable cross-section. This approach, proposed by Lane is the subject matter of this section. On the other hand the regime channel approach proposes to design a channel under dynamic equilibrium while the channel is carrying a small amount of sediment. Design of a non-scouring and non-silting channel is the object of the regime approach. Details of the regime approach proposed by Lacey will be discussed in the next section.

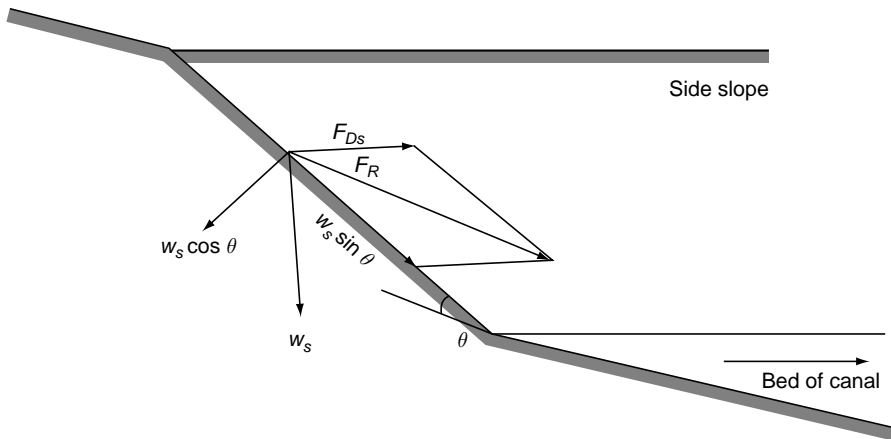
**Stability of a Particle on a Side-slope** Consider a particle on the side of a channel of inclination  $\theta$  to the horizontal, Fig. 11.7. Let

$d$  = size of the particle so that its effective area  $a = C_1 d^2$  where  $C_1$  is a coefficient.

$w_s$  = submerged weight of the particle =  $C_2 (\gamma_s - \gamma) d^3$  where  $C_2$  is a coefficient.

The weight  $w_s$  will have components  $w_s \sin \theta$  along the slope and  $w_s \cos \theta$  normal to the slope. Due to the flow a shear stress  $\tau_w$  exists on the particle situated on the slope. The drag force on the particle due to shear is

$$F_{Ds} = \tau_w a$$



$$F_R = \sqrt{F_{Ds}^2 + w_s^2 \sin^2 \theta}$$

Fig.11.7 Stability of a particle on the side slope of canal

and resultant force tending to move the particle

$$F_R = \sqrt{F_{DS}^2 + w_s^2 \sin^2 \theta}$$

Stabilizing force  $F_s = w_s \cos \theta$

At the condition of incipient motion,  $F_R / F_s = \tan \phi$

Where  $\phi$  = angle of repose of the sediment particles under water.

Thus, 
$$\frac{F_{DS}^2 + w_s^2 \sin^2 \theta}{w_s^2 \cos^2 \theta} = \tan^2 \phi \quad (11.27)$$

On simplifying, 
$$F_{DS} = w_s \cos \theta \cdot \tan \phi \left[ 1 - \frac{\tan^2 \theta}{\tan^2 \phi} \right]^{1/2} \quad (11.28)$$

From Eq. (11.28), when  $\theta = 0$ , the drag force on a particle situated on a horizontal bed at the time of incipient motion is obtained. Thus if  $\tau_b$  = shear stress on the bed of a channel, from Eq. (11.28),

$$F_{DS} = \tau_b a = w_s \tan \phi \quad (11.29)$$

Hence, 
$$\frac{F_{DS}}{F_{Db}} = \frac{\tau_w}{\tau_b}$$

and from Eq. (11.28), 
$$\frac{\tau_w}{\tau_b} = \cos \theta \left[ 1 - \frac{\tan^2 \theta}{\tan^2 \phi} \right]^{1/2} = K_1 \quad (11.30)$$

$$\tau_w = K_1 \tau_b \quad (11.31)$$

### Design Procedure

1. The angle of repose  $\phi$  of the sediment is determined by laboratory tests. For preliminary design Fig. 11.8 giving the variation of  $\phi$  with the particle size and particle shape can be used.
2. The longitudinal slope of the channel is established from topographical considerations. The side slope of the channel is established from practical and constructional aspects. However,  $\theta$  should be much smaller than  $\phi$ .
3. Strickler's formula (Eq 3.17) is used to estimate Manning's coefficient  $n$  for the channel as

$$n = d^{1/6} / 21.1$$

4. Since it is required to have no sediment motion anywhere in the channel, by allowing for factor of safety  $\tau_b$  is taken as

$$\tau_b = K_2 \tau_c \quad (11.32)$$

where  $\tau_c$  = critical shear stress and  $K_2$  = a coefficient of value less than unity and taken as follows

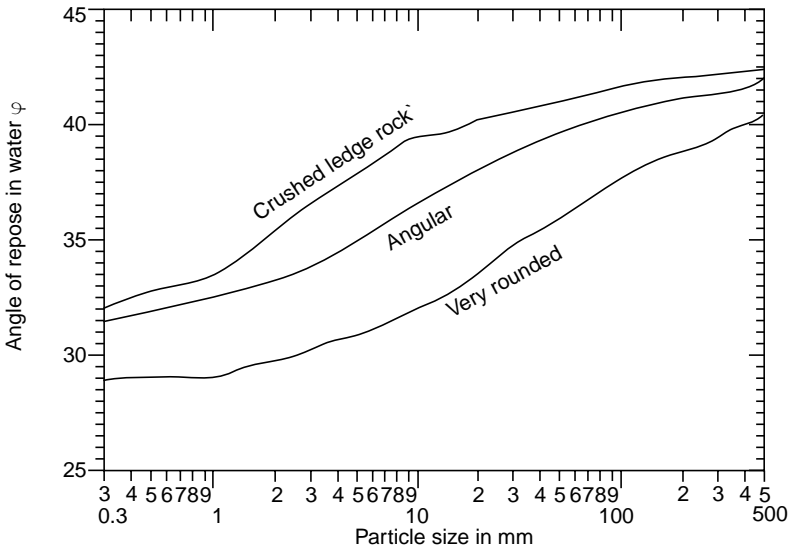


Fig.11.8 Variation of the angle of repose  $\phi$  of particles under water [Ref. 8]

Channel condition	Value of $K_2$
Straight channel	0.90
Slightly curved	0.81
Moderately curved	0.67
Very curved	0.54

From Eq. 11.31

$$\tau_w = K_1 K_2 \tau_c \tag{11.33}$$

- The critical shear stress of the particle is determined by Shields curve or by the appropriate equivalent empirical equation, Eq. 11.2 or 11.3.
- Since there will be considerable variation of the magnitude of shear stress on the perimeter (Fig. 3.6), the non-erodible channel will have to be designed to withstand the maximum shear stress that may occur anywhere in the perimeter of the channel. For a conservative design of a trapezoidal section of normal depth  $y_0$  and longitudinal slope  $S_0$  the maximum shear stress on the sides  $(\tau_w)_{\max}$  and bed  $(\tau_b)_{\max}$  can be safely taken respectively as

$$(\tau_w)_{\max} = 0.75 \gamma y_0 S_0 \tag{11.34}$$

$$(\tau_b)_{\max} = \gamma y_0 S_0 \tag{11.35}$$

Thus for the non-erodibility condition,

$$\tau_w \leq (\tau_w)_{\max}$$

i.e. 
$$K_1 K_2 \tau_c \leq 0.75 \gamma y_0 S_0 \tag{11.36}$$

and

$$\tau_b \leq (\tau_b)_{\max}$$

i.e.

$$K_2 \tau_c \leq \gamma y_0 S_0 \quad (11.37)$$

The lesser of the two values of  $y_0$  obtained from Eqs 11.36 and 11.37 is adopted. The following example illustrates the design procedure well.

**Example 11.6** | Design a stable non-erodible channel to carry 10 m<sup>3</sup>/s of clear water through a 10-mm bed of rounded gravel. A longitudinal slope of 0.0008 and side slope of 2 horizontal: 1 vertical are to be adopted.

*Solution* From Fig. 11.8 for rounded gravel of  $d = 10$  mm,  $\phi = 32^\circ$ .

$$\tan \phi = 0.6249$$

Side slope  $\tan \theta = 1/2 = 0.5$ ,  $\cos \theta = 0.8944$

Sine  $d_{mm} > 6$ , by Eq. 11.2,  $\tau_c = 0.905 \times 10 = 9.05$  Pa

For the bed: By considering a straight channel  $K_2 = 0.9$

$$\tau_b = K_2 \tau_c = 0.9 \times 9.05 = 8.145 \text{ Pa}$$

By making

$$\tau_b = (\tau_b)_{\max} = \gamma y_0 S_0$$

$$y_0 = \frac{8.145}{9790 \times 0.0008} = 1.04 \text{ m} \quad (11.38)$$

For the side: By Eq. 11.30,  $K_1 = \cos \theta \left[ 1 - \frac{\tan^2 \theta}{\tan^2 \phi} \right]^{1/2}$

$$K_1 = 0.8944 \left[ 1 - \left( \frac{0.5000}{0.6249} \right)^2 \right]^{1/2} = 0.536$$

$$\tau_w = K_1 \tau_b = 0.536 \times 8.145 = 4.366 \text{ Pa}$$

Making  $\tau_w = (\tau_w)_{\max} = 0.75 g y_0 S_0$

$$y_0 = \frac{4.366}{0.75 \times 9790 \times 0.0008} = 0.743 \text{ m} \quad (11.39)$$

Adopting the lower of the two values of  $y_0$  given by 11.38 and 11.39

$$y_0 = 0.743 = \text{say } 0.740 \text{ m}$$

To determine the bed width,  $B$ :

$$\begin{aligned} \text{Area } A &= (B + 2 \times 0.74) \times 0.74 \\ &= (B + 1.48) \times 0.74 \end{aligned}$$

$$\text{Perimeter } P = (B + 2 \times 0.74 \times \sqrt{5}) = (B + 3.3094)$$

$$\begin{aligned} \text{By Eq. 3.22, Manning's coefficient } n &= (d)^{1/6} / 21.1 \\ &= (0.01)^{1/6} / 21.1 = 0.022 \end{aligned}$$

$$\text{By Manning's formula, } Q = \frac{1}{n} AR^{2/3} S_0^{1/2}$$

$$\begin{aligned} \text{Hence } Q = 10.0 &= \frac{1}{0.022} \times \frac{(B + 1.48)^{5/3} (0.74)^{5/3}}{(B + 3.3094)^{2/3}} \times (0.0008)^{1/2} \\ (B + 1.48)^{5/3} &= 12.848 (B + 3.3094)^{2/3} \end{aligned}$$

Solving by trial-and-error,  $B = 12.4$  m.

## 11.6 REGIME CHANNELS

The term regime is used in connection with alluvial channels to signify a state of dynamic equilibrium. Lacey (1930) defines a regime channel as one which carries a constant discharge under uniform flow in an unlimited incoherent alluvium having the same characteristics as that transported without changing the bottom slope, shape or size of cross-section over a period of time. Thus in a regime channel, in contrast to the non-erodible channels discussed in the previous section, there will be suspended load, bed load and formation of bed forms. In the initial periods in the life of a channel, there can be changes in the depth, width and longitudinal slope towards attaining the dynamic equilibrium. After the attainment of the regime state, the dimensions of the canal including the longitudinal slope will remain essentially constant over time so long as the discharge and other flow characteristics are not disturbed. The regime channel is thus a channel in dynamic state with neither erosion nor deposition.

A rigid bed canal can be said to have one degree of freedom in the sense that for a given channel a change in the discharge would cause a change in depth only. For an alluvial man-made canal, on the other hand, a change in discharge can cause changes in width, depth and bed slope to achieve a new regime. Thus an alluvial channel has three degrees of freedom. In the same way, a natural alluvial river has four degrees of freedom as its planform can also alter. The basic philosophy of regime concept recognizes the degrees of freedom of an alluvial channel and aims at providing initial conditions which are very near the final regime values.

The regime theory of designing stable channels evolved in India during the late 19th century and early periods of twentieth century by the British engineers. Through keen observations of the behaviour of large number of irrigation canals they recognized that in channels that performed satisfactorily the depth and velocity were such that the water and sediment discharges were in equilibrium. In these canals there were no objectionable scour and deposition and maintenance was minimal. These observations have resulted in empirical relations connecting

the geometry and flow properties of regime channels. Most of the data for the development of regime relations have come from irrigation canals in Indo-Gangetic plain which had a low sediment load ( $< 500$  ppm by weight). Since the regime correlations do not include the sediment load explicitly, these equations should be considered applicable only to channels carrying similar concentrations of sediment load.

Further, the regime method is based on the hypothesis that channels adjust their slope, width and depth until they are in equilibrium with the incoming discharge and sediment load. As both discharges and sediment load vary in time in real canals, in using the term regime it is understood that sediment deposition and scour are balanced over some suitably long period.

**Kennedy Equation** Historically, Kennedy (1895) was the first to propose a relationship between the velocity  $V$  and depth  $y_0$  of a stable channel as

$$V = C y_0^a \quad (11.40)$$

On the basis of observation on Bari-Doab canal system (now in Pakistan) where the channel bed material had a median size of 0.32 mm, Kennedy found the coefficient  $C = 0.56$  and the exponent  $a = 0.64$ . Further, he introduced a coefficient  $m$  (known as critical velocity ratio), to account for the variation of the size of sediments, so that Eq. 11.40 became

$$V = 0.56 m y_0^{0.64} \quad (11.41)$$

In using Eq. 11.41 for designing a stable channel, Manning's formula is used to describe the channel friction. Tables of recommended values of  $B/y_0 = fn$  (discharge) and recommended values of  $m = fn$  (sediment size) are other information needed to estimate the value of  $y_0$  and  $B$  of a stable channel to convey a discharge  $Q$ , in a channel of bed slope  $S_0$ . It is to be noted that Kennedy's method of stable channel design assumes the slope to be independent. In view of many deficiencies, the use of Kennedy equation to design stable channels is now obsolete.

**Lacey's Equations** Lindley (1919) was the first to recognize the need to have three relationships to account for the three degrees of freedom of an alluvial channel. He advanced the basic philosophy of regime concept in his statement<sup>3</sup> "when an artificial channel is used to convey silty water, both bed and banks scour or fill, changing depth, gradient and width until a balance is attained at which the channel is said to be in regime".

Lacey, through systematic analysis of the available stable channel data, perfected the regime concept and gave final forms to it through an adequate set of three primary equations. It is these equations, with minor modifications, that are in general use in India and many other parts of the world as regime equations. Basically, there are three equations of Lacey to represent the three degrees of freedom of an alluvial channel, viz., depth, width and gradient. The role of the sediment size is expressed, in an approximate way, by a fourth equation. These equations are:

$$P = 4.75\sqrt{Q} \quad (11.42)$$

$$R = 0.48 (Q/f_s)^{1/3} \quad (11.43)$$

$$S_0 = 0.0003 (f_s)^{5/3} / Q^{1/6} \quad (11.44)$$

in which

$$f_s = 1.76 \sqrt{d_{mm}} \quad (11.45)$$

where

$P$  = wetted perimeter in m

$R$  = hydraulic radius in m

$Q$  = discharge in the canal in m<sup>3</sup>/s

$S_0$  = longitudinal bed slope

$d_{mm}$  = particle size in mm

$f_s$  = silt factor to account for effect of sediment size on regime dimensions

It is of interest to note that the regime channels have been found to attain a side slope of 0.5 horizontal: 1 vertical at regime due to gradual deposition of fine material. This value of 0.5 H: 1 V is attained irrespective of the initial side slope value provided at the time of construction of the canal. Thus in the design of all regime channels, the final side slope value of 0.5 H: 1 V is taken in the calculation of area, perimeter, etc.

There have been many improvements of the Lacey equations to define the behaviour of regime channels, notable amongst them is the work of Blench<sup>1</sup> and Simons and Albertson<sup>2</sup>. The regime equations of Blench provide for the effect of sediment concentration also on the regime dimension. The Simons and Albertson equations were derived from a larger data set than was available to Lacey and as such are more widely applicable. References 1 through 7 and 9 could be consulted for further details on regime channels. Example 11.7 illustrates use of Lacey equations to design a regime channel.

Based upon these four independent equations of Lacey, (Eq. 11.42 through 11.45) a number of derived relationships between the different parameter have been developed. For example the velocity of flow  $V$  can be expressed as

$$V = 10.8 R^{2/3} S_0^{1/3} \quad (11.46)$$

in a manner similar in form to Manning's formula.

**Example 11.7** | Design a canal by Lacey's theory to convey 40 m<sup>3</sup>/s of water. The canal is to be cut in an alluvial soil of median size 0.6 mm.

**Solution** Silt factor

$$\begin{aligned} f_s &= 1.76 \sqrt{d_{mm}} \\ &= 1.76 \sqrt{0.6} = 1.36 \end{aligned}$$



510 Flow in Open Channels

$$\begin{aligned} \text{Longitudinal slope} \quad S_0 &= \frac{0.0003 \times f_s^{5/3}}{Q^{1/6}} \\ &= \frac{0.0003 \times (1.36)^{5/3}}{(40)^{1/6}} = 2.72 \times 10^{-4} \end{aligned}$$

$$\begin{aligned} \text{Hydraulic radius} \quad R &= 0.48(Q/f_s)^{1/3} \\ &= 0.48 \left( \frac{40}{1.36} \right)^{1/3} = 1.482 \text{ m} \end{aligned}$$

$$\begin{aligned} \text{Wetted perimeter} \quad P &= 4.75\sqrt{Q} \\ &= 4.75 \sqrt{40} = 30.04 \text{ m} \end{aligned}$$

Since the final regime channel will have a side slope of 0.5 horizontal: 1 vertical,

$$P = (B + 2\sqrt{1 + (0.5)^2} y_0) = 30.04 \text{ m} \quad (11.47)$$

$$P = B + 2.236 y_0 = 30.04 \text{ m}$$

$$B = (30.04 - 2.236 y_0)$$

$$A = (B + 0.5 y_0) y_0 = PR = (30.04 \times 1.482)$$

$$= 44.52 \text{ m}^2$$

Substituting for  $B$ ,

$$(30.04 - 2.236 y_0 + 0.5 y_0) y_0 = 44.52$$

$$1.736 y_0^2 - 30.04 y_0 + 44.52 = 0$$

Solving for  $y_0$

$$y_0 = \frac{(30.04 \pm \sqrt{(30.04)^2 - 4 \times 44.52 \times 1.736})}{2 \times 1.736}$$

$$= \frac{30.04 \pm 24.36}{3.472}$$

$$= 15.66 \text{ m and } 1.636 \text{ m}$$

Neglecting the higher value of  $y_0$  as impractical,

$$y_0 = 1.636 \text{ m}$$

$$B = 30.04 - (2.236 \times 1.636) = 26.38 \text{ m}$$

Thus,

$$B = 26.38 \text{ m}$$

$$y_0 = 1.636 \text{ m}$$

$$S_0 = 2.72 \times 10^{-4}$$

Side slope = 0.5 H: 1 V.

**Example 11.8** | A regime Lacey channel having a full supply discharge of  $30 \text{ m}^3/\text{s}$  has a bed material of 0.12-mm median size. What would be the Manning's roughness coefficient  $n$  for this channel?

*Solution*  $f_s = 1.76\sqrt{d_{mm}} = 1.76\sqrt{0.12} = 0.61$

By Eq. (11.44)  $S_0 = \frac{0.0003 f_s^{5/3}}{Q^{1/6}} = \frac{0.0003(0.61)^{5/3}}{(30.0)^{1/6}} = 7.46 \times 10^{-5}$

By Eq. (11.46)  $n = \left( \frac{S_0^{1/6}}{10.8} \right) = \frac{(7.46 \times 10^{-5})^{1/6}}{10.8} = 0.019$

## 11.7 SCOUR

Scour is removal of sediment in a stream due to action of flowing water. In connection with bridges, scour could be defined as the result of erosive action of flowing water excavating and carrying away sediment from the bed and banks of a stream due to interference of structures such as abutments and bridge piers on the flowing water. In an alluvial stream there will be continuous transport of sediment in the stream as a geomorphological process. If however there is additional natural or man induced causes to upset the sediment supply and removal in a reach, such as construction of a barrage or a dam, the stream will have long term changes in the stream bed elevation. If there is progressive build up of stream bed in a reach due to sediment deposition it is called as *aggradation*. Conversely, if there is a progressive long term lowering of the channel bed due to erosion as a result of deficit sediment supply to the reach it is called as *degradation*. In connection with a bridge structure, three types of scour are recognized:

**1. Degradation scour** This is present in the channel at the bridge site due to stream degradation phenomenon in the reach generating from certain causes upstream of the reach.

**2. Contraction scour** Due to constriction of the width of the stream flow at a bridge site, the velocities in the stream would increase and cause erosion resulting in removal of sediment from the bottom and sides of the river. It is also known as *general scour*.

**3. Local scour** Due to the presence of bridge piers and abutments the three dimensional flow around the obstruction would cause vortices that would scoop the sediment in the immediate neighborhood of the abutment and piers and deposit the same at some other location. This results in a deep scour hole around the foundation of bridge elements and may impair the structural safety of the structure. Further, depending upon the sediment movement in the stream, local scour is classified in to two kinds:

**(i) Clear-water scour** This refers to the situation where there is no sediment movement in the bed of the stream and hence no sediment is supplied from upstream into the scour zone. Typical clear water scour situation include (i) coarse bed material streams, (ii) flat gradient streams in low flow (iii) armored stream beds, and (iv) vegetated channels

**(ii) Live-bed scour** This on the other hand, refers to the situation where sediment is continuously being supplied to the scour hole areas. Thus, for example, in a stream where there is dune movement, the scour hole depth will be affected by the movement of a dune in to or out of the scour hole. After a long time there will be some kind equilibrium with the scouring mechanism and bed movement and the equilibrium will be reached asymptotically. The depth of scour will oscillate about a mean position.

**Total scour** The sum of the three types of scour enumerated above, viz., long term degradation, contraction scour and local scour are known as the total depth of scour at the bridge.

The time development of a scour hole in clear water flow and in live bed situation is shown in Fig. 11.9. The main difference between the clear water scour and the live

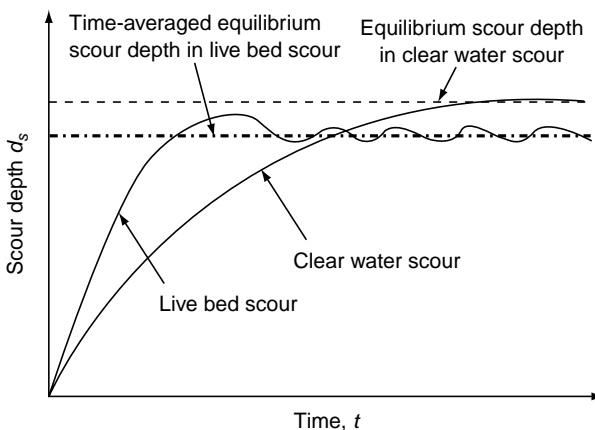


Fig. 11.9 Time development of scour

bed scour is the time taken to reach equilibrium scour; it takes longer in the live bed scour to reach equilibrium. It has been observed in experimental studies that in the live bed scour the equilibrium scour depth is only about 10% smaller than in the corresponding maximum clear water scour depth. The time development of scour is logarithmic in nature.

### 11.7.1 Local Scour

**Scour at a Bridge Pier** Scour caused by flowing water of a stream past a bridge pier or abutment has been recognized as a major cause of bridge failure. Considerable research attention has been devoted since past several decades to understand the scour phenomenon and to design safe and economical bridge structures. A brief description of the scour at a bridge founded on an alluvial stream is given in the following paragraphs.

Figure 11.10 shows a schematic representation of flow around a bridge pier and its scour hole. When the flow approaches a bridge pier, there is a stagnation point at the point of intersection of the flow with the pier, thus in an ideal case a vertical line of stagnation is obtained. Due to the velocity distribution in the approaching flow which is zero at the bed and approaches a maximum at or near the surface, a pressure gradient from top to the bottom is created. Due to this there is a plunging flow and its interaction with the separated boundary layer close to the bed and the main flow results in a set of vortices wrapping most of the upstream part of the pier as shown in Fig. 11.10. The plan view of this set of vortex is in the form of a horseshoe and as such this vortex structure is known as *horseshoe vortex*. In addition to the horse shoe vortex, which is known to be the prime agent responsible

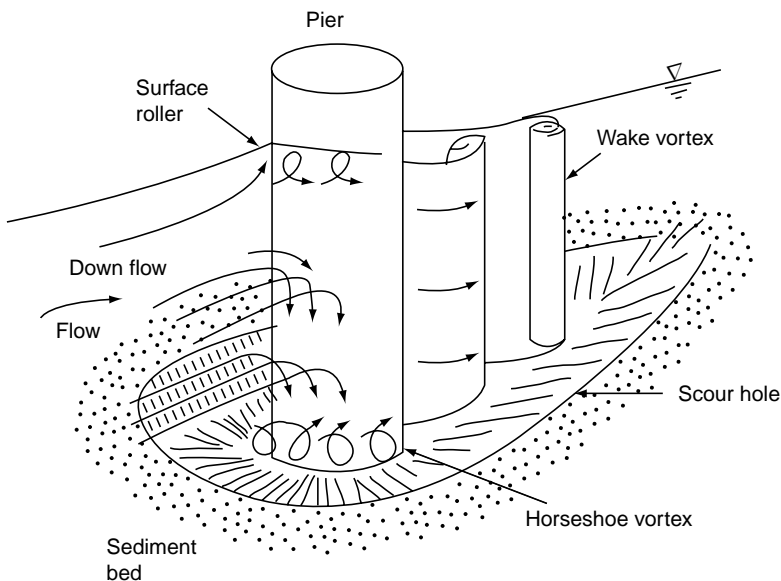


Fig. 11.10 Schematic sketch of vortex system at circular bridge pier

for scour, there exists a wake containing vertical wake vortices in the separation zone in the downstream region of the pier. This system of horseshoe and wake vortices causes the sediment to be lifted up of the bed in the scour hole and carries the sediment out of the separation zone to create a scour hole around the pier.

The action of horseshoe vortex is to remove the bed material from around the base of the pier. When there is live bed condition in the stream, the transport rate of sediment away from the base region of the pier will be greater than the transport rate of sediment in to the region. As the scour hole develops, the strength of the horseshoe vortex is reduced, thereby reducing the transport rate of sediment out of the region. Eventually, an equilibrium is reached between the bed material inflow and outflow and the scour hole development ceases.

In the clear water situation, the scouring action ceases when the shear stress caused by the horseshoe vortex equals the critical shear stress of the sediment particles at the base of the scour hole.

The structure of the vortex has been studied in the laboratory by many investigators. Reference 12 and Ref. 13 explain the mean flow characteristics and turbulent structures of the horseshoe vortex respectively.

Study of local scour at bridge piers has been studied very extensively over several decades and consequently there has been numerous equations purporting to predict the maximum depth of scour. Most of these studies are in the laboratory under simple or idealized conditions and the field studies are rather limited. A review of the studies on scour at bridge piers is available in Ref. 6, 14, 15 and some recent equations are reviewed by Sturm<sup>16</sup>.

The Federal Highway Administration of US Department of Transportation has brought out the Hydraulic Engineering Circular No 18 (HEC-18)<sup>17</sup> in 2001 which presents the state of knowledge and practice for the design, evaluation and inspection of bridges for scour. This document, along with its companion documents HEC-20 and HEC-23, which represents the current recommended procedure relating to Scour for adoption is available in <http://isddc.dot.gov.OLPFiles/FHWA/010590.pdf>

Figure 11.11(a) gives the definition sketch of bridge pier and related scour complex, and Fig. 11.11(b) gives some of the common pier shapes. For the estimation of local scour at bridge piers under situation given in Fig. 11.11, HEC-18 adopts the Colorado State University (CSU) formula of Richardson, Simons and Julien (1990) given by

$$\frac{d_s}{b} = 2.0 K_1 K_2 K_3 K_4 \left( \frac{y_1}{b} \right)^{0.35} F_1^{0.43} \quad (11.48)$$

in which

$d_s$  = Scour depth, (m)

$y_1$  = flow depth directly upstream of the pier, (m)

$K_1$  = correction factor for pier nose shape, Fig (11.11) and Table (11.2)

$K_2$  = correction factor for angle of attack, , Fig (11.11) and Equation 11.49

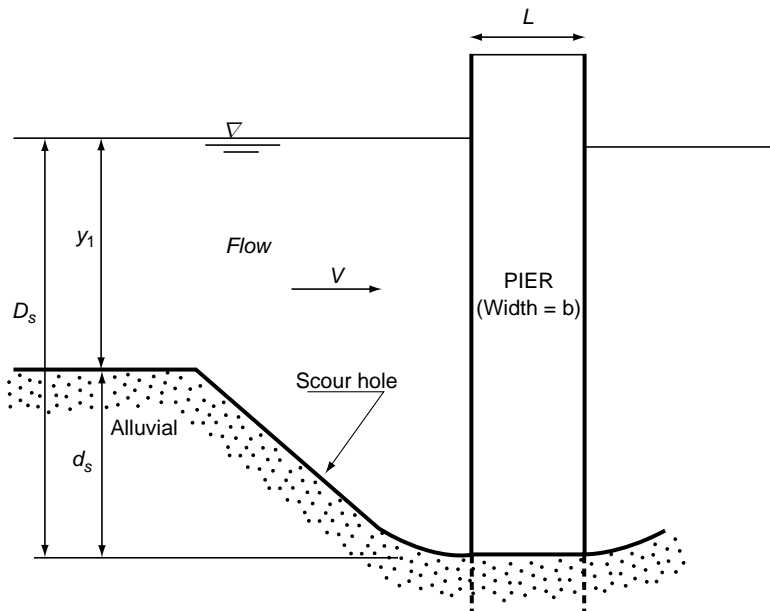


Fig. 11.11 (a) Definition sketch of a scour hole at a bridge pier

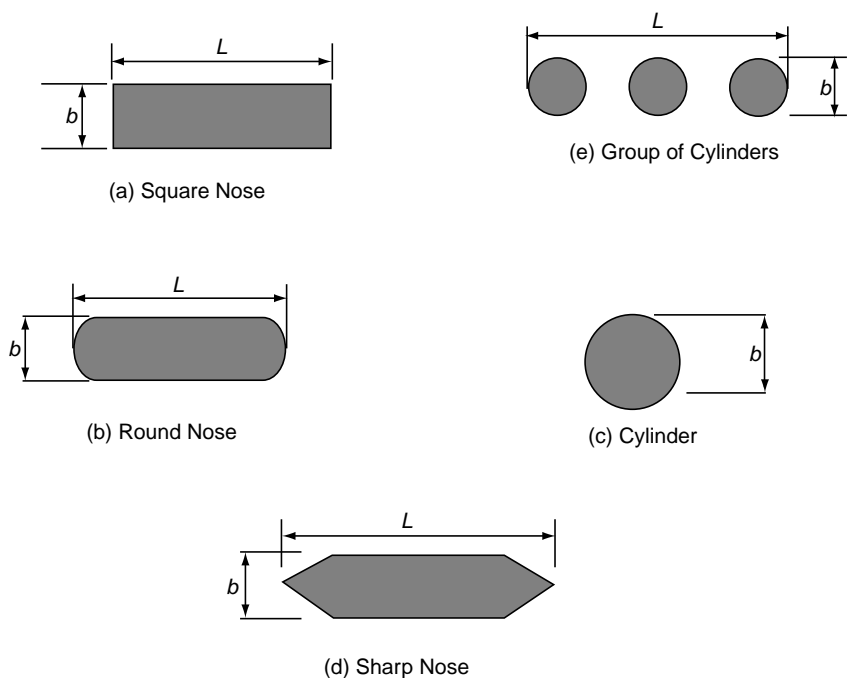


Fig. 11.11 (b) Common pier shapes

**Table 11.2** Correction Factor  $K_1$  for Pier Nose Shapes

Shape of Pier Nose	$K_1$
(a) Square Nose	1.1
(b) Round Nose	1.0
(c) Circular Cylinder	1.0
(d) Group of Cylinders	1.0
(e) Sharp Nose	1.9

**Table 11.3** Correction Factor  $K_2$  for Angle of Attack  $\theta$  of the Flow

Angle $\theta$	$L/b = 4$	$L/b = 8$	$L/b = 12$
0	1.0	1.0	1.0
15	1.5	2.0	2.5
30	2.0	2.75	3.5
45	2.3	3.3	4.3
90	2.5	3.9	5.0

Angle = Skew Angle of Flow,  $L$  = length of Pier (m)

**Table 11.4** Correction Factor  $K_3$  for Bed Condition

Bed Condition	Dune height (m)	$k_3$
Clear water scour	N/A	1.1
Plane bed and Antidune flow	N/A	1.1
Small Dunes	$3 > H \geq 0.6$	1.1
Medium Dunes	$9 > H \geq 3$	1.2 to 1.1
Large Dunes	$H \geq 9$	1.3

$K_3$  = correction for bed condition = as in Table 11.4

$K_4$  = correction factor for armoring by bed material of size from Eqs 11.50 to 11.51a.

$b$  = Pier width (m)

$L$  = length of pier (m)

$$F_1 = \text{Froude number directly upstream of the pier} = \frac{V_1}{\sqrt{gy_1}}$$

$V_1$  = mean velocity of flow

The correction factor  $K_2$  for the angle of attack of the flow  $\theta$  is calculated as

$$K_2 = \left( \cos \theta + \left( \frac{L}{b} \right) \sin \theta \right)^{0.65} \tag{11.49}$$

In Eq. 11.48  $L/b$  is taken as 12.0 even if the actual value exceeds 12.

Armoring is a natural process whereby an erosion resistant layer of relatively large particles is formed due to the removal of finer particles by stream flow. If the bed material consists of relatively large proportion of coarse material, in a scouring action the fines will be eroded first and the larger particles may form an armour coat to resist further scouring thus reducing the maximum depth of scour.

The correction factor  $K_4$  reduces the scour for materials having  $D_{50} \geq 2.0$  mm and  $D_{96} \geq 20$  mm. The correction  $K_4$  is given as follows:

- $K_4 = 1.0$  for  $D_{50} < 2.0$  mm and  $D_{95} < 20.0$  mm
- For  $D_{50} \geq 2.0$  mm and  $D_{96} \geq 20$  mm, the following relationships are used to calculate  $K_4$ :

$$K_4 = 0.4(V_R)^{0.15} \tag{11.50}$$

where

$$V_R = \frac{V_1 - V_{icD50}}{V_{cD50} - V_{icD50}} > 0 \tag{11.50a}$$

$V_{icD_x}$  = approach velocity in m/s required to initiate scour at the pier for the grain size  $D_x$  (m).

$$V_{icD_x} = 0.645 \left( \frac{D_x}{b} \right)^{0.053} V_{cD_x} \tag{11.51}$$

$V_{cD_x}$  = critical velocity in m/s for incipient motion for the grain size  $D_x$ (m)

$$V_{cD_x} = 6.19 y_1^{1/6} D_x^{1/3} \tag{11.51a}$$

In the above  $y_1$  = depth of flow just upstream of the pier, excluding local scour, (m).

$V_1$  = velocity of the approach flow just upstream of the pier (m/s)

$D_x$  = grain size for which x percent of the bed material is finer (m)

The minimum value of  $K_4$  is 0.4.

A study of the above equations reveal the following significant points relating to parameters affecting the scour depth:

- (i) The greater the approach velocity greater will be the scour depth.
- (ii) Similarly, scour depth is directly related to the positive power of the depth of flow.
- (iii) The scour depth increases with an increase in the width of the pier.
- (iv) If the approach flow is at an angle to the pier the projected length of the pier will come in to play and the scour increases.
- (v) Shape of the pier plays an important role on the scour depth.
- (vi) Size and gradation of the bed material do not have an important role on the scour depth; the time taken to achieve maximum scour depth depends on the grain size.
- (vii) Lodging of debris around a pier can increase the width of pier, change its shape and its projected length with consequent increase in the maximum depth of scour



### 11.7.2 Abutment Scour

The mechanism of local scour at an abutment is essentially same as at a bridge pier. Fig. 11.12 shows the formation of horseshoe vortex (primary vortex) and wake vortices. In view of wide range of shape, layout and flow situations possible in abutment scour, the problem is rather complex.

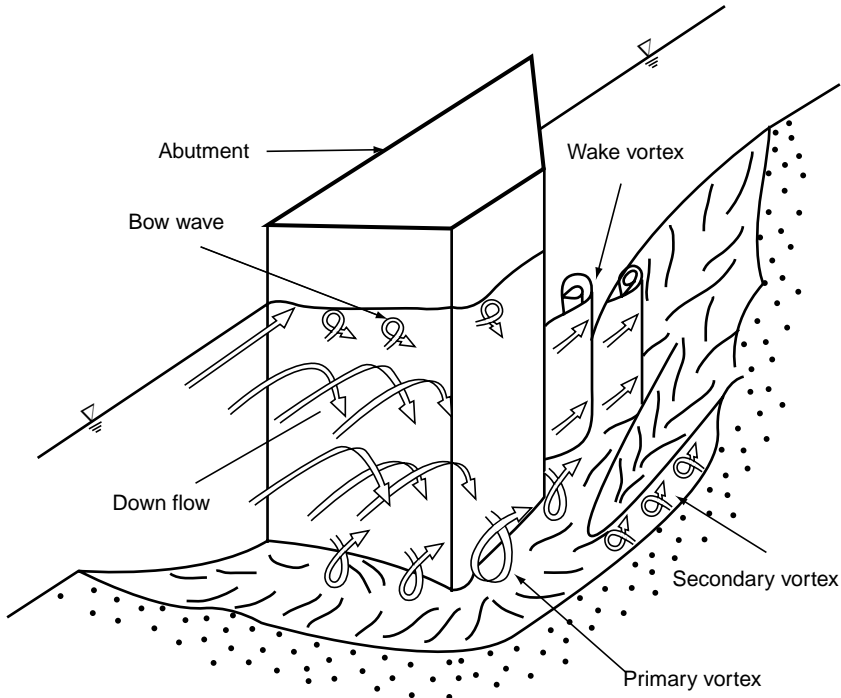


Fig. 11.12 Schematic sketch of flow field at an abutment (Ref. 18)

A detailed review of work done on abutment scour up to 2004 and including all aspects of the scour problem such as flow field, scouring process and scour depth estimation formulae are presented in Ref. 18. Further, relevant useful information related to abutment scour is available in Ref. 16. Detailed survey of abutment scour problem and FHWA recommendations are contained in HEC-18, (Ref. 17)

**Constriction Scour** When there is a contraction in a mobile bed channel there is an increase in the velocity and shear stress in the contracted region which leads to a higher transport rate and change in the sediment transport equilibrium. In live bed contraction scour maximum scour occurs when the shear stress in the contracted portion reduces to a value such that the bed sediment transported in to the section is equal to the bed sediment transported out of the contracted section. In clear water scour case equilibrium is reached when the shear stress in the contracted section reaches the critical shear stress. HEC- 18 contains detailed description of the contraction scour and recommends the following formulae for its estimation.

(i) *Live bed contraction scour*

$$\frac{y_2}{y_1} = \left( \frac{Q_2}{Q_1} \right)^{6/7} \left( \frac{W_1}{W_2} \right)^{K_1} \tag{11.52}$$

and average scour depth  $y_s = y_2 - y_0$  (11.53)

where  $y_1$  = average depth in upstream main channel (m)

$y_2$  = average depth in the contracted channel (m)

$y_0$  = existing depth in the contracting channel before scour (m)

$y_s$  = average scour depth (m)

$Q_1$  = flow in the upstream channel transporting sediment (m<sup>3</sup>/s)

$Q_2$  = flow in the contracted channel (m<sup>3</sup>/s)

$W_1$  = bottom width of the upstream channel that is transporting bed material (m)

$W_2$  = bottom width of the main channel in the contracted section less pier widths (m)

$K_1$  = Exponent determined as below

$V_*/\omega$	$K_1$	Mode of bed material transport
<0.50	0.59	Mostly contact bed material discharge
0.50 to 2.0	0.64	Some suspended material discharge
> 2.0	0.69	Mostly suspended material discharge

Where  $V_*$  = shear velocity in the upstream section (m/s)

=  $\sqrt{g y_1 S_1}$  in which  $S_1$  = slope of the energy grade line in the main channel

$\omega$  = fall velocity of the bed material based on  $D_{50}$  (m/s)

(ii) *Clear water contraction scour*

$$y_2 = \left[ \frac{0.025 Q^2}{D_m^{2/3} W^2} \right]^{3/7} \tag{11.54}$$

and average scour depth  $y_s = y_2 - y_0$  (11.55)

$y_2$  = average equilibrium depth in the contracted section after contraction scour (m)

$Q$  = discharge through the bridge (m)

$D_m$  = diameter of the smallest non-transportable particle in the bed material (taken as equal to  $1.25 D_{50}$ ) (m)

## 520 Flow in Open Channels

$y_0$  = average existing depth in the contracted section (m)

$y_s$  = average scour depth (m)

**Degradation Scour** Long-term degradation of the stream may be the result of some modification of the stream in the upstream regions or in the watershed. The stream may be in equilibrium, or aggrading or degrading at the bridge site. Details of aggradation and degradation phenomenon may be obtained in any treatise on Sediment Transport and is beyond the scope of this book. Details of estimation of degradation of stream at a bridge site are given in HEC-18. Procedures for estimating long-term aggradation and degradation at a bridge site are available in HEC- 20 (Ref. 19).

**Total Scour** The total scour at a bridge site is the sum of degradation scour, local contraction scour and abutment or pier scour. HEC-18 adopts this procedure to get a conservative estimate of scour.

**Example 11.9** | A bridge on an alluvial stream has the following features at the design state:

Upstream depth of flow = 3.5 m

Discharge intensity = 10.5 m<sup>3</sup>/s/m

Bed condition = plane bed. Bed material: median size = 1.0 mm

Piers: Round nosed, 12.0 m long and 1.5 m wide.

Estimate the maximum depth of scour at the bridge piers when the angle of attack of flow with respect to the pier front end is (a) 20° and (b) zero

**Solution** By Eq. 11.48

$$\frac{d_s}{b} = 2.0 K_1 K_2 K_3 K_4 \left(\frac{y_1}{b}\right)^{0.35} F_1^{0.43}$$

$$b = 1.5 \text{ m}, q = 10.5 \text{ m}^3/\text{s}/\text{m} \text{ and } y_1 = 3.5 \text{ m}$$

$$V_1 = 10.5/3.5 = 3.0 \text{ m/s}$$

$$F_1 = \frac{V_1}{\sqrt{gy_1}} = \frac{3.0}{\sqrt{9.81 \times 3.5}} = 0.512 \text{ m}$$

$$y_1/b = 3.5/1.5 = 2.333, L/b = 12.0/1.5 = 8.0$$

$K_1$  = correction factor for pier nose shape from Table (11.2) = 1.0

(a)  $\theta = 20^\circ$

$K_2$  = correction factor for angle of attack from Eq. 11.49

$$= (\cos 20^\circ + 8.0 \sin 20^\circ)^{0.65} = 2.33$$

$K_3$  = correction for bed condition from Table 11.4 for plane bed = 1.1

$K_4$  = correction factor for armoring by bed material for  $D_{50} < 2.00$  mm = 1.0

$$\frac{d_s}{b} = 2.0 \times 1.0 \times 2.33 \times 1.1 \times 1.0 \times (2.333)^{0.35} (0.512)^{0.65} = 5.172 \text{ m}$$

$$d_s = 5.172 \times 1.5 = 7.76 \text{ m below average bed level.}$$

(b) For  $\theta = 0^\circ$ ,  $K_2 = 1.0$

$$\frac{d_s}{b} = 2.0 \times 1.0 \times 1.0 \times 1.1 \times 1.0 \times (2.333)^{0.35} (0.512)^{0.65} = 2.22$$

$$d_s = 2.22 \times 1.5 = 3.33 \text{ m below average bed level.}$$

**The Indian Practice** The current practice followed in India is based on the Lacey equation. Two Codal provisions are available. Indian Railways Standards (1985) and IRC-5 (1998) and IRC-78 (2000) stipulates that in channels with alluvial beds the design scour depth be two times Lacey depth.

The following four Lacey equations are used:

The hydraulic radius of Lacey Eq. 11.43 is considered as depth and as such Eq. 11.43 is written as

$$D_{LQ} = 0.470 \left( \frac{Q}{f_s} \right)^{1/3} \quad (11.56)$$

$$P = 4.75 \sqrt{Q} \quad (11.42)$$

$$f_s = 1.76 \sqrt{d_{mm}} \quad (11.45)$$

Here,  $D_{LQ}$  = normal scour depth (in meters) below the design flood level and is called as Lacey regime depth.

$Q$  = design flood discharge ( $\text{m}^3/\text{s}$ )

$f_s$  = lacey silt factor with  $d_{mm}$  = median diameter of bed particles in mm.

When Lacey 's waterway as given by Eq. 11.42 is not available and restricted waterway is used IRC recommends that that instead of Eq. 11.56 the following equation be used to determine the Lacey depth of scour:

$$D_{Lq} = 1.34 \left( \frac{q^2}{f_s} \right)^{1/3} \quad (11.57)$$

where  $q$  = intensity of discharge under the bridge =  $Q/W_e$

where  $W_e$  = effective waterway.

Based on the analysis of field data by Inglis, a multiplying factor of 2.0 is used to obtain design maximum depth of scour below HFL as

$$D_s = 2.0 D_{LQ} \quad \text{or} \quad D_s = 2.0 D_{Lq} \quad \text{as is appropriate.} \quad (11.58)$$

This method, of estimating design scour depth as above, is sometimes known as Lacey–Inglis method. It is to be noted that in this method there is no separate provision for calculation of degradation scour or contraction scour.

**Example 11.10** Estimate the maximum depth of scour for design for the following data pertaining to a bridge in the Gangetic plain; (Use Lacey – Inglis equations)

Design discharge = 15,000 m<sup>3</sup>/s

Effective Water way = 550.0 m

Median size of bed material =  $d_{mm} = 0.10$  mm

**Solution** By Eq. 11.42,  $P = 4.75\sqrt{Q} = 4.75\sqrt{15000} = 581.8$  m

Since this is greater than  $W_e = 550$  m, use Eq. (11.53)

By Eq. 11.44  $f_s = 1.76\sqrt{d_{mm}} = 1.76\sqrt{0.10} = 0.556$

$$q = 15000/550 = 27.27 \text{ m}^3/\text{s/m}$$

By Eq. 11.57  $D_{Lq} = 1.34 \left( \frac{(27.27)^2}{0.556} \right)^{1/3} = 14.76$  m below HFL

Design scour depth  $D_s = 2.0 D_{Lq} = 2 \times 14.76 = 29.52$  m below HFL



## REFERENCES

1. Blench, T, *Mobile Bed Fluviology*, Univ. of Alberta Press, Edmonton, 1969.
2. Chang, H H, *Fluvial Processes in River Engineering*, John Wiley and Sons, USA, 1988.
3. Davis, C V, and Sorensen. K E, (Ed), *Handbook of Applied Hydraulics*, McGraw-Hill Book Co., New York, 1965.
4. Garde, R J, and Ranga Raju, K G, *Mechanics of Sediment Transportation and Alluvial Stream Problems*, Wiley Eastern Ltd., New Delhi, 2<sup>nd</sup> Ed., 1985.
5. Graf, W H, *Hydraulics of Sediment Transport*, McGraw-Hill Book Co., New York, 1971.
6. Shen, H W, (Ed), *River Mechanics*, Vol, I, II, Shen, H W, Fort Collins, Colo., USA, 1971.
7. Simons, D B, and Senturk F, *Sediment Transport Technology*, Water Resources Publication, Fort Collins, Colo., USA, 1977.

8. Swamee, P K, and Mittal, M K, An Explicit Equation for Critical Shear Stress in Alluvial Streams, *J. of Irrigation and Power*, CBIP, India, Vol. 33, No. 2, pp. 237–239, April 1976.
9. Vanoni, V A, (Ed.), *Sedimentation Engineering*, Manual No. 54, A.
10. Subramanya, K, *Engineering Hydrology*, McGraw-Hill Education (India), 3<sup>rd</sup> Ed, 2008.
11. Yang Xiaqing, ‘Manual on Sediment Management and Measurement’, *WMO – Operation Hydrology Report No. 47*, Secretariat of WMO, Geneva, Switzerland, 2003.
12. Muzzamil, M, and Gangadhariah, T, ‘The Mean Characteristics of a Horseshoe Vortex at a Cylindrical Pier’, *Jour. of Hyd. Research*, IAHR, Vol. 41, No.3, 2003, pp. 285–297.
13. Dey, S, and Raikar, R V, ‘Characteristics of Horseshoe Vortex in Developing Scour holes at Piers’, *Journal of Hydraulic Engineering*, ASCE, Vol. 133, No. 4, 2007, pp. 399–413.
14. Breusers, H N C, Nicollet, G, and Shen, H W, ‘Local Scour around Cylindrical Piers’ *J. Hyd Res.*, IAHR, 15(3), 1977, pp. 211–252.
15. Dargahi, B, ‘Local Scour at Bridge Piers—A Review of Theory and Practice’, *Bull No. Trita, VBI-114*, Hydr. Lab., Royal Institute of Technology, Stockholm, Sweden, 1982.
16. Strum, T W, *Open Channel Hydraulics*, McGraw-Hill Higher Education, Singapore, 2001.
17. Richardson, E V, and Davis, S R, *Evaluating Scour at Bridges*, Fourth Ed., Report No. HEC–18, Federal Highway Administration, US Department of Transportation, Washington DC, May 2001.
18. Barbhuiya, A K, and Dey, S, ‘Local Scour at Abutments: A Review’, *Sadhana*, India, Vol. 29, Part 5, Oct. 2004, pp. 449–476.
19. HEC-20, ‘Stream Stability at Highway Structures’, 3<sup>rd</sup> ed. *Report No. HEC–20*, Federal Highway Administration, US Department of Transportation, Washington DC, 2001.

## PROBLEMS

### Problem Distribution

Topic	Problems
Initiation of motion and Critical shear stress	11.1 to 11.5
Bed forms and Resistance	11.6 to 11.10
Bed load	11.11, 11.12, 11.16 and 11.24
Suspended load	11.13 to 11.15
Total load	11.16, 11.18
Non- Erodible channel	11.17, 11.18
Lacey Regime channel	11.19 to 11.24
Bridge Pier Scour	11.25, 11.26

- 11.1 Estimate the critical shear stress for the following sizes of sediment particles in the bed of a channel:
  - (a) 0.1mm
  - (b) 1.0 mm
  - (c) 10 mm
- 11.2 A wide stream has a sediment bed of median size 0.35 mm. The slope of the channel is  $1.5 \times 10^{-4}$ .
  - (a) If the depth of flow in the channel is 0.25 m, examine whether the bed particles will be in motion or not.
  - (b) What would be the status of the bed when the depth of flow is 0.10 m?

- 11.3 The median size of bed sediment in a wide gravel bed river is 50 mm. The river bed experiences threshold conditions when the energy slope of flow is 0.005. Estimate the depth of flow at this stage.
- 11.4 A wide alluvial channel has a flow which causes incipient motion of the bed particles. The temperature of the water is 25°C ( $\nu = 0.897 \times 10^{-6} \text{ m}^2/\text{s}$ ). It is expected that the temperature would drop to 5°C ( $\nu = 1.519 \times 10^{-6} \text{ m}^2/\text{s}$ ) and all other flow parameters would remain unaltered. Examine, with the help of Shields diagram, the status of the channel bed when the initial shear Reynolds number ( $u_* d/\nu$ ) is (a) 5, (b) 100, and (c) 500. [The change in the densities due to temperature change may be neglected].
- 11.5 A wide rectangular channel carries clear water at a depth of 1.2 m. The channel bed is composed of coarse gravel of  $d_{50} = 40 \text{ mm}$ . Determine the slope of the channel at which incipient conditions exists. What is the discharge per unit width at this slope?
- 11.6 A wide channel in an alluvium of grain size  $d_{50} = 0.30 \text{ mm}$  has plane bed with no motion. The depth of flow is 0.25 m and the bed slope is measured as 0.0002. Estimate the mean velocity and discharge per metre width in this channel.
- 11.7 Two wide alluvial channels A and B have the following features:

	Channel A	Channel B
Depth of flow	1.20 m	1.20 m
Slope	$1.65 \times 10^{-3}$	$1.65 \times 10^{-3}$
Bed material size	1.3 mm	12 mm

Estimate the nature of the bed form in each of these two channels.

- 11.8 A wide alluvial channel has a bed slope of  $6 \times 10^{-4}$  and bed material of median size 0.5 mm. Estimate the maximum depth of flow that can be adopted in this channel while maintaining the ripple and dune type of bed form.
- 11.9 A mobile bed channel with median grain size of 0.8 mm has a longitudinal slope of  $2 \times 10^{-4}$  and carries a discharge of  $10 \text{ m}^3/\text{s}$  at a depth of 1.5 m. The channel is trapezoidal in section and has a bed width of 10 m and side slopes of 1.5 horizontal : 1 vertical. Estimate (a) the Manning's roughness coefficient  $n$ , (b) the shear stress at the bed due to (i) sediment grains, and (ii) bed forms.
- 11.10 An irrigation channel is to be excavated on a slope of 0.0001 through a terrain consisting of coarse sand having  $d_{50} = 0.8 \text{ mm}$  and relative density 2.65. The discharge is to be  $1.5 \text{ m}^3/\text{s}$ . If no sediment transport is to be allowed, determine a suitable width for the channel by assuming it to be wide rectangular and the banks are protected.
- 11.11 Calculate the bed load per unit width in a wide stream having the following data:
- $d_{50} = 0.5 \text{ mm}$   
 $S_0 = 0.0004$   
 $n = \text{Manning's coefficient for the channel} = 0.025$   
 $q = \text{water discharge per unit width} = 3.0 \text{ m}^3/\text{s/m}$
- 11.12 Estimate the bed load for the following canal in coarse alluvium:
- $d_{50} = 12 \text{ mm}$   
 $y_0 = \text{depth of flow} = 5.87 \text{ m}$   
 $B = \text{width} = 46.0 \text{ m}$   
 $S_0 = \text{longitudinal slope} = 6.5 \times 10^{-4}$   
 $n = \text{Manning's coefficient for the channel} = 0.025$

The channel may be assumed to be a wide rectangular channel, with sides protected.

- 11.13 When a sediment of fall velocity  $\omega$  is suspended in water where the mass diffusion coefficient  $\varepsilon_s$  can be assumed constant, show that the concentration  $C$  at a height  $y$  above the bed is given by

$$\frac{C}{C_a} = \exp\left[-\frac{\omega(y-a)}{\varepsilon_s}\right]$$

where  $C_a$  = reference concentration at a level  $a$  above the bed.

- 11.14 In a wide channel with a depth of flow of 3.0 m suspended load samples at depths of 2.0 m and 2.5 m below the water surface indicated concentrations of 1200 ppm and 1800 ppm respectively. Estimate the concentration at a depth of 0.5 m below the water surface.
- 11.15 A wide channel has a slope of 1 in 4500 and a depth of flow of 2.0 m. Suspended load sampling at a height of 0.4 m above the bed revealed a concentration of 800 ppm by weight, consisting of particles having a fall velocity of 0.05 m/s. Estimate the concentration at levels of (a) 0.8 m and (b) 1.2 m above the bed.
- 11.16 A wide alluvial stream has a bed material of 0.25-mm median size and a longitudinal slope of  $2.0 \times 10^{-4}$ . Estimate the bed load and total load per unit width of this stream when the depth of flow is 2.0 m and the water discharge is 1.2 m<sup>3</sup>/s per metre width.
- 11.17 A channel which will carry a discharge of 60 m<sup>3</sup>/s is to be cut on a slope of 0.0005 through coarse, well-rounded gravel having a median size of 25 mm and relative density 2.65. Determine the suitable base width and depth of flow for a non-erodible channel of trapezoidal cross section with a side slope of 2H: 1V for the canal.
- 11.18 A trapezoidal channel of side slopes 2.5 H: 1V is cut in angular gravel of 2.0-mm median size. The base width of the channel is 10.0 m. If this channel is to carry clear water determine the maximum possible longitudinal slope to have a stable channel at a full supply depth of 1.5 m. What is the full supply discharge of this channel at this maximum slope?
- 11.19 Using the primary Lacey equations, show that the velocity of flow in a regime channel is given by

$$V = 10.8 R^{2/3} S_0^{1/2}$$

- 11.20 Fill in the following table relating the elements of a Lacey regime channel:

Sl. No.	$Q$ m <sup>3</sup> /s	$B$ m	$y_0$ m	$S_0$	$V$ m/s	Manning's Coefficient $n$	Silt factor $f_s$
(i)	30.0	—	—	—	—	—	0.80
(ii)	—	—	—	$3.27 \times 10^{-4}$	—	—	1.24
(iii)	—	30.0	1.50	—	—	—	—
(iv)	15.0	—	—	$2.0 \times 10^{-4}$	—	—	—

- 11.21 Design channels by the Lacey theory for the following two cases:
- (a) Discharge = 50 m<sup>3</sup>/s, Median size of alluvium = 0.9 mm
- (b) Discharge = 10m<sup>3</sup>/s, Median size of alluvium = 0.50 mm



- 11.22 A regime channel is designed by Lacey theory to carry  $20 \text{ m}^3/\text{s}$  of full supply discharge in an alluvium of median size  $1.2 \text{ mm}$ . What would be the Manning's roughness coefficient  $n$  of this channel?
- 11.23 Show that the Lacey regime equations would yield the following relationship for the Manning's roughness coefficient  $n$  applicable to a Lacey regime channel:

$$n = \left\{ \frac{0.028 d_{mm}^{5/36}}{Q^{1/36}} \right\}$$

where  $d_{mm}$  = sediment size in mm.

- 11.24 Design a regime channel by Lacey's equations to convey  $15 \text{ m}^3/\text{s}$  of water in an alluvium of median size  $1.2 \text{ mm}$ . What bed load and total load can be expected in this channel?
- 11.25 The following data pertain to a bridge on an alluvial stream at the design state:  
 Upstream depth of flow =  $4.0 \text{ m}$ , Discharge intensity =  $12.0 \text{ m}^3/\text{s}/\text{m}$   
 Bed condition = Small dunes. Bed material: median size =  $1.2 \text{ mm}$   
 Piers: Sharp nosed,  $18.0 \text{ m}$  long and  $1.5 \text{ m}$  wide.  
 Estimate the maximum depth of scour at the bridge piers when the angle of attack of flow with respect to the pier front end is  $5^\circ$ .
- 11.26 For the design of a bridge the following data have been collected:  
 Design flood discharge =  $600 \text{ m}^3/\text{s}$ ; Bed material =  $0.08 \text{ mm}$ .  
 Estimate the design scour for use in the design of the bridge piers.  
 [Use Lacey–Ingilis method].

## OBJECTIVE QUESTIONS

- 11.1 For a gravel of median size  $11 \text{ mm}$ , the critical shear stress is about  
 (a)  $3.2 \text{ Pa}$  (b)  $10 \text{ Pa}$   
 (c)  $0.62 \text{ Pa}$  (d)  $22 \text{ Pa}$
- 11.2 For water flow in coarse alluvium, the minimum size of the particle at which the critical shear stress is independent of the viscosity of water is about  
 (a)  $6 \text{ mm}$  (b)  $6 \text{ cm}$   
 (c)  $0.06 \text{ mm}$  (d)  $3 \text{ mm}$
- 11.3 Shields diagram is a plot of non-dimensional shear stress  $\tau_{*c}$  against  
 (a) Reynolds number of flow  
 (b) relative depth of grain size,  $d/R$   
 (c) Shear Reynolds number,  $u_{*c} d/\nu$   
 (d)  $u_* R/\nu$ , where  $R$  = hydraulic radius.
- 11.4 In Shields diagram the minimum shear Reynolds number  $R_{*c} = \left[ \frac{u_{*c} d}{\nu} \right]$  beyond which the critical shear stress is independent of  $R_{*c}$  is about  
 (a) 10 (b) 2000  
 (c) 2 (d) 400
- 11.5 The size  $d_c$  of a sediment particle that will just remain at rest in the bed of a wide rectangular alluvial channel of depth  $D$  and slope  $S_0$  is given by  $d_c$  equal to  
 (a)  $11 D S_0$  (b)  $10.8 D^{2/3} S_0^{1/3}$   
 (c)  $11 \sqrt{RS_0}$  (d)  $\frac{1}{11} R^{2/3} S_0^{1/2}$

- 11.6 If in an alluvial channel the Manning's  $n$  corresponding to plane bed without sediment is 0.016, the same channel with dunes on the bed will have a Manning's coefficient  $n_d$  such that
- (a)  $n_d < 0.016$                       (b)  $n_d = 0.016$   
 (c)  $n_d > 0.016$                       (d)  $n_d = 0.032$
- 11.7 Indicate the *incorrect* statement in an alluvial channel
- (a) if the bed form is dunes, then the water surface will be out of phase with the bed forms  
 (b) if the bed form is antidunes, then the water surface, will be in phase with the bed form  
 (c) ripples are not formed in sediment of size greater than 0.6 mm  
 (d) if the bed form is dunes, then the Froude number of the flow is greater than unity.
- 11.8 In an ideal laboratory channel with alluvial bed the channel flow is to be observed at various progressively higher shear values. Starting from the plane bed form the following sequence of bed forms can be expected:
- (a) Ripples and dunes–Transition–Antidunes  
 (b) Transition–Dunes–Antidunes  
 (c) Ripples and Dunes–Antidunes–Transition  
 (d) Antidunes–Ripples and dunes–Transition.
- 11.9 The hydraulic radius associated with the grain roughness  $R'$  is related to total hydraulic radius  $R$  as

$$(a) \quad R' = \left[ \frac{n_s}{n} \right]^{3/2} R \qquad (b) \quad R' = \left[ \frac{n_s}{n} \right] R^{3/2}$$

$$(c) \quad R' = \left[ \frac{n_s}{n} \right] R \qquad (d) \quad R' = \left[ \frac{n_s}{n} \right]^{2/3} R$$

where  $n_s$  and  $n$  are Manning's coefficient corresponding to grain roughness and total channel roughness respectively.

- 11.10 *Bed load* is a term used to describe
- (a) the combination of contact load and wash load  
 (b) the combination of contact load and saltation load  
 (c) the combination of contact load and suspended load near the bed  
 (d) the bed material load.
- 11.11 The term *wash load* refers to
- (a) the saltating part of bed material load  
 (b) suspended load during a flood  
 (c) part of suspended load comprising of particles not available in the bed material  
 (d) bed load after the fines have been washed out.
- 11.12 An alluvial channel has a bed material of median size 0.9 mm. The Manning's coefficient  $n$  of this bed when it is plane and without motion of particles is
- (a) 0.0009                      (b) 0.0123  
 (c) 0.0273                      (d) 0.0147

- 11.13 An unlined alluvial channel has trapezoidal section with side slopes of 2.5 horizontal: 1 vertical. If the angle of repose of the bed material is  $35^\circ$ , the ratio of critical shear stress of the sediment particle on the side to that on the bed is  
 (a) 0.61 (b) 0.93  
 (c) 0.65 (d) 0.76
- 11.14 In a trapezoidal channel having a side slope =  $m$  horiz : 1 vertical, depth of flow =  $D$ , longitudinal slope =  $S_0$ , the maximum shear stress on the sides is about  
 (a)  $\gamma DS_0$  (b)  $0.99 \gamma DS_0$   
 (c)  $0.76 \gamma DS_0$  (d)  $\left(\frac{1}{m}\right) \gamma DS_0$
- 11.15 In a regime alluvial channel designed by Lacey's theory,  
 (a) the bed load is zero  
 (b) the suspended load is zero  
 (c) the bed will have dune type of bed form  
 (d) the bed form will be of plane bed with sediment motion.
- 11.16 The Lacey's equations for a regime channel consists of a set of  $x$  independent equations relating to the flow, where  $x$  equal to  
 (a) 1 (b) 3  
 (c) 8 (d) 2
- 11.17 An alluvium with a median size of 0.32 mm has Lacey's silt factor  $f$  of value  
 (a) 1.76 (b) 1.00  
 (c) 0.57 (d) 0.80
- 11.18 A regime canal has a discharge of  $100 \text{ m}^3/\text{s}$ . It will have a perimeter of  
 (a) 4.8 m (b) 10.0 m  
 (c) 47.5 m (d) 22.0 m
- 11.19 A regime channel has a width of 22.2 m and depth of flow of 1.70 m. The discharge in the channel is about  
 (a)  $68 \text{ m}^3/\text{s}$  (b)  $3.0 \text{ m}^3/\text{s}$   
 (c)  $30.0 \text{ m}^3/\text{s}$  (d)  $7.0 \text{ m}^3/\text{s}$
- 11.20 When an alluvial channel attains its regime it will have side slopes  
 (a) of value equal to the angle repose of the alluvium  
 (b) of value equal to the angle of repose of the alluvium under water  
 (c) of value 0.5 vertical : 1 horizontal  
 (d) of value 0.5 horizontal : 1 vertical
- 11.21 The Lacey regime formulae are in general applicable to alluvial channels with sediment concentration in ppm by weight of less than about  
 (a) 10,000 (b) 1000  
 (c) 500 (d) 5000
- 11.22 The mean velocity in a Lacey regime channel is proportional to  
 (a)  $R^{1/3}$  (b)  $R^{1/2}$   
 (c)  $S_0^{1/2}$  (d)  $S_0^{1/3}$
- 11.23 A regime channel of longitudinal slope  $S_0$  will have Manning's roughness coefficient  $n$  given by  $n$  is equal to  
 (a)  $\left[\frac{S_0^{1/6}}{10.8}\right]$  (b)  $[S_0^{1/6}]$   
 (c)  $\left[\frac{R^{1/6}}{10.8}\right]$  (d)  $\left[\frac{1}{R^{1/6}}\right]$



## APPENDIX-A

Table A.1 Physical properties of Water

Temperature. °C	Specific weight $\gamma$ kN/m <sup>3</sup>	Density $\rho$ kg/m <sup>3</sup>	Viscosity $\mu \times 10^3$ . Ns/m <sup>2</sup>	Kinematic viscosity $\nu \times 10^6$ m <sup>2</sup> /s	Surface tension $\sigma$ N/m	Vapour pressure $P_v$ kN/m <sup>2</sup> abs	Vapour pressure head $P_v/\gamma$ m	Bulk modulus of elasticity $K \times 10^{-6}$ kN/m <sup>2</sup>
0	9.805	999.8	1.781	1.785	0.0756	0.61	0.06	2.02
5	9.807	1000.0	1.518	1.519	0.0749	0.87	0.09	2.06
10	9.804	999.7	1.307	1.306	0.0742	1.23	0.12	2.10
15	9.798	999.1	1.139	1.139	0.0735	1.70	0.17	2.14
20	9.789	998.2	1.002	1.003	0.0728	2.34	0.25	2.18
25	9.777	997.0	0.890	0.893	0.0720	3.17	0.33	2.22
30	9.764	995.7	0.798	0.800	0.0712	4.24	0.44	2.25
40	9.730	992.2	0.653	0.658	0.0696	7.38	0.76	2.28
50	9.689	988.0	0.547	0.553	0.0679	12.33	1.26	2.29
60	9.642	983.2	0.466	0.474	0.0662	19.92	2.03	2.28
70	9.589	977.8	0.404	0.413	0.0644	31.16	3.20	2.25
80	9.530	971.8	0.354	0.364	0.0626	47.34	4.96	2.20
90	9.466	965.3	0.315	0.326	0.0608	70.10	7.18	2.14
100	9.399	958.4	0.282	0.294	0.0589	101.33	10.33	2.07

SOME USEFUL WEBSITES RELATED TO OPEN  
CHANNEL HYDRAULICS

1. USGS – Surface Water Field Techniques  
***<http://www.usgs.gov>***
2. US Department of Transportation. Federal Highway Administration  
***<http://www.fhwa.dot.gov/engineering/hydraulics/index.cfm>***
3. US Bureau of Reclamation, USA  
***[http://www.usbr.gov/pmts/hydraulics\\_lab/](http://www.usbr.gov/pmts/hydraulics_lab/)***
4. Hydrologic Centre, US Army Corps of Engineers  
***<http://www.hec.usace.army.mil/>***
5. W M Keck Laboratory of Hydraulics and Water Resources Technical Reports administration.  
***<http://www.caltechkhr.library.caltech.edu/>***
6. Dr. Victor Miguel Ponce – Online Open Channel Hydraulics  
***<http://www.victormiguelponce.com>***  
***<http://onlinechannel.sdsu.edu/>***
7. Fluid Flow Calculations web site of LMNO Engineering Research and Software, Ltd.  
***<http://www.lmnoeng.com>***

## ANSWERS TO PROBLEMS

## CHAPTER 1

1.2 (a)  $\alpha = 2.0$ ,  $\beta = 1.33$

(b)  $\alpha = \frac{1}{(1-a)^2}$ ,  $\beta = \frac{1}{(1-a)}$

1.3  $a = \frac{(n+1)^3}{n^2(n+3)}$   $\beta = \frac{(n+1)^2}{n(n+2)}$

1.4  $\alpha = 5.71$ ,  $\beta = 2.374$

1.6 (a)  $v = \frac{9.9245}{r}$  (b)  $V = 2.0$  m/s

(c)  $\alpha = 1.023$ ,  $\beta = 1.008$

1.7 (a)  $h_{ep} = Z_0 + \frac{(k+1)}{2} h_1$  (b)  $h_{ep} = Z_0 + \frac{(2k+1)}{2} h_1$

1.8  $p/\gamma = 0.466$  y

1.9  $p/\gamma = 1.266$  y

1.13 (a) 1.046 m (b) 1.0473 m (c) 1.0431 m

1.14 (a) At  $x = 1.0$  m,  $h_{ep} = 1.173$  m (b) At  $x = 2.5$  m,  $h_{ep} = 1.101$  m

1.15  $Q = 3618$  m<sup>3</sup>/s

1.16  $q = 0.3889$  m<sup>3</sup>/s/m

1.17  $q = 1.03625$  m<sup>3</sup>/s/m

1.18  $h_m = 8.424$  m

1.19 (a)  $y_1 = 3.818$  m, (b)  $y_2 = 0.232$  m

(c)  $y_2 = 0.244$  m, (d)  $q = 1.843$  m<sup>3</sup>/s/m

1.20  $\Delta z = 0.751$  m,  $\Delta W_x = 0.251$  m

1.21  $H_A = 16.753$  m,  $h_{pA} = 16.280$  m

$H_B = 16.331$  m,  $h_{pB} = 15.782$  m

1.22  $E_L = 0.109$  m

532 Flow in Open Channels

- 1.24 Afflux = 0.056 m
- 1.25  $F_x = 5000 \text{ N/m}$ ,  $F_y = 10182 \text{ N/m}$  width
- 1.26 (a) 51.86 kN/m (b) 61.97 kN/m  
 (c) 62.79 kN/m (d) 33.51 kN/m width
- 1.28  $F = 6.91 \text{ kN/m}$ ,  $E_L = 0.453 \text{ m}$
- 1.29  $F_D = 13.67 \text{ kN/m}$

CHAPTER 2

- 2.3  $\Delta z = -0.857 \text{ m}$
- 2.4 (a) 0.736 m, 1.940 m, (b) 0.936 m, 1.943 m (c) 0.730 m, 1.888 m
- 2.7  $E = 1.5906 \text{ m}$ ,  $y_2 = 0.497 \text{ m}$
- 2.17  $Q = 0.031 \text{ m}^3/\text{s}$ ,  $E = 0.60 \text{ m}$
- 2.18 (a) Subcritical (b)  $y_c = 1.148 \text{ m}$   
 (c)  $E = 1.454 \text{ m}$  (d)  $y_3 = 1.08 \text{ m}$
- 2.19 (a)  $Q = 3.322 \text{ m}^3/\text{s}$ ,  $E_c = 0.75 \text{ m}$   
 (b)  $B = 2.5 \text{ m}$ ,  $E_c = 1.20 \text{ m}$   
 (c)  $y_c = 0.972 \text{ m}$ ,  $E_c = 1.458 \text{ m}$   
 (d)  $Q = 1.585 \text{ m}^3/\text{s}$ ,  $y_c = 0.40 \text{ m}$
- 2.20 (i)  $y_c = 0.283 \text{ m}$ ,  $E_c = 0.978 \text{ m}$   
 (ii)  $Q = 0.164 \text{ m}^3/\text{s}$ ,  $E_c = 0.375 \text{ m}$   
 (iii)  $Q = 0.354 \text{ m}^3/\text{s}$ ,  $y_c = 0.480 \text{ m}$
- 2.21 (a)  $y_c = 0.546 \text{ m}$ ,  $E_c = 0.775 \text{ m}$   
 (b)  $Q = 1.206 \text{ m}^3/\text{s}$ ,  $E_c = 0.422 \text{ m}$   
 (c)  $B = 3.0 \text{ m}$ ,  $E_c = 0.571 \text{ m}$   
 (d)  $y_c = 0.80 \text{ m}$ ,  $Q = 11.068 \text{ m}^3/\text{s}$
- 2.22 (a)  $Q = 0.558 \text{ m}^3/\text{s}$ ,  $E_c = 0.51 \text{ m}$   
 (b)  $Q = 0.741 \text{ m}^3/\text{s}$ ,  $E_c = 0.540 \text{ m}$
- 2.23 (a)  $y_c = 0.947 \text{ m}$ , (b)  $y_c = 1.1644 \text{ m}$
- 2.24  $y_c = 1.185 \text{ m}$
- 2.25  $D = 1.50 \text{ m}$
- 2.26  $Q = 1.216 \text{ m}^3/\text{s}$ ,  $E_c = 0.836 \text{ m}$
- 2.27  $Q = 0.737 \text{ m}^3/\text{s}$
- 2.29  $Q = 11.50 \text{ m}^3/\text{s}$

- 2.32 (i) 3.106, 3.500, 3.833 and 4.200 (ii) 3.96, 3.84 and 4.35
- 2.33  $y_2 = 1.079$  m
- 2.34 (a)  $y_2 = 1.366$  m,  $y_1 = 2.086$  m (b)  $y_2 = 1.651$  m,  $y_1 = 2.00$  m
- 2.35  $\Delta z_m = 0.244$  m
- 2.36  $B_2 = 2.472$  m
- 2.37 (a)  $y_2 = 0.871$  m,  $y_1 = 0.90$  m  
(b)  $y_2 = 0.657$  m,  $y_1 = 0.911$  m
- 2.38  $Q = 3.362$  m<sup>3</sup>/s,  $y_1 = 1.153$  m,  $F_1 = 0.289$   
 $y_2 = 0.261$  m,  $F_2 = 2.683$
- 2.39  $\Delta z = -0.366$  m
- 2.40  $y_1 = 2.171$  m
- 2.41  $y_2 = 0.744$  m,  $\Delta z_m = 0.133$  m
- 2.42  $B_2 = 3.299$  m
- 2.43  $Q = 4.825$  m<sup>3</sup>/s,  $\Delta z = -0.25$  m
- 2.44  $\Delta z = 0.440$  m,  $\Delta y = 0.011$  m

### CHAPTER 3

- 3.1 (a)  $\tau_0 = 1.6187$  N/m<sup>2</sup> (b) rough (c)  $C = 60.9$   
(d)  $n = 0.014$  (e)  $Q_{ch} = 2.314$  m<sup>3</sup>/s,  $Q_{Ma} = 2.458$  m<sup>3</sup>/s
- 3.2  $Q = 9.035$  m<sup>3</sup>/s
- 3.3  $f = 0.0178$ ,  $n = 0.0145$ ,  $C = 66.5$
- 3.6  $n = 0.0181$
- 3.7 38.9%
- 3.8  $n = 0.0474$
- 3.9 (a) 4.206 m<sup>3</sup>/s, (b) 6.373 m<sup>3</sup>/s, (c) 3.773 m<sup>3</sup>/s,
- 3.10  $y_0 = 0.944$  m
- 3.11 (a)  $1.9446 \times 10^{-4}$  (b)  $3.46 \times 10^{-4}$
- 3.12 (a) 12.176 m<sup>3</sup>/s (b)  $y_0 = 1.735$  m
- 3.13  $Q = 0.974$  m<sup>3</sup>/s
- 3.14  $B = 3.656$  m
- 3.15  $n = 0.0188$
- 3.16  $D = 2.00$  m
- 3.17  $Q = 2.73$  m<sup>3</sup>/s,  $y_0 = 0.093$  m



534 Flow in Open Channels

3.18  $B = 4.85 \text{ m}, y_0 = 3.638 \text{ m}$

3.19  $F_0 = 0.197$

3.20  $S_0 = 7.196 \times 10^{-4}$

3.21 0.9615

3.22  $\tau_0 = 0.2674 \text{ N/m}^2$

3.23  $B = 3.465 \text{ m}, y_0 = 1.155 \text{ m}, S_0 = 1.998 \times 10^{-4}$

3.24  $K = 160.5 \text{ m}^3/\text{s}, S_0 = 3.209 \text{ m}^3/\text{s}, F_0 = 0.282, \tau_0 = 2.50 \text{ N/m}^2$

3.25  $Q = 4.48 \text{ m}^3/\text{s}, S_0 = 5.2 \times 10^{-3}$

3.26 (a) 1.179 m, (b) 1.540 m, (c) 1.957 m

3.28  $B = 23.00 \text{ m}, y_0 = 3.105 \text{ m}$

3.29  $B = 13.09 \text{ m}$

3.30  $Q = 271.3 \text{ m}^3/\text{s}$

3.31  $Q = 23.52 \text{ m}^3/\text{s}$

3.32  $y_0 = 2.352 \text{ m}, \tau_0 = 11.537 \text{ Pa}$

3.33  $Q = 18.61 \text{ m}^3/\text{s}$

3.37 (a)  $y = 0.849 B$ , (b)  $y = 1.635 B$

3.38 (i)  $d = 0.3382 a$ , (ii)  $d = 0.4378 a$

3.39  $y_e = 1.597 \text{ m}, B_e = 1.120 \text{ m}$

3.40  $y_e = 4.045 \text{ m}, Q = 32.12 \text{ m}^3/\text{s}$

3.42  $S_0 = 2.609 \times 10^{-4}$

3.44  $B_e = 3.232 \text{ m}, y_e = 5.338 \text{ m}$

3.46  $B_e = 3.57 \text{ m}, y_e = 2.89 \text{ m}, S_0 = 2.7 \times 10^{-4}$

3.47 Lined canal is 14.7% cheaper.

3.48  $y_e = 1.934 \text{ m}, B_e = 2.735 \text{ m}$

3.53  $N = 3.51$

3.54	$m$	$\frac{y}{B} = 0.5$	1.0	2.0
	1.0	$N = 3.7$	4.0	4.4
	1.5	$N = 3.9$	4.3	4.7

3.55 (i) 2.902 m<sup>3</sup>/s (ii) 6.568 m<sup>3</sup>/s

3.56 (i) 2.631 m<sup>3</sup>/s (ii) 6.010 m<sup>3</sup>/s

3.57 (i) 41.450 m<sup>3</sup>/s (ii) 47.99 m<sup>3</sup>/s

3.59  $y_{e1} = 0.250 \text{ m}, y_{e2} = 2.30 \text{ m}$

3.61  $S_c = 0.004447$ , Slope is Mild in the range of depths.

- 3.62  $S_0 = 0.0006939$   
 3.63  $F_0 = 0.5$   
 3.64 (a)  $S_0 = 1.6036 \times 10^{-4}$  (b)  $S_c = 4.009 \times 10^{-3}$  (c)  $y_0 = 3.96$  m  
 3.65 (a)  $S_e = 7.1 \times 10^{-3}$  (b)  $F = 1.07$   
 3.66  $S_{L_c} = 4.166 \times 10^{-3}$   $Q = 0.336$  m<sup>3</sup>/s,  $y_c = 0.2$  m  
 3.67  $S_{*L_c} = 2.28$   
 3.68  $m = 1.5$ ,  $n = 0.015$ ,  $B/y_0 = 10.0$   
 $B = 18.0$  m,  $y_0 = 1.821$  m,  $V = 3.618$  m/s

## CHAPTER 4

- 4.4  $\left( \frac{dy}{dx} - S_0 \right) = -1.437 \times 10^{-4}$   
 4.5  $S_2$  curve  
 4.6 (i)  $M_2$  curve (ii)  $M_1$  curve  
 4.7  $M_3$  curve  
 4.8 (i)  $M_3$  curve, (ii)  $M_2$  curve, (iii)  $M_1$  curve  
 4.9  $S_2$  curve on steeper channel  
 4.10 Jump and  $S_1$  curve  
 4.12 (a) Mild – Steep (b) Mild – Steeper Mild  
 (c) Steep – Mild (d) Mild – Milder Mild  
 4.13 (a)  $[H_3 - J - H_2]$  or  $[J - S_1 - H_2]$   
 (b)  $M_1 - M_3 - J - M_2 - S_2 - J - S_1 - H_2$  or  
 $M_1 - M_3 - J - M_2 - M_2 - S_2 - H_3 - J - H_2$   
 (c)  $[S_2 - J - S_1 - M_1]$  or  $[S_2 - M_3 - J - M_1]$   
 (d)  $S_2 - J - S_1 - S_3 - M_3 - J$   
 (e)  $J - S_1 - M_1 - M_3 - J - M_2$  or  
 $M_3 - J - M_1 - M_3 - J - M_2$   
 (f)  $A_3 - J - A_2 - H_2 - S_2$   
 4.14 (a)  $[J - S_1]$  on the upstream and  $S_1$  on the downstream  
 (b)  $M_1$  on the upstream and  $(M_3 - J - M_2/M_1)$  on the downstream  
 (c) Horizontal on the upstream and  $(H_3 - J - H_2)$  on the downstream  
 4.15 (a)  $M_3$  on A (b)  $M_1$  on A and  $(M_3 - J)$  on B  
 4.16  $M_2$  curve on A and  $S_2$  curve on B  
 4.17  $[S_2 - H_3 - J]$  or  $[S_2 - J - S_1]$   
 4.18  $M_1 - M_3 - J - M_2 - S_2$

**CHAPTER 5**

- 5.5  $M_1$  curve;  $L = 2.28$  km
- 5.7 (a) 9.16 km (b) 130 m
- 5.8 (a) 2.87 m (b) 2.873 m
- 5.9  $y_0 = 1.074$  m
- 5.10  $\alpha = 1.195$ ,  $S_f = 9.795 \times 10^{-6}$
- 5.11  $L = 24,500$  m
- 5.13  $M_1$  profile,  $L = 454$  m
- 5.14  $Q_2 = 105$  m<sup>3</sup>/s,  $Q_R = 55$  m<sup>3</sup>/s
- 5.15  $S_2$  curve,  $L = 70$  m
- 5.16 105.604 m, 106.355 m and 107.313 m.
- 5.17  $S_1$  curve, 69 m
- 5.18 22.5 m
- 5.19  $M_2$  curve, 222 m
- 5.20 2.69 m, 6.16 km
- 5.21 Inlet is submerged
- 5.22  $x = 89$  m
- 5.23 (a) 122.109 m and 121.800 m (b) 11.3 m<sup>3</sup>/s
- 5.24  $Q = 31.13$  m<sup>3</sup>/s,  $L = 222$  m
- 5.25  $Q = 178$  m<sup>3</sup>/s

**CHAPTER 6**

- 6.1  $q = 8.4$  m<sup>3</sup>/s/m;  $E_L = 3.65$  m;  $F_1 = 4.58$
- 6.2  $E_L/E_1 = 72.7\%$

	$V_1$	$y_1$	$q$	$F_1$	$y_2$	$V_2$	$F_2$	$E_L$	$\frac{E_L}{E_1} \%$
(a)	10.33	0.170	1.756	8.00	1.84	0.954	0.225	3.722	66.4
(b)	8.91	0.100	0.891	9.00	1.224	0.728	0.210	2.900	69.9
(c)	8.00	0.250	2.000	5.10	1.683	1.188	0.292	1.750	50.0
(d)	9.54	0.151	1.440	7.84	1.600	0.900	0.227	3.140	65.5
(e)	13.50	0.350	4.725	7.29	3.435	1.375	0.237	6.105	63.3
(f)	13.64	0.068	0.928	16.70	1.574	0.590	0.150	8.00	83.7

- 6.4  $F_2 = 0.296$
- 6.6  $y_1 = 0.198$  m,  $y_2 = 2.277$  m

- 6.8  $F_1 = 4.82$
- 6.9  $F_1 = 13.65, F_2 = 0.235$
- 6.10  $y_1 = 0.348 \text{ m}, y_2 = 3.40 \text{ m}$
- 6.11  $y_1 = 0.90 \text{ m}, y_2 = 6.94 \text{ m}; E_L/E_1 = 55\%$
- 6.12 101.486 m
- 6.13 95.973 m
- 6.14 Repelled jump;  $y_1 = 1.674 \text{ m}, L_j = 26.4, H_3$  curve of length = 81.0 m
- 6.17  $y_t = 26.21 \text{ m}, L_j = 120 \text{ m}, E_L = 40.77 \text{ m}$
- 6.18  $Q = 1.541 \text{ m}^3/\text{s}; F_1 = 2.494; F_2 = 0.441$
- 6.20  $y_2 = 1.875 \text{ m}, E_L = 6.880 \text{ m}$
- 6.21  $y_1 = 0.242 \text{ m}, E_L = 4.695 \text{ m}$
- 6.22  $y_2 = 0.796 \text{ m}$
- 6.23 Jump at 80 m from the gate,  $y_1 = 1.02 \text{ m}, y_2 = 3.99 \text{ m}$ ,
- 6.24  $x = 62.0 \text{ m}, y_1 = 0.96 \text{ m}, y_2 = 3.23 \text{ m}$
- 6.25  $y_{th} = 1.892 \text{ m}, y_{ts} = 3.595 \text{ m}$
- 6.30  $\Delta z = 0.880 \text{ m}$
- 6.31 (i) No free jump is possible. Submerged jump occurs  
(ii) free repelled jump,  $y_1 = 0.467 \text{ m}, y_t = 3.737 \text{ m}$
- 6.32 (a)  $q = 15.31 \text{ m}^3/\text{s}/\text{m}$   
(b) Free – repelled jump,  $y_1 = 1.119 \text{ m}, y_t = 6.0 \text{ m}$   
(c)  $y_{tm} = 6.53 \text{ m}$ .

## CHAPTER 7

- 7.1 0.074 m rise
- 7.2  $P = 1.088 \text{ m}$
- 7.3  $3.512 \text{ m}^3/\text{s}$
- 7.5  $Q_s = 0.0626 \text{ m}^3/\text{s}$
- 7.6  $2.965 \text{ m}^3/\text{s}$
- 7.7 6.38%
- 7.8  $a = 0.592 \text{ m}, H_{d \max} = 1.144 \text{ m}$
- 7.9  $a = 0.231 \text{ m}, H_{d \max} = 1.386 \text{ m}$
- 7.10 (i)  $0.118 \text{ m}^3/\text{s}$ , (ii)  $0.163 \text{ m}^3/\text{s}$ , (iii)  $0.396 \text{ m}$
- 7.11 (i) 38 lit/s, (ii) 9.91 cm

538 Flow in Open Channels

7.12 23.088 m, 23.102m with river bed as datum, 3.8440 m, -1.069m

7.13 34.243 m<sup>3</sup>/s/m

7.14 0.150 m

7.15 59.3 m<sup>3</sup>/s

7.16 11.939 m and 11.950 m above the bed

7.17 0.502 m above the crest

7.18 1240 s

7.19 Broad crested weir; 0.076 m

7.21 16.39 m<sup>3</sup>/s

7.22 0.785 m

7.23  $\eta = 0.657$

7.24  $\eta = 0.7834$

7.25  $\eta = 0.733$

7.26 0.673 m

7.27 (i) 4.815 m<sup>3</sup>/s, (ii) 0.695 m<sup>3</sup>/s, (iii) 0.505 m<sup>3</sup>/s

7.29 1.624 m<sup>3</sup>/s; 7580 N

7.30 0.747 m

7.31 0.487 m

**CHAPTER 8**

8.2  $y_c = 3.14$  m and  $x_c = 43.7$  m

8.3  $y_c = 3.3$  m and  $x_c = 74.75$  m

8.7  $L = 1.353$  m,  $s = 0.79$  m

8.8  $Q_s = 0.206$  m<sup>3</sup>/s

8.9  $Q_s = 0.206$  m<sup>3</sup>/s

8.10  $L = 1.729$  m,  $\Delta z = 0.09$  m or  $B_2 = 1.80$  m

8.12  $L = 0.767$  m

8.13  $Q_d = 3.17$  m<sup>3</sup>/s

**CHAPTER 9**

9.1  $\beta = 29^\circ$

9.2  $y_1 = 0.393$  m

9.5  $\beta_s = 42^\circ$ ,  $y_2 = 0.72$  m

9.6  $\beta_s = 29^\circ$ ,  $y_2 = 0.84$  m,  $E_{L0} = 0.268$  m

9.7 (a) Positive (b) Negative (c) Positive (d) Negative

9.8  $F_m = 13.6$ ,  $\beta_m = 4.217^\circ$ , Width of fan = 4.606°

9.10  $F_2 = 2.86$ ,  $F_3 = 2.384$ ,  $\beta_A = 18.3^\circ$ ,  $\beta_B = 21.87^\circ$ ,  $\beta_c = 25.96^\circ$

9.12  $F_2 = 3.395$ ,  $F_3 = 3.30$ ,  $\beta_1 = 18.5^\circ$ ,  $\beta_2 = 21.5^\circ$ ,  $\beta_3 = 25.5^\circ$ ,  $\beta_4 = 22^\circ$ .

9.13

Sl. No.	$F_1$	$y_1$ (m)	$B_1$ (m)	$F_3$	$y_3$ (m)	$B_3$ (m)	$F_2$	$y_2$ (m)	$\theta$	$\beta_1$	$\beta_2$
1	5.0	0.7	6.0	3.317	1.450	3.00	4.02	1.038	5.2°	16.5°	19.2°
2	6.0	0.5	4.0	3.795	1.155	1.802	4.649	0.803	5.0°	13.5°	17.0°
3	4.0	0.6	4.71	2.622	1.213	2.5	3.194	0.885	6.0°	19.5°	4.0°
4	5.2	0.48	5.04	2.939	1.30	2.0	3.807	0.841	7.5°	8.0°	22.5°

**CHAPTER 10**

10.5 (a)  $V_2 = -2.335$  m/s,  $V_w = -6.17$  m/s

or  $V_2 = 5.335$  m/s,  $V_w = 9.17$  m/s

(b)  $y_2 = 1.265$  m,  $V_2 = 2.535$  m/s

(c)  $y_2 = 2.640$  m,

(d)  $y_1 = 0.385$  m,  $V_2 = -1.459$  m/s

(e)  $V_1 = 0.529$  m/s,  $V_2 = 2.015$  m/s

10.6  $y_1 = 2.60$  m

10.7 = 0.2286 m

10.8  $y_2 = 0.85$  m,  $V_w = 4.95$  m/s

10.9  $\Delta y = 0.501$  m,  $V_w = 2.695$  m/s

10.10  $y_2 = 1.915$  m,  $V_w = 3.0$  m/s, Time = 11 m 6.6 s

10.11 (i)  $h = 0.6$  m,  $V_w = 4.248$  m (directed upstream)

(ii)  $h = 0.216$  m,  $V_w = 6.208$  m

10.12 (a)  $V_w = 4.774$  m/s,  $V_2 = -0.160$  m/s

(b)  $\Delta y = 0.485$  m

10.14 At  $t = 2.0$  s,  $x = 37.585 - 18.792\sqrt{y}$

10.15  $V_2 = 2.778$  m/s,  $y_2 = 1.44$  m

10.16 (a)  $q = 3.27$  m<sup>3</sup>/s/m, (b)  $q_{\max} = 15.103$  m<sup>3</sup>/s/m

**CHAPTER 11**

11.1 (a) 0.159 Pa, (b) 0.532 Pa, (c) 9.05 Pa

11.2 (a) in motion, (b) not in motion

11.3  $y_0 = 0.925$  m

11.4 (a) no motion, (b) motion of bed, (c) incipient conditions

540 Flow in Open Channels

11.5  $S_0 = 0.0031$ ,  $q = 2.69 \text{ m}^3/\text{s per m}$

11.6  $V = 0.456 \text{ m/s}$ ,  $q = 0.114 \text{ m}^3/\text{s/m}$

11.7 Channel A : Transition; Channel B : Dunes

11.8  $y_0 = 1.40 \text{ m}$

11.9  $n = 0.0292$ ;  $\tau_0' = 0.8086 \text{ Pa}$ ;  $\tau_0'' = 1.526 \text{ Pa}$

11.10  $B = 12.0 \text{ m}$

11.11  $q_B = 2.131 \text{ N/s per m}$

11.12  $Q_B = 2091 \text{ N/s}$

11.14  $C_3 = 433.2 \text{ ppm}$

11.15  $C_{08} = 125 \text{ ppm}$ ;  $C_{12} = 27 \text{ ppm}$

11.16  $q_B = 0.1494 \text{ N/s per m}$ ;  $q_T = 0.1.752 \text{ N/s per m}$ ;  $q_x = 1.603 \text{ N/s per metre}$

11.17  $B = 7.10 \text{ m}$ ;  $y_0 = 3.20 \text{ m}$

11.18  $S_0 = 8.5 \times 10^{-5}$ ;  $Q = 9.43 \text{ m}^3/\text{s}$

No.	$Q \text{ m}^3/\text{s}$	$m$	$y_0$	$S_0$	$V \text{ m/s}$	$n$	$f_s$
(i)	30.0	21.93	1.83	$1.17 \times 10^{-4}$	0.718	0.020	0.80
(ii)	5.12	8.74	0.90	$3.27 \times 10^{-4}$	0.618	0.243	1.24
(iii)	49.3	30.00	1.50	$5.23 \times 10^{-4}$	1.07	0.0263	2.06
(iv)	15.0	15.40	1.34	$2.00 \times 10^{-4}$	0.695	0.0224	1.03

11.21 (a)  $S_0 = 3.674 \times 10^{-4}$ ,  $B = 29.95 \text{ m}$ ,  $y_0 = 1.627 \text{ m}$

(b)  $S_0 = 2.943 \times 10^{-4}$ ,  $B = 13.788 \text{ m}$ ,  $y_0 = 0.551 \text{ m}$

11.22  $n = 0.0265$

11.24  $Q_B = 11.12 \text{ N/s}$ ;  $Q_T = 18.86 \text{ N/s}$

11.25  $d_s = 4.13 \text{ m below average bed level.}$

11.26  $D_s = 10.00 \text{ below HFL}$

## ANSWERS TO OBJECTIVE QUESTIONS

### Chapter 1

	0	1	2	3	4	5	6	7	8	9
1.0		<i>b</i>	<i>c</i>	<i>d</i>	<i>d</i>	<i>d</i>	<i>c</i>	<i>a</i>	<i>c</i>	<i>c</i>
1.10	<i>b</i>	<i>c</i>	<i>a</i>	<i>c</i>	<i>b</i>	<i>b</i>	<i>d</i>	<i>c</i>	<i>c</i>	<i>c</i>
1.20	<i>d</i>	<i>b</i>	<i>b</i>	<i>b</i>	<i>d</i>	<i>a</i>	<i>a</i>	<i>a</i>	<i>b</i>	

### Chapter 2

	0	1	2	3	4	5	6	7	8	9
2.0		<i>c</i>	<i>d</i>	<i>c</i>	<i>b</i>	<i>c</i>	<i>a</i>	<i>c</i>	<i>d</i>	<i>b</i>
2.10	<i>d</i>	<i>c</i>	<i>a</i>	<i>a</i>	<i>b</i>	<i>a</i>	<i>d</i>	<i>b</i>	<i>c</i>	<i>a</i>
2.20	<i>d</i>	<i>c</i>	<i>c</i>	<i>c</i>	<i>c</i>	<i>a</i>	<i>a</i>	<i>b</i>		

### Chapter 3

	0	1	2	3	4	5	6	7	8	9
3.00	-	<i>c</i>	<i>d</i>	<i>c</i>	<i>a</i>	<i>c</i>	<i>a</i>	<i>c</i>	<i>d</i>	<i>c</i>
3.10	<i>d</i>	<i>b</i>	<i>a</i>	<i>d</i>	<i>c</i>	<i>b</i>	<i>a</i>	<i>b</i>	<i>b</i>	<i>c</i>
3.20	<i>c</i>	<i>b</i>	<i>b</i>	<i>a</i>	<i>c</i>	<i>c</i>	<i>d</i>	<i>b</i>	<i>a</i>	<i>d</i>
3.30	<i>c</i>	<i>a</i>	<i>d</i>	<i>c</i>	<i>b</i>	<i>b</i>	<i>a</i>			

### Chapter 4

	0	1	2	3	4	5	6	7	8	9
4.0		<i>c</i>	<i>b</i>	<i>b</i>	<i>b</i>	<i>c</i>	<i>a</i>	<i>c</i>	<i>c</i>	<i>c</i>
4.10	<i>c</i>	<i>d</i>	<i>d</i>	<i>a</i>	<i>b</i>	<i>a</i>	<i>a</i>	<i>d</i>	<i>c</i>	<i>b</i>
4.20	<i>c</i>	<i>c</i>	<i>d</i>							

### Chapter 5

	0	1	2	3	4	5	6	7	8	9
5.0	-	<i>d</i>	<i>d</i>	<i>c</i>	<i>b</i>	<i>c</i>	<i>b</i>	<i>d</i>	<i>c</i>	<i>a</i>
5.10	<i>d</i>	<i>b</i>	<i>b</i>	<i>d</i>	<i>c</i>	<i>c</i>	<i>d</i>	<i>a</i>	<i>c</i>	

### Chapter 6

	0	1	2	3	4	5	6	7	8	9
6.0		<i>d</i>	<i>b</i>	<i>d</i>	<i>a</i>	<i>d</i>	<i>c</i>	<i>c</i>	<i>b</i>	<i>d</i>
6.10	<i>a</i>	<i>c</i>	<i>a</i>	<i>b</i>	<i>c</i>					



**Chapter 7**

	0	1	2	3	4	5	6	7	8	9
7.0	-	<i>d</i>	<i>b</i>	<i>d</i>	<i>b</i>	<i>a</i>	<i>c</i>	<i>a</i>	<i>c</i>	<i>b</i>
7.10	<i>d</i>	<i>b</i>	<i>d</i>	<i>d</i>	<i>c</i>	<i>b</i>	<i>a</i>	<i>b</i>	<i>b</i>	<i>c</i>
7.20	<i>c</i>	<i>a</i>	<i>a</i>	<i>b</i>	<i>c</i>	<i>d</i>	<i>d</i>	<i>d</i>	<i>c</i>	<i>c</i>
7.30	<i>a</i>									

**Chapter 8**

	0	1	2	3	4	5	6	7	8	9
8.0		<i>b</i>	<i>c</i>	<i>d</i>	<i>b</i>	<i>b</i>	<i>c</i>	<i>c</i>	<i>c</i>	<i>a</i>
8.10	<i>a</i>	<i>d</i>	<i>b</i>	<i>a</i>	<i>b</i>					

**Chapter 9**

	0	1	2	3	4	5	6	7	8	9
9.0		<i>a</i>	<i>b</i>	<i>a</i>	<i>d</i>	<i>c</i>	<i>b</i>	<i>d</i>	<i>a</i>	<i>b</i>
9.10	<i>d</i>	<i>d</i>	<i>c</i>	<i>d</i>						

**Chapter 10**

	0	1	2	3	4	5	6	7	8	9
10.0		<i>c</i>	<i>c</i>	<i>d</i>	<i>a</i>	<i>b</i>	<i>a</i>	<i>d</i>	<i>b</i>	<i>d</i>
10.10	<i>d</i>	<i>d</i>	<i>c</i>	<i>a</i>	<i>d</i>	<i>a</i>				

**Chapter 11**

	0	1	2	3	4	5	6	7	8	9
11.00	-	<i>b</i>	<i>a</i>	<i>c</i>	<i>d</i>	<i>a</i>	<i>c</i>	<i>d</i>	<i>a</i>	<i>a</i>
11.10	<i>b</i>	<i>c</i>	<i>d</i>	<i>d</i>	<i>c</i>	<i>c</i>	<i>c</i>	<i>c</i>	<i>c</i>	<i>c</i>
11.20	<i>d</i>	<i>c</i>	<i>d</i>	<i>a</i>						

# Index

## A

Abel's form of integral equation, 313  
Abutment Scour, 519  
Advanced Numerical Methods, 203  
Adverse slope, 161, 169  
Aeration, 301  
Aeration of the nappe, 364  
Afflux, 36, 333  
Aggradation, 512  
Air entrainment, 368  
Alluvial channels, 139  
Alluvium, 2, 484, 508  
Alternate depths, 43, 73  
Antidunes, 488  
Antoine Chezy, 86  
Apron floor, 288  
Armoring, 517

## B

Backwater, 157  
Backwater curve, 165, 197, 218  
Baffle blocks, 279, 291  
Baffle wall, 291  
Baffles, 291  
Bakhmeteff, 42, 123  
Base weirs, 315  
Bazin's formula, 91  
Bed forms, 488  
Bed irregularities, 488  
Bed load, 495, 502  
Bed shear stresses, 484  
Bernoulli equation, 22  
Blasius formula, 87  
Bore, 438  
Bottom rack, 80, 378, 389  
Bottom Slots, 396  
Boundary layer, 258, 259  
Boussinesq equation, 338  
Boussinesq, 19  
Break in Grade, 172  
Bresse's function, 196  
Bresse's solution, 195, 196  
Brink depth, 335  
Broad-crested weirs, 295, 326

## C

Calibration, 220  
Canal-design practice, 139

Cavitation, 316  
Celcrity, 469  
Central Water Commissions (CWC), 139  
Channel, 369  
Channel with a Hump, 60  
Channels of the first kind, 105  
Channels of the second kind, 106  
Channels with Large Slope, 12  
Channels with Small Slope, 11  
Characteristic, 412, 450  
Characteristic grid method, 451  
Chezy coefficient, 86  
Chezy formula, 86, 90  
Choked conditions, 69, 70, 184  
Choppy Jump, 254  
Chute blocks, 280  
Circular Channel, 56, 112  
Circular culvert, 271  
Circular hydraulic jump, 291, 292  
Circular jump, 291  
Clear-water scour, 513  
Clinging nappe, 296  
Coefficient of contraction, 298, 347  
Coefficient of discharge, 298, 318  
Coherence method, 128  
Colebrook-White equation, 88  
Complimentary weir, 307, 312  
Composite roughness, 101  
Compound channels, 125  
Compound sections, 211  
Concave curvilinear flow, 15  
Concave Wall, 409  
Confined nappe, 336  
Constriction Scour, 519  
Contact load, 495  
Continuity equation, 19, 30, 347  
Contracted Weir, 302  
Contraction scour, 513  
Contractions, 433  
Control point, 169  
Control section, 169  
Control volume, 26, 28, 29, 85  
Convex corner, 433  
Convex curvilinear flow, 13  
Convex Wall, 410  
Conveyance, 104, 123  
Courant condition, 452  
Critical depth, 43, 73

Critical depth in circular channels, 49  
 Critical discharge, 51  
 Critical motion, 485  
 Critical shear stress, 485  
 Critical slope, 131, 132, 136, 161  
 Critical slope channel, 131  
 Critical tractive force, 485  
 Critical velocity ratio, 509  
 Critical-flow condition, 43  
 Cubic parabola, 43  
 Culvert, 295, 352  
 Curvilinear flow, 13

**D**

Dam break, 443  
 Dam Break problem, 475  
 Darcy–Weisbach equation, 87  
 Darcy–Weisbach friction factor, 87  
 Datum constant, 312, 313  
 De Marchi Coefficient CM, 382, 383  
 De Marchi Equation, 382, 383  
 De Marchi varied flow function, 383  
 Degradation, 512  
 Degradation scour, 513  
 Delivery of, 227  
 Design head, 317  
 Design-energy head, 318  
 Diagonal Interface Method, 127  
 Differential equation of GVF, 190, 201  
 Diffusing scheme, 453  
 Diffusion coefficient, 498  
 Diffusion scheme, 454  
 Direct integration, 189  
 Direct Numerical Methods, 452  
 Direct-Step method, 203  
 Divided channel, 219  
 Divided Channel method (DCM), 127  
 Drowned jump, 282  
 Dunes, 488  
 Dynamic equation of GVF, 159

**E**

Effective length, 318  
 Effective piezometric head, 10, 16, 17, 19  
 Empirical formulae, 100  
 Empirical Methods, 128  
 End contractions, 324  
 End depth, 295, 335  
 End sill, 280  
 Energy Dissipator, 248, 279  
 Energy equation, 22, 30

Energy loss in the jump, 260  
 Equation of continuity, 19  
 Equivalent roughness, 101, 102, 127  
 Equivalent sand-grain roughness, 87  
 Euler's equation, 10  
 Exchange Discharge Model, 128  
 Expansion, 433  
 Explicit method, 449, 453  
 Exponential channel, 75

**F**

FHWA, 358  
 Finite crest width weir, 364  
 Finite-difference schemes, 449  
 Finite-element method, 449  
 First hydraulic exponent, 51, 73  
 Fluid, 1  
 Flood banks, 150  
 Flood plain, 125  
 Flood routing, 439  
 Flood wave, 38  
 Free Board, 141  
 Free flow, 296, 347  
 Free jumps, 282  
 Free overfall, 34, 37, 334  
 Free repelled jump, 283  
 Free surface, 1  
 Free-mixing zone, 259  
 Free-surface flow, 189  
 Friction slopes, 430  
 Froude line, 412  
 Froude number, 44, 47, 48, 49  
 Full rough flow, 87

**G**

Ganguillet and Kutter Formula, 91  
 General scour, 513  
 General Transition, 71  
 Generalised – flow relation, 134, 180  
 Generalized slope, 150  
 Gradually varied flow, 3, 4, 157  
 Graphical method, 189  
 Grit chamber, 315  
 GVF equation, 183  
 GVF profile, 194

**H**

HDS-5, 352  
 HEC-18, 20, 23, 515  
 HEC-RAS, 218  
 Helical secondary, 126

Horizontal bed, 161  
 Horseshoe vortex, 514  
 Horton's formula, 102, 103  
 Hump height, 60  
 HY-8, 358  
 Hydraulic drop, 229  
 Hydraulic exponents, 199  
 Hydraulic jump, 36, 248  
 Hydraulic radius, 86  
 Hydraulically efficient, 119  
 Hydraulically efficient  
   trapezoidal, 120  
 Hydraulically smooth wall, 87  
 Hydrostatic, 157  
 Hydrostatic distribution, 14  
 Hydrostatic pressure, 10  
 Hydrostatic Pressure  
   Distribution, 11

**I**

Ideal contraction, 424  
 Implicit method, 449, 454  
 Inception of cavitation, 319  
 Incipient motion, 485  
 Incompressible fluid, 1  
 Indian Practice, 522  
 Initiation of motion, 485  
 Inlet control, 352  
 Interface, 125  
 Irrigation Engineering, 139  
 Island-type flow, 223

**J**

Jump profile, 257  
 Jumps on a Sloping Floor, 274, 275

**K**

Karman-Prandtl equation, 87  
 Keifer and Chu's method, 200  
 Kennedy Equation, 509  
 Kerb outlets, 390  
 Kinetic Energy, 7  
 Kinetic energy correction factor, 8  
 Kutta-Merson Method, 221

**L**

Lacey's Equations, 509  
 Lacey-Inglis method, 523  
 Laminar sublayer, 87, 485  
 Lateral flow, 368

Lateral spillway, 369  
 Lateral weir, 380  
 Law of the Wall, 92  
 Lax-Wendroff schemes, 454  
 Leap-Frog, 454  
 Limit slope, 132, 136  
 Linear Proportional Weir, 306  
 Linear-momentum equation, 26  
 Live-bed scour, 513  
 Local phenomenon, 295  
 Local scour, 513  
 Location of the jump, 281  
 Long-crested weir, 327  
 Longitudinal Slope, 140  
 Lower nappe, 296

**M**

Manning's formula, 89, 90, 377  
 Manning's  $n$ , 90  
 Maximum discharge, 117  
 Mechanics, 1  
 Median drain, 356  
 Median size, 485  
 Membrane analogy, 95  
 Method (DCM), 220  
 Method of characteristics, 430  
 MIKE 21, 218  
 Mild slope, 161  
 Mild slope channel, 131  
 Minimum specific energy, 73  
 Mobile bed channels, 484  
 Mobile boundary channels, 2  
 Modular limit, 300, 329, 350  
 Momentum, 8  
 Momentum correction factor, 8  
 Momentum equation, 26, 30  
 Momentum equation in  
   conservation form, 443  
 Momentum exchange, 125  
 Monoclinical wave, 480  
 Moody chart, 88  
 Moody diagram, 145, 485  
 Most Efficient Channels, 121  
 Most efficient section, 121  
 Mostkow Equations, 391  
 Moving Hydraulic Jump, 465  
 Moving-boat method, 33  
 Multi-island-type flow, 223, 225  
 Multi-roughness type  
   perimeter, 101

**N**

Narrow channels, 93  
 Narrow-crested, 328  
 Natural channel, 6, 9, 218  
 Natural streams, 100  
 Negative disturbance, 410  
 Negative surge, 459, 468, 480  
 Negative Wave, 469  
 Non-prismatic channel, 151  
 Non-rectangular channel, 265  
 Non-uniform flow, 3  
 Normal Acceleration, 14  
 Normal depth, 81, 105, 110,  
 Notch, 295  
 Notch-orifice, 314  
 Numerical Method, 128, 189, 448

**O**

Oblique jump, 415  
 Oblique shock, 433  
 Oblique shock wave, 414  
 Ogee Crest, 317  
 Ogee spillway, 316  
 One-dimensional analysis, 7, 126  
 Open channel, 1, 88  
 Orifice, 314  
 Oscillating jump, 253, 293  
 Outlet control, 352  
 Overflow spillways, 295, 262, 316  
 Overland flow, 5  
 Overrun, 446

**P**

Parabolic, 305  
 Parshall Flume, 334  
 Pavlovski formula, 91, 103  
 Performance curve, 357  
 Permissible Velocities, 140  
 Piezometric head, 12  
 Plane bed, 488  
 Positive surge, 459, 480  
 Prandtl, 86  
 Prandtl's mixing length theory, 497  
 Prandtl-Meyer fan, 413, 429  
 Prandtl-Meyer function, 408  
 Preissmann Scheme, 455  
 Pressure, 10  
 Pressure distribution, 10, 30  
 Preston tube, 5, 95  
 Primary vortex, 519  
 Prismatic channels, 1, 85, 207

Profile analysis, 183  
 Projecting barrel, 353  
 Proportional weir, 305  
 P-weirs, 306

**Q**

Quadrant plate weir, 309  
 Quadratic weir, 312, 361

**R**

Rapidly varied flows, 3, 4, 295  
 Rectangular Section, 47  
 Rectangular Weir, 295  
 Rectangular-grid method, 452  
 Regime channel, 504, 508  
 Rehbock formula, 298  
 Relative roughness, 87  
 Repelled jump, 282, 284  
 Reynolds number, 93, 298  
 Rigid bed channels, 484  
 Rigid channels, 2  
 Ripples, 488  
 Robert Manning, 89  
 Roll waves, 431  
 Roller, 259, 460  
 Rough turbulent-flow, 89  
 Roughness, 140  
 Rouse equation, 498  
 Runge-Kutta methods, 221

**S**

Saint Venant equations, 443  
 Saltation load, 495  
 Scales, 259  
 Scour, 512  
 SCS, 142  
 Second hydraulic exponent, 123  
 Secondary currents, 5  
 Section factor, 51  
 Sediment, 484  
 Sediment engineering, 2  
 Sediment load, 495  
 Sediment rating curve, 503  
 Sediment transport, 2, 101, 484  
 Sedimentation Engineering, 484  
 Self-similar, 259  
 Separation, 319  
 Sequent Depth Ratio, 250  
 Sequent depths, 248  
 Shallow waves, 402  
 Sharp-crested weirs, 295

- Shear Reynolds number, 485
  - Shear stress, 86
  - Shear velocity, 87, 259, 485
  - Shear-stress distribution, 2
  - Shields curve, 485
  - Shock fronts, 404
  - Shock wave, 71, 404, 406
  - Side weir, 380
  - Side-channel spillway, 367
  - Sill, 279, 298
  - Simple-island-Type Flow, 224
  - Siphon tube irrigation systems, 378
  - Skijump spillway, 34
  - Slope-discharge-continuity theorem, 311
  - Sloping apron, 290
  - Sluice gate, 25, 295, 347
  - Spatially varied flow, 5, 20, 38, 367
  - Special Weirs, 315
  - Specific energy, 42, 73
  - Specific Force, 30
  - Spillway bucket, 16
  - Spillway crest, 32
  - St. Venant's equations, 217
  - Stability, 431, 433, 468
  - Stability analysis, 431
  - Stable flows, 431
  - Stagnation point, 514
  - Standard lined canal sections, 114
  - Standard lined trapezoidal section, 114
  - Standard lined triangular section, 114
  - Standard-step Method, 203, 207, 211
  - Standing wave, 491
  - Standing-wave flume, 332
  - Steady flow, 2, 19, 26
  - Steady jump, 293
  - Steady uniform flow, 3
  - Steep slope, 161
  - Steep slope channel, 131
  - Stilling basin, 279, 280
  - Straub's Equations, 273
  - Streamlined transition, 422
  - Strickler formula, 100
  - Strickler's Equation, 493
  - Strong jump, 293
  - Subcritical flow, 44, 60
  - Submerged, 282
  - Submerged flow, 300, 329, 350
  - Submerged jump, 282, 283
  - Submerged sluice-gate, 34
  - Submergence, 300
  - Submergence factor, 282
  - Submergence limit, 300
  - Submergence ratio, 300
  - Sudden drop, 172
  - Super elevation, 142
  - Super critical expansions, 427
  - Supercritical Flow, 62
  - Supercritical flow region, 44
  - Supercritical streams, 402
  - Supersonic flows, 408
  - Supersonic nozzles, 428
  - Suppressed weirs, 302
  - Surface of zero shear, 127, 128
  - Surface of zero shear stress, 127
  - Surface tension, 1, 298, 303
  - Surface velocity, 7
  - Surges, 438, 459
  - Suspended load, 495, 502
  - Sutro Weir, 304, 361
  - SVF with increasing discharge, 367
- T**
- Tailwater depth, 280, 282
  - Tailwater level, 282
  - The section factor for uniform-flow computations, 104
  - Thin plate weir, 295
  - Throated flume, 332
  - Tidal bores, 464
  - Top width, 44
  - Torrents, 9
  - Total bed material load, 495, 500
  - Total energy, 42, 151
  - Total load, 495
  - Total scour, 513
  - Transients, 438
  - Transition, 60, 66, 73, 426
  - Transitional depth, 180
  - Transitional profile, 370, 371, 400
  - Trapezoidal Channel, 49
  - Trapezoidal Method, 222
  - Trench weir, 390
  - True broad-crested weir, 327
  - Turbulent flows, 87
  - Turbulent regime, 1
  - Two-stage channel, 125
- U**
- Unconfined nappe, 336
  - Uncontracted, 302
  - Underdesigning of the spillway, 320
  - Undular jump, 253